The Use of Solid Biomass Stoves for Heating: An Investigation Into the Effects of Fuel Properties and Operational Practices on Pollutant Emissions

Andrew Price-Allison

Submitted in accordance with the requirements for the degree of
Doctor of Philosophy

The University of Leeds
School of Chemical and Process Engineering

June, 2022

The candidate confirms that the work submitted is his/her own, except where work which has formed part of jointly-authored publications has been included. The contribution of the candidate and the other authors to this work has been explicitly indicated below. The candidate confirms that appropriate credit has been given within the thesis where reference has been made to the work of others.

1. Price-Allison, A., Lea-Langton, A.R., Mitchell, E.J.S., Gudka, B., Jones, J.M., Mason, P.E., Williams, A., 2019, Emissions performance of high moisture wood fuels burned in a residential stove, Fuel, 239, pp.1038-1045
2. Price-Allison, A., Mason, P.E., Jones, J.M., Barimah, E.K., Jose, G., Brown, A.E., Ross, A.B., 2021, The impact of fuelwood moisture content on the emission of gaseous and particulate pollutants from a wood stove, Combustion Science and Technology

Publication #1 has been included in **Chapter 5** with some modifications. Publication #2 has been included in **Chapter 6** with some modifications. The candidate principally designed the experiments, conducted the experimental work, conducted the data analysis and drafted the manuscripts.

Regarding publication #1, Dr. Eddy Mitchell and Dr. Bijal Gudka assisted in experimental work. Dr. Patrick Mason assisted in results analysis and statistics. Dr. Patrick Mason, Prof. Jenny Jones and Prof. Alan Williams assisted in the drafting of the manuscript.

Regarding publication #2, Dr. Eric Barimah, Dr. Aaron Brown, Dr. Jeanine Williams, Dr. Adrian Cunliffe and Dr. Alexander Kulak assisted in experimental work. Dr. Patrick Mason, Prof. Jenny Jones and Prof. Alan Williams assisted in the drafting of the manuscript.

Acknowledgements

Abstract

There is considerable public interest in the emission of pollutants, especially smoke, from wood burning stoves in the UK. The popularity of residential combustion appliances has increased in recent years which has contributed in poor urban air quality. Additionally, the use of inadequate fuels and limitations in stove testing methods may suggest that the negative impact of such appliances is worse than currently predicted.

Combustion testing was undertaken on a HETAS approved 5.7 kW Waterford Stanley Oisin SF NB multifuel heating stove. A custom LabVIEW development platform was constructed for measuring various combustion properties including burning rate, flue gas flowrate and temperature. Gaseous pollutant analysis was undertaken using fourier transform infrared (FTIR) spectroscopy and electrochemical sensors. Particulate pollutant sampling was undertaken using a Dekati PM_{10} Impactor system. Independent studies investigated changes in combustion conditions and pollutant formation associated with (*i*) changes in the properties of the fuel and (*ii*) the influence of the stove operator. Predominantly, the impact of fuelwood moisture content, cold-start operation and reproducibility where reviewed.

Moisture content (MC%) was shown to significantly affect the properties of the combustion reaction. The combustion of wet fuelwood resulted in lower combustion temperatures and a prolonged burning period (reduced burning rate). The emission of CO, CH_4, non-methane volatile organic compound (NMVOC) and CH_2O was shown to increase with (*i*) an increase in MC% and (*ii*) the subsequent reduction in combustion temperature. The average CO emission for dry fuelwood (MC is <20%) was 59.0 ± 22.4 g/kg_{fuel} and for wet fuelwood (MC is >20%) was 105.6 ± 12.3 g/kg_{fuel}. The average CH_4 emission for dry fuelwood was 1.32 ± 0.76 g/kg_{fuel} and for wet fuelwood was $5.01.6\pm2.48$ g/kg_{fuel}. The average NMVOC emission for dry fuelwood was 2.14 ± 1.26 g/kg_{fuel} and for wet fuelwood was 8.51 ± 4.17 g/kg_{fuel}. The average CH_2O emission for dry fuelwood was 0.47 ± 0.36 g/kg_{fuel} and for wet fuelwood was 2.00 ± 1.09 g/kg_{fuel}. Both NOx and SO_2 emission was shown to be generally unaffected by MC% and was dependent upon fuel nitrogen and sulphur content. Particulate matter (PM) emission was also found to vary depending on MC%. The combustion of dry fuelwood produced lower PM emissions (2.03 ± 1.06 g/kg_{fuel}) than wet fuelwood (7.20 ± 4.85 g/kg_{fuel}). As a result, combusting fuelwood which maintains *Ready to Burn* certified moisture contents contributes in a PM emission reduction of 112%. In addition, the structure and morphology of soot generated by the combustion of dry and wet fuelwood was also found to differ. Dry fuelwood produced soot comprising long chains of spherical particulate matter which

presented a higher elemental carbon (EC) fraction. Alternatively, wet fuelwood produced amorphous tar-like material which presented a higher organic carbon (OC) fraction.

The impact of repeat stove testing was examined in order to determine the effect of prolonged operational practices and emission inventory sample size on the properties of the combustion process and results confidence. An increase in the inventory size resulted in an improvement in results confidence to an extent. Issues relating to reproducibility were observed when additional batches were applied to the stove. An increase in combustion temperature was identified during prolonged stove operation which improved combustion efficiency and reduced reproducibility. Poor stove operation was also presented during prolonged operation in response to limitations in the fuel. Finally, individual events relating to the dynamic nature of the combustion reaction limited reproducibility. These events, such as a fuel particle falling from the heated grate, leads to an increase in emissions and is identified as an uncontrollable factor.

Finally, the inclusion of cold-start operation within standard operating practices and emission inventories was investigated. Cold-start testing is often negated from standardised testing procedures due to the difficulties in attaining repeatable results. The findings of this work revealed a notable increase in the average emission of CO by a factor of 2.9, total hydrocarbon (THC) by a factor of 2.4 and PM by a factor of 1 when cold-start data was included. Data from stove testing is applied in the regulation of appliances and in climate modelling. These results show that by neglecting cold-start data from accreditation and testing practices, emission inventories may be underestimating the true impact of stove operation. This is of greater importance in urban locations where air quality problems persist, and stove operational duration may be confined to a single cold-start batch only.

Table of Contents

List of Tables

List of Figures

Nomenclature

AAE	Absorption Ångström Exponent
af	As fired basis
ar	As received basis
BB or B	Biomass briquettes
BC	Black carbon
Bfl	Fuelwood batch mass
BL	Beech logs
BrC	Brown carbon
BW	Bound water
C	Concentration
CBT	Characteristic burning time
cDAQ	Compact data acquisition
CDF	Cumulative distribution function
CE	Combustion efficiency
CI	Confidence interval
CL	Confidence level
CN	Cetane number
CODT	CO conc. in dilution tunnel
COF	CO conc. in flue
CO_{FTIR}	CO conc. via FTIR
CO_{Testo}	CO conc. via Testo 340
cpm	Cycle(s) per minute
cps	Cycle(s) per second
CS	Cold start
CV	Calorific value
daf	Dry ash free basis
db	Dry basis
DF	Dilution factor

dp	Differential pressure
D_{rel}	Relative darkness
DSC	Differential scanning calorimeter
EC	Elemental carbon
EDX	Energy Dispersive X-Ray spectroscopy
EF	Emission factor
F	Fuelwood
FC or FC%	Fixed carbon
FCB	Fresh cut beech
FCS	Fresh cut spruce
FID	Flame ionization detector
$Flue_v$	Flue gas velocity
FSP	Fibre saturation point
FTIR	Fourier-transform infrared
$Fuel_N$	Fuel nitrogen
$Fuel_S$	Fuel sulphur
FW	Free water
GJ	Gigajoule
GHG	Greenhouse gas
HACA	Hydrogen abstraction-carbon addition
HAP	Household air pollution
HHV	Higher heating value
K	Kindling
KDB	Kiln dried beech
KDS	Kiln dried spruce
LHV	Lower heating value
MC or MC%	Moisture content
$MC\%_{Probe}$	Moisture content determined via probe
$MC\%_{Prox.}$	Moisture content determined via proximate analysis

MCE	Modified combustion efficiency
MJ	Megajoule
NCV	Net calorific value
NDIR	Nondispersive infrared
NI	National Instruments
NMHC	Non-methane hydrocarbon
NMVOC	Non-methane volatile organic compound(s)
NTP	Normal temperature and pressure
OC	Organic carbon
OGC	Organic gaseous carbon
OH	Hydroxyl
OM	Organic matter
PAH	Polyaromatic hydrocarbon(s)
PC	Particulate carbon
PCDD/F	polychlorinated dibenzo-dioxines/dibenzofurans
PM	Particulate matter
PM_t	Total particulate matter fraction
ppm	Parts per million
PTFE	Polytetrafluoroethylene
Py-GC-MS	Pyrolysis gas chromatography
R	Pearson's correlation coefficient
RBG	Red, blue, green
RHI	Renewable Heat Incentive
RSF	Residential solid fuel
SB	Seasoned beech
SCA	Smoke control area(s)
SDFGV	Specific dry flue gas volume
SE	Standard error
SEM	Scanning electron microscopy

SOVC	Semi-volatile organics
SS	Seasoned spruce
STP	Standard temperature and pressure
T	Torrefied briquettes
TB	Test batch
TC	Total carbon
TGA	Thermogravimetric analysis
TN	Total nitrogen
TOA	Thermo-optical analysis
TOC	Total organic carbon
UV-Vis	Ultraviolet visible
VFA	Volatile fatty acid
VI	Virtual instrument
VM or VM%	Volatile material
VOC	Volatile organic compound(s)
vol-%	Volume percent
wb	Wet basis
WS	Warm start
Wt or Wt%	Weight percent

Chapter 1
Background and Context

1.1 Climate Change and Bioenergy

Climate change is the single most important issue facing the world today. Anthropogenic driven modification of the natural world has resulted in negative consequences for both the environment and future human development. Though there remains uncertainty regarding the magnitude of change in global temperature trends associated with greenhouse gas (GHG) emissions (Held and Soden, 2006) the general consensus indicates a global average increase between 1.5°C and >4°C by the end of the 21st century (IPCC, 2021). The impact of climate change is complex and not fully understood with likely environmental impacts relating to desertification, land degradation, ecological deterioration, sea-level-rise, drought, and an increase in the frequency of extreme weather events (Singh, 2019). In addition, such processes are likely to present a direct and detrimental impact upon the anthroposphere including food and water insecurity, social displacement, increase in regional disease prevalence, economic impacts, and conflict (IPCC, 2018).

Pollutant emissions associated with global warming include water vapour, N_2O, CH_4, O_3 and CO_2 with the latter being the most prevalent. Atmospheric CO_2 concentrations are known to have increased from 280 ppm, during the pre-industrial period, to 417 ppm in 2022 (MacFarling Meure et al., 2006; NORA, 2022). Similarly, CH_4 has been shown to increase by 160% since preindustrial times while average atmospheric N_2O is increasing at a rate of 1.20 ppm/year (Bruhwiler et al., 2021). **Figure 1.1** shows the increase in atmospheric GHG and CO_2 emissions and the likely impact upon average temperature anomaly.
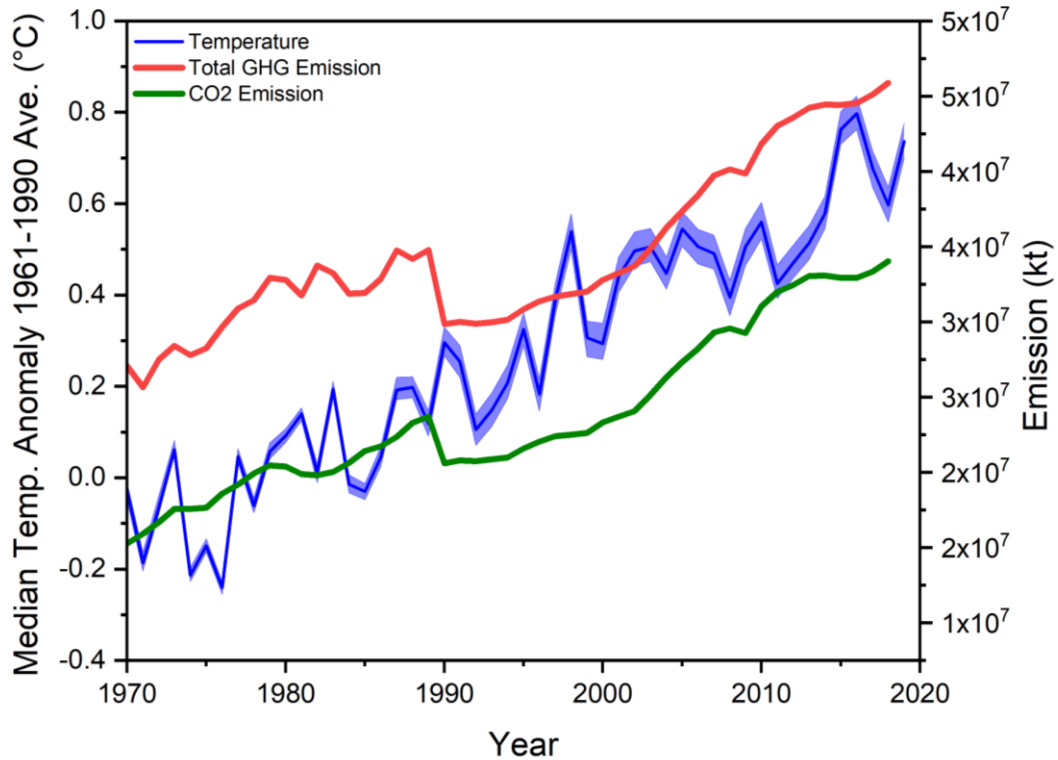
Figure 1.1 Variation in median temperature anomaly from the 1961-1990 global average including upper and lower 95% CI (TheWorldBank.org, 2022a). CO_2 emission is presented in kt and Total GHG in kt of CO_2 equivalent (TheWorldBank.org, 2022b; TheWorldBank.org, 2022c).

The IPPC outlines a number of primary GHG sources associated with human activity including; energy supply (29.3%), transport (19.5%), industry (19%), residential and commercial (11.5%), agriculture (11.3%), waste management (3.2%), international aviation (3.0%), international navigation (3.0%) and other sources (0.2%) (EEA, 2016). GHG emission relating to combustion may be separated into two sectors; energy supply associated with large scale power generation and residential processes relating to heating and cooking practices.

In 2008, the UK established the Climate Change Act which proposed a reduction in GHG emissions by 100% relative to 1990 baseline levels by the year 2050 (GOV, 2008). The Act is responsible for ensuring all seven GHG pollutants outlined within the Kyoto Protocol (CO_2, CH_4, N_2O, HFC's, PFC's, SF_6 and NF_3), signed by 192 countries including the UK, remain below a level that would prevent what is described as "dangerous anthropogenic interference" to global climate systems (UNFCCC, 2022b). This commitment was further developed with the signing of the 2016 Paris Agreement which set the limit of minimising global warming to 1.5-2°C compared to pre-industrial temperatures (UNFCCC, 2022a). Renewable energy generation is identified as a promising approach to achieving these targets. The Renewable Energy Directive (2009/28/EC) defines renewable resources as "energy

from renewable non-fossil sources, namely wind, solar, aerothermal, geothermal, hydrothermal and ocean energy, hydropower, biomass, landfill gas, sewage treatment plant gas and biogases" (EU, 2009). As such, the 2009/28/EC outlines the requirement of member states to replace 30% of power generation, 12% of heat generation and 10% of transport with renewable alternatives by 2020 (GOV, 2022). As of 2020 the total UK energy supplied from renewable resources equated to 21.5%, an increase of 11.4% from 2010 levels. Additionally, bioenergy was identified as the most significant renewable energy resource in 2020, contributing 37% of the total renewable derived supply (BEIS, 2021).

1.2 Residential Combustion

Fuelwood combustion is the most significant renewable energy resource for domestic heating in Europe (Wöhler et al., 2016). Residential combustion maintains a significant contribution towards both UK and European GHG emissions. Wood use is increasing. In 2010, residential emission contributed 15% towards the total UK greenhouse gas emissions of which 94.9% was derived from domestic combustion (AEA, 2012). Similarly, in 2005 European household emissions from solid-fuel combustion contributed 45% of the total $PM_{2.5}$ equating to more than three times the pollution generated by road transport (Amann et al., 2005).

Domestic combustion practices have changed significantly in recent years. Processes of social preference, the inherent opinion of biomass combustion as a clean and sustainable energy resource, relatively reduced fuel costs, and governmental incentives have resulted in the substantial increase in the combustion of biomass across Europe (Viana et al., 2016). In the UK most stove use is identified as a "lifestyle choice" with 46% of users being from high earning AB social grades (higher and intermediate professional occupations). Of the stove users it is estimated that 28% use appliances recreationally for aesthetic reasons, 18% use is based upon tradition and 8% is out if necessity (KANTAR, 2020).

The quantity of biomass consumed for the purpose of residential heating increased by 56% between 1991 and 2011 (DEFRA, 2017). In response to increased consumer demand, the Stove Industry Alliance (SiA) estimate that more than 1 million homes currently maintain a wood burning stove or open-fireplace with an additional 175,000 new devices installed annually (SiA, 2017). A similar trend is observed in Europe with more than 65 million direct heating appliances (Mudgal et al., 2009) and 8 million indirect heating appliances (Krecl et al., 2008) currently installed (Cincinelli et al., 2019). An increase in the bioenergy capacity for the UK has been observed in recent years however this coincides with an increase in the quantity of fuelwood combusted from 138 ktoe in 1990 to 1,115 ktoe in 2020 (BEIS,

2021). This is a likely response to several governmental incentives which has seen an increase in the use of fuelwood for residential and industrial heating practices. Specifically, the domestic and non-domestic Renewable Heat Incentive (RHI) encouraged the development of combustion technologies which contributed in an increase in woodburning practices.

DUKES identifies more than 35% of renewable heat and 5.4% of renewable energy is generated from small-scale, domestic wood consumption (MacLeay et al., 2014). Though reliance on fuelwood remains low with 80% of consumers relying on residential solid fuel (RSF) as a secondary source of heating only (BEIS, 2016b), an increasing awareness within both the literature and governmental legislation regarding the detrimental consequences of domestic combustion on both health and environment, calls into question the use of such devices within the urban setting. Lee (2005) estimates that domestic combustion is responsible for between 30% and 80% of net polyaromatic hydrocarbon emissions (PAH) and 10% of polychlorinated dibenzo-pdioxines and dibenzofurans (PCDD/F) emissions (Wild and Jones, 1995; Wenborn, 1999; Lee, 2005) with residential sources responsible for significant $PM_{2.5}$ contribution (Gelencser et al., 2007; DEFRA, 2012). In line with recent legislation, the use of stoves in urban locations will require greater control and regulation.

Though solid fuel consumption is identified as a minority source of domestic heat generation in the UK, global trends indicate a significant reliance particularly when associated with cooking practices. Though advances have been made towards universal electrification, projections indicate that more than 2.3 billion people will maintain a continued primary reliance upon solid fuel, or kerosene for cooking by the year 2030 (IEA, 2017); a reduction from 2.5 billion predicted in 2006 (IEA, 2006). Such processes are particularly pronounced in sub-Saharan Africa and Asia where between 80-90% of rural populations rely on solid fuel for cooking activities (GAFCC, 2016). **Figure 1.2** presents variability in solid fuel consumption and use of fuelwood as a resource for cooking. In addition, regional variation is presented in response to premature mortalities due to household air pollution (HAP); a process of particular importance in the context of the current research and contemporary challenges (GAFCC, 2016; BEIS, 2016b).
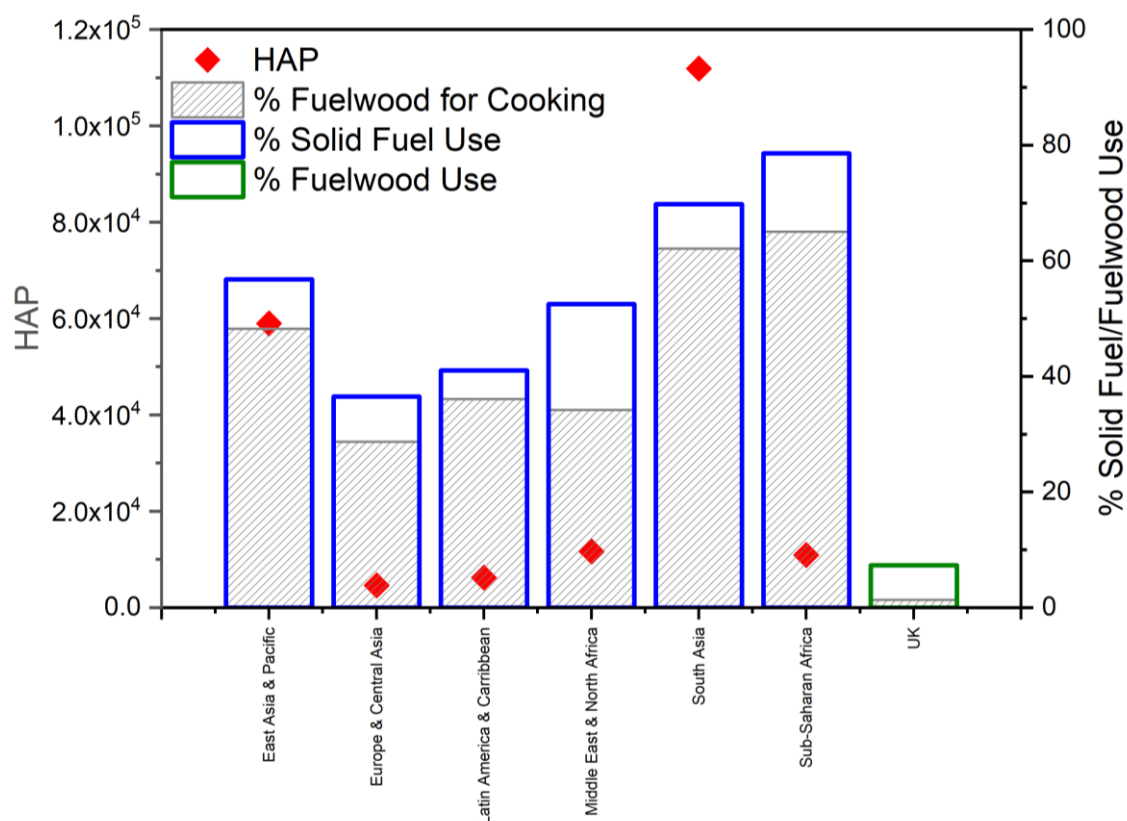
Figure 1.2 Differences in solid fuel and fuelwood use, the use of fuelwood applied in cooking practices, and mortalities relating to household airborne pollution (HAP) (GAFCC, 2016; BEIS, 2016b).

1.3 Information on Wood and Solid Fuel Use in the UK

Fuelwood combustion has increased significantly in recent years with an estimated 2.41 Mt consumed in the UK between 2018-2019 (DEFRA, 2020). The extent of use and operating practices regarding residential heating appliances in the UK is largely unknown. Uncertainty is particularly prevalent when attributing the use of fuelwood within the domestic heating sector. Residential solid fuels (RSW) are often designed to standardised practices which place limitations on fuel characteristics with fuelwood graded under BS EN 17225-5: 2021 and BS EN 14961-5: 2011. However, a significant fraction of fuelwood consumed within the UK originates from an informal or "grey" market where fuel standardisation practices are not adhered to. As much as 31% of total fuelwood is sourced from the grey market within the UK and is likely sourced from the end users own land or by gathering practices (BEIS, 2016a). The exact quantity of fuelwood consumed from unregulated sources is likely to be underestimated due to significant uncertainty in domestic heating practices (KANTAR, 2020). In terms of residential combustion, the most significant concern is the use of fuelwood with an inappropriate moisture content.

1.4 The Impact of Moisture Content (MC)

The informal nature of fuelwood acquisition in the UK raises questions on the quality of material being consumed within the domestic heating sector. The primary concern relates to the MC of the fuel and the potential impact upon emissions. Fuelwood is generally categorised based upon the MC of the material. Wet wood is often freshly felled and can have a moisture content within the range of 50-60% (Jones et al., 2014; Černý et al., 2016). Seasoned wood has been stored for a duration allowing the MC to naturally diminish to approximately 20% (DEFRA, 2020). The seasoning duration has an effect on MC% with 12 months of storage being described as part-seasoned and presenting a MC of between 30-35%. Subsequently, prolonged storage of 24 months, further reduces the moisture content to within the range of 20-25% (Rolls, 2013). Kiln-dried material is a fuel which has been mechanically dried so that the MC% is low for improved combustion performance. The MC of this material is generally found within the range of 8-12% (Rolls, 2013; DEFRA, 2020). A recent report outlined the likely consumption of fuelwood based on MC within the UK. A summary of the type of fuelwood used is shown in **Figure 1.3**. Most material consumed was seasoned with a predicted MC value of 20%. Of significant concern is the high quantity of wet material and low quantity of dry material commonly combusted equating to 26.7% and 18.1% of the total fuelwood consumed (DEFRA, 2020).
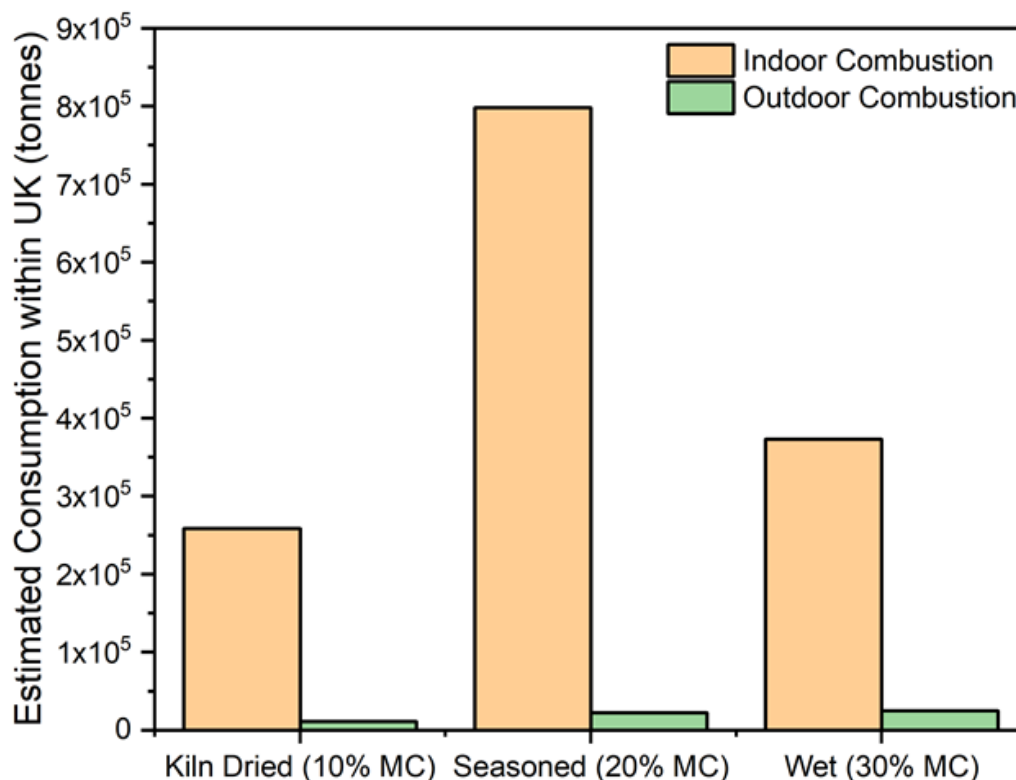
Figure 1.3 Estimated extent of fuelwood combustion within the UK. Indoor combustion refers to the use of fuelwood in residential heating appliances including stoves and open fires. Outdoor combustion refers to the combustion of fuelwood in bonfires and chimineas etc (DEFRA, 2020).

Due to the quantity of high moisture content materials being used, there is growing concern relating to the effect on emissions. Several studies have been undertaken which attempt to assess the impact of such conditions on pollutant formation, however, the general consensus remain unclear. The impact of moisture during fuelwood combustion is therefore complex (Shen et al., 2013) with some authors presenting a positive impact (Lu et al., 2009), others presenting a negative impact (Bignal et al., 2008; Chomanee et al., 2009), and some showing no clear or an indifferent effect (Roden et al., 2006).

1.5 Accuracies in Testing Methods

The testing of stove and fuel performance is undertaken to assess emission criteria, before market deployment. The testing of combustion appliances is generally undertaken in accordance with standardised testing procedures. A number of procedures are available including BS EN 13240 in Europe, BS PD 6436 in the UK and DIN Plus in Germany. The purpose of standardised testing is to allow for accreditation of appliance performance in terms of thermal output, emission generation and safety. Due to the dynamic nature of combustion reactions, the

results of such tests are often highly variable leading to poor repeatability (Trojanowski et al., 2018; Haslett et al., 2018). This results in the quality of contemporary emission inventories, such as the NAEI inventory, generated by standardised testing practices, being called into question (Klauser et al., 2020).

The number of tests required for stove accreditation is outlined within the standard protocols. The number of tests undertaken does however vary depending upon the standard method in question. Additionally, the number of tests applied within the literature is variable with the number ranging between 1-7 (Kinsey et al., 2009; Vu et al., 2012; Cerqueira et al., 2013; Ozgen et al., 2013; Calvo et al., 2014; Phillips et al., 2016; Seljeskog et al., 2017). Additional batch testing may be applied as a method of improving confidence in emission and stove performance analysis (Scott, 2005; Schmidl et al., 2011; Wilton, 2012; Wilton and Bluett, 2012; Wang et al., 2014; Stewart, 2017). Alternatively, it is predicted that the variable nature of combustion reactions inherently limits the capacity for repeatability and increasing the number of tests will not improve results confidence (Coulson et al., 2015).

Standardised combustion practices often require the stove to be under a nominal operating temperature before the initiation of testing. In response, emission from the cold-start batch observed shortly after ignition is often disregarded from the testing procedure, meaning that values are often not incorporated into emission inventories. Cold-start operation is often associated with higher emissions than those observed during warm-start operation (Shelton and Gay, 1986; Nussbaumer et al., 2008; Ozgen et al., 2013). Subsequently, the results generated by means of standardised testing practices, present combustion values that are not representative of real-world domestic application (Houck et al., 2008; Reichert and Schmidl, 2018). This indicates that the effect of stove operation upon air quality and emissions is likely underestimated.

Further work is therefore required to quantify unpredictability in stove testing outcomes to assess the adequate number of tests required for improved result confidence and assess the effect of cold-start operation on emission results.

1.6 Research Gaps

The use of biomass as an alternative method for residential heating has been increasing in Europe in recent years, however, there remains a question as to the carbon neutrality and associated sustainability (Cincinelli et al., 2019). Biomass combustion is identified as a renewable resource under the Renewable Energy Directive (2009/28/EC) and accounted for 45% of the gross EU renewables contribution in 2016, a value which is predicted to rise to between 55-75% by 2050

(Wagner et al., 2010). Despite this, issues remain as to the likely effect of biomass combustion appliance in terms of GHG emission and air quality.

As previously mentioned, a significant proportion of fuelwood consumed within the UK maintains a higher moisture content. The combustion of wet fuelwood leads to reduced efficiency and an increase in pollutant emission (Orang and Tran, 2015; Magnone et al., 2016; Fachinger et al., 2017). This is of real concern from air quality and health points of view and was identified as one of the key research gaps to be addressed in this thesis. In 2017, a preliminary report completed as part of this thesis (**Chapter 5**) was undertaken for the purpose of advising DEFRA on the impacts of fuelwood MC during domestic heating. Results from this investigation assisted in the development of the UK *Ready to Burn* strategy. This resulted in an increased control of wet fuelwood sales within UK markets. Notwithstanding, the use of high moisture fuelwood remains prevalent due to the acquisition of materials from the grey market. Additional research is therefore required to fully understand the effect of such materials on stove performance and aspects relating to air quality.

In addition, a variety of testing approaches may be applied when investigating stove operation and emission formation. Most notably is the process of disregarding cold-start information from testing criteria which may lead to an underestimation of emission trends in contemporary inventories. Furthermore, due to the dynamic nature of combustion reactions and the limited number of repeated tests applied under standardised methods, there remains a high level of uncertainty relating to the quality of these inventories.

It is therefore of particular importance that more research is undertaken assessing the impact of fuelwood moisture content on emission formation and likely shortcomings regarding emission inventories.

1.7 Aims and Objectives

The overall objective of this thesis is to investigate the effect of fuel properties and stove operational techniques on pollutant emission formation. The primary aims of this work include:

Aim 1: To assess the impact of fuelwood moisture content on emission generation and thermal performance in a small residential heating appliance. This work was organised by the following objectives:

Objective 1a: To identify and review the theoretical processes associated with wood-moisture interaction including an assessment of previous research undertaken on the effect of moisture content on pollutant formation.

Objective 1b: To undertake combustion testing of various fuelwood material incorporating different moisture contents and assess emission and thermal performance outcomes.

Objective 1c: To examine the impact of moisture content on soot formation, specifically the soot fraction incorporating particles which are <1μm in diameter.

Aim 2: To assess the different testing methods for the determination of weight percent moisture in fuelwood particles (MC). This work was organised by the following objectives.

Objective 2a: To identify and review methods of moisture content determination which are suitable for fuelwood analysis.

Objective 2b: To undertake analysis of moisture using different methods in order to determine accuracy and evaluate how error could affect combustion testing practices.

Aim 3: To assess the limitations of testing procedures and how these restrictions could have detrimental impacts on emission inventories. This work was organised by the following objectives:

Objective 3a: To identify and review standardised testing methods which are used to define residential combustion appliance performance (thermal and emission performance).

Objective 3b: To investigate the effect of cold-start operation and understand how the incorporation of such values could affect emission inventory data.

Objective 3c: To ascertain the impact of repeatability and duration of testing on statistical confidence or uncertainty.

1.8 Thesis Structure

The following is a breakdown of the thesis structure including publication submissions and co-author acknowledgments.

Chapter 2: Literature Review

This chapter provides an overview of the principals and processes associated with residential combustion and emission formation. The chapter offers a breakdown of the processes of fuel and moisture interaction, methods of MC% determination and methods of moisture content management. Additionally, the chapter outlines the effect of MC% on combustion and emission performance as well as describing other recent findings from within the wider literature.

Chapter 3: Experimental Methodology and Design

This chapter outlines the development of the experimental procedures applied within the experimental work. This chapter includes an overview of the combustion facility design and operation as well as describing the principals of equipment operation. In addition, the chapter outlines the methods of quantifying emissions and methods of post-sampling and fuel characterisation analysis.

Chapter 4: Moisture Content Determination via a Digital 2-Pin Electrical Resistance Meter

This chapter evaluates the use of digital resistance-type meters for the determination of fuelwood moisture content. The principal operation of this type of device is shown as well as alternative methods of MC% determination. The chapter describes the differences in MC% values depending upon the analytical method applied.

Chapter 5: Emissions Performance of High Moisture Wood Fuels Burned in a Residential Stove; Preliminary Study

Citation and Co-authorship: Price-Allison, A., Lea-Langton, A.R., Mitchell, E.J.S., Gudka, B., Jones, J.M., Mason, P.E., Williams, A., 2019, Emissions performance of high moisture wood fuels burned in a residential stove, Fuel, 239, pp.1038-1045

This chapter evaluates the effect of fuel moisture content on stove performance and emissions from a small residential heating appliance. The impact of MC% on burning rate, combustion temperature and gaseous emission profiles are assessed. In addition, particulate matter is evaluated regarding material size distribution and EC/TC composition.

Chapter 6: The Impact of Fuelwood Moisture Content on the Emission of Gaseous and Particulate Pollutants from a Wood Stove

Citation and Co-authorship: Price-Allison, A., Mason, P.E., Jones, J.M., Barimah, E.K., Jose, G., Brown, A.E., Ross, A.B., 2021, The impact of fuelwood moisture content on the emission of gaseous and particulate pollutants from a wood stove, Combustion Science and Technology

This chapter further develops the findings outlined in Chapter 5. Stove and emission performance is presented during the combustion of low moisture and high moisture fuelwood. Specific research is undertaken on the variation in soot physical properties via Py-GC-MS, Raman Nanostructure Analysis and assessment of soot colouration, and what this implies.

Chapter 7: The Effect of Cold-Start Operation on Combustion Conditions and Pollutant Formation

This chapter is a study on the differences in stove and emission performance during cold-start and warm-start operation. Under standardised testing practices the cold-start phase of testing is disregarded due to inconsistencies in operation. This work attempts to investigate the differences in the cold-start phase of testing and the impact of associated emission factors.

Chapter 8: Impact of Replicate Number on Repeatability of Results and the Minimisation of Error when Calculating Emission Factors from a Domestic Stove

This chapter investigates the effect of repeatability during stove testing. Analysis of stove and emission performance was undertaken across a prolonged testing regime to statistically evaluate the effect of the number of repeat tests on results confidence.

Chapter 9: Conclusions

This chapter outlines the key conclusions of the included work as well as offering examples of potential future research.

1.9 References

AEA 2012. Residential: GHG inventory summary factsheet [Online]. Available from: https://www.gov.uk/government/publications/greenhouse-gas-inventory-summary.

Amann, M., Bertok, I., Cofala, J., Gyarfas, F., Heyes, C., Klimont, Z., Schopp, W. and Winiwarter, W. 2005. Baseline scenarios for the Clean Air for Europe (CAFE) programme [Online]. Available from: https://iiasa.ac.at/web/home/research/researchPrograms/air/policy/CAFE-baseline-full.pdf.

BEIS 2016a. Special feature - Domestic wood use survey [Online]. [Accessed 18 May 2020]. Available from: www.gov.uk/government/statistics/digest-of-united-kingdom-energy-statistics-dukes-2014-printed-version.

BEIS 2016b. Summary results of the domestic wood use survey [Online]. Available from: www.gov.uk/government/statistics/digest-of-united-kingdom-energy-statistics-dukes-2014-printed-version.

BEIS 2021. UK energy in brief 2021 [Online]. Available from: https://assets.publishing.service.gov.uk/government/uploads/system/uploads/attachment_data/file/1032260/UK_Energy_in_Brief_2021.pdf.

Bignal, K.L., Langridge, S. and Zhou, J.L. 2008. Release of polycyclic aromatic hydrocarbons, carbon monoxide and particulate matter from biomass combustion in a wood-fired boiler under varying boiler conditions. Atmospheric Environment. 42(39), pp.8863–8871.

Bruhwiler, L., Basu, S., Butler, J.H., Chatterjee, A., Dlugokencky, E., Kenney, M.A., McComiskey, A., Montzka, S.A. and Stanitski, D. 2021. Observations of greenhouse gases as climate indicators. Climate Change. 165.

Calvo, A.I., Tarelho, L.A.C., Alves, C.A., Duarte, M. and Nunes, T. 2014. Characterization of operating conditions of two residential wood combustion appliances. Fuel Processing Technology. 126, pp.222–232.

Černý, D., Malaťák, J. and Bradna, J. 2016. Influence of biofuel moisture content on combustion and emission characteristics of stove.

Cerqueira, M., Gomes, L., Tarelho, L. and Pio, C. 2013. Formaldehyde and acetaldehyde emissions from residential wood combustion in Portugal. Atmospheric Environment. 72, pp.171–176.

Chomanee, J., Tekasakul, S., Tekasakul, P., Furuuchi, M. and Otani, Y. 2009. Effects of Moisture Content and Burning Period on Concentration of Smoke Particles and Particle-Bound Polycyclic Aromatic Hydrocarbons from Rubber-Wood Combustion. Aerosol and Air Quality Research. 9(4), pp.404–411.

Cincinelli, A., Guerranti, C., Martellini, T. and Scodellini, R. 2019. Residential wood combustion and its impact on urban air quality in Europe. Current Opinion in Environmental Science & Health. 8, pp.10–14.

Coulson, G., Bian, R. and Somervell, E. 2015. An investigation of the variability of particulate emissions from woodstoves in New Zealand. Aerosol and Air Quality Research. 15(6), pp.2346–2356.

DEFRA 2020. Estimating UK domestic solid fuel consumption, using Kantar data.

DEFRA 2012. Fine particulate matter ($PM_{2.5}$) in the United Kingdom [Online]. Available from: https://ukair.defra.gov.uk/assets/documents/reports/cat11/1212141150_AQEG_Fine_Particulate_Matter_in_the_UK.pdf.

DEFRA 2017. The Potential Air Quality Impacts from Biomass Combustion.

EEA 2016. Sectoral greenhouse gas emissions by IPCC sector. Data visualisation. [Online]. [Accessed 13 April 2022]. Available from: https://www.eea.europa.eu/data-and-maps/daviz/change-of-CO_2-eq-emissions-2#tab-dashboard-01.

EU 2009. Directive 2009/28/EC of the European Parliament and of the Council [Online]. Available from: https://www.legislation.gov.uk/eudr/2009/28/data.pdf.

Fachinger, F., Drewnick, F., Giere, R. and Borrmann, S. 2017. How the user can influence particulate emissions from residential wood and pellet stoves: Emission factors for different fuels and burning conditions. Atmospheric Environment. 158, pp.216–226.

GAFCC. 2016. Country profiles. Global Alliance for Clean Cookstoves. [Online]. Available from: http://archive.cleancookingalliance.org/country-profiles/index.html.

Gelencser, A., May, B., Simpson, D., Sanchez-Ochoa, A., Kasper-Giebl, A., Puxbaum, H., Caseiro, A., Pio, C. and Legrand, M. 2007. Source apportionment of $PM_{2.5}$ organic aerosol over Europe: Primary/secondary, natural/anthropogenic, and fossil/biogenic origin. Journal of Geophysical Research. 112.

GOV 2022. 2020 renewable heat and transport targets. Publications and Records. [Online]. [Accessed 20 April 2022]. Available from: https://publications.parliament.uk/pa/cm201617/cmselect/cmenergy/173/17302.htm.

GOV 2008. The Climate Change Act 2008 [Online]. Available from: https://www.legislation.gov.uk/ukpga/2008/27/contents.

Haslett, S.L., Thomas, J.C., Morgan, W.T., Hadden, R., Liu, D., Allan, J.D., Williams, P.I., Keita, S., Liousse, C. and Coe, H. 2018. Highly controlled, reproducible measurements of aerosol emissions from combustion of a common African biofuel source. Atmospheric Chemistry and Physics. 18(1), pp.385–403.

Held, I.M. and Soden, B.J. 2006. Robust response of the hydrological cycle to global warming. Journal of Climate. 19(21), pp.5686–5699.

IEA 2006. World Energy Outlook 2006 [Online]. Available from:
https://iea.blob.core.windows.net/assets/390482d0-149a-48c0-959b-
d5104ea308ca/weO$_2$006.pdf.

IEA 2017. World Energy Outlook 2017 [Online]. Available from:
https://iea.blob.core.windows.net/assets/4a50d774-5e8c-457e-bcc9-
513357f9b2fb/World_Energy_Outlook_2017.pdf.

IPCC 2021. Climate Change 2021 - The Physical Science Basis. Sixth Assessment
Report [Online]. Available from:
https://www.ipcc.ch/report/ar6/wg1/downloads/report/IPCC_AR6_WGI_Full_Report.
pdf.

IPCC 2018. Special Report: Global Warming of 1.5°C.

Jones, J.M., Lea-Langton, A.R., Ma, L., Pourkashanian, M. and Williams, A. 2014.
Pollutants Generated by the Combustion of Solid Biomass Fuels. London: Springer.

KANTAR 2020. Burning in UK homes and gardens.

Kinsey, J.S., Kariher, P.H. and Dong, Y. 2009. Evaluation of methods for the
physical characterization of the fine particle emissions from two residential wood
combustion appliances. Atmospheric Environment. 43(32), pp.4959–4967.

Klauser, F., Carlon, E., Kistler, M., Schmidl, C., Schwabl, M., Sturmlechner, R.,
Haslinger, W. and Kasper-giebl, A. 2020. Emission characterization of modern
wood stoves under real-life oriented operating conditions. Atmospheric
Environment. 192, pp.257–266.

Krecl, P., Larsson, E.H., Strom, J. and Johansson, C. 2008. Contribution of
residential wood combustion and other sources to hourly winter aerosol in Northern
Sweden determined by positive matrix factorization. Atmos. Chem. Phys. 8,
pp.3639–3653.

Lee, R.G.. 2005. Emission factors and importance of PCDD/F's, PCB's, PCN's,
PAH's and PM$_{10}$ from the domestic burning of coal and wood in the UK.
Environmental Science and Technology. 39(6), pp.1436–1447.

Lu, H., Zhu, L. and Zhu, N. 2009. Polycyclic aromatic hydrocarbon emission from
straw burning and the influence of combustion parameters. Atmospheric
Environment. 43(4), pp.978–983.

MacFarling Meure, C., Ethridge, D., Trudinger, C., Steele, P., Langenfelds, R., van
Ommen, T., Smith, A. and Elkins, J. 2006. Law Dome CO_2, CH_4 and N_2O ice core
records extended to 2000 years BP. Geophysical Research Letters. 33(14).

MacLeay, I., Harris, K. and Annut, A. 2014. Digest of United Kingdom energy
statistics 2014 [Online]. Available from:
https://assets.publishing.service.gov.uk/government/uploads/system/uploads/attach
ment_data/file/338750/DUKES_2014_printed.pdf.

Magnone, E., Park, S.K. and Park, J.H. 2016. Effects of Moisture Contents in the Common Oak on Carbonaceous Aerosols Generated from Combustion Processes in an Indoor Wood Stove. Combustion Science and Technology. 188(6), pp.982–996.

Mudgal, S., Turbe, A. and Roy, N. 2009. Lot 15 solid fuel small combustion installations. Task 2: Economic and market analysis. Preparation studies for eco-design requirements of EuPs (II) in contract for the European Commission DG TREN.

NORA 2022. Trends in atmospheric carbon dioxide. Carbon cycle greenhouse gases. [Online]. [Accessed 13 April 2022]. Available from: https://gml.noaa.gov/ccgg/trends/global.html.

Nussbaumer, T., Czasch, C., Klippel, N., Johansson, L. and Tullin, C. 2008. Particulate emissions from biomass combustion in IEA countries - Survey on measurements and emission factors.

Orang, N. and Tran, H. 2015. Effect of feedstock moisture content on biomass boiler operation. Tappi Journal. 14(10), pp.629–637.

Ozgen, S., Cernuschi, S. and Giugliano, M. 2013. Experimental evaluation of particle number emissions from wood combustion in a closed fireplace. Biomass and Bioenergy. 50(0), pp.65–74.

Phillips, D., Mitchell, E.J.S., Lea-Langton, A.R., Parmar, K.R., Jones, J.M. and Williams, A. 2016. The use of conservation biomass feedstocks as potential bioenergy resources in the United Kingdom. Bioresource Technology. 212, pp.271–279.

Roden, C., Bond, T., Conway, S. and Pinel, A. 2006. Emission factors and real-time optical properties of particles emitted from traditional wood burning cookstoves. Environmental Science and Technology. 40, pp.6750–6757.

Rolls, W. 2013. The Log Book. East Meon: Permanent Publications.

Schmidl, C., Luisser, M., Padouvas, E., Lasselsberger, L., Rzaca, M., Ramirez-Santa Cruz, C., Handler, M., Peng, G., Bauer, H. and Puxbaum, H. 2011. Particulate and gaseous emissions from manually and automatically fired small scale combustion systems. Atmospheric Environment. 45(39), pp.7443–7454.

Scott, A. 2005. Real-life emissions from residential wood burning appliances in New Zealand [Online]. Available from: http://www.crc.govt.nz/publications/Reports/air-report-emissions-residential-wood-burning-appliances-nz-000805.pdf.

Seljeskog, M., Sevault, A., Østnor, A. and Skreiberg, Ø. 2017. Variables Affecting Emission Measurements from Domestic Wood Combustion. Energy Procedia. 105(1876), pp.596–603.

Shelton, J.W. and Gay, L.W. 1986. Evaluation of low-emission wood stoves [Online]. Sacramento, California. [Accessed 12 June 2020]. Available from:

https://www.arb.ca.gov/sites/default/files/classic//research/apr/past/a3-122-32_exsum.pdf.

Shen, G., Tao, S., Chen, Y., Zhang, Y., Wei, S., Xue, M., Wang, B., Wang, R., Lv, Y., Shen, H., Huang, Y. and Chen, H. 2013. Emission characteristics for polycyclic aromatic hydrocarbons from solid fuels burned in domestic stoves in rural China. Environmental Science and Technology. 47(24), pp.14485–14494.

SiA 2017. The contribution wood burning stoves can make to carbon reduction and sustainable energy. Available from:
http://www.stoveindustryalliance.com/newsarticle/?LatestNews_ID=10000&pPK=618f83d6-c438-%0A4b35-9515-8c3b1aa76bf9.

Singh, R.B. 2019. The science and impact of climate change [Online]. Singapore: Springer Nature. Available from:
https://link.springer.com/content/pdf/10.1007%2F978-981-13-0809-3.pdf.

Stewart, R. 2017. Assessment of particulate emissions from wood log and wood pellet heating appliances [Online]. Harwell. Available from: https://uk-air.defra.gov.uk/assets/documents/reports/cat07/1801291425_170201_Defra_NAEI_appliance_testing_summary_Issue1_Final_copy.pdf.

TheWorldBank.org 2022a. CO_2 and greenhouse gas emissions. [Accessed 8 April 2022]. Available from: https://ourworldindata.org/CO_2-and-other-greenhouse-gas-emissions.

TheWorldBank.org 2022b. CO_2 emissions (kt) - World. [Accessed 4 August 2022]. Available from:
https://data.worldbank.org/indicator/EN.ATM.CO_2E.KT?locations=1W.

TheWorldBank.org 2022c. Total greenhouse gas emissions (kt of CO_2 equivalent) - World. [Accessed 8 April 2022]. Available from:
https://data.worldbank.org/indicator/EN.ATM.GHGT.KT.CE?locations=1W.

Trojanowski, R., Butcher, T., Wei, G. and Celebi, Y. 2018. Repeatability in Particulate and Gaseous Emissions from Pellet Stoves for Space Heating. Energy and Fuels. 32(3), pp.3543–3550.

UNFCCC 2022a. The Paris Agreement. Process and Meetings. [Online]. [Accessed 20 April 2022]. Available from: https://unfccc.int/process-and-meetings/the-paris-agreement/the-paris-agreement.

UNFCCC 2022b. What is the United Nations Framework Convention on Climate Change. Process and Meetings. [Online]. [Accessed 20 April 2022]. Available from: https://unfccc.int/process-and-meetings/the-convention/what-is-the-united-nations-framework-convention-on-climate-change.

Viana, M., Alastuey, A., Querol, X., Guerreiro, C., Vogt, M., Colette, A., Collet, S., Albinet, A., Fraboulet, I., Lacome, J.-M., Tognet, F. and de Leeuw, F. 2016.

Contribution of residential combustion to ambient air pollution and greenhouse gas emissions.

Vu, B., Alves, C.A., Gonçalves, C., Pio, C., Gonçalves, F. and Pereira, R. 2012. Mutagenicity assessment of aerosols in emissions from wood combustion in Portugal. Environmental Pollution. 166, pp.172–181.

Wagner, F., Amann, M., Bertok, I., Cofala, J., Heyes, C., Kilmont, Z., Rafaj, P. and Schopp, W. 2010. NEC Scenario Analysis Report Nr. 7. Baseline emission projections and further cost-effective reductions of air pollution impacts in Europe – a 2010 perspective. Laxenburg.

Wang, Yungang, Sohn, M.D., Wang, Yilun, Lask, K.M., Kirchstetter, T.W. and Gadgil, A.J. 2014. How many replicate tests are needed to test cookstove performance and emissions? - Three is not always adequate. Energy for Sustainable Development. 20(1), pp.21–29.

Wenborn, M.J. 1999. Speciated PAD inventory for the UK.

Wild, S.R. and Jones, K.C. 1995. Polynuclear aromatic hydrocarbons in the United Kingdom environment: A preliminary source inventory and budget. Environmental Pollution. 88(1), pp.91–108.

Wilton, E. 2012. Review - particulate emissions from wood burners in New Zealand [Online]. Available from: https://www.niwa.co.nz/sites/niwa.co.nz/files/WoodburnerReportFinal.pdf.

Wilton, E. and Bluett, J. 2012. Wood Burner Testing Christchurch 2009 : Diurnal variation in emissions , wood use , indoor temperature and factors influencing start-up Prepared for Ministry of Science and Innovation [Online]. Available from: https://www.niwa.co.nz/sites/niwa.co.nz/files/2 - AKL 2012-020 Woodburner testing Chch 2009.pdf.

Wöhler, M., Andersen, J.S., Becker, G., Persson, H., Reichert, G., Schön, C., Schmidl, C., Jaeger, D. and Pelz, S.K. 2016. Investigation of real life operation of biomass room heating appliances - Results of a European survey. Applied Energy. 169, pp.240–249.

Chapter 2
Literature Review

2.1 Wood Fuel Characteristics

Moisture content (MC%) of a fuel resource is the most significant property controlling the effectiveness of a material as an energy resource (Koppejan and Loo, 2008; Phillips, 2018). The use of biomass and solid-fuel resources are therefore controlled based upon MC% while material drying to a specific condition is commonly employed to improve suitability. High MC% has been shown to reduce the efficiency of energy from biomass application throughout the production and supply-chain processes (Obernberger, 1998; Rupar and Sanati, 2003; Koppejan and van Loo, 2008; Murphy et al., 2012; Sosa et al., 2015). The most significant affect relates to the control of combustion quality where higher MC% content inhibits thermal efficiency resulting in incomplete combustion and an increase in pollutant formation (Bignal et al., 2008; Magnone et al., 2016). MC% is an important property associated with biomass because of the relatively high inherent water-content (Choudhury et al., 2015; Orang, 2015). Additionally, the interaction of MC% and biomass is complex and highly variable meaning that the restriction of such parameters requires significant consideration and control (Koppejan and Loo, 2008; Laurila, 2013). The importance of MC% is therefore common for all types of energy extraction from biomass resources (Acharjee et al., 2011; Hermansson et al., 2011; Zhao et al., 2014; Price-Allison et al., 2021).

2.2 Water in Wood

Water availability is considered the most significant control over global flora abundance and distribution (McElrone et al., 2013). Moisture absorbance through root systems operate under a negative water pressure allowing for an uptake of solubilized mineral material from ambient sediment horizons. Though prominent in the development of plant growth, water loss via evapotranspiration results in less than a 5% water retention within the body of the tree (McElrone et al., 2013). Nonetheless, recently felled fuelwood stems present inherently high moisture contents with water composition incorporating up to 50-60% of the total fresh-cut weight (Svoboda et al., 2009; Jones et al., 2014; Černý et al., 2016). As such, the physical characteristics of fresh fuelwood stems may provide for inappropriate fuel for domestic combustion.

2.3 Water Storage in Wood

The interaction of wood and water is a dominant process affecting not only the growth development of a tree but also the biochemical and physical properties of the material. As such, the uptake and transfer of water is a fundamental process affecting nutrient uptake from the soil through root systems and CO_2 transfer across stomata cells in leaves (Green et al., 2003). The mass of water within green wood may incorporate as much as 50% of the material weight (Jones et al., 2014). The minimum MC% generally observed in sapwood is found between 35-60%$_{db}$ and 60-75%$_{db}$ for ring-pored and diffuse-pored angiosperm species and 75-100%$_{db}$ in non-pored gymnosperm species (Stewart, 1967). Once stored within wood, water may be identified as either free or bound depending upon storage location within the tree structure. Free water is generally described as water stored within lumen capillary structures which may incorporate photosynthetic products. Alternatively, bound water is chemically bonded water interacting with wood polymers, including cellulose, hemicellulose and to a lesser extent lignin, via hydroxyl (O-H) bonds (Shmulsky and Jones, 2011; Engelund et al., 2013). In addition, bound-water may be stored in the void spaces between cellulose chains and in the micropores of cell walls (Kekkonen et al., 2013).

Bound-water is the result of the inherent hygroscopic nature of wood (Reeb, 1995). As such, the inherent moisture content is noted to vary with an increase or a decrease in the relative humidity (Hoadley, 2000). The occurrence of bound water, or fixed water, within the tree is the result of strong hydroxyl-bonding between water (H_2O) and wood materials (cellulose, hemicellulose and lignin) as identified in **Figure 2.1**. Two types of water-cell wall interactions are identified within the literature including freezing bound water and non-freezing bound water (Engelund et al., 2013). Freezing bound-water is water which undergoes a phase change between -10 °C and -20 °C and is believed to be less confined with reduced bonding to the cell wall (Engelund et al., 2013). Non-freezing bound-water does not present a phase change down to temperatures of -70 °C (Berthold et al., 1996). The application of a differential scanning calorimeter (DSC) appears to suggest crystallisation peaks at -18 °C for free-water within the lumen of cellulosic biomass while a second bound-water peak may be observed between -13 °C and -23 °C. In addition, a fraction of the bound-water appears non-crystallised at a temperature of 203 K (Nakamura et al., 1981). Such processes may indicate differentiation in the extent to which bound-water interacts with and bonds within cellulosic cell walls (Engelund et al., 2013). However, there is limited evidence to suggest that this process occurs in wood (Thygesen et al., 2010; Engelund et al., 2013) with such processes only occurring in lignocellulosic compounds maintaining weak or strong

acid groups (Berthold et al., 1996; Engelund et al., 2013). Free-water or capillary water is non-bound water molecules located principally within the lumen of green-wood which incorporates concentrations of minerals required for plant growth (Reeb, 1995; Engelund et al., 2013).
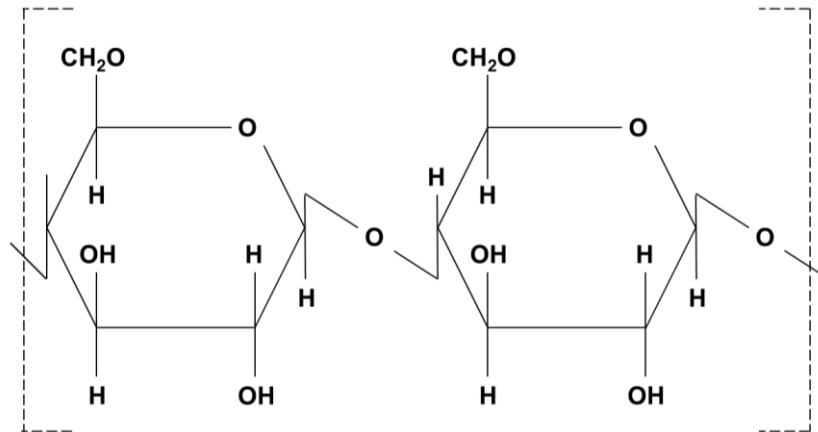
Figure 2.1 The integration of bound-water within the microfibres of a cell wall; the structure identifies the water molecule bound between two cellulose formations (Reeb, 1995).

Initial water loss occurs when there is a reduction in free-water within the wood structure only; bound-water volume remains constant until all the free-water has been lost. Opposingly, water accumulation begins with the storage of bound-water followed by the accumulation of free-water within the lumen (Gezici-Koc et al., 2017). The Fibre Saturation Point (FSP) is the point at which all the free-water has been lost and only bound-water remains within the cell walls. Further drying results in loss of moisture from the bound-water reserve resulting in further mass loss and a shrinkage of the wood structure. Similarly, the addition of further moisture, following FSP, results in an initial increase in bound-water volume until saturation were water is gained within the lumen (Reeb, 1995). Non-bound, free-water is lost initially in response to the limited physical interaction with the biomass material while bound-water is fully integrated within the molecular structure of wood. As such, a greater amount of energy is required to remove bound-water from the cellulose material in response to the demand for breaking molecular bounds (Espenas, 1951).

2.4 Water Transport in Wood

The motion of water transport in trees is driven by passive differential pressure and chemical potential gradients. Water movement through plants is driven by a negative pressure gradient dictated by the loss of water via transpiration in the

leaves (McElrone et al., 2013). Most plants are regarded as highly inefficient in relation to water retention following absorption. The majority of water loss occurs through leaf canopies during evapotranspiration processes (Whiley et al., 1988). Moisture loss, principally through the stomata of leave structures, occurs during the absorption of CO_2; another compound fundamental to tree development. The extent to which trees lose water is significant with some species losing more than 400 molecule of H_2O per molecule of CO_2 absorbed. As such, tree species may retain as little as 5% of the total volume of water absorbed by the root systems (McElrone et al., 2013). This is the fundamental process by which water is drawn through a plant stem under a negative differential pressure. This differential pressure process is identified as the cohesion-tension theory and allows for the creation of a tension gradient along which the flow of water through the xylem is maintained (Bentrup, 2017). This process results in the movement of water from the soil to the root system to the stem to the branches and finally to the atmosphere which is regulated by the stomata in leaves (Beedlow et al., 2017). The process of stomatal regulation is complex and occurs in response to a large number of variables including leaf CO_2 concentration and the soil water potential (Zweifel et al., 2007). Generally, loss of water through evaporation within the leaf canopy which reduces the pressure of the water remaining within the leaf system relative to the atmospheric pressure. In turn, the reduced pressure elevates liquid out of the soil via the root system and up the tree structure via the xylem system (Wheeler and Stroock, 2008). This mechanism is subject to the cohesive nature of water occurring in response to the O-H bonding and allows for significant water-tension up to 30 MPa (McElrone et al., 2013).

Processes of water transport have been shown to differ between hardwood (angiosperm) and softwood (gymnosperm) tree species in response to differences in the cellular microstructure of the material (Gezici-Koc et al., 2017). The principal differences relate to the types of cells present within the wood materials with softwoods incorporating only longitudinal tracheid and transversely orientated ray cells while hardwood species incorporate a series of cell types adjusted for specific functions within the plant (Thomas, 1991; Sjostrom, 1993). Longitudinal tracheids and ray cells which incorporate between 90-95% and 5-10% of the wood cells respectively (Sjostrom, 1993). Longitudinal tracheids are described as very long, hollow cells with a length between 3 mm and 5 mm. In contrast the cell width is very small often 100 times narrower than the cell length. Unlike hardwood cells, the longitudinal tracheids present a duel function offering both strength and rigidity to the wood structure but also allowing for water movement through convection (Thomas, 1991). The cells are generally dead and contain a hollow centre, known as a lumen, through which water and chemicals may be transfer throughout the total tree structure (Wheeler, 2008). The structure of the cells is noted to change

between earlywood and latewood. Early wood is often associated with a larger cross-sectional area, thinner cell walls and a large hollow lumen throughout the centre of the structure. As such, early wood cells are more commonly applied for water transport under convection. Alternately, latewood cells present a smaller cross-sectional area, thicker cell walls and a smaller lumen structure. Late wood tracheids are therefore more responsible for strengthening (Thomas, 1991).

A fundamental feature of tracheids cells relates to pitting within the cell walls. Generally, three types of pits are present including large boarded pits which connect tracheids cells in a vertical direction towards the height of the tree, smaller boarded pits which connect tracheids cells with ray tracheids cells and half-boarded connected with ray parenchyma cells (Howard and Manwiller, 1969). All pitting is described as a gap within the secondary cell wall which allows through flow of liquids between lumen structures via semi-permeable membranes. Earlywood may contain up to 200 pits per tracheid cell often located within the radial walls while latewood tracheids may contain as few as 10 pits (Sjostrom, 1993). Water movement generally occurs between bordered pit pairs whereby a margo, or small opening at the centre of the pit dome structure is connected to that of a second longitudinal tracheid. The connection of two pits allows for the free movement of liquids between two lumen structures (Thomas, 1991).

Liquids are transferred from longitudinal tracheids to ray parenchyma cells via half-bordered pits through convection (Sjostrom, 1993). Ray cells, most commonly ray parenchyma cells form a ray structure in softwood species. Ray structures are commonly associated with biosynthesis, storage and transfer of chemicals within a tree. The ray structure is formed from a series of ray parenchyma cells structured in a brick-type pattern (Wiedenhoeft, 2012). Larger structures assist in lateral movement of materials through contact with longitudinal cells with rays including both tracheid and parenchyma cells (Côté Jr, 1963). Resin canal features are also present in a number of softwood tree species including spruce and pine. The canals incorporate intercellular spaces through which resins may be transferred; the canal structures may be found in longitudinal and transverse directions (Thomas, 1991). Unlike softwood species, the microstructure of hardwood is more complex resulting in a broader array of cell types and structures. Most commonly, hardwood cells include vessel elements, fibres, ray parenchyma and longitudinal parenchyma, the latter of which is specifically rare in softwood species but may incorporate up to 23% of the cellular mass of hardwoods (Thomas, 1991).

While longitudinal tracheids are responsible for fundamental lateral water transfer and strengthening within softwood species, hardwood species incorporate specialised cells known as vessel elements or perforated elements for convection

processes. A vessel structure operates as a longitudinal tube which can transfer water from the roots to the top of the tree structure (Conners, 2015). In addition, water transfer may occur laterally through interaction of vessels with other cellular elements through half-boarded pits (Côté Jr, 1963). Vessel structures incorporate a series of vessel elements which are developed as a stack and eventually form an uninterrupted tube allowing for improved water convection. The formation of a specific tube allows for much improved water convection when compared with softwood water movement (Sjostrom, 1993). Individual vessel elements, upon contact, may pass material between individual structures through a perforation plate. Unlike pits, a perforation plate does not include a membrane and occurs following the loss of the element structure during the formation of the unified tube (Wiedenhoeft, 2012). The size and volume of vessel elements may vary between species, and between earlywood and latewood samples of the same tree, however a typical range of a single element length may be between 0.18 mm and 1.33 mm with a diameter between 50 um and 200 um. In addition, the total wood volume associated with vessel structures may be between 6% and 55% depending upon hardwood species (Thomas, 1991; Wiedenhoeft, 2012). Intervessel pitting occurs between vessel elements allowing for water translocation between vessel structures (Wiedenhoeft, 2012).

2.5 Fuelwood Drying

A suitably low moisture content is the basis for high efficiency fuel conversion in small residential appliances (Strehler, 2000; Visser et al., 2014). Green fuelwood often presents a moisture content within the range of 50-63% (Holmberg and Ahtila, 2004; Obernberger et al., 2006). Fuel drying leads to a number of benefits including lower emissions during combustion, a reduction in fuel handling and transportation costs and lower material loss through inhibited microbial degradation (Koppejan and Loo, 2008; Hofmann et al., 2018; Price-Allison et al., 2019). Additionally, fuelwood maintaining a lower MC% presents a higher calorific value which, in practical terms, means that the greater the drying requirement the lower the calorific value of the fuel thereby resulting in a lower thermal output from a stove appliance (**Figure 2.2**). Drying is therefore applied as a method of maximising material utilisation while minimising degradation and waste (Mathewson, 1930). A variety of methods may be applied during the drying of biomass and can be separated into two types: active drying and natural drying. A variety of active drying methods may be utilized including kiln-drying, heated-air drying (Holmberg and Ahtila, 2004), solar convection (Raitila and Tsupari, 2020) and mechanical compression (Yoshida

et al., 2010). Kiln drying and natural drying are the most common approaches applied during commercial and residential fuelwood preparation.
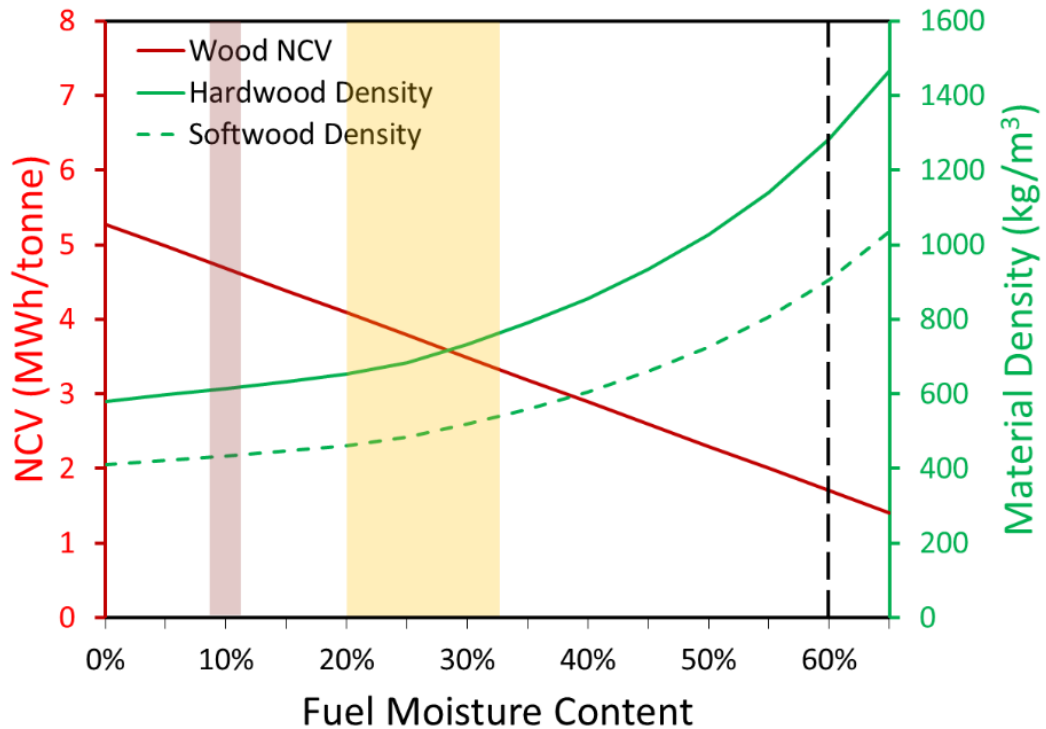
Figure 2.2 An estimation of the effect of fuelwood moisture content upon net calorific value (NCV) and the impact of material density (kg/m^3) on moisture content. An estimation of the theoretical maximum MC% for combustion (60%) and the suggested MC% value for fuelwood following seasoning (20-35%) and kiln-drying (8-12%) pre-treatment is also presented (Koppejan and Loo, 2008; Rolls, 2013; Forest-Research, 2019).

2.5.1 Mechanical Drying

Mechanical drying is the process of actively reducing the moisture content via a thermal treatment process. Kiln drying is the process of reducing the moisture content of fuelwood under mechanically heated conditions. Generally, fuelwood is stacked within an oven and exposed to heated air for a specific duration depending upon the desired moisture content. A variety of kiln systems may be applied in the drying of fuelwood utilizing a number of heat sources including steam, direct fire (biomass powered), electricity, hot-water and solar (Simpson, 1991). Kiln-drying is undertaken at a variety of temperatures depending upon the properties of the wood and the desired moisture content. Generally, drying is undertaken at low temperatures within the range of 21-49°C, moderate temperatures within the range of 43-82°C and high temperatures in excess of 100°C (Oltean et al., 2011). The drying temperature affects the length of the drying period where an increase in the

temperature reduces the amount of time required (Simpson et al., 1987). Maviglio (1986) observed a reduction in moisture content from 50% to 15-20% when drying split maple in a kiln-drier at 60-93°C for three days. Similarly, Simpson et al. (1987) shows a drying period of 257 hours at 60°C, 92 hours at 82°C and 32 hours at 104°C is required when reducing the moisture content of split spruce from 52% to <20%.

Mechanical drying of fuelwood provides several advantages namely the ability to produce dried firewood all year round and the ability to create fuel of a specific moisture content by changing the drying schedule. However, kiln drying is associated with several limitations. The drying of fuelwood at higher temperatures may result in the loss of VM from the fuel (Matthews, 2010). VOC loss via evaporation occurs at low temperatures for softwood species and at higher temperatures for hardwood. Englund and Nussbaum (2000) identifies a loss of between 20-50% of fuel VOC during the heating of softwood at 60°C. Similarly, the heating of hardwood at 105°C may result in a loss of between 12-70% (Englund and Nussbaum, 2000; Samuelsson, Nilsson, et al., 2006; Matthews, 2010). The quantity of emissions generated during the drying of biomass in a kiln-dryer is dependent upon the temperature. Generally, the greater the drying temperature the greater the emission concentration (Holmberg and Ahtila, 2004). Emission formation at low temperatures is associated with gaseous and condensable lipophilic, monoterpenes, fatty acid and resin acid compounds. Alternatively, drying at higher temperatures results in the formation of acetic acids, aldehydes, furfurals, carbohydrates and CO_2 during the thermal breakdown of the fuel (Fagernäs and Sipilä, 1997). Additionally, depending upon the heating method the mechanical removal of moisture from fuelwood may be a financially costly exercise (Gebgeegziabher et al., 2013) with the methods of heat generation also often associated with other limitations including pollutant formation.

2.5.1 Natural Drying

The most cost-effective method of fuelwood drying is by natural drying in a heap or structured pile outdoors during summer months. This process, commonly referred to as seasoning may be applied to reduce the moisture content from 50% to 30% (Koppejan and van Loo, 2008). In practice, seasoning generally involves storing recently felled green wood within a pile or structure either outdoors or under a shelter for a prolonged duration. The capacity for drying by this mechanism is subject to the conditions of storage namely temperature, relative-humidity, tree species, material volume and air-circulation within the pile (Mathewson, 1930; Bergman, 2010; Nurmi and Lehtimaki, 2011). Additionally, seasonality has been

shown to affect drying capacity and effectiveness is known to vary between geographical regions (Heiskanen, 1953; Nurmi and Lehtimaki, 2011). Assuming appropriate storage conditions, the moisture content of a fuelwood pile may be reduced from 50% (green fuelwood) to between 30-35% and 20-25% following 12 months and 24 months of seasoning (Rolls, 2013). Achieving a MC% between 20-30% is attainable within 3-12 months of seasoning depending upon climate and seasoning conditions (Rogge et al., 1998). Given the capacity for bulk-drying this process is often considered as a pre-treatment prior to additional drying within a kiln (Bergman, 2010).

The principal advantage of natural drying is the ability to dry large quantities of fuelwood in-situ encouraging for a seasonal supply of low-MC% material. However, natural drying removes only the free-water within the wood structure thereby restricting the total water-loss potential. Additional energy is required to remove the chemically bound-water fraction; a process which limits the drying capacity of the process (Kofman and Kent, 2009). Furthermore, effective natural drying requires specific conditions meaning the method is restrictive to regional climate conditions (Kofman and Kent, 2009). Finally, the storage of fuelwood within a pile exposes individual particles to differing seasoning conditions. This process, often attributed to differences in solar or precipitation exposure, result in differences in MC% thereby leading to the formation of a heterogeneous material. A summary of the effect of pile storage on MC% uniformity is presented in **Chapter 4**.

2.6 Methods of MC% Determination

Moisture content is generally presented on a wet-basis (wb) or a dry-basis (db). MC% on a wet-basis is presented as a percentage of the total mass of the sample considering the combined mass of the biomass sample and water content. MC% of biogenic fuels maybe presented on both a dry-basis and wet-basis (Reeb and Milota, 1999; Govett et al., 2010). A number of methods may be applied for the determination of moisture content (Govett et al., 2010). The most commonly applied method is the oven drying approach in accordance with BS EN ISO 18134-1, BS EN 14774-3 and ASTM D4442 and presented in **Chapter 3**. This approach is associated with a number of limitations which can lead to error in the determination of MC%. The heating of biomass at 105±2 ºC can result in the loss of VOC's within the biomass effecting the measured volatile fraction (VM%) and resulting in additional mass loss presenting as MC% (Reeb and Milota, 1999; Samuelsson, Burvall, et al., 2006). Samuelsson, Nilsson, et al. (2006) shows VOC emittance as a percentage of MC% between 0.002% and 0.119% during the drying of different biomass at 105ºC. The devolatalisation of VM% during biomass drying results in

the formation of a number of VOC compounds including 2,6-dimethylbicyclohept-2-ene, furfural, phenol, α-pinene and hexanal (Samuelsson, Nilsson, et al., 2006). Similarly, Rupar and Sanati (2003) identify terpene formation, specifically monoterpenes and sesquiterpenes, during the drying of biomass under heated air and steam-medium. The loss of VM% during drying at temperatures presented in BS EN ISO 18134-1 (105±2 ºC) is believed to be negligible and should not present a significant impact upon the MC% value (Price-Allison et al., 2019).

Fuelwood moisture content may be determined through the electrical resistivity of the material (James, 1988). A detailed review of the process, accuracy and limitations of this technique is provided in **Chapter 4**. Several alternative methods for the determination of fuel MC% may also be applied. The moisture content of a milled biomass sample may be determined through the heating of sample using a microwave-oven (Govett et al., 2010). MC% is determined following a similar gravimetric method to what is outlined in the oven-drying approach and is undertaken in accordance with ASTM E1358-97. This method is often applied for the determination of moisture in agronomy biomass (Anwar, 2010), organic samples (Routledge and Sabey, 1976) and woody biomass (Maruf Hossain et al., 2012) but is considered not appropriate for the testing of large fuelwood samples (such as logs) in response to combustion risk (Govett et al., 2010). The determination of biomass MC% may also be achieved through freeze-drying of sample material (Samuelsson, Burvall, et al., 2006). Freeze-drying is based upon the principal of lyophilization whereby water content is firstly frozen before being removed from a sample by sublimation under vacuum conditions before being desorbed (Nireesha et al., 2013). A comparison of MC% determined via an oven-drying approach and freeze-drying revealed that the derived moisture content is generally underestimated in the latter technique (Samuelsson, Burvall, et al., 2006). However, this process may result in a reduction in MC% loss when compared with sampling heating practices (Bjurman and Jirjis, 1994). An additional method is based upon the principal of distillation with xylene or toluene and is undertaken in accordance with TAPPI T208 WD (Krause, 2000; Samuelsson, Burvall, et al., 2006). In this method the xylene/toluene is applied to distil out the water fraction within a biomass sample given that H_2O is not miscible with the chemical additives. The extracted H_2O forms in a boundary horizon above the xylene/toluene where it can be extracted and quantified (Krause, 2000). Previous work identified low accuracy of this method in comparison to an oven-drying approach in response to the very small sample mass associated with the technique resulting in samples not being representative of the complete biomass. In addition, the collected moisture content is quantified by reading the volume from a scale on a moisture trap where the accuracy is subject to the readability of the scale (Samuelsson, Burvall, et al.,

2006). A number of advanced instrumental methods of MC% determination are also applied including near-infrared, nuclear, magnetic resonance and x-ray analysis (Fridh et al., 2014).

2.7 Moisture Content and the Combustion of Biomass

Fuelwood moisture content is a significant factor affecting the combustion process (Jones et al., 2014). Freshly felled wood, depending upon species, felling period and location, may present an inherently high moisture content up to 50% of the total mass (Obernberger et al., 2006). Moisture content can affect the ignition and combustion efficiency of biomass fuels applied in residential stove and boiler systems. Unprocessed biomass materials are inherently hygroscopic meaning that it has a tendency to absorb water (Bach and Skreiberg, 2016). Fuelwood MC% is variable and subject to the inherent bound water content and extrinsic processes including weather conditions or ambient humidity. Extrinsic processes are commonly associated with dead-biomass material and may be derived from absorption, desorption, evaporation or precipitation while the storage of water within living biomass is intrinsic and subject hydrostatic operation (Mckendry, 2002; Parmar et al., 2008). Green fuelwood is likely to present a moisture content in excess of 50-60% (Jones et al., 2014; Černý et al., 2016) and so the addition of 1kg of recently-felled and unprocessed fuelwood to a stove is the equivalent of adding 500ml of water to the combustion reaction (Rolls, 2013). As a result, fuelwood MC% has a direct effect on the combustion process leading to energy loss, incomplete combustion and finally, higher pollutant formation.

2.7.1 Stages of Biomass Combustion

2.7.1.1 Drying Phase

A drying phase is required as a precursor to ignition and stable flaming combustion within domestic heating devices. Drying temperature requirements are generally low (<100°C) which result in the evaporation of water from exposed biomass particles (Koppejan and Loo, 2008). Radiative heat derived from the combustion of smaller biomass particles or an external heating source leads to an increase in ambient temperatures around a fuel pack resulting in moisture loss through evaporation. Fuelwood MC% impacts the temperature and efficiency of the combustion reaction where fuels maintaining a higher MC% require additional heating for the elimination of water-content prior to ignition (Bahadori et al., 2014). Alternatively, an increase in fuel particle MC% requires higher temperature heating or a prolonged drying period to remove a sufficient water content to initiate

combustion leading to greater energy losses and a reduction in the burning rate (Rogge et al., 1998; Simoneit, 2002; Koppejan and Loo, 2008; Guofeng Shen et al., 2013; Guerrero et al., 2019). Prior to ignition, much of the fuel moisture must be removed given the capacity of water vapour for minimising combustion zone temperatures and transporting heat away from the fuel pack (Koppmann et al., 2005). The combustion of very wet fuelwood therefore requires an additional support fuel so as to maintain sufficient temperatures for drying during start-up (Svoboda et al., 2009).

An increase in the MC% leads to an increase in the energy requirement during initial vaporization contributing to poor ignition, lower combustion temperatures and a prolonged drying phase (Amos, 1998; Simoneit, 2002; Yang et al., 2007; Koppejan and Loo, 2008; Gebgeegziabher et al., 2013). Given the required energy demand during drying it is assumed that fuel maintaining a moisture content in excess of 60%$_{wb}$ will not burn due to energy loss and low temperatures below which are required for sustainable combustion (USEPA, 1984; Koppejan and Loo, 2008; Al-Shemmeri et al., 2015) however a theoretical maximum MC% of 60-65% may be combusted in larger systems (Svoboda et al., 2009). The quantity of energy lost during evaporation is proportional to inherent fuel moisture content (Raman et al., 2013). It is generally assumed that the energy requirement for the vaporization is 3.21 MJ per kilogram of water (BMZ, 2013) however other parameters including particle size and material density will have an effect. The energy-value of dried fuelwood is typically within the range of 18-21 MJ/kg while the energy requirement for the heating and evaporation of 1 kg of water stored within green fuelwood is in excess of 2.6 MJ/kg (Svoboda et al., 2009). As a result, start-up is still possible if ambient radiative heating is sufficient (Van Wagner, 1977). Orang and Tran (2015) show significantly extended drying periods during the combustion of fuelwood maintaining a moisture content in excess of 30%. In addition, the devolatalisation period was shown to be slightly extended when a higher moisture content was present however the char burnout phase remained unaffected. Predominant moisture loss is observed during the initial stages of devolatalisation prior to the establishment of a sustainable flame. As such, the detrimental effects of high MC% are generally associated with the period immediately following fuel start-up or stove reloading. This process, known as ignition delay, is generally extended with an increase in the moisture content (Saito et al., 2001). Following the loss of fuel bound water during the devolatalisation phase the material will burn similar to what is observed during kiln-dried fuel combustion (Koppejan and Loo, 2008).

The process of drying during heating is complex. **Figure 2.3** presents the process of water loss by evaporation during heating. During exposure to an external heat

flux the majority of the free water within the fuelwood particle is lost via evaporation as the combustion temperature approaches 100°C (Yang et al., 2003; Bartlett et al., 2019). Following heating a fraction of the water vapor may re-condense in the cooler inner structure of the fuel particle (White and Schaffer, 1981; Schmid et al., 2015) leading to the formation of higher localized moisture values (Bartlett et al., 2019). During drying the free water is transported through voids in the material structure via capillary flow assuming that the water content is in excess of the FSP. As the drying process proceeds the moisture content at the particle surface reaches a maximum sorptive point creating an evaporation front which progresses vertically through the particle structure. Behind the evaporation front remains a sorption zone where bound water vapor is transferred via a diffusive mechanism. Assuming a sufficient external heat flux the dried fuel horizon behind the evaporation front progresses into a pyrolysis phase whereby volatile loss occurs (Grønli and Melaaen, 2000; Bartlett et al., 2019). The initial moisture content and external heat flux affect the longevity of the drying period and, as a result, the time requirement for particle ignition. An increase in the moisture content results in both an increase in energy loss causing reduced combustion temperatures and a prolonged drying period thereby delaying the onset of ignition (Orang and Tran, 2015). The final phase occurs when the volatile loss is complete leading to the formation of a char phase (Grønli and Melaaen, 2000; Bartlett et al., 2019).
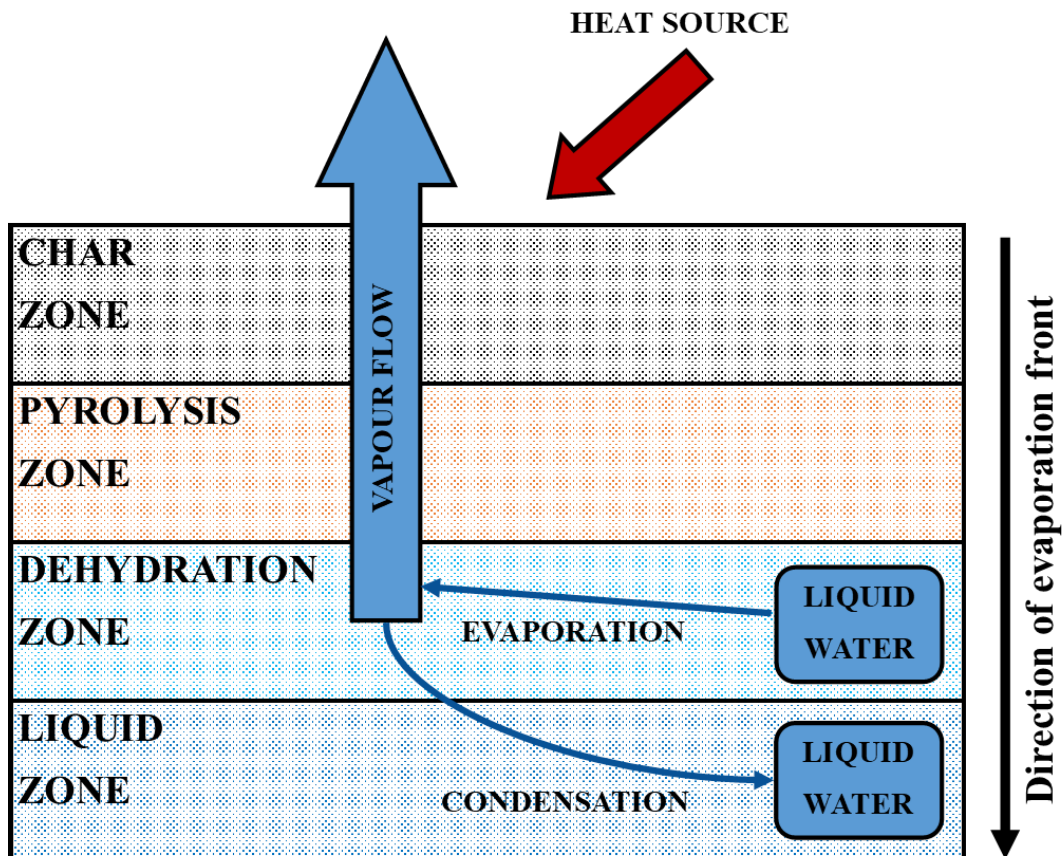
Figure 2.3 Transition of fuel particle moisture content during heating and the onset of moisture zones. Adapted from (Bartlett et al., 2019).

During exposure to start-up temperatures, and under pre-ignition conditions, it is common for some loss of highly volatile organic compounds including aromatic and ether extractives (Koppmann et al., 2005). During the initial start-up, while combustion temperatures remain low (<100°C), some devolatilisation of highly volatile organics occur. A series of methanol, light aldehydes, formic acid and acetic acid are released during the thermal decomposition of hemicellulose and lignin (Koppmann et al., 2005). The heating of larger particles may therefore result in simultaneous drying and devolatilisation of the centre and external surface of the material respectively.

2.7.1.2 Devolatilisation/Pyrolysis Phase

The process of devolatilisation is the initial combustion step producing an array of products in different quantities often dependent upon the individual characteristics of the fuel particle (Biagini et al., 2006). During heating, compounds within the fuel structure start to pyrolyse, hydrolise, oxidise or dehydrate allowing for the formation of combustible volatile products (Simoneit, 2002). Loss of volatiles occurs under

different temperature conditions during the combustion of coal compared to biomass. The process occurs in response to the onset of pyrolysis conditions whereby thermochemical decomposition of a particle structure causes chemical bonds to sever. The ease of thermochemical degradation is in response to the strength of bonding; i.e. the breakage of weak bonds require lower temperatures while stronger bonds require higher temperatures (Saxena, 1990). As such, the point at which devolatilisation begins also differs between coal and biomass particles with the former starting around 350°C and the latter between 160-250°C (Jones et al., 2014). The extent of total devolatilised product formation is identified as a function of the fuel material. The increased volatile composition of biomass fuels and residues, in comparison to coal products, leads to generally more extensive devolatilisation and lower ignition temperatures (Mando, 2013).

As previously identified, the decomposition of chemical components within a fuel particle occur at different temperatures. Biomass products and residues are made up of a mixed composition of three polymeric incorporations; lignin, cellulose and hemicellulose (Burhenne et al., 2013). The extent of each polymer within a fuel is highly variable between biomass resources thereby providing a source of inherent variability upon the combustion process. Cellulose is a long-chain homopolyer incorporating carbon, hydrogen and oxygen atoms arranged as $C_6H^{10}O^5n$ where n is representative of the degree of polymerisation. Cellulose is formed following β-1-4 glyosidic bonding of two of more glucose molecules which become connected by a series of strong hydroxyl (OH) bonds (Mulinari et al., 2013). Hemicellulose is located within the primary and secondary cell walls of living plant cells and incorporate a series of polysaccharides which bond with cellulose microfibrils during the formation of a matrix structure. The hemicellulose material may make up between 20-30% of the total dry mass of wood (Whistler, 1991; Bonnin et al., 2009; Postek et al., 2011; Moon et al., 2011). The substance operates as a binding matrix between cellulose and amorphous lignin located with the cell wall as such, the presence of hemicellulose is for the purpose of offering strength and rigidity to the plant (Pandey, 1999). Lignin is a series of complex aromatic heteropolymers which operate as a stiffening material within the secondary cellular walls for the purpose of providing strength and rigidity (Grabber, 2005). In addition, the material is described as having a cross-linked structure incorporating phenylpropanoid units which are linked by C-O-C and C-C bonds (Basso et al., 2017). Variation in bonding structures associated with the three primary polymers comprising all biomass fuels results in marked devolatilisation points during the combustion process (Burhenne et al., 2013). Slower heating rates (and lower temperature) tend to be associated with the breakage of weaker chemical bonds thereby resulting in the evaluation of water molecules and the thermal decomposition of hemicellulose and lignin. This

process may be observed during lower heating rates below 100 °C/min (Yang et al., 2006).

Thermogravimetric analysis of the three biomass components may be applied to determine temperature dependent devolatilisation conditions. Yang et al. (2006) identified decomposition of hemicellulose within the range of 220-260°C and cellulose within the range of 315-390°C. Generally higher TGA peaks are identified for cellulose and hemicellulose across very specific temperature and heating rate bounds. Alternatively, lignin decomposition is presented as a very low DTG peak with a marginal increase in devolatilisation rate likely between 750-850°C. It is likely that gradual decomposition of lignin occurs between 250-500°C. As a result, the final product of combustion, commonly referred to as char, incorporates a high pyrolysed lignin concentration (wt.%) following the rapid decomposition of cellulose and hemicellulose components (Yang et al., 2006; Chen and Kuo, 2011; Burhenne et al., 2013; Reza et al., 2014).

A variety of products are derived from the devolatilisation phase of the combustion process. Generally, biomass compounds thermally decompose in the order of hemicellulose, cellulose and finally lignin decomposition rates becomes appreciable (Jones et al., 2014). Low temperature heating of hemicellulose and lignin leads to the emission of methanol, light aldehyde, formic acid and acetic acid. These products are derived following the thermal cracking of polysaccharide chains within the biomass constituents. An increase in devolatilisation occurs within an increase in temperature resulting in a significant loss of particle mass (approximately 80% in woody biomass). This often leads to a spike in volatile emission during the decomposition of the fuel material. A further increase in temperature results in the release of methane, aldehydes, methanol and furans. In addition, a series of aromatic compounds including benzene, toluene and phenol is released between temperatures of 250-500°C. The extent and rate of devolatilisation depends on the inherent characteristics of the fuel, specifically the fuel moisture content, and additional variables specific to the combustion device including fuel placement, heat exposure and excess air availability (Koppmann et al., 2005). It is estimated that the gaseous and volatile products of devolatilisation correspond to approximately 70-95% of the total pyrolysis phase derivatives which are combusted during the flaming phase (Jones et al., 2014).

2.7.1.3 Flaming Phase

An increase in temperature results in the combustion of devolatilised products in the form of a yellow flame. When temperatures within the combustion chamber reach the point of ignition the volatile compounds, including gases and tars, combust in an

exothermic reaction (Simoneit, 2002). The composition of the devolatilised products, incorporating both gases, tars and char, is dependent upon both the temperature and the heating rate. As such, the temperature conditions within the combustion zone have a direct influence on the calorific value (CV) of the products (Jones et al., 2014). If adequate air flow is supplied to the combustion zone, derived volatile gases are combusted in the presence of oxygen. The importance of primary air flow is therefore identified as a paramount concept during the design and development of domestic heating appliances (Yin et al., 2004). Error in the estimation of air supply may lead to delayed combustion of products resulting in lower operational temperatures and increased pollutant emissions. The rate of devolatilised product combustion is very fast, in contrast to char, with an increase in total volatiles leading to a reduction in the residence time within the stove combustion zone. A generalised model for the combustion of volatiles in presented in **Equation 2.1** whereby total volatiles (CHxOy) are completely reacted in the presence of oxygen to form first CO and H$_2$O, then CO$_2$ based upon the availability of CO and O$_2$ (Mando, 2013). The extent to which the gaseous and tar compounds are combusted is dependent upon the extent of combustion completeness; the process is fully dependent upon conditions within the combustion zone (Simoneit, 2002).

$$(\mathbf{2.1}) \quad CH_xO_y + O_2 \rightarrow CO + H_2O + \text{Ash}$$
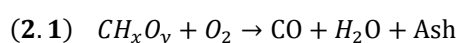
2.7.1.3 Char Burnout

Smouldering is the flameless combustion, or solid phase oxidation, of the remaining fuel on the grate. The smouldering process begin following the loss of volatiles during the pyrolysis and flaming combustion phases (Chandler et al., 1983). The process involves the diffusion of oxygen to the surface of the char particle whereby it reacts with the remaining carbon fraction of the fuel at temperatures greater than 430°C producing carbon monoxide. In addition, an increase in particle heating during this period to temperatures within the range of 630-700°C allows for the formation of carbon dioxide (Reid et al., 2005). The process involves the thermal degradation of remaining charcoal contributing in the emission of high carbon monoxide concentrations. In addition, NO emissions may be higher during smouldering combustion when temperatures in the combustion zone are reduced while solid PM emission are reduced. A reduction in PM formation is likely in response to limited volatile formation and reduced burning rates during this period (Reid et al., 2005; Jones et al., 2014; Mitchell et al., 2016). Remaining char comprises 90% carbon, 5% oxygen and 3% hydrogen leading to a limitation in the

formation of volatile products thereby inhibiting flaming combustion (Koppmann et al., 2005).

2.8 Pollutant Emissions

2.8.1 Incomplete Combustion

Soot and gaseous pollutants are produced during the incomplete combustion of biomass and fossil fuels (Atiku et al., 2016; Jones et al., 2018). Unlike coal and smokeless solid-fuels, biomass maintains a high VM content which, following heating, forms higher volatile concentrations within the combustion zone (Wang et al., 2018). Under an idealised combustion condition, a cellulosic fuel, defined as CHxOy, is completely oxidised where all volatile products are consumed during the reaction leading to the formation of CO_2, water-vapour and ash. Incomplete combustion occurs when the conditions within the combustion zone are not sufficient to completely oxidise the volatile and inorganic components which are subsequently expelled from the combustion zone within the entrained flue gas.

It is impossible to achieve complete combustion of a biomass fuel within small heating appliances due to the complexity of the reaction and limitations in the capacity of the device (Demirbas, 2007). Incomplete combustion is therefore an inevitable consequence of the combustion of residential solid fuel (RSF) in domestic heating appliances leading to the formation of soot, CO, VOC's and PAH's (Jantunen, 1985; Bignal et al., 2008; Ozil et al., 2009). Several factors may result in the incomplete combustion within heating appliances which commonly relate to the ratio of well mixed air and mass of fuel, the combustion temperature, and the residence time of products within the combustion zone (Smith, 1987). Most notably, in relation to fuelwood combustion, the impact of MC% is known to effect the extent of volatile oxidation. An increase in the moisture content reduces the adiabatic temperature and increases the air requirement resulting in the need for an increased residence to ensure complete combustion (Koppejan and van Loo, 2008; L'Orange et al., 2012).

2.8.1.1 CO

Carbon monoxide (CO) is a common pollutant produced during the incomplete combustion of all carbonaceous fuels. The initial formation of CO occurs within the flaming phase where hydrocarbons are rapidly oxidised (Williams, 1990). The concentration of carbon monoxide derived from a combustion reaction is also principally controlled by the temperature and residence time where reduced

pollutant formation is generally in response to improved combustion conditions (Vakkilainen, 2017). As such, the presence of CO may be applied as a mechanism for understanding the efficiency of combustion and thereby applied as an indicator for other pollutant species formation (Koppejan and Loo, 2008; Vakkilainen, 2017). Under ideal combustion conditions, CO is oxidised leading to the formation of carbon dioxide (CO_2) where temperature and O_2 availability are shown as a rate limiting control (Koppejan and Loo, 2008; Vakkilainen, 2017). CO formation generally occurs when the supply of primary air within the combustion zone is less than the stoichiometric requirement thereby resulting in high CO and inhibited oxidation leading to lower CO_2 (Ndiema et al., 1998). In response, CO is generally associated with smouldering combustion while CO_2 is generally observed during the flaming phase of combustion.

2.8.1.2 NOx and SOx

Nitrogen oxides (NOx) are pollutant species formed during the oxidation of fuel nitrogen ($fuel_N$) during biomass combustion. The primary pollutants generated during the oxidation of $fuel_N$ is nitrogen oxide (NO), accounting for 90-95% of total NOx, and nitrogen dioxide (NO_2), accounting for 5-10% of total NOx (Koppejan and van Loo, 2008; Ma et al., 2021). There are three routes of NOx formation observed during biomass combustion including fuel-NOx, thermal-NOx and prompt-NOx. Both thermal-NOx and prompt-NOx formation is observed during high temperature combustion in excess of 1300°C. Biomass combustion in heating stoves generally occurs at a lower temperature, within the range of 800-1200°C, meaning that NOx formation via these routes is likely negligible when attributed to residential combustion (Skreiberg et al., 1997; Stubenberger et al., 2008; Mitchell et al., 2016). Fuel-NOx is considered the most common route of formation during biomass combustion and is directly derived from the conversion of $fuel_N$ (Glarborg et al., 2003; Koppejan and Loo, 2008; Sommersacher et al., 2012; Bugge et al., 2020). The process involves the thermal decomposition of nitrogen-containing compounds within the fuel during devolatilisation. The combustion of fuels maintaining a higher $fuel_N$ content, including coal and peat (0.5-2.5%), generally corresponds with an increase in NOx formation in contrast to low $fuel_N$ materials such as wood (0.003-1.0%) (Glarborg et al., 2003). **Figure 2.4** identifies the effect of varying $fuel_N$ content on subsequent NOx formation. Under the mechanism nitrogen is provided to the reaction from the fuel source while oxygen is provided from the air within the combustion chamber (Wielgosinski, 2012).
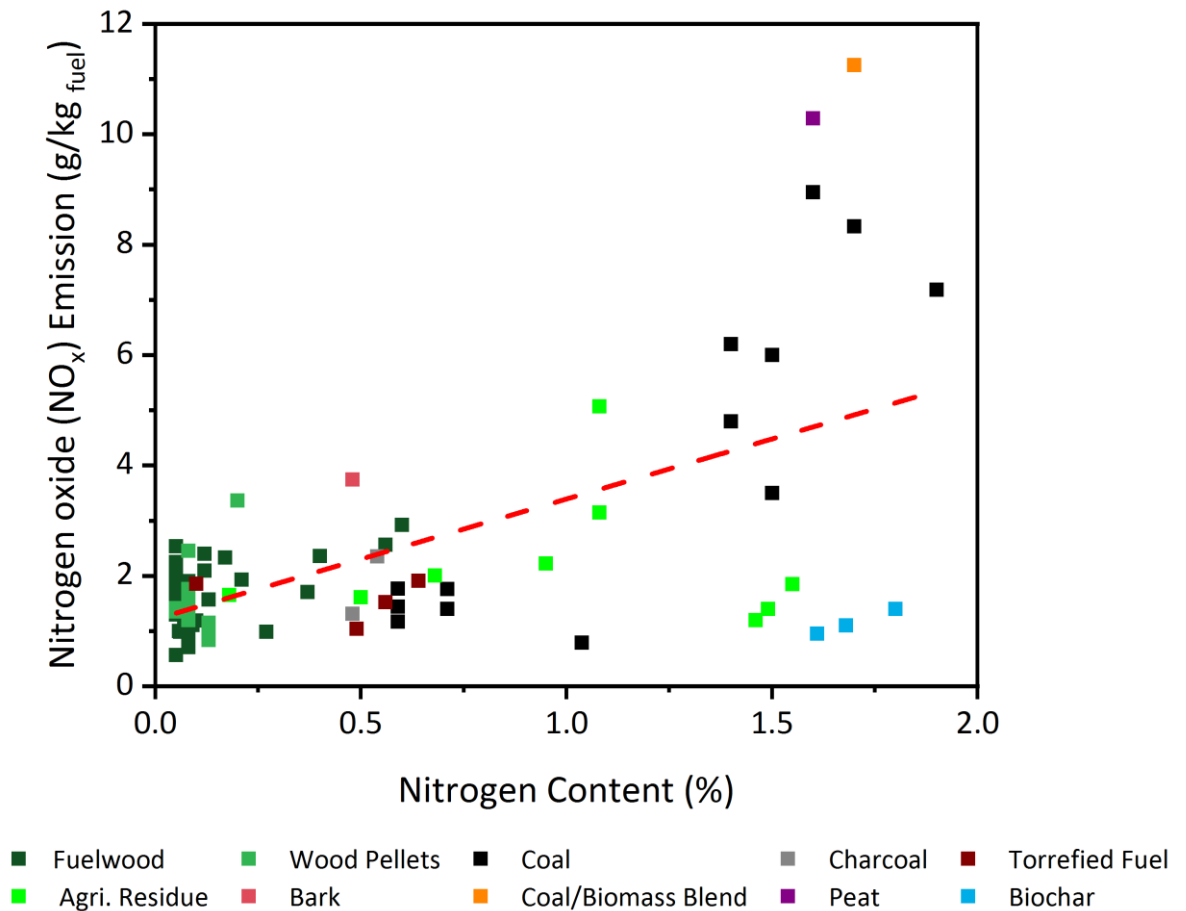
Figure 2.4 Correlation of fuel nitrogen content (%) and NOx formation during combustion testing for various fuels outlined within the literature (Ellegård, 1993; Johansson et al., 2004; Bäfver et al., 2011; Kistler et al., 2012; Guofeng Shen, Tao, Wei, et al., 2012; Mitchell et al., 2016; Sevault et al., 2017; Du et al., 2017; Liu et al., 2018; Price-Allison et al., 2019; Maxwell et al., 2020; Guo et al., 2020; Champion et al., 2020).

Sulphur oxide (SOx) formation occurs during the oxidation of fuel sulphur (fuel$_S$). Fuel-bound sulphur is heated and emitted within the gas-phase during devolatilisation in the form of H_2S, COS, SO_2 and CS_2 while some of the fuel$_S$ content is retained within the char fraction until later phases of fuel conversion. Generally, SO_2 comprises 95%> of total SOx. Following char burnout, a minor fraction of the fuel$_S$ may be retained as a non-combusted product within the bottom ash. A further fraction may also be converted to a salt (K_2SO_4) or emitted at H_2S at lower combustion temperatures (Koppejan and Loo, 2008). In total, between 57-65% of fuel$_S$ may be released and entrained within the flue gas while between 35-43% remains within the char (Houmoller and Evald, 1999). The extent of SOx formation is associated with the fuel$_S$ content. Sulphur is applied within all plants for the purpose of plant growth and development via the biosynthesis of proteins, enzymes and amino-acids (Gigolashvili and Kopriva, 2014). As such, sulphur

availability is likely influenced by the soil conditions where the biomass is grown (Jones et al., 2014). Notwithstanding, typical biomass fuels present only a low $fuel_S$ composition thereby inhibiting the potential for SOx formation. Coal derived fuels present a much higher $fuel_S$ composition which is maintained in the form of pyrite and organic sulphur (Glassman et al., 2015). **Figure 2.5** presents the relationship between $fuel_S$ and SO_2 formation in a series of different domestic combustion devices. A trend is apparent however the correlation is statistically limited likely due to sulphur being retained within the ash.
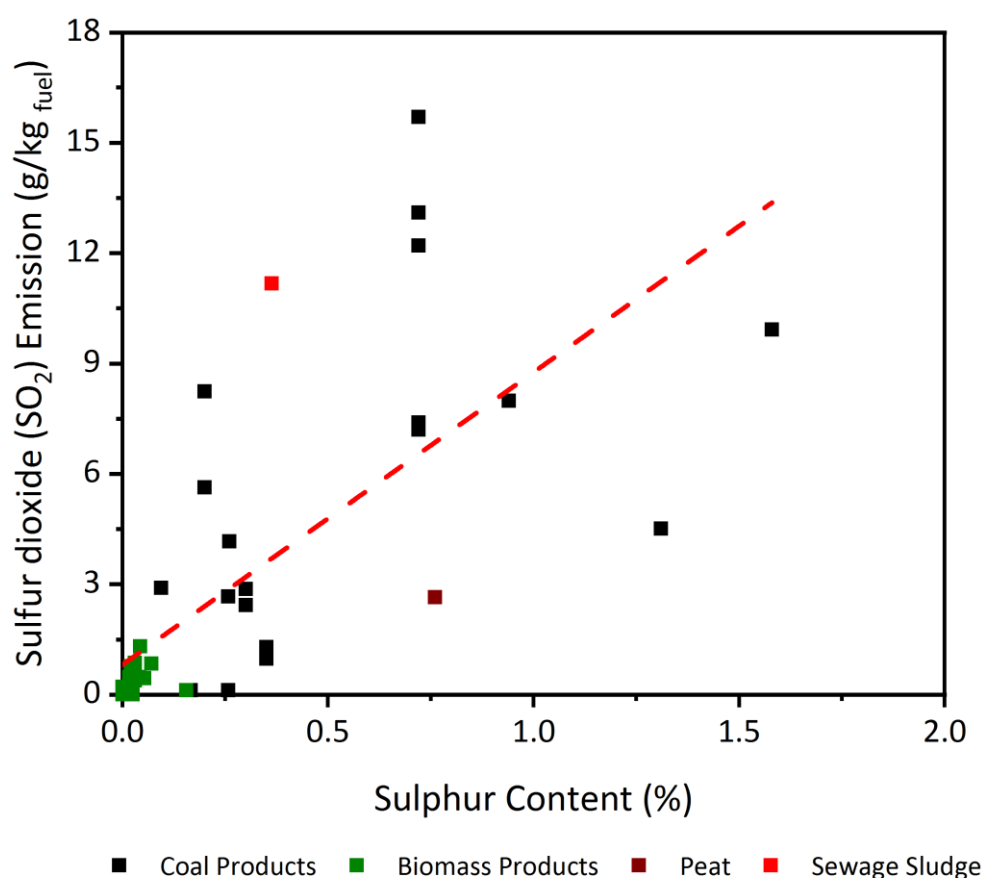
Figure 2.5 Relationship between fuel sulphur content (%) and emission of SO_2 (as SOx) during combustion in a variety of devices (Zhang et al., 2000; Reddy and Venkataraman, 2002; Ge et al., 2004; Krugly et al., 2014; Du et al., 2016; Cereceda-balic et al., 2017; Liu et al., 2018; Price-Allison et al., 2019)

2.8.1.3 Aldehyde

Aldehyde formation occurs during the oxidation of cellulose and hemicellulose during combustion (Kopczyński et al., 2015). In biomass combustion, more than 50% of the total aldehyde emittance is formaldehyde (CH_2O) and acetaldehyde (CH_3CHO). The ratio of CH_2O and CH_3CHO formation has been found between 2.1-2.9 (Cerqueira et al., 2013). The extent of aldehyde formation is known to vary

depending upon the phase of combustion, the fuel type, fuel conversion rate, fuel moisture content, the characteristics of the combustion appliance and the combustion temperature (Liparl et al., 1984; Mcdonald et al., 2000; Schauer et al., 2001; Hedberg et al., 2002; Koppmann et al., 2005). The effect of combustion temperature and burning rate on CH_2O emission is shown in **Figure 2.6**.
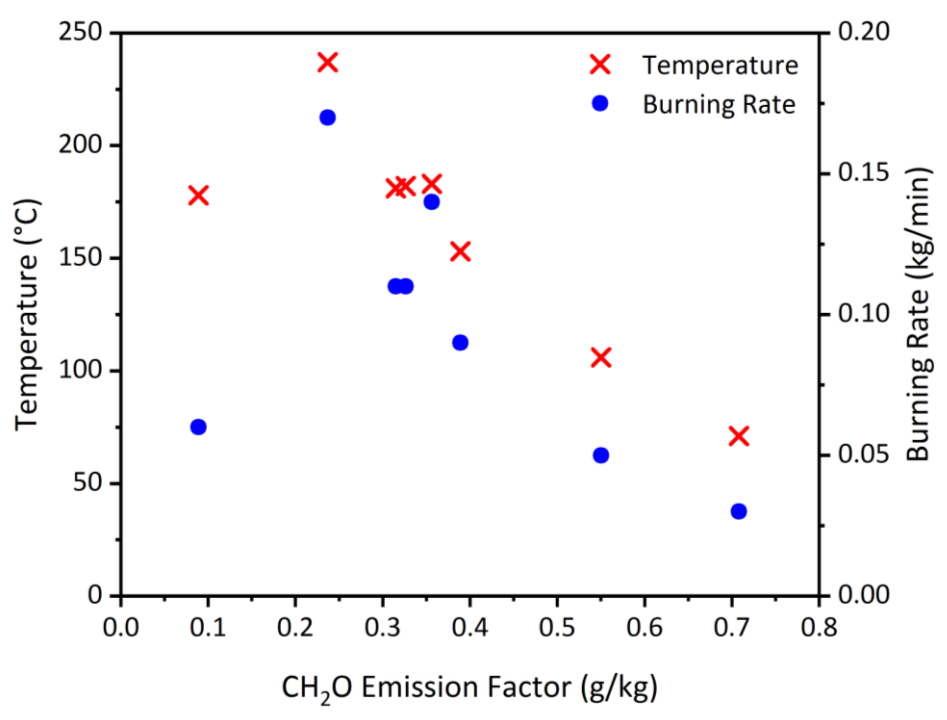
Figure 2.6 Variation in CH_2O formation under different temperature and burning rate condition (Liparl et al., 1984).

2.8.1.4 Volatile Organic Compounds

Volatile organic compounds (VOC's) are organic compounds maintaining a high vapour pressure and are generally identified in two groups; methane and non-methane (NMVOC). NMVOC includes all hydrocarbon species excluding CH_4, polyaromatic hydrocarbons (PAH) and heavy hydrocarbons associated with the formation of soot particles (Koppejan and Loo, 2008). CH_4 is presented separately from NMVOC due to its high atmospheric concentration and relative inertness in comparison to other VOC's (Koppmann, 2007). CH_4, like NMVOC's, is an intermediate pollutant commonly attributed to lower stove temperatures within the range of 250-500°C, reduced residence time within the combustion zone and low O_2 availability resulting in the incomplete combustion (Koppejan and Loo, 2008). During the pyrolysis carbon and hydrogen within fuel are converted into a series of gaseous hydrocarbons leading to the formation of CH_4 which, assuming complete combustion, is totally converted into CO_2 and H_2O. NMVOC's include, but are not

limited to, ethane (C_2H_6), ethylene (C_2H_4), propane (C_3H_8), hexane (C_6H_{14}), acetylene (C_2H_2) and benzene (C_6H_6). A total of 148 VOC species have been identified during combustion reactions (Fingas, 2017).

2.8.1.5 Polyaromatic Hydrocarbons (PAH)

Polyaromatic hydrocarbons include a group of several hundred organic compounds which incorporate two or multiple aromatic rings and tend to exist in complex mixtures (Lee, 2010). PAHs are generally identified separately from other hydrocarbon species in response to their carcinogenic effects. However, the formation pathway is similar in that PAH is an intermediate species between fuel-carbon to CO_2 and fuel-hydrogen to H_2O (Koppejan and van Loo, 2008). PAH formation may also be described as occurring via competing routes which differ to oxidation pathways and are intermediates in soot formation. Pyrene ($C_{16}H_{10}$) is the most common PAH associated with biomass combustion while retene ($C_{18}H_{18}$) is also common (Vicente et al., 2020). Pettersson et al. (2011) found pyrene concentrations of 6400 µg/mg$_{fuel}$ with additional high concentrations of phenanthrene ($C_{14}H_{10}$) and fluoranthene ($C_{16}H_{10}$) during the combustion of wood logs and pellets. Similarly, Hedberg et al. (2002a) and Ozgen et al. (2014) report $C_{16}H_{10}$ concentrations between 0.066-16.0 mg/kg depending upon fuel and appliance type. PAH is of particular importance due to the likely health impacts relating to mutagenic and carcinogenic properties (Nystrom et al., 2017).

2.8.1.6 Soot, Elemental Carbon (EC) and Organic Carbon (OC)

The term smoke is used to refer to the whole particulate matter (PM) fraction and includes ash, inorganic aerosols, amalgamated tar particles, PAH, soot and small fragments of char (Jones et al., 2014). Of particular interest to this work is the development of soot during combustion reactions. The physiochemical process of soot formation during combustion is complex and may results from a single or multiple formation pathways (Bartle et al., 2011). Smoke formation may occur through the formation of PAH via monocycles by the hydrogen abstraction-carbon addition (HACA) mechanism (Fitzpatrick et al., 2008). Additionally, for biomass combustion, formation may occur through the generation of cyclopentadienyl (CPDyl) radicals via phenoxy radicals leading to the formation of naphthalene and indene. More complex PAH structures are subsequently produced through interaction with the HACA mechanism or additional reactions with CPDyl radicals. Finally, soot formation may occur through the direct coupling of PAH structures which are released during the combustion reaction or produced via the HACA or CPDyl routes (Bartle et al., 2011).

Soot particles consist of amalgamated agglomerations of carbonaceous spherules. These spherules are generally between 20-100 nm in nominal diameter with soot particles generally less than 1 μm (Jones et al., 2018). The composition of soot particles may be determined as containing varying fractions of elemental carbon (EC) and organic carbon (OC). EC is a term which is often interchangeably used with black carbon (BC), soot, and the light absorbing soot fraction. The IPCC applies the term soot to determine the fraction of emittance from incomplete combustion which presents light absorbing properties while BC is a term specifically used to determine the light absorbing properties of a carbonaceous material (Karanasiou et al., 2015). The characteristic of emitted smoke is dependent upon the properties of the fuel and the condition of the combustion reaction (Jones et al., 2014). PM emission maintaining a higher EC fraction are generally associated with higher combustion temperatures while the inverse is shown for high OC formation (Bond et al., 2004; Gonçalves et al., 2011; Mitchell et al., 2016; Obaidullah et al., 2018). A summary of the effect of fuel moisture content on EC and OC emission is presented in **Chapter 6**.

2.9 Impact of MC% on Pollutant Formation

Moisture content has been shown to affect combustion processes in residential combustion appliances (Price-Allison et al., 2019; Price-Allison et al., 2021). Biomass is regularly burned with a variety of moisture values with processes relating to cost and accessibility affecting use. Notwithstanding, the impact of moisture during fuelwood combustion is complex (G. Shen et al., 2013) and has shown to have a positive (Lu et al., 2009), negative (Bignal et al., 2008; Chomanee et al., 2009) or indifferent effect (Roden et al., 2006). The MC% of fuelwood consumed in residential appliances is not known however values range from 50-60% for green (Černý et al., 2016), 20-35% for seasoned wood (Rolls, 2013; CertainlyWood.co.uk, 2022) and 8-20% for kiln-dried fuel (Rolls, 2013; HETAS, 2018). Several New Zealand studies have been undertaken investigating the MC% of fuelwood consumed in residential combustion practices. MC% was found within the range of 7-35% (Lamb, 1999a) with more than 36% of fuel maintaining a water concentration in excess of 30% (Lamb, 1999b). The wide variation in fuel MC% identified in these studies is likely in response to the origin of most fuel materials. In New Zealand it has been identified that approximately 50% of fuel is obtained from alternative sources (Lamb, 2003). These sources are likely associated with a '*grey*' market and are often not subject to adequate drying or fuel quality monitoring. In the UK it is assumed that up to 31% of fuelwood is obtained through a similar mechanism (BEIS, 2016). An ideal MC% has been estimated to be between 20%

and 30% (Core et al., 1982; Core et al., 1984; Simoneit, 2002). An increase in the moisture content corresponds with increased energy losses during the combustion of the dry biomass fraction with additional heat required during the evaporation of water. Regarding the impact upon combustion, moisture is likely to affect fuel and appliance efficiency, combustion temperature and burn duration, excess air availability and pollutant formation (Černý et al., 2016).

2.9.1 Combustion Conditions

Moisture in fuel has a similar effect to a heat sink thereby affecting combustion efficiency (CE) (Ballard-Tremeer, 1997). Fundamentally, the effect of MC% on combustion efficiency relates to energy losses during water vaporisation. This has a significant effect on combustion conditions and fundamentally leads to a reduction in temperature (Černý et al., 2016). During the combustion of wet fuel, energy loss is expected as water must first be removed via evaporation (Bahadori et al., 2014). An increase in the MC%, results in an increase in the required temperature and/or heating duration, before ignition is achieved (Rogge et al., 1998; Simoneit, 2002; Koppejan and Loo, 2008; Guofeng Shen et al., 2013; Bahadori et al., 2014; Guerrero et al., 2019). It is assumed that the heat requirement for the evaporation of 1 kg of water from biomass is in excess of 2.6 MJ/kg with most dry biomass feedstock maintaining a heating value of 18-21 MJ/kg (Svoboda et al., 2009). The effect of this process is a reduction in CE, in response to energy loss during water vaporisation and lower temperatures within the combustion zone (S. Bhattacharya et al., 2002). The process of moisture loss prior to ignition is discussed in **Chapter 6**.

Lower operating temperatures and fuel energy loss are commonly identified during the combustion of higher MC% materials (Yuntenwi and Ertel, 2008). Guerrero et al. (2019) presents a reduction in CE from 93% and a maximum temperature of 537°C to 49% and a maximum temperature of 236°C when the MC% was increased from 0% to 25%. G. Shen, Tao, et al. (2012) identifies a connection between fuelwood moisture content and reduced combustion temperatures due to energy losses during the vaporisation phase. Bhattacharya et al. (2002) reported a reduction in cookstove CE between 20-43% when the MC% is increased from 10-25%. Similarly, Kumar et al. (2013) identifies an average reduction in efficiency between 3-7% when the moisture content of fuelwood was increased from 10-25%. Additionally, combustion conditions are noted to vary across the duration of a batch. High MC% fuel samples are therefore likely to show inhibited ignition conditions however, following drying, the material is likely to combust similar to dry fuel (Orasche et al., 2013). Evidence of the effect of MC% is also likely during prolonged

stove operation where temperature variation, in accordance with MC%, may be exacerbated over a prolonged operating period due to energy losses and the cooling effect of water within the combustion chamber. The effect of higher combustion temperatures also results in a higher burning rate; as a result, the use of high MC% fuel results in a lower rate of combustion (Purvis et al., 2000). MCE is often used as an indicator for CE and is adversely effected by the moisture content. The reduction in MCE, and therefore CE, is often identified by an exponential increase in CO and an exponential decrease in CO_2 with an increase in MC% (Possell and Bell, 2012).

The use of fuels maintaining a very low MC% inhibited combustion conditions. Fuels maintaining a very low MC% are generally consumed at a higher burning rate than wet fuels (Price-Allison et al., 2021). This is due to higher combustion temperatures and low energy losses during the drying phase. The problem generally arises when the burning rate reaches a point where there is an exceedance in the air supply to the reaction. This insufficient air supply can result in the formation of an oxygen deficiency within the combustion chamber thereby inhibiting CE and subsequently affecting pollutant formation (Rogge et al., 1998; G. Shen, Wei, et al., 2012). Therefore MC% may be applied as a control to improve CE (Yuntenwi and Ertel, 2008). Alternatively, Shen et al. (2017) shows limited variation in the combustion condition when varying moisture between 10-30%.

2.9.2 Moisture and Combustion Conditions

Moisture has been shown to affect the combustion characteristics in residential heating and cooking appliances. This process is observed for a variety of fuel resources including coal, lignite (Man et al., 2015), crop residues (Possell and Bell, 2012) and woody biomass including fuelwood. As previously stated, this process occurs in response to lower combustion temperatures resulting in processes of incomplete combustion. The effect of increased moisture content results in a lower combustion efficiency leading to the formation of higher quantities of incomplete combustion products. This occurs when energy is lost during the vaporisation process (Simoneit, 2002). Furthermore, the presence of vapourised water within the combustion zone is believed to further affect temperature via change to the relative humidity as well as affecting condensation processes (Shen, Wei, et al., 2012; Magnone et al., 2016). The presence of MC% is believed to be significant after a real-world study undertaken in New Zealand revealed that MC% accounted for 43% of the variability in emissions (Wilton and Bluett, 2012).

2.9.2.1 Negative Impact of MC% on Emissions

It is generally agreed that the combustion of high moisture fuels results in an increase in emissions. Regarding particulate formation; Shen et al. (2010) identifies MC% as the principal control on emission formation accounting for between 63% and 83% soot concentration variability. Guofeng Shen et al. (2013) determined an increase in PM from 3.4 g/kg$_{fuel}$ to 4.1 g/kg$_{fuel}$ when the MC% was increased from 14% to 27%. Similarly, Purvis et al. (2000) reported a reduction in PM emissions from 10.29 g/kg$_{fuel}$ to 4.24 g/kg$_{fuel}$ when the moisture content was reduced from 30% to 22%. Furthermore, Magnone et al. (2016) identifies a 275% increase in PM emission concentrations when the moisture content was increased from 10.34% (1.07 g/kg$_{fuel}$) to 56.31% (4.02 g/kg$_{fuel}$). This occurs in response to energy loss during the vaporisation phase contributing in maximum flue gas combustion temperatures of 505°C in contrast to a maximum temperature of 562°C observed when dry fuelwood was burned. A study undertaken by Butcher and Sorenson (1979) generally identify an increase in the particulate emission concentration with other variables including draft and fuel load also maintaining an influence on pollutant formation. Guerrero et al. (2019) identifies an increase in PM$_{2.5}$ and PAH emission concentrations from 2.01 to 22.9 g/kg$_{fuel}$ and 5215 to 7644 ng/g respectively when the moisture content of eucalyptus fuelwood was increased from 0% to 25%.

As previously stated, when wet fuelwood is added to a hot grate the combustion reaction is slowed leading to a drop in temperature and the formation of pollutants derived from incomplete combustion. It should however be stated that once the moisture has been evaporated from the fuel it will burn in a manner similar to a drier particle. Chomanee et al. (2015) shows this where a wet particle (MC% = 37.4%) and a dry particle (MC% = 76.6%) produced 23.35 mg/m^3 and 47.54 mg/m^3 during peak combustion. This was then stabilised following prolonged heating where the wet particle produced a PM concentration of 4.57 mg/m^3 and the dry produced a concentration of 3.65 mg/m^3. This occurs as the level of incomplete combustion is reduced as the remaining water within the fuel particle is lost. A summary of the effect of MC% on PM emission is presented in **Figure 2.7**.
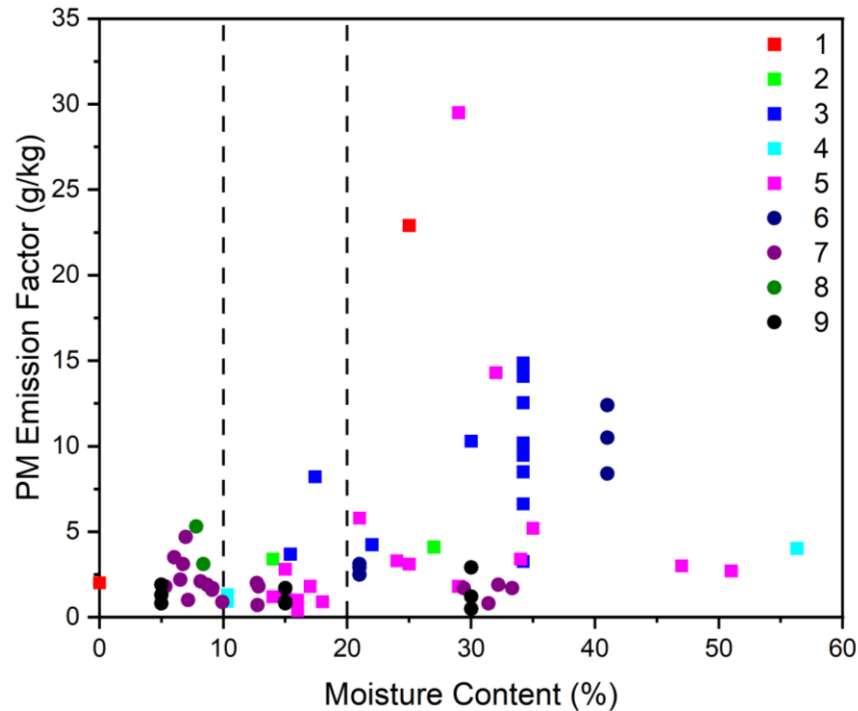
Figure 2.7 Effect of moisture content on PM emission factor values within the literature (1) (Guerrero et al., 2019), (2) (Guofeng Shen et al., 2013), (3) (Purvis and McCrillis, 2000), (4) (Magnone et al., 2016), (5) (Wilton and Bluett, 2012), (6) (Shelton and Gay, 1986), (7) (G. Shen, Wei, et al., 2012), (8) (Mitchell et al., 2016), (9) (Yuntenwi and Ertel, 2008). Dashed lines identify the ideal fuel MC% in accordance with *Ready to Burn* certification.

Fuel moisture content can also affect the particulate size distribution following combustion. When low moisture fuelwood is burned the temperature within the combustion zone is generally higher and so the conditions for producing smaller particles are generally more favourable (Guofeng Shen, Wei, Wei, et al., 2012). The chemical composition of soot is also noted to change depending upon MC%. Guofeng Shen et al. (2013) determined that the fraction of OC was shown to increase from 1.7 g/kg_{fuel} to 4.3 g/kg_{fuel} as the fuel MC% was increased. Higher OC values are likely caused by lower combustion temperatures which inhibit the oxidation of the volatile fraction into CO_2. Similarly, Magnone et al. (2016) reported a lower OC fraction when burning dry fuelwood (29.15 mg/m^3) compared to wet fuelwood (39.06 mg/m^3). Similarly, van Zyl et al. (2019) shows a decrease in the EC fraction of soot produced during the combustion of wet fuelwood. Furthermore, Tissari et al. (2019) shows a reduction in BC emissions by a factor of 1.8-2.8 when the fuelwood moisture was increased from 11% to 18%. However, the combustion of wet wood maintaining a higher MC% of 28% revealed an increase in BC and OC but the concentration remained less than that observed during dry fuelwood combustion. The formation of EC occurs in response to combustion temperature. As a result, the combustion of wet fuel, at a lower temperature, will always result in lower EC formation as identified in Guofeng Shen et al. (2013)

The effect of moisture content on gaseous emissions is also investigated within the literature. Like with PM formation, the effect of reduced combustion temperatures results in an increase in gaseous pollutant formation when the fuel moisture content is increased. Bhattacharya et al. (2002) shows an increase in CO and NOx and a decrease in CO_2 when the fuel MC% was increased. CO and NOx is shown to reduce due to lowered oxidation rates under lower combustion temperatures, the CO_2 concentration was reduced due to the smaller quantity of fuel available to the combustion reaction on a dry basis. The formation of CH_4 remained unaffected by the moisture content. van Zyl et al. (2019) identifies an increase in CO by 84%, formaldehyde by 216% and benzene by 82% when fuelwood moisture content was increased from 5% to 25% in a cookstove appliance. In addition, Tissari et al. (2019) presents an increase in CO emissions when the MC% of fuelwood, applied in a sauna stove, was increased. In the study the CO concentration increased by a factor of 1.15-1.35 when the MC% was increased from 11% to 18%.

Variation in the impact of MC% throughout the combustion process is highly likely. The process of combustion is dynamic meaning that the inherent moisture content of a fuel particle prior to ignition will not be the same following exposure to the heated grate (Zhao et al., 2021). The impact of moisture is also apparent during flaming and smouldering phases of combustion. Bignal et al. (2008) presents generally higher soot formation during the flaming phase and lower concentrations during the smouldering phase. The soot concentration was reduced from 352 mg/m^3 to 50 mg/m^3 during flaming combustion and from 131 mg/m^3 to 45 mg/m^3 during smouldering combustion when the moisture content was reduced from >40% to <25%. As a result, considering only the initial MC% may be a shortcoming when attributing a relationship between fuel properties and emission performance. Zhao et al. (2021) identifies a gradual reduction in the fuel particle moisture content following heating which results in an increase in the combustion temperature and improved MCE. In response, the effect of fuel moisture content should be considered dynamic due to the effect of moisture loss during heating. Assessing a fuel particle based on the inherent moisture content may be considered a methodological limitation.

2.9.2.2 Positive Impact of MC% on Emissions

The presence of some moisture within a combustion reaction is also believed to be beneficial. A sufficient MC% concentration within a fuel particle allows for the suppression of the pyrolysis reaction. The use of very dry fuel particles may lead to processes of pyrolysis far from the flame as, with a reduced drying period, volatile loss occurs more readily. A combination of volatile loss and char combustion away

from the combustion zone results in incomplete combustion (Smith, 1987; Yuntenwi and Ertel, 2008). The presence of moisture within a fuel particle may therefore control and localise the combustion zone thereby reducing the escape of volatile components before burnout is complete (Yuntenwi and Ertel, 2008). Additionally, the presence of water vapour within the combustion zone may provide additional OH radicals which promote the combustion reaction (Baldwin, 1987). Furthermore, regarding soot formation; it is possible that an increase in fuel MC% reduces flame temperature away from the ideal condition required for PAH formation (Korenaga et al., 2001).

Huangfu et al. (2014) provides evidence for a negative correlation between fuel MC% and pollutant formation. An increase in the fuel moisture content resulted in a reduction in PM and CO emissions leading to an improved combustion efficiency. PM emission concentrations reduced from 581.7 mg/MJ to 194.8 mg/MJ when the MC% was increased from 5.9% to 22.1%. The occurrence of this negative correlation is the result of the type of combustion appliance operated in the study. The device, a top-lit natural-draft semi-gasification cookstove burning pelletised fuel, operated more efficiently during the combustion of wet fuel as the reaction was slowed leading to a prolonged residence time. The prolonged residence time and secondary air feeding system contributed in more complete combustion. Additionally, when using gasification-type combustion appliance the presence of water vapour within the gas products affects the chemistry of the reaction via water shift reactions thereby increasing the hydrogen content (OH radicals) of the synthesis gas (Acharjee et al., 2011). This process is not likely during the combustion of fuelwood particles in stove appliances. Similarly, L'Orange et al. (2012) improved combustion conditions resulting in a reduction in CO and PM emissions when the MC% was increased from 4%, to 7% and to 13%. An increase in emissions was only observed when very wet fuelwood maintaining an MC% of 30% was applied to the cookstove appliance.

Yuntenwi and Ertel (2008) identified a reduction in the emission of CO when a moderate MC% fuelwood was applied to a cookstove appliance. This process was found to be affected by other parameters within the study and was related to cooking pot placement and air availability controlled by the cookstove structure. Additionally, fuelwood combusted in an open fire with a moisture content of 15% produced low PM emission concentrations with a small increase observed at 5% moisture and a large increase observed at 30% moisture. A reduction in PM emission was also observed with an increase in fuel MC% in two cookstove appliances.

2.9.2.3 Complex Interaction

The impact of MC% of emissions is complex and it is difficult to discern a clean conclusion from within the literature (Tissari et al., 2019). Variation in MC% can lead to differences in efficiency and emissions. Evidence within the literature suggests that an increase in MC% leads to an increase in pollutant formation. Alternatively, it is possible that the combustion of very dry fuelwood can also lead to increased emissions. Several studies have highlighted this process whereby very low and very high moisture fuels lead to poor combustion quality while a moderate amount of moisture, often around 20%, leads to improved combustion quality (Korenaga et al., 2001; Tissari et al., 2019).

This process is presented by Wilton and Bluett (2012) where the combustion of fuelwood maintaining a MC% of 10-20% and 30-40% lead to higher emissions while fuelwood with a MC% of 20-30% lead to lower emissions. The effect of MC% is therefore likely parabolic. Additionally, the work undertaken by L'Orange et al. (2012) presents a similar parabolic function whereby the combustion of dry fuelwood (<10%) and wet fuelwood (30%) produce higher emissions that fuelwood maintaining a moderate MC% (13%). A similar trend is presented by Tissari et al. (2019). **Figure 2.8** shows this process for the three authors. The guidance provided by HETAS via the Ready to Burn scheme also identifies a similar process where fuelwood with a MC% less than 8% and more than 25% should not be burned while an ideal moisture content is likely within the range of 10-20% (HETAS, 2018).
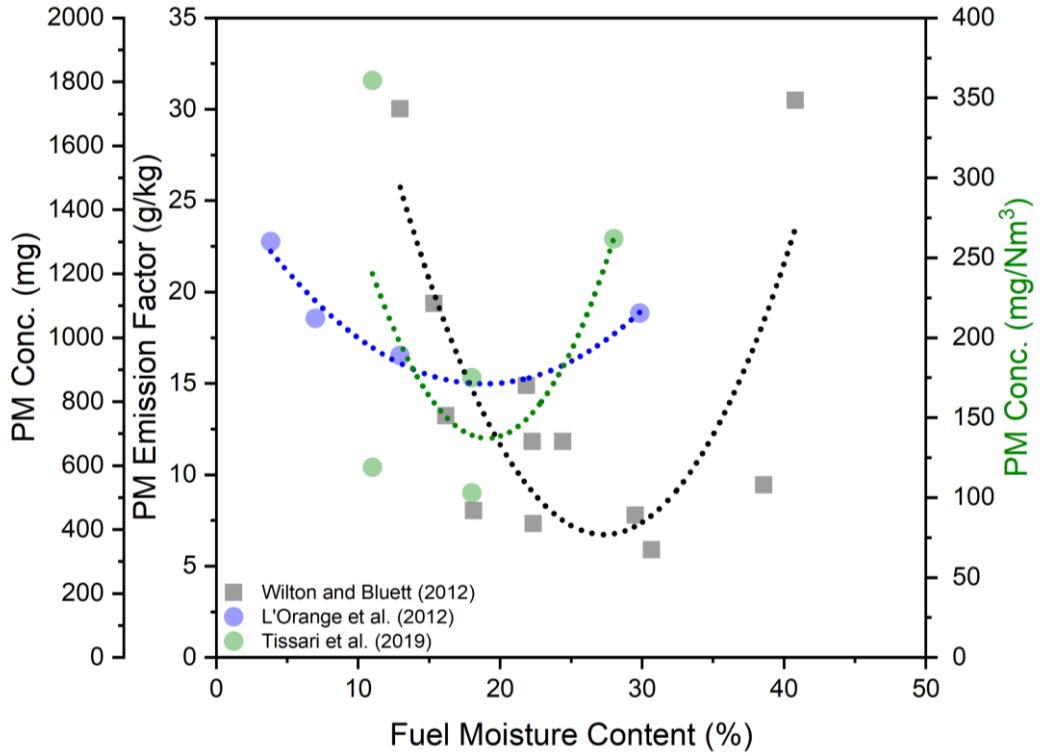
Figure 2.8 The parabolic effect of fuel MC% on particulate emission factor
(Wilton and Bluett, 2012) and particulate concentration mass in mg and
mg/Nm^3 (L'Orange et al., 2012; Tissari et al., 2019)

2.10 Legislation and Control of Fuelwood

As this thesis progressed, the research was able to contribute to legislative
changes to control the sale and consumption of high moisture fuels within the UK.
Ready to Burn is a commercial certification scheme designed to limit the sale of
fuelwood and biomass briquettes subject to moisture content. The scheme is
outlined within The Air Quality (Domestic Solid Fuels Standards) (England)
Regulations (2020) provides certification for fuel suppliers who meet fuel current
moisture standards (Woodsure, 2021a). Under the scheme, and associated Air
Quality Regulation, fuelwood sold is volumes up to 2 m^3 should not maintain a
moisture content in excess of the established prohibited level of 20%. Fuelwood
sold in quantities larger than 2 m^3 requires the supplier to provide advice to the
consumer on seasoning prior to combustion (Woodsure, 2021b). **Figure 2.9** shows
the identification for fuelwood sold inline within the Ready to Burn criteria. The
Ready to Burn scheme is also outlined within the Clean Air Strategy 2019.

Figure 2.9   Logo of Ready to Burn scheme, UK (Woodsure, 2021b)

The Clean Air Act (1993) prohibits the emission of dark smoke from a residential chimney however it does not stipulate fuel conditions relating to moisture. The establishment of Smoke Control Areas (SCA) prohibits the use of residential combustion appliances in some urban locations. Regarding fuelwood, the legislation stipulates that only appropriate and exempted appliances may be operated in these locations. These appliances, including wood burning and multi-fuel stoves, have been exempted under the Clean Air Act (1993) subject to sufficient testing and DEFRA approval. Furthermore, fuelwood burned on DEFRA approved appliances within SCA locations should meet *Ready to Burn* criteria. This is further supported by the Clean Air Plan for Wales (Griffiths, 2020) and the Clean Air for Scotland 2 strategy (McAllan, 2021).

2.11 References

Acharjee, T.C., Coronella, C.J. and Vasquez, V.R. 2011. Effect of thermal pretreatment on equilibrium moisture content of lignocellulosic biomass. Bioresource Technology. 102(7), pp.4849–4854.

Al-Shemmeri, T.T., Yedla, R. and Wardle, D. 2015. Thermal characteristics of various biomass fuels in a small-scale biomass combustor. Applied Thermal Engineering. 85, pp.243–251.

Amos, W.A. 1998. Report on Biomass Drying Technology [Online]. [Accessed 27 October 2020]. Available from: http://www.doe.gov/bridge/home.html.

Anwar, S.I. 2010. Determination of moisture content of bagasse of jaggery unit using microwave oven. Journal of Engineering Science and Technology. 5(4), pp.472–478.

Atiku, F.A., Mitchell, E.J.S., Lea-Langton, A.R., Jones, J.M., Williams, A. and Bartle, K.D. 2016. The Impact of Fuel Properties on the Composition of Soot Produced by the Combustion of Residential Solid Fuels in a Domestic Stove. Fuel Processing Technology. 151, pp.117–125.

Bach, Q. and Skreiberg, Ø. 2016. Upgrading biomass fuels via wet torrefaction : A review and comparison with dry torrefaction. Renewable and Sustainable Energy Reviews. 54, pp.665–677.

Bäfver, L.S., Leckner, B., Tullin, C. and Berntsen, M. 2011. Particle emissions from pellets stoves and modern and old-type wood stoves. Biomass and Bioenergy. 35(8), pp.3648–3655.

Bahadori, A., Zahedi, G., Zendehboudi, S. and Jamili, A. 2014. Estimation of the effect of biomass moisture content on the direct combustion of sugarcane bagasse in boilers. International Journal of Sustainable Energy. 33(2), pp.349–356.

Baldwin, S.F. 1987. Biomass stoves: engineering design. Development, and Dissemination, Volunteers in Technical Assistance.

Ballard-Tremeer, G. 1997. Emissions of rural wood-burning cooking devices.[Online] University of Witwatersrand. Available from: https://www.researchgate.net/profile/Grant-Ballard-Tremeer/publication/265361292_Emissions_of_Rural_Wood-Burning_Cooking_Devices/links/54e35ebb0cf2be54da85c125/Emissions-of-Rural-Wood-Burning-Cooking-Devices.pdf.

Bartle, K.D., Fitzpatrick, E.M., Jones, J.M., Kubacki, M.L., Plant, R., Pourkashanian, M., Ross, A.B. and Williams, A. 2011. The combustion of droplets of liquid fuels and biomass particles. Fuel. 90(3), pp.1113–1119.

Bartlett, A.I., Hadden, R.M. and Bisby, L.A. 2019. A Review of Factors Affecting the Burning Behaviour of Wood for Application to Tall Timber Construction. Fire Technology. 55, pp.1–49.

Basso, M.C., Pizzi, A., Delmotte, L. and Abdalla, S. 2017. Analysis of the cross-linking reaction of lignin with triethyl phosphate by MALDI-TOF and13C NMR. Polymers. 9(6), p.206.

Beedlow, P.A., Waschmann, R.S., Lee, E.H. and Tingey, D.T. 2017. Seasonal patterns of bole water content in old growth Douglas-fir (Pseudotsuga menziesii (Mirb.) Franco). Agricultural and Forest Meteorology. 242, pp.109–119.

BEIS 2016. Summary results of the domestic wood use survey [Online]. Available from: www.gov.uk/government/statistics/digest-of-united-kingdom-energy-statistics-dukes-2014-printed-version.

Bentrup, F.-W. 2017. Water ascent in trees and lianas: the cohesion-tension theory revisited in the wake of Otto Renner. Protoplasma. 254, pp.627–633.

Bergman, R. 2010. Drying and control of moisture content and dimensional changes In: Wood handbook: Wood as an engineering material. Madison: Forest Products Laboratory, pp.1–20.

Berthold, J., Rinaudo, M. and Salmeń, L. 1996. Association of water to polar groups; Estimates by an adsorption model for ligno-cellulosic materials In: Colloids and Surfaces A: Physicochemical and Engineering Aspects. Elsevier Science B.V., pp.117–129.

Bhattacharya, S., Albina, D. and Myint Khaing, A. 2002. Effects of selected parameters on performance and emission of biomass-fired cookstoves.

Bhattacharya, S.C., Albina, D.O. and Salam, P.A. 2002. Emission factors of wood and charcoal-fired cookstoves. Biomass and Bioenergy. 23, pp.453–469.

Biagini, E., Barontini, F., Tognotti, L. and Diotisal, V. 2006. Devolatilization of Biomass Fuels and Biomass Components Studied by TG / FTIR Technique. Industrial & Engineering Chemistry Research. 45(13), pp.4486–4493.

Bignal, K.L., Langridge, S. and Zhou, J.L. 2008. Release of polycyclic aromatic hydrocarbons, carbon monoxide and particulate matter from biomass combustion in a wood-fired boiler under varying boiler conditions. Atmospheric Environment. 42(39), pp.8863–8871.

Bjurman, J. and Jirjis, R. 1994. A possible reason for variations in the determination of dry matter losses in logging residues In: Proceedings of IEA/BA joint workshop. Garpenberg, Sweden, pp.42–45.

BMZ 2013. Micro-gasification: cooking with gas from dry biomass [Online]. Available from: https://energypedia.info/images/0/05/Micro_Gasification_2.0_Cooking_with_gas_from_dry_biomass.pdf.

Bond, T.C., Streets, D.G., Yarber, K.F., Nelson, S.M., Woo, J.H. and Klimont, Z. 2004. A technology-based global inventory of black and organic carbon emissions from combustion.pdf. Journal of Geophysical Research2. 109(D14).

Bonnin, E., Ralet, M.-C., Thibault, J.-F. and Schols, H.A. 2009. Enzymes for the valorisation of fruit- and vegetable-based co-products. Handbook of Waste Management and Co-Product Recovery in Food Processing., pp.257–285.

Bugge, M., Skreiberg, Ø., Haugen, N.E.L. and Carlsson, P. 2020. Predicting NOx emissions from wood stoves using detailed chemistry and computational fluid dynamics. Energy Procedia. 75(1876), pp.1740–1745.

Burhenne, L., Messmer, J., Aicher, T. and Laborie, M. 2013. Journal of Analytical and Applied Pyrolysis The effect of the biomass components lignin , cellulose and hemicellulose on TGA and fixed bed pyrolysis. Journal of Analytical and Applied Pyrolysis. 101, pp.177–184.

Butcher, S.S. and Sorenson, E.M. 1979. A Study of Wood Stove Particulate Emissions. Journal of the Air Pollution Control Association. 29(7), pp.724–728.

Cereceda-balic, F., Toledo, M., Vidal, V., Guerrero, F., Diaz-robles, L.A., Petit-breuilh, X. and Lapuerta, M. 2017. Science of the Total Environment distributions from the combustion of wood species using a new controlled combustion chamber 3CE. Science of the Total Environment. 584–585, pp.901–910.

Černý, D., Malaťák, J. and Bradna, J. 2016. Influence of biofuel moisture content on combustion and emission characteristics of stove.

Cerqueira, M., Gomes, L., Tarelho, L. and Pio, C. 2013. Formaldehyde and acetaldehyde emissions from residential wood combustion in Portugal. Atmospheric Environment. 72, pp.171–176.

CertainlyWood.co.uk 2022. Kiln-dried vs seasoned logs - is there a difference. [Accessed 17 March 2022]. Available from: https://www.certainlywood.co.uk/blogs/news/kiln-dried-vs-seasoned-logs-is-there-a-difference.

Champion, W.M., Warren, S.H., Kooter, I.M., Preston, W., Krantz, Q.T., DeMarini, D.M. and Jetter, J.J. 2020. Mutagenicity- and pollutant-emission factors of pellet-fuelled gasifier cookstoves: Comparison with other combustion sources. Science of the Total Environment. 739, p.139488.

Chandler, C., Cheney, P., Thomas, P., Trabaud, L. and Williams, D. 1983. Fire in forestry. Volume 1. Forest fire behaviour and effects. Volume 2. Forest fire management and organisation. New York: John Wiley & Sons, Inc.

Chen, W. and Kuo, P. 2011. Torrefaction and co-torrefaction characterization of hemicellulose , cellulose and lignin as well as torrefaction of some basic constituents in biomass. Energy. 36(2), pp.803–811.

Chomanee, J., Tekasakul, S., Tekasakul, P. and Furuuchi, M. 2015. Effects of Moisture Content and Burning Period on Concentration of Smoke Particles and Particle-Bound Polycyclic Aromatic Hydrocarbons from Rubber- Effects of Moisture Content and Burning Period on Concentration of Smoke Particles and Particle-Bound Polyc. Aerosol and Air Quality Research. 9, pp.404–411.

Chomanee, J., Tekasakul, S., Tekasakul, P., Furuuchi, M. and Otani, Y. 2009. Effects of Moisture Content and Burning Period on Concentration of Smoke Particles and Particle-Bound Polycyclic Aromatic Hydrocarbons from Rubber-Wood Combustion. Aerosol and Air Quality Research. 9(4), pp.404–411.

Choudhury, H.A., Chakma, S. and Moholkar, V.S. 2015. Biomass Gasification Integrated Fischer-Tropsch Synthesis: Perspectives, Opportunities and Challenges In: A. Pandey, T. Bhaskar, M. Stöcker and R. K. Sukumaran, eds. Recent Advances in Thermo-Chemical Conversion of Biomass. Elsevier, pp.383–435.

Conners, T. 2015. Distinguishing Softwoods from Hardwoods. Agriculture and Natural Resources Publications. 105.

Core, J.E., Cooper, J.A. and Houck, J.E. 1982. Residential wood combustion study. Task 7. Indoor air quality. Final Report. Woodburn.

Core, J.E., Cooper, J.A. and Neulicht, R.M. 1984. Current and projected impacts of residential wood combustion on Pacific Northwest air quality. Journal of the Air Pollution Control Association. 34(2), pp.138–143.

Côté Jr, W.A. 1963. Structural factors affecting permeability of wood. Journal of Polymer Science Part C. 2(1), pp.231–42.

Demirbas, A. 2007. Environmental Effects Hazardous Emissions from Combustion of Biomass Hazardous Emissions from Combustion of Biomass. Energy Sources, Part A: Recovery, Utilization, and Environmental Effects. 7036, pp.170–178.

Du, Q., Zhang, C., Mu, Y., Cheng, Y., Zhang, Y., Liu, C., Song, M., Tian, D., Liu, P., Liu, J., Xue, C. and Ye, C. 2016. An important missing source of atmospheric carbonyl sulfide: Domestic coal combustion. Geophysical Research Letters., pp.8720–8727.

Du, W., Shen, G., Chen, Y., Zhu, X., Zhuo, S., Zhong, Q., Qi, M., Xue, C., Liu, G., Zeng, E., Xing, B. and Tao, S. 2017. Comparison of air pollutant emissions and household air quality in rural homes using improved wood and coal stoves. Atmospheric Environment. 166, pp.215–223.

Ellegård, A. 1993. The Maputo coal stove project. Environmental assessment of a new household fuel. Energy Policy. 21(5), pp.598–614.

Engelund, E.T., Thygesen, L.G., Svensson, S. and Hill, C.A.S. 2013. A critical discussion of the physics of wood-water interactions. Wood Science and Technology. 47(1), pp.141–161.

Englund, F. and Nussbaum, R.M. 2000. Monoterpenes in Scots pine and Norway spruce and their emission during kiln drying. Holzforschung. 54(5), pp.449–456.

Espenas L. D. (United States Department of Agriculture Forest Service) 1951. Some Wood-Moisture Relations. Wisconsin.

Fagernäs, L. and Sipilä, K. 1997. Emissions of Biomass Drying In: Developments in Thermochemical Biomass Conversion [Online]. Springer Netherlands, pp.783–797. [Accessed 23 March 2021]. Available from: https://link.springer.com/chapter/10.1007/978-94-009-1559-6_63.

Fingas, M. 2017. In Situ Burning: An Update In: M. Fingas, ed. Oil Spill Science and Technology. Gulf Professional Publishing, pp.483–676.

Fitzpatrick, E.M., Jones, J.M., Pourkashanian, M., Ross, A.B., Williams, A. and Bartle, K.D. 2008. Mechanistic Aspects of Soot Formation from the Combustion of Pine Wood. Energy and Fuels. 22, pp.3771–3778.

Forest-Research 2019. Effect of Moisture Content. Tools and Resources.

Fridh, L., Volpé, S. and Eliasson, L. 2014. An accurate and fast method for moisture content determination. International Journal of Forest Engineering. 25(3), pp.222–228.

Ge, S.U., Xu, X.U., Chow, J.C., Watson, J., Sheng, Q., Liu, W., Bai, Z., Zhu, T.A.N. and Zhang, J. 2004. Emissions of Air Pollutants from Household Stoves : Honeycomb Coal versus Coal Cake. Environmental Science and Technology. 38(17), pp.4612–4618.

Gebgeegziabher, T., Oyedun, A.O., Zhang, Y. and Hui, C.W. 2013. Effective optimization model for biomass drying In: Computer Aided Chemical Engineering. Elsevier B.V., pp.97–102.

Gezici-Koc, O., Erich, S.J.F., Huinink, H.P., van der Ven, L.G.J. and Adan, O.C.G. 2017. Bound and free water distribution in wood during water uptake and drying as measured by 1D magnetic resonance imaging. Cellulose. 24, pp.535–553.

Gigolashvili, T. and Kopriva, S. 2014. Transporters in plant sulfur metabolism. Frontiers in Plant Science. 5, p.442.

Glarborg, P., Jensen, A.D. and Johnsson, J.E. 2003. Fuel nitrogen conversion in solid fuel fired systems. Progress in Energy and Combustion Science. 29(2), pp.89–113.

Glassman, I., Yetter, R.A. and Glumac, N.G. 2015. Combustion 5th ed. Elsevier.

Gonçalves, C., Alves, C., Fernandes, A.P., Monteiro, C., Tarelho, L., Evtyugina, M. and Pio, C. 2011. Organic compounds in $PM_{2.5}$ emitted from fireplace and woodstove combustion of typical Portuguese wood species. Atmospheric Environment. 45(27), pp.4533–4545.

Govett, R., Mace, T. and Bowe, S. 2010. A practical guide for the determination of moisture content of woody biomass.

Grabber, J.H. 2005. How do lignin composition, structure, and cross-linking affect degradability? A review of cell wall model studies. Crop Science. 45(3), pp.820–831.

Green, S.R., Vogeler, I., Clothier, B.E., Mills, T.M. and Van Den Dijssel, C. 2003. Modelling water uptake by a mature apple tree. Australian Journal of Soil Research. 41(3), pp.365–380.

Griffiths, L. 2020. The Clean Air Plan for Wales [Online]. Available from: https://gov.wales/sites/default/files/publications/2020-08/clean-air-plan-for-wales-healthy-air-healthy-wales.pdf.

Grønli, M.G. and Melaaen, M.C. 2000. Mathematical Model for Wood Pyrolysis Comparison of Experimental Measurements with Model Predictions. Energy and Fuels. 14, pp.791–800.

Guerrero, F., Yanez, K., Vidal, V. and Cereceda-Balic, F. 2019. Effects of wood moisture on emission factors for $PM_{2.5}$, particle numbers and particulate-phase PAHs from Eucalyptus globulus combustion using a controlled combustion chamber for emissions. Science of the Total Environment. 648, pp.737–744.

Guo, Z., Wu, J., Zhang, Y., Wang, F., Guo, Y., Chen, K. and Liu, H. 2020. Characteristics of biomass charcoal briquettes and pollutant emission reduction for sulfur and nitrogen during combustion. Fuel. 272, p.117632.

Hedberg, E., Kristensson, A., Ohlsson, M., Johansson, C., Johansson, A., Swietlicki, E., Vesely, V., Wideqvist, U. and Westerholm, R. 2002a. Characterisation of particulate matter emissions from a modern wood burner under varying burner conditions. Atmospheric Environment. 36, pp.4823–4837.

Hedberg, E., Kristensson, A., Ohlsson, M., Johansson, C., Johansson, A., Swietlicki, E., Vesely, V., Wideqvist, U. and Westerholm, R. 2002b. Chemical and physical characterization of emissions from birch wood combustion in a wood stove.

Heiskanen, V. 1953. Summary on the drying of firewood and on its consideration in storage. Communicationes Instituti Forestalis Fenniae. 41(4), p.41.

Hermansson, S., Lind, F. and Thunman, H. 2011. On-line monitoring of fuel moisture-content in biomass-fired furnaces by measuring relative humidity of the flue gases. Chemical Engineering Research and Design. 89(11), pp.2470–2476.

HETAS 2018. HETAS Technical Bulletin #9: Ready to Burn Special Edition [Online]. Available from: https://woodsure.co.uk/ready-burn-technical-bulletin/.

Hofmann, N., Mendel, T., Schulmeyer, F., Kuptz, D., Borchert, H. and Hartmann, H. 2018. Drying effects and dry matter losses during seasonal storage of spruce wood chips under practical conditions. Biomass and Bioenergy. 111, pp.196–205.

Holmberg, H. and Ahtila, P. 2004. Comparison of drying costs in biofuel drying between multi-stage and single-stage drying. Biomass and Bioenergy. 26(6), pp.515–530.

Houmoller, S. and Evald, A. 1999. Sulphur Balances for Biofuel Combustion Systems In: 4th Biomass Conference of the Americas.

Howard, E.T. and Manwiller, F.G. 1969. Anatomical characteristics of southern pine stemwood. Wood Science. 2(2), pp.77–86.

Huangfu, Y., Li, H., Chen, X., Xue, C., Chen, C. and Liu, G. 2014. Effects of moisture content in fuel on thermal performance and emission of biomass semi-gasified cookstove. Energy for Sustainable Development. 21, pp.60–65.

James, W.L. 1988. Electric moisture meters for wood [Online]. Madison. [Accessed 12 May 2020]. Available from: https://www.fs.usda.gov/treesearch/pubs/9823.

Jantunen, M.J. 1985. Problematic emissions of wood combustion compared with other fuels [Online]. Available from: https://www.osti.gov/etdeweb/biblio/8321094.

Johansson, L.S., Leckner, B., Gustavsson, L., Cooper, D., Tullin, C. and Potter, A. 2004. Emission characteristics of modern and old-type residential boilers fired with wood logs and wood pellets. Atmospheric Environment. 38, pp.4183–4195.

Jones, J., Mitchell, E., Williams, A., Jose, G., Hondow, N., Lea-langton, A., Jones, J., Mitchell, E., Williams, A., Jose, G., Hondow, N. and Combustion-generated, A.L.E. 2018. Examination of Combustion-Generated Smoke Particles from Biomass at Source : Relation to Atmospheric Light Absorption Examination of Combustion-Generated Smoke Particles from Biomass at Source : Relation to Atmospheric Light Absorption. Combustion Science and Technology. 00(00), pp.1–14.

Jones, J.M., Lea-Langton, A.R., Ma, L., Pourkashanian, M. and Williams, A. 2014. Pollutants Generated by the Combustion of Solid Biomass Fuels. London: Springer.

Karanasiou, A., Minguillon, M.C., Viana, M., Alastuey, A., Putaud, J.P., Maenhaut, W., Panteliadis, P., Mocnik, G., Favez, O. and Kuhlbusch, T.A.J. 2015. Thermal-optical analysis of the measurement of elemental carbon (EC) and organic carbon (OC) in ambient air: A literature review. Atmos. Meas. Tech. Discuss. 8, pp.9649–9712.

Kekkonen, P.M., Ylisassi, A. and Telkki, V.-V. 2013. Absorption of Water in Thermally Modified Pine Wood As Studied by Nuclear Magnetic Resonance.

Kistler, M., Schmidl, C., Padouvas, E., Giebl, H., Lohninger, J., Ellinger, R., Bauer, H. and Puxbaum, H. 2012. Odor, gaseous and PM 10 emissions from small scale combustion of wood types indigenous to Central Europe. Atmospheric Environment. 51, pp.86–93.

Kofman, P.D. and Kent, T. 2009. Storage and seasoning of conifer and broadleaf firewood. Dublin.

Kopczyński, M., Plis, A. and Zuwała, J. 2015. Thermogravimetric and kinetic analysis of raw and torrefied biomass combustion. Chemical and Process Engineering - Inzynieria Chemiczna i Procesowa. 36(2), pp.209–223.

Koppejan, J. and Loo, S. van 2008. The Handbook of Biomass Combustion and Co-firing. London: Routledge.

Koppejan, J. and van Loo, S. 2008. The Handbook of Biomass Combustion and Co-firing. London: Routledge.

Koppmann, R. 2007. Volatile Organic Compounds in the Atmosphere [Online]. Blackwell Publishing Ltd. Available from: https://onlinelibrary.wiley.com/doi/book/10.1002/9780470988657.

Koppmann, R., Von Czapiewski, K. and Reid, J.S. 2005. A review of biomass burning emissions, part I A review of biomass burning emissions, part I: gaseous emissions of carbon monoxide, methane, volatile organic compounds, and nitrogen containing compounds. Atmos. Chem. Phys. Discuss. 5, pp.10455–10516.

Korenaga, T., Liu, X. and Huang, Z. 2001. The influence of moisture content on polycyclic aromatic hydrocarbons emission during rice straw burning. Chemosphere - Global Change Science. 3(1), pp.117–122.

Krause, A.M. 2000. Method of wood chip moisture analysis. , pp.1–8.

Krugly, E., Martuzevicius, D., Puida, E., Buinevicius, K., Stasiulaitiene, I., Radziuniene, I., Minikauskas, A. and Kliucininkas, L. 2014. Characterization of Gaseous- and Particle-Phase Emissions from the Combustion of Biomass-Residue-Derived Fuels in a Small Residential Boiler. Energy and Fuels. 28, pp.5057–5066.

Kumar, A., Prasad, M. and Mishra, K.P. 2013. Comparative study of the effect of different parameters on performance and emission of biomass cook stoves. International Journal of Research in Engineering and Technology. 1(3), pp.121–126.

L'Orange, C., DeFoort, M. and Willson, B. 2012. Influence of testing parameters on biomass stove performance and development of an improved testing protocol. Energy for Sustainable Development. 16(1), pp.3–12.

Lamb, C.G. 1999a. Firewood moisture content survey: A survey of the moisture content of firewood in Metropolitan Christchurch (Report No. U99/58).

Lamb, C.G. 2003. Public survey: wood burner operation and wood type survey of Christchurch residents.

Lamb, C.G. 1999b. Wood moisture survey - Winter 1998 (Report No. U99/6).

Laurila, J. 2013. Moisture content, weight loss and potential of energy wood in South and Central Ostrobothnia regions in western Finland. University of Helsinki.

Lee, B. 2010. Sources, Distribution and Toxicity of Polyaromatic Hydrocarbons (PAHs) in Particulate Matter In: Air Pollution. London: IntechOpen.

Liparl, F., Dasch, J.M. and Scruggs, W.F. 1984. Aldehyde emissions from wood-burning fireplaces. Environmental Science and Technology1. 18(5), pp.326–330.

Liu, Y., Zhang, Y., Li, C., Bai, Y., Zhang, D., Xue, C. and Liu, G. 2018. Air pollutant emissions and mitigation potential through the adoption of semi-coke coals and improved heating stoves : Field evaluation of a pilot intervention program in rural China *. Environmental Pollution. 240, pp.661–669.

Lu, H., Zhu, L. and Zhu, N. 2009. Polycyclic aromatic hydrocarbon emission from straw burning and the influence of combustion parameters. Atmospheric Environment. 43(4), pp.978–983.

Ma, W., Ma, C., Liu, X., Gu, T., Thengane, S.K., Bourtsalas, A. and Chen, G. 2021. NOx formation in fixed-bed biomass combustion: Chemistry and modelling. Fuel. 290, p.119694.

Magnone, E., Park, S.K. and Park, J.H. 2016. Effects of Moisture Contents in the Common Oak on Carbonaceous Aerosols Generated from Combustion Processes in an Indoor Wood Stove. Combustion Science and Technology. 188(6), pp.982–996.

Man, C., Zhu, X., Gao, X. and Che, D. 2015. Combustion and pollutant emission characteristics of lignite dried by low temperature air. Drying Technology. 33(5).

Mando, M 2013. Biomass Combustion and Co-Firing In: L. Rosendahl, ed. Biomass Combustion Science, Technology and Engineering. Oxford: Woodhead Publishing.

Mando, M. 2013. Direct combustion of biomass In: L. Rosendahl, ed. Biomass combustion science, technology and engineering. Oxford: Woodhead Publishing, pp.61–83.

Maruf Hossain, A.M.M., Park, S., Kim, J.S. and Park, K. 2012. Volatility and mixing states of ultrafine particles from biomass burning. Journal of Hazardous Materials. 205–206, pp.189–197.

Mathewson, J.S. 1930. The air seasoning of wood. Technical Bulletin No.174.

Matthews, S. 2010. Effect of drying temperature on fuel moisture content measurements. International Journal of Wildland Fire. 19, pp.800–802.

Maviglio, S. 1986. From stump to stove in three days. Yankee. 50(12), pp.95–96.

Maxwell, D., Gudka, B.A., Jones, J.M. and Williams, A. 2020. Emissions from the combustion of torrefied and raw biomass fuels in a domestic heating stove. Fuel Processing Technology. 199.

McAllan, M. 2021. Clean Air for Scotland 2 [Online]. Available from: https://www.gov.scot/publications/cleaner-air-scotland-2-towards-better-place-everyone/documents/.

Mcdonald, J.D., Zielinska, B., Fujita, E.M., Sagebiel, J.C., Chow, J.C. and Watson, J.G. 2000. Fine particle and gaseous emission rates from residential wood combustion. Environmental Science and Technology. 34(11), pp.2080–2091.

McElrone, A.J., Choat, B., Gambetta, G.A. and Brodersen, C.R. 2013. Water Uptake and Transport in Vascular Plants. Nature Education Knowledge. 4(5), p.6.

Mckendry, P. 2002. Energy production from biomass (part 1): overview of biomass. Bioresource Technology. 83(2002), pp.37–46.

Mitchell, E.J.S., Lea-Langton, A.R., Jones, J.M., Williams, A., Layden, P. and Johnson, R. 2016a. The impact of fuel properties on the emissions from the combustion of biomass and other solid fuels in a fixed bed domestic stove. Fuel Processing Technology. 142, pp.115–123.

Moon, R.J., Martini, A., Nairn, J., Simonsen, J. and Youngblood, J. 2011. Cellulose nanomaterials review: Structure, properties and nanocomposites.

Mulinari, D.R., Barros, C.C. and Rocha, G.J.M. 2013. Composites of Thermosetting Polymers Reinformed with Natural Fibres In: V. K. Thakur and A. S. Singha, eds. Biomass-based Biocomposites. Shawbury: Smithers, p.85.

Murphy, G., Kent, T. and Kofman, P.D. 2012. Modelling air drying of Sitka spruce (Picea sitchensis) biomass in off-forest storage yards in Ireland. Forest Products Journal. 62(6), pp.443–449.

Nakamura, K., Hatakeyama, T. and Hatakeyama, H. 1981. Studies on heat capacity of cellulose and lignin by differential scanning calorimetry. Polymer. 51(9), pp.607–613.

Ndiema, C.K.W., Mpendazoe, F.M. and Williams, A. 1998. Emission of pollutants from a biomass stove. Energy Conversion and Management. 39(13), pp.1357–1367.

Nireesha, G.R., Divya, L., Sowmya, C., Venkateshan, N., Niranjan Babu, M. and Lavakumar, V. 2013. Lyophilization/freeze drying-A review. International Journal of Novel Trends in Pharmaceutical Sciences. 3(4), pp.87–98.

Nurmi, J. and Lehtimaki, J. 2011. Debarking and drying of downy birch (Betula pubescenes) and Scots pine (Pinus sylvestris) fuelwood in conjunction with multi-tree harvesting. Biomass and Bioenergy. 35, pp.3376–3382.

Nystrom, R., Lindgren, R., Avagyan, R., Westerholm, R., Lundstedt, S. and Boman, C. 2017. Influence of wood species and burning conditions on particle emission characteristics in a residential wood stove. Energy and Fuels. 31(5), pp.5514–5524.

Obaidullah, M., Bram, S. and Ruyck, J. De 2018. An Overview of PM Formation Mechanisms from Residential Biomass Combustion and Instruments Using in PM Measurements. International Journal of Energy and Environment. 12(May), pp.41–50.

Obernberger, I. 1998. Decentralized biomass combustion: State of the art and future development. Biomass and Bioenergy. 14(1), pp.33–56.

Obernberger, I., Brunner, T. and Bärnthaler, G. 2006. Chemical properties of solid biofuels-significance and impact. Biomass and Bioenergy. 30(11), pp.973–982.

Oltean, L., Teischinger, A. and Hansmann, C. 2011. Influence of low and moderate temperature kiln drying schedules on specific mechanical properties of Norway spruce wood. Journal of Wood and Wood Products. 69(3), pp.451–457.

Orang, N. 2015. Effect of feedstock moisture content on biomass boiler operation. Tappi J. 14, pp.629–637.

Orang, N. and Tran, H. 2015. Effect of feedstock moisture content on biomass boiler operation. Tappi Journal. 14(10), pp.629–637.

Orasche, J., Schnelle-Kreis, J., Schön, C., Hartmann, H., Ruppert, H., Arteaga-Salas, J.M. and Zimmermann, R. 2013. Comparison of emissions from wood combustion. Part 2: Impact of combustion conditions on emission factors and characteristics of particle-bound organic species and polycyclic aromatic hydrocarbon (PAH)-related toxicological potential. Energy and Fuels. 27(3), pp.1482–1491.

Ozgen, S., Caserini, S., Galante, S., Giugliano, M., Angelino, E., Marongiu, A., Hugony, F., Migliavacca, G. and Morreale, C. 2014. Emission factors from small scale appliances burning wood and pellets. Atmospheric Environment. 94, pp.144–153.

Ozil, F., Tschamber, V., Haas, F. and Trouvé, G. 2009. Efficiency of catalytic processes for the reduction of CO and VOC emissions from wood combustion in domestic fireplaces. Fuel Processing Technology. 90, pp.1053–1061.

Pandey, K.K. 1999. A study of chemical structure of soft and hardwood and wood polymers by FTIR spectroscopy. Journal of Applied Polymer Science. 71(12), pp.1969–1975.

Parmar, R.S., Welling, M., Andreae, M.O. and Helas, G. 2008. Water vapor release from biomass combustion. Atmos. Chem. Phys. 8, pp.6147–6153.

Pettersson, E., Boman, C., Westerholm, R., Bostrom, D. and Nordin, A. 2011. Stove Performance and Emission Characteristics in Residential Wood Log and Pellet Combustion, Part 2: Wood Stove. Energy Fuels. 25, pp.315–323.

Phillips, D. 2018. The UK's forest resource and its potential as a sustainable feedstock for bioenergy. University of Leeds.

Possell, M. and Bell, T.L. 2012. The influence of fuel moisture content on the combustion of Eucalyptus foliage. International Journal of Wildland Fire. 22(3), pp.343–352.

Postek, M.T., Vladár, A., Dagata, J., Farkas, N., Ming, B., Wagner, R., Raman, A., Moon, R.J., Sabo, R., Wegner, T.H. and Beecher, J. 2011. Development of the metrology and imaging of cellulose nanocrystals. Measurement Science and Technology. 22(2).

Price-Allison, A., Lea-Langton, A.R., Mitchell, Edward J.S. Gudka, B., Jones, J.M., Mason, P.E. and Williams, A. 2019. Emissions Performance of High Moisture Wood Fuels Burned in a Residential Stove. Fuel. 239, pp.1038–1045.

Price-Allison, A., Mason, P.E., Jones, J.M., Barimah, E.K., Jose, G., Brown, A.E., Ross, A.B. and Williams, A. 2021. The Impact of Fuelwood Moisture Content on the Emission of Gaseous and Particulate Pollutants from a Wood Stove. Combustion Science and Technology.

Purvis, C.R. and McCrillis, R.C. 2000. Fine Particulate Matter (PM) and Organic Speciation of Fireplace Emissions. Environmental Science and Technology. 34, pp.1653–1658.

Purvis, C.R., Mccrillis, R.C. and Kariher, P.H. 2000. Fine particulate matter (PM) and organic speciation of fireplace emissions. Environmental Science and Technology. 34(9), pp.1653–1658.

R. Bruce Hoadley 2000. Understanding Wood: A Craftsman's Guide to Wood. Newtown: The Taunton Press.

Raitila, J. and Tsupari, E. 2020. Feasibility of Solar-Enhanced Drying of Woody Biomass. BioEnergy Research. 13, pp.210–221.

Raman, P., Sakthivadivel, M.D. and Vigneswaran, V.S. 2013. Performance evaluation of three types of forced draft cook stoves using fuel wood and coconut shell. Biomass and Bioenergy. 49, p.2013.

Reddy, M.S. and Venkataraman, C. 2002. Inventory of aerosol and sulphur dioxide emissions from India. Part II F biomass combustion. Atmospheric Environment. 36, pp.699–712.

Reeb, J.E. 1995. Wood and Moisture Relationships [Online]. Available from: https://catalog.extension.oregonstate.edu/em8600.

Reeb, J.E. and Milota, M. 1999. Moisture content by the oven-dry method for industrial testing.

Reid, J.S., Koppmann, R., Eck, T.F. and Eleuterio, D.P. 2005. A review of biomass burning emissions part II: intensive physical properties of biomass burning particles. Atmos. Chem. Phys. 5, pp.799–825.

Reza, M.T., Becker, W., Sachsenheimer, K. and Mumme, J. 2014. Hydrothermal carbonization (HTC) - Near infrared spectroscopy and partial least-squares regression for determination of selective components in HTC solid and liquid products. Bioresource Technology. 161, pp.91–101.

Roden, C., Bond, T., Conway, S. and Pinel, A. 2006. Emission factors and real-time optical properties of particles emitted from traditional wood burning cookstoves. Environmental Science and Technology. 40, pp.6750–6757.

Rogge, W.F., Hildemann, L.M., Mazurek, M.A. and Cass, G.R. 1998. Sources of Fine Organic Aerosol . 9 . Pine , Oak , and Synthetic Log Combustion in Residential Fireplaces. Environmental Science and Technology. 32(1), pp.13–22.

Rolls, W. 2013. The Log Book. East Meon: Permanent Publications.

Routledge, D.B. and Sabey, B.R. 1976. Use of a microwave oven for moisture determination in a soil science laboratory. Journal of Agronomic Education. 5(1), pp.25–27.

Rupar, K. and Sanati, M. 2003. The release of organic compounds during biomass drying depends upon the feedstock and/or altering drying heating medium. Biomass and Bioenergy. 25, pp.615–622.

Saito, M., Amagai, K., Ogiwara, G. and Arai, M. 2001. Combustion characteristics of waste material containing high moisture. Fuel. 80(9), pp.1201–1209.

Samuelsson, R., Burvall, J. and Jirjis, R. 2006. Comparison of different methods for the determination of moisture content in biomass. Biomass and Bioenergy. 30(11), pp.929–934.

Samuelsson, R., Nilsson, C. and Burvall, J. 2006. Sampling and GC-MS as a method for analysis of volatile organic compounds (VOC) emitted during oven drying of biomass materials. Biomass and Bioenergy. 30(11), pp.923–928.

Saxena, S.C. 1990. Devolatalisation and combustion characteristics of coal particles. Progress in Energy and Combustion Science. 16(1), pp.55–94.

Schauer, J.J., Kleeman, M.J., Cass, G.R. and Simoneit, B.R.T. 2001. Measurement of emissions from air pollution sources. 3. C1-C29 organic compounds from fireplace combustion of wood. Environmental Science and Technology. 35(9), pp.1716–1728.

Schmid, J., Klippel, M. and Zurich, E. 2015. The Reduced Cross-Section Method for Evaluation of the Fire Resistance of Timber Members: Discussion and Determination of the Zero-Strength Layer. Fire Technology. 51, pp.1285–1309.

Sevault, A., Khalil, R.A., Enger, B.C., Skreiberg, O., Goile, F., Wanf, L., Seljeskog, M. and Kempegowda, F. 2017. Performance evaluation of a modern wood stove using charcoal In: 9th International Conference on Applied Energy. Cardiff, pp.192–197.

Shelton, J.W. and Gay, L.W. 1986. Evaluation of low-emission wood stoves [Online]. Sacramento, California. [Accessed 12 June 2020]. Available from: https://ww2.arb.ca.gov/sites/default/files/classic//research/apr/past/a3-122-32_exsum.pdf.

Shen, G., Preston, W., Ebersviller, S.M., Williams, C., Faircloth, J.W., Jetter, J.J. and Hays, M.D. 2017. Polycyclic aromatic hydrocarbons in fine particulate matter emitted from burning kerosene, liquid petroleum gas, and wood fuels in household cookstoves. Energy Fuels. 31(3), pp.3081–3090.

Shen, G., Tao, S., Chen, Y., Zhang, Y., Wei, S., Xue, M., Wang, B., Wang, R., Lv, Y., Shen, H., Huang, Y. and Chen, H. 2013. Emission characteristics for polycyclic aromatic hydrocarbons from solid fuels burned in domestic stoves in rural China. Environmental Science and Technology. 47(24), pp.14485–14494.

Shen, Guofeng, Tao, S., Wei, S., Zhang, Y., Wang, R., Wang, B., Li, W., Shen, H., Huang, Y., Chen, Y., Chen, H., Yang, Y., Wang, W., Wang, X., Liu, W. and Simonich, S.L.M. 2012. Emissions of parent, nitro, and oxygenated polycyclic aromatic hydrocarbons from residential wood combustion in rural China. Environmental Science and Technology. 46(15), pp.8123–8130.

Shen, G., Tao, S., Wei, S., Zhang, Y., Wang, R., Wang, B., Li, W., Shen, H., Huang, Y., Chen, Y., Chen, H., Yang, Y., Wang, W., Wang, X., Liu, W. and Simonich, S.L.M. 2012. Emissions of Parent, Nitro, and Oxygenated Polycyclic Aromatic Hydrocarbons from Residential Wood Combustion in Rural China. Environmental Science and Technology. 46, pp.8123–8130.

Shen, G., Wei, S., Wei, W., Zhang, Y., Min, Y., Wang, B., Wang, R., Li, W., Shen, H., Huang, Y., Yang, Y., Wang, W., Wang, X., Wang, X. and Tao, S. 2012. Emission factors, size distributions, and emission inventories of carbonaceous particulate matter from residential wood combustion in rural China. Environmental Science and Technology. 46(7), pp.4207–4214.

Shen, Guofeng, Wei, S., Wei, W., Zhang, Y., Min, Y., Wang, B., Wang, R., Li, W., Shen, H., Huang, Y., Yang, Y., Wang, W., Wang, Xilong, Wang, Xuejun and Tao, S. 2012. Emission factors, size distributions, and emission inventories of carbonaceous particulate matter from residential wood combustion in rural China. Environmental Science and Technology. 46(7), pp.4207–4214.

Shen, Guofeng, Xue, M., Wei, S., Chen, Y., Zhao, Q., Li, B., Wu, H. and Tao, S. 2013. Influence of fuel moisture, charge size, feeding rate and air ventilation conditions on the emissions of PM, OC, EC, parent PAHs, and their derivatives from residential wood combustion. Journal of Environmental Sciences (China). 25(9), pp.1808–1816.

Shen, G., Yang, Y., Wang, W., Tao, S., Zhu, C., Min, Y., Xue, M., Ding, J., Wang, B., Wang, R., Shen, H., Li, W., Wang, X. and Russell, A.G. 2010. Emission factors of particulate matter and elemental carbon for crop residues and coals burned in typical household stoves in China. Environmental Science and Technology. 44(18), pp.7157–7162.

Shmulsky, R. and Jones, P.D. 2011. Forest Products and Wood Science: An Introduction. Chichester: John Wiley & Sons, Inc.

Simoneit, B.R.T. 2002. Biomass burning - A review of organic tracers for smoke from incomplete combustion.

Simpson, W.T. 1991. Dry Kiln Operators Manual [Online]. [Accessed 14 May 2020]. Available from: https://books.google.co.uk/books?id=cBjZE-bNWWAC&pg=PA1&lpg=PA1&dq=Lumber+drying+is+one+of+the+most+time-+and+energy+consuming+steps+in+processing+wood+products.+The+anatomical+structure+of+wood+limits+how+rapidly+water+can+move+through+and+out+of+wood.+I.

Simpson, W.T., Boone, R.S., Chern, J. and Mace, T. 1987. Kiln-Drying Time of Split Oak Firewood.

Sjostrom, E. 1993. Wood Chemistry - Fundamentals and Applications. San Diego: Academic Press, Inc.

Skreiberg, Ø., Hustad, J. and Karlsvik, E. 1997. Empirical NOx-Modelling and Experimental Results from Wood Stove Combustion In: Developments in Thermochemical Biomass Conversion. Dordrecht: Springer, pp.1462–1476.

Smith, K.R. 1987. Biofuels, Air Pollution and Health. New York: Plenum Press.

Sommersacher, P., Brunner, T. and Obernberger, I. 2012. Fuel indexes: A novel method for the evaluation of relevant combustion properties of new biomass fuels In: Energy and Fuels. American Chemical Society, pp.380–390.

Sosa, A., Acuna, M., McDonnell, K. and Devlin, G. 2015. Managing the moisture content of wood biomass for the optimisation of Ireland's transport supply strategy to bioenergy markets and competing industries. Energy. 86, pp.354–368.

Stewart, C.M. 1967. Moisture content of living trees. Nature. 214, pp.138–140.

Strehler, A. 2000. Technologies of wood combustion. Ecological Engineering. 16(1), pp.25–40.

Stubenberger, G., Scharler, R., Zahirovic, S. and Obernberger, I. 2008. Experimental investigation of nitrogen species release from different solid biomass fuels as a basis for release models. Fuel. 87, pp.793–806.

Svoboda, K., Martinec, J., Pohorely, M. and Baxter, D. 2009. Integration of biomass drying with combustion/gasification technologies and minimisation of emissions of organic compounds. Chemical Papers. 63(1), pp.15–25.

Thomas, R.J. 1991. Wood: Formation and Morphology In: M. Lewin and I. S. Goldstein, eds. Wood Structure and Composition. New York: Marcel Dekker, Inc, pp.7–49.

Thygesen, L.G., Tang Engelund, E. and Hoffmeyer, P. 2010. Water sorption in wood and modified wood at high values of relative humidity. Part I: Results for untreated, acetylated, and furfurylated Norway spruce. Holzforschung. 64(3), pp.315–323.

Tissari, J., Väätäinen, S., Leskinen, J., Savolahti, M., Lamberg, H., Kortelainen, M., Karvosenoja, N. and Sippula, O. 2019. Fine particle emissions from sauna stoves: effects of combustion appliances and fuel, and implications for the Finnish Emission Inventory. Atmosphere. 10(12), p.775.

USEPA 1984. Residential Wood Combustion Study [Online]. Available from: https://nepis.epa.gov/Exe/ZyPDF.cgi/20008ZNS.PDF?Dockey=20008ZNS.PDF.

Vakkilainen, E.K. 2017. Steam Generation from Biomass. Oxford: Butterworth-Heinemann.

Vicente, E.D., Vicente, A.M., Evtyugina, M., Tarelho, L.A.C., Almeida, S.M. and Alves, C. 2020. Emissions from residential combustion of certified and uncertified pellets. Renewable Energy. 161, pp.1059–1071.

Visser, R., Berkett, H. and Spinelli, R. 2014. Determining the effect of storage conditions on the natural drying of radiata pine logs for energy use. New Zealand Journal of Forestry Science. 44(1), pp.1–8.

Van Wagner, C. 1977. Conditions for the start and spread of crown fire. Canadian Journal of Forest Research. 7(1), pp.23–34.

Wang, X., Bai, S., Jin, Q., Li, S., Li, Y., Li, Y. and Tan, H. 2018. Soot formation during biomass pyrolysis: Effects of temperature, water-leaching, and gas-phase residence time. Journal of Analytical and Applied Pyrolysis. 134, pp.484–494.

Wheeler, E. 2008. Softwood Anatomy: Longitudinal tracheids. Nature. 455.7210, pp.208–212.

Wheeler, T.D. and Stroock, A.D. 2008. The transpiration of water at negative pressures in a synthetic tree. Nature. 455.7210, pp.208–212.

Whiley, A.W., Chapman, K.R. and Saranah, J.B. 1988. Water loss by floral structures of avocado (Persea americana cv. Fuerte) during flowering. Australian Journal of Agricultural Research. 39(3), pp.457–467.

Whistler, R.L. 1991. Hemicelluloses In: M. Lewin and I. Goldstein, eds. Wood Structure and Composition. New York: Marcel Dekker, Inc, pp.287–313.

White, R.H. and Schaffer, E.L. 1981. Transient moisture gradient in fire-exposed wood slab. Wood Fiber Sci. 13, pp.17–38.

Wiedenhoeft, A.C. 2012. Structure and Function of Wood In: R. M. Rowell, ed. Handbook of Wood Chemistry and Wood Composits. Boca Raton: CRC Press - Taylor & Francis Group, pp.9–30.

Wielgosinski, G. 2012. Pollutant Formation in Combustion Processes In: Z. Nawaz and S. Naveed, eds. Advances in Chemical Engineering., pp.295–324.

Williams, A. 1990. Combustion of Liquid Fuel Sprays. London: Butterworths.

Wilton, E. and Bluett, J. 2012. Factors influencing particulate emissions from NEW compliant woodburners in Nelson, Rotorua and Taumarunui 2007.

Wilton, Emily and Bluett, J. 2012. Wood Burner Testing Christchurch 2009 : Diurnal variation in emissions , wood use , indoor temperature and factors influencing start-up Prepared for Ministry of Science and Innovation [Online]. Available from: https://www.niwa.co.nz/sites/niwa.co.nz/files/2 - AKL 2012-020 Woodburner testing Chch 2009.pdf.

Woodsure 2021a. Ready to Burn. Available from: https://www.readytoburn.org/.

Woodsure 2021b. Woodsure appointed by DEFRA to run Ready to Burn certification scheme. [Accessed 25 March 2022]. Available from: https://woodsure.co.uk/woodsure-appointed-by-defra-to-run-ready-to-burn-certification-scheme/.

Yang, H., Yan, R., Chen, H., Zheng, C., Lee, D.H., Uni, V., V, N.D., March, R. V, Re, V., Recei, M. and September, V. 2006. In-Depth Investigation of Biomass Pyrolysis Based on Three Major Components : Hemicellulose , Cellulose and Lignin. Energy and Fuels. 20(17), pp.388–393.

Yang, L., Chen, X., Zhou, X. and Fan, W. 2003. The pyrolysis and ignition of charring materials under an external heat flux. Combustion and Flame. 133(4), pp.407–413.

Yang, Y.B., Newman, R., Sharifi, V., Swithenbank, J. and Ariss, J. 2007. Mathematical modelling of straw combustion in a 38 MWe power plant furnace and effect of operating conditions. Fuel. 86, pp.129–142.

Yin, C., Rosendahl, L., K, S.K. and Condra, T.J. 2004. Use of numerical modelling in design for co-firing biomass in wall-fired burners. Chemical Engineering Science. 59, pp.3281–3292.

Yoshida, T., Sasaki, H., Takano, T. and Sawabe, O. 2010. Dewatering of high-moisture wood chips by roller compression method. Biomass and Bioenergy. 34(7), pp.1053–1058.

Yuntenwi, E.A.T. and Ertel, J. 2008. Laboratory study of the effects of moisture content on heat transfer and combustion efficiency of three biomass cook stoves. Energy for Sustainable Development. 12(2), pp.66–77.

Zhang, J., Smith, K.R., Ma, Y., Ye, S., Jiang, F., Qi, W., Liu, P., Khalil, M.A.K., Rasmussen, R.A. and Thorneloe, S.A. 2000. Greenhouse gases and other airborne pollutants from household stoves in China: A database for emission factors. Atmospheric Environment. 34(26), pp.4537–4549.

Zhao, N., Li, B., Ahmad, R., Ding, F., Zhou, Y., Li, G., Zayan, A.M.I. and Dong, R. 2021. Dynamic relationships between real-time fuel moisture content and combustion-emission-performance characteristics of wood pellets in a top-lit updraft cookstove. Case Studies in Thermal Engineering. 28(101484).

Zhao, P., Shen, Y., Ge, S., Chen, Z. and Yoshikawa, K. 2014. Clean solid biofuel production from high moisture content waste biomass employing hydrothermal treatment. Applied Energy. 131, pp.345–367.

Zweifel, R., Steppe, K. and Sterck, F.J. 2007. Stomatal regulation by microclimate and tree water relations: Interpreting ecophysiological field data with a hydraulic plant model. Journal of Experimental Botany. 58(8), pp.2113–2131.

van Zyl, L., Tryner, J., Bilsback, K., Good, N., Hecobian, A., Sullivan, A., Zhou, Y., Peel, J.L. and Volckens, J. 2019. Effects of fuel moisture content on emissions from a rocket-elbow cookstove. Environmental Science and Technology. 53, pp.4648–4656.

Chapter 3
Experimental Methodology and Design

3.1 Combustion Experiments

3.1.1 Combustion Appliance

Combustion testing was undertaken using a HETAS approved Waterford Stanley Oisin multifuel heating stove. The appliance is not DEFRA approved meaning that it has not been certified for use in smoke control locations. The same stove has been used in previous studies providing a comparable inventory of different fuels and combustion conditions (Mitchell et al., 2016; Phillips et al., 2016; Price-Allison et al., 2019; Maxwell et al., 2020). An image of the appliance is presented in **Figure 3.1a,b**. The appliance is representative of common domestic combustion appliances used within the UK maintaining a nominal radiant heat output of 5.7 kW and a thermal efficiency of 79% during the combustion of fuelwood. The stove is a medium-sized cast-iron appliance maintaining a gross weight of 74 kg and external dimensions of 535 mm, 408 mm and 415 mm (H, W, D). The internal dimensions of the firebox are 250 mm, 270 mm and 190 mm (D, W, D) (Mitchell et al., 2016). An internal deflector plate creates two separate combustion zones within the device. Primary and secondary combustion zones maintain a volume of $8{\times}10^{-3}$ m^3 and $1.4{\times}10^{-3}$ m^3 providing a residence time of 0.9 s and 0.2 s respectively (Atiku et al., 2016). A series of refractory firebricks are positioned across the rear and side faces of the firebox for the purpose of increasing thermal insulation and inhibiting corrosion.
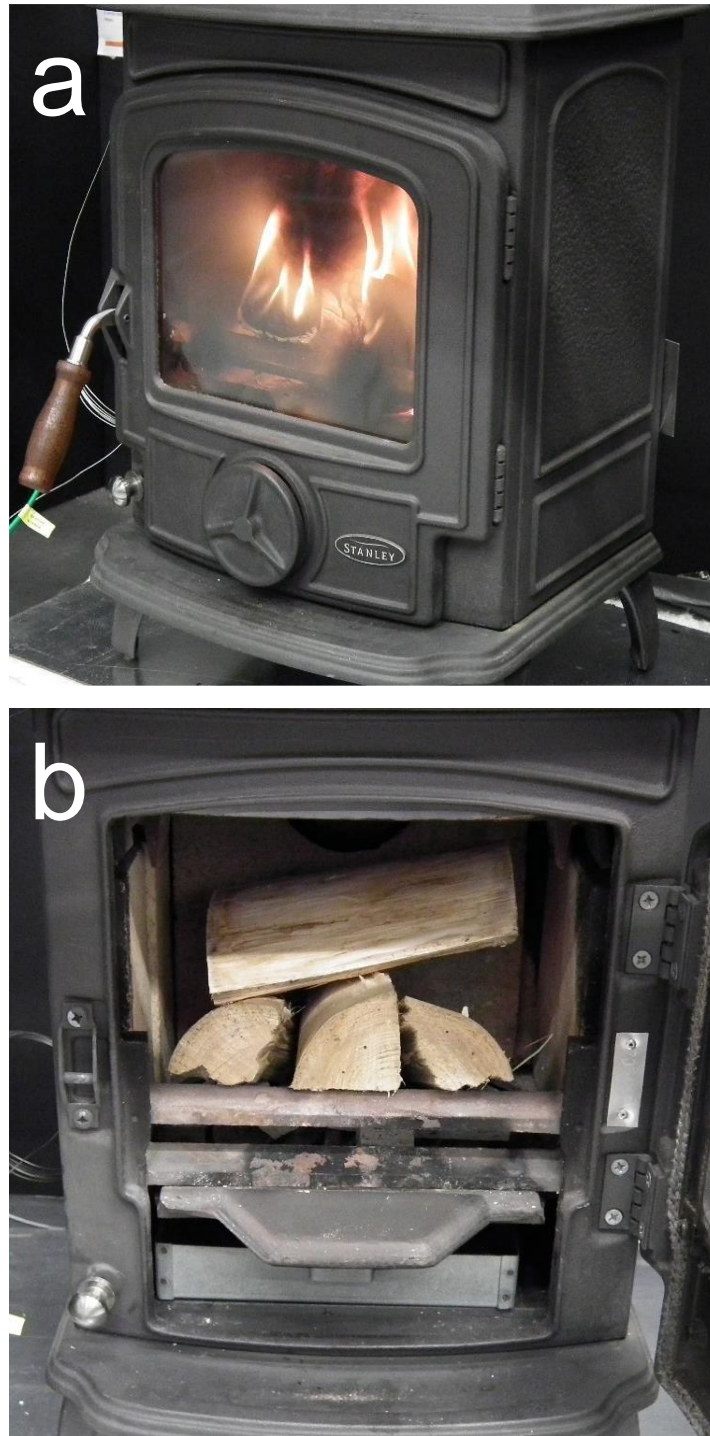
Figure 3.1 (a) External image of Waterford Stanley Oisin stove appliance during operation and (b) internal configuration of the device during fuel loading including ashpan and fire-fence

Primary air was supplied to the firebox via an air control damper located on the stove door below the fixed grate. The extent of the air supply was increased by turning the damper in a counter-clockwise direction. During combustion experiments the air inlet was opened to 10 mm by means of the manual damper. The air availability was not adjusted throughout the experimental procedure or across the individual combustion cycle. The fixed grate encompasses a total area of

616 cm^2. A slotted proportion of the grate, maintaining an area of 314 cm^2, allows for air flow while an interconnected rocker mechanism allows for deashing. A detail description of the grate design is provided in Mitchell et al. (2016). **Figure 3.1b** presents the internal configuration of the stove during fuel loading.

A 300 mm riser was applied at the top of the stove above which a 125 mm ID twin-skin flue was fitted. A series of sampling ports were installed approximately 1430 mm above the top of the firebox for gaseous emission sampling and particulate emission sampling as well as for the monitoring of differential pressure and flue gas temperature. The flue was located directly below a collection hood which was connected to both the dilution tunnel and extraction system.

3.1.2 Stove Operational Procedure

Stove testing was performed following a method similar to BS EN 13240 for a heating stove burning under nominal intermittent conditions. A pre-test batch of fuel was placed across the bottom grate in a manner designed to ensure reproducibility of ignition. The fuel pack was ignited using a mixture of firelighters and kindling with the placement designed to ensure repeatable start-up conditions. The pre-test batch was identified as complete when the mass of fuel and ash remaining in the stove reached a specified mass. A series of subsequent test batches were applied to investigate the repeatability of results under hot start conditions. The number of hot-start tests varied between two and five. Each of the fuels were investigated across a minimum of two combustion series. A reload point was determined for each of the hot-start test batches based upon the mass of unburned fuel and ash residue remaining within the stove. The reload points for each batch were maintained across testing series. The operation of the stove and placement of the fuel was designed to ensure repeatability of results and uniform combustion of the fuel pack.

The required mass of each fuel batch is subject to the fuel moisture content and is calculated from the nominal stove heat output, the recommended refuelling period, the stove efficiency and the fuel LHV (kJ/kg). The appliance specifications are as follows: the rated room output is 5.7 kW, the net efficiency is 79.4% and the refuel period is 0.75 hours during fuelwood combustion. Calculating and pre-weighing the fuel material will allow for similar masses of fuel on a dry basis to be applied within the stove thereby negating the effect of variable moisture content. The batch requirement is calculated as per BS EN 13240-2001 + A2:2004 with the method presented in **Equation 3.1**. **Figure 3.2** presents the effect of MC on the required fuel mass loading in accordance with standard operating practice.

$$(\mathbf{3.1}) \quad B_{fl} = \frac{(3.6 \times 10^5 \times P_n \times T_b)}{(H_u \times \eta)}$$

B_{fl} is the mass of fuel load, in kg

P_n is the nominal heat output, in kW

H_u is the lower calorific value of the test fuel, on a fired basis, in kJ/kg

H is the minimum efficiency according to this appliance standard or a higher value declared by the manufacturer, in %

t_b is the minimum refuelling interval, in hours, or duration as declared by the manufacturer
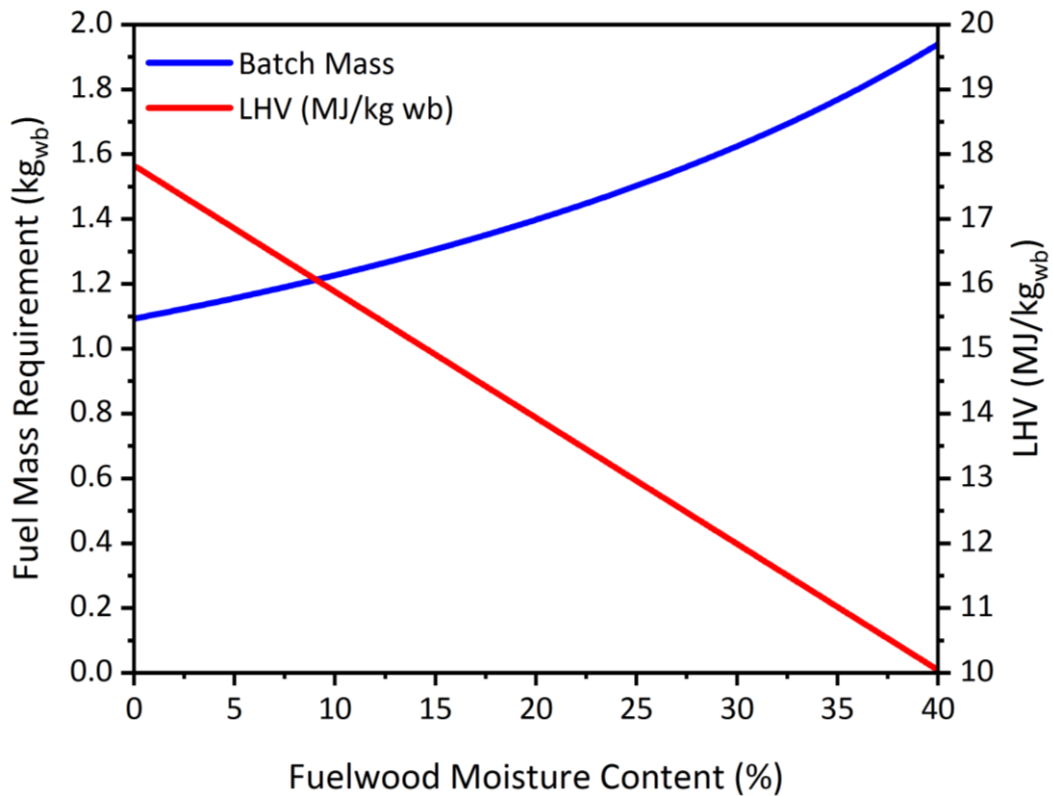
Figure 3.2 Variation in B_{fl} requirement (kg) and LHV (MJ/kg) dependent upon fuelwood moisture content.

3.2 Combustion Testing Facility

A diagram of the combustion facility design in presented in **Figure 3.3**. A 2D schematic of the combustion rig is also shown in **Figure 3.4**. The stove was mounted upon a mass balance [Kern, DE 300k5DL] to record the mass of fuel. A series of K-type thermocouples were placed around the stove to measure the temperature of the stove body and surrounding surfaces. Additional thermocouples were placed inside the stove to measure the temperature of the bottom grate and the combustion chamber. Thermocouples were placed in the flue to measure flue

gas and diluted gas temperature. A precision manometer device [Furness Controls, FCO560 or Wohler, DC100] was used to measure the differential pressure (dp) across an S-type pitot tube positioned in the flue. The manometer also measured ambient barometric pressure within the laboratory. Experimental data (from the balance, thermocouples and manometer) was acquired using a LabVIEW [National Instruments] data acquisition and control system at a sample rate of 1 Hz. Sample gas was analysed in real-time using a Fourier-transform infrared (FTIR) spectrometer [Gasmet, DX4000]. Following sampling and passing through the FTIR spectrometer, the exhaust gases were condensed in deionised water via an impinger. Additional online gas analysis was undertaken using a series of electrochemical sensors located in a dilution duct which was designed in accordance with BS EN 13240 and NS 3058. Particulate sample material was collected using three methods which included size defined collection via impaction under diluted conditions, gravimetric collection at 70 ºC within the flue and gravimetric collection at room temperature within the flue (PM sampled via a non-heated filter).
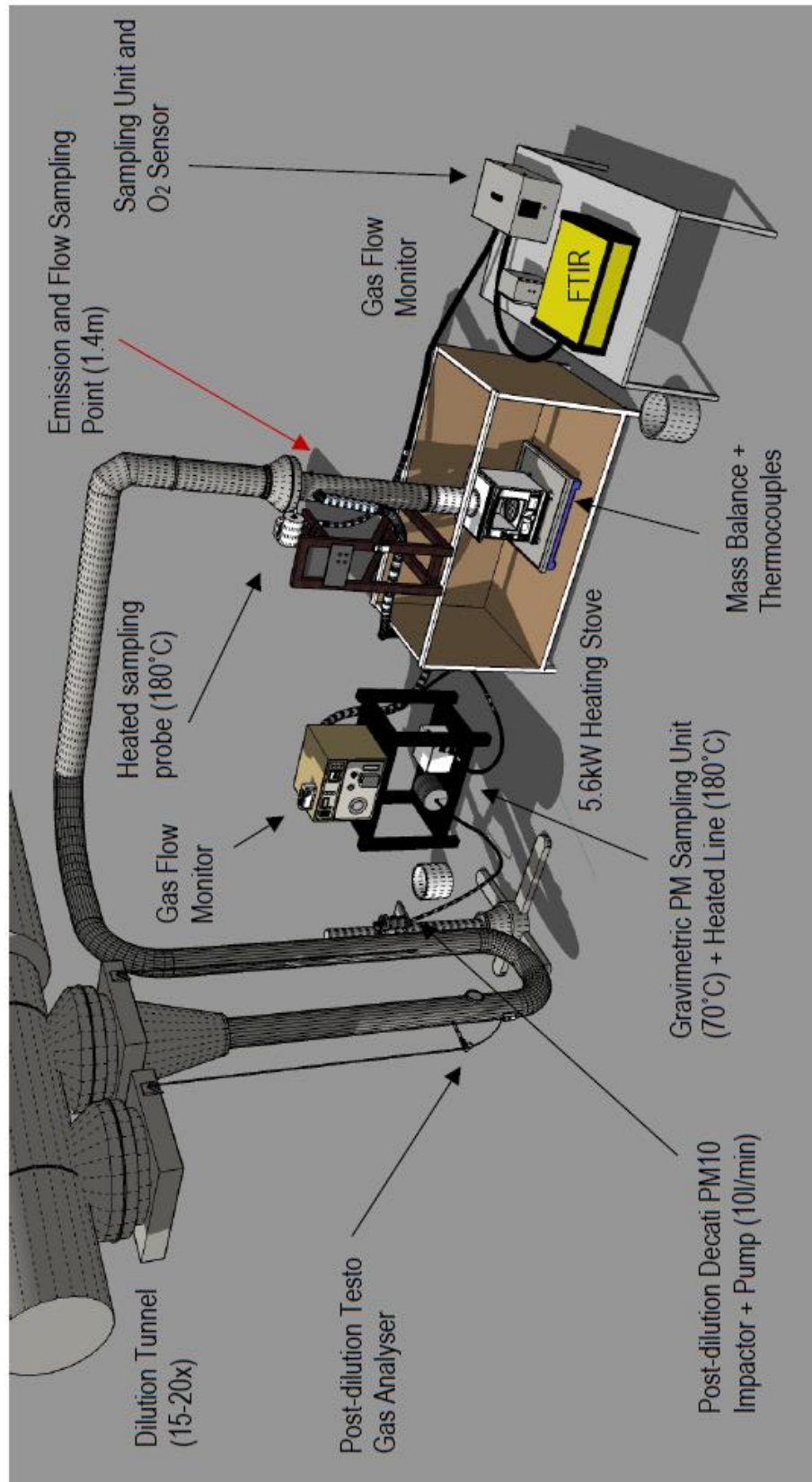
Figure 3.3 Diagram of the combustion facility
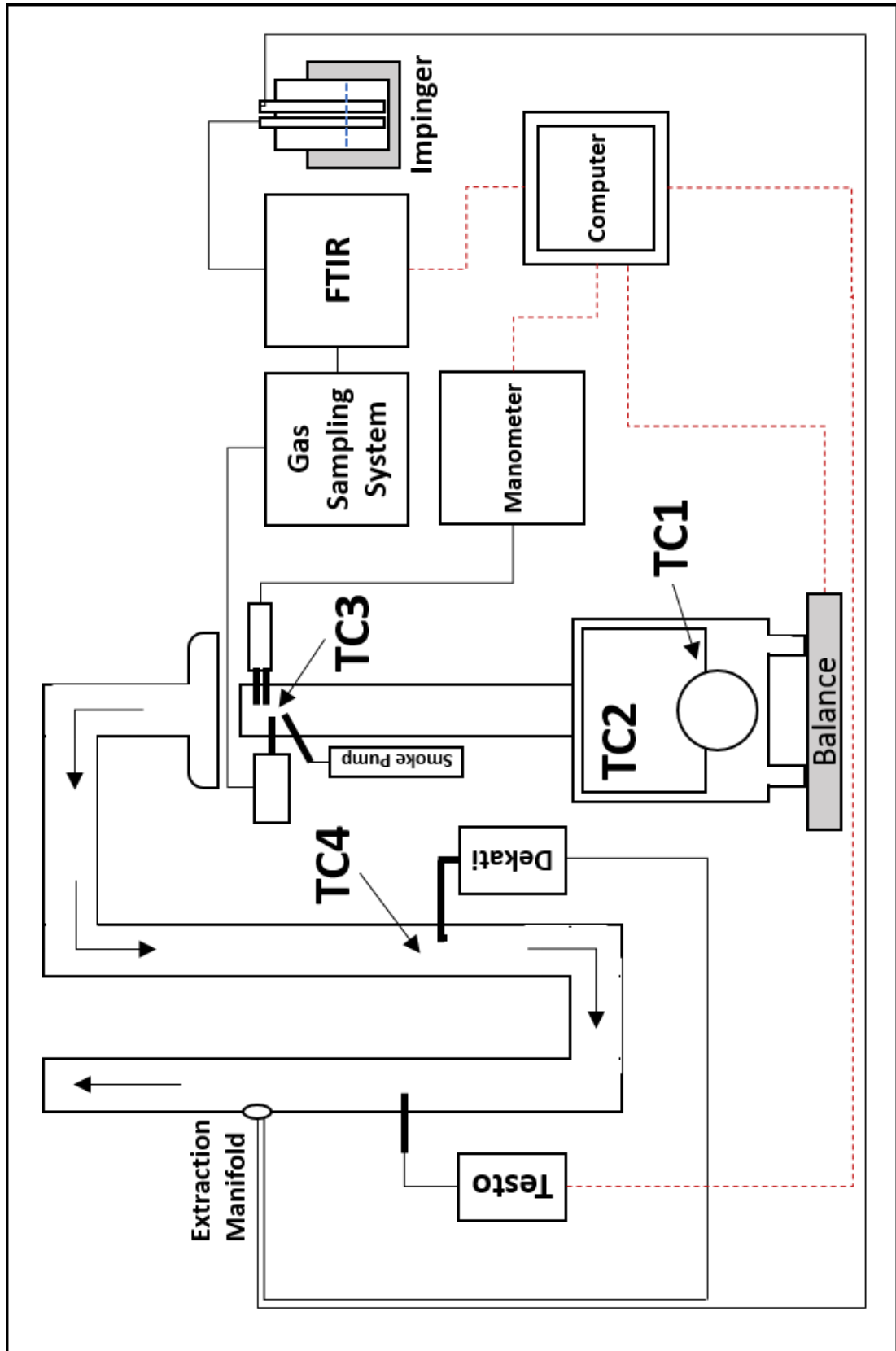
Figure 3.4 2D schematic of combustion rig indicating points of sampling, sampling line (—) and DAQ acquisition (- - -). TC1 is the average grate temperature, TC2 is the flame temperature, TC3 is the flue gas temperature and TC4 is the dilution tunnel temperature.

3.2.1 Gaseous Emission Sampling

3.2.1.1 Fourier Transform Infrared (FTIR) Analysis

Gaseous emission monitoring was undertaken within the flue 1430 mm above the top of the firebox via Fourier Transfer Infrared (FTIR) spectroscopy using a Gasmet DX4000 instrument. FTIR is an instrumentation technique allowing for the determination of organic and inorganic compounds within a gaseous mixture by measuring their absorption of infrared radiation across a range of wavelengths (Berna, 2017). During sampling a beam of light is generated and subsequently split by a Michelson interferometer. The first beam fraction is sent to a fixed Zinc selenide (ZnSe) mirror while the second fraction is sent to a motorized moving mirror; both beams are then recombined before passing through the gaseous sample. A signal interferogram is generated when the recombined beam of light is reflected into a Peltier-cooled detector. This process is undertaken prior to combustion testing and emission sampling thereby providing a background interferogram. Following Fourier transformation and background subtraction an absorption spectrum is generated. Chemical compounds absorb light at different wavelengths depending upon the types of atoms and chemical bonding present. The following gaseous species were monitored during combustion testing; CO_2, CO, N_2O, NO, NO_2, SO_2, NH_3, HCl, HF, CH_4, C_2H_6, C_2H_4, C_3H_8, C_6H_{14}, CH_2O, C_6H_6, C_2H_2, $C_2H_4O_2$, $C_5H_4O_2$ and HCN.

Gaseous emission sampling was undertaken under pre-diluted conditions within the flue throughout the combustion experiment. The flue gas sample was extracted using a portable sampling system with a pump [PSS, Gasmet] connected to a stainless-steel heated probe operating at 180 ºC [PSP4000-H, M&C]. The probe included a 0.1 µm sintered stainless-steel filter element for removing particulate matter from the sample matrix prior to analysis. A second phase of filtering was undertaken using a 0.1 µm PTFE filter element within the Portable Sampling Unit. The rate of flue gas sampling was 10 L/min with gas sampled for a total of 57 s followed by a 3 s analysis period. Independent O_2 concentrations were measured using a zirconia (ZrO_2) sensor located within the PSS. The ZrO_2 sensor range was 0.1–25 vol-% with an error of ±2%. Sample gas was transferred throughout the FTIR system using PTFE lines heated to a nominal temperature of 180 ºC. Following sampling and analysis, the exhaust gases were condensed in deionised water via an impinger.

The FTIR and PSS sampling system where serviced annually by the manufacturer. Additionally, leak checks, gas purging and equipment cleaning were undertaken to limit contamination by laboratory air and previous experiments. The associated

errors for some of the analysed gases are 6.5% for CO, 5.6% for NO, 9.2% for SO_2, 6.0% for water vapour and 6.1% for CH_4 (MCERTS, 2016).

3.2.1.2 Electrochemical Analysis

Gaseous emission monitoring was undertaken within the dilution tunnel using a series of electrochemical sensors and a Testo 340 industrial flue gas analyser. The Testo 340 device applies ion-selective potentiometry as a method of determining gaseous emission composition by means of a series of electrodes located within an electrolytic matrix specific for the determination of a particular species (Testo, 2020). Emission species monitored using this method included O_2, CO_2, CO, NO and NO_2. The accuracy (calibration range) of the electrochemical sensors was ±0.2% for O_2, ±0.2% for CO_2, ±10% for CO, ±5% for NO and ±5% for NO_2. Emission monitoring was undertaken at a sampling flow rate of 0.6 L/min throughout the combustion experiment by means of a 335 mm stainless steel probe housed within the dilution tunnel. A PTFE filter element was placed within the sampling probe to reduce the risk of instrumentation damage by particulate emissions and moisture. The logging rate was variable between experiments but was nominally applied at a rate of 1 Hz (1 S/s). In addition, the Testo 340 instrument was applied as a method of determining the dilution ratio for the dilution tunnel. The dilution ratio, or dilution factor (*DF*), was calculated as a function of the CO concentration (ppm) in the dilution tunnel (CO_{DT}) and in the flue (CO_F) or the ratio between the Testo 340 (CO_{Testo}) and the DX4000 FTIR (CO_{FTIR}) as shown in **Equation 3.2**.

$$(3.2) \quad DF = \frac{CO_{DT}}{CO_F} \, or \, \frac{CO_{Testo}}{CO_{FTIR}}$$

The Testo 340 and sampling system where periodically serviced by the manufacturer. Additionally, leak checks and equipment cleaning were undertaken to limit contamination by laboratory air and previous experiments.

3.2.2 Particulate Emission Sampling

3.2.2.1 PM$_{10}$ Impactor

Soot sampling was undertaken under dilution using a heated (30ºC) impactor [Dekati, PM$_{10}$] with a pump and flow controller [Bronkhorst, Mass View] at a sampling rate of 10.0±0.1 L/min. The applied device was a three-stage cascade impactor allowing for the collection of particles based upon the following mass size

distributions: ≥10 µm, 2.5-10 µm and 1.0-2.5 µm. Cascade impaction operates on the process of curvilinear motion where entrained particles within a streamline are separated based upon their specific gravity and the impact velocity of the gas stream at each phase of the impactor (Maheshwari et al., 2018). In principle, particles are sampled from the dilution tunnel before entering the impactor. The gas flow passes through a series of impaction plates designed for the separation of particles by size fraction. The sorting of particles by aerodynamic separation involves the application of nozzles maintaining a reducing diameter at each phase of the impactor construct (Brouwer et al., 2014). The smaller the nozzle size at a specific flow volume leads to an increase in the gas flow velocity. As the flow velocity is increased larger particles maintaining a higher inertia are more likely to collect on the impaction plates while smaller particles with a lower inertia may flow around the plate thereby remaining entrained within the diverted streamline (Finlayson-Pitts and Pitts, 2000). The impaction plate causes significant disruption or bending to the streamline causing the ejection of particles of a specific inertia from the gas flow (Ali, 2010). **Figure 3.6** presents the method of particle entrainment and deposition based upon particle properties. The size classified particles are then impacted upon a collection matrix or substrate. **Equation 3.3** presents the process of particle separation and subsequent impaction as identified in Finlayson-Pitts and Pitts (2000). **Figure 3.5** is an example of the PM collection obtained during the combustion of fuelwood.

$$(3.3) \quad \eta = \frac{D^2 \times V \times \rho}{18 \times \mu \times D_b}$$

D   is the soot particle diameter
V   is the flow velocity of the sampled combustion gas and air matrix
ρ   is the soot particle density
µ   is the viscosity of the sampled combustion gas and air matrix
D_b is a constant relating to the physical properties of the impactor relating to the processes of divergence from the air flow streamline
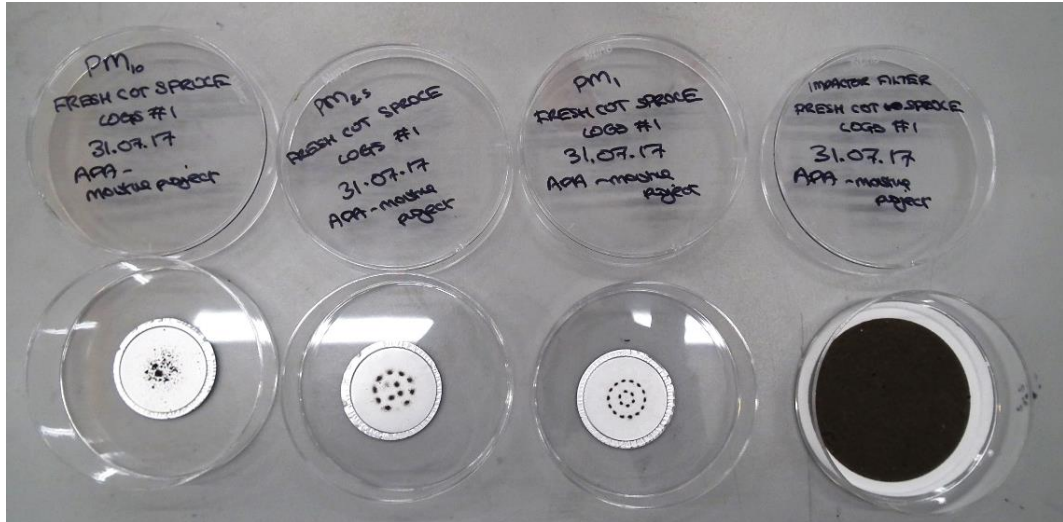
Figure 3.5 Soot sample material collected via impaction during the combustion of fuelwood. Sample material is collected on greased aluminium foils for particle size distribution ≥PM_{10}, $PM_{2.5}$-PM_{10} and PM_1-$PM_{2.5}$ (left). Soot sample material of size distribution <PM_1 is collected upon a micro-quartz filter paper (right).

Particulate emissions were collected on 25mm greased aluminium foils for size fractions of ≥PM_{10}, $PM_{2.5}$-PM_{10} and PM_1-$PM_{2.5}$ µm [CFG-225, Dekati]. A 47 mm Polytetrafluoroethylene (PTFE) backup filter with a pore size of 0.2 µm [10411411, Whatman] or 50 mm micro-quartz backup filter with a pore size of 0.3 µm [RF-360-050, Gilson] was applied to collect PM emissions below PM_1 µm. Filter preparation and weighing was undertaken in accordance with BS EN 13284-1: 2002. Total soot (PM_t) concentration was quantified on a mass basis and is calculated as the sum of each phase of particle collection (PM_t = ≥PM_{10} + $PM_{2.5}$-PM_{10} + PM_1-$PM_{2.5}$ + <PM_1 µm). A calculation workbook provided by the supplier [Impactor Processing Sheet for Microsoft Excel - Version 1.6, Dekati] was used to calculate PM_t concentration on a complete batch basis. Similar methods have been previously applied for soot collection during the combustion of solid fuels in residential heating appliances (Sippula et al., 2007; Stranger et al., 2009; Popovicheva et al., 2016).
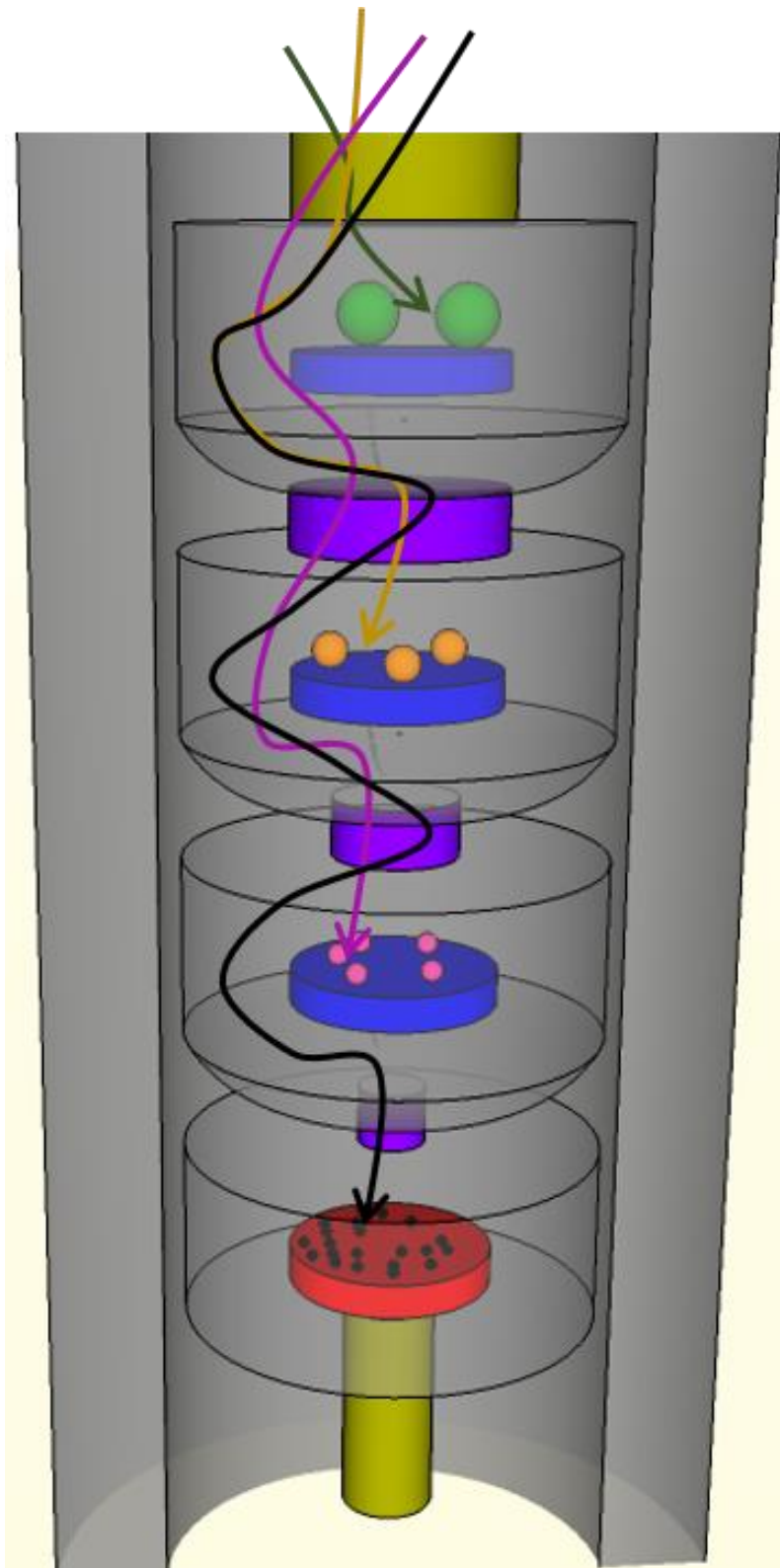
Figure 3.6 Schematic of Dekati PM_{10} Impactor operation. Arrows represent the directional flow of entrained particulate matter depending upon specific inertia and sample density. ● is >PM_{10}, ● is $PM_{2.5}$-PM_{10}, ● is PM_1-$PM_{2.5}$ and ● is <PM_1. ■ is Impactor inlet/outlet, ■ is impaction plate, ■ is specific velocity nozzle and ■ is backup-filter paper. Diagram is adapted from Maheshwari et al. (2018) and Finlayson-Pitts and Pitts (2000).

3.2.2.2 Direct PM$_t$ Flue Sampling

PM$_t$ sampling was undertaken under pre-dilution using a gravimetric smoke meter [Smoke Meter, Richard Oliver]: by means of a sampling probe and a heated filter holder. Particulate matter sampling was undertaken within the stack approximately 1430 mm above the top of the firebox. Sampled flue-gas was transferred through a heated line at 120°C, to a filter-block (70±5°C) housing containing two filter-sheets (Mitchell, Ting, Allan, Lea-Langton, et al., 2019). A heated filter temperature of 70±5°C was selected so as to allow for the condensation and collection of lower volatility organic compounds. A combination of 47 mm glass-fiber filters [10411411, Whatman] and 50mm micro-quartz filters [Gilson, RF-360-050] were applied for PM$_t$ capture with the latter utilized as a method of sample collection for elemental carbon (EC) and black carbon (BC) analysis only. PM$_t$ sampling was undertaken on a temporal basis which was dependent upon fuel type, phase of combustion and the rate of particulate loading.

3.2.2.3 Manual Smoke Pump

PM$_t$ sampling was undertaken under pre-dilution within the stack approximately 1430 mm above the stop of the firebox using a small manual-suction pump device [Smoke Pump, Testo] designed in accordance with DIN 51402 and ASTM D2156. The suction pump sampled a fixed flue gas volume of 1.63±0.07 m^3 across a 2-5 second period. Sample flue gas was drawn across a filter media where entrained soot particles where fixed. Sampling was undertaken every 2-5 min during selected experiments. The device allowed for high resolution sampling of soot from the flue for the purpose of optical and colouration analysis only.

3.2.2.4 Issues Associated with PM Sampling via Gravimetric Filtration

During PM$_t$ sampling and gravimetric analysis a negative particulate mass accumulation was sometimes observed following exposure to smoke. Such anomalies were also observed when visible sampling had occurred on the filter surface. A study by the National Physical Laboratory (NPL) identified a number of potential reasons for the loss of mass during stack sampling. The report identifies potential losses in filter material during placement of filters within a holder and during mechanical manipulation of the material. Such processes can cause notable losses of material, a process particularly prevalent when using brittle and laser cut filters (Robinson et al., 2007). Such processes can lead to a misrepresentation of particle mass accumulation during smoke filtering (Robinson et al., 2007; Charlton, 2011). Additionally, fibrous and brittle filter application can result in difficulties when

attempting to removal of PM sample from a material surface without damaging and simultaneously removing a fraction of collection matrix (Mitchell, Ting, Allan, Lea-Langton, et al., 2019). The use of Teflon (PTFE) filters is identified as a more robust method of sampling with a mitigated risk of fiber loss during handling.

3.2.2.4 Sampling Temperature

The temperature at which particulate matter is sampled influences the material composition. Generally, higher sampling temperatures result in the collection of the EC fraction while low temperature sampling results in OC being more dominant (Mitchell et al., 2016). Sampling at temperatures which are too high or too low can result in the underestimation of overestimation of the OC fraction respectively (Schon and Hartmann, 2018). Because of this consideration of the filter temperature is required when attributing emission factors of EC and OC fractions (Jones et al., 2017). Stove testing standards dictate temperatures of 70°C when conducted in accordance with EN 13240 in Europe, DIN-plus in Germany and BS PD 6436 in the UK. Alternatively, testing in accordance with NS 3058 in Norway, ASTM E2515 in the USA and AS/NZS 4012 in Australia/New Zealand require sampling temperatures <35°C (Seljeskog et al., 2013). Additionally, temperatures of 180°C and 120°C may be applied when sampling undiluted flue gas in accordance with VDI 2066 BLATT 10 in Germany/Austria and EPA Method 5H in the USA respectively (Nussbaumer et al., 2008; Schon and Hartmann, 2018). When sampling diluted flue gas within the Dilution Tunnel a heated filter temperature of 30°C was selected. This value, in accordance with NS 3058, allows for a controlled ambient condition which negates the significant loss of OC fraction often observed at higher temperatures (Nussbaumer et al., 2008). Furthermore, the use of the Dilution Tunnel system reduces the sample temperature to within the range expected at the point of a standard chimney outlet (Schon and Hartmann, 2018). A similar use of low temperature is presented in Orasche et al. (2012) during combustion testing while the positive impact of low temperature sampling on PAH accumulation is shown in (Jones et al., 2017). This procedure is also implemented in the recent Ecodesign regulation (EU 2015/1185) whereby a filter temperature at ambient conditions is applied.

3.2.3 Deviation from Standard Methods for Sampling and Analysis of Emissions

Gaseous emission sampling in accordance with Ecodesign directive 2015/1185 requires the continuous and extractive monitoring of organic gaseous carbon (OGC), CO and NOx (Commission Regulation (EU), 2015). NOx is derived from the

sum of NO and NO_2 and should be expressed as the latter. In accordance with the standardised procedure the analysis technique for each species is as follows; OGC via flame ionisation detection, CO via infrared detection and NOx via chemiluminescence detection. BS EN 13240 outlines the requirement for the monitoring of CO, CO_2 and O_2 however no advise is provided as to the method of analysis required (BSi, 2001). As previously stated, gaseous emission monitoring is undertaken primarily via FTIR. The use of FTIR provides a number of advantages over the advised standardised methods. FTIR is an extractive and continuous technique allowing for the simultaneous determination of a series of inorganic and organic species observed during flaming and smouldering combustion reactions (Stockwell et al., 2016). The fundamental advantage of the technique over that suggested in Ecodesign directive 2015/1185 is that it allows for the simultaneous monitoring of multiple trace species beyond those outlined within standardised testing methods. Additionally, unlike canister sampling techniques, FTIR analysis is not subject to the effects of gaseous artifact formation during emission sampling and storage given that all molecules within the complex flue gas mixture provide a unique infrared signature (Christian et al., 2004). The analysis of gaseous pollutant species arising from small-scale residential combustion appliances via FTIR has been successfully demonstrated within the literature and previous work (Hedman et al., 2006; Tissari et al., 2008; Stockwell et al., 2016; Sevault et al., 2017; Maxwell et al., 2020; Price-Allison et al., 2019; Mitchell et al., 2020).

The analysis of gaseous emissions via electrochemical sensors is undertaken under dilution for the purpose of identifying a dilution factor only.

3.2.4 Data Acquisition and Analysis: National Instruments cDAQ and LabVIEW System

A National Instruments[TM] Compact DAQ (cDAQ) 4-slot USB chassis [cDAQ-9174] was applied as a method of instrumentation control and online data acquisition. The output voltage signal was recorded at a rate of 1 cycle per second (cps) or 1 Hz (1 S/s) under high-resolution operation mode throughout the experimental procedure. Instrumentation interfacing via the cDAQ system was achieved by incorporating a 16-channel thermocouple interface card [NI-9213] and 8-channel ±10 V 12-Bit analogue AI module [NI-9201]. The instrument error associated with the NI-9213 thermocouple module is 0.02 ºC. The acquisition instrument error associated with the NI-9201 ±10 V module is 1.23% assuming an uncalibrated range of 10.53 V. The complete cDAQ, NI-9213 and NI-9201 assembly is shown in **Figure 3.7**.
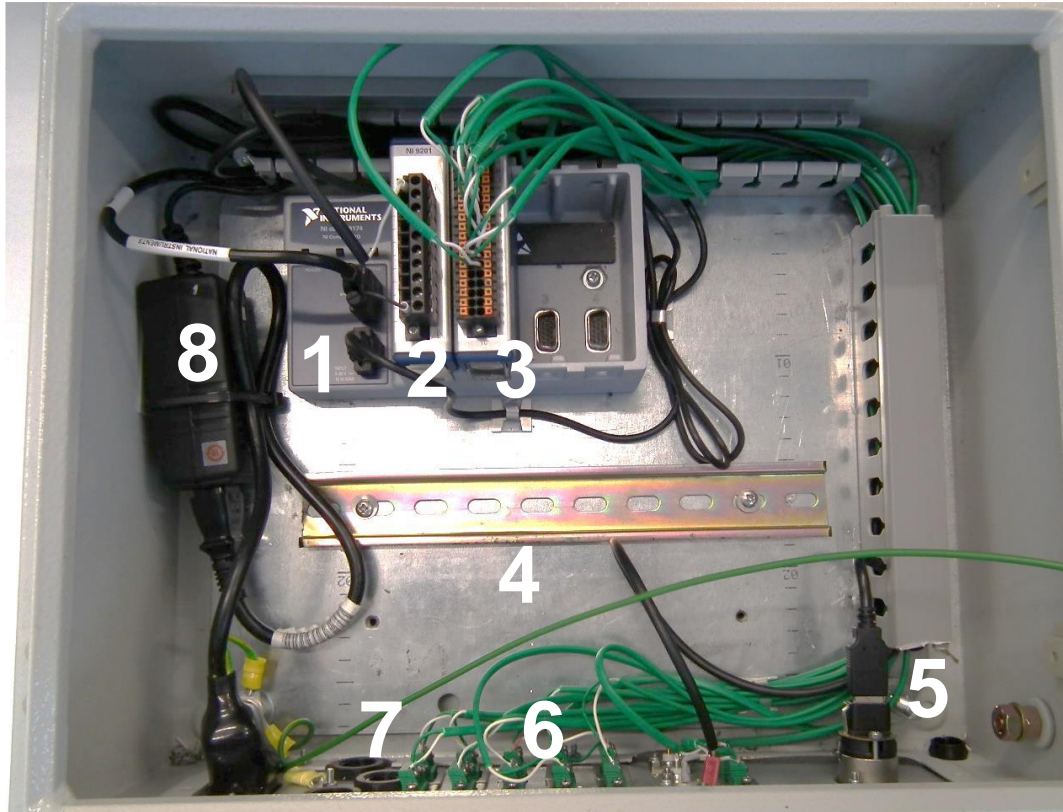
Figure 3.7 Instrumentation and configuration of National Instruments hardware for data logging and control during combustion experiments. The set-up includes [1] cDAQ-9174, [2] NI-9201, [3] NI-9213, [4] DIN rail, [5] USB-b connection. [6] thermocouple input, [7] coaxial input and [8] power supply.

Control and data acquisition for the combustion facility was undertaking using a custom LabVIEW™ platform with USB and RS-232 communication between the cDAQ, or independent instrumentation, and a laboratory PC computer. Thermocouple control and logging was undertaken using the cDAQ with NI-9213 module via a DAQ Assistant virtual instrument (VI). The control and logging for the precision manometer [FCO560] was undertaken using the cDAQ with NI-9201 under a DAQ Assistant VI and with additional control from an independent software [Furness Controls, FBus Utility] with communication via a direct RS-232-PC interface. Fuel weight and mass loss was recorded using a modified Kern™ VI [Kern™ DS Waage v1.0] within the LabVIEW™ platform with communication via a direct USB-PC interface. Optical recording of the combustion experiment was undertaken using a small webcam device under a Vision Acquisition Express VI and logged at a rate of 1 cycle per min (cpm) or 0.02 Hz. **Figure 3.8** shows the user interface for the combustion testing facility as designed within the custom LabVIEW platform.
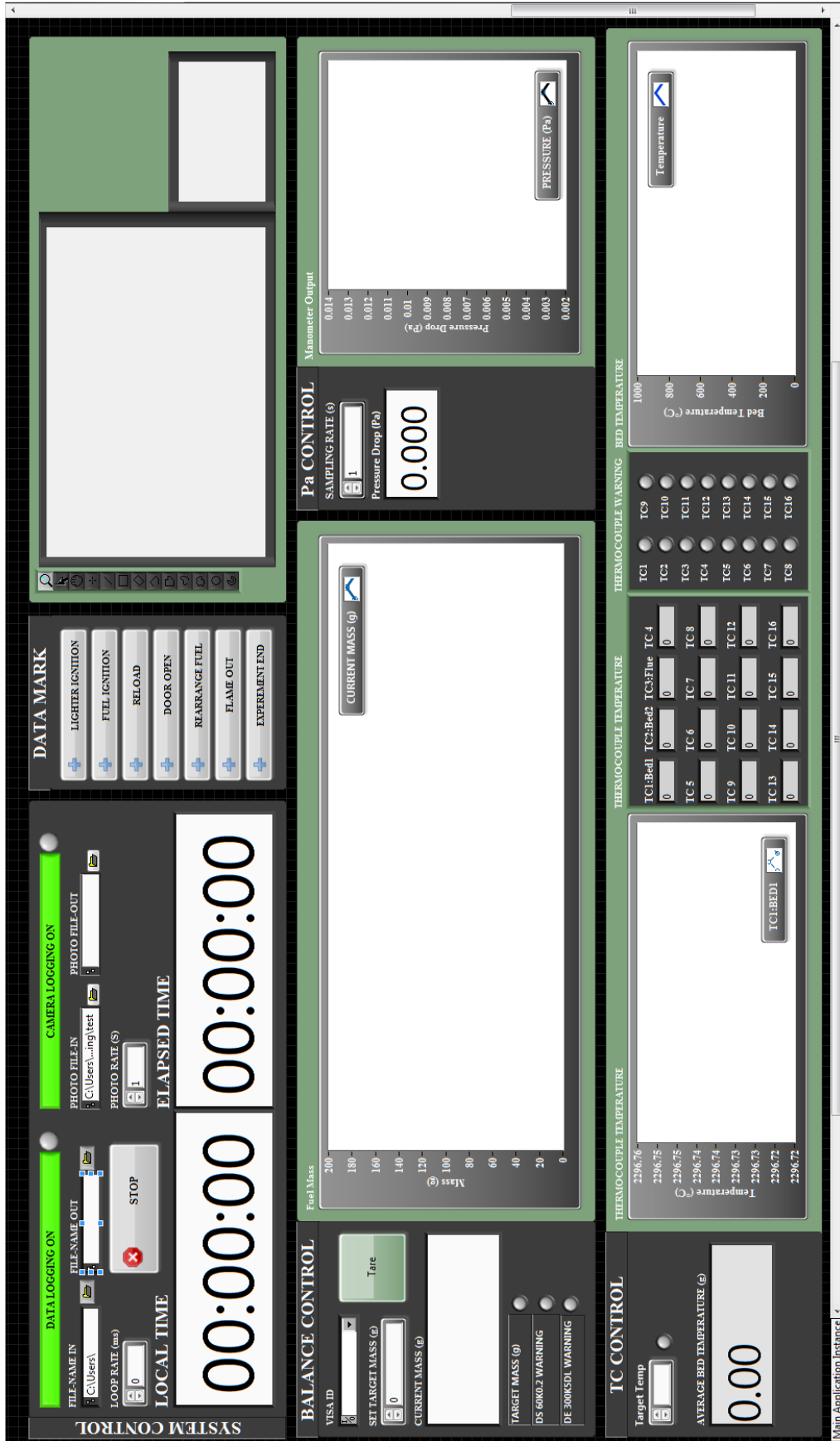
Figure 3.8 User interface front-panel of LabVIEW combustion testing platform

3.2.4.1 Combustion Temperature

Combustion temperature data was recorded at a rate of 1 Hz throughout the experimental procedure. Earlier works utilized a thermocouple data logger [Picolog, TC-08] maintaining an accuracy of 0.2%. Subsequent upgrades replaced this unit with a NI-9201 module maintaining an accuracy of 0.02 ºC which was integrated within the LabVIEW™ platform. An array of insulated stainless-steel K-type thermocouples where applied for temperature monitoring within the combustion appliance, dilution tunnel and surrounding trihedron. A 5 mm thermocouple was situated within the stack approximately 1430 mm above the stove appliance for the purpose of monitoring flue gas temperature at the point of gaseous emission sampling. In addition, a series of 3 mm thermocouples were positioned inside the firebox, upon the grate and at 150 mm above the grate within the flame phase. The temperature at the point of PM_t sampling within the dilution tunnel was also recorded. Finally, the external surface temperature of the firebox and surrounding temperatures within the trihedron were monitored to observe changes in the heat output. **Figure 3.9** identifies the positions of temperature monitoring across the testing rig.
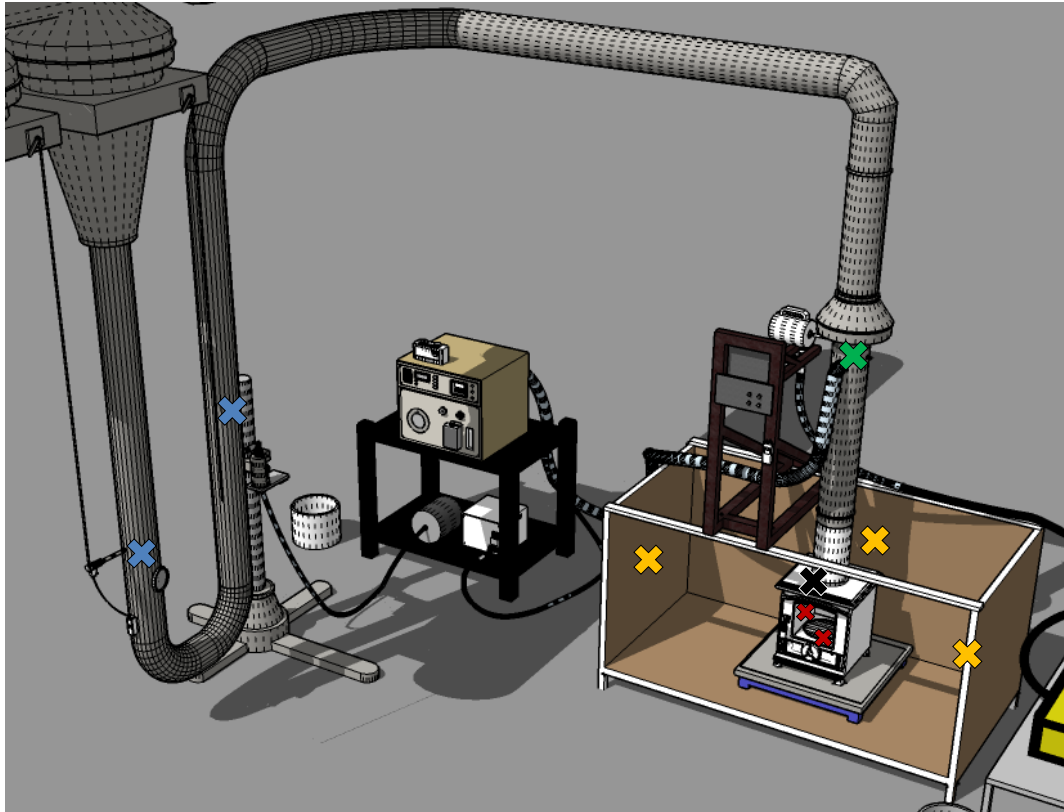
Figure 3.9 Positions of temperature monitoring across the combustion rig and dilution tunnel system. Thermocouple placement is presented as follows: ✖ is grate and flame temperature, ✖ is top of stove temperature, ✖ is trihedron temperature, ✖ is flue gas temperature and ✖ is dilution gas temperature.

Given the likely correlation between flue gas temperature and the combustion temperature within the firebox the former is often applied as a proxy for reaction temperature (Alves et al., 2011; Fachinger et al., 2017). **Figure 3.10** shows a regression analysis between flue gas temperature (*x*), grate temperature (*y1*) and flame temperature (*y2*) sampled during the combustion of a variety of fuels. A weak positive correlation ($R^2 = 0.31$) is shown between flue gas temperature and average grate temperature. A strong positive correlation ($R^2 = 0.84$) is shown between flue gas temperature and flame temperature. The flue gas temperature may therefore be applied as a proxy for the combustion temperature in the flame/gas phase however a poor representation of grate temperature is indicated. Grate temperature is difficult to monitor using thermocouples given the dynamic nature of fixed-grate combustion.
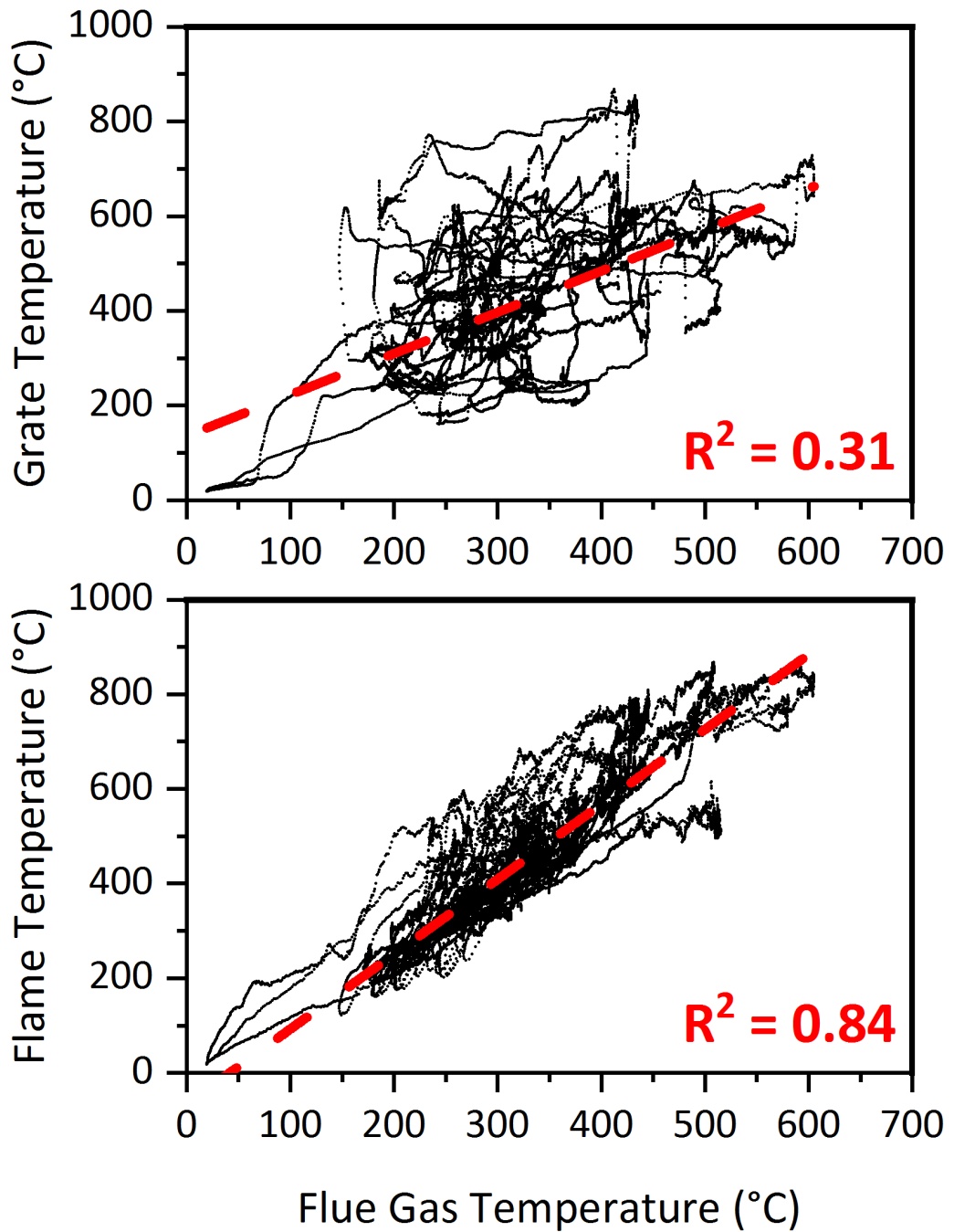
Figure 3.10 Suitability of flue gas temperature as a proxy for the internal combustion temperature of the appliance firebox. A liner correlation coefficient is presented between flue gas temperature and the internal firebox temperature (flame temperature, grate temperature) (n = 46,285). The grate temperature is presented as an average temperature of all thermocouples located on the grate.

3.2.4.2 Fuel Burning Rate

Fuel mass loss (kg) was measured by means of a Kern [DE 300K5DL] platform mass balance. The load cell maintained an instrument error of ±10 g and a mass resolution of 5 g. Mass loss sampling was undertaken by means of the LabVIEW platform at an acquisition rate of 1 Hz (1 S/s). The burning rate (kg/hour) was derived from the difference is fuel mass (Δm) observed across a specific period of analysis (Δt). **Equation 3.4** provides the method of calculating the burning rate.

$$(3.4) \quad \mathrm{kg/hour} = \frac{\Delta m}{\Delta t}$$

The average rate of fuel conversion was calculated on a complete batch basis thereby incorporating aspects of ignition, flaming combustion and smouldering. The average rate was used for comparison between different fuels, operational processes and experiments by other authors. In addition, the burning rate was calculated at the rate of fuel mass acquisition, 1 Hz or 1 S/s, to observe variation in the rate of fuel conversion throughout the combustion cycle. Data processing via an adjacent averaging technique was applied as a method of smoothing noise within the burning rate profile with noise occurring in response to instrumentation error and the sampling resolution of the load cell device.

3.2.4.3 Flue Gas and Volumetric Flow Rate

Differential Pressure (dp) was measured within the flue approximately 1430 mm above the firebox by means of an S-type pitot-tube. In earlier works, a Wohler [DC100] differential pressure computer was used to measure dp within the flue at a rate of 0.5 S/min. The instrument maintained a sampling resolution of 0.01 Pa and an error of ±5%. In later works a precision manometer [Furness Controls, FCO 560] was applied for monitoring dp within the flue at a rate of 1 S/s. The FCO 560 unit maintained a sampling resolution of 0.01 Pa and an error of 0.03 Pa. The barometric pressure (P) within the lab was also recorded by both the FCO 560 precision manometer and GX4000 FTIR as the absolute pressure.

The method of calculating flue gas velocity (v_i) from dp varied between instrumentation. **Equation 3.5** presents the method of determining v_i in accordance with BS EN ISO 16911-1.

$$(3.5) \quad v_i = \alpha \times \sqrt{\left(\frac{2 \times dp}{\rho}\right)}$$

α   is the Pitot tube coefficient and a constant which includes a Pitot tube correction factor that is specific to the type and design of the device. The α value for the S-type pitot tube us 0.84.

dp   is the flue gas differential pressure at the measurement point that is calculated by the device that is measure in Pa.

ρ   is the uncompressed wet flue gas density at ambient temperature at the measurement point. A value of 1.293 kg/m^3 is assumed that is the predicted density of air at standard temperature and pressure.

The method for calculating the flue gas velocity at standard temperature (ºC) and standard pressure (101325 Pa) from the differential pressure within the flue as defined by the FCO 560 device is outlined in **Equation 3.6**.

$$(3.6) \quad v_i = 23.96 \times \sqrt{\left(\frac{\Delta P}{K}\right) \times \left(\frac{T}{P}\right) \times \left(\frac{1}{\rho_{rel}}\right)}$$

ΔP   is the differential pressure (*dp*) within the flue at the point of measurement in Pa.

K   is the inverse of α and is the pitot tube coefficient and a constant which includes a Pitot tube correction factor. The *K* value for the S-type pitot tube us 1.4.

T   is the static temperature of the flue gas at the point of measurement in ºK.

P$_{rel}$ is the relative gas density at the point of measurement. This value is assumed to be 1 kg/m^3 for air at standard temperature and pressure.

Volumetric flow (Q_v) was calculated at the point of flue gas sampling in m^3/min and at STP and on a dry basis. Standard pressure is assumed to be 101325 Pa and standard temperature is assumed to be 0 ºC (273.15 K). Alternatively, emission concentrations may be presented at normal temperature and pressure (NTP) which is the condition of air at 20 ºC and 101325 Pa. The method for determining Q_v from vi at STP is presented in in **Equation 3.7**.

$$(3.7) \quad Q_v = v_i \times \left(\pi \times \left(\frac{D}{2} \right)^2 \right) \times \left(\frac{P}{101325} \right) \times \left(\frac{T}{273.14} \right) \times \left(\frac{100 - MC}{100} \right)$$

Q_v is the volumetric flow rate of flue gas at STP in m^3/min.

D is the diameter of the flue gas pipe that is 0.125 m.

P is the absolute pressure in the pipe at the point of measurement in Pa.

T is the temperature of the flue gas at the point of measurement in ºK.

C is the flue gas moisture content measured by FTIR in vol-%.

3.2.5 Combustion and Emission Factor Calculations

3.2.5.1 Normalisation of Emission Concentrations

Gaseous emission concentration is often recorded in parts per million (ppm) or volume percent (vol-%). These values are converted into an emission concentration normally in mg of pollutant per m^3 of combustion gas (mg/m^3) at standard temperature and pressure (STP). STP is specified as 0ºC and 101325 Pa. **Equation 3.8** presents the method of conversion where V_{mol} is assumed to be the molar volume of one molar of ideal gas at STP or 22.41 L/mol. The Mmol is variable and specific to the volume of each pollutant species (EPA, 2018). The emission concentration may be presented on a dry basis (db) and/or at a reference oxygen concentration depending upon the method of emission factor quantification applied. A reference O$_2$ concentration of 13% was applied within this study and an indication is presented where the correction has been applied.

$$(3.8) \quad C \frac{mg}{m^3} = C \times \frac{M_{mol}}{V_{mol}} \times \frac{21 - O_{2_{ref}}}{21 - O_{2_i}} \times \frac{100}{100 - MC}$$

$C\ mg/m^3$ is the pollutant concentration in mg/m^{3}db at STP at a reference O$_2$%

C is concentration of pollutant species in ppm or vol-%

V_{mol} is the volume of one molar of ideal gas at STP in L/mol

M_{mol} is the molecular mass of the pollutant species in g/mol

$O_{2\ ref}$ is the reference O$_2$ concentration on a dry basis in vol-%

$O_{2\ i}$ is the recorded O$_2$ concentration on a dry basis in vol-%

MC is the moisture content of the flue gas in vol-%

3.2.5.2 SDFGV Method

Emission factor values may be determined using the specific dry flue gas volume (SDFGV). The method requires the estimation of the theoretical stochiometric dry

flue gas volume at a specific O_2 concentration. The SDFGV is calculated as the dry flue gas volume per GJ net heat input (m^3/GJ) at STP, at a specific O_2 concentration and on a dry basis (db) (Stewart, 2012). A method of determining SDFGV (m^3/GJ) via the carbon (C), hydrogen (H), sulphur (S), oxygen (O) and nitrogen (N) composition as indicated in BS EN 12952-15:2003, is shown in **Equation 3.9**. In addition, a number of reference SDFGV values at specific O_2 concentrations are presented by Stewart (2012).

$$(3.9) \quad SDFGV = 88930_{\gamma_C} + 209724_{\gamma_H} + 33190_{\gamma_S} - 26242_{\gamma_O} + 0.7997_{\gamma_N}$$

The SDFGV is subject to variation depending upon the reference O_2 condition and elemental composition of the fuel. **Figure 3.11** presents the effect of the reference O_2 concentration on the SDFGV. Data includes the reference SDFGV for wood and hay as identified in Stewart (2012), BS EN 14961:1 and fuelwood samples from **Chapter 5** (Price-Allison et al., 2019) modelled under different O_2 conditions.
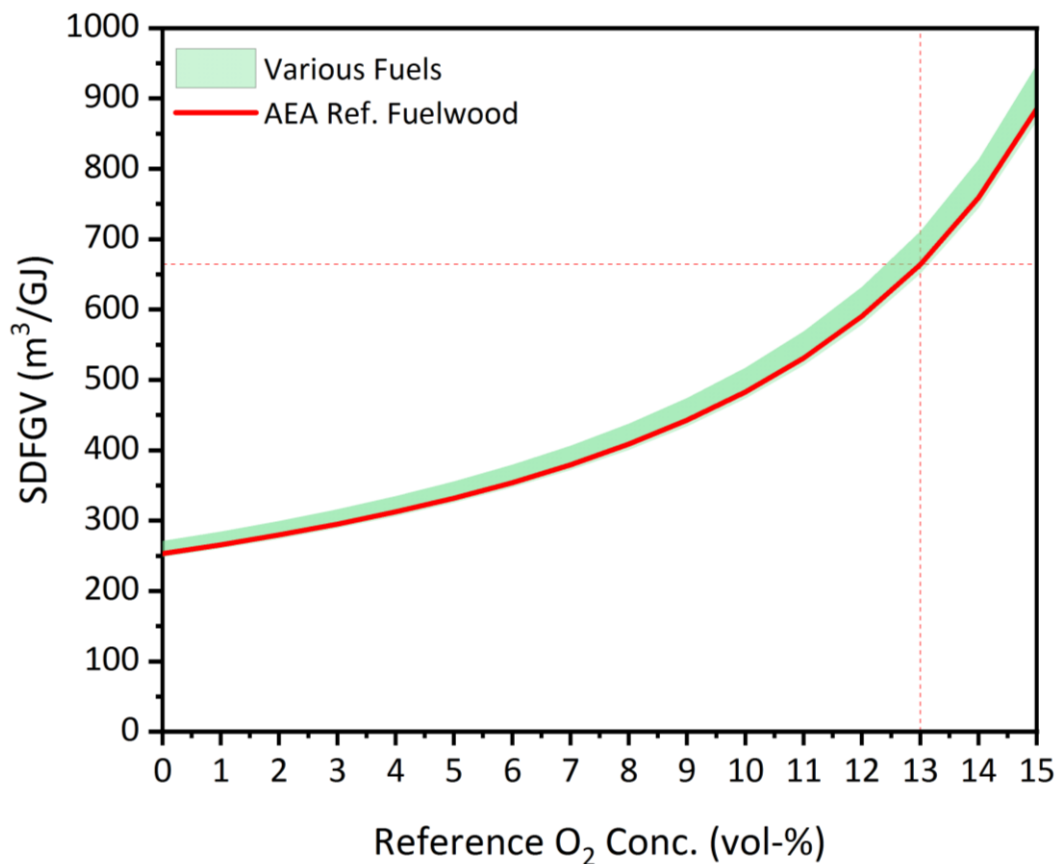
Figure 3.11 Variation in SDFGV (m^3/GJ) under different reference O_2 conditions. The AEA Ref. Fuelwood represents a SDFGV of 253 m^3/GJ at an O_2 reference concentration of 0% resulting in a value of 664 m^3/GJ at 13% O_2. Various fuels represents the SDFGV from fuels presented in BS EN 14961:1, Stewart (2012) and Price-Allison et al. (2019).

An emission factor is derived from the SDFGV (m^3/GJ_{db} at STP and O_2 ref) and the emission concentration of a pollutant species (*i*) (Stewart, 2012; Olave et al., 2017). An average emission concentration is often applied to account for variation in combustion conditions across a complete test batch. The emission concentration (mg/m^3) should be corrected to the same temperature, pressure, moisture and O_2 reference concentration conditions as the SDFGV. The method of calculating an emission factor in g/GJ from the SDFGV and conversion to g/kg_{fuel} using the HHV is presented in **Equation 3.10**. The calculation of the HHV is undertaken using the method outline in Friedl et al. (2005) and presented in **Equation 3.22**.

$$(3.10) \quad EF = \frac{\left[\left(\frac{[Conc_i] \times SDFGV}{1000}\right) \times HHV\right]}{1000}$$

EF is emission factor in g/kg_{fuel} (or g/GJ without the HHV conversion)
Conc$_i$ is the average emission concentration of pollutant species i in mg/m^3
SDFGV is the reference SDFGV value in m^3/GJ at 13% O_2
HHV is the higher heating value for the fuel, in MJ/kgdb

The method is useful for quantifying approximate emission factor values from the SDFGV and emission concentration without the need for monitoring combustion temperature, mass of fuel consumed and flow rate. This is however a fundamental limitation in that key processes for accurately calculating EF values are not included. Furthermore, the method is designed for application on large residential boiler type appliances which often present consistent O_2 concentrations. O_2 concentration is known to vary throughout the combustion reaction in small residential heating appliances. As such, high O_2 concentration during the ignition and smouldering phases can generate erroneous emission concentrations when an O_2 correction is applied. This process is presented in **Figure 3.12** whereby an emission concentration of 100 mg/m^3 is shown to vary under differing O_2 concentrations. As such, derived emission factor values may be substantially higher than what is expected given the observed emission concentration. This method is applied in **Chapter 5** only.
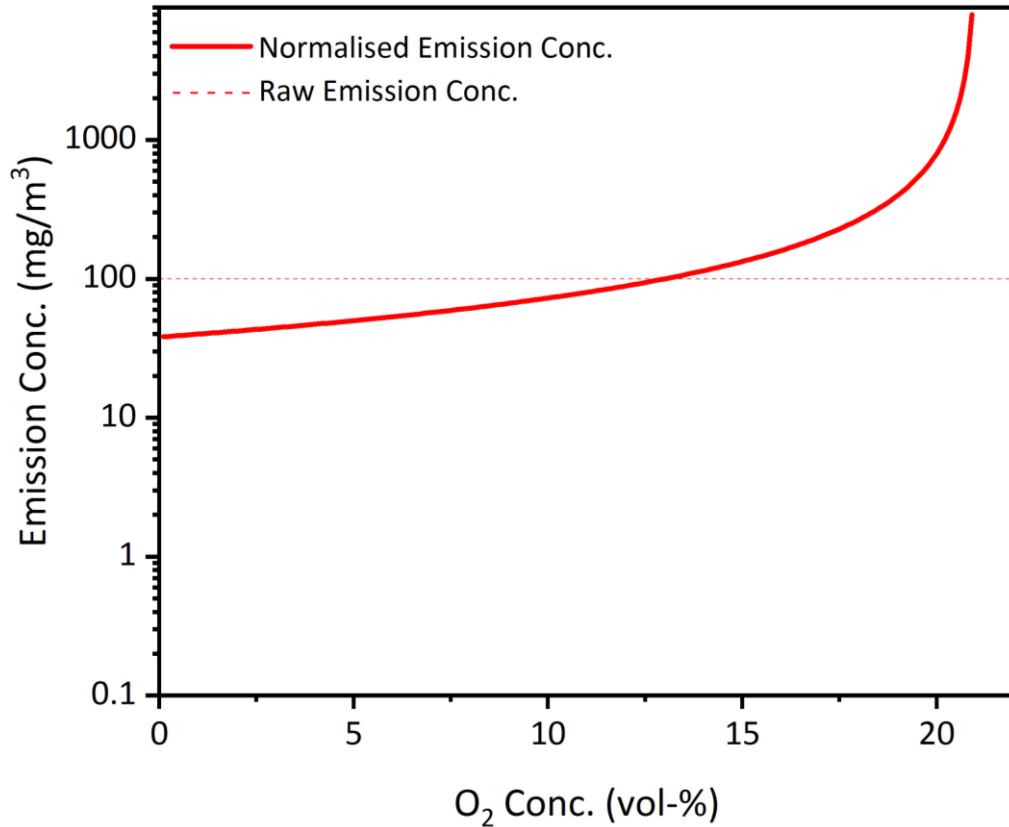
Figure 3.12 Effect of O_2 correction assuming a raw emission concentration of 100 mg/m^3. The range of the modelled O_2 concentration is between 0.1 vol-% and 20.9 vol-% and assumed a O_2 reference value of 13.0 vol-%.

3.2.5.3 Total Capture Method

Emission factor values may be calculated from the emission concentration of pollutant species *i* measured within the stack or collection hood. Gaseous emission concentrations were monitored within the flue while particulate emission sampling was undertaken within the dilution tunnel. EF values were calculated following the method highlighted in ISO 19867-1 and applied in Mitchell et al. (2019). Unlike the SDFGV method, the total flow method incorporates additional processes associated with the combustion reaction including mass of fuel consumed and the total combustion gas flow. In addition, a method of integration is applied between specific temporal periods, as opposed to average emission concentrations used in other methods. The method is presented in **Equation 3.11** where E_t is the total pollutant emitted during the test phase and F_t is the total fuel consumed during the test phase on a dry basis. Emission factor values are presented in g/kg$_{fuel}$ on a dry basis and where obtained across the complete combustion cycle thereby incorporating periods of ignition, flaming combustion and smouldering. This is the primary method for calculating emission factors in this thesis.

$$(3.11) \quad EF = \left(\frac{E_t}{T_f}\right) = \int_{t_0}^{t} \left(\frac{C_i \times Q}{m}\right) dt$$

EF is emission factor in g/kg$_{fuel}$

C_i is the is the total pollutant integral (mg/m^3$_{db}$) for species i at STP

Q is the volumetric flow in m^3/min$_{db}$ at STP

m is the mass of fuel consumed (kg$_{db}$)

3.2.5.4 Modified Combustion Efficiency

Combustion efficiency (CE) is measured as the molar ratio of emitted gaseous CO_2 and fuel carbon burned within a combustion reaction (Yokelson et al., 1996). The CE assumes that the fuel carbon burned within the combustion reaction correlates within the quantity of carbonaceous emission sampled during the experimental phase. As such, the fuel carbon quantity is measured as the sum of CO_2, CO, CH_4, non-methane hydrocarbon (NMHC) species and particulate carbon (PC) concentrations [C]. *CE* is calculated in **Equation 3.12** (Ferek et al., 1998).

$$(3.12) \quad CE = \frac{[C]_{CO_2}}{[C]_{CO_2} + [C]_{CO} + [C]_{NMHC+CH_4} + [C]_{PC}}$$

CE is difficult to measure accurately meaning that a modified combustion efficiency (MCE) is often applied (Ferek et al., 1998; Akagi et al., 2011). MCE may be calculated as an approximation of the fuel carbon fraction converted into CO_2 during a combustion reaction assuming that the total gaseous CO_2 and CO emittance is equal to the total fuel carbon burned (Yokelson et al., 1996; Fachinger et al., 2017). This is a simplified model as it does not require monitoring of all gaseous hydrocarbon species (CH_4 and NMHC) and PM_t carbon content (Ferek et al., 1998). In addition, the MCE is often an accurate representation of the CE which is generally true to within a few percent (Akagi et al., 2011). The calculation also provides an approximation of the extent of flaming and smouldering combustion during a reaction. The method of calculating the MCE is presented in **Equation 3.13** (Stockwell et al., 2015). A high MCE value (0.90>) suggests relatively low CO and high CO_2 emissions thereby signifying efficient flaming combustion. Under such conditions a greater fraction of VOC products will be fully consumed within the flaming phase. A low MCE value (<0.90) suggests relatively high CO and low CO_2 emissions often synonymous with smouldering combustion where reduced combustion temperatures result in an increase in the emission of pollutant species (Reid et al., 2005; Mitchell et al., 2017). Applied only as a predictive method, an

MCE value of 1.00 and 0.80 is indicative of total flaming and total smouldering combustion respectively while an MCE value of 0.90 may indicate an equal mixture of flaming and smouldering within the combustion zone (Yokelson et al., 1996). Akagi et al. (2011) suggests that the reported MCE under smouldering combustion may be between 0.65 and 0.85 and present across a larger range than under the flaming phase. Alternatively, differentiation between the flaming phase and smouldering phase maybe identified by a significant step change in the MCE time series (Fachinger et al., 2017).

$$(3.13) \quad MCE = \frac{\Delta CO_2}{\Delta CO_2 + \Delta CO} = \frac{1}{1 + \left(\frac{\Delta CO}{\Delta CO_2}\right)}$$

3.3 Post-Sampling Analysis

3.3.1 Particulate Sample

3.3.1.1 Elemental Carbon (EC) and Organic Carbon (OC)

Thermogravimetric analysis (TGA) was applied as a method of determining Elemental Carbon (EC) and Organic Carbon (OC) fractions within the soot using a Netzsch STA449 instrument. A 20.1 cm^2 filter cutting with entrained particulate sample material was removed and placed directly into a large TGA crucible before being purged with nitrogen at a rate of 40 ml/min. The temperature was increased from 30°C to 100°C at a rate of 20 K/min before a hold period of 10 min. The OC fraction was determined by measuring the mass-loss while increasing the temperature from 100°C to 550°C at a rate of 20 K/min followed by a subsequent hold period of 10 min. The EC fraction was determined by measuring the mass-loss after exchanging the N_2 supply for an air atmosphere and allowing full oxidation of the remaining sample compounds. An example of the heating profile and mass loss-time-series is shown in **Figure 3.13**. The Total Carbon (TC) was determined as a sum of the EC and OC fractions (TC = OC + EC). A correction was applied to the mass loss results during heating to compensate for the buoyance effects associated with the larger crucible mass. As a control, a blank filter was applied under the same heating conditions to confirm that mass loss from the substrate and binder was negligible. A similar method for determining OC and EC fractions via TGA has been previously described by Atiku et al. (2016) and Jones et al. (2018).
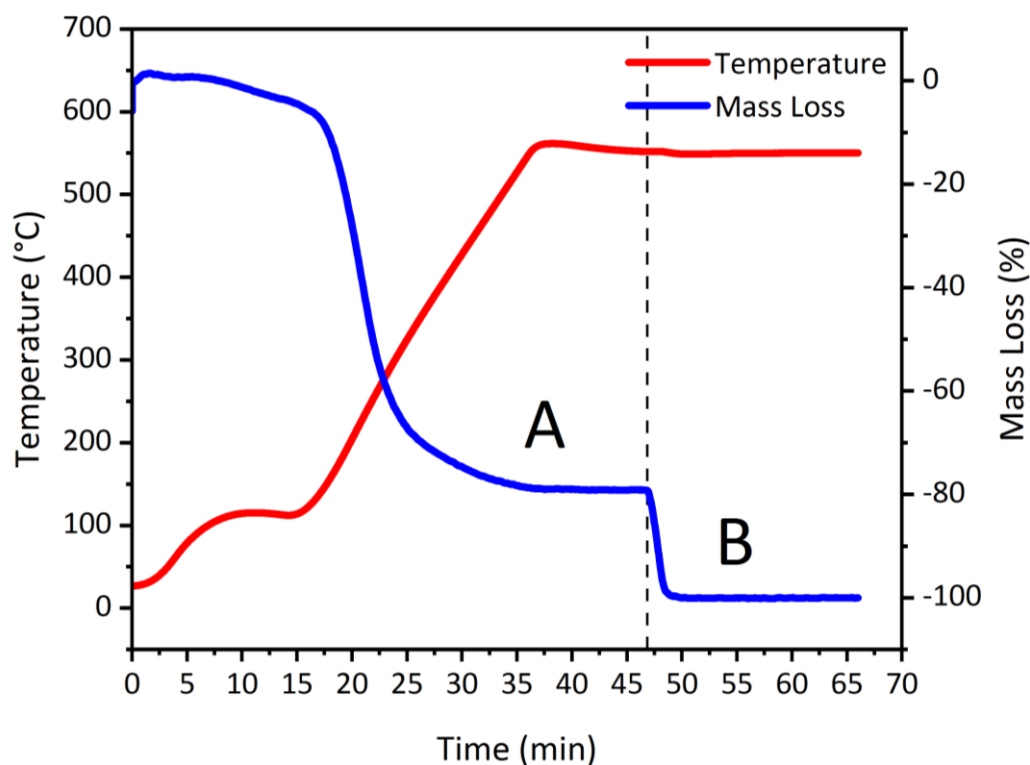
Figure 3.13 Temperature profile and mass loss curve for the OC fraction (A) under N_2 and EC fraction (B) under air of soot collected on a filter.

EC and OC fractions were identified in earlier work (**Chapter 5**) by thermo-optical analysis (TOA) in accordance with the NIOSH 5040 using a Sunset Laboratory Carbon Aerosol Analyser [Sunset Laboratory]. EC and OC fractions are generally identified via TOA by observing the evolution of PM fractions at predetermined plateau temperatures (Phuah et al., 2009). A 10mm x 10mm section of filter paper was sampled and thermally desorbed under an initially inert He atmosphere and secondary oxidizing (2% O_2, 98% He) atmosphere. A total of four heating steps are applied for the quantification of OC with heating plateaus defined at 250ºC, 500ºC, 650ºC and 850ºC (Grover et al., 2012). Following vaporization, organic compounds are oxidized forming CO_2 before being reduced to CH_4 in a methanator oven. The CH_4 concentration, and thus the concentration of desorbed organic material is quantified using a flame ionization detector (FID) (Sunset-Laboratory, 2020b). Low temperature pyrolysis of the OC fraction is also observed during the early phases of heating leading to the formation of elemental carbon; the extent of conversion is monitored via transmittance and reflectance of the sampled filter surface using a laser (Wu et al., 2012; Grover et al., 2012). Subsequently, The He atmosphere is replaced with an oxidizing atmosphere and the temperature is increased from 525ºC to 850ºC so as to convert sample EC and EC derived from the pyrolysis of organic compounds previously to CO_2. A series of heating plateaus are defined at 650ºC, 750ºC and 850ºC (Grover et al., 2012). The CO_2 is then converted to CH_4

and identified by FID as previously discussed. The instrumentation range of analysis was 0.05-45 µg/cm^2 and 0.05-400 µg/cm^2 for EC and OC respectively (Sunset-Laboratory, 2020a).

3.3.1.2 Microscope Raman

The physiochemical structure of soot collected on micro quartz filter papers was analysed using a Renishaw inVia Raman Spectrometer. Soot samples collected during dry and wet fuelwood combustion were excited using a 514.5 nm green argon laser. The Raman shift spectrum was evaluated in the range from 500 to 2500 cm^{-1}. **Equation 3.14** presents the method of converting from spectral wavelength and excitation wavelength to wavenumber of the observed shift.

$$(3.14) \quad Raman\ shift\ (cm^{-1}) = \frac{10^7}{\lambda_{ex}[nm]} - \frac{10^7}{\lambda[nm]}$$

Λ is the Raman spectrum wavelength, in nanometres

Λ_{ex} is the excitation wavelength, in nanometres

Analysis was undertaken for a period of 90 seconds at a maximum power of 90 mW so as to minimise damage or change to the sample material. Prior to the analysis of Raman spectral features a background subtraction was applied using a 2nd order polynomial function as identified in Ferralis et al. (2016). Raman microscopy (RM) is applied as a method of determining variability in the structure of soot particles collected during dry and wet fuelwood combustion. The first order spectra of soot particles are widely reported in the literature and generally consists of two overlapping peaks located at approximately 1350cm^{-1} and 1585cm^{-1} attributed as the G-band and D-band respectively (Dippel et al., 1999; Sadezky et al., 2005; Ess et al., 2016). The G-band (1585cm^{-1}), often designated the 'Graphitic band', is characteristic of ideal graphitic lattice type structures maintaining an E$_{2g}$ symmetry. The D-band (1350cm^{-1}), or 'Defect band', applies to the disordered fraction of graphitic materials (Ferrari and Robertson, 2000; Sadezky et al., 2005; Ivleva et al., 2007). The quantification of nanostructural order may be inferred from the peak intensity height-ratio as described in Ferrari and Robertson (2000) and Ess et al. (2016). The height-ratio, calculated as I$_D$/I$_G$, indicates the degree of order of the soot material where a value <1 is indicative poor ordering and a value >1 suggests an improved order. This method may also be applied as a non-destructive method of estimating EC and OC material fractions.

3.3.1.3 Electron Microscopy

Fuel particle morphology and physical structure was analysed using a FEI Nova NanoSEM 450 device operating at 3 kV. Soot samples collected on micro-quartz filter papers were placed on copper tape and mounted under vacuum within the SEM device. A copper mounting membrane was selected given the generally carbonaceous nature of the soot sample material. In addition, Energy Dispersive X-Ray spectroscopy (EDX) analysis was applied as a method of determining the elemental composition of the soot samples using an EDAX AMTEK analyser operating at 18 kV.

3.3.1.4 Pyrolysis Gas-Chromatography (Py-GC-MS)

The composition of organic soot fractions were analysed using Py-GC-MS as identified in Atiku et al. (2016) and Maxwell et al. (2020). Analysis was undertaken using a CDS Pyroprobe [Model 5000] connected to a Shimadzu GC-MS [Model QP2010E] operated under trap-mode conditions and a 10:1 sample split. Helium was applied as a carrier gas during analysis. A 60m rtx1701 fused silica capillary column (0.25mm internal diameter) was applied during sample analysis. The column was heated to a hold temperature of 40°C for 2 min before being ramped at a rate of 4°C/min to 250°C before a final hold period of 30 min. Resulting chromatographs where identified using the NIST Mass Spectral Library Database.

3.3.1.5 Spectrodensitometer

An evaluation of the colour and optical density of the soot deposited on the filter papers was analysed using an X-Rite [504] spectrodensitometer. The optical density is reported here as a darkness factor, D, where white is represented as D=0 and black is D=100. The colour of soot samples was estimated using GIMP GNU [2.8.14] image manipulation and analysis software expressed using red, green or blue (RGB) additive colour model (Nishad and Chezian, 2013). **Table 3.1** presents the effect of variation in the red, green and blue shift on colour. Soot sample material derived from biomass combustion is generally known to be black, brown or tan-like in colour. Red (R), green (G) and blue (B) are measured across the range of 0-250 with other colour variants dependent upon the ratio of each. This allows variation in the soot sample colour to be characterised qualitatively (Jones et al., 2018).

Table 3.1 RGB colouration shift

Component	Range	Red	Green	Blue	Yellow	Brown	White	Black
R	0,255	255	0	0	255	150	255	0
G	0,255	0	255	0	255	75	255	0
B	0,255	0	0	255	0	0	255	0
Example								

3.3.1.6 Ultraviolet Visible Spectroscopy

The light absorption potential of soot particles entrained on filter papers was measured via ultraviolet visible (UV-Vis) spectroscopy. Analysis was undertaken using a UV-Vis-NIR spectrophotometer [Perkin Elmer, Lambda 950] over the range 250-850 nm.

3.3.2 Condensate Analysis

Entrained gaseous combustion products were extracted from the flue at a rate of 10.00 L/min via a gas sampling unit [Gasmet, Portable Sampling System] and condensed in deionised water (150 ml) via a chilled impinger system. Condensate collection was undertaken continuously throughout the combustion experiment incorporating both pre-test phase products and gaseous compounds generated during the combustion of each subsequent test batch. The acidity of process substrate was determined via a digital pH probe [HQ40d HACH pH Meter]. The total phenolic concentration, incorporating both ortho- and meta-substituted phenolic components, was determined following mixing with 4-aminoantipyrine [HACH, LCK346 5-200 mg/L] resulting in a colour-shift within the solution and quantified via spectrophotometry [Dr. Lange, Lasa100 photometer]. The total organic carbon (TOC) fraction within the process water was determined differentially via a nondispersive infrared sensor (NDIR) [Analytik-jena]. Volatile Fatty Acid (VFA) compounds where determined via gas chromatography with flame ionisation detector or GC-FID (Agilent, 7890A). Prior to analysis the acidity of the condensate was stabilised to pH 2.0±0.1 using phosphoric acid. VFA constituents were analysed via the GC using a DB-FFAP column under He. The column length, thickness and diameter where 30 m, 0.5 um and 0.32 mm respectively. The GC was operated in split-mode with a split-ratio of 5:1. The oven temperature was held at 600°C for 4 minutes before increasing at a rate of 10°C/min to 1,400°C before increasing again to 2,000°C at a ramp-rate of 40°C/min. The temperature was then maintained at 2,000°C for 5 minutes. The FID was operated at 2,000°C using N_2 as a make-up gas.

3.4 Fuel Characterisation

3.4.1 Sample Preparation

Prior to analysis, fuel samples were milled and sieved to a maximum nominal diameter of 100 μm using a combination of cutting-mill [Retsch SM100] and cryo-mill [Retsch CryoMill] devices. Given the difficulty in sampling and characterising biomass due to the heterogeneity of the material (Mitchell et al., 2016), a cone and quartering technique was applied to ensure representative sampling. Following milling, additional sampling was undertaken to ensure homogeneity with each batch of material tested in duplicate. Sample preparation and selection was undertaken following BS EN 14780.

3.4.2 Proximate Analysis

The composition of fuel and firelighter materials was determined via proximate analysis. Constituents defined by proximate analysis include moisture content (MC%), volatile matter (VM%), fixed carbon (FC%) and ash (Ash%). MC%, VM% and Ash% are measured while FC% is calculated by difference.

3.4.2.1 Moisture Content Determination

Moisture content (MC%) was determined following a method similar to that defined in BS EN ISO 18134: 2015. MC% was calculated on a wet basis as identified in **Equation 3.15**. Complete logs were placed within a drying oven [Memmert] and heated in the presence of air to a maximum temperature of 105±2˚C. The drying process generally included a high temperature drying phase during the day (105±2˚C) before a low temperature drying phase during the night (60±2˚C). This was undertaken to mitigate the risk of material combustion during heating. Sample drying was undertaken until a constant mass was determined or the mass loss was <1% across a 24h heating duration. **Figure 3.14** identifies the loss of moisture during the heating of fuelwood biomass at low temperature (L) and high temperature (H) conditions.

$$(\textbf{3.15}) \quad MC\% = \left(\frac{m_1}{100 - m_2} \right) \times 100$$

m_1 is the mass of the empty tray, in mg

m_2 is the mass of the empty tray and the fuel sample before drying, in mg

The method presented above has a number of discrepancies from that outlined in BS EN 18134: 2015 namely the mass of sample applied. In accordance with the standard procedure a sample mass of up to 300 g should be heated in a pile maintaining particles incorporating a nominal top-size of 30 mm. The water distribution in fuelwood logs is highly variable and generally presents higher concentrations in the centre of the fuel particles. As such, complete log samples were exposed to heating for a prolonged observation period to ascertain the complete moisture content of the particle as a whole.
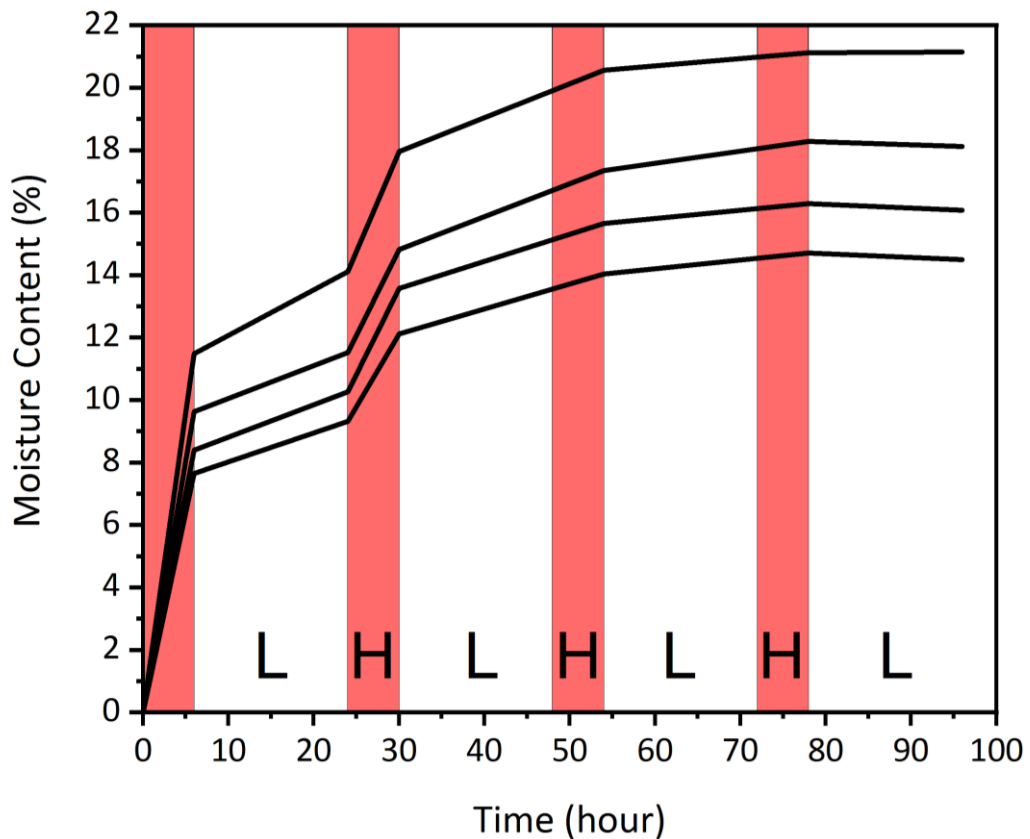
Figure 3.14 Moisture loss profile of four fuelwood particles (beech) collected from the same pile and heating profile during prolonged drying operation at low (L, 60°C) and high (H, 105°C) temperatures.

3.4.2.2 Volatile Matter Determination

Volatile matter (VM%) determination was undertaken in accordance with BS EN 15148:2009. The method includes heating sample material which has been milled to a nominal top-size of 1 mm and sampled in accordance with BS EN 14780: 2011 for a period of 7 min to a maximum temperature of 900±10 ˚C. The sample mass is 1.0±0.1 g which is heated in absence of oxygen using closed-lid crucibles. **Equation 3.16** presents the method for calculating VM% as a function of mass loss

during heating and adjustment for initial moisture loss via the MC% value
determined in line with BS EN ISO 18134: 2015.

$$(3.16) \quad VM\% = \left[\frac{100 \times m_2 - m_3}{m_2 - m_1} - MC\%\right] \times \frac{100}{100 - MC\%}$$

m_1 is the mass of the empty crucible and lid, in mg

m_2 is the mass of the empty crucible, lid and the fuel sample before heating, in mg

m^3 is the mass of the empty crucible, lid and the fuel sample after heating, in mg

MC%   is the sample moisture content

3.4.2.3 Ash Determination

Ash (Ash%) determination was undertaken in accordance with BS EN 14775: 2009.
The method includes heating sample material which has been milled to a nominal
top-size of 1 mm and sampled in accordance with BS EN 14780: 2011. The sample
is heated in the presence of air to 250⁰C at a rate of approximately 4.5-7.5 ºC/min.
A subsequent hold period of 1 h is then observed allowing for the removal of VM
from the sample material. The temperature is then increased to 550⁰C at a rate of
10 ºC/min followed by a hold period of 2 h. **Equation 3.17** presents the method for
calculating Ash% as a function of mass loss during heating and adjustment for
initial moisture loss via the MC% value determined in line with BS EN ISO 18134:
2015.

$$(3.17) \quad Ash\% = \left[\frac{m_3 - m_1}{m_2 - m_1}\right] \times 100 \times \frac{100}{100 - MC\%}$$

m_1 is the mass of the empty crucible, in mg

m_2 is the mass of the empty crucible and the fuel sample before heating, in mg

m^3 is the mass of the empty crucible and the fuel sample after heating, in mg

MC%   is the sample moisture content

3.4.2.4 Fixed Carbon Determination

Fixed carbon (FC%) determination was undertaken by difference and was
calculated as a function of the VM% and Ash% on a dry basis. The method is
shown in **Equation 3.18**.

$$(3.18) \quad FC\% = 1 - (VM\% + Ash\%)$$

FC%   is the sample fixed carbon content, in percent

VM%   is the sample volatile matter content, in percent

Ash%   is the sample ash content, in percent

3.4.2.5 Thermogravimetric Analysis

In addition, thermogravimetric analysis (TGA) was undertaken on each of the fuels with heating rates and temperatures set to those outlined in BS EN 14774-3 for moisture (MC%), BS EN 15148 for volatile matter (VM%) and BS EN 14775 for ash (Ash%). MC% is determined by heating the sample under N_2 (50 ml/min) from 30°C to 105°C at a rate of 20°C/min prior to a hold period of 10 minutes. VM% is then determined by heating the sample under N_2 from 105°C to 550°C at a rate of 20°C/min prior to a hold period of 10 minutes. Ash% is determined by sample oxidation in the presence of air (50 ml/min) at 550°C for a period of 30 minutes. FC% is determined by difference as identified in **Equation 3.18**. The temperature profile for the proximate analysis of biomass is shown in **Figure 3.15**.
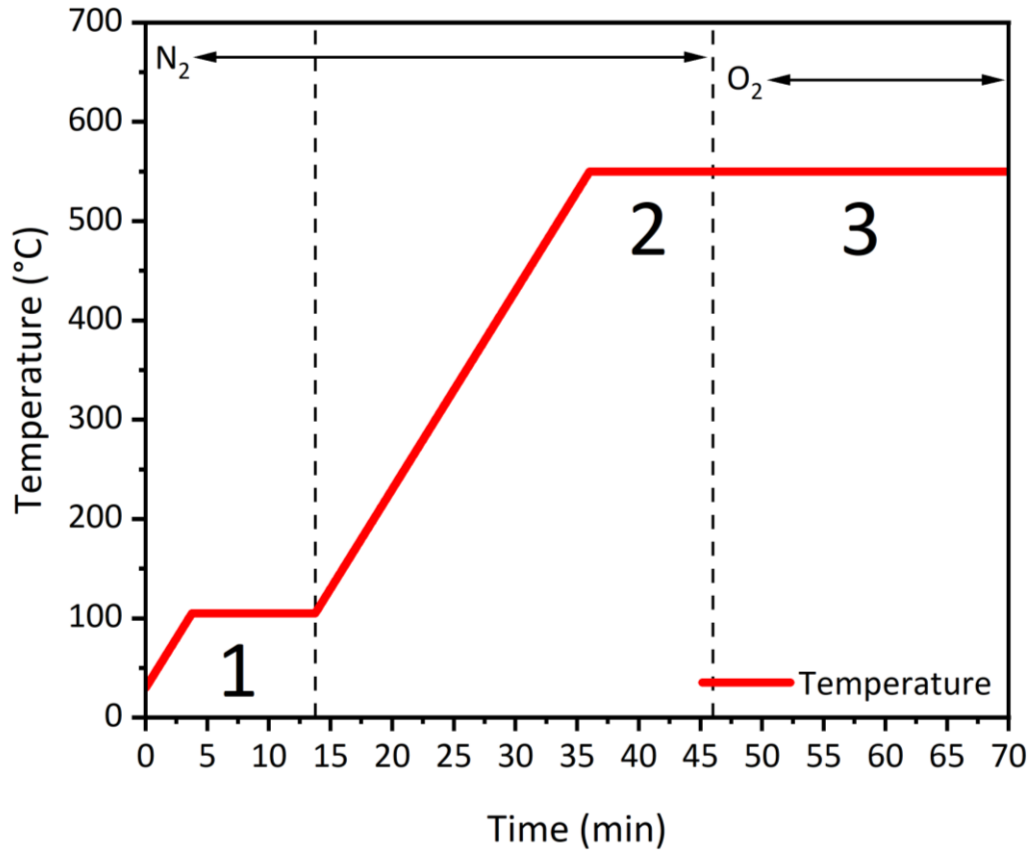
Figure 3.15 Temperature profile of Proximate Analysis by TGA. Vertical lines identify the periods of analysis for each fuel constituent where [1] is MC%, [2] is VM% and [3] is Ash%. [1] and [2] are determined under N_2 while [3] is measured under O_2.

3.4.3 Ultimate Analysis

Ultimate Analysis (CHNS) was undertaken via a Thermo Scientific EA2000 or CE Instruments Flash EA1112 elemental analyser and in accordance with BS EN ISO 16948: 2015. Approximately 2-3 mg of sample material maintaining a nominal top-size diameter of <100μm was applied for testing. The sample is heated at 900ºC under He as a carrier-gas before pure oxygen is applied to ensure complete combustion. The sample is subsequently oxidized forming ash and a series of combustion products with C, H, N and S forming CO_2, H_2O, NO_2 and SO_2 respectively. The evolved gas species are separated within a gas chromatography column before the concentration of each is analysed using thermal conductivity. A standard reference material was analysed during sample testing and included 2,5-Bis(5-tert-butyl-2-benzo-oxazol-2-yl) thiophene (BBOT). In addition, reference material was analysed simultaneously and included Oatmeal and Olive stone. Finally, Total Nitrogen (TN) was determined for some biomass fuels in response to the inherently low nitrogen content of the materials [Analytik Jena Multi 500] via

chemiluminescence detection. The CHN value for the standard and reference materials is presented in **Table 3.2**.

Table 3.2 CHN microanalytical composition of standard and reference sample materials applied during Ultimate Analysis.

Standard	C	H	N	S	O
BBOT	72.56	6.11	6.49	7.40	7.41
Oatmeal (B2170)	47.06	6.35	0.204	-	-
Olive Stone (B2276)	47.00	6.67	2.03	0.16	-

The microanalytical fuel composition (Proximate and Ultimate Analysis) was presented on a dry basis as shown in **Equation 3.19**.

$$(3.19) \quad C, N, S_{db} = n_{wb} \times (\frac{100}{100 - MC\%}$$

C,N,S_{db} is the carbon, nitrogen or sulphur content on a dry basis, in percent

N_{wb} is the carbon, nitrogen or Sulphur concentration on a wet basis, in percent

$MC\%$ is the sample moisture content

The hydrogen content is calculated using a correction factor taking into account the hydrogen content associated with the sample water fraction. The method for correcting the hydrogen content is shown in **Equation 3.20** where 8,937 is half the molar mass of H_2O (H = 1.008 u and O = 15.999 u) as presented in BS EN ISO 16948: 2015. The oxygen concentration may be subsequently calculated by difference as a function of the CHNS and ash content as shown in **Equation 3.21**.

$$(3.20) \quad H_{db} = \left(H_{wb} - \frac{MC\%}{8.937}\right) \times \frac{100}{100 - MC\%}$$

H_{db} is the hydrogen content on a dry basis, in percent

H_{wb} is the hydrogen concentration on a wet basis, in percent

$MC\%$ Is the sample moisture content

$$(3.21) \quad O_{db} = 100 - (C_{db} + H_{db} + N_{db} + S_{db} + Ash_{db})$$

O_{db} is the oxygen content on a dry basis, in percent

C_{wb} is the carbon content on a dry basis, in percent

H_{wb} is the hydrogen content on a dry basis, in percent

N_{wb} is the nitrogen content on a dry basis, in percent

S_{wb} is the sulphur content on a dry basis, in percent

Ash_{db} is the ash content on a dry basis, in percent

3.4.4 Calorific Value

An approximation of the higher heating value (HHV) or gross calorific value (GCV) was made empirically using the formula outlined in Friedl et al. (2005). The method for calculating the HHV in MJ/kgdb from the elemental composition of the fuel is shown in **Equation 3.22**.

$$(3.22) \quad HHV = \frac{(3.55 \times C^2) - (232 \times C) - (2230 \times H) + (51.2 \times C \times H) + (131 \times N) + 20,600}{1,000}$$

HHV   Is the higher heating value, in MJ/kg

C   is the wt% carbon content on a dry basis, in percent

H   is the wt% hydrogen content on a dry basis, in percent

N   is the wt% nitrogen content on a dry basis, in percent

The lower heating value (LHV) or net calorific value (NCV) was calculated as a function of the HHV, the fuel hydrogen content and the fuel moisture content. As outlined in Koppejan and Loo (2008), the method for calculating the LHV in MJ/kgdb from the elemental composition of the fuel is shown in **Equation 3.23**.

$$(3.23) \quad LHV = HHV \times \left(1 - \left(\frac{X}{100}\right)\right) - 2.444 \times \frac{MC\%}{100} - 2.444 \times \frac{H}{100} \times 8.936 \times \left(1 - \left(\frac{MC\%}{100}\right)\right)$$

LHV   is the lower heating value, in MJ/kg$_{db}$

HHV   is the lower heating value, in MJ/kg

H   is the hydrogen content on a dry basis, in percent

MC%   is the fuel moisture content, in percent

3.5 References

Akagi, S.K., Yokelson, R.J., Wiedinmyer, C., Alvarado, M.J., Reid, J.S., Karl, T., Crounse, J.D. and Wennberg, P.O. 2011. Emission factors for open and domestic biomass burning for use in atmospheric models. Atmospheric Chemistry and Physics. 11(9), pp.4039–4072.

Ali, M. 2010. Pulmonary Drug Delivery In: V. S. Kulkarno, ed. Handbook of Non-Invasive Drug Delivery Systems. William Andrew Publishing, pp.209–246.

Alves, C., Gonçalves, C., Fernandes, A.P., Tarelho, L. and Pio, C. 2011. Fireplace and woodstove fine particle emissions from combustion of western Mediterranean wood types. Atmospheric Research. 101(3), pp.692–700.

Atiku, F.A., Mitchell, E.J.S., Lea-Langton, A.R., Jones, J.M., Williams, A. and Bartle, K.D. 2016. The Impact of Fuel Properties on the Composition of Soot Produced by the Combustion of Residential Solid Fuels in a Domestic Stove. Fuel Processing Technology. 151, pp.117–125.

Berna, F. 2017. Fourier Transform Infrared Spectroscopy (FTIR) In: A. S. Gilbert, ed. Encyclopedia of Geoarcheology. Dordrecht: Springer.

Brouwer, D.H., Lidén, G., Asbach, C., Berges, M.G.M. and van Tongeren, M. 2014. Monitoring and Sampling Strategy for (Manufactured) Nano Objects, Agglomerates and Aggregates (NOAA): Potential Added Value of the NANODEVICE Project In: U. Vogel, K. Savolainen, Q. Wu, M. van Tongeren, D. Brouwer and M. Berges, eds. Handbook of Nanosafety: Measurement, Exposure and Toxicology. Academic Press, pp.173–206.

Charlton, A.J. 2011. Characterisation of urban particulates and their potential health effects. University of Leeds.

Dippel, B., Jander, H. and Heintzenberg, J. 1999. NIR FT Raman spectroscopic study of Ñame soot. phys. 1, pp.4707–4712.

EPA 2018. Emissions monitoring guidance note (AG2) [Online]. [Accessed 15 July 2020]. Available from: https://www.epa.ie/pubs/advice/air/emissions/Emission_Monitoring_Guidance_AG2_May2018.pdf.

Ess, M.N., Ferry, D., Kireeva, E.D., Niessner, R., Ouf, F. and Ivleva, N.P. 2016. In situ Raman microspectroscopic analysis of soot samples with different organic carbon content : Structural changes during heating. Carbon. 105, pp.572–585.

Fachinger, F., Drewnick, F., Gieré, R. and Borrmann, S. 2017. How the user can influence particulate emissions from residential wood and pellet stoves: Emission factors for different fuels and burning conditions. Atmospheric Environment. 158, pp.216–226.

Ferek, R.J., Reid, J.S., Hobbs, P. V., Blake, D.R. and Liousse, C. 1998. Emission factors of hydrocarbons, halocarbons, trace gases and particles from biomass burning in Brazil. Journal of Geophysical Research: Atmospheres. 103(D24), pp.32107–32118.

Ferralis, N., Matys, E.D., Knoll, A.H., Hallmann, C. and Summons, R.E. 2016. Rapid , direct and non-destructive assessment of fossil organic matter via microRaman spectroscopy. Carbon. 108, pp.440–449.

Ferrari, A.C. and Robertson, J. 2000. Interpretation of Raman spectra of disordered and amorphous carbon. The American Physical Society: Physical Review B. 61(20), pp.95–107.

Finlayson-Pitts, B. and Pitts, J.N. 2000. Analytical Methods and Typical Atmospheric Concentrations for Gases and Particles In: J. N. P. Barbara J. Finlayson-Pitts, ed. Chemistry of the Upper and Lower Atmosphere. Academic Press, pp.547–656.

Friedl, A., Padouvas, E., Rotter, H. and Varmuza, K. 2005. Prediction of heating values of biomass fuel from elemental composition In: Analytica Chimica Acta. Elsevier, pp.191–198.

Grover, B.D., Kleinman, M., Eatough, N.L., Eatough, D.J., Cary, R.A., Hopke, P.K. and Wilson, W.E. 2012. Journal of the Air & Waste Management Association Measurement of Fine Particulate Matter Nonvolatile and Semi-Volatile Organic Material with the Sunset Laboratory Carbon Aerosol Monitor Measurement of Fine Particulate Matter Nonvolatile and Semi-Volatile Organic Material with the Sunset Laboratory Carbon Aerosol Monitor. Journal of the Air & Waste Management Association. 58(1), pp.72–77.

Ivleva, N.P., Mckeon, U., Niessner, R. and Pöschl, U. 2007. Raman Microspectroscopic Analysis of Size- Resolved Atmospheric Aerosol Particle Samples Collected with an ELPI : Soot , Humic-Like Substances , and Inorganic Compounds Raman Microspectroscopic Analysis of Size-Resolved Atmospheric Aerosol Particle Sample. Aerosol Science and Technology. 41(7), pp.655–671.

Jones, J.M., Ross, A.B., Mitchell, E.J.S., Lea-Langton, A.R., Williams, A. and Bartle, K.D. 2017. Organic carbon emissions from the co-firing of coal and wood in a fixed bed combustor. Fuel. 195, pp.226–231.

Jones, J., Mitchell, E., Williams, A., Jose, G., Hondow, N., Lea-langton, A., Jones, J., Mitchell, E., Williams, A., Jose, G., Hondow, N. and Combustion-generated, A.L.E. 2018. Examination of Combustion-Generated Smoke Particles from Biomass at Source : Relation to Atmospheric Light Absorption Examination of Combustion-Generated Smoke Particles from Biomass at Source : Relation to Atmospheric Light Absorption. Combustion Science and Technology. 00(00), pp.1–14.

Koppejan, J. and Loo, S. van 2008. The Handbook of Biomass Combustion and Co-firing. London: Routledge.

Maheshwari, R., Todke, P., Kuche, K., Raval, N. and Tekade, R.K. 2018. Micromeritics in Pharmaceutical Product Development In: R. K. Tekade, ed. Dosage Form Design Considerations: Volume I. Academic Press, pp.599–635.

Maxwell, D., Gudka, B.A., Jones, J.M. and Williams, A. 2020. Emissions from the combustion of torrefied and raw biomass fuels in a domestic heating stove. Fuel Processing Technology. 199.

MCERTS. 2016. Product Conformity Certificate for the DX4000 FTIR.

Mitchell, E.J.S. 2017. Emission from residential solid fuel combustion and implications for air quality and climate change. University of Leeds.

Mitchell, E.J.S., Coulson, G., Butt, E.W., Forster, P.M., Jones, J.M. and Williams, A. 2017. Heating with Biomass in the United Kingdom: Lessons from New Zealand. Atmospheric Environment. 152, pp.431–454.

Mitchell, E.J.S., Lea-Langton, A.R., Jones, J.M., Williams, A., Layden, P. and Johnson, R. 2016. The impact of fuel properties on the emissions from the combustion of biomass and other solid fuels in a fixed bed domestic stove. Fuel Processing Technology. 142, pp.115–123.

Mitchell, E.J.S., Ting, Y., Allan, J., Lea-Langton, A.R., Spracklen, D. V, Mcfiggans, G., Coe, H., Routledge, M.N., Williams, A. and Jones, J.M. 2019. Combustion Science and Technology Pollutant Emissions from Improved Cookstoves of the Type Used in Sub-Saharan Africa. Combustion Science and Technology. 17, pp.1–21.

Mitchell, E.J.S., Ting, Y., Allan, J., Spracklen, D. V, Mcfiggans, G., Coe, H., Routledge, M.N., Williams, A., Jones, J.M., Ting, Y., Allan, J. and Spracklen, D. V 2019. Pollutant Emissions from Improved Cookstoves of the Type Used in Sub-Saharan Africa Pollutant Emissions from Improved Cookstoves of the Type Used in Sub-Saharan Africa. Combustion Science and Technology., pp.1–21.

Nussbaumer, T., Czasch, C., Klippel, N., Johansson, L. and Tullin, C. 2008. Particulate emissions from biomass combustion in IEA countries - Survey on measurments and emission factors.

Olave, R.J., Forbes, E.G.A., Johnston, C.R. and Relf, J. 2017. Particulate and gaseous emissions from different wood fuels during combustion in a small-scale biomass heating system. Atmospheric Environment. 157, pp.49–58.

Phillips, D., Mitchell, E.J.S., Lea-Langton, A.R., Parmar, K.R., Jones, J.M. and Williams, A. 2016. The use of conservation biomass feedstocks as potential bioenergy resources in the United Kingdom. Bioresource Technology. 212, pp.271–279.

Orasche, J., Seidel, T., Hartmann, H., Schnelle-Kreis, J., Chow, J.C. and Ruppert, H. 2012. Comparison of emissions from wood combustion. Part 1: Emission factors and characteristics from different small-scale residential heating appliances considering particulate matter and polycyclic aromatic hydrocarbon (PAH)-related toxicological potential o. Energy Fuels. 26, pp.6695–6704.

Phuah, C.H., Peterson, M.R., Richards, M.H., Turner, J.R. and Dillner, A.M. 2009. A Temperature Calibration Procedure for the Sunset Laboratory Carbon Aerosol Analysis Lab Instrument. Aerosol Science and Technology. 43(10), pp.1013–1021.

Popovicheva, O.B., Engling, G., Diapouli, E., Saraga, D., Persiantseva, N.M., Timofeev, M.A., Kireeva, E.D., Shonija, N.K., Chen, S.-H., Nguyen, D.L., Eleftheriadis, K. and Lee, C.-T. 2016. Impact of Smoke Intensity on Size-Resolved Aerosol Composition and Microstructure during the Biomass Burning Season in Northwest Vietnam. Aerosol and Air Quality Research. 16, pp.2635–2654.

Price-Allison, A., Lea-Langton, A.R., Mitchell, Edward J. S.Gudka, B., Jones, J.M., Mason, P.E. and Williams, A. 2019. Emissions Performance of High Moisture Wood Fuels Burned in a Residential Stove. Fuel. 239, pp.1038–1045.

Reid, J.S., Koppmann, R., Eck, T.F. and Eleuterio, D.P. 2005. A review of biomass burning emissions part II: intensive physical properties of biomass burning particles. Atmos. Chem. Phys. 5, pp.799–825.

Robinson, R.A., Whiteside, K., Elliott, R., Clack, M. and Curtis, D. 2007. Study into the loss of material from filters used for collecting particulate matter during stack emissions monitoring.

Sadezky, A., Mucjenhuber, H., Grothe, H., Niessner, R. and Poschl, U. 2005. Raman microspectroscopy of soot and related carbonaceous materials: Spectral analysis and structural information. Carbon. 43, pp.1731–1742.

Sippula, O., Hytönen, K., Tissari, J., Raunemaa, T. and Jokiniemi, J. 2007. Effect of Wood Fuel on the Emissions from a Top-Feed Pellet Stove.

Schon, C. and Hartmann, H. 2018. Status of PM emission measurement methods and new developments.

Seljeskog, M., Goile, F. and Sevault, A. 2013. Particle emission factors for wood stove firing in Norway.

Stewart, R. 2012. Conversion of biomass boiler emission concentration data for comparison with Renewable Heat Incentive emission criteria [Online]. [Accessed 16 July 2020]. Available from: https://uk-air.defra.gov.uk/assets/documents/reports/cat07/1205310837_Conversion_of_biomass_boiler_emission_data_rep_Issue1.pdf.

Stockwell, C.E., Veres, P.R., Williams, J. and Yokelson, R.J. 2015. Characterisation of biomass burning emissions from cooking fires, peat, crop residue, and other fuels

with high-resolution proton-transfer-reaction time-of-flight mass spectrometry. Atmos. Chem. Phys. 15, pp.845–865.

Stranger, M., Potgieter-Vermaak, S.S. and Van Grieken, R. 2009. Particulate matter and gaseous pollutants in residences in Antwerp, Belgium. Science of the Total Environment. 407(3), pp.1182–1192.

Sunset-Laboratory 2020a. Carbon Aerosol Particulate Analysis Instruments - Sunset Lab. Sunset Laboratory, Methodology. [Online]. [Accessed 26 October 2020]. Available from: https://www.sunlab.com/about-us/methodology/.

Sunset-Laboratory 2020b. Sunset Laboratory Instrument Brochure - OCEC Lab Instrument, Model 5 [Online]. Available from: https://sunlab.com/wp-content/uploads/Lab-Instrument-brochure.pdf.

Testo 2020. What are Electrochemical sensors? Common Testing Questions. [Online]. Available from: https://www.testo.com/en-US/Common+Testing+Questions/us_products_350_testing_questions.

Testo 2022. Testo 340 – Flue gas analyser for use in industry [Online]. Available from: https://www.testo.com/en-UK/testo-340/p/0632-3340#tab-technicalData

Wu, C., Man Ng, W., Huang, J., Wu, D. and Zhen Yu, J. 2012. Determination of Elemental and Organic Carbon in PM 2.5 in the Pearl River Delta Region: Inter-Instrument (Sunset vs. DRI Model 2001 Thermal/Optical Carbon Analyzer) and Inter-Protocol Comparisons (IMPROVE vs. Institute of Tropical and Marine Meteorology. 46(6), pp.610–621.

Yokelson, R.J., Griffith, D.W.T. and Ward, D.E. 1996. Open-path Fourier transform infrared studies of large-scale laboratory biomass fires. Journal of Geophysical Research: Atmospheres. 101(D15), pp.67–80.

Chapter 4
Moisture Content Determination via a Digital 2-Pin Electrical Resistance Meter

4.1 Introduction

4.1.1 Use of Resistance Meter for the Determination of Fuelwood Moisture Content

Digital 2-pin resistance meter devices are commonly applied as a method of determining the moisture content of fuelwood. This method is a low-cost and simple process for estimating the moisture content of fuel prior to the testing of residential combustion appliances (Hedberg et al., 2002; Weatherburn et al., 2011; Price-Allison et al., 2018). Fuelwood moisture content has been shown previously to effect both stove performance and emissions (Butcher and Sorenson, 1979; Bhattacharya et al., 2002; Price-Allison et al., 2018) while an increase in emissions is correlated with detrimental climate and human health effects (DEFRA, 2018; Mitchell et al., 2019). A series of legislative controls restricting the combustion of high moisture fuels have recently been established via the Clean Air Strategy 2019. In addition, fuelwood certification schemes, including Ready to Burn, have been implemented to control the sale of high moisture fuelwood for domestic application. Notwithstanding, a significant proportion of fuelwood combusted at the domestic level is sourced from the grey-wood market (BEIS, 2016b). Such fuels may encompass as much as 31% of the total quantity burned within the UK and are not subject to quality control and restrictions (BEIS, 2016a). These grey-wood materials are often seasoned by the end-user with the moisture content determined via the aid of low-cost resistance-type moisture meter devices. These devices provide a simple and non-destructive method for determining fuelwood moisture content but commonly exhibit several limitations inhibiting accuracy (James, 1963; James, 1988; Skaar, 1988; Tarvainen and Forsén, 2000; Price-Allison et al., 2018). The following work attempts to provide an insight into the variation in the measurable moisture content of fuelwood particles when tested in accordance with BS EN 13183-2: 2002 using resistance-type moisture probes and BS EN ISO 18134-2 using oven-drying with gravimetric measurement techniques.

4.1.2 The Determination of Moisture Content

Fuelwood moisture presents a significant control upon combustion efficiency and pollutant formation (Koppejan & van Loo, 2008). As such, moisture content is often determined prior to combustion using oven-drying with gravimetric approach or via

the use of electrical moisture probe devices. Oven-drying in accordance with BS EN ISO 18134-2 is by fuelwood and lumber suppliers, during fuelwood accreditation and in analytical laboratories prior to combustion testing. A summary of the process of moisture content determination in accordance with BS EN ISO 18134-2 (Solid biofuels, determination of moisture content) is shown in **Chapter 3**. A little discussed limitation in the standard method is the assumption that the sampled fuelwood particles maintain a moisture content which is representative of the fired fuel. Fuelwood is generally stored within a stack during seasoning and prior to or following treatment via kiln-drying. Fuelwood moisture content is subject to variation depending upon several factors outlined in **Chapter 2**. Such factors include the tree felling period, the duration and temperature of drying by seasoning and mechanical methods, location of fuelwood particle within a stack and origin within the tree structure (Mytting, 2015; Wetzel et al., 2017). Location of the fuelwood particle within the pile during seasoning and during storage prior to or following kiln-drying is important since variation in sun exposure and shading, exposure to wind and the effect or humidity or precipitation lead to potential changes include rewetting (Eliasson et al., 2020). In this study, fuelwood particles selected for combustion testing were sampled from a stack based on similar physical characteristics, dimensions and mass. As stated, the logs stored within a pile may exhibit a high variance in moisture content. Following selection, a subsequent phase of sampling was undertaken prior to the determination of moisture using BS EN ISO 18134-2. It is assumed that these logs present a moisture content which is representative of the pile but are not subsequently used during combustion testing due the destructive nature of the analysis. Given the high degree of variation likely present within a fuelwood pile it stands to reason that the particles tested for moisture may not be representative of those fired during stove testing. As such, it is very difficult to make solid conclusions as to the true moisture content of a batch of fired fuelwood using standard means. The determination of moisture using resistance-type moisture meter devices may offer a solution as an alternative non-destructive approach for the testing of individual fuelwood particles prior to firing.

4.1.2 Appliance Principle

An estimation of the fuelwood moisture content ($MC\%_{Probe}$) is derived through the measurement of electrical resistance (R) of the material between two nail-like electrode pins (James, 1963). Resistance is observed as a function of Ohm's Law and may be calculated as a derivative of voltage (V) and current (I) as identified in **Equation 4.1** (Ohm, 1827). Electrical resistance is measured in ohms (Ω) and is a material property quantifying the capacity to resist the flow of an electrical current.

Electrical resistivity (ρ) is measured in ohm-meters (Ω·m) and is the intrinsic property and quantified resistance property of a specific sample. Electrical conductance is the reciprocal of resistance while electrical conductivity (σ) is the reciprocal of resistivity where the former is measured in siemens (S), and the latter is measured in siemens per meter (S/m). Electrical resistivity is therefore a measure of the opposition to the flow of electrons through the fuel particle structure.

$$(4.1) \quad I = \frac{V}{R}$$

The fuelwood moisture content is estimated via the known resistance value R and factors a and b calibrated within the instrument function which are derived from the analysis of observed resistance under different moisture conditions. Factors a and b are often species specific and derived from the testing of an appliance using a specific type of sample or biomass species. For example, the calculation of the MC%$_{Probe}$ of pinewood incorporates an *a* value of -0.039 and b value of 1.061 within the instrument internal algorithm (Tarvainen and Forsén, 2000). If such factors are not known and resistance curves are not available, the use of resistance-based moisture analysers is for indication purposes only. The a and b calibration values are instrument specific with some instruments providing an option for specification based upon the type or biomass species or sample material. **Equation 4.2** presents the algorithm for the determination of MC%$_{Probe}$ (Tarvainen and Forsén, 2000).

$$(4.2) \quad MC\% = (\log{(\log{(R)} + 1 - b)/a)})$$

Electrical properties of fuelwood are highly variable and fundamentally dependent upon the moisture content. Water content in fuelwood is known to vary depending upon period of felling (Belart et al., 2019), method of seasoning (Raitila et al., 2015) and processes of treatment including kiln-drying (Wallace and Avramidis, 2016). Variability in water properties may span up to ten orders of magnitude over the moisture content range typically observed for fuelwood (Glass et al., 2010). An estimation of the moisture content of a fuelwood particle may be found though electrical resistance when the sample is placed under voltage within a circuit. The magnitude of the resistance at a known electromotive force, or voltage, suggests the resistance of a material is dependent upon the length of the conductor (L) in mm, the cross-sectional area of the conductor (A) in mm² and the resistivity of the material (ρ) subject to temperature (T).
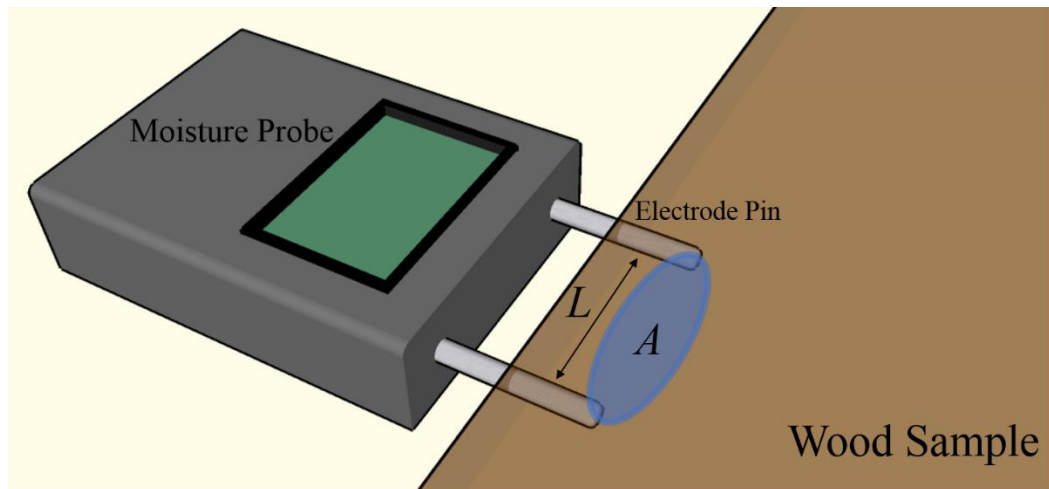
Figure 4.1 Schematic of electrode application within a fuelwood particle subject to electrode separation (L) and the cross-sectional area of the sampled location (A)

Figure 4.1 depicts a pin-type electrode circuit within a biomass sample relative to L and A. The L is subject to the electrode separation length while the cross-sectional area is of an unknown dimension but incorporates an area between the electrode pins. Previous research has identified a limited impact of variance in length on sample resistance (Apneseth & Hay, 1992; Tarvainen & Forsén, 2000). The resistance of a material sample may be expressed as shown in **Equation 4.3** (Skaar, 1988; Glass et al., 2010).

$$(\mathbf{4.3}) \quad R = \rho \times \left(\frac{L}{A}\right)$$

R is the sample resistance, in Ω

L is the distance of electrode separation, in mm

A is the cross-sectional area through which the current travels, in mm^3

ρ is the resistivity, in $\Omega \cdot m$

Water is a good conduit of electron transfer resulting in a reduction in resistance when the moisture content is high and an increase in resistance when the moisture content is low. Moisture content is the primary control of fuelwood resistivity (Darveniza et al., 1967). As such, low moisture fuelwood is a good insulator inhibiting the flow of current with a resistivity of approximately 1017 ohm-meters. R is known to reduce exponentially with an increase in moisture content within the hygroscopic range of a sample. Relatively dry fuelwood presents an approximate resistivity of 1011 ohm-meters at room temperature (Skaar, 1988).

A correlation is observed between resistance and moisture when the fuelwood particle maintains a moisture content within the hygroscopic range that is no greater than the point of fibre saturation (Stamm, 1927; James, 1988). The fibre saturation point (FSP) of wood is generally observed within the range of 26-30% (Simpson, 2001; Verbist et al., 2019) and is identified as the point during the drying process where only bound water within the plant cell walls remain. At this point all free water within the wood sample has been removed (Smith, 1986; Babiak and Kudela, 1995). Between the FSP and the oven dried condition there is an approximately linear relationship between the logarithm of resistance and the logarithm of inherent moisture content (James, 1988). Some divergence is presented in samples maintaining a moisture content of approximately 25% and in samples maintaining a moisture content <7%. **Figure 4.2** presents this linear relationship between resistance and moisture content between the FSP and the point of oven-dried as defined by James (1988). A range of R values are presented and show a reduction in the resistance with an increase in the wood moisture content. Typical resistance values for softwood are shown to be 1,654 MΩ, 3.4 MΩ and 0.63 MΩ for wood moisture contents of 10%, 20% and 25% respectively. A similar trend is also displayed for hardwood species. A linear regression fit (y = (a + b) · x) is applied to all softwood and hardwood species. A strong negative correlation is presented between R and moisture content for both softwood and hardwood species where the R^2 value and Pearson's r value of the former are 0.97 and -0.98. and for the latter are 0.93 and -0.96. Similar correlations (R^2 is > 0.90) between R and moisture content have been described within the literature (Tarvainen and Forsén, 2000). Observations in the electrical properties of wood may therefore be applied as a non-destructive mechanism for determining the moisture content of a fuelwood particle prior to combustion.
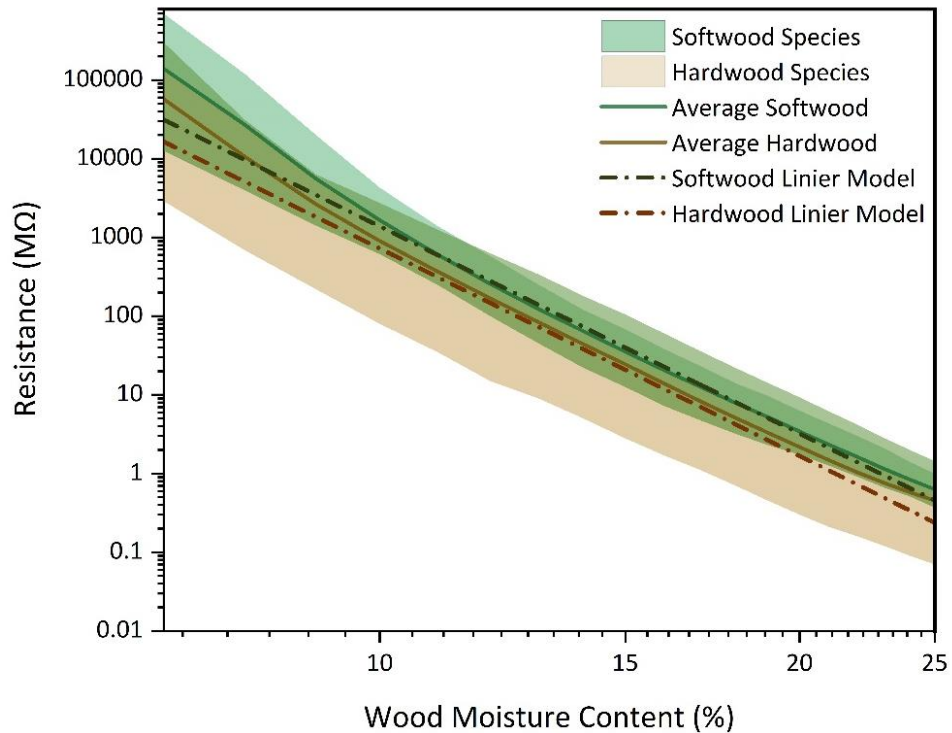
Figure 4.2 The effect of moisture content in hardwood and softwood samples on electrical resistivity. ▨ and ▨ represent the range in resistivity observed during the testing of different hardwood and softwood tree species. Data is presented in a Log10 scale. A linear regression fit is applied to the average data where y = a + b · x. Data is derived from James (1988).

During operation, the pin-type electrodes are driven into an individual side of the fuel particle. The measured resistance is therefore observed across a selected point on a single plain that is parallel to the fuel surface and not across the cross-section of sample (James, 1988). The integrated electrodes of resistance-type moisture meters may be insulated or uninsulated. Uninsulated pins are exposed to the sample material across the complete surface of the electrode. As such, uninsulated pins will record the highest conductance along the exposed length of the electrode surface. Moisture content is known to vary across a gradient where high water content is generally observed in the centre of the particle and a lower moisture content is presented at the log surface. In kiln-dried sample material the moisture content observed at the surface of the particle is likely affected by the ambient condition whereby the wood reaches a moisture equilibrium dependent upon humidity (Baker, 1956). This can affect the estimated moisture content (MC%$_{Probe}$) value presented during the application of uninsulated pins as the water content is likely to vary across the electrode depending upon depth. Insulated pins provide an estimate of the moisture content at the peak of the pin only. Previous work has discussed the effect of electrode type, design and spacing on current resistance through fuelwood samples (Tarvainen and Forsén, 2000). Such methods therefore provide for an estimate of the moisture content of the fuel particle at a

specific depth (Engineering Toolbox, 2008). A schematic of the operational principal for such devices is present in **Figure 4.3**.
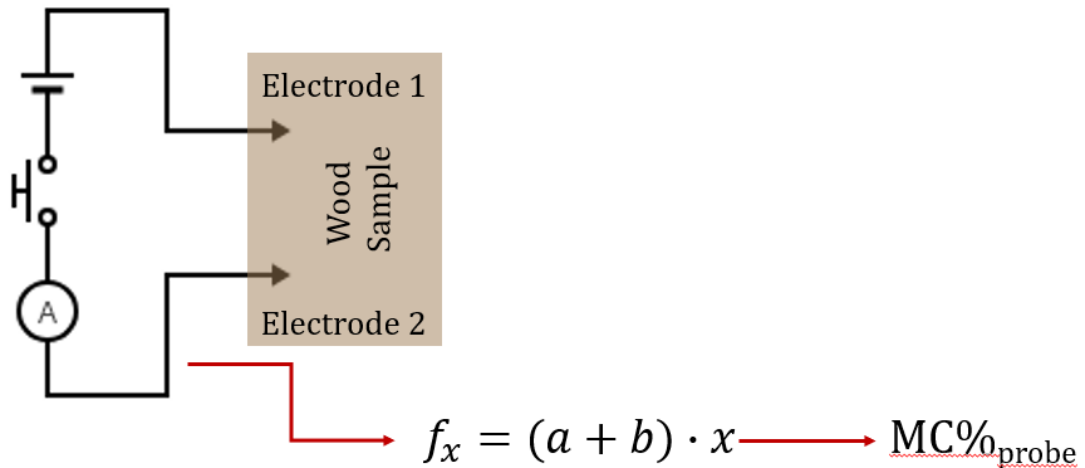
Figure 4.3 Electrical component schematic and algorithm for the determination of MC%$_{Probe}$ from R.

The resistivity of fuelwood is variable and fundamentally dependent upon the temperature (Tarvainen and Forsén, 2000; Engineering Toolbox, 2003). An increase in the temperature of the fuelwood particle leads to an increase in the material conductivity which can erroneously be interpreted as a higher moisture content (James, 1963; Skaar, 1988; James, 1988; Slávik et al., 2019). Such processes are opposite to what is generally observed in metallic materials. This is likely in response to the part ionic mechanism of current transfer in wood samples where an increase in mobility occurs in response to an increase in the sample temperature. Assuming a wood sample maintains a water content of 10%, the conductance of the sample may double with each increase in temperature of 10°C (James, 1988).

The method for determining the change in ρ (in **Equation 4.3**) involves varying the sampling temperature as shown in **Equation 4.4** where $d_ρ$ is change in resistivity (Ω m^2/m), α is an empirical temperature coefficient (1/°C) and T (°C) is the material temperature during sampling. T_0 and $ρ_0$ is the reference temperature for the device (°C) and the material resistivity at the reference temperature (Ω) (Glass et al., 2010). Sampling undertaken at room temperature (20 °C) does not require a temperature correction as this is likely to be the standard temperature for the instrument calibration (Tarvainen and Forsén, 2000).

$$(\mathbf{4.4}) \quad d_p = \rho_0 \times \left(1 + \alpha \times (T - T_0)\right)$$

4.1.2 Limitations in Moisture Content Determination via Electrical Resistance

Resistance-type devices are simple to use and provide an estimate of the fuel particle water content. However, this method of moisture determinisation is subject to variation depending upon several factors. The moisture estimation is based upon an empirical calculation derived from the recorded resistance. Such derivations are based upon fuel particle type, often based upon sample density and dependent upon species, sample thickness, electrode thickness and type, grain direction and the temperature at which the recording was undertaken (James, 1963; Skaar, 1988; Slávik et al., 2019). Electrical conductance is known to vary between different species of fuelwood. As such, a correction should be applied depending upon the type of fuelwood tested. This correction is not always available when testing fuelwood via a handheld digital moisture meter leading to an estimated error of ±2% (James, 1988). Furthermore, users should be aware that superficial water located on the surface of the sample material may lead to an increase in conductance beyond what is expected throughout the cross-section of the fuel particle. Sources of superficial water may include rainwater and is dependent upon methods of storage (James, 1988). Variation in the location of water within a sample may also affect the accuracy of moisture content estimates following this method. Fuelwood moisture content is shown to be significantly higher across the middle-surface of a split log than in the end-grain (Glass et al., 2010). Estimated moisture contents may be higher by a factor of 1.4 depending upon the location of sampling (Price-Allison et al., 2018) due to accelerated drying at the end-grain resulting in an increased loss of bound water via evaporation. Such processes are also important with regards to the thickness of the fuel particle assuming an uneven gradient in water location throughout the particle (James, 1988). It is assumed that fuelwood which has been allowed to dry naturally via seasoning will present a higher water content in the centre of the particle and a lower water content at the particle surface. Given that the range of depth to which electrode pins penetrate the sample surface is relatively small (1-5 mm), it is unlikely that an accurate estimate of the fuelwood moisture content will be determined if the sample maintains a large thickness. Due to the high variability in the distribution of moisture within a fuelwood log it is recommended that sampling is undertaken at multiple locations across the exposed surface (Woodsure, 2018). The primary variable effecting the accuracy of digital resistance type probes is the operator. Variation in the methods applied in the assessment of moisture within a fuel particle can lead to significant changes in the derived moisture value (James, 1988). Therefore, it may be difficult to reconcile

probe values collected at different testing facilities under differing conditions or using different probe appliances.

4.2 Materials and Methods

Moisture testing was undertaken on seasoned European ash (Fraxinus excelsior L.) and seasoned European beech (Fagus sylvatica L.) fuelwood logs [Ashtrees Ltd, Leeds, West Yorkshire]. All bark on the fuelwood logs was removed to mitigate potential sources of mass loss through particle fragmentation and the vaporisation of incorporated surface contaminants (Obernberger et al., 2006; Phillips et al., 2016). A total of three samples of each species were selected for the determination of moisture. Prior to testing the fuel particles were stored in a sheltered outdoor woodstore at the same humidity and temperature conditions so as to allow for equilibrium. The estimated density of European ash and European beech is 700-900 kg/m^3 and 710 kg/m^3 respectively (Toolbox, 2004).

The moisture content of the logs was determined using two methods:

i.   using a resistance-type digital moisture meters based on BS EN 13183-2: 2002, manufacturer guidance and (HETAS, 2018) recommendation.

ii.   oven-drying method to a maximum temperature of 105°C based on BS EN ISO 18134-2: 2015 (Proximate analysis of the whole logs).

4.2.1 Estimation of Fuel Particle Moisture Content via Electrical Resistance

In accordance with BS EN 13183-2: 2002, HETAS (2018) and the manufacturer guidance an estimation of the fuelwood moisture content was undertaken via the application of a series of 2-pin resistance-type handheld digital moisture meters. Because of the possibility of free water on the particle surface and the effect of the water gradient through the cross-sectional area of the logs only insulted-type electrodes were applied. The insulated electrode pins were pressed into the surface of the exposed fuel particle to a maximum depth of 1-5 mm (Price-Allison et al., 2018). Electrode penetration was undertaken at 90º to the grain direction. This contrasted with the suggested method provided in BS EN 13183-2: 2002 however the direction of electrode orientation has been shown to offer limited effect (Tarvainen and Forsén, 2000). A stabilisation period of 5 s was applied before recording the estimated moisture content. In order to account for the likely variation in moisture across the length and cross-section of a fuelwood particle the method was repeated at six locations across two of the exposed particle faces. A numerical average ($\bar{x}$) and standard deviation ($\sigma\bar{x}$) was calculated for each of the particles

analysed. The point of sampling was undertaken at similar distances for each of the particles and was spaced to avoid interference from inconsistent physical characteristics including bark-residue, knots and resin pockets.

4.2.2 Measurement of Fuel Particle Moisture Content via Oven-Drying

Following a method similar to BS EN ISO 18134-2: 2015 the moisture content of the log sample was calculated via mass loss during oven drying in air at a temperature not exceeding 105°C±2°C (so called Proximate analysis). The loss of volatile components is believed to be negligible at this temperature (Price-Allison et al., 2018). Each of the fuelwood particles were placed on a pre-weighed tray in a drying oven [Memmert] until a mass loss of <1% is observed per 24 h period. The fuelwood moisture content was determined on a wet basis (**Equation 4.5**) where m_1 is the mass of the empty tray, m_2 is the mass of the empty tray plus the mass of the wet fuel particle and m_3 is the mass of the empty tray plus the mass of the oven-dried fuel particle. Gravimetric measurements where made using a bench-top mass balance [Kern] and reported to the nearest 0.1%. This method is outlined in detail in **Chapter 3**.

$$(4.5) \quad MC\% = \left(\frac{m_2 - m_3}{m_2 - m_1} \right) \times 100$$

4.2.3 Resistance Moisture Meter Devices

A total of three 2-pin resistance type moisture meter devices were tested on each of the fuelwood particles prior to the determination of MC% via the oven-drying procedure. Each of the devices incorporated 2-pin type electrodes which were insulated so as to negate the effect of surface water and the moisture gradient in the fuel particle. A summary of the device characteristics is provided in **Table 4.1**. The WM01 and FIR 421 model appliances provided an internal calibration of a and b based upon the species of fuelwood being tested. Alternatively, the MD 812 model did not provide an option for species calibration. Estimated moisture (MC%$_{Probe}$) testing via the probe devices was undertaken under standard laboratory temperature and pressure conditions.

Table 4.1 Information regarding the digital moisture probes applied within this study

Name	Tacklife	Dr Meter MD 812	Valiant FIR 421
MC% Range	2%-70%	5%-40%	6%-48%
MC% Error	±0.5%	±1%	±2%
Voltage	-	9v	9v
Internal Calibration	✔	✚	✔

4.5 Results and Discussion

Figure 4.4 presents the recorded moisture content of the beech and ash fuelwood as a function of time (t) during oven drying at 105±2°C (Proximate analysis method). The majority of mass loss is observed within the initial 24 h of drying via evaporation of bound and remaining free, or residual, water from the fuelwood material, and was 13.4±1.5% and 14.2±4.0% for beech and ash samples respectively. A subsequent 48 h of drying revealed a further mass loss of 0.4±0.1% and 0.2±0.0% for beech and ash samples. The moisture content of beech logs was found to be between 12.1% and 14.8% and present a range of 2.7% with an average moisture content of 13.9±1.5%. The moisture content of ash logs was found to be between 12.2% and 13.0% and present a range of 0.8% with an average moisture content of 12.5±0.5%.
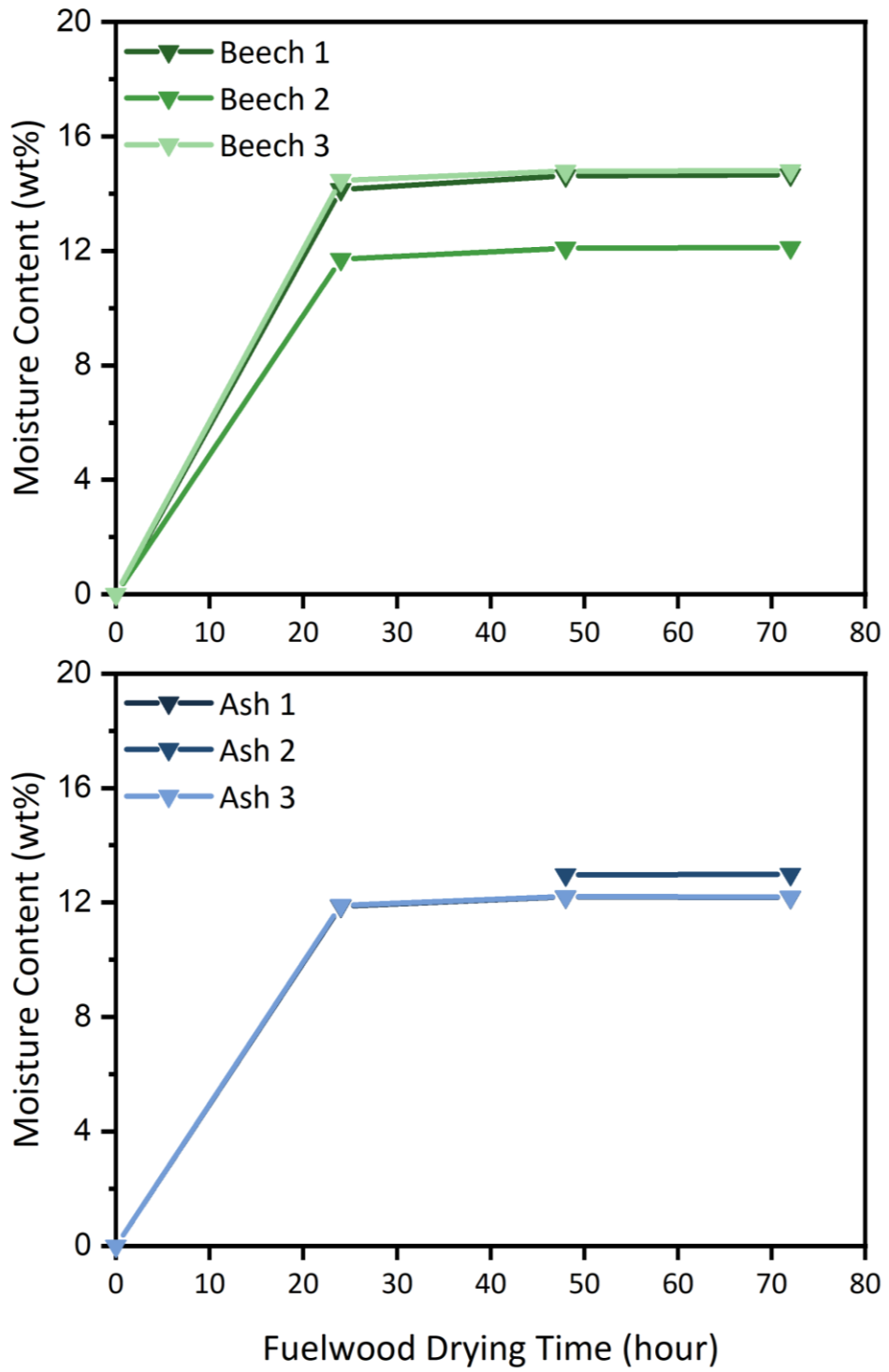
Figure 4.4 Fuelwood drying profile as a function of t for beech and ash logs. Fuelwood drying was undertaken in accordance with BS EN 18134-1 at a maximum operating temperature of 105±2°C.

4.3.1 Variation in Moisture Content Between particles

A summary of the fuel particle mass and MC (determined in accordance with BS EN ISO 18134-2: 2015 and BS EN 13183-2: 2002) is presented in **Table 4.2**. Some variation in the moisture content determined through oven drying is presented for beech sample material (σ=1.5%) while ash samples appear to be more consistent (σ=0.5%). Variation in moisture is likely the result of a number of variables relating to the fuelwood sample and material storage following splitting. Fundamentally, the drying profile of green wood is subject to the temperature of the particle, the ambient humidity and the water gradient of the sample (Simpson, 1991). Sample material was collected from a pile suggesting that fuelwood logs may have originated from different tree specimens or different locations within an individual tree. The distribution of water is known to vary across the tree structure and stem height. The volume and distribution of water within a tree is noted to vary with the majority of the total content located within the sapwood at the butt (base) of the tree structure (Espenas, 1951). The stem structure contains a significant volume of stored water, incorporating between 6-28% of the total daily water budget of an individual tree (Carrasco et al., 2014) however the volume may range between 30% and 200% of the dry mass of the tree depending upon location (Espenas, 1951). In addition, variation in the density of the fuelwood particle, often dependent upon species, has been shown to affect the storage and transport of water within a standing stem (Carrasco et al., 2014). Change in wood porosity is noted to vary between hardwood and softwood species due to the density, orientation and structure of the biomass cells. Such processes often mean that softwood and low-density samples dry quickly while hardwood and high-density samples require a prolonged drying period. Similarly, variation in the drying potential between heartwood and sapwood may be observed following felling (Perre and Keey, 2014). The location of the fuelwood particle within the pile, following felling and splitting, may also lead to variation in the moisture content. Fuelwood particles located on the surface of the pile may dry faster in response to increased exposure to sunlight, improved air circulation and separation from ground humidity. Alternatively, inadequate storage may lead to an increase in the particle moisture content due to high humidity and rainfall exposure. Seasonality may also provide an impact of the moisture content of a log pile with trees felled within the summer presenting a higher moisture content than trees felled in winter month. This process, however, will not affect the moisture content of the sampled particles given the similar felling period under which the material was acquired. This variation is of significant importance during fuelwood combustion testing as it is likely that the moisture content determined during oven-drying practices will not be representative of the

fuelwood pile as a whole given the complexity of the drying process and material
characteristics.

Table 4.2 Fuel particle mass (g) and moisture content (%) determined by oven-drying and digital moisture probe

Material	Sample ID	Wet Mass (g)	Dry Mass (g)	MC%$_{Prox.}$ (%)	MC%$_{Probe}$ (%)
Beech	Sample 1	1433.6	1109.1	14.1	13.6±1
Beech	Sample 2	786.7	642.2	12.1	13.8±1
Beech	Sample 3	1266.4	1002.8	14.8	13.6±1
Ash	Sample 1	1000.8	817.3	12.2	13.8±1
Ash	Sample 2	1048.0	847.7	13.0	15.4±2
Ash	Sample 3	804.0	654.7	12.2	13.8±1

It is possible that the size of the fuelwood particle could affect the inherent moisture
content of the sample where an increase in the mass leads to an increase in the
water content (Simpson, 1991). **Figure 4.5** presents the variation in fuelwood
moisture for each of the samples as a function of particle mass. A generally linear
positive relationship is presented whereby an increase in the particle mass
generally corresponds with an increase in the sample moisture content. Pearson's
correlation analysis indicates a r coefficient of 0.98 between particle mass and
moisture content. The mass of particles analysed was in the range of 642.2 g and
1109.1 g for beech samples and 654.7 g and 847.7 g for ash samples. Such
disparity may therefore account for some of the variance in observed wt% moisture
content between the fuelwood particles. As such, the selection of variably sized
fuelwood samples from a pile may result in an unrepresentative measure of particle
moisture content. This indicates a limitation in the determination of moisture via
oven-drying given that the particles tested are not the same particles applied during
combustion testing.
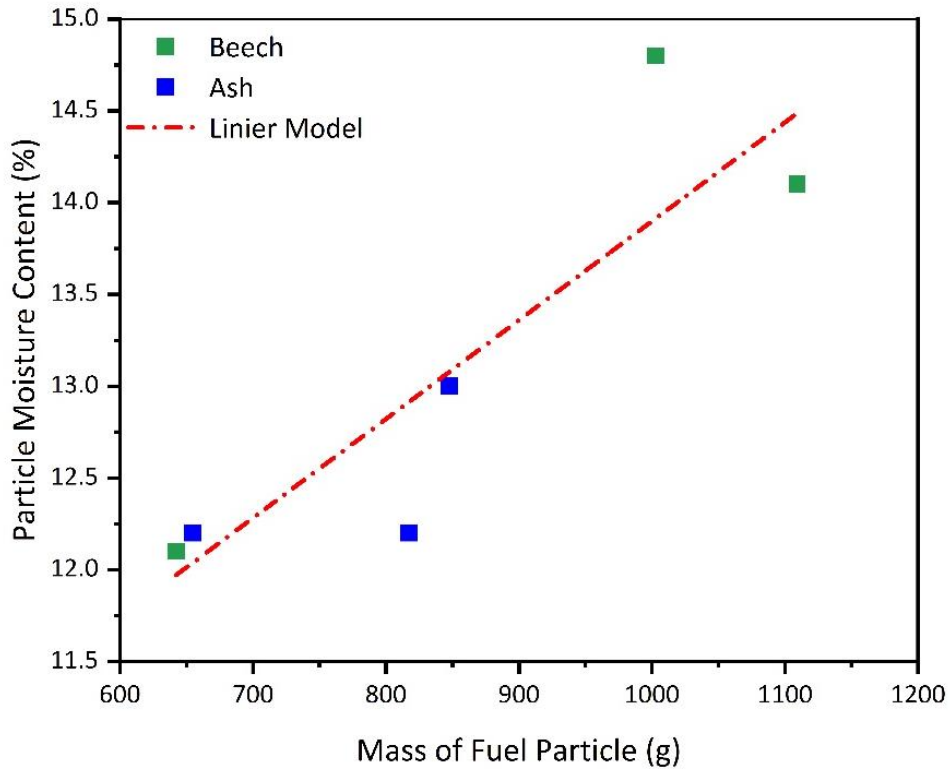
Figure 4.5 The effect of dry fuel particle mass (g) on moisture content (%). A linear regression fit is applied to the average data where y = a + b · *x.*

4.3.2 Variation in Determined Moisture Content Between BS EN ISO 18134-2: 2015 and BS EN 13183-2: 2002 Methods

Figure 4.6 presents the recorded values determined via electrical resistance for each of the beech particles. **Figure 4.7** presents the recorded values determined via electrical resistance for each of the ash particles.

The analysis of beech particles via both BS EN ISO 18134-2: 2015 and BS EN 13183-2: 2002 methods determined similar results. The average moisture content determined for the three beech fuelwood particles via oven drying (MC%$_{Prox.}$) was 13.9±1.5% compared to 13.7±0.9% via electrical resistance (MC%$_{Probe}$). In contrast, the average moisture content determined for the three ash fuelwood particles via oven drying was 12.5±0.5% compared to 14.3±1.5% via electrical resistance. The instrument error associated with resistant type moisture meters is determined to be ±0.5-2.0%. As such, the average MC%$_{Probe}$ falls approximately within the bounds of the fuel particle MC%.

A comparison of the MC%$_{Probe}$ for individual moisture probe devices reveals some disparity to the fuel particle MC% derived from oven-drying. The average beech MC%$_{Probe}$ was found to be 13.9±0.6%, 14.3±1.0% and 12.9±0.3% for devices WM01, MD-812 and FIR-421 respectively. The average ash MC%$_{Probe}$ was found to

be 14.2±0.8%, 15.7±1.6% and 13.1±0.6% for devices WM01, MD-812 and FIR-421 respectively.

Probe MD-812 presents the highest degree of error for beech (σ = 1.0) and ash (σ = 1.6) with MC%$_{Probe}$ recorded within the range of 12% and 16% for beech samples and 13% and 18% for ash samples. For this probe the MC%$_{Probe}$ was 13.9±1.0, 14.8±1.0 and 14.3±0.8 for beech sample 1, 2 and 3 respectively, and 14.7±0.5, 17.5±0.5 and 14.9±1.5 for ash sample 1, 2 and 3 respectively. Therefore, for this probe, MC%$_{Probe}$ values were inaccurate and overestimated the moisture content by a factor of 0.97 for beech fuelwood and 0.79 for ash fuelwood. The instrument error associated with this device is ±1%.

Probe WM01 had the second highest degree of error for beech (σ = 0.6) and ash (σ = 0.8) with MC%$_{Probe}$ recorded within the range of 12% and 14.5% for beech samples and 13% and 16.5% for ash samples. The MC%$_{Probe}$ by this probe was 14.05±0.6, 13.75±0.8 and 13.75±0.5 for beech sample 1, 2 and 3 respectively, and 13.9±0.5, 15±0.6 and 13.9±0.7 for ash sample 1, 2 and 3 respectively. The average MC%$_{Probe}$ value was found to be equal to the moisture content derived by oven drying for beech fuelwood but the probe overestimating the moisture content by a factor of 0.9 for ash fuelwood. The instrument error associated with this device is ±0.5%.

Finally, probe FIR421 presents the lowest degree of error for beech (σ = 0.3) and ash (σ = 0.6) with MC%$_{Probe}$ recorded within the range of 12.1% and 13.5% for beech samples and 11.9% and 14.2% for ash samples. The MC%$_{Probe}$ was 12.8±0.4, 13±0.3 and 12.8±0.4 for beech sample 1, 2 and 3 respectively, and 12.9±0.4, 13.7±0.4 and 12.7±0.6 for ash sample 1, 2 and 3 respectively. The average MC%$_{Probe}$ value was an underestimate of the moisture content by a factor of 1.1 for beech fuelwood and overestimate the moisture content by a factor of 0.95 for ash fuelwood. The instrument error associated with this device is ±2%.
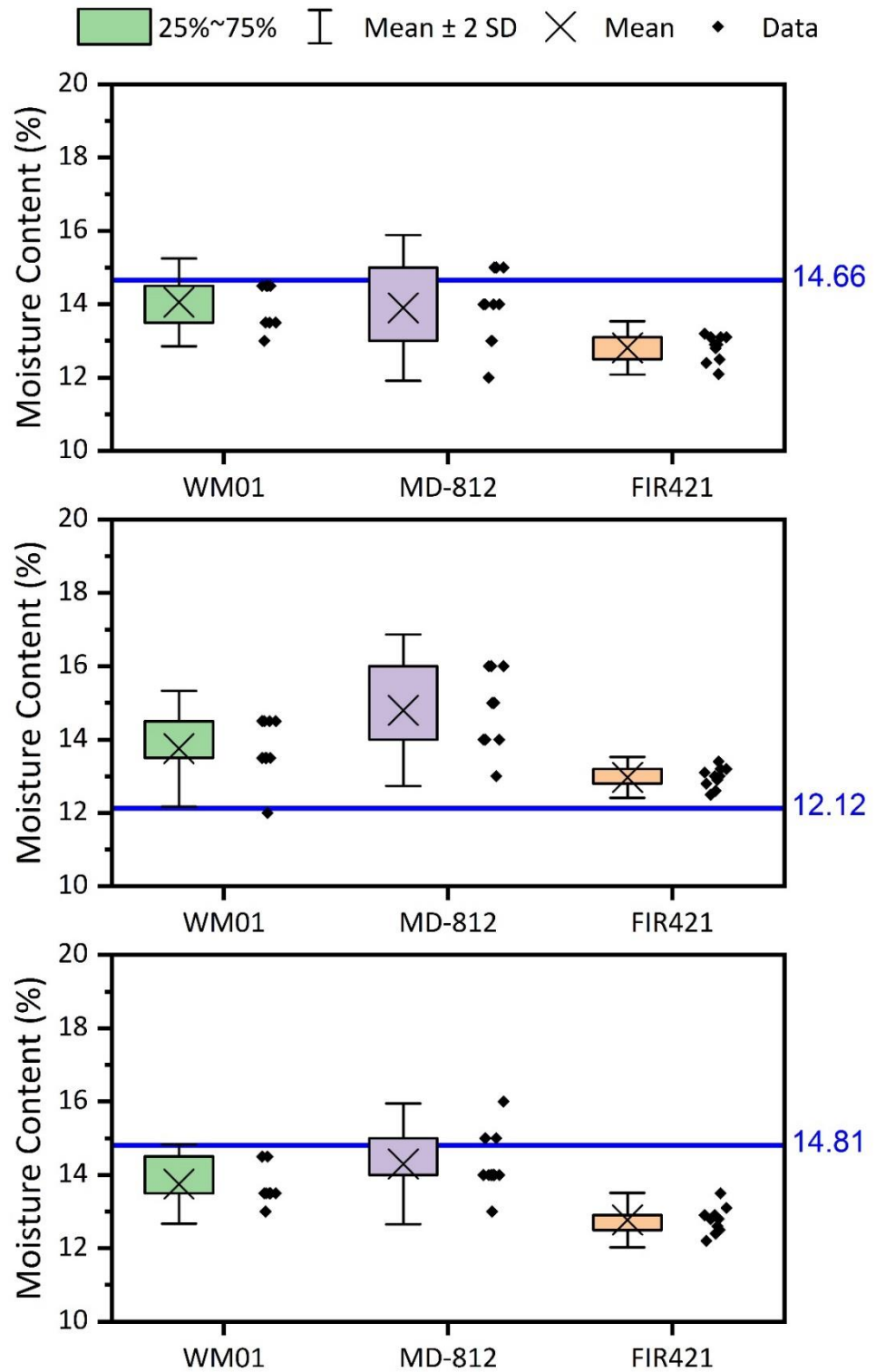
Figure 4.6 Variation in estimated moisture content (%) of beech fuelwood using different test devices. Error bars represent the numerical mean ±2σ. ▬ is the moisture content (%) derived from the oven-drying method undertaken in accordance with BS EN 18134-1.
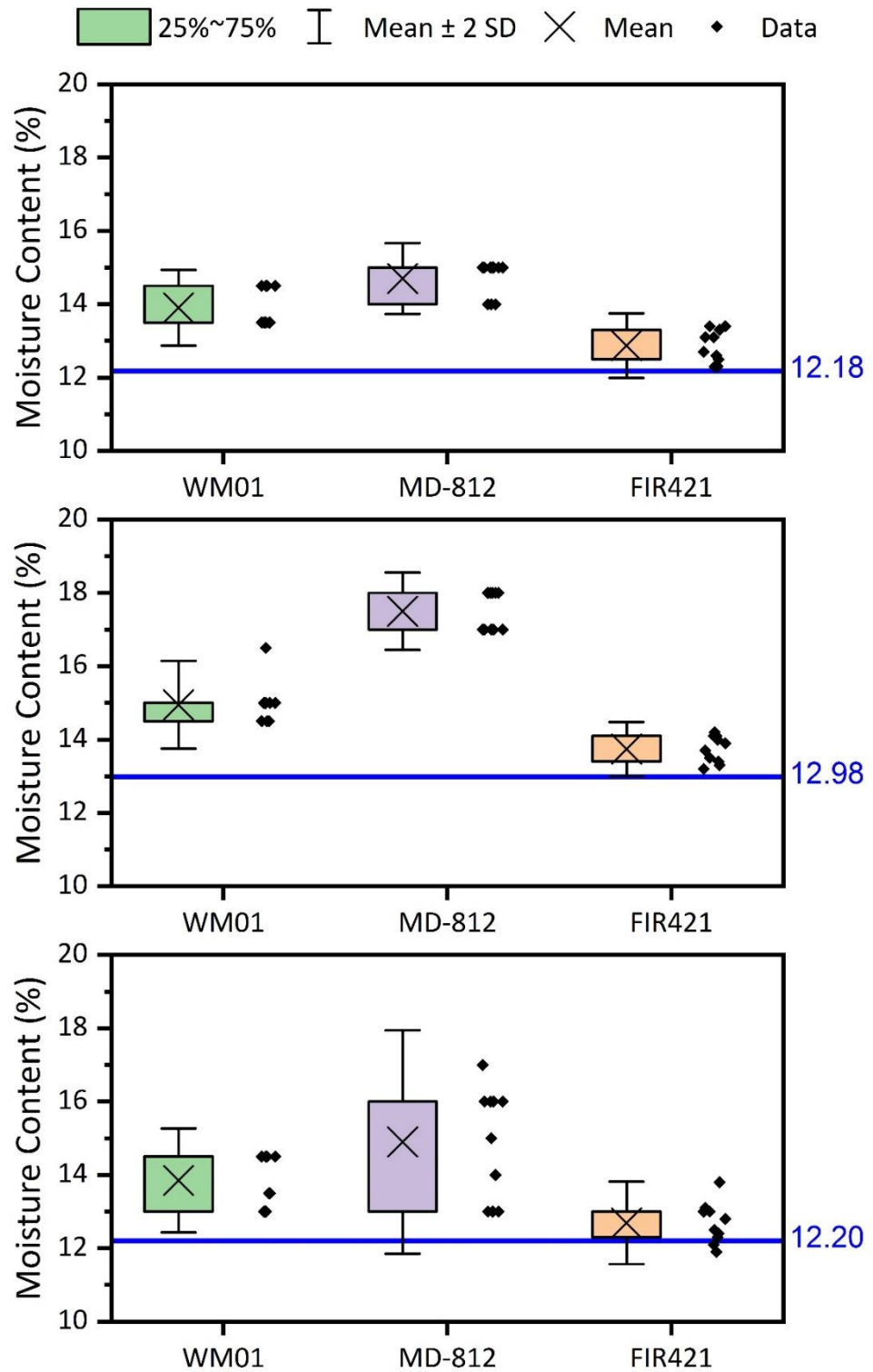
Figure 4.7 Variation in estimated moisture content (%) of ash fuelwood using different test devices. Error bars represent the numerical mean ±2σ. ── is the moisture content (%) derived from the oven-drying method undertaken in accordance with BS EN 18134-1.

The MC%$_{Probe}$ determined via electrical resistance was found to be variable between appliances. A non-parametric Mann-Whitney U test was conducted to establish whether the MC%$_{Probe}$ recorded by two probe devices was statistically different. A two-tailed significance value (ρ) of <0.05 was applied to test the null hypothesis of the comparison. For example, the mean lattice of MC%$_{Probe}$ values for beech fuelwood samples obtained using probe WM01 and MD-812 devices were 13.9±0.6% and 14.3±1.0%; the distribution of the two groups is found to have differed significantly at a statistical level where U = 310.5 (n_1 = n_2 = 90) and ρ = 0.036. Similarly, the mean lattice of estimated moisture values derived from probe WM01 and FIR-421 devices were 13.9±0.6% and 12.9±0.3%; the distribution of the two groups is found to differed significantly at a statistical level where U = 59.0 (n_1 = n_2 = 90) and ρ = 0.00. Finally, the mean lattice of estimated moisture values derived from probe MD-812 and FIR-421 devices were 14.3±1.0% and 12.9±0.3%; the distribution of the two groups is found to have differed significantly at a statistical level where U = 74.0 (n_1 = n_2 = 90) and ρ = 0.00. A similar statistical variance was observed between the MC%$_{Probe}$ derived from each device when testing ash fuelwood particles.

4.3.3 Difference in Moisture Content Determined via Electrical Resistance and Oven-Drying

Table 4.3 presents a ratio of the difference between the methods of determining fuel particle moisture content. The variation factor, as shown in **Equation 4.6**, indicates which probe provides a MC%$_{Probe}$ most similar to that observed when analysing moisture content in accordance with BS EN 18134-2: 2015. A factor of 0.0 would therefore indicate equal moisture content determination when using a resistance type moisture probe and oven-drying. The WM01 probe the most accurate device when measuring the MC%$_{Probe}$ of beech fuelwood particles with an average variation factor of 0.08. The FIR421 probe is the most accurate device when measuring the MC%$_{Probe}$ of ash fuelwood particles with an average variation factor of 0.05. Furthermore, the FIR421 is shown to be the most reliable device for measuring MC%$_{Probe}$ relative to measured MC% across all particles. The MD-812 is shown to be most unreliable; likely in response to the inability to correct MC%$_{Probe}$ for different fuelwood species.

$$(\mathbf{4.6}) \quad Variance\ Factor = 1 - \left(\frac{MC\%_{Proximate}}{MC\%_{Probe}}\right)$$

Table 4.3 Variation in estimated moisture content (%) of beech and ash fuelwood using different test devices.

Sample		Proximate	WM01		MD812		FIR421	
		MC%	MC%	Variation Fac.	MC%	Variation Fac.	MC%	Variation Fac.
Beech	1	14.7	14.1	0.04	13.9	0.05	12.8	0.13
Beech	2	12.1	13.8	0.13	14.8	0.22	13.0	0.07
Beech	3	14.8	13.8	0.07	14.3	0.03	12.8	0.14
Ash	1	12.2	13.9	0.14	14.7	0.21	12.9	0.06
Ash	2	13.0	15.0	0.15	17.5	0.35	13.7	0.06
Ash	3	12.2	13.9	0.14	14.9	0.22	12.7	0.04

4.3.4 Disparity Between Proximate Moisture Content and the Moisture Content of Combusted Fuelwood Samples: The Effect of a Varying Moisture Content within a Pile

The moisture content of fuelwood is recommended to be determined via oven drying of logs in accordance with BS EN 18134-1 (Proximate analysis). Proximate analysis of whole logs is time-consuming and often made in duplicate, triplicate or more so as to minimise sampling error in the determination of MC%$_{Prox.}$; this value is then applied across the pile. As previously suggested, the moisture content of fuelwood stored in a pile may differ depending upon environmental and physical conditions. Furthermore, the value used for MC%$_{Prox.}$ is important since it is applied to the entire fuel pack mass during testing in accordance with BS EN 13240 and when calculating emission factor values. Consequently, the moisture content of fuelwood determined via oven-drying may not be representative of the logs used during combustion testing.

This section evaluates the differences in fuel particle moisture content determined by oven-drying and using a moisture probe prior to combustion. The Low MC% beech and high MC% beech samples refer to fuels tested in **Chapter 6**. The kiln dried beech refers to fuel tested in **Chapter 8**. A sample of fuel was selected and used to determine MC% via oven-drying. This value was used in the determination of batch mass and in the calculation of emission factors. The MC%$_{Probe}$ values of fired fuelwood particles was determined prior to the firing of each fuelwood particle.

Figure 4.8 presents the disparity between moisture content values of fuelwood particles sampled from a pile and determined via proximate analysis in accordance with BS EN 18134-1, and the moisture content of fired fuelwood particles estimated via electrical resistance prior to combustion. The proximate moisture content of previously kiln-dried beech was observed within the range of 14.5% and 21.1% with

an average MC% of 17.45±2.86. The MC%_{Probe} for combusted logs was within the range of 14.6±3.5% and 27.8±3.3% with an average MC%$_{Probe}$ of 22.3±5.5% determined across all combusted particles. The difference is moisture content determined between sampled material and combusted material as well as between oven drying and electrical resistance methods was 4.9%. In this case, the disparity of moisture content between the proximate MC% and MC%$_{Probe}$ is likely in response to inaccuracies associated with the determination of moisture content by electrical resistance and variability in moisture content between sample particles and combusted particles. The average moisture content is shown to vary by a factor of 0.8 between methods. A similar process is observed when determining the moisture content of fuelwood particles maintaining a low and high moisture content. In the case of fuelwood presenting a low moisture content the use a resistance type moisture meter determined an MC%$_{Probe}$ value below that observed when testing samples via oven-drying. In the case of fuelwood presenting a low moisture content the use a resistance type moisture meter determined an MC%$_{Probe}$ value above that observed when testing samples via oven-drying. The average moisture content is shown to vary by a factor of 1.1 and 0.9 between methods for low moisture and high moisture fuelwood respectively. The proximate moisture content is shown to be within the range of average MC%$_{Probe}$ with consideration of instrument error (±2%) for low MC% beech however there is a notable disparity between the proximate MC% and fuelwood MC%$_{Probe}$ for high moisture beech and kiln dried beech samples. Such disparity is likely in response to two factors:

i.   The fuelwood samples selected for proximate analysis in accordance with BS EN 18134-1 were not representative of the pile likely in response to variations in the environmental and physical properties of individual fuel particles.

ii.   The use of a resistance-type moisture probe was not suitable for deriving an accurate MC%$_{Probe}$ relative to the findings of an oven drying approach.

It therefore stands to reason that both the techniques are suitable but potentially not comparable at a high degree of accuracy. Furthermore, careful selection and a high replicant number should be applied when determining the moisture content of a pile in accordance with BS EN 18134-1 given the heterogeneous nature of the fuel particles. Similarly, the attribution of a moisture content value via electrical resistance should only be applied when considering the error and limitations of the instrument.
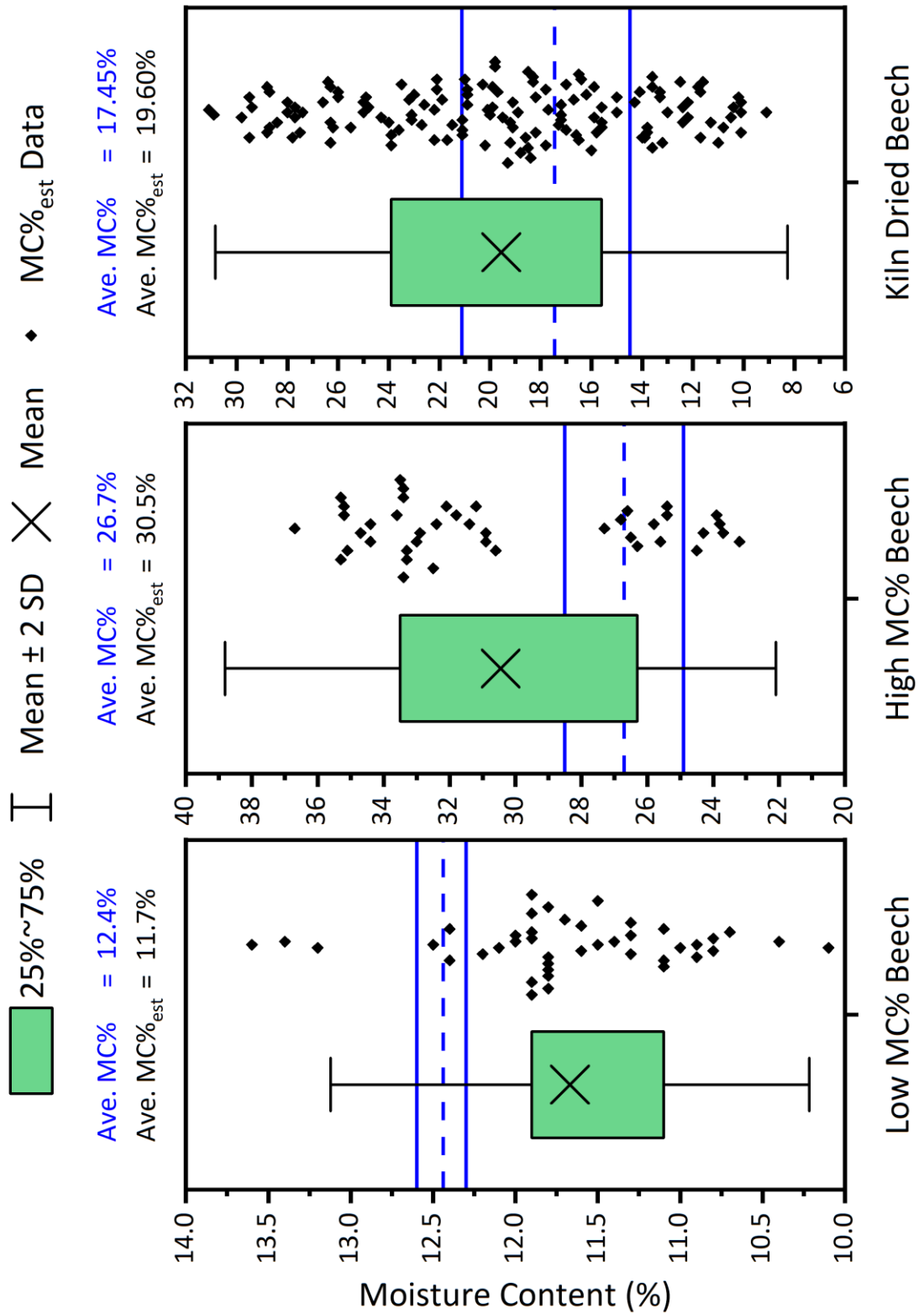
Figure 4.8 Disparity of MC% and MC%$_{Probe}$ values between sampled particles and fuelwood applied for combustion testing. Error bars represent the numerical mean ±2σ. — is the range and - - - is the average of MC% derived from the oven-drying method undertaken in accordance with BS EN 18134-1. Data for Low MC% Beech, High MC% Beech and Kiln Dried Beech is derived from **Chapters 5**, **6** and **8**. MC%$_{Probe}$ determined via electrical resistance was determined using a FIR 421 probe device.

4.3.5 Variation in Moisture Content Between End-Grain and Heartwood

The rate of water loss during seasoning is changeable across the structure of a fuelwood particle (Chen and Lamb, 2007). Such processes lead to inconsistency in water distribution within a particle which can affect measurements of MC%$_{Probe}$ using 2-pin resistance type moisture probes (Price-Allison et al., 2018). The rate of water transfer is greatest in a longitudinal direction via the end-grain of the cut log (Glass et al., 2010). This may result in a generally lower moisture content at the end of the particle than in the centre of the log in response to accelerated drying at the position of the exposed end-grain (James, 1988).

This section evaluates the differences MC%$_{Probe}$ values determined by sampling at the end-grain and centre of fuelwood particles. The fuelwood samples include kiln-dried, seasoned and fresh-cut particles from the study described in **Chapter 5**. The MC%$_{Prox.}$ value was determined using the method described in **Chapter 4.2.2**. The MC%$_{Probe}$ values were found by taking six readings at the end-grain positions and six readings in the centre of the split log using the MD-812 device.

Figure 4.9 identifies the variation in MC%$_{Probe}$ at the end-grain position and within the centre of split log particles. In freshly-cut sample material the average MC%$_{Probe}$ was found to be 28.9±5.2% in the centre of the particle and 20.7±1.0% at the end-grain. Similarly, seasoned sample material presents an average MC%$_{Probe}$ of 25.5±4.2% in the centre of the particle and 19.8±1.0% at the end-grain. Wood which had been exposed to kiln-drying presents the lowest moisture content however the variation in MC%$_{Probe}$ between the centre of the particle and the end-grain is still prevalent: the moisture content is shown to be 4.4 ± 2.7% at the centre of the particle and 3.5±1.9% at the point of the end-grain. As such, the moisture content within the end-grain was lower by a factor of between 0.72 and 0.82 when compared with the MC%$_{Probe}$ recorded in the centre of the particle. The drying profile of wood relates to the inherent porosity of the material; an increase in the porosity leads to an increase in the rate of water loss and absorption. The wood permeability in a longitudinal direction, along the grain, is significantly greater than the permeability in a transverse direction. As such, the majority of water is transported along the grain allowing for an increased rate of moisture loss at the end of the particle (Chen and Lamb, 2007). The process of water loss at the end-grain is driven through the exposed longitudinal capillary structure under atmospheric tension (Baker, 1956). The estimation of fuelwood moisture content via electrical resistance techniques should therefore consider only the MC%$_{Probe}$ values recorded at the centre of fuelwood particles in response to the likely high-water loss observed at the sample end-grain.
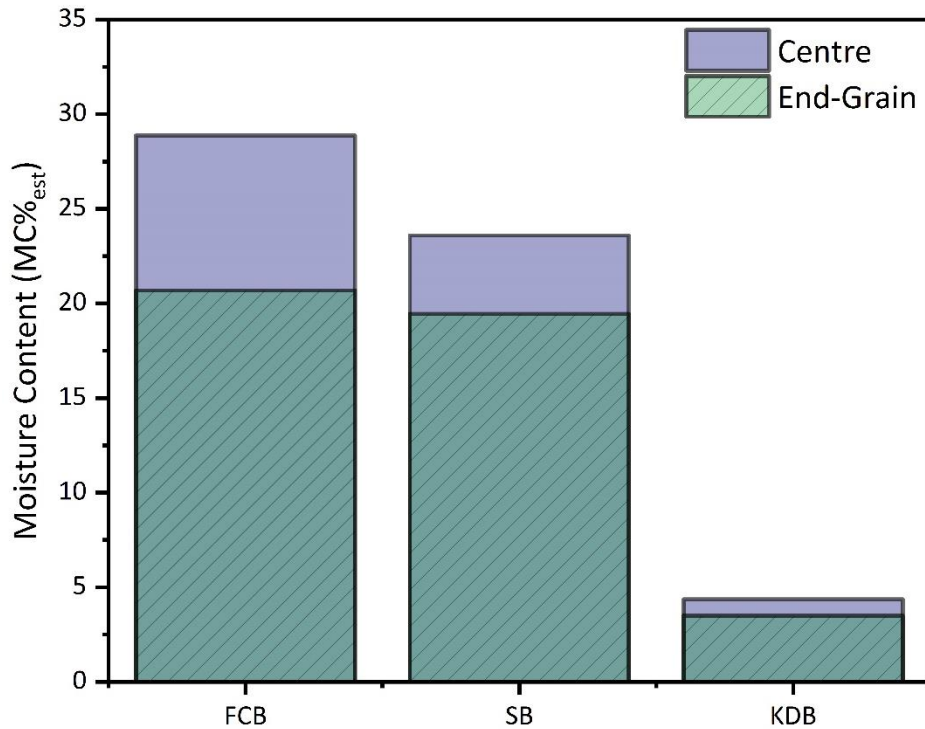
Figure 4.9 Variation in MC%_{Probe} during moisture sampling in the particle centre and end-grain. The three fuels analysed include fresh cut beech (FCB), seasoned beech (SB) and kiln-dried beech (KDB) representing a spectrum of particle moisture contents. Data is taken from **Chapter 5** and (Price-Allison et al., 2018).

4.4 Conclusions

A study was undertaken to investigate the effect of analysis method on the determination of fuelwood moisture content. Moisture content was determined via electrical resistance using three different digital 2-pin moisture meter devices. In addition, the moisture content of fuel logs was determined using oven drying in accordance with BS EN 18134-1 (Proximate analysis). A review of the proximate moisture values and estimated moisture values was undertaken so as to establish variation between analytical techniques and probe devices. Furthermore, the variation in the MC%_{Prox.} and MC%_{Probe} values of materials sampled from a pile for oven-drying and fuelwood particles, tested using a moisture probe, and used in combustion experiments was examined. Disparity of moisture content between proximate analysis sample material and fuelwood particles remaining within a pile was analysed. In addition, analysis was undertaken on the effect of measurement location on electrical resistance with respect to centre-grain and end-grain. The following conclusions have been made:

i.   The proximate moisture content of beech particles and ash particles was found to be 13.9±1.5% and 12.5±0.5% respectively. A higher degree of

variation in particle moisture content was identified in beech fuelwood particles due to specific particle properties including mass and environmental factors relating to storage.

ii. The MC%$_{Probe}$ of beech particles and ash particles was found to be 13.7±0.9% and 14.3±1.5% respectively. These values were different to that determined via oven drying with variation attributed to limitations in the method of MC%$_{Probe}$ determination and instrument error. MC%$_{Probe}$ was determined to overestimate the moisture content of beech samples by a factor of 1.01. Alternatively, MC%$_{Probe}$ was determined to underestimate the moisture content of ash samples by a factor of 0.87.

iii. Variation in the MC%$_{Probe}$ determined by different moisture probe devices was observed and was found to be statistically and significantly different. The disparity of MC%$_{Probe}$ was likely in response to the internal calibration for constants a and b relative to R whereby probes WM01 and FIR-421 allow for user calibration subject to material type while MD-812 limits this capacity.

iv. The WM01 probe is presented to be the most accurate device when measuring the MC%$_{Probe}$ of beech fuelwood particles with an average variation factor of 0.08. The FIR421 probe is presented to be the most accurate device when measuring the MC%$_{Probe}$ of beech fuelwood particles with an average variation factor of 0.05. Furthermore, the FIR421 is shown to be the most reliable device for measuring MC%$_{Probe}$ relative to measured MC% across all particles. The MD-812 is shown to be most unreliable likely in response to the inability to correct MC%$_{Probe}$ for different fuelwood species.

v. Some degree of variation in MC% and MC%$_{Probe}$ may be attributed to the storage of logs within a pile. The locality of logs within a pile may result in increased rates or drying or water absorbance depending upon environmental conditions. The selection of fuelwood particles for proximate analysis and combustion testing should therefore consider such processes so as to ensure heterogeneity of fuel material. The use of homogenous fuel particles should be considered to remove the effect of fuel mass on water storage. In addition, both the sampled particles used during MC%$_{Prox.}$ analysis and MC%$_{Probe}$ analysis (prior to combustion testing) should be stored within a humidity-controlled environment to ensure equalisation of fuel moisture content.

vi. A potential linear relationship between fuelwood particle mass and moisture content was determined whereby an increase in the weight of the post-drying log corresponded with an increase in moisture content. A

strong r correlation of 0.98 was presented between the variables. The selection of large fuelwood particles for proximate analysis and combustion testing may result in derivation of a moisture content that is not representative of the pile. Careful log selection for the measure of moisture content and combustion testing should therefore be undertaken so as to ensure uniformity of fuel particles.

vii.   Moisture content derived for the oven drying of sample material was revealed to differ to the MC%$_{Probe}$ values obtained from fuelwood particles prior to combustion testing. It therefore stands to reason that; the fuelwood samples selected for proximate analysis in accordance with BS EN 18134-1 were not representative of the pile likely in response to variations in the environmental and physical properties of individual fuel particles. Alternatively, the use of a resistance type moisture probe may not be suitable for deriving an accurate MC%$_{Probe}$ relative to the findings of an oven drying approach.

viii.   The MC%$_{Probe}$ sampled in the centre of fuelwood particles was found to differ from those collected within the material end-grain. MC%$_{Probe}$ was revealed to be lower at the end-grain than in the centre of the particle likely in response to the increased rate of drying at the end of the particle.

ix.   The determination of fuelwood moisture content via MC%$_{Probe}$ is for estimation only. The calculation of accurate moisture values requires adequate sampling and testing in accordance with BS EN 18134-1. However, the MC%$_{Probe}$ was generally found to represent the particle moisture content with consideration for instrumentation error (generally found to be ±0.5-2%). Such methods may therefore provide a reasonable indication of fuelwood moisture content during domestic seasoning practices prior to combustion.

x.   It is difficult to accurately determine the moisture content of fuelwood for the purpose of combustion testing. The destructive nature of accurate MC% determination means that the particles sampled for proximate analysis are not the same as the fuelwood logs applied during combustion experiments. Therefore, there is a high likelihood that the MC%$_{Prox.}$ value will not be representative of the fired fuelwood. This is a significant limitation in the application of oven-drying of fuels to be characterised for the purpose of combustion testing given the substantial effect of moisture upon the combustion reaction. As such, the use of moisture probe devices should be considered for all proximate and fired

fuelwood particles to ensure approximate homogeneity of moisture content.

xi.   If the wood within the pile is very dry following kiln-drying and appropriate storage, there should not be much in the way of discrepancy between the MC%$_{Prox.}$ values and the MC%$_{Probe}$ values. The difference between these values will likely fall within the instrument error associated with the method of application. The main problem occurs when the pile is very wet or has not been stored in an appropriate manner. In this event it is likely that the differences between MC%$_{Prox.}$ and MC%$_{Probe}$ will be more significant.

xii.   Following the completion of this work it is recommended that MC%$_{Probe}$ values are obtained from devices which have specific calibrations for the test material. The FIR-421 device appears most appropriate from the selection included within this study. Notwithstanding, the used of digital moisture meter devices should be used for the selection of fuelwood particles prior to firing only. The technique is not suitable for the accurate determination of fuelwood moisture content and an oven-drying approach should instead be considered. Finally, variation in fuel moisture content is likely when sampling from a pile. A method of mitigating erroneous results or combusting fuelwood particles which are not representative of the pile would be to ensure greater control of the storage conditions. The use of atmospheric controlled environments allow for the selection of ambient pressure, humidity and temperature which should mitigate significant differences in moisture content during storage.

4.5 References

Babiak, M. and Kudela, J. 1995. A contribution to the definition of the fiber saturation point. Wood Science and Technology. 29, pp.217–226.

Baker, W.J. 1956. How Wood Dries.

BEIS 2016a. Special feature - Domestic wood use survey [Online]. [Accessed 18 May 2020]. Available from: www.gov.uk/government/statistics/digest-of-united-kingdom-energy-statistics-dukes-2014-printed-version.

BEIS 2016b. Summary results of the domestic wood use survey [Online]. Available from: www.gov.uk/government/statistics/digest-of-united-kingdom-energy-statistics-dukes-2014-printed-version.

Belart, F., Sessions, J. and Murphy, G. 2019. Seasonal Changes in Live Tree Branch Moisture in Oregon, USA: Four Case Studies. Forest Science. 65(1), pp.100–107.

Bhattacharya, S., Albina, D. and Myint Khaing, A. 2002. Effects of selected parameters on performance and emission of biomass-fired cookstoves.

Butcher, S.S. and Sorenson, E.M. 1979. A Study of Wood Stove Particulate Emissions. Journal of the Air Pollution Control Association. 29(7), pp.724–728.

Carrasco, L.O., Bucci, S.J., di Francescantonio, D., Lezcano, O.A., Campanello, P.I., Scholz, F.G., Rodríguez, S., Madanes, N., Cristiano, P.M., Hao, G.-Y., Holbrook, N.M. and Goldstein, G. 2014. Water storage dynamics in the main stem of subtropical tree species differing in wood density, growth rate and life history traits. Tree Physiology. 35, pp.354–365.

Chen, Z. and Lamb, F.M. 2007. Analysis of the Vacuum Drying Rate for Red Oak in a Hot Water Vacuum Drying System. Drying Technology. 25(3), pp.497–500.

DEFRA 2018. Clean Air Strategy 2018 [Online]. [Accessed 18 May 2020]. Available from: https://consult.defra.gov.uk/environmental-quality/clean-air-strategy-consultation/user_uploads/clean-air-strategy-2018-consultation.pdf.

Engineering Toolbox 2010. Resistance and Conductance. Resistance and Conductance. [Online]. [Accessed 11 May 2020]. Available from: https://www.engineeringtoolbox.com/resistance-conductance-d_1654.html.

Engineering Toolbox 2008. Resistance and Resistivity. Resistance and Resistivity. [Online]. [Accessed 11 May 2020]. Available from: https://www.engineeringtoolbox.com/resistance-resisitivity-d_1382.html.

Engineering Toolbox 2003. Resistivity and Conductivity - Temperature Coefficients for Common Materials. [Accessed 11 May 2020]. Available from: https://www.engineeringtoolbox.com/resistivity-conductivity-d_418.html.

Espenas, L.D. 1951. Some wood-moisture relations.

Glass, Samuel V, Zelinka and Samuel L 2010. Moisture Relations and Physical Properties of Wood In: Wood Handbook: Wood as an Engineering Material., 4.1-4.19.

Hedberg, E., Kristensson, A., Ohlsson, M., Johansson, C., Johansson, A., Swietlicki, E., Vesely, V., Wideqvist, U. and Westerholm, R. 2002. Characterisation of particulate matter emissions from a modern wood burner under varying burner conditions. Atmospheric Environment. 36, pp.4823–4837.

HETAS 2018. HETAS Technical Bulletin #9: Ready to Burn Special Edition [Online]. Available from: https://woodsure.co.uk/ready-burn-technical-bulletin/.

James, W.L. 1988. Electric moisture meters for wood [Online]. Madison. [Accessed 12 May 2020]. Available from: https://www.fs.usda.gov/treesearch/pubs/9823.

James, W.L. 1963. Electric moisture meters for wood - William L. James, Forest Products Laboratory (U.S.) - Google Books [Online]. [Accessed 7 May 2020]. Available from: https://books.google.co.uk/books?hl=en&lr=&id=jwvHCYOSmCoC&oi=fnd&pg=PA29&dq=pin+moisture+meter+wood&ots=_fCGsLNIDu&sig=Ga8oOo-8IEZNROnABl4namPZ6gI&redir_esc=y#v=onepage&q=pin%20moisture%20meter%20wood&f=false.

Mitchell, E.J.S., Ting, Y., Allan, J., Lea-Langton, A.R., Spracklen, D. v, Mcfiggans, G., Coe, H., Routledge, M.N., Williams, A. and Jones, J.M. 2019. Combustion Science and Technology Pollutant Emissions from Improved Cookstoves of the Type Used in Sub-Saharan Africa. Combustion Science and Technology. 17, pp.1–21.

Obernberger, I., Brunner, T. and Bärnthaler, G. 2006. Chemical properties of solid biofuels-significance and impact. Biomass and Bioenergy. 30(11), pp.973–982.

Perre, P. and Keey, R. 2014. Drying of wood: principles and practices In: A. S. Mujumdar, ed. Handbook of Industrial Drying. Taylor and Francis.

Phillips, D., Mitchell, E.J.S., Lea-Langton, A.R., Parmar, K.R., Jones, J.M. and Williams, A. 2016. The use of conservation biomass feedstocks as potential bioenergy resources in the United Kingdom. Bioresource Technology. 212, pp.271–279.

Price-Allison, A., Lea-Langton, A.R., Mitchell, Edward J. S.Gudka, B., Jones, J.M., Mason, P.E. and Williams, A. 2018. Emissions Performance of High Moisture Wood Fuels Burned in a Residential Stove.

Raitila, J., Heiskanen, V.P., Routa, J., Kolström, M. and Sikanen, L. 2015. Comparison of Moisture Prediction Models for Stacked Fuelwood. Bioenergy Research. 8(4), pp.1896–1905.

Simpson, W.T. 1991. Dry Kiln Operators Manual [Online]. [Accessed 14 May 2020]. Available from: https://books.google.co.uk/books?id=cBjZE-

bNWWAC&pg=PA1&lpg=PA1&dq=Lumber+drying+is+one+of+the+most+time-
+and+energy+consuming+steps+in+processing+wood+products.+The+anatomical+
structure+of+wood+limits+how+rapidly+water+can+move+through+and+out+of+wo
od.+I.

Simpson, W.T. 2001. Wood: Dimensional Change from Moisture In: K.H. Jürgen
Buschow, R. W. Cahn, M. C. Flemings, B. Ilschner, E. J. Kramer, S. Mahajan and
P. Veyssière, eds. Encyclopedia of Materials: Science and Technology. Elsevier,
pp.9627–9629.

Skaar, C. 1988. Electrical Properties of Wood In: Water-Wood Relations. Springer,
Berlin, Heidelberg, pp.207–262.

Slávik, R., Čekon, M. and Štefaňák, J. 2019. A nondestructive indirect approach to
long-term wood moisture monitoring based on electrical methods. Materials. 12(15).

Smith, H.H. 1986. Fiber saturation point: a new definition. 37th Meeting Western
Dry Kiln Association., pp.9–12.

Stamm, A.J. 1927. The electrical resistance of wood as a measure of its moisture
content. Industrial and Engineering Chemistry1. 19(9), pp.1021–1025.

Tarvainen, V. and Forsén, H. 2000. Accuracy and functionality of hand held wood
moisture content meters [Online]. Available from: http://www.inf.vtt.fi/pdf/.

Toolbox, E. 2004. Density of Various Wood Species. Density of Various Wood
Species. [Online]. [Accessed 13 May 2020]. Available from:
https://www.engineeringtoolbox.com/wood-density-d_40.html.

Verbist, M., Nunes, L., Jones, D. and Branco, J.M. 2019. Service life design of
timber structures In: Bahman Ghiassi and P. B. Lourenço, eds. Long-term
Performance and Durability of Masonry Structures: Degradation Mechanisms,
Health Monitoring and Service Life Design. Woodhead Publishing, pp.311–336.

Wallace, J. and Avramidis, S. 2016. Impact of airflow on hem-fir kiln drying. Drying
Techology. 34(11), pp.1354–1358.

Weatherburn, David C, Ancelet, T., Davy, P.K., Trompetter, W.J., Markwitz, A. and
Weatherburn, D C 2011. Characterisation of particulate matter emissions from a
modern wood burner under varying burner conditions. Air Quality and Climate
Change. 45(2), pp.21–27.

Woodsure 2018. Ready to Burn Technical Bulletin [Online]. [Accessed 12 May
2020]. Available from: https://www.readytoburn.org/special-edition-ready-burn-
technical-bulletin/.

Chapter 5
Emissions Performance of High Moisture Wood Fuels Burned in a Residential Stove; Preliminary Study

5.0 Chapter Overview

This Chapter represents an initial investigation of the effect of fuel moisture content on emissions from a wood burning domestic stove, which has been published in Fuel. (2019). 239(1), pp.1038-1045. Two fuel types were studied: beech which is a hardwood, and spruce which is a softwood. The moisture contents investigated were for a freshly felled wood, a seasoned wood and a kiln dried wood. The effect of the moisture measurement method was considered using a commercial electrical conductivity probe moisture meter which was compared with laboratory analysis by drying in an oven at 105°C. It was shown that the probe can significantly underestimate the actual moisture content in certain cases. Correlations were made of the burning rate, the Emission Factors for the formation of gaseous and particulate pollutants as a function of the moisture content. We also studied the ratio of Black Carbon to Total Carbon (BC/TC) to obtain information on the organic content of the particles. The impact of moisture content on NOx emissions from thus type of stove is also explored although it is expected that NOx would only be dependent on the fuel-nitrogen content.

5.1 Introduction

The use of wood as a fuel is common throughout the world, although the extent varies from country to country depending on their energy requirements and the supply situation. The trend in wood usage has increased in recent years and has resulted in high particulate and air pollution emissions within urban locations with consequential adverse effects on human health (Kocbach Bølling et al., 2009; Orasche et al., 2013) and on climate forcing (Bond et al., 2013). The same situation applies to the use of cookstoves in developing countries where often less attention is paid to the quality of the fuel. There is increasing concern over the impacts of wood stoves on air quality in the UK and worldwide, especially in terms of particulate pollution.

Recent improvements in stove design have resulted in a potential reduction in air pollution by improved control over the supply of air in the primary and secondary combustion chambers. However, increased particulate and pollution formation will result during cold-starting and reloading of fuel (refueling). Thus, lower emissions are dependent on operational practices but also on the fuel properties (L'Orange et

al., 2012; Ozgen et al., 2014; Fachinger et al., 2017). The use of pellet stoves and boilers and wood pellets with suitably defined fuel specifications has greatly improved the environmental impact in regions where it is economical to use these processed fuels. However, in many cases logs are used and there are inadequacies in fuel properties with regard to size and moisture content (MC). High moisture contents contribute to limited thermal performance and enhanced pollutant emissions following slow or incomplete combustion, and some studies have been made of this aspect (Shen, Wei, et al., 2012; Orang, 2015; Magnone et al., 2016; Fachinger et al., 2017).

The effect of biomass moisture content on combustion and emissions has been the subject of a number of investigations. However, a difficulty is that it can vary depending on the initial moisture content in the wood and the humidity of the surrounding air. In the case of logs, as seen in **Chapter 4,** moisture can be lost or gained via the end grain so that the moisture is unevenly distributed throughout the log (Jirjis, 1995). There is an issue that the practical definition of moisture content into loosely defined categories such as kiln dried, seasoned and freshly harvested, is at present insufficient to define the use of wood as a fuel. Some schemes have been implemented in which the wood is certified to have a moisture content less than 20%, but so far there is still limited data available from real stove studies about their impact.

Several papers have studied emissions from the combustion of biomass with various moisture contents. Shen et al. (2013) observed higher emission factors for smoke and polycyclic aromatic hydrocarbons (PAH) for fuels with high moisture content. Bignal et al. (2008) identified greater PAH and CO emissions in biomass fuels with high moisture content. It was observed that the combustion of dry biomass may result in rapid burning resulting in excessive consumption of oxygen within the stove and consequential production of greater smoke concentrations. Chen et al. studied the effect of moisture on wildfires (Chen et al., 2010), however these combustion systems are different to that in a domestic stove.

This Chapter seeks to address the gaps in knowledge by measuring emissions from a wood burning stove which approximates real world conditions. The study determines the effects of the fuel moisture content on the burning rate and emission factors, using batch feeding in a single combustion chamber stove. In particular the work examines the particulate size and composition in terms of black carbon (BC), total carbon (TC) and brown carbon as well as organic carbon (OC). As discussed in **Chapter 4**, wood stove users are often reliant on 'probe' moisture analysers (Tarvainen and Forsén, 2000) for determining wood moisture content. The work in

Chapter 4 is extended here to further testing using an electrical conductivity probe device compared against laboratory analysis using a drying oven.

5.2 Material and Methods

5.2.1 Fuel Preparation

Two species of wood, beech (a hard wood) and spruce (a soft wood) were supplied as logs (by Certainly Wood, Hereford, UK) and each wood was supplied with three moisture contents (MC%); they were designated as (i) fresh cut, expected MC% > 40%, (ii) seasoned, expected MC% 25–35% and (iii) kiln dried, expected less than 20% MC.

The logs were prepared as follows. The fuels were stored as 2.5m cords in-situ for a period of weeks following felling and these provide the fresh cut samples. Following removal from the woodland, each of the cords were cut into 25 cm logs and seasoned by storing outdoors for 24–48 days, noting that the weather had been frequently damp. The kiln dried logs were prepared by heating in a kiln for a period of 50 h at~100 °C. After receipt, the logs were kept in a covered, outdoor stores. The bark was removed prior to all combustion experiments and laboratory analysis, and for combustion studies the dimensions were approximately 25 cm×7 cm.

The wood moisture contents were determined using two techniques. A handheld two pin probe digital moisture meter (Dr Meter MD-812, supplied by Amazon UK) was applied to both lengths of the 'end grain' and in two locations across the exposed centre of the log. The use of the moisture meter provides an approximate moisture concentration at a depth of 1–5mm depth, depending on the hardness of the wood (beech is much harder to penetrate. The meter is suitable for the range of 5–40% moisture content and is accurate to a resolution of 1% point. Measurements were made in a laboratory under conditions well within the operating specifications of 0–40 °C and a relative humidity of 0–70% RH. The total moisture content was also determined using a technique based on the Oven Dry method (BS EN ISO 18134-1: 2015) on the logs being used for the combustion experiments. The temperature used during drying was such that the loss of volatile components, such as oils, in the wood is negligible.

5.2.2 Combustion Experiments

A fixed bed 5.7 kW maximum capacity Waterford Stanley Oisin multi-fuel domestic stove was operated under batch loading conditions previously described (Mitchell et al., 2016; Atiku et al., 2016).

This approach approximates typical 'real world' conditions but in these experiments the flue gases from the stack entered a dilution tunnel. The stove was mounted on a balance in order to measure the burning rate. Sampling ports were positioned on the flue-stack 1.43m above the combustion chamber. A FTIR analyser (Gasmet DX4000) with an integrated oxygen sensor was used for gaseous emission analysis. A pitot tube was used to measure the flue gas velocity. Particulate matter was sampled within the stack using a gravimetric method as described before, using a heated line at 120 °C leading to a filter-block (70±5 °C) housing 50mm micro quartz (Munktell) filter papers for sample collection for black carbon (EC) and organic carbon (OC) determination. Particulate matter (PM) concentrations and size-distribution were calculated post-dilution using a Dekati PM_{10} Impactor set up to separate for $>PM_{10}$, PM_{10}-$PM_{2.5}$, $PM_{2.5}$-PM_1 and $< PM_1$. The flue-gas sampling rate for this was 10±0.5 l/min and the temperature of the diluted air was 64±1 °C. Greased 25mm aluminium foils were used for the collection of the particulate matter and an additional 47mm (Whatman GF/F) was placed at the base of the impactor for $<PM_1$ emission collection. The carbon monoxide concentrations pre- and post-dilution were used to determine the dilution-factor in the dilution tunnel as CO is sufficiently unreactive at this temperature to permit it to be used in this way. Cross-contamination between experimental runs was minimised by removing soot from the stove and flue between experimental runs and cleaning the sampling probes and measurement equipment.

Each fuel was tested in duplicate, and each experiment consisted of two combustion cycles, a cold ignition cycle and a warm refuelling cycle. The cold start or 'ignition batch' was followed by a subsequent reload, this cycle was used for the measurement of gaseous and particulate emissions during the phases, ignition, flaming and smouldering. Means of replicate tests are reported. Both fuel batches incorporated a measured fuel mass between 1.2 kg and 1.8 kg and ignition was achieved by means of kerosene-based firelighters (Zip High Performance) with a mass of 100 g. As such, less fuel is used for testing fresh and seasoned fuelwood compared to kiln-dried fuelwood on an energy basis. This was a deliberate decision since it reflects user behaviour where a consistent number of logs would be used. Both firelighters and fuel were arranged in the stove in a reproducible geometrical arrangement for each of the experiments. Gaseous emissions were analysed by the

FTIR using 60 s resolution. In addition, mass and differential pressure were measured at 120 s sampling resolution.

Emission factors (EF) for the different species (n), were determined as [species (n)] g/kg_{fuel} [fuel] using effectively the method described by Fachinger et al. (2017) (although that paper uses thermal units). The method of determining EF is previously discussed in detail within **Chapter 3**. The emission factors obtained in this paper incorporate results over the whole combustion cycle and are sampled throughout the ignition, combustion and smouldering phases: initially they are obtained in mg/m^3 dry flue gas at 0 °C, 101.25 kPa and 13% O_2 and then converted to g/kg_{fuel}.

5.3 Experimental Results

5.3.1 Fuel Analysis

Logs were selected in duplicate, split, milled and sieved to an approximate nominal top size of 1.0 mm. A representative sample was used for proximate and ultimate analyses using the appropriate British Standard methods, analysis was undertaken in triplicate and means are reported. Proximate analyses are given in **Table 5.1**, where the entries are on a dry basis and accurate to ±0.5 wt% and were obtained using milled samples. Ultimate analysis results are also given on a dry ash free basis and are accurate to ±0.2 wt%, are also given in **Table 5.1**. The Higher Heating Values were calculated from the composition using the method given by (Friedl et al. (2005). They are accurate to ±2%.

As expected, the three beech samples and the three spruce samples have similar elemental compositions. There are some variations due to the natural variability in samples taken from different parts of the tree; typically, the moisture varies as discussed in the next section.

Table 5.1 Proximate and Ultimate fuel analysis

Fuel	Fresh Cut Beech	Seasoned Beech	Kiln Dried Beech	Fresh Cut Spruce	Seasoned Spruce	Kiln Dried Spruce
Designation	FCB	SB	KDB	FCS	SS	KDS
VM (db)	85.0	84.8	86.1	85.0	83.5	84.2
FC (db)	14.7	14.7	13.7	14.8	16.2	15.8
Ash (db)	0.3	0.5	0.02	0.2	0.3	<0.1
C (%) (daf)	49.9	48.9	49.0	50.0	50.9	49.9
H (%) (daf)	6.07	6.18	6.11	6.19	6.13	6.12
N (%) (daf)	0.12	0.08	0.09	0.08	0.08	0.08
S (%) (daf)	0.02	0.02	0.02	0.03	0.02	0.02
O (%) (daf)	43.7	44.6	44.6	43.6	42.8	43.9
HHV (db) (MJ/kg)	19.8	19.3	19.5	19.9	20.2	19.9

5.3.2 Fuel Moisture Contents (MC%)

The accurate determination of the moisture content in logs (MC wt %) is difficult and the two methods previously described were used. Firstly, a commercial digital moisture probe was used as a method of estimating the fuel moisture content for each log consumed. This is the method typically available to stove users. Manual sampling of moisture content was determined across both the exposed centre of the log after splitting, which is the recommended measurement method, and within the end-grain. The results, some of which are at the extremity of the range of the meter, are summarised in **Table 5.2**. The errors shown there are the instrumental errors.

The second method was to use a drying oven in order to determine the total water content in the samples by heating whole logs at 105 °C for 96 h; after this period of time the mass loss was constant within 2%. As discussed in **Chapter 4**, this method is considered to give the actual moisture content, but we estimate the overall error to be ±5%. These results are shown in **Table 5.2**.

Table 5.2 Comparison of moisture contents of the different fuels.

Fuel	Actual MC% (Heated 96 h in Drying Oven) (Error ±5%)	MC% Estimate 1. (Probe, middle surface)	MC% Estimate 2. (Probe, end grain)
FCB	36.4	29±1	21±2
SB	29.7	24±1	19±2
KDB	3.6	4±1	3±2
FCS	42.9	22±1	21±2
SS	39.8	22±1	21±2
KDS	7.1	5±1	7±2

It is evident that the highest moisture values are those obtained by laboratory analysis using the Drying Oven method with the difference up to 100% between the two methods. The results for kiln dried logs are the only ones in agreement for the laboratory and probe tests. The outside measurements at a depth of 5mm were approximately similar, but the result for the end-grain were significantly lower. This is because the moisture in the logs is not uniformly distributed throughout and this inhomogeneity is greater for the highest moisture logs that have tended to dry from the end surfaces first. The values used in this study for moisture content of the logs are those by the Oven Drying method. The differences between this and the outside measurements are significant and in the case of logs with high moisture content this will influence the combustion behaviour; the centre of the logs will remain cooler for much of the combustion cycle.

5.3.3 Burning Rate Studies

Each experimental run incorporated an ignition cycle, during which the ease of ignition was investigated, followed by a subsequent reload and emissions test cycle for particulate and pollutant emission analysis. Fuel consumption and burning characteristics were made at 120 s increments and include visual recordings of the phase of combustion.

The cold start 'ignition batch' testing identifies significant difficulty in wet-fuel ignition when compared with the kiln-dried materials. Additional firelighter batches were often required following the end of flaming combustion while fuel material remained. Both seasoned and fresh-cut fuel presented difficulty in achieving fuel ignition; both kiln dried beech and kiln-dried spruce required only the initial batch of firelighters. Typical results for the burning rate expressed as mass against time for beech wood samples are shown in **Figure 5.1**; duplicate runs (numbered 1, 2) for the kiln dried,

seasoned and freshly cut are given. The results for spruce are not shown because they behave in a similar way and show similar trends to the Beech.
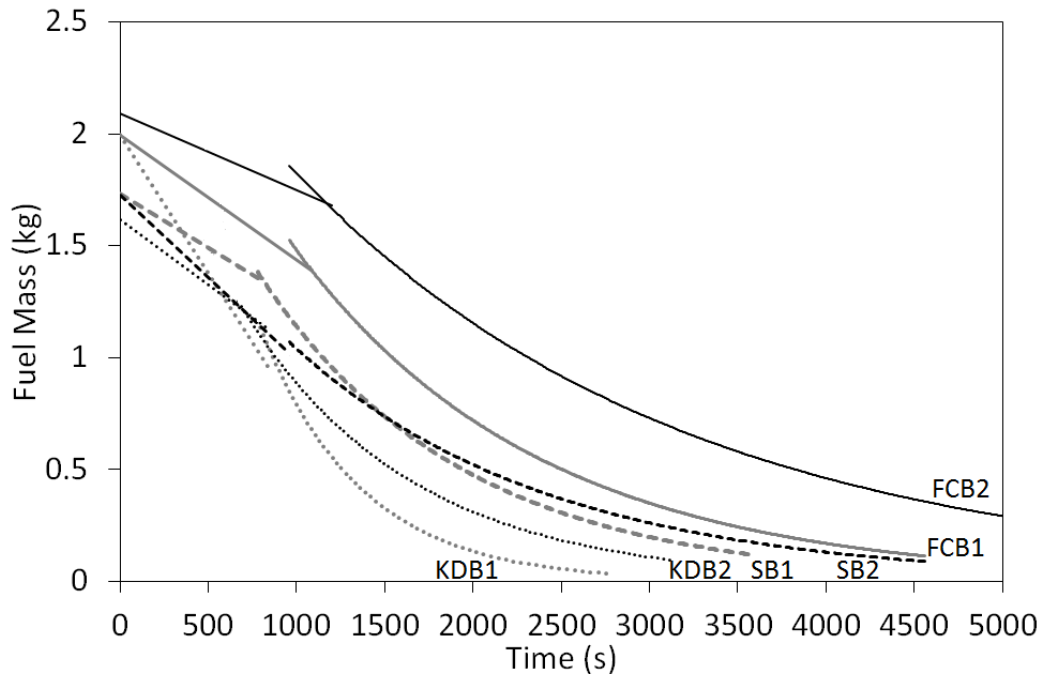
Figure 5.1 Plot of fuel mass against burning time for the beech and spruce wood samples.

The burning rates were quantified in terms of a characteristic burning time, tb, of the exponential part of the combustion as tb=1/bc, where bc is the burning rate coefficient. The burning rate coefficient is a function of moisture, oxygen level, reactivity and the surface area. It is analogous to the function used in fluid bed combustion. The relationship between moisture content and characteristic burning time (below) shows what one would expect: drier burns faster, but the relationship is more complex than just that. **Figure 5.1** shows the mathematical fit of the equations used in the case of all the samples.

Statistical analysis showed that the coefficients of determination, R^2, for the exponential part of the curves are as follows: FCB: 0.998 and 0.999; KDB: 0.995 and 0.937; SB: 0.999 and 0.997; FCS: 0.961 and 0.997SS: 0.999 and 0.964; KDS: 0.918 and 0.870. In most cases, the regression fit is good to very good. The exponential decay function is consistent with the expected mass loss during the period of consistent combustion. As a metric for comparing the behaviours of the various fuels, this is considered a reasonable criterion. It is observed that the curve for KDS is a less good fit. However, they are not sufficiently divergent from the 'exponential decay' model to require altering model or the criterion which works well in all other cases.

Given the inherent variability in fuel moisture content, and resultant combustible fuel mass, a Characteristic Burning Time (CBT) (1/s), or the time required for the fuel batch to lose 37% mass, was used as a method of comparing burning rate independent of initial mass. Estimated values of CBT are plotted against fuel moisture content (%) so as to identify the effect of moisture content on burning rate. **Figure 5.2a** and **5.2b** presents the variability in CBT against moisture content (MC%) obtained following the application of linear regression and estimated moisture content at the time of the combustion experiment. Whilst the data points are few and scattered there is an apparent dependency in the cases studied here and this is indicated by applying a regression line. The linearity of the relationship should not be assumed from this and more evidence is required. The errors in the MC% are estimated to be ±5% and in the CBT±10%.

It is seen that the characteristic burning time increases with the moisture content but also that beech burns more rapidly than spruce and with approximately the same dependence on moisture content. Beech has only a slightly higher volatile content than spruce but as a hard wood has a significantly higher density (beech 721 kg/m^3, spruce 450 kg/m^3), higher (and more reactive) hemicellulose content, and the thermal conductivity of beech is about three times that of spruce (Mason et al., 2016), although this does change as well with the moisture content. The increase in burning rate is consistent with the increased heat transfer rate due to the changes in the thermal conductivity.

The temperature in the combustion chamber as a result of first gas phase flaming combustion and then smouldering bed combustion determines the characteristic burning times. These temperatures are reflected in the flue temperatures and the general behaviour has been observed by our previous studies (Mitchell et al. 2016, Maxwell et al. 2020) with this stove and other research groups, most recently by Fachinger et al. (2017). At the beginning of the combustion cycle there is an initial increase in the burning rate and flue gas temperature resulting from the initial devolatilisation followed by combustion of the partially decomposed biomass and char during the smouldering phase. The emission of smoke is higher over this short initial flaming period.
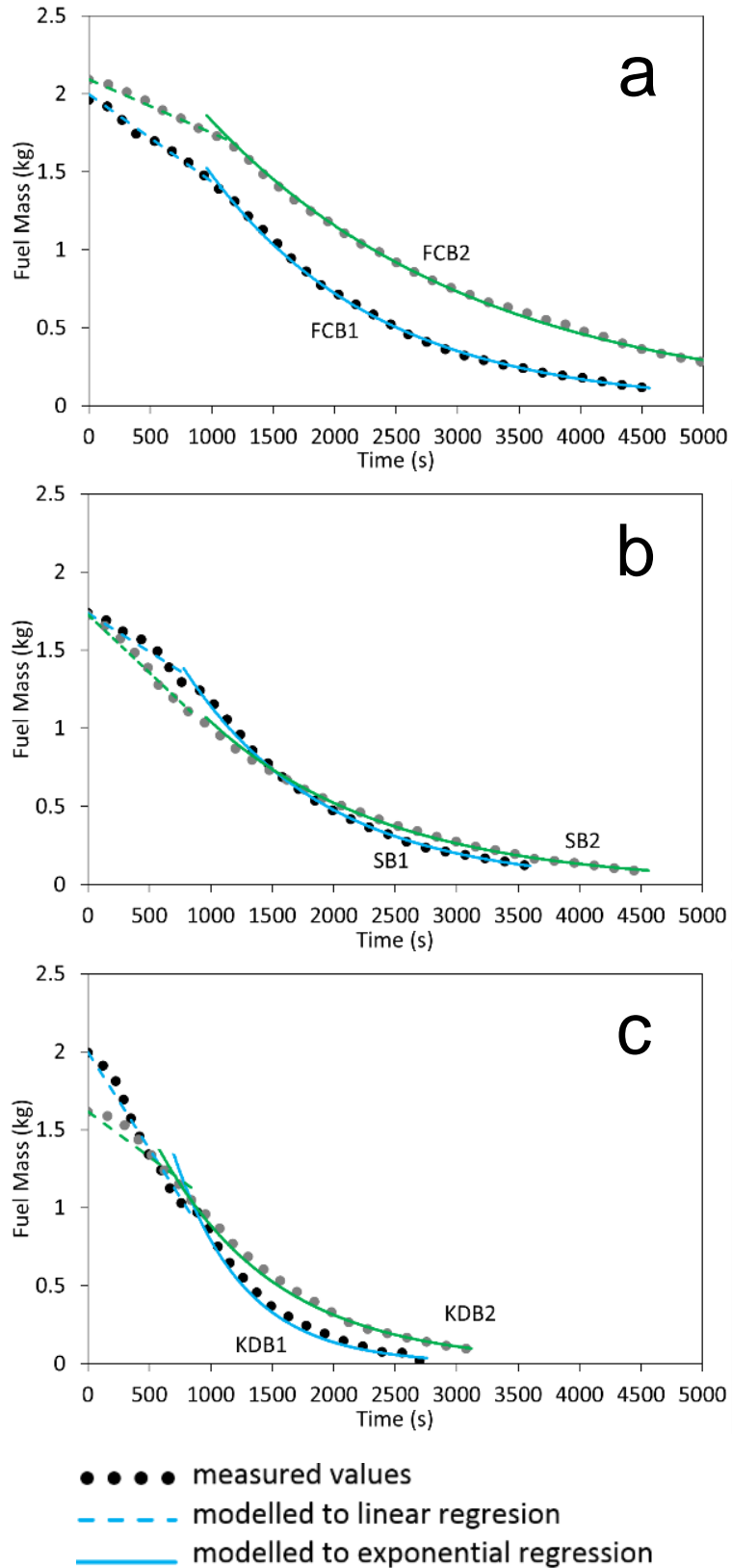
Figure 5.2a Plots of the measured mass of the fuel throughout combustion with initial period of mass loss modelled to a linear function and the established combustion period modelled to an exponential function. The characteristic burning time is derived from the exponential function. (a) Fresh cut beech; (b) seasoned beech; (c) kiln dried beech.
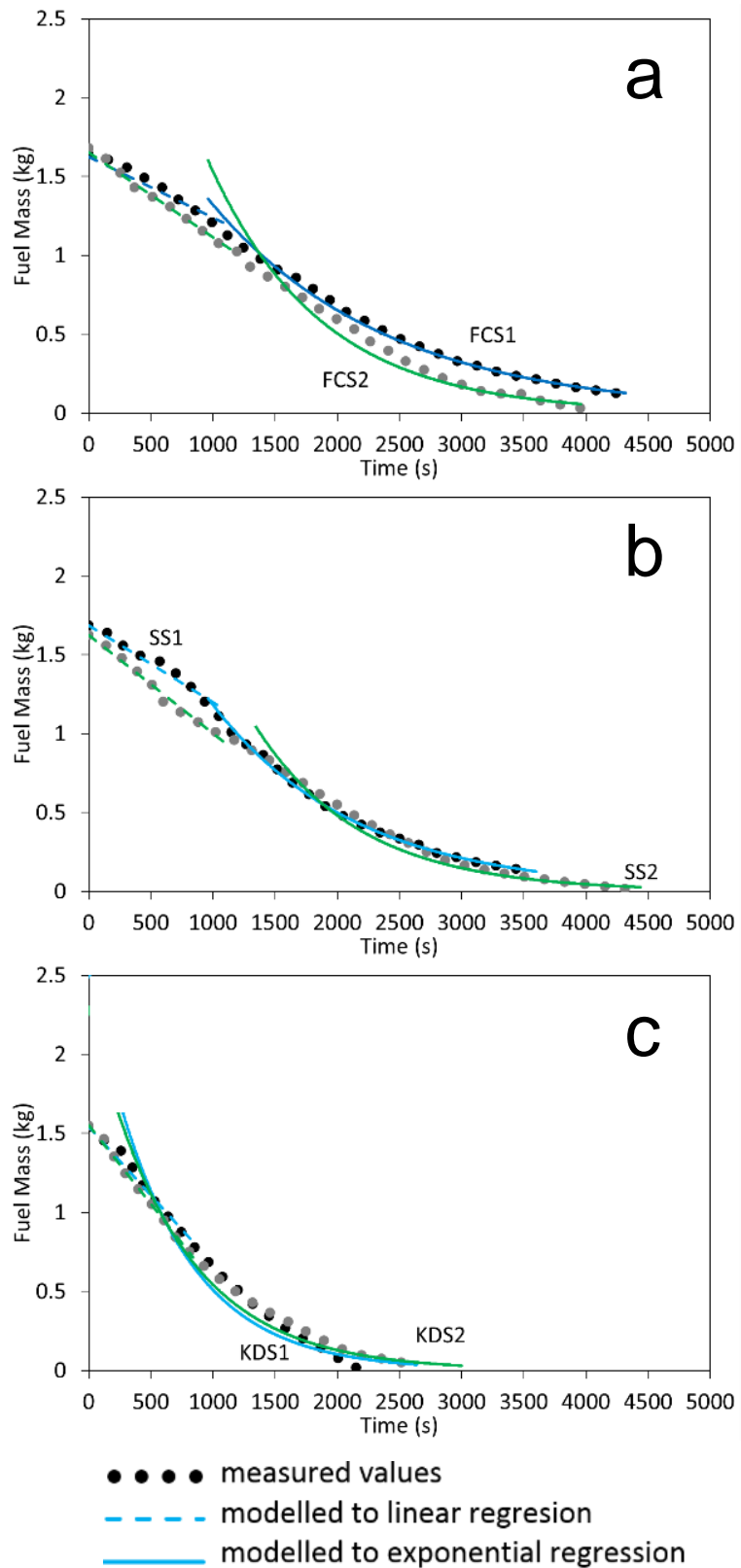
Figure 5.2b Plots of the measured mass of the fuel throughout combustion with initial period of mass loss modelled to a linear function and the established combustion period modelled to an exponential function. The characteristic burning time is derived from the exponential function. (a) fresh cut spruce; (b) seasoned spruce; (c) kiln dried spruce.

There are differences in flue gas temperature for both beech and spruce fuels. Kiln dried fuels gave a much higher temperature, with peak conditions associated with a higher rate of combustion (**Figure 5.3**). This is particularly the case during the early phases of combustion. The enhanced burning rates associated with the drier fuel types results in higher peaks in the flue gas temperature. Significant variation in temperature is identified between kiln dried and fresh cut fuels, with experimental errors of ±5 °C. Here kiln dried beech has initial flue gas temperatures of about 620 °C declining to about 150 °C at the end of the smouldering phase. In contrast, fresh cut beech has an initial temperature of about 325 °C declining to the same final temperature, 150 °C. Seasoned beech is intermediate in behaviour depending on the exact MC. Spruce, which has a lower mass burning rate produces temperatures which are slightly lower during the initial flaming phase. Kiln dried spruce gives an initial peak temperature of 580 °C eventually reducing to 150–180 °C. Fresh cut spruce gives a higher temperature of 300 °C and this is about halfway through the burning cycle; this is the result of the difficulty in the initial ignition process and the slow burning rate.
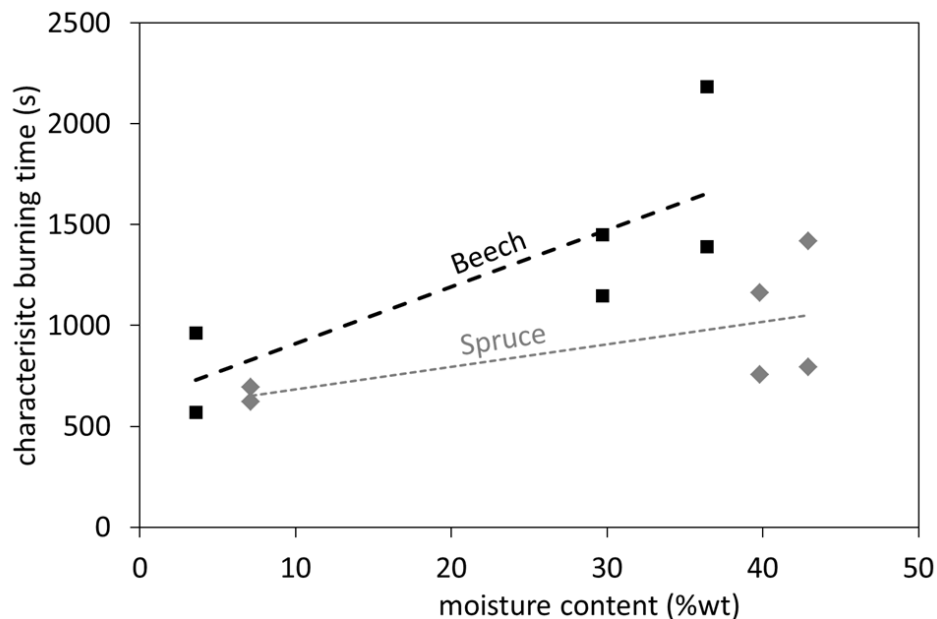
Figure 5.3 Plot of characteristic burning time against moisture content for all the samples: ▪, beech; □ spruce.

5.3.4 Gaseous Emissions Analysis

Emissions measurements were made for both the ignition batch and re-load batch cycles but only the reload batch results are used here. Data is presented in mg/m³ under a standardised condition and on a dry gas basis. The nature of the emission curves follows the conventional pattern observed by other research groups, for

example, Fachinger et al. (2017). Mean values of the Emission Factors are given in **Table 5.3** for all the fuels studied here. The percentage-estimated errors for the gaseous pollutants are ±8% and for the particulate matter (PM) ±10%. It should be noted that trace species measured by FTIR and recorded as 'benzene' and 'CH_2O' may also include other similar species.

The behaviour of some of the emission profiles from fuels with high moisture content does not follow the conventional pattern. The flaming combustion phase and the char combustion phase are far less distinct, and it was observed that some volatile material was released in spikes towards the end of the smouldering phase. The emissions of CH_2O and C_6H_6 can be measured throughout the cycle and there is an emphasis the emissions of unburned species towards the end of the cooler, smouldering phase. It is likely that the centre of wetter logs remains relatively cooler and unreacted biomass is 'trapped' there and decomposes later. The resulting low temperature pyrolysis of wood produces complex organic compounds such as PAH and Brown Carbon (Atiku et al., 2016).

NOx and SO_2 emissions are shown to be unaffected by the fuelwood moisture content. Unlike other organic species the emission of NOx and SO_2 does not increase during the combustion of higher moisture content materials. Given the higher combustion temperatures associated with dry fuelwood combustion and the similarity in emission between fuels it is assumed that NOx and SO_2 formation occurs in response to the fuel NOx mechanism.

Table 5.3 Overall cycle gaseous and total PM Emission Factors in g/kg$_{fuel}$ for the different woods. The % moisture contents of the woods are shown in parenthesis. Emission factor values in this table are updated since publication.

Fuel	CO	CH_4	CH_2O	C_6H_6	SO_2	NOx	PM
FCB 36.4%	119.2±20.7	7.0±6.0	2.2±1.6	2.7±2.3	0.4±0.1	1.5±0.3	8.9±7.7
SB 29.7%	96.8±13.2	3.4±1.9	1.3±0.1	1.5±0.1	0.5±0.2	1.4±0.0	2.3±0.3
KDB 3.6%	70.0±25.4	0.74±0.2	0.2±0.0	0.3±0.2	0.2±0.1	1.1±0.1	3.6
FCS 42.9%	106.9±1.0	5.2±0.4	1.7±0.6	2.2±0.5	0.0±0.0	0.8±0.0	9.0±4.2
SS 39.8%	103.6±3.9	3.8±0.7	1.2±0.6	1.5±0.6	0.8±0.0	0.7±0.0	3.6
KDS 7.1%	116.1±9.9	1.6±0.1	0.2±0.0	0.4±0.0	0.4±0.1	1.0±0.0	1.0

5.3.5 Particulate Matter Emissions

The results obtained by the Dekati Impactor in the dilution tunnel are shown in **Figure 5.4**. Here the PM emissions are expressed in mass/m^3 as measured directly by the Impactor. For each of the wood samples the experiments shown in **Figure 5.4** are in duplicate and the experimental errors are shown on the figures.

It is seen that at the extremities of moisture content, i.e. very dry or high moisture – the beech produces more smoke than the spruce. The high particulate emission associated with the kiln dried wood was also associated with measurement of extremely low oxygen concentrations in the flue, indicating that the air flow was insufficient to permit complete combustion at this high burning rate. Beech was shown (**Figure 5.3**) to burn more rapidly than spruce resulting in the different in the total particulate produced.
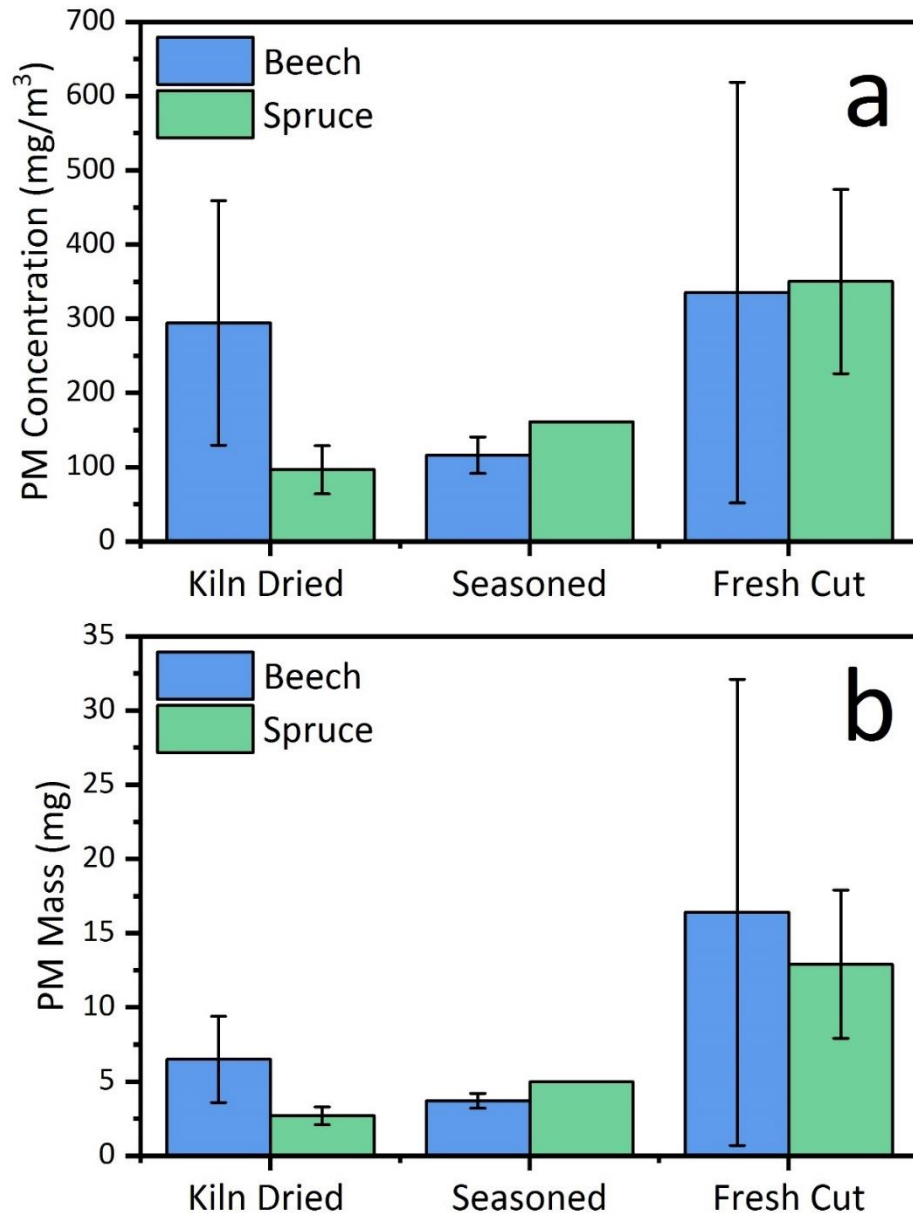
Figure 5.4 Particulate emission obtained by the Dekati Impactor of the smoke concentrations (mg/m^3) and PM mass (mg) for refuelled cycles plotted for all fuels studied. Error bars are presented as the standard deviation.

5.3.6 Particulate Size Distribution

The particle size distributions obtained using the Dekati Impactor are given in **Table 5.4.** It is clear that the majority (at least 92%) of the particulate matter on a mass basis is less than 1 μm in diameter. The relative (%) error here is ±10%. The other fractions produced, PM_1-$PM_{2.5}$, $PM_{2.5}$-PM_{10}, >PM_{10}, are all less than 3 wt% which means that the mass collected is very small, and here the relative (%) error is estimated to be ±30% The fact that most of the soot is <PM_1 has implications in

relation to the number density of the soot and the effect on human health (Kocbach Bølling et al., 2009; Torvela et al., 2014).

Table 5.4 Overall cycle gaseous and total PM Emission Factors in g/kg$_{fuel}$ for the different woods. The % moisture contents of the woods are shown in parenthesis.

Fuel	<PM$_1$	PM$_1$-PM$_{2.5}$	PM$_{2.5}$-PM$_{10}$	> PM$_{10}$	EC/TC
FCB (36.4%)	98.6	0.7	0.3	0.5	0.15
SB (29.7%)	95.4	1.4	1.2	2.1	0.21
KDB (3.6%)	92.6	3.9	1.8	1.7	0.28
FCS (42.9%)	97.3	1.1	0.7	0.9	0.015
SS (39.8%)	92.2	2.6	2.6	2.6	0.15
KDS (7.1%)	92.5	3.1	3.0	1.4	0.51

5.3.7 Elemental Carbon/Total Carbon (EC:TC) Ratio

Particulate samples taken from the dilution tunnel using the Dekati Impactor for the <PM$_1$ fraction were collected on a filter paper and analysed for the ratio EC/TC, (Elemental Carbon/Total Carbon), by Sunset Laboratory Inc, a method used previously (Atiku et al., 2016) and described in **Chapter 3**. The results are given in **Figure 5.5** and **Table 5.4**. The % relative errors for EC/TC are ±15%.

It is apparent that the values for EC/TC are in the sequence kiln dried > seasoned > fresh cut, for both the beech and the spruce, but the values for spruce kiln dried are the highest than for beech. These results are slightly surprising because the fuel chemical analyses of the woods are similar; however, the cellulose content for spruce and beech respectively are 45 and 37 wt%, for hemicellulose 27 and 35 wt% and for lignin 27 and 21 wt%, which would explain the low values of EC/TC observed for beech (that is, high values of OC). The Modified Combustion Efficiency (MCE), which is given by the ratio [CO$_2$]/[CO and CO$_2$], has been used as a measure of combustion inefficiency but more recently Pokhrel et al. (2016) have shown that the ratio EC/OC provides a better correlation. Since TC=EC+OC then the data in in **Figure 5.5** shows the increase in combustion inefficiency as the moisture content increase for both woods. Shen et al have shown that there is a correlation between EF (PM) and OC (Shen, Tao, et al., 2012).

Samples were also taken directly from the undiluted flue gases using the smoke meter and deposited on filter papers. Because the kiln dried beech burns the most rapidly, only four filters could be collected (one every 10 min); six filters were collected for the other two fuels for which the test lasted longer. It was seen for the

kiln dried and the seasoned beech that the samples obtained during the initial flaming phase were black but those obtained during the later smouldering phase are slightly brown. These last samples are brown carbon as observed using this stove before (Atiku et al., 2016). Increasing the MC in the samples increases the combustion time at lower fuel temperatures. Thus, the Seasoned and Fresh Cut Wood samples produced increasingly greater amounts of 'Brown Carbon', and this is especially the case with the Fresh Cut wood, presumably caused by low temperature reactions inside the logs. This effect does not seem to have been observed before although Butcher and Sorenson (1979) observed that 42–77 mass % of wood fire soot could be extracted with benzene, and more recently Fachinger et al. (2017) observed that the organics in PM_1 from wood stoves was 40%. Purvis et al. looked at organic speciation and concluded that the temperature at which the particle size sample is collected has a major impact on the measured distribution of organic material (Purvis et al., 2000). Burning high moisture wood has a deleterious effect on both environment and climate change because of both the increased emission of Black Carbon and also Brown and Organic Carbon.
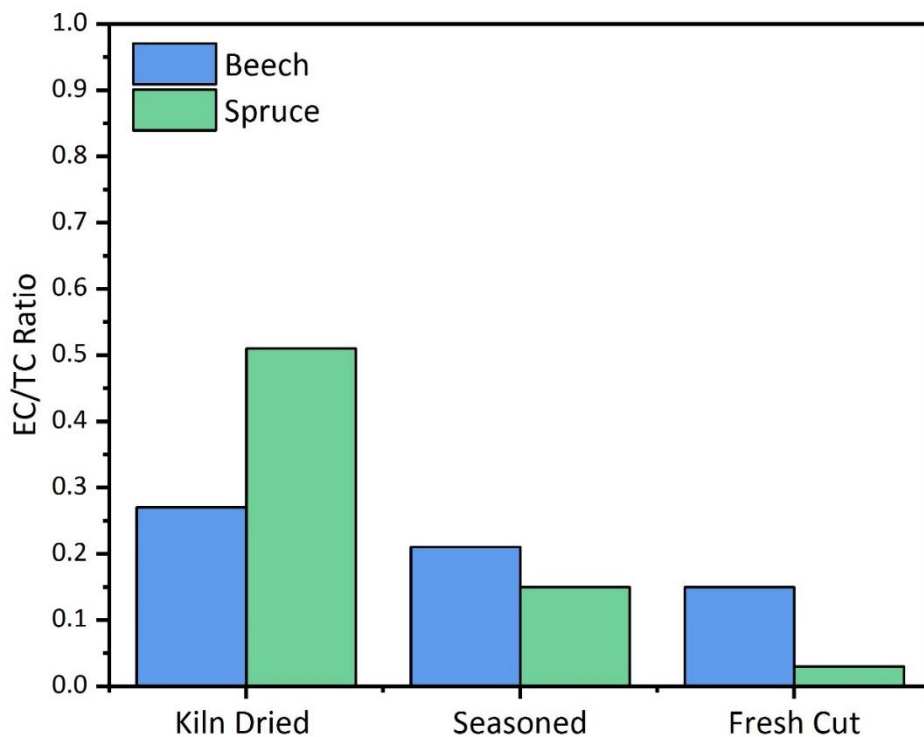
Figure 5.5 Measurements of the particulate EC/TC ratio for all samples over the whole cycle taken in the dilution tunnel using a refuelled batch.

5.4 Discussion

5.4.1 General Features of the Effects of Moisture

A study has been made of the effects of moisture in lump firewood (small logs) under real world conditions. As discussed in **Chapter 4**, there are some interesting issues about measuring the moisture content because of the nonuniformity of the distribution of the moisture in the wood which causes uncertainties here as well as in the interpretation of emissions quoted in previous publications.

5.4.2 Comparison With Other Published Results

The effects of moisture are complex affecting the burning rate and the formation of secondary combustion products. Emission factors are given for the gaseous and particulate species but there are only a few other studies in which the results can be directly compared. For example, Fachinger et al. (2017) made studies of EF for PM_1 from a wood stove but did not specifically give the moisture contents of the fuels studied and averaged results for a number of woods which were in a narrow range; they also stated that very dry wood resulted in elevated particulate emissions. Other examples are Tihay-Felicelli et al. (2017) using green waste, Chomanee et al. (2009) with rubber wood, Bahadori et al. (2014) with bagasse and Lu et al. (2009) using straw. This work identified a reduction in total PAH combustion generated emissions from dried rice and bean straw following an increase in moisture content up to 30. This was attributed to a reduced combustion temperatures.

Of particular interest from both an environmental and a health point of view is the extent of the emission of particulate matter and associated organic matter. This has been the subject of a number of investigations, but there are difficulties in comparing experimental results from other research groups because of differences in the combustion units but also because of different methodologies used to collect sample. The particulate matter consists of carbonaceous soot particles together with a layer of PAH, associated particulate organic matter as well as fragments of ash and char. The amount of organic matter that is deposited on the collection filter depends on the temperature of the collection filter (Jones et al., 2017), which is 64 °C in these experiments, but is often not specified. It is seen from the data for EC/TC in **Table 5.4** that the amount of organic matter present is considerable, the values of EC/TC are low.

The results from the present experiments for the emission of total particulate matter from fuels with different moisture content are given in **Figure 5.6**. Also shown are data from other researchers where they have used stoves which have a similar

design and method of operation to the present work. Data from Fachinger et al. (2017) and Bäfver et al. (2011) as well as Mitchell et al. (2016) using the same stove as the present experiments are given: in most cases results have had to be averaged. Shen et al. (2013) have obtained data for different moisture levels (5–27%) for a range of woods (mainly Chinese Popular) for a brick cooking stove but these are not included in **Figure 5.6** because the stove type (designed for cooking) and PM sampling arrangements are different. However, the results parallel our results in **Figure 5.6** but are ca. 20% higher. NIWA (2007) produced a report in 2007 showing that the in situ wet weight particulate emission factor was 3.3 g/kg$_{fuel}$ and was about three times smaller than the emission factor of 11 g/kg$_{fuel}$ for pre-1994 wood burners. These results are constant over the range of 13–54 % moisture content. This is in contrast to the pre-1994 results which showed a strong parabolic variation with moisture content, and with the results in this paper and those of Shen et al. (2013). It raises an interesting issue about how the present results can be scaled and applied to other stove with different designs and thermal capacities.

It is seen from present results in **Figure 5.6** and **Table 5.4** the similarity of the behaviour of the particulate matter, benzene, which is an important intermediate in soot formation, formaldehyde and methane (which are indicators of the decomposition products from biomass). The EF for soot are in accord with previous investigations, namely that above 25% MC the smoke increases markedly (Bäfver et al., 2011; Magnone et al., 2016). However, this work indicates that below 5%MC here is no increase in smoke emission over the whole cycle, although there is for a short initial part of the cycle during ignition or refuelling. The main advantage of using very dry wood is the ease of ignition, but this comes at a cost, the energy required to dry the wood.
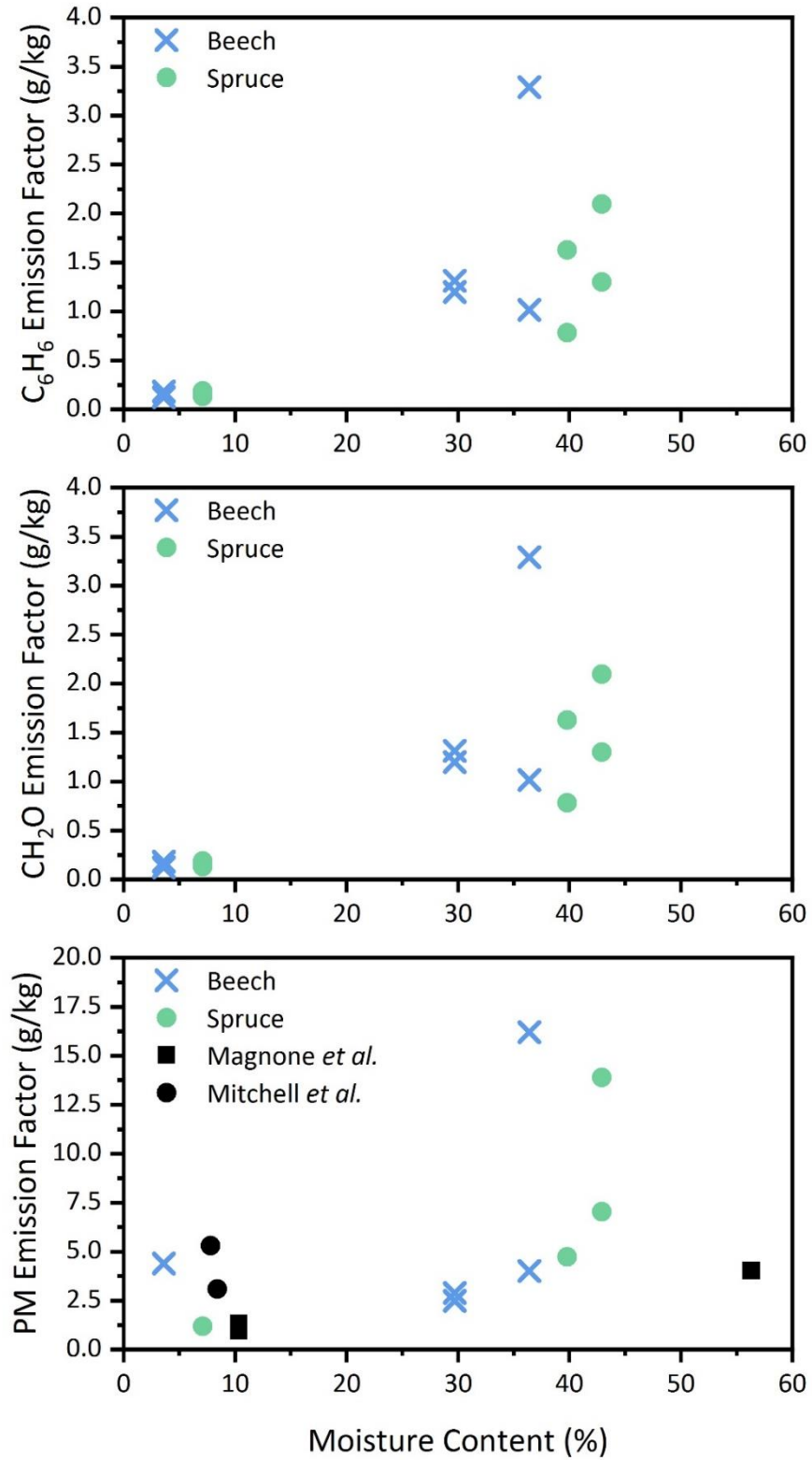
Figure 5.6 Plot of the Emission Factors for (a) C_6H_6, (b) CH_2O and (c) total PM against Moisture Content. Data is also included from Magnone et al. (2016) and Mitchell et al. (2016).

5.4.2 Effects on the Combustion Process

Optimum moisture content is considered to be between about 8 and 20%MC where the effect of moisture on emissions is not significant other than changing the heat available on a mass basis. The type of wood is significant, whether it is hard or soft or indeed an agri-residue based fuel such as straw. Visually it is observed that if very dry log wood is ignited the process occurs smoothly and transition to flaming combustion soon occurs. But when the stove is refuelled with very dry wood it burns rapidly initially with the copious release of soot, and this process changes during the transition to flaming combustion. Very wet wood (> 40% moisture) burns badly; moderately wet partially seasoned wood retains moisture within the wood which results in overlapping combustion stages as a result of delayed pyrolysis which forms decomposition products during smouldering, releasing CH_4,

CH_2O, C_6H_6 and also forming brown carbon etc. NOx was not the primary focus of this study, since it is well established that at the low temperatures observed in this type of stoves, NOx formation is dominated by $Fuel_N$ as discussed by Mitchell et al. (2016) and the references listed in that paper. This is supported by the experimental results for spruce, which are within experimental error for all fuels. NOx formation was higher during the combustion of Beech fuelwood and it is assumed that moisture content may be having an impact on the nature of the emission of the nitrogen species. Both Chen et al. (2010) and Shen, Tao, et al. (2012) found that moisture affects the partitioning of nitrogen between NOx and NH_3, but further research is required to fully understand the impact of moisture on nitrogen partitioning amongst NOx, NH_3 and N-PAH.

5.5 Conclusions

A study was undertaken to investigate the effect on the moisture content in the range 3.6 – 42.9 wt% on the combustion of wood logs in a domestic stove, and the following conclusions were made:

i.   The measurement of moisture in wood logs can lead to different results depending on the method used; analysis of the actual moisture contents determined by the Drying Oven method were different in some cases to those given by a handheld probe analyser. The results from the former were adopted.

ii.   Mass burning rates were a function of moisture content and wood type and have been quantified for the cases studied here.

iii.   The emissions of particulate matter over a whole combustion cycle were found to increase with increasing wood moisture in the range studied;

this was paralleled by the emissions of benzene (and similar aromatic species) and formaldehyde.

iv.   Measurements of the ratio EC/TC (elemental to total carbon) indicate that the emissions of organic carbon decrease as the wood is drier.

v.   In all cases studied the particulate matter mainly consisted of PM_1. For both woods the PM_1 was higher for freshly cut wood than for kiln dried.

vi.   NOx emissions were not seen to be affected by fuel moisture in these stoves, only by the $Fuel_N$ content.

5.7 References

Atiku, F.A., Mitchell, E.J.S., Lea-Langton, A.R., Jones, J.M., Williams, A. and Bartle, K.D. 2016. The Impact of Fuel Properties on the Composition of Soot Produced by the Combustion of Residential Solid Fuels in a Domestic Stove. Fuel Processing Technology. 151, pp.117–125.

Bäfver, L.S., Leckner, B., Tullin, C. and Berntsen, M. 2011. Particle emissions from pellets stoves and modern and old-type wood stoves. Biomass and Bioenergy. 35(8), pp.3648–3655.

Bahadori, A., Zahedi, G., Zendehboudi, S. and Jamili, A. 2014. Estimation of the effect of biomass moisture content on the direct combustion of sugarcane bagasse in boilers. International Journal of Sustainable Energy. 33(2), pp.349–356.

Bignal, K.L., Langridge, S. and Zhou, J.L. 2008. Release of polycyclic aromatic hydrocarbons, carbon monoxide and particulate matter from biomass combustion in a wood-fired boiler under varying boiler conditions. Atmospheric Environment. 42(39), pp.8863–8871.

Bond, T.C., Doherty, S.J., Fahey, D.W., Forster, P.M., Berntsen, T., Deangelo, B.J., Flanner, M.G., Ghan, S., Kärcher, B., Koch, D., Kinne, S., Kondo, Y., Quinn, P.K., Sarofim, M.C., Schultz, M.G., Schulz, M., Venkataraman, C., Zhang, H., Zhang, S., Bellouin, N., Guttikunda, S.K., Hopke, P.K., Jacobson, M.Z., Kaiser, J.W., Klimont, Z., Lohmann, U., Schwarz, J.P., Shindell, D., Storelvmo, T., Warren, S.G. and Zender, C.S. 2013. Bounding the role of black carbon in the climate system: A scientific assessment. Journal of Geophysical Research Atmospheres. 118(11), pp.5380–5552.

Butcher, S.S. and Sorenson, E.M. 1979. A Study of Wood Stove Particulate Emissions. Journal of the Air Pollution Control Association. 29(7), pp.724–728.

Chen, L.-W.A., Verburg, P., Shackelford, A., Zhu, D., Susfalk, R., Chow, J.C. and Watson, J.G. 2010. Moisture effects on carbon and nitrogen emission from burning of wildland biomass. Atmospheric Chemistry and Physics. 10(14), pp.6617–6625.

Chomanee, J., Tekasakul, S., Tekasakul, P., Furuuchi, M. and Otani, Y. 2009. Effects of Moisture Content and Burning Period on Concentration of Smoke Particles and Particle-Bound Polycyclic Aromatic Hydrocarbons from Rubber-Wood Combustion. Aerosol and Air Quality Research. 9(4), pp.404–411.

Fachinger, F., Drewnick, F., Gieré, R. and Borrmann, S. 2017. How the user can influence particulate emissions from residential wood and pellet stoves: Emission factors for different fuels and burning conditions. Atmospheric Environment. 158, pp.216–226.

Friedl, A., Padouvas, E., Rotter, H. and Varmuza, K. 2005. Prediction of heating values of biomass fuel from elemental composition In: Analytica Chimica Acta. Elsevier, pp.191–198.

Jirjis, R. 1995. Storage and drying of wood fuel. Biomass and Bioenergy. 9(1–5), pp.181–190.

Jones, J.M., Ross, A.B., Mitchell, E.J.S., Lea-Langton, A.R., Williams, A. and Bartle, K.D. 2017. Organic carbon emissions from the co-firing of coal and wood in a fixed bed combustor. Fuel. 195, pp.226–231.

Kocbach Bølling, A., Pagels, J., Yttri, K.E., Barregard, L., Sallsten, G., Schwarze, P.E. and Boman, C. 2009. Health effects of residential wood smoke particles: the importance of combustion conditions and physicochemical particle properties. Particle and Fibre Toxicology. 6(1), pp.1–20.

L'Orange, C., DeFoort, M. and Willson, B. 2012. Influence of testing parameters on biomass stove performance and development of an improved testing protocol. Energy for Sustainable Development. 16(1), pp.3–12.

Lu, H., Zhu, L. and Zhu, N. 2009. Polycyclic aromatic hydrocarbon emission from straw burning and the influence of combustion parameters. Atmospheric Environment. 43(4), pp.978–983.

Magnone, E., Park, S.K. and Park, J.H. 2016. Effects of Moisture Contents in the Common Oak on Carbonaceous Aerosols Generated from Combustion Processes in an Indoor Wood Stove. Combustion Science and Technology. 188(6), pp.982–996.

Mason, P.E., Darvell, L.I., Jones, J.M. and Williams, A. 2016. Comparative Study of the Thermal Conductivity of Solid Biomass Fuels. Energy and Fuels. 30(3), pp.2158–2163.

Maxwell, D., Gudka, B.A., Jones, J.M. and Williams, A. 2020. Emissions from the combustion of torrefied and raw biomass fuels in a domestic heating stove. Fuel Processing Technology. 199, pp.106266

Mitchell, E.J.S., Lea-Langton, A.R., Jones, J.M., Williams, A., Layden, P. and Johnson, R. 2016. The impact of fuel properties on the emissions from the combustion of biomass and other solid fuels in a fixed bed domestic stove. Fuel Processing Technology. 142, pp.115–123.

NIWA 2007. Factors influencing particulate emissions from NES compliant woodburners in Nelson, Rotorua and Taumarunui 2007 [Online]. Auckland, New Zealand. [Accessed 26 June 2020]. Available from: https://niwa.co.nz/sites/niwa.co.nz/files/1 - NIWA Report AKL 2012-013.pdf.

Orang, N. 2015. Effect of feedstock moisture content on biomass boiler operation. Tappi J. 14, pp.629–637.

Orasche, J., Schnelle-Kreis, J., Schön, C., Hartmann, H., Ruppert, H., Arteaga-Salas, J.M. and Zimmermann, R. 2013. Comparison of emissions from wood combustion. Part 2: Impact of combustion conditions on emission factors and characteristics of particle-bound organic species and polycyclic aromatic hydrocarbon (PAH)-related toxicological potential. Energy and Fuels. 27(3), pp.1482–1491.

Ozgen, S., Caserini, S., Galante, S., Giugliano, M., Angelino, E., Marongiu, A., Hugony, F., Migliavacca, G. and Morreale, C. 2014. Emission factors from small scale appliances burning wood and pellets. Atmospheric Environment. 94, pp.144–153.

Pokhrel, R.P., Wagner, N.L., Langridge, J.M., Lack, D.A., Jayarathne, T., Stone, E.A., Stockwell, C.E., Yokelson, R.J. and Murphy, S.M. 2016. Parameterization of single-scattering albedo (SSA) and absorption Ångström exponent (AAE) with EC / OC for aerosol emissions from biomass burning. Atmospheric Chemistry and Physics. 16(15), pp.9549–9561.

Purvis, C.R., Mccrillis, R.C. and Kariher, P.H. 2000. Fine particulate matter (PM) and organic speciation of fireplace emissions. Environmental Science and Technology. 34(9), pp.1653–1658.

Shen, G., Tao, S., Wei, S., Zhang, Y., Wang, R., Wang, B., Li, W., Shen, H., Huang, Y., Chen, Y., Chen, H., Yang, Y., Wang, W., Wang, X., Liu, W. and Simonich, S.L.M. 2012. Emissions of parent, nitro, and oxygenated polycyclic aromatic hydrocarbons from residential wood combustion in rural China. Environmental Science and Technology. 46(15), pp.8123–8130.

Shen, G., Wei, S., Wei, W., Zhang, Y., Min, Y., Wang, B., Wang, R., Li, W., Shen, H., Huang, Y., Yang, Y., Wang, W., Wang, Xilong, Wang, Xuejun and Tao, S. 2012. Emission factors, size distributions, and emission inventories of carbonaceous particulate matter from residential wood combustion in rural China. Environmental Science and Technology. 46(7), pp.4207–4214.

Shen, G., Xue, M., Wei, S., Chen, Y., Zhao, Q., Li, B., Wu, H. and Tao, S. 2013. Influence of fuel moisture, charge size, feeding rate and air ventilation conditions on the emissions of PM, OC, EC, parent PAHs, and their derivatives from residential wood combustion. Journal of Environmental Sciences (China). 25(9), pp.1808–1816.

Tarvainen, V. and Forsén, H. 2000. Accuracy and functionality of hand held wood moisture content meters [Online]. Available from: http://www.inf.vtt.fi/pdf/.

Tihay-Felicelli, V., Santoni, P.A., Gerandi, G. and Barboni, T. 2017. Smoke emissions due to burning of green waste in the Mediterranean area: Influence of fuel moisture content and fuel mass. Atmospheric Environment. 159, pp.92–106.

Torvela, T., Tissari, J., Sippula, O., Kaivosoja, T., Leskinen, J., Virén, A., Lähde, A. and Jokiniemi, J. 2014. Effect of wood combustion conditions on the morphology of freshly emitted fine particles. Atmospheric Environment. 87, pp.65–76.

Chapter 6
The Impact of Fuelwood Moisture Content on the Emission of Gaseous and Particulate Pollutants from a Wood Stove

6.1 Introduction

Air pollution from residential biomass combustion has been shown to cause detrimental effects on both climate and human health (Bond et al., 2013; Mitchell et al., 2019). While such effects have been inaccurately attributed to being only regional (Scandinavian) issues or historical issues in Europe, recent research suggests increased contemporary pollution in a number of urban locations including London, Berlin and Paris amongst others (Fuller et al., 2013; Fuller et al., 2014). EU 2020 strategy targets require 20% of energy generation by renewable means and social issues including fuel poverty and ease of access to low-cost grey fuelwood resources have all been associated with increased domestic biomass combustion practices (Wagner et al., 2010; DEFRA, 2017). Though UK policy has attempted to mitigate the effect of domestic combustion, through Ecodesign 2022 and Clean Air Strategy 2019 legislation, processes of user behaviour are shown to provide a significant control on overall pollutant formation and appliance efficiency (Ozgen et al., 2014; Wöhler et al., 2016; Fachinger et al., 2017). The moisture content of fuelwood has been shown to have significant effects on combustion conditions and pollutant formation in small-scale residential heating and cooking appliances (Simoneit, 2002; Shen, Wei, et al., 2012; Magnone et al., 2016; Fachinger et al., 2017; Price-Allison et al., 2019). A number of previous studies have investigated such effects. However, given the complexity of the combustion reaction and the many variables to be considered, further exploration is required to better understand the issue (Houck and Tiegs, 1998; Magnone et al., 2016).

It is well established that the combustion of biomass and other solid fuels leads to the formation of a complex mixture of gaseous pollutant species (Koppmann et al., 2005) and carbon-based aerosols commonly identified as soot (Magnone et al., 2016). These products are formed as a result of the incomplete combustion of carbonaceous materials, including wood, and small-scale combustion appliances have been identified as a significant source (Bond et al., 2004). Previous work has identified an increase in the formation of particulate emissions corresponding to higher moisture content of the fuelwood (Price-Allison et al., 2019). During heating and prior to flaming combustion, water vapour, resinous compounds and pyrolysis products, derived from the parent hemicellulose and lignin composition, are liberated from the fuel at a specific temperature range. During this process, water vapour acts as a rate limiting influence creating a cooling effect within the firebox

thus requiring additional heat energy for fuel drying. The greater the quantity of water vapour, the greater the energy requirement prior to ignition (Simoneit, 2002; Shen, Wei, et al., 2012). Studies reported in the literature have generally shown a positive correlation between fuel moisture content and pollutant emission formation, predominantly in response to the cooling effect of water within the combustion reaction resulting in lower combustion temperatures and inhibited combustion efficiency (Shen, Tao, et al., 2012).

The relationship between fuel moisture content and pollutant formation is more complex. A number of studies have revealed the detrimental impact of moisture content on pollutant formation associated with small-scale domestic combustion. There is evidence that the total particulate (PM_t) formation increases during the combustion of fuels comprising a higher moisture content with a number of examples found within the literature (Purvis and McCrillis, 2000; Shen et al., 2013; Chomanee et al., 2015; Magnone et al., 2016; Price-Allison et al., 2019). It has been estimated that moisture content may account for 43% and 38% variance in particulate emission formation and combustion temperature respectively (Wilton and Bluett, 2012). Conversely, the effect of fuel moisture content has also be shown to reduce PM_t formation in systems with improved oxygen availability and controlled burning rates (Zhao et al., 2008; Lu et al., 2009). There is also evidence that the composition of soot is varies with the combustion of higher moisture fuels generally resulting in a high organic carbon (OC) and low elemental carbon (EC) fraction (Price-Allison et al., 2019). Magnone et al. (2016) previously identified variability in the OC fraction of soot samples collected during the combustion of low moisture (10.34%) and high moisture (56.31%) fuels in response to differences in the temperature of the combustion reactions. In that study, the burning of low moisture fuel resulted in higher temperatures (344°C) and a lower organic fraction (29.15 mg/m^3) while high moisture fuel resulted in lower temperatures (320°C) and a higher organic fraction (39.06 mg/m^3). Similarly, Shen et al. (2013) found that an increase in the moisture content of the fuel leads to a corresponding increase in PM_t and OC formation while the elemental carbon (EC) fraction was shown to reduce in response to inhibited combustion efficiency and lower temperatures.

The importance of understanding the effect of fuel moisture content upon soot formation and physiochemical characteristics relates to both the detrimental health effects during exposure and global climate change. Fuelwood maintaining an inappropriate moisture range is commonly combusted in small-scale heating and cooking appliances. The application of such fuelwood is fundamentally in response to the origin of the fuel material with the majority of logs combusted within residential appliance coming from a "grey market" and maintain no certification or

control on fuel properties including moisture content (BEIS, 2016). Such practices are likely to result in the formation of varied gaseous and particulate carbonaceous species commonly associated with respiratory disorders and climate forcing. Combustion of fuels at optimum moisture conditions is therefore desirable to inhibit detrimental effects commonly attributed to such emissions. The purpose of this study is to evaluate the effect of fuel moisture content on pollutant formation and stove efficiency in this context. The findings of the preliminary study (Chapter 5) identified gaps within the emission inventory which aimed to assess the impact of moisture on emissions. Additional testing is therefore required to fully quantify this process. Furthermore, the study examines how the subsequent changes in combustion conditions result in differences in the structure and composition of derived soot materials.

6.2 Materials and Methods

6.2.1 Fuels

Combustion experiments were undertaken using 'low-moisture' and 'high-moisture' hardwood beech (Fagus sylvatica L.) logs [Ashtrees Ltd, Leeds, West Yorkshire] as a principal fuel. The moisture content of the 'low-moisture' fuel was 12.4±0.2% and was prepared following a kiln-drying method for a period of 24 hours at 50°C in accordance with HETAS and Woodsure certification. The 'high-moisture' fuel maintained a moisture content of 23.6±2.6% and was prepared following a short seasoning period. The moisture content was determined using two methods:

i.   oven-drying method to a maximum temperature of 105°C based on BS EN 18134-1

ii.   using a digital moisture meter as previously described in Price-Allison et al. (2018).

All bark on the fuelwood logs was removed so as to mitigate potential sources of contamination and increased emissions from secondary sources (Obernberger et al., 2006; Phillips et al., 2016). Finally, fuel particles where cut to an average length and width of 224±1.4mm and 80±1.2mm respectively.

6.2.2 Combustion Experiments

Combustion testing was undertaken on a HETAS approved Waterford Stanley Oisin multi fuel heating stove. A review of the combustion testing facility, procedure and instrumentation is presented in **Chapter 3**.

Each experimental procedure generally consisted of three warm-start test batches with each burn consisting between 1132 g and 1454 g of fuelwood. The mass of fuel within the stove was selected based on the inherent moisture content in accordance with BS EN 13240. Particulate sampling using the manual-suction pump device was undertaken in a separate testing series whereby dry-fuel and wet-fuel where subsequently applied following burnout. The Cold-start testing was undertaken using a mixture of dried fuelwood with kindling or an alternative dried fuel [briquetted biomass, Hotmax] with ignition achieved using a kerosene-based firelighter [Zip, High Performance]. As such, cold-start data is disregarded and is not evaluated in this work. The point of fuel reloading was selected based upon the mass of unburned fuel and bottom ash present upon the grate.

The sampling of entrained soot within the flue gas was undertaken using two methods:

i.   Total soot (PM_t) sampling was undertaken under diluted conditions using a heated (30°C) impactor [Dekati, PM_{10}] with a pump and flow controller [Bronkhorst, Mass View] at a sampling rate of 10.0±0.1 L/min. Particulate emissions were collected on 25mm greased aluminium foils for size fractions of ≥10 µm, 2.5-10 µm and 1.0-2.5 µm [CFG-225, Dekati]. A 50 mm micro-quartz backup filter with a pore size of 0.3 µm [Gilson, RF-360-050] was applied to collect PM emissions below 1.0 µm. Soot samples collected from the impaction method where applied for emission factor quantification (PM_t) and soot composition analysis.

ii.   A second method of soot sampling was undertaken within the flue using a small manual-suction pump device [Testo Smoke Pump] designed in accordance with DIN 51402 and ASTM D2156. The suction pump was applied within the flue and sampled a fixed flue gas volume of 1.63±0.07 m^3 across a 2-5 second period. Sample flue gas was drawn across a filter media where entrained soot particles where fixed with a sample taken every 2 min – 5 min.

6.2.3 Fuelwood Characterisation

Fuel analysis was undertaken via TGA using a sequential temperature program outlined BS EN 14774-3, BS EN 15148 and BS EN 14775. The elemental composition of the fuel was analysed using a CE Instruments Flash EA1112 analyser (CHNS) in accordance with BS ISO 17247. Fuel sampling and preparation was undertaken in accordance with BS EN 14780. A summary of the results are shown in **Table 6.1**.

Table 6.1 Proximate and Ultimate analysis of test fuel material.

Fuel Type	Beech Fuelwood	
VM% (%db)	75.8±0.4	
Ash%	10.5±0.6	
FC%	13.7±0.4	
Bulk MC% (%ar)	Dry Fuel	Wet Fuel
	12.4±0.2	26.7±2.6
HHV (MJ/kgdb)	18.2	18.2
LHV	11.8	14.6
C (%db)	46.1±0.6	
H	5.7±0.1	
N	0.4±0.01	
S	0.00*	
O	37.3±0.9	

*value is recorded below the detection limit; db indicates dry basis; ar indicates as received basis

6.2.4 Sample Analysis

Particulate sample material was collected via gravimetric sampling and impaction as presented in **Chapter 3**. Particulate colour and sample density analysis was undertaken using an X-Rite spectrodensitometer. The sample darkness was therefore calculated as (d) = 100 – L. The colour-shift of soot samples where estimated using GIMP GNU [2.8.14] image manipulation and analysis software and expressed using a red, green or blue (RGB) additive colour model (Nishad, 2013). The physiochemical structure of soot collected on micro quartz filter papers was analysed using a Renishaw inVia Raman Spectrometer. The Raman shift spectrum was evaluated in the range from 500 to 2500 cm^{-1}. In addition, Thermogravimetric analysis (TGA) was applied as a method of determining Elemental Carbon (EC) and Organic Carbon (OC) fractions within the soot using a Netzsch STA449 instrument. The composition of the organic soot fraction was determined by pyrolysis-GC-MS. An optical investigation of the soot particle morphology and physical structure was undertaking using a FEI Nova NanoSEM 450 device operating at 3 kV with energy dispersive x-ray spectroscopy (EDX). The absorption and light attenuation of highly organic soot and highly elemental soot was determined by way of ultra-violet visible spectroscopy (UV-Vis). A summary of the analytical techniques is provided in **Chapter 3**.

6.3 Results

6.3.1 Moisture Content Determination

As previously discussed, the moisture content of the fuelwood logs was determined following two methods:

i. Firstly, a representative sample was selected and heated at a temperature not exceeding 105 °C in accordance with BS EN 18134-1. The fuelwood samples continued to be heated until the change in measured mass loss reduced to less than 1% over a 24-hour period. The overall measured mass loss value determines the bulk MC% and incorporates all of the moisture within the sample material as identified in our previous work (Price-Allison et al., 2019).

ii. The second method of MC% determination was applied using a digital moisture meter [Valiant FIR421]. This method involves penetrating the fuel particle to a maximum depth of 5 mm with two electrode pins. An estimation of the MC% value is determined through measurement of the electrical resistance, or corresponding conductance, of the material between the two pins. The presence of a higher water content acts as a conduit for current transfer and, as a result, a lower resistance. The accuracy of the device is ±2% with a range of 6-48% water content. The analysis device is maintained and calibrated empirically by the manufacturer to ensure accuracy. This method was applied at six locations across the exposed surface of each fuelwood particle prior to combustion testing. **Figure 6.1** shows the distribution of moisture probe results and the range of bulk drying results for the low moisture and high moisture fuels. The bulk MC% value was determined to be 12.4±0.2 and 26.7±2.6 for low moisture and high moisture fuels respectively. The deviation of results is higher for wet fuelwood samples in response to the inhomogeneity of sample material.
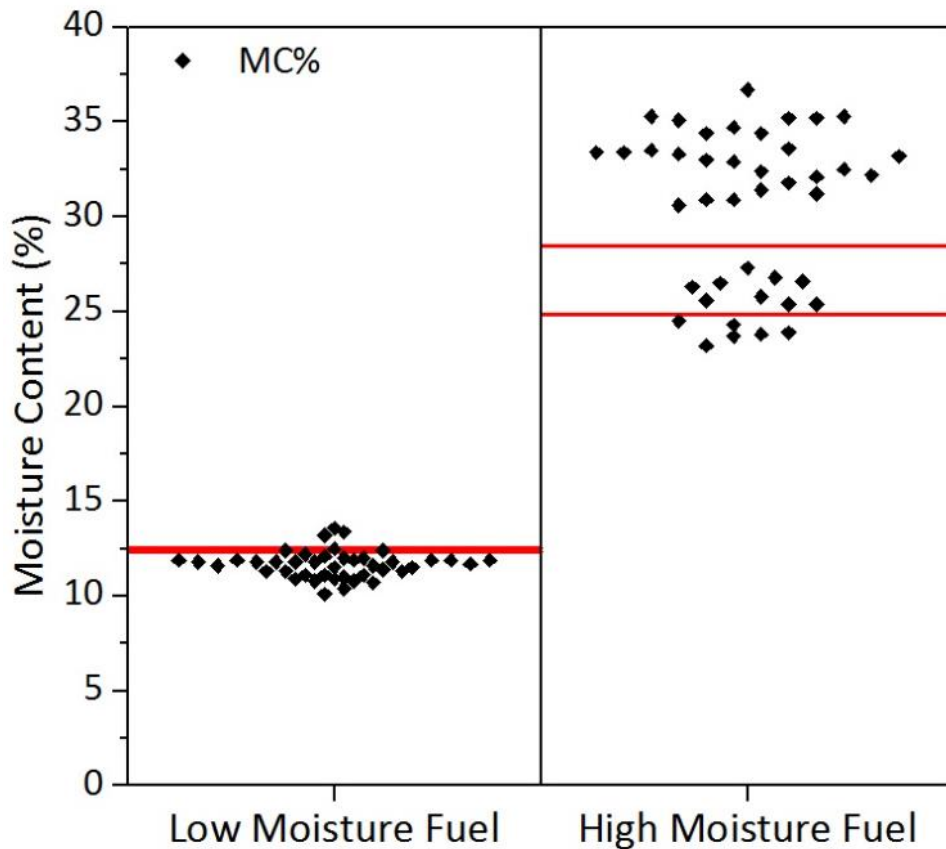
Figure 6.1 Distribution of fuelwood moisture content values using two methods of MC% determination. • indicates the moisture content as determined by the digital moisture meter. The horizontal lines (—) indicate the range of bulk moisture content values determined through drying the sample material at 105°C.

6.3.2 Burning Rate and Combustion Temperature

Monitoring of mass loss, combustion temperature and flue gas velocity allow determination of combustion conditions within the stove. Higher combustion temperatures generally correspond to an increase in the fuel conversion rate while lower combustion temperatures tend to correspond with detrimental combustion conditions (Alves et al., 2011; Fachinger et al., 2017). The flue gas temperature is taken as indicative of combustion temperature while burning rate (kg/hour) is calculated as a function of measured mass loss over time.

Fuel conversion rate is presented in two formats:

    i.   Firstly, the rate is shown on a min/min basis (**Figure 6.2**) so as to establish the variance in conversion during ignition, flaming combustion and smouldering phases.

ii.   Secondly, the rate is calculated on a complete batch basis for the
         purpose of comparing the effect of fuelwood moisture content across the
         complete combustion cycle (**Table 6.2**).

Burning rate is quantified as kg/hour on an 'as-fired' basis. The rate of conversion is shown to vary throughout the combustion experiment. Initially, there is a short period of slow burning which occurs during the fuel drying phase which varies significantly depending upon the moisture content of the fuel and the temperature within the firebox. This is followed by a period of rapid fuel conversion during the flaming phase prior to a period of slowed burning during the smouldering phase. Similar fuel conversion profiles are shown by Mitchell et al. (2016) and Maxwell et al. (2020) when burning fuelwood logs in the same domestic heating appliance. This process is similar for both dry fuelwood and wet fuelwood combustion. The rate of conversion appears to vary depending upon the moisture content of the fuel with the combustion of dry fuel generally corresponding with higher burning rates. A maximum burning rate of 6.6 kg/hour and 3.6 kg/hour was observed during dry fuelwood and wet fuelwood combustion respectively. The burning rate was shown to increase on a batch-basis with a reduction in the fuel moisture content as presented in **Table 6.2**. The rate of conversion increases after each consecutively applied batch of fuel when the moisture content is low. However, the opposite effect is observed when the moisture content is high. The reduction in burning rate following subsequent batch addition, when applying a wet fuel, is likely a consequence of the cooling effect of water vapourisation and subsequent energy loss associated with the enthalpy of vapourisation. The rate of conversion is affected by a number of variables including reactivity of the fuel particle, oxygen availability and surface area. However, combustion temperature is likely to be the primary control (Price-Allison et al., 2019).
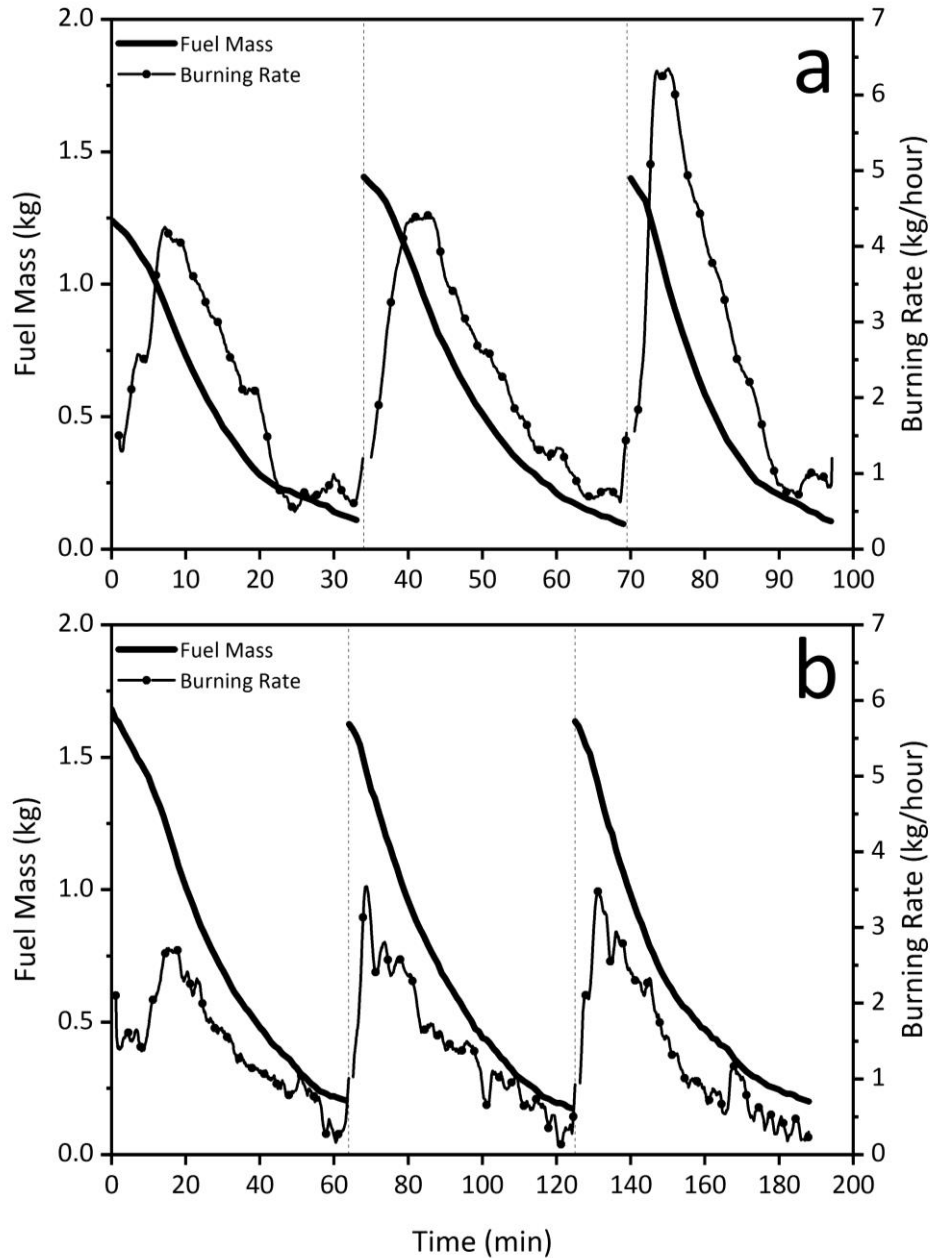
Figure 6.2 Measured mass loss (kg) and derived fuel conversion rate (kg/hour) during the combustion of: a) low moisture and; b) high moisture fuel. --- identifies periods of fuel reloading.

The temperature within the combustion zone is variable and controlled by a number of factors previously described. There is a difficulty in measuring combustion temperature inside the stove, principally because of the dynamic variability of the combustion reaction. Since the flue gas temperature can be measured more consistently, it may be taken as a proxyindicator for the conditions within the firebox. This approach is consistent with other studies in the literature (Lamberg et al., 2011; Fachinger et al., 2017; Price-Allison et al., 2019). Corresponding with burning rate, the heat release from a fuel particle varies depending upon the phase

of combustion. Following reloading, the slowed combustion reaction caused by the presence of moisture within the fuel leads to a reduction in both burning rate and temperature. During the fuel particle ignition and devolatilisation phases the temperature increases to a peak in the presence of flames followed by a period of cooling during smouldering. This process occurs during the combustion of both wet and dry fuel however the presence of water content within the fuelwood particles inhibits the combustion reaction and, as a result, reduces the temperature. Maximum temperatures of 605°C and 355°C were observed during dry fuelwood and wet fuelwood combustion respectively. Furthermore, the average temperature was notably higher during the combustion of dry fuelwood when compared with fuelwood with a higher moisture content (**Table 6.2**). In a similar pattern as observed with the burning rate, the peak combustion temperature increases for each subsequent batch of dry fuelwood while a reduction in temperature occurs for each subsequent batch of high moisture fuel. This is consistent with the higher energy loss resulting from the drying (enthalpy of vapourisation) of high moisture fuels and the cooling effect of water vapour within the combustion zone.

Table 6.2 Variation in fuel burning rate and flue gas combustion temperature between test batches for high moisture and low moisture fuelwood. Burning rate, combustion temperature and oxygen concentration are measured on a complete batch basis.

Test Number	Low Moisture Fuel			High Moisture Fuel		
	Burning Rate (kg/hour)	Temperature (°C)	Oxygen (vol-%)	Burning Rate (kg/hour)	Temperature (°C)	Oxygen (vol-%)
TB1	2.0	394.9	15.8	1.4	289.9	16.22
TB2	2.2	421.7	14.8	1.4	288.2	14.8
TB3	2.9	472.9	11.1	1.4	271.0	13.6
Average	2.4±0.4	429.8±39.6	13.9	1.4±0.03	283.0±10.5	14.9

The average Combustion temperature is shown to vary depending upon the inherent moisture content of the fuelwood particles where an increase in moisture content generally corresponds with a reduction in temperature. **Figure 6.3** identifies the relationships between combustion temperature and burning rate and flue gas velocity for both dry and wet fuelwood. Variation in the flue has velocity may be applied as an indicator of change in the pyrolysis product retention time within the combustion zone. Generally, an increase in combustion temperature corresponds with an increase in the burning rate and the flue gas velocity. Pearson's correlation

analysis indicates a coefficient of 0.981 for temperature and burning rate. Similarly, a correlation coefficient of 0.986 is indicated for temperature and flue gas velocity. These correlations of temperature with fuel conversion rate and flue gas retention time are shown to be statistically significant to a level of $P<0.01$.
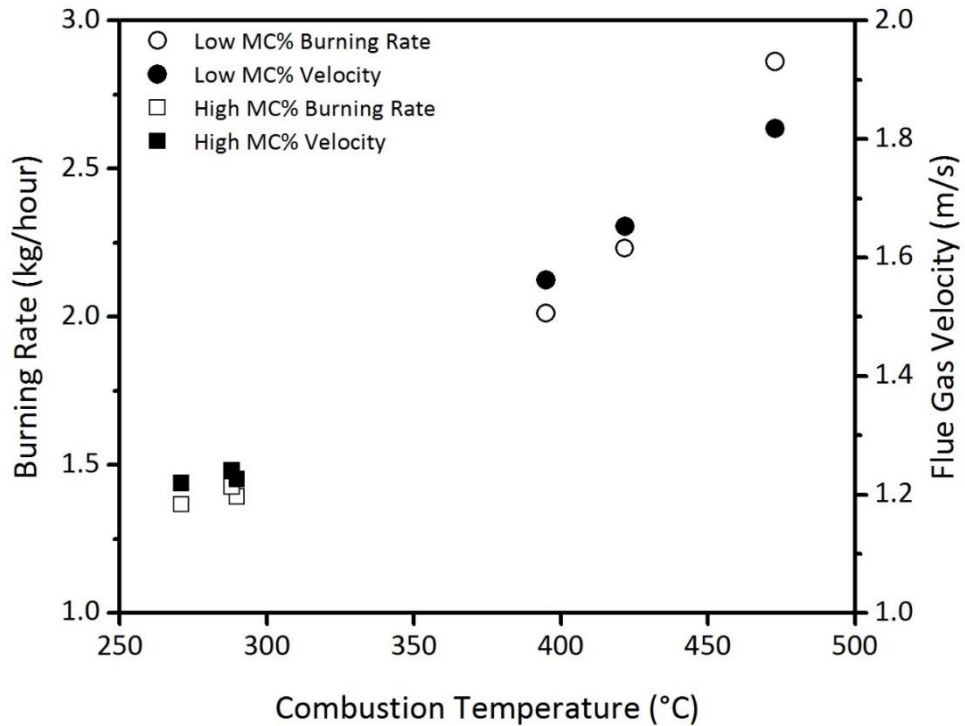
Figure 6.3 Comparison of the effect of flue gas temperature on burning rate and flue gas velocity for low moisture and high moisture fuelwood.

6.3.3 Combustion Efficiency

The fuel conversion efficiency is calculated as the MCE as identified in **Chapter 3** and presented within the literature (Yokelson et al., 1996; Fachinger et al., 2017). **Figure 6.4** shows the variation in MCE and CO_2 concentration during the combustion of low moisture fuelwood (a) and high moisture fuelwood (b). During the combustion of dry fuel, the MCE follows a distinct and repeatable trend whereby efficiency increases to a peak following ignition and the onset of flaming combustion. A plateau period is then presented during flaming combustion often beginning during the point of peak combustion temperature. A steep decline in MCE and CO_2 is subsequently observed following the end of the flaming phase and during the onset of smouldering combustion (Fachinger et al., 2017). The prolonged plateau period suggesting improved combustion conditions results in an MCE of 0.94, 0.96 and 0.94 for TB1, TB2 and TB3 respectively. The average MCE observed during the combustion of dry fuelwood is 0.94±0.01. Alternatively, during the combustion of wet fuel, the MCE and CO_2 concentration is shown to oscillate

with poor repeatability between test batches. Following ignition, a steep rise in MCE and CO_2 is presented in response to the presence of a flame within the combustion zone. No stabilisation or plateau phase is presented in response to a prolonged drying period and extended phases of smouldering combustion. In addition, the CO_2 concentration is shown to be significantly lower than that observed during the combustion of dry fuelwood. Periods of heavy smouldering with limited flaming result in high CO formation where the CO_2 concentration is negligible thereby inhibiting the application of MCE for determining efficiency. Oscillation in MCE also occurs in response to manual manipulation of the fuel bed undertaken so as to maintain the combustion reaction. An increase in the fuel moisture content results in an increased drying period and a reduction in the combustion temperature contributing in the onset of a smouldering-type combustion reaction. A low MCE of 0.92, 0.89 and 0.87 is therefore observed during the combustion TB1, TB2 and TB3 respectively. The average MCE observed during the combustion of wet fuelwood is 0.89±0.03.
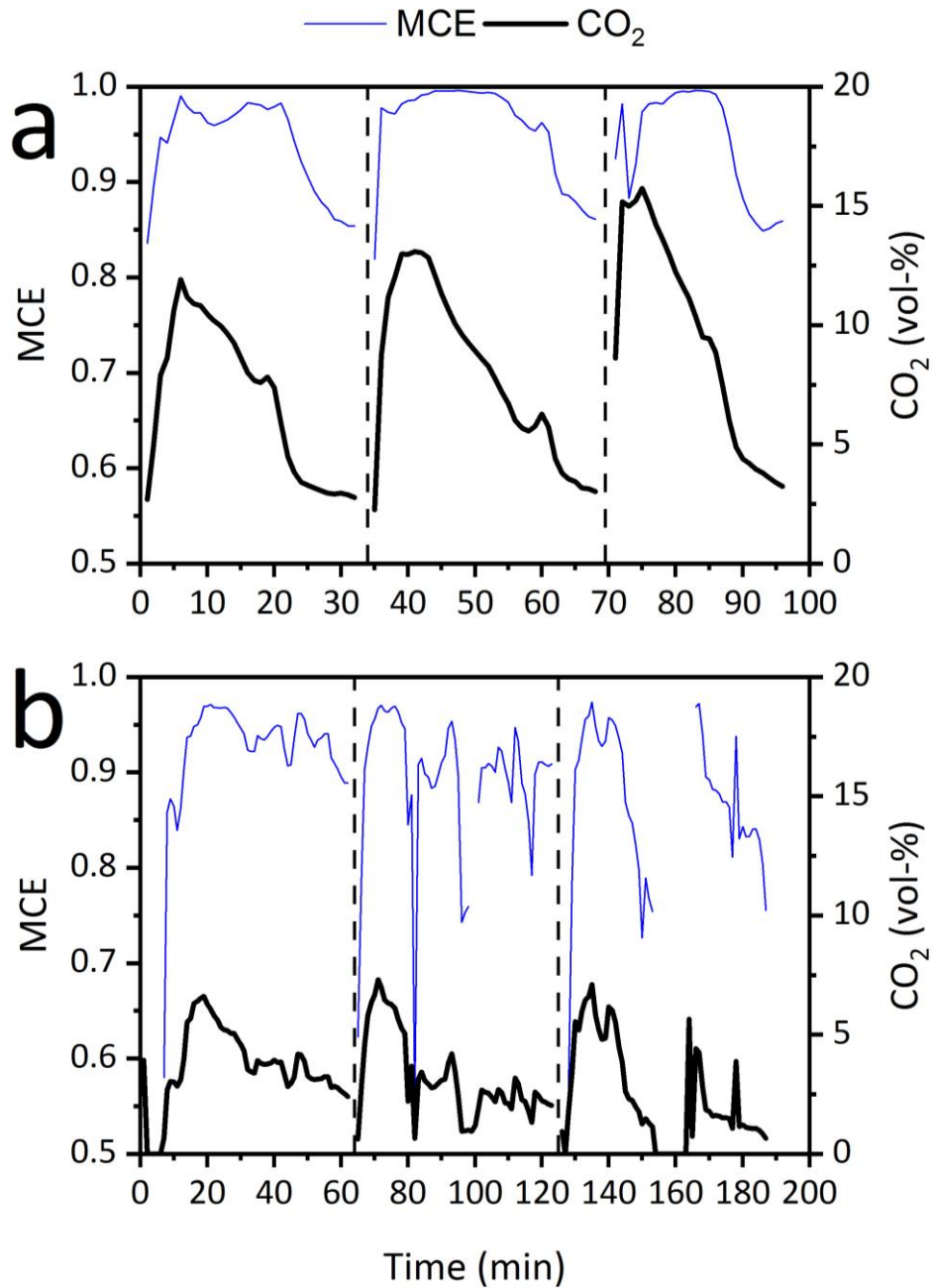
Figure 6.4 Variation in modified combustion efficiency (MCE) and CO_2 formation during the combustion of low moisture fuelwood (a) and high moisture fuelwood (b).

6.3.4 Gaseous Emissions

Gaseous emissions monitoring was undertaken during the combustion of each batch of fuel and during each phase of particle combustion as such incorporating aspects of ignition, flaming combustion and smouldering. **Figure 6.5** presents the emissions measurements for organic and inorganic gaseous species in mg/Nm^3. It should be noted that pollutant species identified as benzene (C_6H_6) and Formaldehyde (CH_2O) are likely to include a series of other trace species. The

nature and pattern of the emission profiles were found to generally correspond with similar measurements presented in earlier works (Pettersson et al., 2011; Maxwell et al., 2020). There is a 120 second data-gap in the emission profile at the point of manual reloading. The measurements in this period are invalidated by the effect of air inundating the firebox while the stove door is opened. During the combustion of dry fuelwood, the CO concentration measurements follow a typical profile whereby formation is low during the flaming phase and higher during particle ignition and smouldering. During the combustion of wet fuelwood, the CO concentration measurements show a different profile, remaining high throughout the combustion cycle with the highest pollutant formation following fuel addition. This is primarily due to the higher MC% content of the fuel particles and the prolonged drying period required prior to ignition. CO formation is therefore generally higher throughout the combustion cycle where combustion temperatures are inhibited during the flaming phase (Vakkilainen, 2017).

Nitric oxide formation is observed to be variable throughout the combustion cycle with higher emissions during periods where the rate of fuel conversion was highest (**Figure 6.5**). NO is the most common nitric species in the flue gas composition and incorporates 90% of total NOx. Fuel bound NOx is considered the most common route of formation and is derived from the conversion of nitrogen within the fuel composition to NO and NO_2 (Glarborg et al., 2003; Koppejan and Loo, 2008; Bugge et al., 2020). The process of conversion is known as the fuel NOx mechanism and involves the thermal decomposition of nitrogen-containing compounds within the fuel during devolatilisation. The combustion of fuels with a higher $Fuel_N$ composition, such as coal and peat (0.5-2.5%), generally corresponds with increased NOx formation when compared to low $Fuel_N$ materials such as fuelwood (0.003-1.0%). NO formation is shown to be similar during the combustion of wet and dry fuelwood with formation following a similar trend to the fuel particle burning rate. Formation is generally highest during the flaming phase and lowest during smouldering. However, the total formation is shown to be unaffected by combustion temperature where the correlation coefficient (r) for the combustion temperature and emission factor is 0.693. Total NOx formation is therefore unlikely to be affected by alternative routes of formation, including the thermal NOx mechanism, as the combustion temperature remains relatively low (<1400 °C) (Bugge and Haugen, 2014). Instead, formation is affected by the burning rate and subsequent rate of devolatilisation of the fixed nitrogen content within the fuel. Given the uniformity of the fuel nitrogen content, only the rate of NO formation appears to vary. Similarly, SOx formation is derived from the fuel sulphur content with SO_2 identified as the principal pollutant species. During typical stove operation between 57-65% of fuel sulphur may be released and entrained within the flue gas while

between 35-43% remains within the char (Houmoller and Evald, 1999). As with NOx formation, the rate of SO_2 emittance is paralleled with the fuel conversion rate however there is some correspondence with the combustion temperature where the correlation coefficient (r) for the relationship between the combustion temperature and SO_2 formation is 0.818. Variation between SO_2 emissions is presented during the combustion of dry fuelwood and wet fuelwood samples with the former generally associated with higher concentrations.

Concentrations of gaseous organic species are shown to vary throughout the combustion cycle. Formaldehyde (CH_2O) and Acetic acid ($C_2H_4O_2$) formation generally peak immediately following stove reloading with a subsequent reduction throughout the flaming and smouldering phases. The trend appears similar during the combustion of dry and wet fuelwood however concentration of these species is significantly higher for the latter. The average organic concentration was found to be 130 mg/Nm^3 for Formaldehyde and 214 mg/Nm^3 for Acetic acid during the combustion of wet fuelwood. The concentration was shown to be significantly lower during dry fuelwood combustion testing where the average formation was 17 mg/Nm^3 and 23 mg/Nm^3 for Formaldehyde and Acetic acid respectively. Differences between the trends are likely a result of variation in combustion temperature with moisture content acting as an inhibitor. Spikes in the pollutant emission concentrations are likely to be a result of delayed ignition following reloading. This results in the fuel being heated and undergoing devolatilisation before ignition of the gases and the appearance of flaming combustion. The devolatilisation contributing in heavy production of smoke which further inhibits ignition. Such processes are less pronounced during the combustion of dry fuel in response to the reduced drying period. Similar trends are observed for hydrocarbon species where emission concentration is shown to mirror that of the organic species indicating similar causation with regards to reloading, delayed ignition and combustion temperature. Methane (CH_4) and Benzene (C_6H_6) were shown to be the most prevalent hydrocarbon emissions during the combustion of both dry and wet fuelwood. Furthermore, hydrocarbon emission concentrations are generally shown to be lower with an increase in the molecular mass (g/mol) of the gaseous species. For example, Methane with a mass of 16.04 g/mol is found in abundance while the heavier hydrocarbons including Hexane (86.17 g/mol) are only found at trace levels. A number of mid-batch peaks are observed which are evidence of the inherent variability in combustion conditions. Consistent with previous work, wet fuel appears to produce high emissions throughout the combustion cycle with high concentration of organic and hydrocarbon species identified during the cooler smouldering phase. The high moisture content in the wet fuel inhibits fuel particle heating leading to

unreactive biomass fractions retaining volatile constituents for a prolonged period under heating (Price-Allison et al., 2019).
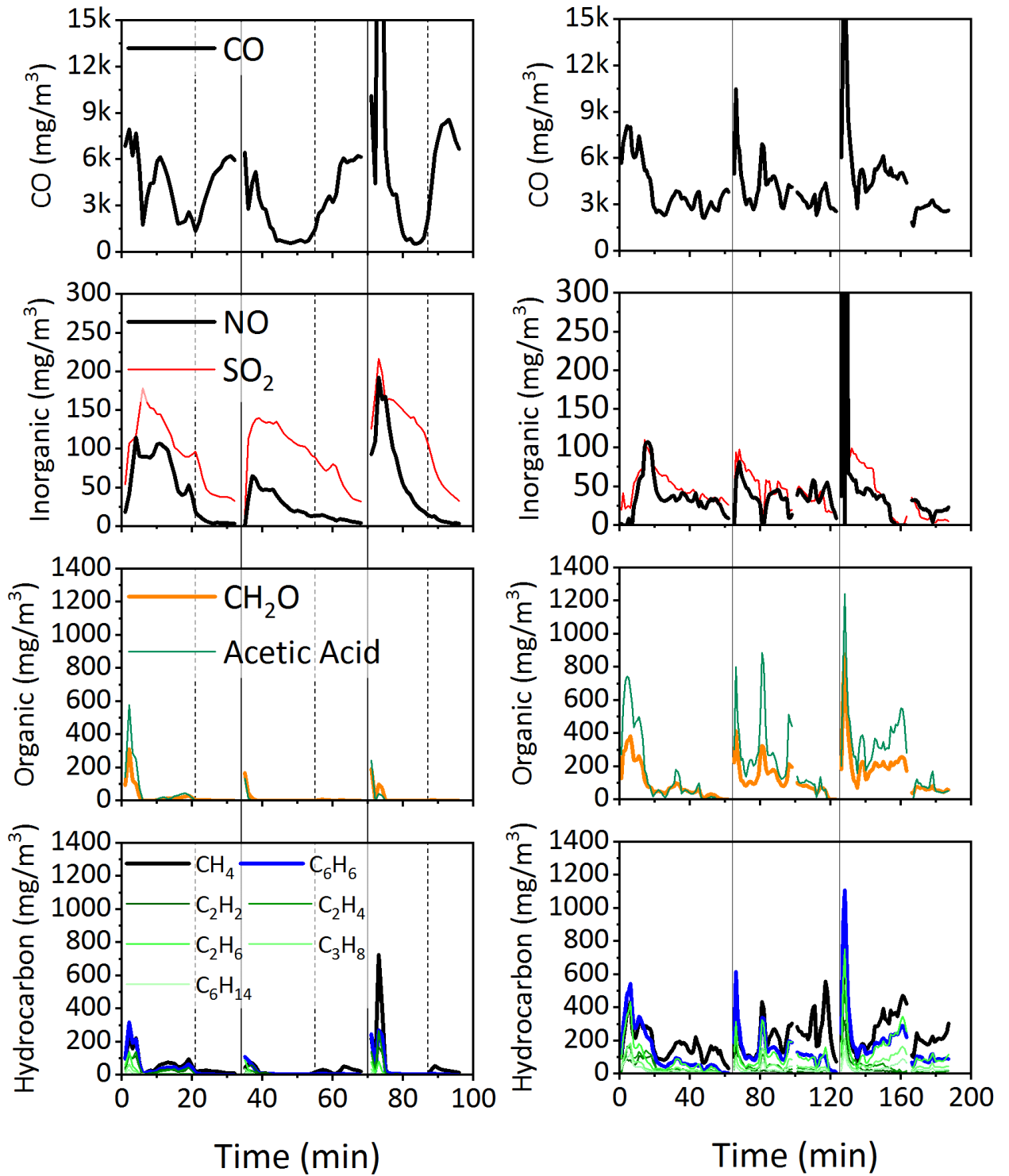
Figure 6.5 Gaseous emission concentrations (mg/Nm$^3_{db}$) for (a) low moisture fuelwood and (b) high moisture fuelwood. Solid vertical line indicates the point of fuel reloading. Dashed vertical line indicates the shift from the flaming phase to the smouldering phase.

Gaseous emission factors were calculated for each of the pollutant species using a total flow method as identified in **Chapter 3**. The values are presented in grams of pollutant per kilogram of dry-fuel combusted (g/kg_{fuel}) and are calculated on a complete batch basis thereby including aspects of ignition, flaming combustion and smouldering. **Table 6.3** presents the numerical average emission factors calculated for the three test batches where the stated error is the standard deviation of the sample. The standard deviation (σ) is quantified as the square root if the variance.

A scaling factor is calculated to numerically quantify the variation in average emission factor values between fuel types. The factor is calculated as a ratio of the emission factor from high moisture combustion and low moisture combustion ($EF_{High}:EF_{Low}$). The variation is the pollutant emission factor values follow a similar trend to that presented in the emission concentrations. Carbon monoxide is shown to be higher during wet fuel combustion in response to reduced flaming and prolonged smouldering phases. Organic and hydrocarbon species are also shown to be higher during wet fuel combustion in response to reduced combustion temperatures with CH_4, C_6H_6, CH_2O and Acetic acid the predominant species. In all cases, gaseous pollutant species derived from wet fuelwood combustion were higher with scaling factors within the range of 12-15 for organic species and 3-23 for hydrocarbon species. The formation of hydrocarbon pollutants appears to be influenced by the combustion temperatures and the molecular weight of the species with larger (heavier) products generally only present in trace quantities. CH_4 is the most prevalent alkane species with the lowest molecular mass and saturated bonds. Products with a higher molecular weight correspond to lower levels in the gaseous mixture, likely as a result of the thermal cracking of compounds. Higher molecular weight compounds including C_3H_8 and C_6H_{14} are less stable and more likely to be degraded under heating, thus leading to the formation of small alkane and alkene chains. Alkene compounds, C_2H_2 and C_2H_4, are less chemically stable and are a precursor to C_6H_6 and soot formation (Damodara et al., 2017).

Table 6.3 Numerical average emission factor values calculated from the complete combustion cycle for low and high moisture fuelwood in g/kg$_{fuel}$

Pollutant Species	Molecular Weight (g/mol)	Low Moisture Fuel (12.44%)	High Moisture Fuel (26.68%)	Scaling Factor (EF$_{High}$/EF$_{Low}$)
CO	28.01	57.80±13.70	102.80±12.72	1.78
SO$_2$	64.06	0.52±0.20	0.94±0.18	1.81
NOx	30.01	1.30±0.08	1.11±0.11	0.85
CH$_4$	16.04	0.61±0.28	5.39±1.33	8.84
C$_2$H$_6$	30.07	0.12±0.05	2.70±1.04	22.50
C$_2$H$_4$	28.05	0.21±0.15	1.14±0.21	5.43
C$_3$H$_8$	44.10	0.07±0.04	1.19±0.46	17.00
C$_6$H$_{14}$	86.17	0.04±0.02	0.61±0.22	15.25
C$_2$H$_2$	26.04	0.23±0.13	0.69±0.14	3.00
C$_6$H$_6$	78.11	0.44±0.23	3.68±1.02	8.36
CH$_2$O	30.03	0.26±0.15	3.13±1.07	12.04
C$_2$H$_4$O$_2$	60.05	0.35±0.35	5.15±1.60	14.71

The behaviour of emission concentration profiles is shown to be dependent upon the combustion temperature. Combustion temperatures are shown to be higher during the combustion of dry wood as a result of lower energy loss during fuel particle drying and heat transfer within the subsequent water vapour matrix. **Figure 6.6** presents the correlation between combustion temperature and emission formation of organic and hydrocarbon species. Combustion temperatures are determined as an average of the flue gas temperature throughout the combustion cycle for each batch of fuel applied thereby incorporating periods of ignition, flaming combustion and smouldering. Analysis of the Pearson correlation coefficient (r) between temperature and emission formation shows a statistically significant correlation where an increase in temperature leads to a reduction in pollutant: CH$_2$O: 0.913, C$_2$H$_4$O$_2$: 0.926, CH$_4$: 0.925, C$_6$H$_6$: 0.928, C$_2$H$_2$: 0.899, C$_2$H$_4$: 0.927, C$_2$H$_6$: 0.899, C$_3$H$_8$: 0.901, C$_6$H$_{14}$: 0.915. Average combustion temperatures are shown to be significantly higher during the combustion of dry fuelwood (**Table 6.3**). Fuel moisture content is shown to inhibit combustion temperature which, in turn, leads to an increase in gaseous pollutant formation.
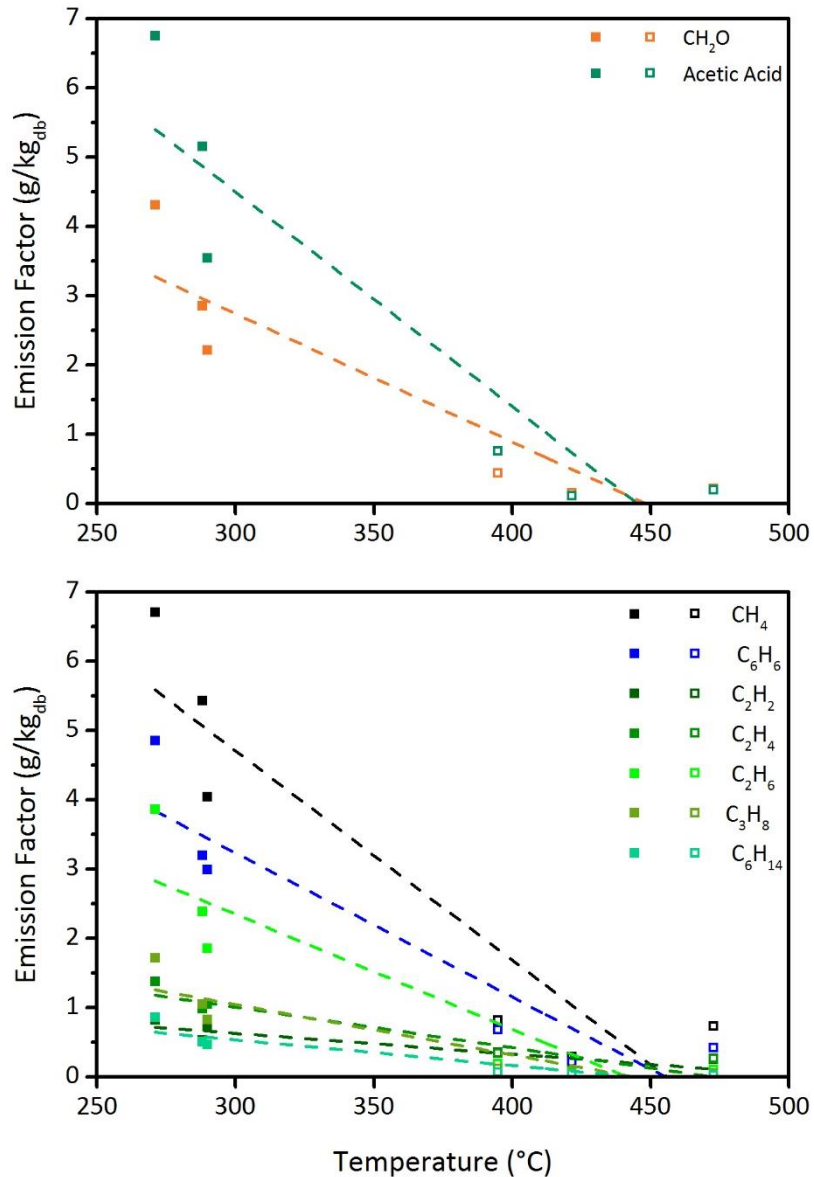
Figure 6.6 The impact of combustion temperature upon organic (a) and hydrocarbon species (b) pollutant formation. Plotted results present the variation in temperature and emission formation trends for both higher moisture fuelwood ■ and low moisture fuelwood □.

6.3.4.1 Flue Gas Condensate Analysis

Entrained gaseous combustion products were extracted from the flue at a rate of 10.00 L/min via a gas sampling unit [Gasmet, Portable Sampling System] and condensed in deionised water via a chilled impinger system. Condensate collection was undertaken throughout the combustion experiment incorporating both pre-test phase products and gaseous compounds generated during the combustion of subsequent test batches. A summary of the condensate analysis is presented in **Table 6.4**.

Table 6.4 Concentration of organic compounds in mg/L sampled within fuel gas condensate

Condensate Composition	Chemical Formula	Molecular Mass (g/mol)	Low Moisture Fuel (12.44%)	High Moisture Fuel (26.68%)
pH	-	-	3.6	3.27
TOC	-	-	396.1±0.8	1727.5±13.0
Total Phenols	-	-	31.5±0.5	80.0±2.3
Acetic Acid	CH_3CO_2H	60.05	143.1±25.9	109.9±0.1
Propanoic Acid	$CH_3CH_2CO_2H$	74.08	10.5±5.1	28.9±0.2
Isobutryic Acid	$C_4H_8O_2$	88.1	3.2±0.2	8.8±0.2
Butyric Acid	$C_4H_8O_2$	88.1	1.5±0.2	6.0±0
Isovaleric Acid	$C_5H_{10}O_2$	102.13	2.2±0.5	3.9±1.0
Valeric Acid	$C_5H_{10}O_2$	102.13	1.8±0.1	0.8±0.1
Isocaproic Acid	$C_6H_{12}O_2$	116.16	2.0±0.1	1.9±0.1
Caproic Acid	$C_6H_{12}O_2$	116.16	1.9±0.6	0.5±0.1
Heptanoic Acid	$C_7H_{14}O_2$	130.18	3.5±1.0	10.6±0.3
Organic Acid	Total	-	169.7	171.2

The total organic carbon (TOC) content of flue gas condensate was analysed using nondispersive infrared analysis (NDIR). TOC is identified as the total concentration (mg/L) of all organic carbon containing compounds in a condensate sample. Organic carbon molecules are described as compounds containing carbon bonded with hydrogen and often including oxygen. Organic carbon species may include protein, sugar, fat, alcohol and hydrocarbon formations. In the context of condensate derived from biomass combustion emissions the sample matrix is likely to include a mixture of methyl group hydrocarbons, carboxyl group acid compounds and alcohols derived from the thermal degradation of cellulose and lignin during the combustion reaction. **Figure 6.7** presents the concentrations of TOC generated during the combustion of low moisture and high moisture fuelwood. As previously described, increased fuelwood moisture content leads to adverse combustion conditions resulting in increased pollutant formation. TOC formation is shown to be higher during the combustion of wet fuelwood by a factor of 4.4. These results correspond with increased pollutant formation identified in the gas phase as a result of reduced temperatures in the combustion zone.
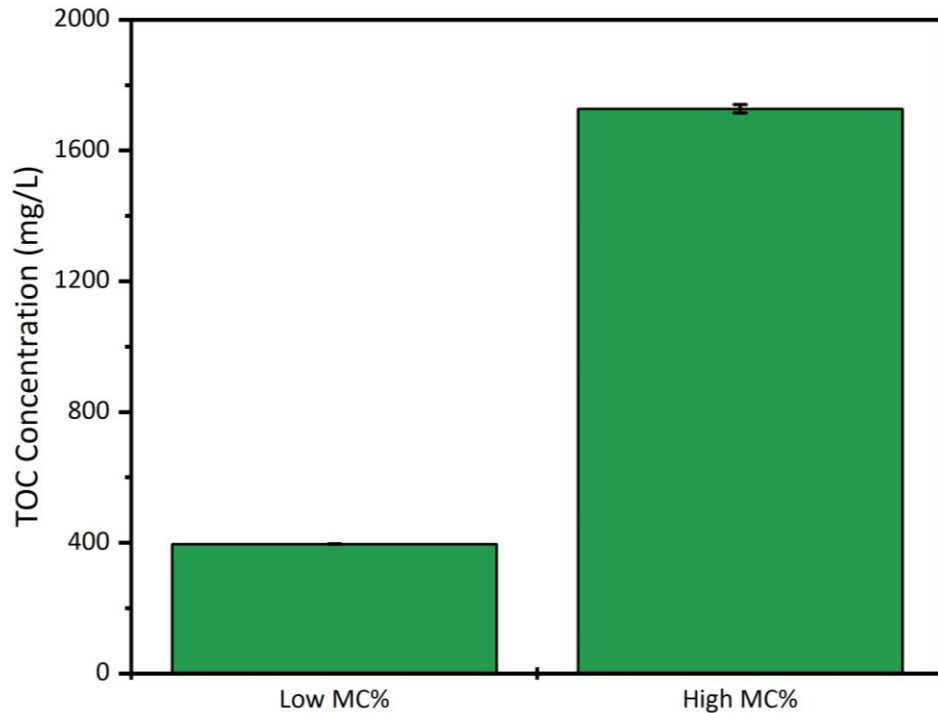
Figure 6.7 Total Organic Carbon (TOC) concentration of flue gas condensate collected during the complete combustion run

Total phenolic content was identified by mixing with 4-aminoantipyrine ($C_{11}H_{13}N_3O$) resulting in a colour-shift within the solution and quantified via spectrophotometry. Phenolic molecules are identified as cyclic compounds including aromatic hydrocarbon rings bonded with phenyl hydroxyl groups (-OH) or associated radical compounds (Dyakov et al., 2007; Clarke, 2008). Phenolic compounds in woodsmoke have been shown to include a complex mixture of methylphenols and nitrophenols generated during the thermal degradation of lignin in woody biomass (Faix et al., 1990; Kjällstrand and Petersson, 2001; Li et al., 2020). Nitrated phenolic compounds are identified as a common product associated with the incomplete combustion of biomass or in response to the oxidation of phenolic precursors (Li et al., 2020). Such products are attributed with phytotoxic properties presenting detrimental effects on human and plants (Huang et al., 1995; Harrison et al., 2005; Morville et al., 2006). Phenolic molecule formation is in response to the pyrolysis of lignin within the parent fuel material. **Figure 6.8** presents the variation in total phenolic compounds generated during the combustion of low moisture and high moisture fuelwood. As previously described, an increase in the fuelwood moisture content leads to adverse combustion conditions resulting in an increase in pollutant formation. Total phenolic compound formation is shown to be higher during the combustion of wet fuelwood by a factor of 2.5. Under ideal combustion

conditions these molecules are consumed by the thermal reaction and oxidized. During the combustion of fuelwood maintaining a higher moisture content the combustion temperature is reduced resulting in incomplete combustion. Derived phenolic compounds are emitted as gaseous pollutants or within particulate emissions.
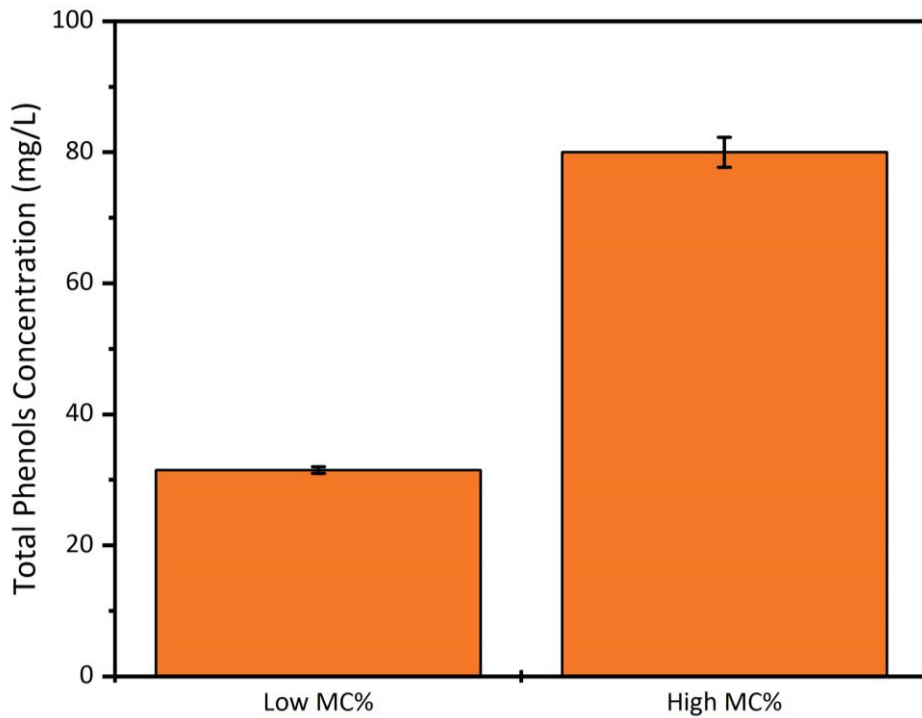
Figure 6.8 Total Phenolic concentration of flue gas condensate collected during the complete combustion run

Volatile Fatty Acid (VFA) compounds and simple alcohol condensates were determined using gas chromatography with flame ionisation detection (GC-FID). **Figure 6.9** presents the concentrations of VFA produced during the combustion of low moisture and high moisture fuelwood. A series of short-chain VFA's were identified within the sample matrix including propionic acid ($CH_3CH_2CO_2H$), isobutryic and butyric acid ($C_4H_8O_2$), isovaleric and valeric acid (C5H10O2), and acetic acid (CH_3COOH). Long-chain VAF's identified in the matrix included isocaproic and caproic acid ($C_6H_{12}O_2$) and heptanoic acid ($C_7H_{14}O_2$). The condensate collected during dry fuelwood and wet fuelwood combustion was found to be acidic with, approximately, pH 3.6 and pH 3.27 respectively. The total carboxyl acid concentration was found to be similar with dry fuelwood combustion producing 169.7 mg/L and wet fuelwood combustion producing 171.2 mg/L. VFA formation occurs in response to the thermal degradation of cellulose during the

pyrolysis of biomass within the combustion zone. The concentration of carboxyl acid species is shown to reduce with an increase in the molecular mass. Acetic acid, with a molecular mass of 60.05 g/mol, is presented as the most common organic acid within the condensate incorporating 84.3% and 64.2% of the total organic acid composition sampled during dry fuelwood and wet fuelwood combustion respectively. Propanoic acid (74.08 g/mol) is also predominant within the condensate equating to 6.2% during dry wood combustion and 16.9% during wet wood combustion. Lower combustion temperatures are observed during the application of fuels maintaining a higher moisture content. A higher fraction of long-chain VFA's maintaining a higher molecular mass are observed during the combustion of wet fuelwood. Such compounds are only observed in trace concentrations during the combustion of dry fuelwood in response to the thermal degradation of such molecules under higher operating temperatures.
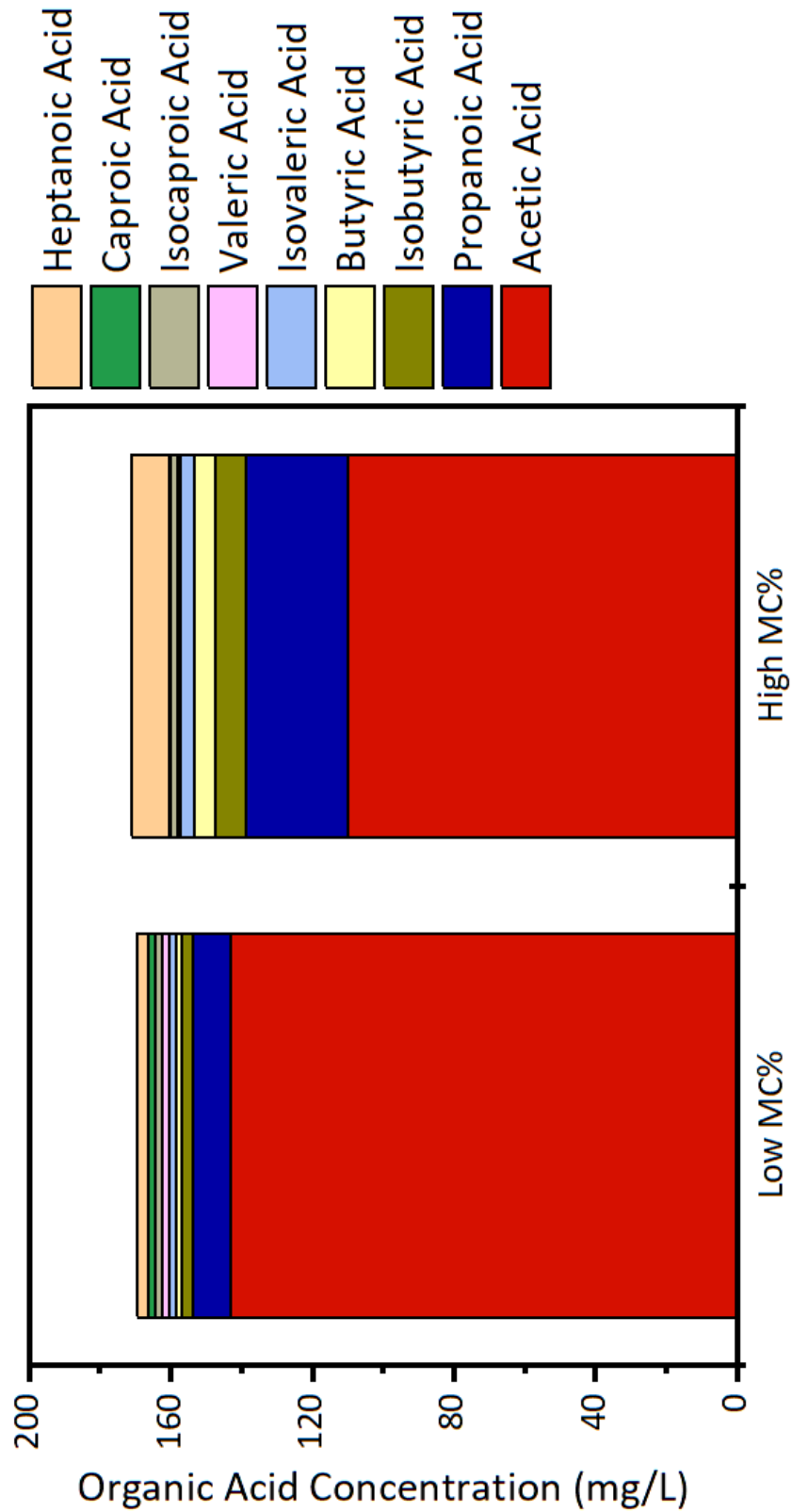
Figure 6.9 Flue gas condensate analysis for organic acid compounds collected during a complete combustion experiment. Sampling was undertaken during the pre-test batch and subsequent test batches at a rate of 10.0 L/min.

6.3.5 Particulate Emissions

Total particulate emission (PM_t) sampling was undertaken via impaction with size separation as per the specific gravity of aerosol constituents. Soot emission factors were found to vary during the combustion of low moisture and high moisture fuelwood with the former being lower by a factor of 2.9. Emission factors for each of the test batches are presented in **Table 6.5**. The average emission factors are shown to be 3.1±0.6 g/kg$_{fuel}$ and 9.3±4.9 g/kg$_{fuel}$ for low moisture and high moisture fuel respectively. In addition, the quantity of aerosol emission is shown to increase with each batch of fuel applied to the stove device; such processes appear prevalent for both dry and wet fuelwood combustion however the range of observed results is notably lower when the moisture content is reduced. Correlation is observed between average combustion temperature and oxygen availability (**Table 6.5**) and the increase in particulate formation following subsequent fuel addition signifying potential oxygen starvation and increased smoking under enhanced stove operating temperatures (Rogge et al., 1998; Shen, Wei, et al., 2012).
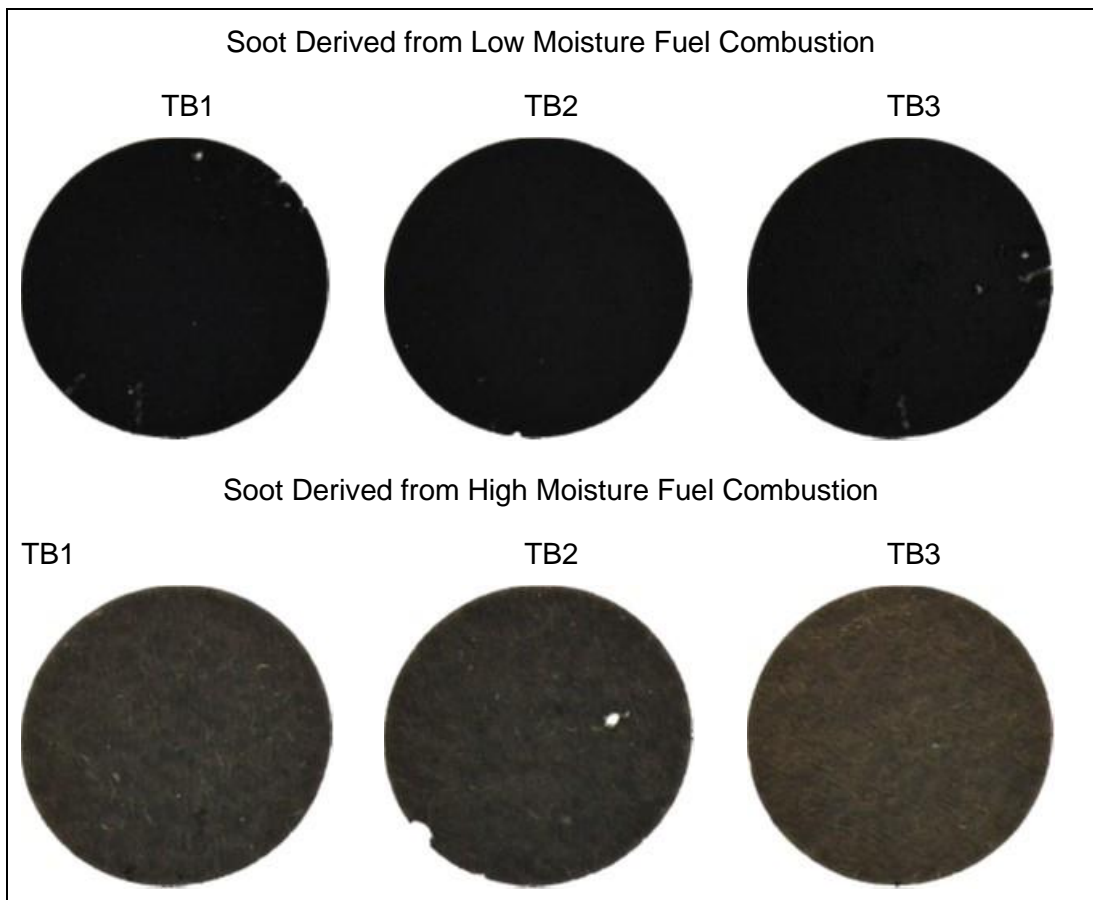
Figure 6.10 Soot samples collected via an impaction device showing the variability in colour caused by the combustion of low moisture and high moisture fuelwood.

6.3.5.1 Elemental Carbon/Total Carbon (EC:TC) Ratio

Analysis of the elemental and organic carbon fractions of sample particulate matter was undertaken on the $<PM_1$ soot fraction via thermal decomposition (**Figure 6.11**). A notable variation is observed between the elemental carbon and organic carbon fractions of soot derived from fuelwood of differing moisture contents. Low moisture fuel is shown to predominantly form EC, or black carbon, with a smaller OC, or brown carbon, fraction. The variation in the colour of soot samples is presented in **Figure 6.10**. The soot produced during wet fuelwood combustion has a much larger organic fraction with only trace fractions of EC. The EC fraction of soot is shown to increase with each batch of dry fuelwood applied to the stove. The increased fraction is as a result of increased combustion temperatures resulting in the thermal decomposition of the organic fraction within the combustion zone. Similarly, an increase in the OC fraction during wet fuel combustion is shown following subsequent reloading in response to a reduction in the combustion temperature.
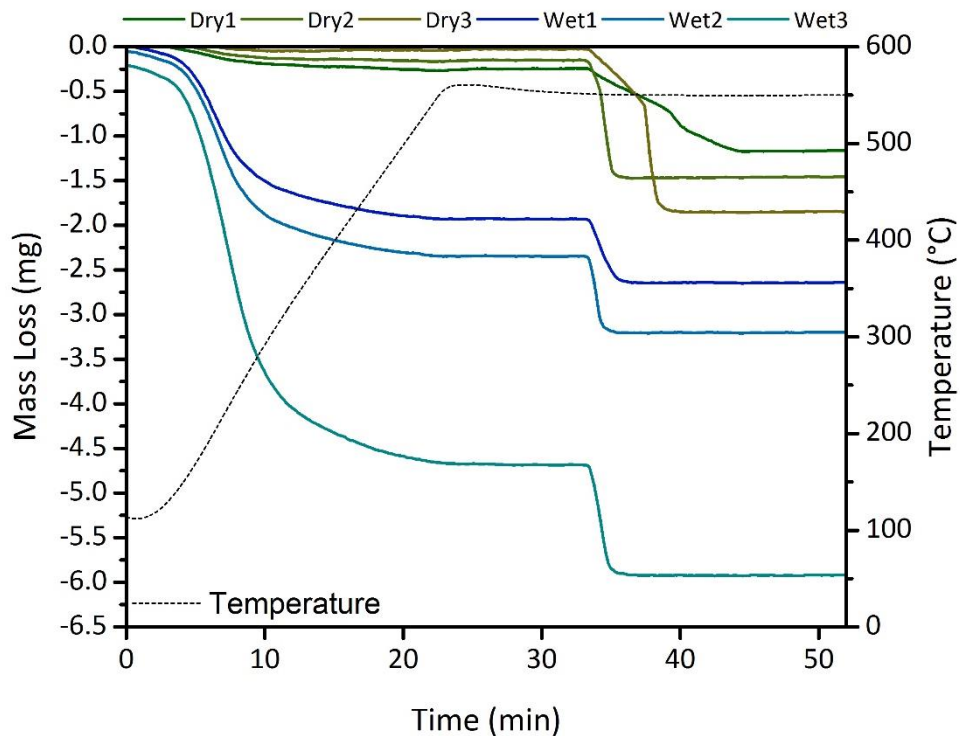
Figure 6.11 TGA results for soot samples collected during the combustion of low moisture and high moisture fuelwood batches. Mass loss is presented on a mass basis (mg) for the period of OC (105-550°C) in the presence of N_2 and EC loss (550°C) in the presence of air.

EC:TC may be applied as an indication of combustion efficiency with higher values corresponding with improved combustion conditions and higher temperatures. An

average EC:TC of 0.84±0.09 and 0.25±0.03 was calculated for dry fuelwood and wet fuelwood respectively. A statistical analysis of the correlation between combustion temperature and EC:TC revealed a Pearson r value of 0.990 which was statistically significant at the 0.01 level. As such, an increase in the ratio of EC and TC during the combustion of dry fuelwood suggests a larger fraction of the organic aerosol fraction being consumed under improved combustion conditions.

The observed colour shift in soot sample material is quantified across the RBG spectrum. Soot sample material collected during low moisture fuelwood combustion appears to present a black colouration with an average RGB value of 17.4, 17.6, 17.7. This colouration is very similar to absolute black where the RGB value is equal to 0, 0, 0. The colouration is shown to be similar for each of the soot samples derived for dry fuel combustion. Soot collected during the combustion of high moisture fuelwood presents a dark brown colouration. The average RBG value is shown to be 56.5, 51.8, 43.1 where absolute brown is shown to be 150, 75, 0. Some variation is presented in the colour shift for soot derived for high moisture fuelwood combustion and appears to correspond with variations in the EC:TC.

Table 6.5 Elemental Carbon and Organic Carbon composition of soot samples analysed via TGA. EC and OC values are presented on a mass basis (mg) and weight percent basis (wt. %) where TC=EC+OC.

| Fuel | ID | EF | EC | | OC | | TC | EC:TC | MCE | Colour |
		g/kg_{fuel}	%	mg	%	mg	%	a/b	a/b	RGB Shift
Low MC% (12.44%)	TB1	2.97	0.92	75.41	0.3	24.59	1.22	0.754	0.94	
	TB2	3.69	1.31	83.97	0.25	16.03	1.56	0.840	0.96	
	TB3	4.63	1.83	92.89	0.14	7.11	1.97	0.929	0.94	
High MC% (26.68%)	TB1	6.46	0.71	26.89	1.93	73.11	2.64	0.269	0.92	
	TB2	8.93	0.85	27.16	2.28	72.84	3.13	0.272	0.89	
	TB3	17.57	1.23	21.62	4.46	78.38	5.69	0.216	0.87	

Figure 6.12 presents the effect of efficiency on the formation of EC and OC (presented as EC/TC) by the combustion reaction. The combustion of wet fuelwood results in a reduction in the MCE resulting in lower EC/TC values. Alternatively, the combustion of dry fuelwood results in an increase in the MCE resulting in higher EC/TC values. **Figure 6.12** presents a generally linear correlation ($R^2 = 0.691$) between EC/TC and MCE whereby an increase in the former results in an increase in the latter. Pervez et al. (2019) presents similar findings during the combustion of solid fuel in a cookstove appliance where smouldering combustion was generally

associated with a reduction in MCE and a lower EC fraction. Alternatively, higher temperatures during flaming combustion, resulting in a higher MCE, are generally shown to correspond with an increase in the EC fraction (Reid et al., 2005; Pervez et al., 2019).
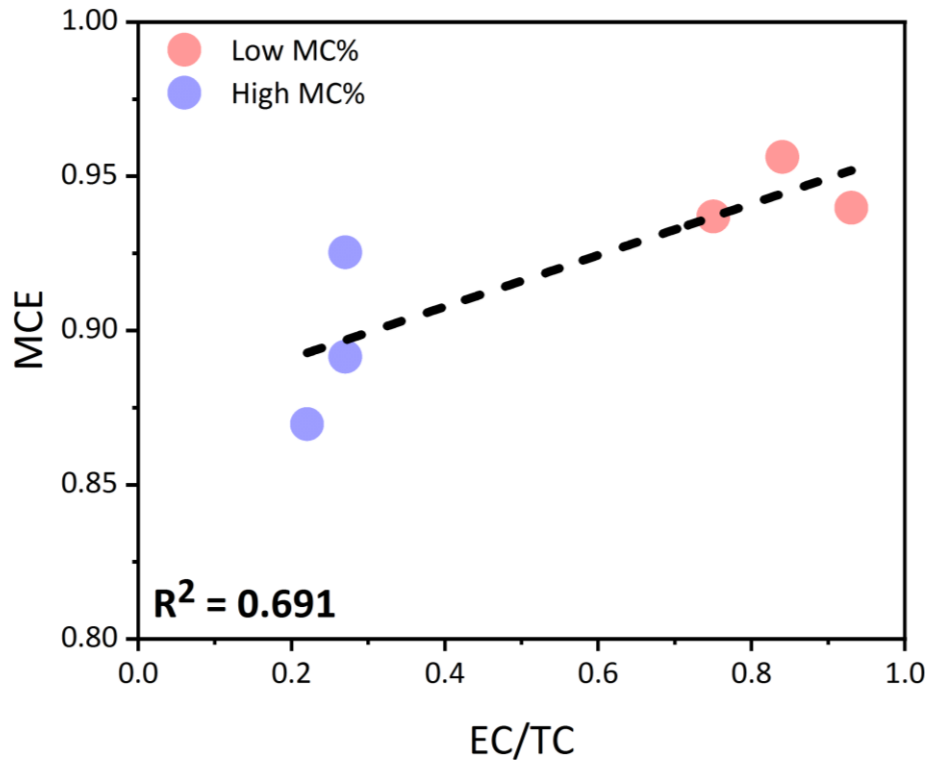
Figure 6.12 Correlation of EC/TC and the average MCE calculated on a complete batch basis.

6.3.5.2 Soot Particle Size Distribution

Previous work has identified the prevalence of the $<PM_1$ soot fraction which often incorporates more than 95% of the total aerosol composition (Price-Allison et al., 2019; Maxwell et al., 2020). Similar findings have been outlined within the literature whereby soot particles from biomass combustion were generally below 2µm (Oros and Simoneit, 2001). The dominance of such fractions are shown to be of particular importance with regards to human health given the toxicity of the associated compounds and likely contact with the respiratory tract given the particle dimension (Kocbach Bølling et al., 2009; Min et al., 2011; Mitchell et al., 2019). The combustion of dry fuelwood appears to produce a slightly higher fraction of larger soot particles (PM_{10}>, $PM_{2.5}$-PM_{10} and PM_1-$PM_{2.5}$) when compared with soot from a lower temperature reaction. A summary of the size fractionation of soot particles is shown in **Table 6.6**.

Table 6.6 Particle size distribution on a mass basis (mg) and percentage basis (wt%) for low moisture and high moisture fuelwood.

Size Fraction	Low Moisture Fuel (12.44%)		High Moisture Fuel (26.68%)	
μm	mg	%	mg	%
$PM_{10} >$	0.04±0.02	0.76±0.51	0.04±0.02	0.41±0.22
$PM_{2.5}$ - PM_{10}	0.08±0.03	1.61±0.53	0.04±0.01	0.37±0.10
PM_1 - $PM_{2.5}$	0.25±0.09	4.60±0.29	0.15±0.10	1.26±0.93
$<PM_1$	5.00±1.46	93.03±0.82	12.05±5.26	97.96±1.13

6.3.5.3 Structure of Soot Samples

The composition of soot samples collected during these experiments has been shown to vary depending upon the moisture content of the fuelwood. As discussed, the combustion of dry fuelwood resulted in a lower soot loading with the sample material incorporating a high elemental carbon and a low organic carbon fraction. Alternatively, the combustion of wet fuelwood resulted in a higher soot loading with the sample material containing a majority organic composition, as described in **Figure 6.11**. SEM with EDX was applied so as to assess the structure and material composition of the soot sample. **Figure 6.13** show long chains of spherical particulate matter amassed within the filter matrix and maintaining a diameter of approximately 50 nm. These chains are synonymous with the elemental carbon fraction derived from dry fuelwood combustion. Alternatively, **Figure 6.14** shows a more amorphous tar-like material which has developed into strands and globules across the filter matrix. This tar-like material is likely the organic carbon fraction previously discussed. Similar findings are presented in **Figure 6.15**. PM_t emission factor values are shown to increase with each batch of fuel applied within the stove device (**Table 6.5**). Optical analysis of the dry fuelwood soot samples do not appear to show an increase in loading however this is likely in response to the layering effect of the gravimetric sampling method and chain-like structure of the sample material. PM_t is also shown to increase with each batch of wet fuelwood applied within the stove however visual inspection of the sample matrix reveals an increase in sample loading. Processes of loading reveal an increase in the thickness of the strands of tar-like material across the filter substrate.
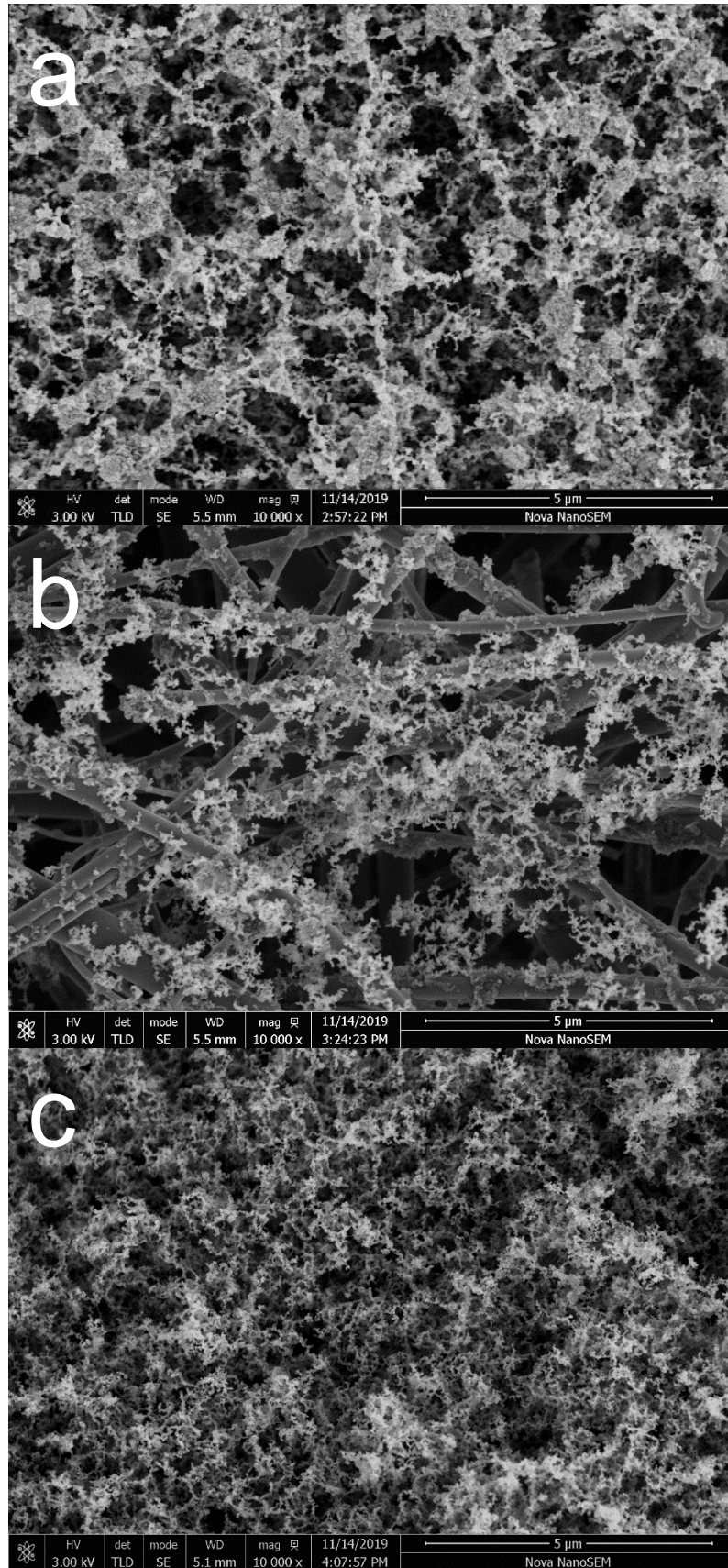
Figure 6.13 SEM images of soot samples (<1 um) from Low Moisture Fuel combustion. Figure a, b and c soot images are from TB1, TB2 and TB3 which show higher particulate formation which is representative of the elemental carbon fraction.
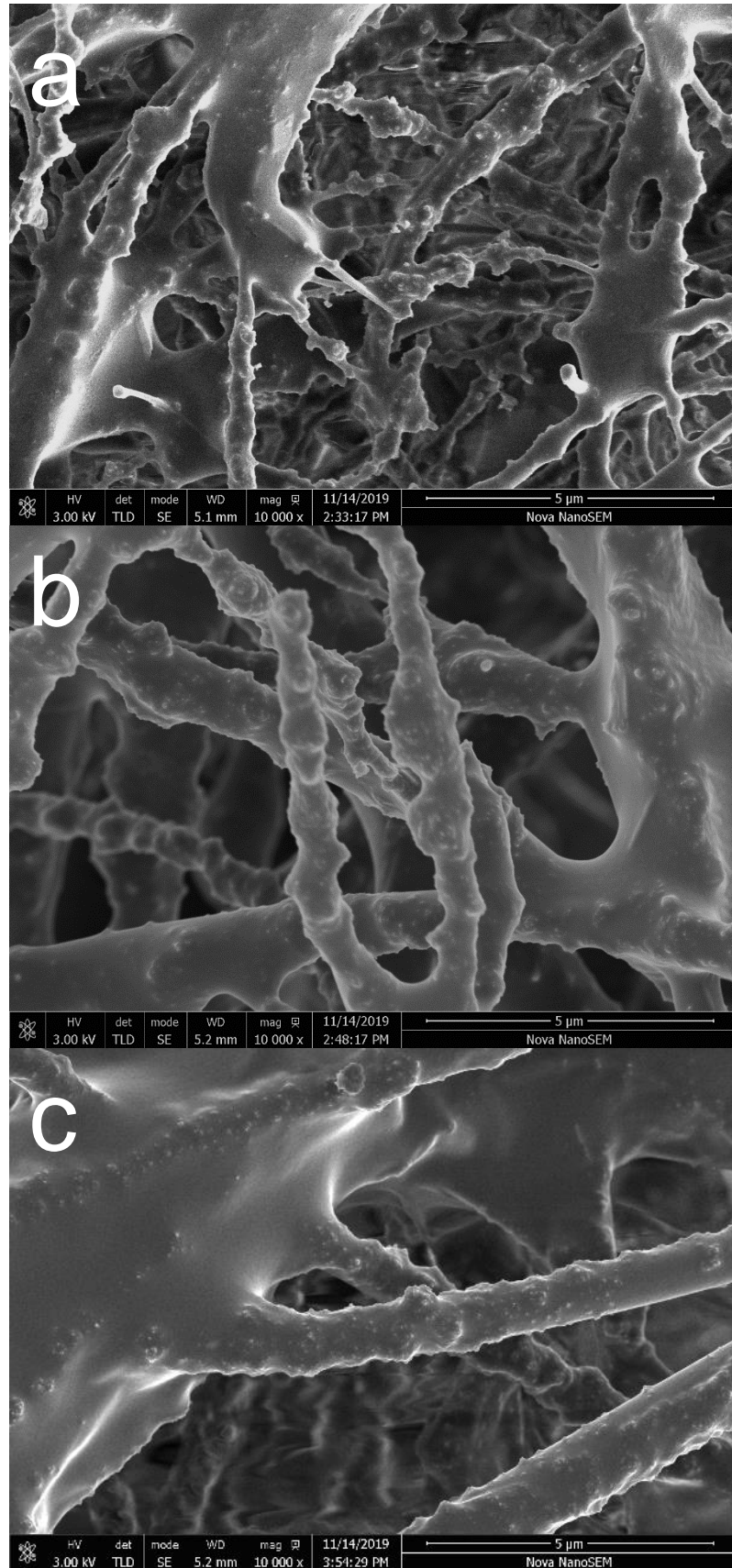
Figure 6.14 SEM images of soot samples (<1 um) from High Moisture Fuel combustion. Figure a, b and c soot images are from TB1, TB2 and TB3 which show higher tar formation which is representative of the organic carbon fraction.
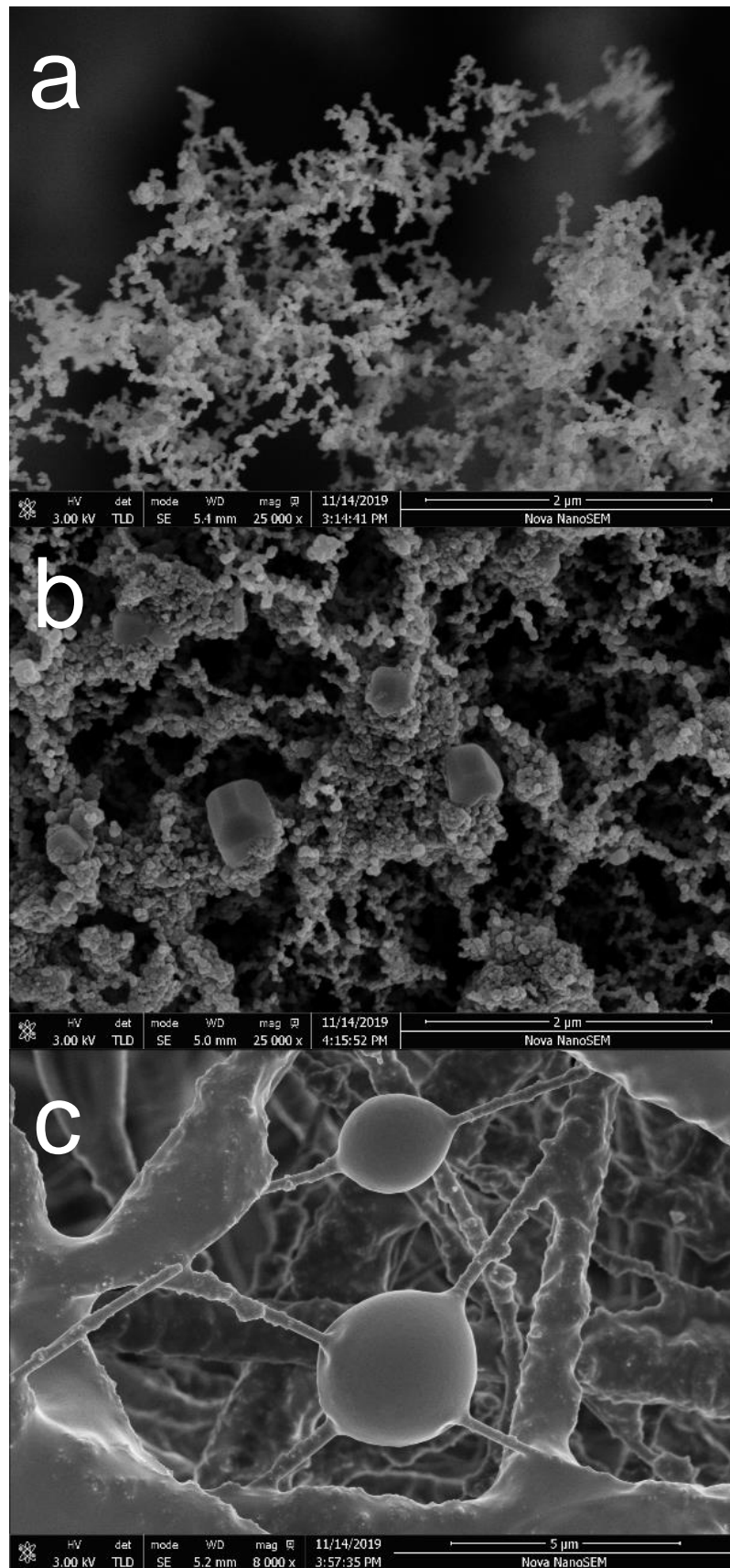
Figure 6.15 SEM image of soot sample showing (a) chain of particulate amalgamates, (b) potassium chloride crystalline structures and (c) amorphous tar-like material

Chemical microanalysis and classification of soot samples was undertaken using energy-dispersive x-ray spectroscopy (EDX). Soot samples generated during the combustion of both dry fuelwood (high temperature) and wet fuelwood (low temperature) contained a predominant organic fraction incorporating carbon and oxygen. As previously described, the formation of soot generated during low temperature combustion generally corresponds with a higher organic fraction incorporating tars and other volatile compounds while dry fuelwood combustion corresponds with an increased elemental carbon fraction (**Figure 6.12**). **Figure 6.16** presents the EDX spectra for soots collected during the combustion of low moisture and high moisture fuelwood. The spectra produced from soot samples generated during higher temperature combustion show higher inorganic fractions including sulphur (S), chlorine (Cl) and potassium (K) compounds likely in the form of potassium chloride (KCl) and potassium sulphide (K2SO4) crystals. High combustion temperatures generally correspond with an increase in the inorganic components within the sampled soot material. The lower peaks in the spectra observed from the testing of high moisture fuelwood indicate a lower presence of such species within the soot composition.
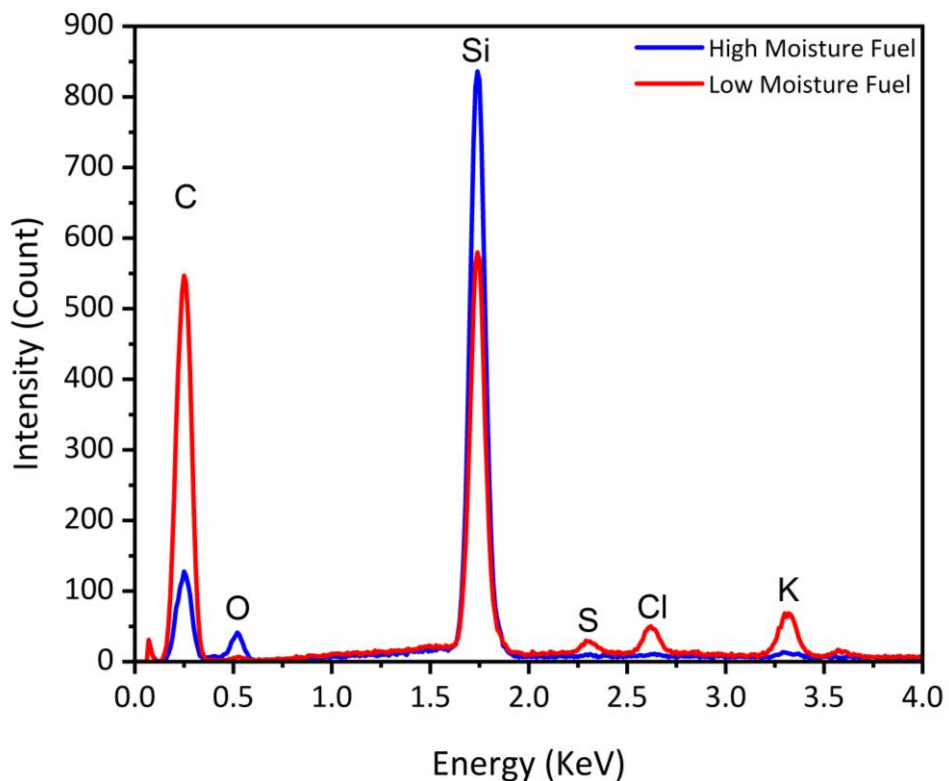
Figure 6.16 Elemental composition analysis via EDX of soot from low moisture and high moisture fuelwood.

Inorganic constituents in the fuel are typically liberated at temperatures exceeding 500°C with a minor, fractional loss at lower temperatures in the range of 180-500°C (Olsson et al., 1997). The concentration of alkali metal species within the soot liberated during the combustion reaction is proportional to the inherent metal composition of the parent material. Chlorine is identified as a primary trace element in biomass feedstocks and fuels. Higher Cl content in the fuel generally results in higher concentrations in emissions (Olsson et al., 1997; Johansson et al., 2003). Dayton et al., (1995) identified the impact of metal content in fuels on the release of alkaline species to the gas phase during the combustion of switchgrass containing chlorine (Cl) and potassium (K). An increase in the fuel inorganic compound concentration generally results in an increase in the subsequent emission, often in the form of potassium chloride (KCl) (Dayton et al., 1995; Mason et al., 2016). Variation in the combustion conditions has also been shown to have an effect on the liberation of alkali species from the fuel including the fuelwood moisture content, combustion temperature and O_2 availability within the combustion zone (Dayton et al., 1995; Johansson et al., 2003). Obernberger et al. (2001) presents a potential mechanism for KCl and K2SO4 formation during the combustion of woody biomass. The mechanism involves the liberation of potassium, sulphur and chlorine from the parent fuel during heating at high temperature. Microparticles of calcium (Ca) are simultaneously released during the combustion reaction and entrained within the flue gas remaining in a crystalline form due to its higher melting point. KCl and K2SO4 occurs within the gas phase and formation subsequently condenses onto the calcium crystal surface while addition formation may occur via nucleation (Obernberger et al., 2001; Johansson et al., 2003). In addition to the vapourisation and condensation, or nucleation routes, inorganic particle formation may occur through the breakdown of residual fly-ash fragments entrained within the flue gas or maintained on condensed on fine organic soot particles initially produced as a function of incomplete combustion as identified in **Figure 6.17** (Wiinikka and Gebart, 2004; Obaidullah et al., 2012). Given the relatively high activation energy required for the vaporisation of chlorine and potassium (168-238 kJ/mol), the formation of inorganic constituents within soot generally only occurs during high temperature combustion (Johansson et al., 2003). Similar findings have been reported by Rau (1989) whereby cold-stove combustion lead to the formation of tan-coloured soot comprising 55-60% organic carbon with minor traces of inorganic constituents. The combustion of biomass at high temperatures led to the formation of black-coloured soot comprising 20-60% carbon with high concentrations of inorganic constituents including potassium (11%), sulphur (1%) and chlorine (3%) (Rau, 1989). The increased concentration of sulphur, potassium and chlorine during the combustion of dry fuelwood is likely in response to the increased combustion

temperatures associated with the reaction. Reduced concentrations are observed during the combustion of high moisture fuelwood in response to the energy loss and cooling effect associated with water vapour within the combustion zone.
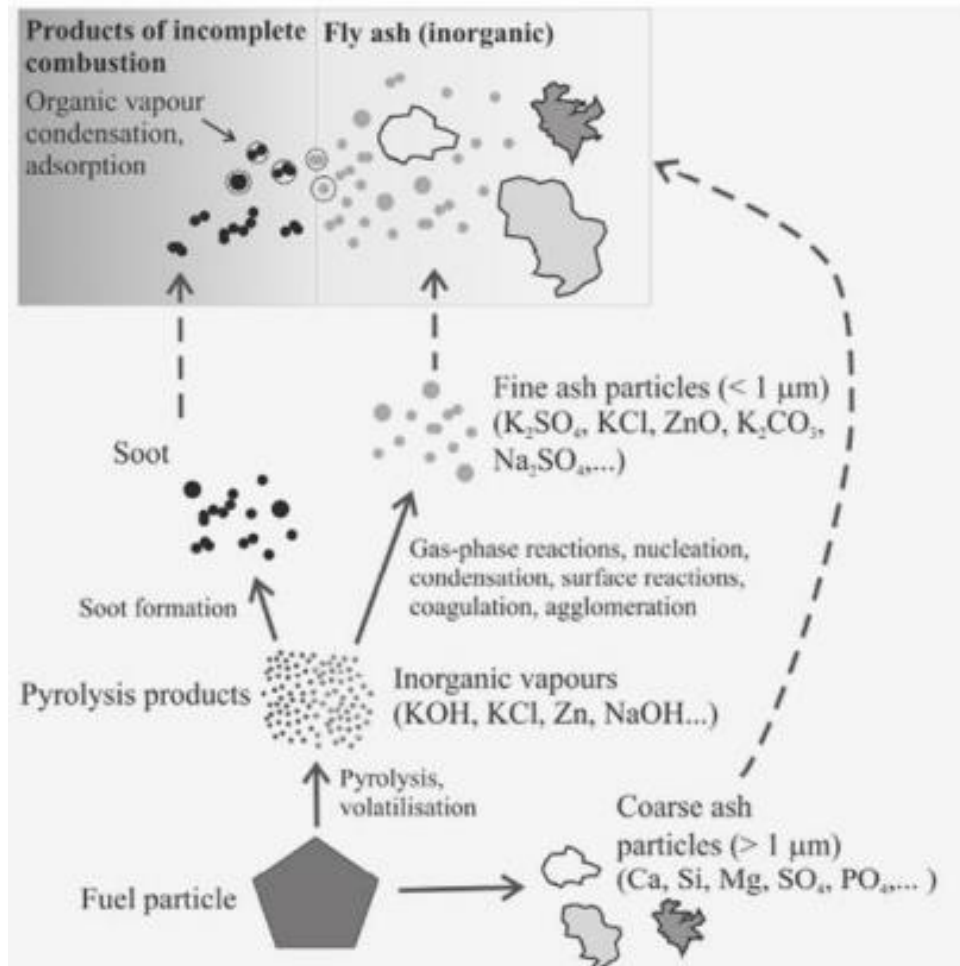
Figure 6.17 Soot particle and inorganic component formation during the combustion of biomass (Sippula et al., 2009; Sippula, 2010; Obaidullah et al., 2012).

6.3.5.4 Py-GC-MS

Evidence on the nature of the tar-like material was obtained by using PY- GC-MS analysis on the samples from the same quartz micro-filters. The resulting chromatogram for the high moisture wood is shown in **Figure 6.18**. The low moisture sample showed a similar chromatogram but with a much lower intensity. The fraction also contains peaks from organic acids which might explain the difference between the concentration of acetic acid measured by FTIR (given in **Table 6.3**) and the measured speciated lower molecular weight acid data in **Table 6.4**.
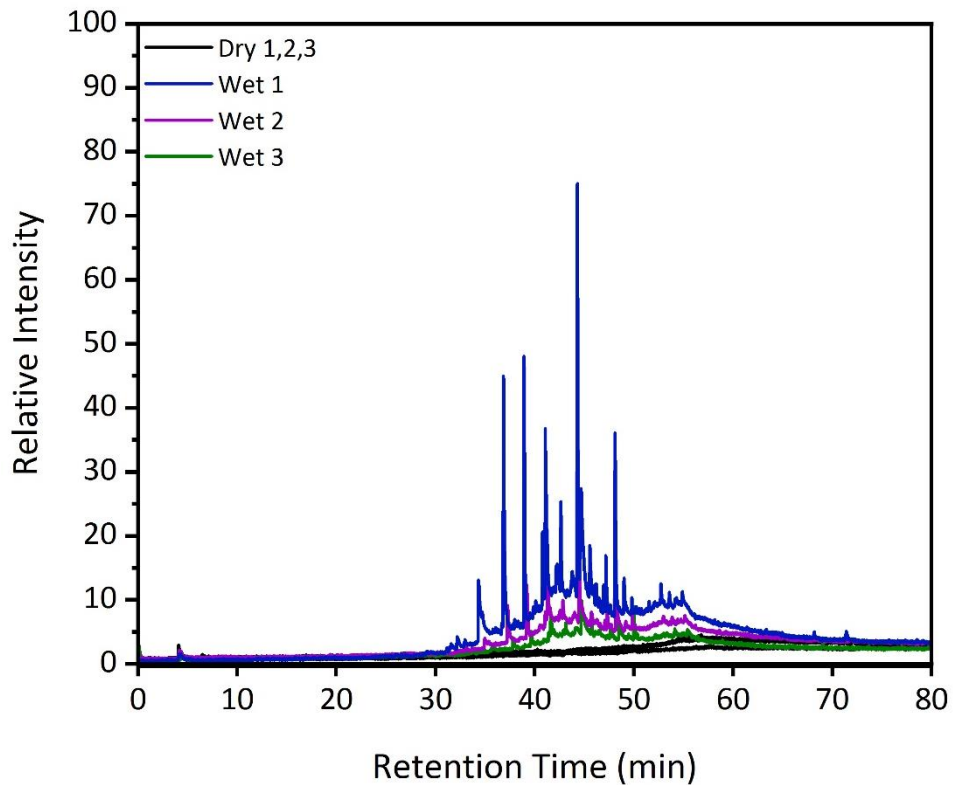
Figure 6.18 Py-GC-MS chromatogram of soot material collected during low moisture and high moisture fuelwood combustion.

6.3.5.5 Raman Nanostructure Analysis

The first order Raman spectra of soot particles have been widely reported in the literature. A typical spectrum generally consists of two overlapping peaks located at approximately $1350cm^{-1}$ and $1585cm^{-1}$ (Dippel et al., 1999; Sadezky et al., 2005; Ess et al., 2016). This banding is clearly visible in **Figure 6.19** where the same band conditions are present in both dry fuelwood and wet fuelwood combustion. The position of the graphitic and defect peaks maintains limited variation between when comparing spectra attained during dry soot and wet soot analysis. The D-peak is identified at $1372\pm8cm^{-1}$ and $1373\pm4cm^{-1}$ for soot derived from low moisture and high moisture fuel respectively. Similarly, the position of the G-peak within the spectra is at $1590\pm4cm^{-1}$ and $1575\pm2cm^{-1}$ respectively for soots from dry and wet fuelwood combustion.

The height-ratio (I_D/I_G) of the D-peak and G-peak may be applied as a method of characterising the nanostructural order of the soot material as identified in Ferrari and Robertson (2000) and Ess et al. (2016). A higher value of I_D/I_G is indicative of an increased structural order of the soot material. For example, spectra of a highly graphitic nature will present a high I_D/I_G value indicating high structural order while soot and other organic materials will present a low I_D/I_G and reduced structural

order. The intensity of the D-peak and G-peak and I_D/I_G ratio is presented in **Table 6.7**. The I_D/I_G values of soot samples collected during dry fuelwood combustion appear to be relatively high ($I_D/I_G = 0.93\pm0.04$). The soot samples collected during wet fuelwood combustion present a significantly lower I_D/I_G value indicating lower graphitic order ($I_D/I_G = 0.69\pm0.03$). Furthermore, the I_D/I_G appears to be affected by the OC of the soot material. For example, Dry3 presents the lowest OC fraction and has an I_D/I_G value of 0.90 suggesting a higher structural order. The Wet3 sample was collected during very cool combustion conditions and was associated with a prolonged smouldering period leading to the formation of a higher OC fraction. The sample presents a significantly lower I_D/I_G value (0.65) indicating a more defective (less ordered) structure. The nanostructural order of the carbon within the amorphous material increases as the OC fraction of the material decreases. Though presenting a higher nanostructural order, the inherent amorphous nature of the soot means that the I_D/I_G values are lower than that observed in the literature for true graphitic materials (Ferrari and Robertson, 2000; Ivleva et al., 2007; Ess et al., 2016). The enhanced intensity of the spectra from wet fuelwood combustion is also likely in response to a higher degree of florescence from the OC increased OC fraction. Lower intensity from the soot derived from dry fuelwood combustion is likely to be as a result of thermal decomposition of the OC fraction due to higher combustion temperatures (Ess et al., 2016).

Table 6.7 Effect of OC fraction upon derived I_D/I_G value

Fuel	Sample ID	OC (%)	D Band Intensity	G Band Intensity	I_D/I_G
Low Moisture	Dry1	24.6	269	315	0.85
	Dry2	16.0	382	404	0.95
	Dry3	7.1	317	353	0.90
High Moisture	Wet1	73.1	1671	2356	0.71
	Wet2	72.8	1211	1738	0.70
	Wet3	78.4	1912	2924	0.65

Highly graphitic carbon materials may include only a single peak centred at approximately 1580cm^{-1} as identified in Tuinstra and Koenig (1970). As previously discussed, amorphous and soot like materials tend to incorporate a pair of overlapping bands consisting of both a Graphitic and Defect peak (Dippel et al., 1999; Ferrari and Robertson, 2000; Sadezky et al., 2005; Seong and Boehman, 2013; Ess et al., 2016). A number of works (Sadezky et al., 2005; Ess et al., 2016)

have theorised the presence of a number of bands located within the D and G peaks which correspond with the nanostructural nature of the carbonaceous material. These bands include a G band centred at $1580cm^{-1}$ and D1 band centred $1350cm^{-1}$ representing ideal graphitic lattice type structures and disordered graphitic lattice structures respectively. In addition, a D3 band is centred between the D and G peaks ($1500cm^{-1}$) and represents interstitial defects and amorphous carbon vibrations. Furthermore, A D2 band ($16200cm^{-1}$) identified as a shoulder of the G peak and D4 band ($1200cm^{-1}$) as a shoulder of the D peak represent disordered graphitic lattices comprising polyenes, ionic impurities and organic compounds (Sadezky et al., 2005; Ess et al., 2016). A number of works have attempted to investigate fitting options for the identification of such bands with a combination of four Lorentzian (G, D1, D2 and D4) and one Gaussian (D3) providing the most accurate representation of the sample material (Sadezky et al., 2005; Seong and Boehman, 2013).

The shape of the Raman spectra is observed to differ between soot derived from dry fuelwood and wet fuelwood combustion. Soot developed during the combustion of dry fuelwood appears to be characterised by a lower D peak and an exaggerated G peak. The Raman spectra of soot generated during wet fuelwood combustion is characterised by two peaks of a similar intensity. The intensity of the spectra between the two peaks is identified as the D3 band and represents amorphous carbon materials. The resolution between the two peaks is shown to be reduced for soot samples collected during wet fuelwood combustion. The reduced resolution, in response to an increased intensity at $1500cm^{-1}$, suggests an increase in the OC and amorphous carbon content of the material. The amorphous fraction is identified as polycyclic aromatic compounds with other inorganic and organic components (Sadezky et al., 2005). An increased resolution in the peak-to-plateau of soot derived from dry fuelwood combustion suggests a reduction in OC and a minor amorphous fraction as identified by the EC/TC of dry fuelwood soot (Sadezky et al., 2005; Ivleva et al., 2007; Ess et al., 2016). Furthermore, the D-peak shoulder, identified as a D4 band at $1200cm^{-1}$ in Sadezky et al. (2005), is shown to increase in intensity for soot materials generated during wet fuelwood combustion. The resultant effect is a reduction in the slope gradient between $1200cm^{-1}$ and $1350cm^{-1}$. The D4 band is attributed to C-C and C=C stretching vibrations of polyene hydrocarbon structures (Dippel et al., 1999; Sadezky et al., 2005; Ivleva et al., 2007; Ess et al., 2016).

The stronger intensity spectra of the high moisture fuel soot samples is due to greater florescence from the higher OC benzenoid content. Though presenting a higher nano-structural order, the inherent amorphous nature of the soot means that

the I_D/I_G values are lower than that observed in the literature for true graphitic materials (Ferrari and Robertson, 2000; Ivleva et al., 2007; Ess et al., 2016).
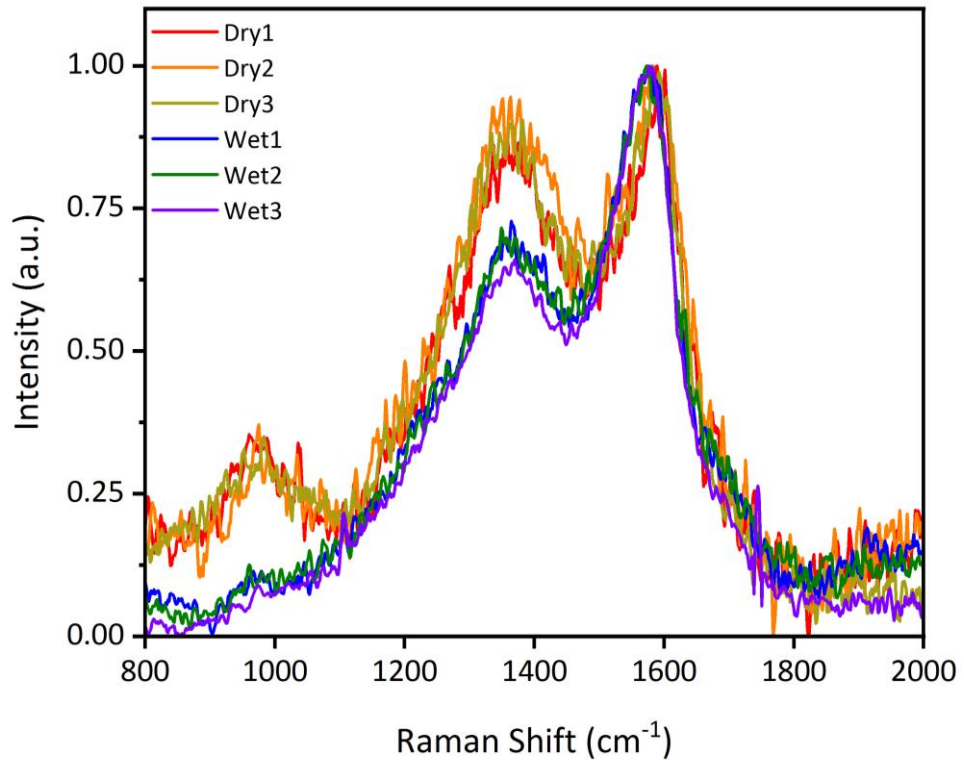
Figure 6.19 Normalised Raman spectra of soot sample material collected during dry and wet fuelwood combustion. Raman spectra is presented between 800 cm^{-1} and 2000 cm^{-1}.

6.3.5.6 Variation in Soot Colour and Sample Density

Additional soot sampling was undertaken by means of a small manual-suction pump device [Testo Smoke Pump] designed in accordance with DIN 51402 and ASTM D2156. Soot sampling was undertaken from the entrained flow in the centre of the flue approximately 1430 mm above the stove (1680 mm above the grate). A fixed flue gas volume of 1.63±0.07 m^3 was sampled for a 2-5 second period at a rate of 20-49 m^3/min. The sampled flue gas was drawn across a filter media where entrained soot particles were captured. This method allows an approximate estimate of soot concentration, in accordance with ASTM D2156, and allows for the retrieval of sample media from the flue at a higher sampling frequency. Soot sampling was undertaken at 2-5 min intervals. Soot material collected via this method are representative of PM_t with no separation by specific gravity. Similar methods of soot collection are outlined within the literature with applications in engine emission monitoring (Dantas Neto et al., 2013) and stack gas sampling from boiler heating systems (McDonald, 2009; Mante et al., 2015). Stove operation was

maintained under similar conditions to those outlined previously. The combustion testing procedure incorporated a preliminary cold-start batch of dry fuelwood (CS-D) followed by two subsequent warm-start batches. The initial warm-start batch incorporated dry fuelwood (WS-D) while the second incorporated wet fuelwood (WS-W). Following sampling, soot colour and darkness was analysed via a spectrodensitometer. The device was calibrated to measure optical density (L) where L=0 is represents black and L=100 represents white. The relative darkness is therefore a function of L and is calculated as 100-L.

Variation in combustion conditions between the combustion of low moisture and high moisture fuelwood are shown to be consistent with previous testing. The mass of fuel batches was 1505±30 g, 1255±107 g and 1412±46 g for the CS-D, WS-D and WS-W batches respectively. The mass of fuel applied is below that of the conditions described in BS EN 13240 and is representative of an underloaded grate. The cold-start batch included 192 g of softwood kindling with a moisture content of 16.5±1.4% and 32 g of kerosene-based firelighter [Zip, High Performance]. As previously described (**Chapter 3**), the fuel reloading pattern was undertaken on a mass basis.

Figure 6.20 presents the measured temperature, flue gas velocity and burning rates under different starting conditions (cold-start and warm-start) and fuel types (low moisture and high moisture fuelwood). As previously presented (**Chapter 5**), the combustion of fuelwood with a high moisture content resulted in a reduced burning rate and a prolonged combustion cycle. The average burning rate of low moisture and high moisture fuelwood under warm-start conditions was 2.29 kg/hour and 1.40 kg/hour respectively. The average burning rate of low moisture fuelwood under cold-start conditions was 1.68 kg/hour in response to the reduced combustion temperature. The introduction of high moisture fuelwood into the combustion zone appears to correspond with a spike in the rate of mass loss followed by a prolonged period of reduced combustion. The initial spike in mass loss is likely to be the result of loss of surface moisture from the fuel following initial contact with the hot grate/bed. The prolonged period of reduced combustion is in response to a prolonged drying period and the cooling effect of moisture within the combustion zone. Similarly, the combustion of fuelwood with a higher moisture content resulted in a reduced combustion temperature. The average flue gas temperature observed during the combustion of low moisture and high moisture fuelwood under warm-start conditions was 383°C and 279°C respectively. The flue gas velocity is shown to follow a similar trend to the combustion temperature in response to the effects of buoyancy and increased draft. An increase in the

combustion temperature results in a greater flue gas flow rate and fuel conversion rate.
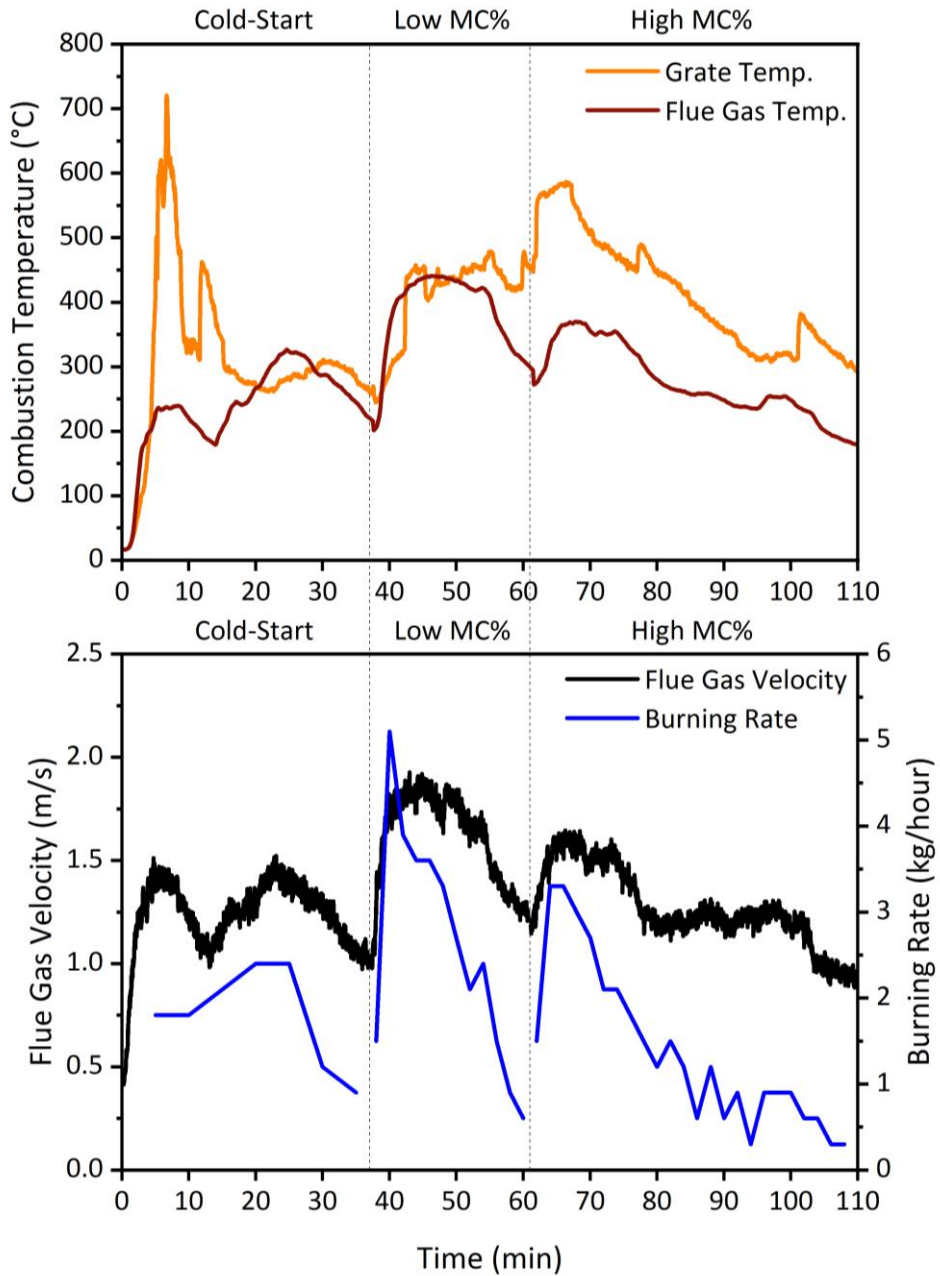
Figure 6.20 Combustion temperature (°C), fuelwood burning rate (kg/hour) and flue gas velocity (m/s) for dry fuelwood under cold-start conditions (CS-D), dry fuelwood under warm-start conditions (WS-D) and wet fuelwood under warm-start conditions (WS-W). The burning rate is presented for each of the soot sampling points and is calculated across a 60 second period. Temperature and velocity results were sampled at a rate of 1 Hz.

The colouration and 'darkness' of soot samples collected is presented in **Table 6.8-10**. A noticeable/significant colour difference is observed between the samples obtained during testing of the low moisture and high moisture fuelwood. Dry fuelwood combustion generally results in formation of darker and higher density samples whereby the colour is dark brown or black. The combustion of high moisture fuelwood or fuels under cold-start conditions results in the formation of soot samples presenting lower density and light brown or tan colouration. Similar findings have been presented in the literature (Rau, 1989; Mitchell et al., 2016; Jones et al., 2018) whereby the colour-shift is in response to variation in the EC and OC content of the soot. Soot samples presenting a lower density and light brown or tan colouration correspond to an increase in the OC fraction of the material while soot samples presenting a higher density and a dark brown or black colouration correspond with an increase in the EC formation of the material (Rau, 1989). Mitchell et al. (2016) identified brown or tan-colouration in soot samples collected under cold-start operation while soot collected under higher temperature combustion were black. This colour shift from black to brown was in response to a higher tar-phase formation on the soot surface resulting in a higher organic fraction (Mitchell et al., 2016). Similarly, Jones et al. (2018) identified a shift in the visible colour of soot samples collected during different phases of combustion and related such processes in response to variation in the combustion efficiency and EC/TC. As such, darker and black soot samples are representative of periods of higher temperature and efficiency combustion while lighter brown, tan, yellow and grey soot samples are indicative of reduced combustion efficiency and fuel smouldering (Jones et al., 2018). Such findings are important given the application of soot colouration and optical analysis in climate forcing models.

Given the capacity of high moisture fuelwood combustion via improper seasoning and grey fuelwood procurement routes the fraction of brown carbon particles may be higher than initially predicted in climate models. Further assessment is therefore required when assessing the impact of residential combustion on climate forcing.

Table 6.8 Soot characteristics generated under cold-start combustion using low moisture fuelwood.

Sample time (min)	5	10	15	20	25	30	35
Filter							
Colour Shift							
Darkness (100-L)	25.6	19.0	18.0	19.0	25.2	17.4	27.8
Burning Rate (kg/hour)	1.8	1.8	2.1	2.4	2.4	1.2	0.9
Temperature (°C)	227	220	205	267	323	287	244

Table 6.9 Soot characteristics generated under warm-start combustion using low moisture fuelwood.

Sample time (min)	38	40	42	44	46	48	50	52	54	56
Filter										
Colour Shift										
Darkness (100-L)	26.5	44.2	32.7	27.6	26.2	21.7	26.8	35.3	55.9	20.6
Burning Rate (kg/hour)	1.5	5.1	3.9	3.6	3.6	3.3	2.7	2.1	2.4	1.5
Temperature (°C)	205	363	411	432	440	440	433	422	422	373

Table 6.10a Soot characteristics generated under warm-start combustion using high moisture fuelwood.

Sample time (min)	62	64	66	68	70	72	74	76	78	80
Filter										
Colour Shift										
Darkness (100-L)	15.5	21.5	20.3	18.5	18.6	13.9	13.1	13.7	17.6	18.6
Burning Rate (kg/hour)	1.5	3.3	3.3	3	2.7	2.1	2.1	1.8	1.5	1.2
Temperature (°C)	276	331	365	370	355	352	353	328	302	280

Table 6.10b Soot characteristics generated under warm-start combustion using high moisture fuelwood.

Sample time (min)	82	84	86	88	90	92	94	96	97	98
Filter										
Colour Shift										
Darkness (100-L)	15.02	15.36	12.67	14.0	11.8	14.0	24.8	19.1	20.2	17.1
Burning Rate (kg/hour)	1.5	1.2	0.6	1.2	0.6	0.9	0.3	0.9	0.9	0.9
Temperature (°C)	266	262	258	257	248	239	236	245	254	253

Table 6.10c Soot characteristics generated under warm-start combustion using high moisture fuelwood.

Sample time (min)	100	102	104
Filter			
Colour Shift			
Darkness (100-L)	10.37	14.46	4.44
Burning Rate (kg/hour)	0.9	0.6	0.6
Temperature (°C)	266	262	258

Figure 6.21 presents the variation in soot colour, subject to combustion temperature and burning rate, during the combustion of low moisture fuelwood under cold-start and warm-start conditions, and wet fuelwood under warm-start conditions. Initially, the burning rate appears as a function of the combustion temperature. In addition, the combustion temperature and subsequent burning rate is shown to be low during cold-start operation and during the combustion of wet fuelwood. Both combustion temperature and burning rate are shown to be significantly higher during the combustion of fuelwood maintaining a lower moisture content. Reduced temperatures are also observed within the range of 200-300 °C during the combustion of dry fuelwood in response to periods of ignition and smouldering combustion. Similarly, higher temperatures (300 °C>) are also observed during the combustion of wet fuelwood during periods where the inherent water content has been devolatilised by the combustion reaction. Variation in

colouration occurs in response to change in the soot composition but also in response to the sample density. The soot generated during low temperature combustion including those observed during ignition periods, during smouldering reactions, during cold-start operation and during the combustion of wet fuelwood appears to be more tan and brown-coloured. This is likely in response to the high EC/TC associated with low temperature combustion and reduced PM_t loading relative to the sampling period (5 seconds) and rate of fuel conversion. The soot generated during the combustion of dry fuelwood appears to present dark-brown and black colouration. This is likely in response to the high EC/TC previously identified during high temperature conditions associated with dry fuelwood combustion. In addition, the higher rate of fuel conversion results in an increase in PM_t formation. In response to the short sampling period the sample appears as a darker material in response to a high sample density.
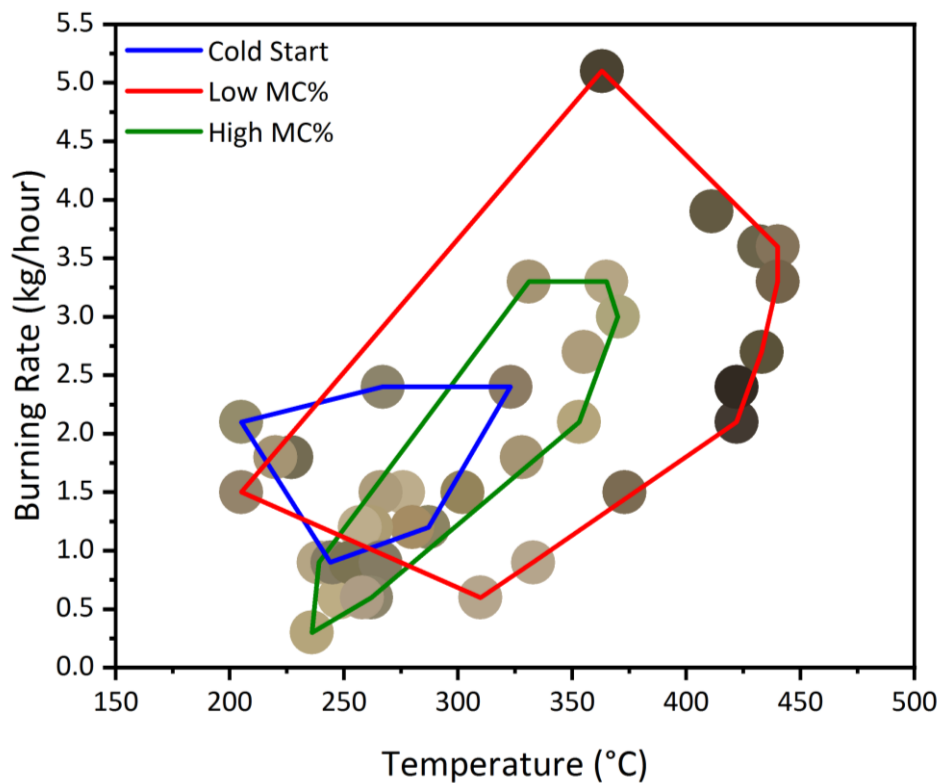
Figure 6.21 Variation in soot colouration and density observed during cold-start operation (blue band), low MC% fuelwood combustion (red band) and high MC% fuelwood combustion (green band). Colouration of the symbols is representative of the RGB colouration identified for each soot sample.

Absorption Ångström Exponent (AAE) is applied as a method of investigating aerosol optical property variation through wavelength absorption in the visible and near-infrared spectral region (Ångström, 1929; Liu et al., 2018). AAE is therefore an equation which represents the optical absorption of an aerosol as a function of wavelength (Liu et al., 2018). It is generally assumed that BC, generated under low moisture fuelwood combustion, presents an AAE value of 1.0 while soot samples that are visually brown in colour present an AAE greater than 2.0 (Kirchstetter et al., 2004; Russell et al., 2010; Liu et al., 2016; Liu et al., 2018). Climate model predictions make assumptions on the fraction of black carbon, brown carbon and EC/TC fraction emitted under a combustion reaction (Jones et al., 2018). An increase in brown carbon emission is prevalent during the combustion of high moisture fuelwood while black carbon is generally only associated with high temperature combustion. It is interesting to compare the results obtained previously using a total soot sample analyser (Jones et al., 2018). Of note is the fact that for this <1μm sample the colours are black or brown. Lighter colours such as yellows are seemingly associated with larger particles containing organic molecules. The present results are compared with previous published results from this stove, and from a model compound, furfural, which are presented in **Table 6.11**. The association of colour and the nature of the carbon is clearly apparent.

Table 6.11 Published data from (Jones et al., 2018) on optical properties and MCE.

Fuel	AAE	EC/TC	Colour of Sample	MCE
Furfural	1.18	0.98	Black	1.0
Pine wood, flaming	0.99	0.5	Black	0.93
Pine wood, transient	1.91	0.3	Brown	0.65
Pine wood, smouldering	3.33	0.1	Yellow	0.63

The AAE is defined as: $b_{abs} = a \lambda\ AAE$ where b_{abs} is the absorption coefficient for filter papers covered with soot samples and measured by a spectrophotometer. The constant, a, is independent of wavelength but is dependent on the thickness of the absorbing sample. For small spherical soot particles AAE equals 1.

UV-Vis analysis of the ASTM soot samples have been made using the same method in Jones et al. (2018). Previously it has been seen that mature soot particles with a low OC had AAEs close to 1, whereas soot containing higher OC had high values of AAEs. In these experiments there is a very significant difference between the soot produced during combustion of low moisture wood compared to the high moisture wood as shown in **Figure 6.22a** and **6.22b**. In the former, spectra

for soot produced during flaming combustion are close together and separated from the spectra for soots from smouldering combustion. In the latter, all curves are also close together indicating that the products are optically similar in both phases.

In this analysis, the shapes of the spectra are dictated by enhanced absorption by semi-volatile organics (SOVC) such as the compounds shown from PY-GC-MS analysis, or due to the soot-forming species (the building bricks). As a consequence, it is not possible to get a power-function to fit in the AAE equation although the results are similar. This may be the result of higher levels of samples and thicker optical paths for the measurement. During short sampling times (0-5 min) it is possible to see a number of different colours but these are lost when we collect soot over a long period of time (Dekati sampling method), so we only see brown and black soot samples.
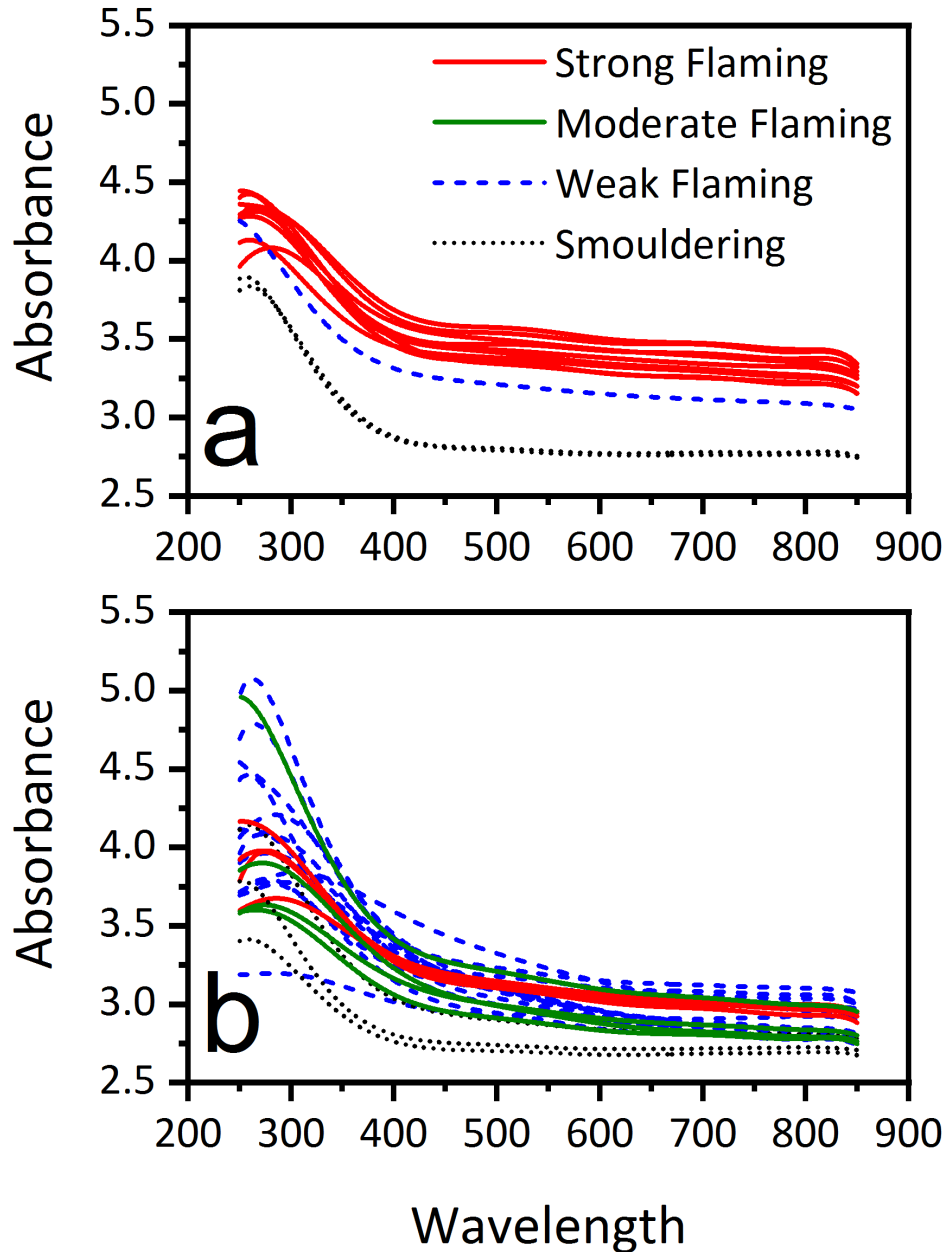
Figure 6.22 UV-Vis light absorbance of soot samples collected during the combustion of low moisture [a] and high moisture [b] samples.

6.4 Discussion

6.4.1 Variation in Fuel Particle Moisture Content

Bulk drying of a representative sample was undertaking in accordance with BS EN 18134-1 so as to determine the approximate moisture content of the fuelwood. In addition, an approximation of the moisture content for each fuel particle was determined via electrical conductance. The variability in derived moisture values

appears low when testing fuelwood which has undergone a kiln-drying pre-treatment while freshly-cut particles present a broader range of values (**Figure 6.1**). Dry fuelwood and wet fuelwood maintain a bulk moisture content range of 0.23 wt% and 3.64 wt% respectively. The variation is likely in response to the storage of water within the biomass structure, general inhomogeneity of biomass materials and water transfer processes during fuelwood storage (Kenney et al., 2014; Raitila et al., 2015). As described in previous work (Price-Allison et al., 2019), a notable variation between bulk MC% and probe MC% values is presented within the figure. Results obtained from the lower moisture fuelwood generally correspond with the bulk MC% however a much larger variation is observed during wet fuelwood testing. The primary limitation of the digital moisture meter device is the relatively small sampling area of the device. The device probes are inserted to a maximum depth of 5mm identifying the surface moisture content of the material only. The inaccuracy of the probe is therefore based upon the uneven distribution of water across the cross-sectional area of the fuel sample. For example, the sap wood structure at the base of the tree is likely to maintain a higher moisture content than heart wood, bark or sapwood at a higher elevation up the stem (Espenas, 1951). Variation in bulk MC% and probe MC% results are also presented within the literature for fuelwood and other biomass materials (Byler et al., 2009; Chesser Jr et al., 2012; Davis et al., 2017; Price-Allison et al., 2019).

6.4.2 Impact of Moisture Content Upon Combustion Conditions

Previous work has identified the negative effects of high fuel moisture content on combustion conditions and the related effects upon stove performance (Price-Allison et al., 2019). Results identify a reduction in temperature during the combustion of higher moisture fuelwood. Such processes are in response to the increased energy requirement needed during the vaporisation of the fuel moisture (Simoneit, 2002; Shen, Wei, et al., 2012; Magnone et al., 2016). As such, the amount of fuel energy lost during the vaporisation phase is proportional to the amount of energy available for efficient combustion as well as the subsequent heat output of the stove device. Furthermore, the presence of higher water vapour within the firebox likely resulted in a further cooling effect of entrained gases thereby inhibiting high temperature combustion (Shen, Tao, et al., 2012). **Figure 6.23** presents the effect of moisture content on water vapour within the combustion zone and flue gas temperature. As previously described, the combustion temperature is significantly higher during low moisture fuelwood combustion. The water vapour concentration is shown to increase significantly during dry fuelwood combustion suggesting the effect of higher temperatures upon the vaporisation process.

Maximum water vapour concentrations are lower during wet fuelwood combustion however the total vapoured volume is significantly higher. Similar effects on combustion temperature have been reported within the literature whereby higher concentrations generally lead to reduced stove performance (Yuntenwi and Ertel, 2008; Wilton and Bluett, 2012; Shen, Tao, et al., 2012; Magnone et al., 2016).
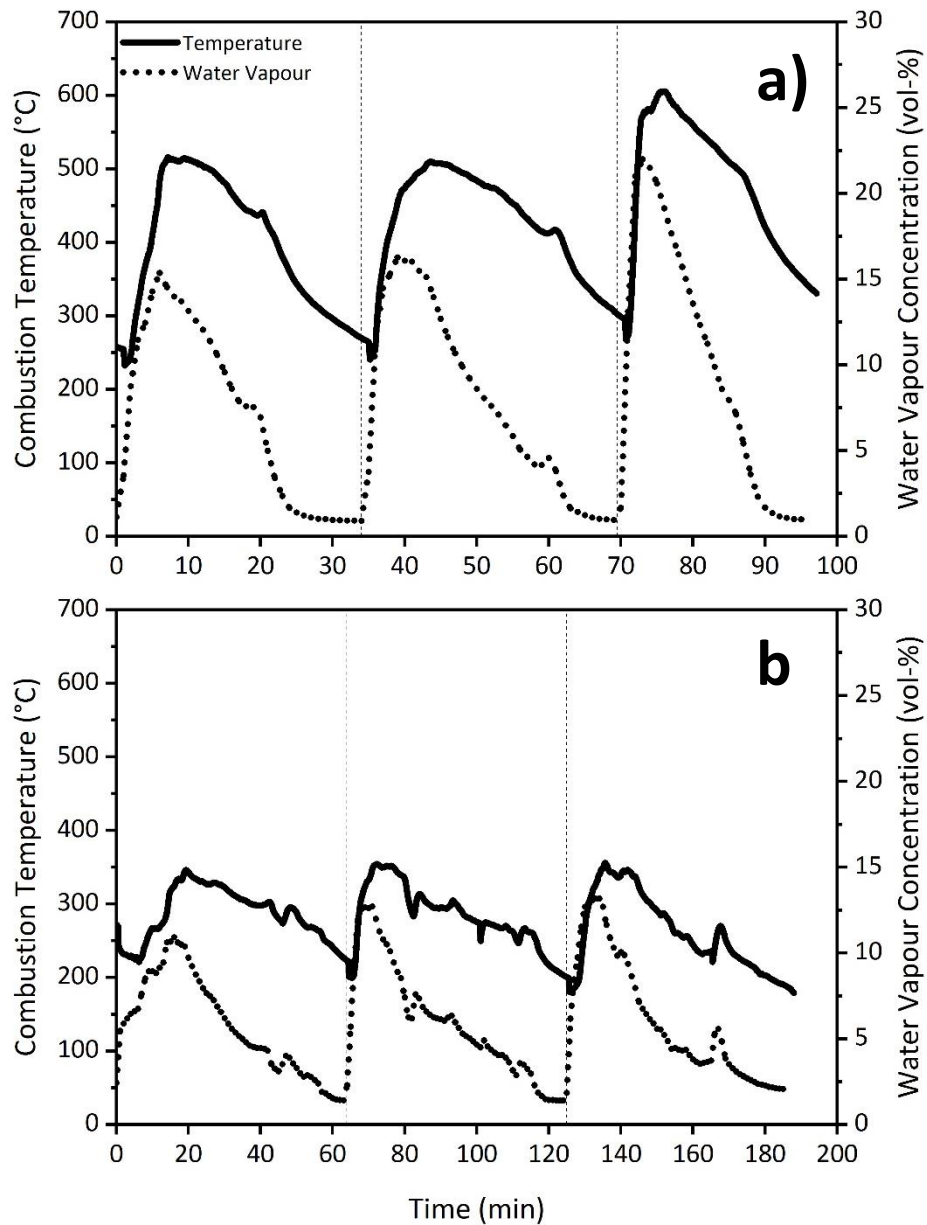
Figure 6.23 The effect of fuelwood moisture content upon combustion temperature and fuel water vaporisation during a) dry fuelwood combustion and b) wet fuelwood combustion.

Oxygen availability and burning rate are shown to vary with fuelwood moisture content and are statistically dependent upon the temperature within the combustion zone. An increase in the moisture content was shown to reduce the burning rate and increase the oxygen availability while the inverse effect was observed when burning lower moisture fuel. Fuels maintaining a higher moisture content have traditionally been applied as a method of managing burning rate and O_2 availability in both heating stove and cookstove appliances. The presence of water within the combustion system operates as a suppressant preventing the rate of combustion exceeding the availability of oxygen (Rogge et al., 1998; Pettersson et al., 2011;

Shen, Wei, et al., 2012). As such, the burning of very dry fuelwood may result in increased emission formation as a result of incomplete combustion however the O_2 availability however the moisture content of fuels tested within this work appear suitable for negating such effects. Furthermore, the rate of fuel conversion appears similar to that outlined within the literature (Mitchell et al., 2016; Fachinger et al., 2017). The reduced combustion temperatures appear to inhibit the conversion of fuel maintaining a higher moisture content likely in response to the prolonged drying period and suppressive nature of water within the combustion reaction.

6.4.3 Impact of Fuelwood Moisture Content on Gaseous and Particulate Emission Formation

Particulate emission factor values have been shown to increase during the combustion of fuelwood maintaining a higher moisture content. Particulate emission factor values were found to be 3.1 ± 0.6 g/kg$_{fuel}$ and 9.3 ± 4.9 g/kg$_{fuel}$ during the combustion of dry and wet fuelwood respectively. Similar findings have been identified within the literature with results suggesting a positive correlation between fuelwood moisture content and carbonaceous aerosol formation. Similarly, Chomanee et al. (2015) identifies an increase in smoke formation in response to incomplete combustion conditions when burning rubber-wood fuels of a higher water content. Interestingly, the smoke concentration was shown to reduce over time in response to fuel particle drying. This suggests that a period of low emission combustion may occur at the end of the combustion cycle when all of the water content has been vaporised. In addition, Magnone et al. (2016) found an increase in soot formation when burning oak maintaining moisture contents of 10.34% and 56.31% in a wood burning appliance. PM_t emission factor values were found to be within the range of 0.93 g/kg$_{fuel}$ and 1.32 g/kg$_{fuel}$ during dry wood combustion and 4.02 g/kg$_{fuel}$ during wet fuel combustion. Purvis and McCrillis (2000) present the effect of fuel moisture in two different domestic combustion appliances under different operating conditions. PM_t was shown to increase during the combustion of fuels maintaining a higher moisture content however the combustion efficiency is presenting as having a greater influence. Furthermore, Johansson et al. (2004) identified a negative impact of moisture content when burning high moisture fuelwood (38%) on PM_t emissions in modern boiler systems however limited variability was observed when burning fuelwood at moderate (26%) and low (15%) moisture values. Such processes are also observed in small cookstove devices where a positive correlation between PM_t emission and fuel water content is found (Bignal et al., 2008; Shen, Tao, et al., 2012; Shen, Wei, et al., 2012; Shen et al., 2013; Mitchell et al., 2019).

The formation of hydrocarbon and organic gaseous species is shown to increase during the combustion of fuelwood maintaining a higher moisture content. As identified in Pettersson et al. (2011), CH_4 was shown to be the most prevalent hydrocarbon species generated during both low moisture and high moisture fuel combustion. Emission factor values where in the range of 0.29 g/kg_{fuel} and 0.81 g/kg_{fuel} in low moisture combustion and 4.04 g/kg_{fuel} and 6.70 g/kg_{fuel} during high moisture combustion. Similarly, Orasche et al. (2013) shows an increase in CH_4 formation when burning fuelwood of a higher moisture content generating emission factor values of 0.72 g/kg_{fuel}, 0.92 g/kg_{fuel} and 2.167 g/kg_{fuel} at moisture contents of 1.6%, 15% and 19% respectively. Similar processes resulting in the formation of CH_4 have also been reported in the literature during uncontrolled green-waste combustion (Tihay-Felicelli et al., 2017) and during cookstove operation (Mitchell et al., 2019). Similar processes where observed in the formation of other non-methane volatile organic compounds (NMVOC) species whereby a reduction in fuel moisture content leads to increased temperature and combustion efficiency and a reduction in emissions. NMVOC species including C_2H_2, C_2H_4, C_2H_6, C_3H_8, and C_6H_{14} are found to be common in biomass combustion and maintain a significant influence on global climate conditions (Lanz et al., 2008; Pandey and Sahu, 2014). The impacts of stove operation upon VOC formation have been previously explored (Pettersson et al., 2011; Evtyugina et al., 2014) however information on the influence of fuel moisture content on emissions remains limited. Reduced temperatures, occurring in response to the presence of water vapour within the combustion zone, inhibits the breakdown of pyrolysis products contributing in high VOC concentration levels within the flue gas composition. VOC products, including benzene species, are likely to be fully consumed during ideal combustion conditions. The presence of moisture within the combustion system therefore offers some degree of uncertainty in emission formation given the inhomogeneity of fuels applied on the domestic market.

Fuelwood moisture content was shown to have an impact upon the total phenolic compound emission sampled as a fuel gas condensate. Phenolic molecules are identified as cyclic compounds including aromatic hydrocarbon rings bonded with phenyl hydroxyl groups (-OH) or associated radical compounds (Dyakov et al., 2007; Clarke, 2008). Phenolic compounds in woodsmoke are shown to include a complex mixture of methylphenols and nitrophenols generated during the thermal degradation of lignin in woody biomass (Faix et al., 1990; Kjällstrand and Petersson, 2001; Li et al., 2020). The majority of phenol derivative products originate via the thermal degradation of lignin however some compounds may also originate as products of cellulose and hemicellulose pyrolysis. Nowakowski and Jones (2008) identifies phenol (C_6H_6O) and a series of methoxyphenol compounds

derived from the pyrolysis of lignin including 2-methoxy-4-(2-propenyl)-phenol ($C_{10}H_{12}O_2$) and 2,6-dimethoxyphenol ($C_8H_{10}O_3$). Phenolic compound formation was also shown to occur during the pyrolysis of cellulose and hemicellulose depending upon the potassium content of the parent material. Such products include phenol with methoxyphenol and dimethoxyphenol derivatives in lower concentrations (Nowakowski and Jones, 2008). Similar findings have been identified during the pyrolysis of various types of raw biomass, pre-treated biomass and synthetic biomass materials (Nowakowski et al., 2007). In addition, nitrated phenolic compounds are identified as a common product derived from the pyrolysis of lignin in woody biomass and coal as well as other combustion sources including vehicle emissions (Harrison et al., 2005; Mohr et al., 2013; Li et al., 2020). Such compounds have been shown to include nitrophenol ($C_6H_5NO_3$), methylnitrophenol ($C_7H_7NO_3$) and dinitrophenol ($C_6H_4N_2O_5$) amongst others which incorporate a fraction of brown carbon emissions presenting both light absorption properties and detrimental effects on human health (Huang et al., 1995; Mohr et al., 2013). Similar compounds have been identified in the soot phase generated during the combustion of pine fuelwood from a small-residential heating device (Jones et al., 2018). Methoxyphenol and nitrophenol compounds are derived from the pyrolysis and thermal degradation of lignin. Derived compounds are oxidised under high flame temperatures such as those observed during the combustion of low moisture fuelwood. An increased fuelwood moisture content often corresponds with reduced combustion temperatures resulting in higher phenolic compound emissions from the flue or stack. The emittance of such compounds generally occurs within the temperature range of 250-500 °C, however, in the event of higher moisture concentrations within the parent fuelwood the period of emittance is increased in response to a lower rate of temperature increase (Koppmann et al., 2005).

6.4.4 Effect of Fuel Moisture Content upon Combustion Efficiency

The combustion efficiency of residential heating applies is often determined using the MCE. Based upon the molar ratio of emitted CO_2 and fuel bound carbon consumed during the combustion reaction the method provides a simple approach for accurately estimating CE (Yokelson et al., 1996; Akagi et al., 2011). During the combustion of dry fuelwood the method may be used as a proxy for the determination of the phase of combustion. This technique has been applied by numerous authors previously (Yokelson et al., 1996; Akagi et al., 2011; Fachinger et al., 2017). Though average MCE values may be quantified during the combustion of high moisture fuelwood it is difficult to ascertain specific information regarding the

phase of combustion in response to poor repeatability and oscillation in the time-series associated with the presence of a high water content in the fuel. Regarding phase identification, flaming combustion and smouldering combustion present values of MCE=1.0 and MCE=0.8 respectively while an equal mixture of both processes presents a value of MCE=0.9 (Yokelson et al., 1996). Alternatively, the phase of combustion may be determined by visual evaluation of the time series and identification of significant changes in the CO or CO_2 emission (Fachinger et al., 2017). In response to significantly inhibited combustion the formation of CO_2 is often minimal in contract to CO and other pollutant species when burning wet fuelwood. This leads to inaccuracy in the estimation of accurate MCE time series trends. In addition, non-uniformity and poor repeatability of the fuel bed leads to unpredictable oscillations in CO_2 formation leading to changeable peaks in the time series. This process is also exacerbated by the need to manually manipulate the fuel pack to promote combustion. As such, it may be difficult to accurately estimate the burning efficiency via the MCE approach and subsequently identify phases of combustion for fuels maintaining a high moisture content.

6.4.5 Variation in Physiochemical Properties of Soot

6.4.5.1 Effect of Moisture Content upon Particulate Physiochemical Structure

The nanostructure of the soot was found to differ depending upon the moisture content of the parent fuel material. Soot samples formed during dry fuelwood combustion appear to produce long chains of spherical particulate matter maintaining a diameter of approximately 50 nm. Particles of a similar size and formation have been found during the combustion of liquid (Huang et al., 2017) and solid fuels (Tissari et al., 2008; Atiku et al., 2016) within the literature. Alternatively, soot derived from wet fuelwood combustion maintained a more amorphous tar-like material which has developed into strands and globules across the filter matrix. These globules appear to increase in density and concentration between test batches in line with the increase in PM_t emission factor and OC fraction. As such, the structural nature of soot is likely to vary in response to the EC and OC composition with processes of incomplete combustion resulting in a higher organic fraction and amorphous structure (Ess et al., 2016). Atiku et al. (2016) identified similar agglomerations, presented as the OC fraction, during smouldering combustion of fuelwood maintaining a moisture content of 8%. Unlike this current study, the globular OC structure was only observed during the low temperature smouldering phase while fine spherical particulate matter was observed during

flaming combustion. Similar findings have been reported in Tissari et al. (2008) whereby smouldering combustion resulted in OC agglomerates forming carbonaceous soot particles. EC particles generated within the flame zone may act as a nucleus for the condensation of organic compounds derived from low temperature combustion. During high temperature oxidation the EC particles are observed in an uncoated form however in smouldering or low temperature combustion spherical particles comprising a high OC fraction may be produced which do not present a visible EC nuclei (Reid et al., 2005). The very high tar concentration suggests highly inhibitory combustion conditions suggesting limited burnout of volatile organic compounds within the combustion zone. As such, the lower combustion temperatures observed during wet fuelwood combustion appear to result in the formation of soot maintaining a higher OC fraction and differing physical structure to soot formed under higher temperatures.

The size distribution of soot particles was found to include a majority $<PM_1$ size material with additional fractions of $<PM_{2.5}$, $<PM_{10}$ and $PM_{10}>$ present in lower quantities. The small size fraction was found to be within the range of 96.7% and 98.7% during wet fuelwood combustion and between 92.2% and 93.9% during dry fuelwood combustion. These findings where corroborated through SEM where PM was found to include long chains of spherical material maintaining a nominal diameter of approximately 50 nm. Similar findings where outlined in previous work whereby PM_1 was the predominant size fraction with higher moisture fuel generally resulting in a higher fraction of smaller particles (Price-Allison et al., 2019; Maxwell et al., 2020).

6.4.5.2 Physiochemical Structure of Biomass Derived Soot

EC and OC fractions within soot samples are shown to vary depending upon moisture content. Fuels maintaining a higher moisture value appear to exhibit a larger OC fraction and subsequent lower EC fraction while the inverse is shown for dry fuelwood. Soots derived from biomass combustion incorporate a Black Carbon (BC) fraction which predominantly incorporates EC. The BC fraction is commonly designated as the light absorbing constituent within the soot matrix while the EC is defined as the thermally stable aspect of the material (Bahadur et al., 2012; Lack et al., 2014; Atiku et al., 2016). As such, BC incorporates a mixture of both elemental and organic fractions (Chow et al., 2009). The OC fraction maintains a more volatile design and can include a large mixture of compounds resulting from incomplete combustion processes. A secondary OC fraction identified as Brown Carbon (BrC) is designated as the light absorbing fraction within the OC composition (Bahadur et al., 2012). The BC and BrC fractions are of importance due to the positive radiative

forcing effects associated while OC is identified as to having a potentially negative forcing effects. The OC fraction is also important with regards to the detrimental health effects associated following inhalation in response to the associated oxy-PAH composites (Atiku et al., 2016).

The mass fraction of OC and EC within the soot matrix varied significantly during the combustion of dry fuelwood and wet fuelwood. In addition, the EC:TC is noted to change between test batches in response to changes in the combustion temperature. The EC fraction was found to be within the range of 75.41% and 92.89% during dry fuelwood combustion and between 21.62% and 26.89% during wet fuelwood combustion. As such, a much higher OC fraction was observed at higher fuel moisture contents. The concentration of OC and EC fractions within the soot matrix is dependent upon the combustion conditions during sampling (Mcdonald et al., 2000; Atiku et al., 2016). Heringa et al. (2011) identifies notable differences in the organic matter (OM) and BC fractions of soot collected in different residential combustion appliances with combustion efficiency and phase of combustion maintaining a principal influence. Similarly, Grieshop et al. (2009) identifies the influence of combustion efficiency upon the organic component formation whereby smouldering fires produce a higher OC fraction and flaming fires produce a higher EC fraction. Reduced OC formation is also reported when burning briquetted fuels rather than fuelwood particles due to the disintegration of the particle structure resulting in improved air availability and higher oxidation of devolatilised products (Schmidl et al., 2008). Mitchell et al. (2016) found that the EC:TC ratio differed throughout the combustion process with a higher ratio present during ignition and flaming combustion followed by a lower ratio during smouldering. The combustion of dry fuelwood is shown to maintain a predominant flaming phase while wet fuelwood is described as a smouldering reaction as indicated by the EC:TC results (**Table 6.5**). Direct results comparison with other authors is difficult given the variability and effects of differing sampling temperatures (Atiku et al., 2016) and analysis techniques (Chow et al., 1993). Notwithstanding, the impact of combustion efficiency outlined within the literature corresponds with findings presented in this work. **Figure 6.24** presents the effect of combustion temperature as an indication of combustion efficiency upon EC and OC formation. The EC fraction is also shown to increase following each batch of dry fuel added to the stove in response to the increase in combustion temperature. The detrimental effects of a higher water volume within the combustion chamber is observed when burning wet fuelwood resulting in the formation of a higher OC fraction after each batch. The energy loss associated with fuel drying and inherent cooling effect of water vapour results in a reduction in combustion temperature and efficiency. Such processes lead to limited burnout of VOC and oxy-PAH compounds which

subsequently attenuate in the formation of the OC fraction. As identified in Heringa et al. (2011) and Grieshop et al. (2009), improved combustion conditions result in an increase in EC and a reduction in OC. Such processes are therefore directly controlled by the fuel moisture content and, as a result, the conditions within the stove.
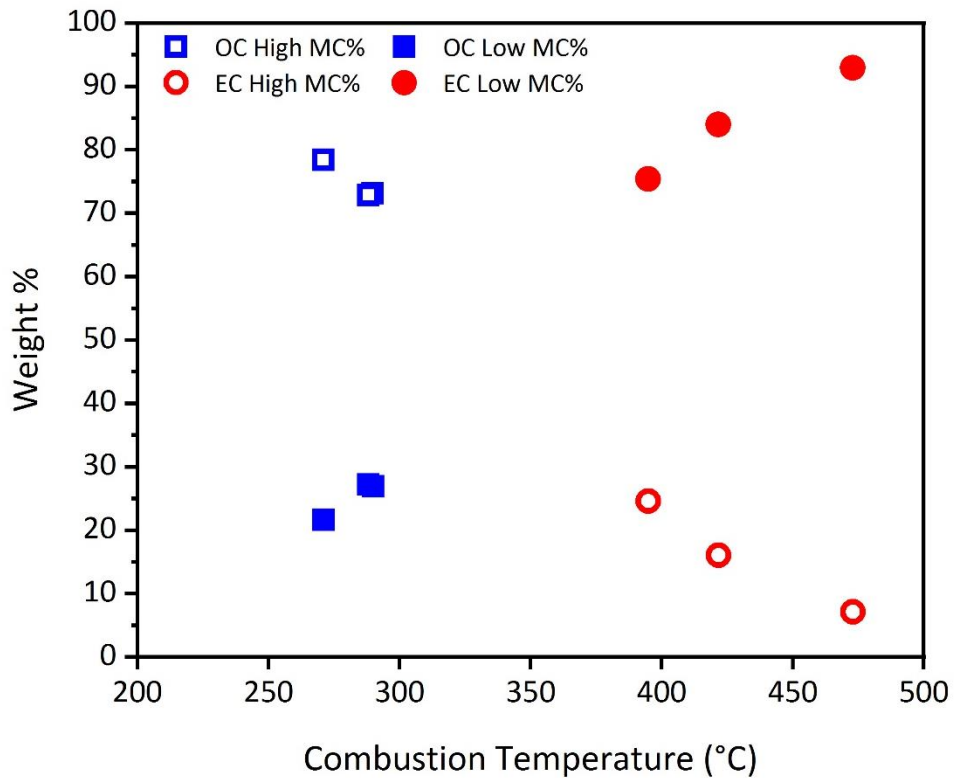
Figure 6.24 The effect of fuel combustion temperature upon OC and EC fractional formation within soot samples.

Raman analysis has been applied as a method of determining variation in the nanostructure of soot samples collected during the combustion of dry and wet fuelwood. The Raman spectra of soot generally consists of two broad overlapping peaks centred at approximately $1350cm^{-1}$ and $1585cm^{-1}$ (Dippel et al., 1999; Sadezky et al., 2005; Ess et al., 2016). Similar findings have been reported here whereby a D-peak and G-peak are present for soot materials collected during the combustion of both fuel types. The I_D/I_G ratio was applied as a method of determining the structural order of soot samples as identified in Ferrari and Robertson (2000). An increase in the I_D/I_G was presented during the combustion of dry fuelwood in response to the higher combustion temperatures resulting in a larger fraction of EC. During the combustion of wet fuelwood the inhibited combustion conditions, in response to an increased moisture content, was shown to

lead to incomplete combustion and a larger OC fraction. As such, the I_D/I_G was shown to be reduced indicating a more significant amorphous carbon structure. In addition, the I_D/I_G appears to directly correspond with variation in the OC content of the soot material. Ess et al. (2016) suggests similar findings where the I_D/I_G was shown to be directly proportional the OC composition of the propane flame derived soot. In the study propane soot maintaining an OC fraction of 4%, 47% and 87% produced an I_D/I_G of 1.19, 1.03 and 0.96 respectively while Pintrex XE2 (very low OC fraction) and Humic acid (very high OC fraction) presented an I_D/I_G of 1.51 and 0.90. **Figure 6.25** shows a linear correlation between I_D/I_G and OC. The increased I_D/I_G of wood derived soot is likely in response to the higher volatile composition of the parent material leading to the formation of amorphous soot compounds. The combustion of wet fuelwood results in a reduced combustion temperature inhibiting the burnout of organic carbon compounds within the smoke. Furthermore, the application of optical Raman analysis, as a non-destructive optical technique, may be applied as a method of determining the elemental carbon and organic carbon of a soot sample given.
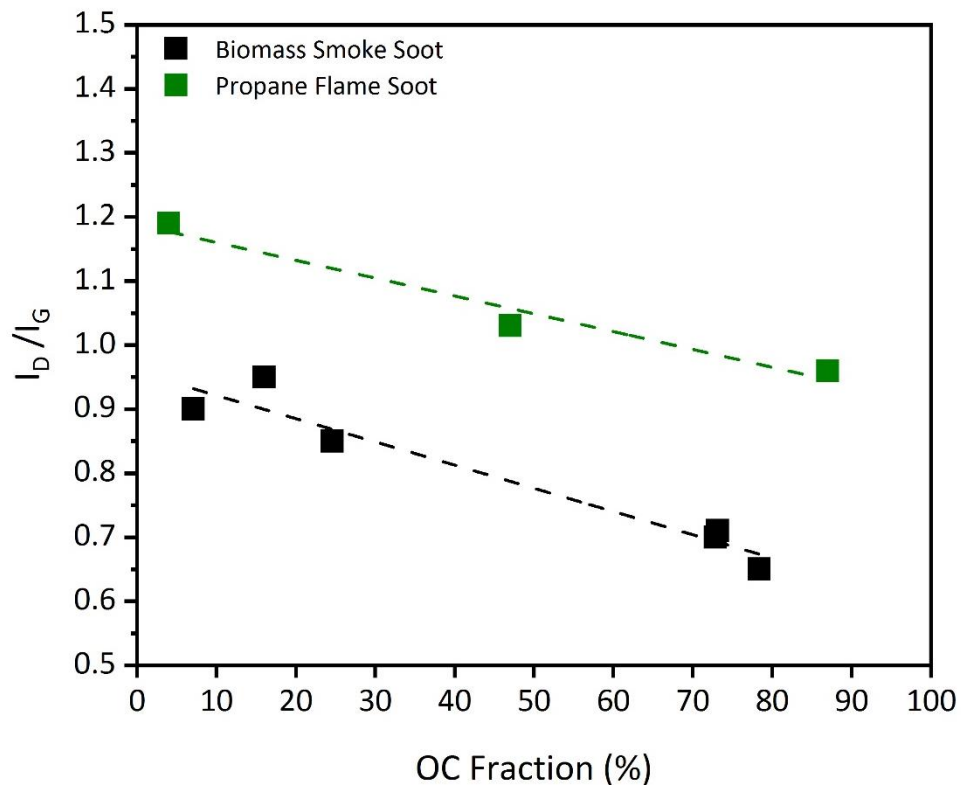
Figure 6.25 Variation in I_D/I_G values with differences in the OC fraction of soot derived from biomass smoke (this work) and propane smoke (Ess et al., 2016).

6.4.5.3 Impact of Combustion Conditions upon Soot Colouration

The colour and density of soot samples collected from the flue and extracted from the dilution tunnel was shown to differ during the combustion of low moisture and high moisture fuelwood. Soot samples generated during the combustion of low moisture fuelwood was shown to be dark brown or black while soot collected during the combustion of high moisture fuelwood where light brown or tan (Price-Allison et al., 2019). Variation in the OC between black and brown soot samples, and subsequent colour shift, has been shown to corresponds with variation in the chemical composition of the material (Atiku et al., 2016). The colouration of soot samples is likely in response to variation in the EC and OC composition. As previously discussed, soot samples collected during the combustion of high moisture fuelwood present a high OC fraction and low EC fraction and present a corresponding brown or tan colour shift. Alternatively, soot samples collected during the combustion of low moisture fuelwood present a low OC fraction and high EC fraction and present a corresponding black colour shift. Similar findings have been identified within the literature attributing variation in the OC fraction during inefficient combustion phases and subsequent effects on soot colouration (Rau, 1989; Mitchell et al., 2016; Jones et al., 2018).

Soot sample material was shown to vary in terms of darkness as a function of colour and density. Soot darkness was measured via spectrodensitometry as a function of light, darkness = 100-L, where L is the material lightness on the CIELAB colour spectrum. Soot concentration is often estimated for residential boiler and engine exhaust systems in accordance with DIN 51402 and ASTM D2156 (McDonald, 2009; Dantas Neto et al., 2013; Mante et al., 2015). An estimation of flue gas concentration requires a known volume of flue gas to be drawn across a filter media before the colour and density of the sample is compared across a known concentration scale. Given the significant variation in both soot colour and the density of the particles collected during fuelwood combustion it may be more applicable to measure sample darkness as a proxy for PM_t generation under different firebox conditions. **Figure 6.26** identified the effect of fuelwood burning rate (kg/hour) on the darkness of PM_t sample material. The darkness of the sample material is seen to vary in response to both the sample colour and the density of the soot collected upon the filter. Soot samples generated during the combustion of low moisture fuelwood under warm-start conditions generally present the highest darkness factor and are generated under the highest fuel conversion rate. Soot samples generated during the combustion of high moisture fuelwood under warm-start conditions generally present the lowest darkness factor and are generated under the lowest fuel conversion rate. Soot samples generated during the

combustion of low moisture fuelwood under cold-start conditions is an intermediate in terms of both sample darkness and burning rate. Such processes are likely in response to increased soot darkness during high temperature combustion where elemental, or black, carbon is a primary constituent. In addition, an increase in the burning rate likely leads to an increase in the rate of PM_t formation across a reduced combustion period. This process combined with increased soot entrainment under higher flue gas velocity rates results in an increase in the darkness and density of soot samples. The relatively low burning rate presented during the combustion of high moisture fuelwood results in a lower flue gas velocity and a slower rate of PM_t formation over a prolonged period. Such processes are an important consideration when applying soot sampling and estimation PM_t concentrations under DIN 51402 and ASTM D2156. High resolution soot sampling under known PM_t concentrations (mg/m^3) could be used to develop an accurate concentration scale based upon the darkness of the sample material similar to the method presented in DIN 51402 and ASTM D2156. The development of a large dataset could be applied as a method of soot concentration monitoring for residential and cookstove appliances where online analytical equipment is not available.
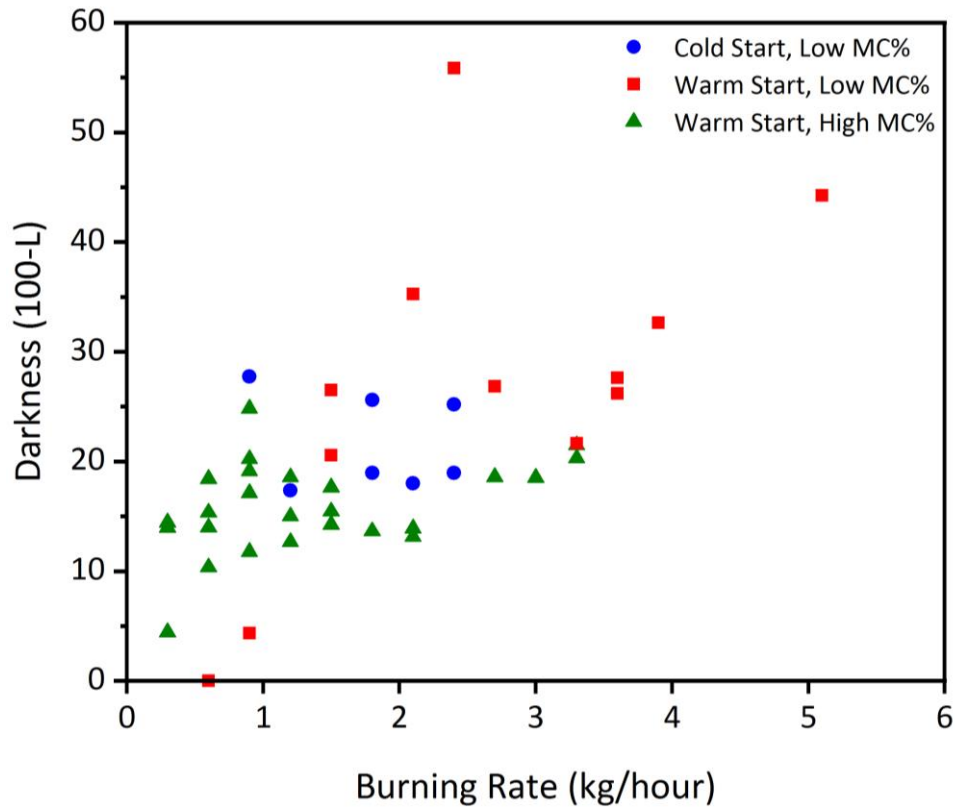
Figure 6.26 The impact of fuelwood moisture content and combustion conditions upon the colouration and loading of soot particles collected from the flue via an ASTM smoke pump device. The relative darkness (D_{rel}) is a measure of the colour variation in the soot samples collected using an ASTM Smoke Pump device (Testo, Smoke Pump) and is the inverse of colour lightness. D_{rel} = 100-L.

6.5 Conclusions

A study was undertaken to investigate the effect of fuelwood moisture content on gaseous and particulate pollutant formation from a small fixed-bed residential heating stove. A series of combustion experiments where undertaken using a method based upon BS EN 13240. Fuels included within this study include low moisture logs (beech) maintaining a moisture content of 12.44% and high moisture logs (beech) maintaining a moisture content of 26.68%. Gaseous emissions where monitored throughout the combustion cycle via an online FTIR analyser. Size-separated soot particles where collected within a dilution tunnel using a gravimetric impaction device. PM_t sample material was collected from the flue using a small handheld gravimetric suction device. Flue gas condensate was analysed to identify the effect of fuelwood moisture content and combustion conditions upon organic acid, TOC and total phenolic compound concentrations. Various physiochemical properties relating to different types of soot collected during the combustion of

different fuels have been made via spectrodensitometry, microscope Raman, py-GC-MS, TGA, SEM and EDX. The following conclusions have been made:

i. The moisture content of bulk fuel samples is difficult to determine via electrical resistance using small handheld digital moisture meter with values often varying from the true moisture content determined via an oven-drying method (BS EN 1813-1). Moisture probe values for low moisture content fuels appear similar to the true MC% value as a result of a more uniform moisture content throughout the fuel particle. Moisture probe values obtained from high moisture fuels often differed from the true MC% value as a result of an uneven distribution of moisture throughout the fuel particle. It may therefore be concluded that digital moisture meter devices are suitable for providing rough estimate of the fuel particle moisture content only.

ii. Fuelwood burning rates were shown to be significantly different depending upon the moisture content of the fuel. It was observed that an increase in the fuel moisture content generally led to a reduction in the rate of fuel conversion. Such processes where attributed to a reduction in the combustion temperature and loss of energy during a prolonged drying period. A strong correlation was observed between the temperature of the combustion reaction and the rate of fuel conversion.

iii. Gaseous pollutant species where shown to be higher during the combustion of high moisture fuelwood. In all cases, gaseous pollutant species derived from wet fuelwood combustion where higher with scaling factors within the range of 12-15 for organic species and 3-23 for hydrocarbon species. A statistically significant correlation between hydrocarbon pollutant species and combustion temperature was observed. As such, it may be concluded that the combustion of low moisture fuelwood results in increased combustion temperatures and, as a result, lower pollutant formation.

iv. The concentration of gaseous hydrocarbon species was shown to be dependent upon the molecular mass of the compound. Species with a lower molecular weight (CH_4) where identified in higher concentrations than high molecular compounds. An increase in the molecular weight corresponds with a reduction in prevalence within the gaseous mixture likely in response to the thermal cracking. High molecular weight compounds including C_3H_8 and C_6H_{14} are less stable and more likely to be degraded under heating leading to the formation of small alkane and alkene chains.

v. The concentrations of TOC and total phenolic content was shown to be significantly higher during the combustion of high moisture fuelwood. The pyrolysis of lignin and cellulose structures within the fuel particle composition results in the formation of protein, sugar, fat, alcohol, hydrocarbon and phenols. Such compounds are emitted as pollutant species in response to inefficient conditions within the firebox during the combustion of high moisture fuelwood. Such processes have a detrimental effect on both climate forcing and human health.

vi. The combustion efficiency was calculated using the MCE method. Dry fuelwood presented a high combustion efficiency than wet fuelwood. A repeatable MCE time series was identified during the combustion of dry fuelwood indicating periods of flaming and smouldering combustion. Oscillations in the MCE were identified during the combustion of high moisture fuelwood in response to variable combustion conditions, periods of prolonged smouldering and the need for manually adjusting the fuel pack. It is therefore possible to ascertain combustion efficiency via the MCE when burning dry fuelwood however it is difficult to accurately determine an MCE time series if the fuel moisture content is high. Furthermore, MCE is shown to correlate with EC/TC in response to variation in the combustion temperature depending upon fuel type.

vii. PM_t emissions generated during the combustion of low moisture and high moisture fuelwood where 3.1 ± 0.6 g/kg$_{fuel}$ and 9.3 ± 4.9 g/kg$_{fuel}$ respectively. Soot samples collected during low fuelwood combustion presented a black appearance and included a high EC fraction and a low OC fraction. Soot samples collected during high fuelwood combustion presented a brown appearance and included a low EC fraction and a high OC fraction. The organic content fraction of soot was shown to reduce during the combustion of low moisture fuelwood in response to increased combustion temperatures.

viii. The physical nature of the $<PM_1$ particulate matter was shown to vary depending upon the fuelwood moisture content of the parent material and OC fraction. Soot samples maintaining a high OC fraction are presented as amorphous tar-like material. Soot samples collected during high temperature combustion and maintaining a high EC fraction are presented as long chains of spherical particulate matter maintaining a diameter of approximately 50 nm.

ix. Raman spectra of soot was presented as two overlapping bands located at approximately 1350cm^{-1} and 1585cm^{-1}. The first peak, identified as the D-band, is representative of disordered carbon structures and the

second-peak, identified as the G-band, is representative of graphitic carbon structures. An increase in the I_D/I_G was presented during the combustion of dry fuelwood in response to the higher combustion temperatures resulting in a larger fraction of EC. In addition, the intensity of the spectra between the two peaks is identified as the D3 band and represents amorphous carbon materials. This band was shown to be higher in soot samples collected during the combustion of wet fuelwood suggesting a higher OC fraction.

6.7 References

Akagi, S.K., Yokelson, R.J., Wiedinmyer, C., Alvarado, M.J., Reid, J.S., Karl, T., Crounse, J.D. and Wennberg, P.O. 2011. Emission factors for open and domestic biomass burning for use in atmospheric models. Atmospheric Chemistry and Physics. 11(9), pp.4039–4072.

Alves, C., Gonçalves, C., Fernandes, A.P., Tarelho, L. and Pio, C. 2011. Fireplace and woodstove fine particle emissions from combustion of western Mediterranean wood types. Atmospheric Research. 101(3), pp.692–700.

Ångström, A. 1929. On the atmospheric transmission of sun radiation and on dust in the air. Geografiska Annaler. 11, pp.156–166.

Atiku, F.A., Mitchell, E.J.S., Lea-Langton, A.R., Jones, J.M., Williams, A. and Bartle, K.D. 2016. The Impact of Fuel Properties on the Composition of Soot Produced by the Combustion of Residential Solid Fuels in a Domestic Stove. Fuel Processing Technology. 151, pp.117–125.

Bahadur, R., Praveen, P.S., Xu, Y. and Ramanathan, V. 2012. Solar absorption by elemental and brown carbon determined from spectral observations. Proceedings of the National Academy of Sciences of the United States of America. 109(43), pp.17366–17371.

BEIS 2016. Summary results of the domestic wood use survey [Online]. Available from: www.gov.uk/government/statistics/digest-of-united-kingdom-energy-statistics-dukes-2014-printed-version.

Bignal, K.L., Langridge, S. and Zhou, J.L. 2008. Release of polycyclic aromatic hydrocarbons, carbon monoxide and particulate matter from biomass combustion in a wood-fired boiler under varying boiler conditions. Atmospheric Environment. 42(39), pp.8863–8871.

Bond, T.C., Doherty, S.J., Fahey, D.W., Forster, P.M., Berntsen, T., DeAngelo, B.J., Flanner, M.G., Ghan, S., Kärcher, B., Koch, D. and Kinne, S. 2013. Bounding the role of black carbon in the climate system: a scientific assessment. Journal of Geophysical Research: Atmospheres. 118(11), pp.5380–5552.

Bond, T.C., Streets, D.G., Yarber, K.F., Nelson, S.M., Woo, J.H. and Klimont, Z. 2004. A technology-based global inventory of black and organic carbon emissions from combustion.pdf. Journal of Geophysical Research2. 109(D14).

Bugge, M. and Haugen, N.E.L. 2014. NOx emissions from wood stoves - a CFD modelling approach In: Proc. of 22nd EU BC&E., pp.674–679.

Bugge, M., Skreiberg, Ø., Haugen, N.E.L. and Carlsson, P. 2020. Predicting NOx emissions from wood stoves using detailed chemistry and computational fluid dynamics. Energy Procedia. 75(1876), pp.1740–1745.

Byler, R.K., Pelletier, M.G., Baker, K.D., Hughs, S.E., Buser, M.D., Holt, G.A. and Carroll, J.A. 2009. Cotton bale moisture meter comparison at different locations. Applied engineering in agriculture. 25(3), pp.315–320.

Chesser Jr, G.D., Davis, J.D., Purswell, J.L. and Lemus, R. 2012. Moisture determination in windrowed switchgrass using electrical resistance probes. Applied engineering in agriculture. 28(5), pp.623–629.

Chomanee, J., Tekasakul, S., Tekasakul, P. and Furuuchi, M. 2015. Effects of Moisture Content and Burning Period on Concentration of Smoke Particles and Particle-Bound Polycyclic Aromatic Hydrocarbons from Rubber- Effects of Moisture Content and Burning Period on Concentration of Smoke Particles and Particle-Bound Polyc. Aerosol and Air Quality Research. 9, pp.404–411.

Chow, J.C., Watson, J.G., Doraiswamy, P., Chen, L.A., Sodeman, D.A., Lowenthal, D.H., Park, K., Arnott, W.P. and Motallebi, N. 2009. Aerosol light absorption , black carbon , and elemental carbon at the Fresno Supersite , California. Atmospheric Research. 93(4), pp.874–887.

Chow, J.C., Watson, J.G., Pritchett, L.C., Pierson, W.R., Frazer, C.A. and Purcell, R.G. 1993. The dri thermal/optical reflectance carbon analysis system: description, evaluation and applications in U.S. air quality studies. Atmospheric Environment. 27(8), pp.1185–1201.

Clarke, S. 2008. Essential chemistry for aromatherapy. Churchill Livingstone.

Damodara, V., Chen, D.H., Lou, H.H., K.M., R., Richmond, P., Wang, A. and Li, X. 2017. Reduced combustion mechanism for C1-C4 hydrocarbons and its application in computational fluid dynamics flare modelling. Journal of air waste management association. 67(5), pp.599–612.

Dantas Neto, A.A., Fernandes, M.R., Barros Neto, E.L., Castro Dantas, T.N. and Moura, M.C.P.A. 2013. Effect of biodiesel/diesel-based microemulsions on the exhaust emissions of a diesel engine. Brazilian Journal of Petroleum and Gas. 7(4), pp.141–153.

Davis, J., Matovic, D. and Pollard, A. 2017. The performance of resistance , inductance , and capacitance handheld meters for determining moisture content of low-carbon fuels. Fuel. 188, pp.254–266.

Dayton, D.C., French, R.J. and Milne, T.A. 1995. Direct Observation of Alkali Vapor Release during Biomass Combustion and Gasification. 1. Application of Molecular Beam/Mass Spectrometry to Switchgrass Combustion. Energy and Fuels. 9(5), pp.855–865.

DEFRA 2017. The Potential Air Quality Impacts from Biomass Combustion.

Dippel, B., Jander, H. and Heintzenberg, J. 1999. NIR FT Raman spectroscopic study of Ñame soot. phys. 1, pp.4707–4712.

Dyakov, Y., Dzhavakhiya, A. and Korpela, T. 2007. Comprehensive and molecular phytopathology. Elsevier.

Espenas L. D. (United States Department of Agriculture Forest Service) 1951. Some Wood-Moisture Relations. Wisconsin.

Ess, M.N., Ferry, D., Kireeva, E.D., Niessner, R., Ouf, F. and Ivleva, N.P. 2016. In situ Raman microspectroscopic analysis of soot samples with different organic carbon content : Structural changes during heating. Carbon. 105, pp.572–585.

Evtyugina, M., Alves, C., Calvo, A., Nunes, T., Tarelho, L., Duarte, M., Prozil, S.O., Evtuguin, D. V and Pio, C. 2014. VOC emissions from residential combustion of Southern and mid- European woods. Atmospheric Environment. 83, pp.90–98.

Fachinger, F., Drewnick, F., Giere, R. and Borrmann, S. 2017. How the user can influence particulate emissions from residential wood and pellet stoves: Emission factors for different fuels and burning conditions. Atmospheric Environment. 158, pp.216–226.

Faix, O., Meier, D. and Fortmann, I. 1990. Thermal degradation of wood. Holz aks Rohund Werkstoff. 48, pp.281–285.

Ferrari, A.C. and Robertson, J. 2000. Interpretation of Raman spectra of disordered and amorphous carbon. The American Physical Society: Physical Review B. 61(20), pp.95–107.

Fuller, G.W., Sciare, J., Lutz, M., Moukhtar, S. and Wagener, S. 2013. New Directions : Time to tackle urban wood burning ? Atmospheric Environment. 68(2013), pp.295–296.

Fuller, G.W., Tremper, A.H., Baker, T.D., Espen, K. and Butter, D. 2014. Contribution of wood burning to PM_{10} in London. Atmospheric Environment. 87, pp.87–94.

Glarborg, P., Jensen, A.D. and Johnsson, J.E. 2003. Fuel nitrogen conversion in solid fuel fired systems. Progress in Energy and Combustion Science. 29(2), pp.89–113.

Grieshop, A.P., Logue, J.M., Donahue, N.M. and Robinson, A.L. 2009. and Physics Laboratory investigation of photochemical oxidation of organic aerosol from wood fires 1: measurement and simulation of organic aerosol evolution. Atmos. Chem. Phys.2. 9, pp.1263–1277.

Harrison, M.A.J., Barra, S., Borghesi, D., Vione, D., Arsene, C. and Iulian Olariu, R. 2005. Nitrated phenols in the atmosphere: A review. Atmospheric Environment. 39(2), pp.231–248.

Heringa, M.F., Decarlo, P.F., Chirico, R., Tritscher, T., Dommen, J., Weingartner, E., Richter, R. and Wehrle, G. 2011. and Physics Investigations of primary and secondary particulate matter of different wood combustion appliances with a high-resolution time-of-flight aerosol mass spectrometer. atmo. 11, pp.5945–5957.

Houck, J.E. and Tiegs, P.E. 1998. Residential Wood Combustion Technical Review: Volume 1. Technical Report.

Houmoller, S. and Evald, A. 1999. Sulphur Balances for Biofuel Combustion Systems In: 4th Biomass Conference of the Americas.

Huang, D., Guo, C. and Shi, L. 2017. Experimental investigation on the morphology of soot aggregates from the burning of typical solid and liquid fuels. Journal of Nanoparticle Research. 19(3), p.96.

Huang, Q., Wang, L. and Han, S. 1995. The genotoxicity of substituted nitrobenzenes and the quantitative structure-activity relationship studies. Chemosphere. 30(5), pp.915–923.

Ivleva, N.P., Mckeon, U., Niessner, R. and Pöschl, U. 2007. Raman Microspectroscopic Analysis of Size- Resolved Atmospheric Aerosol Particle Samples Collected with an ELPI : Soot , Humic-Like Substances , and Inorganic Compounds Raman Microspectroscopic Analysis of Size-Resolved Atmospheric Aerosol Particle Sample. Aerosol Science and Technology. 41(7), pp.655–671.

Johansson, L.S., Leckner, B., Gustavsson, L., Cooper, D., Tullin, C. and Potter, A. 2004. Emission characteristics of modern and old-type residential boilers fired with wood logs and wood pellets. Atmospheric Environment. 38, pp.4183–4195.

Johansson, L.S., Tullin, C., Leckner, B. and Sjovall, P. 2003. Particle emissions from biomass combustion in small combustors. Biomass and Bioenergy. 25, pp.435–446.

Jones, J., Mitchell, E., Williams, A., Jose, G., Hondow, N., Lea-langton, A., Jones, J., Mitchell, E., Williams, A., Jose, G., Hondow, N. and Combustion-generated, A.L.E. 2018. Examination of Combustion-Generated Smoke Particles from Biomass at Source : Relation to Atmospheric Light Absorption Examination of Combustion-Generated Smoke Particles from Biomass at Source : Relation to Atmospheric Light Absorption. Combustion Science and Technology. 00(00), pp.1–14.

Kenney, K.L., Smith, W.A., Gresham, G.L., Westover, T.L., Kenney, K.L., Smith, W.A., Gresham, G.L. and Westover, T.L. 2014. Understanding biomass feedstock variability. Biofuels. 4(1), pp.111–127.

Kirchstetter, T.W., Novakov, T. and Hobbs, P. V. 2004. Evidence that the spectral dependence of light absorption by aerosols is affected by organic carbon. Journal of Geophysical Research: Atmospheres. 109(21).

Kjällstrand, J. and Petersson, G. 2001. Phenolic antioxidants in wood smoke. Science of the Total Environment. 277(1–3), pp.69–75.

Kocbach Bølling, A., Pagels, J., Yttri, K.E., Barregard, L., Sallsten, G., Schwarze, P.E. and Boman, C. 2009. Health effects of residential wood smoke particles: the importance of combustion conditions and physicochemical particle properties. Particle and Fibre Toxicology. 6(1), pp.1–20.

Koppejan, J. and Loo, S. van 2008. The Handbook of Biomass Combustion and Co-firing. London: Routledge.

Koppmann, R., Von Czapiewski, K. and Reid, J.S. 2005. A review of biomass burning emissions, part I A review of biomass burning emissions, part I: gaseous emissions of carbon monoxide, methane, volatile organic compounds, and nitrogen containing compounds. Atmos. Chem. Phys. Discuss. 5, pp.10455–10516.

Lack, D.A., Moosmuller, H., McMeeking, G.R., Chakrabarty, R.K. and Baumgardner, D. 2014. Characterizing elemental, equivalent black, and refractory black carbon aerosol particles: a review of techniques, their limitations and uncertainties. Analytical and Bioanalytical Chemistry. 406, pp.99–122.

Lamberg, H., Nuutinen, K., Tissari, J., Ruusunen, J., Yli-Pirilä, P., Sippula, O., Tapanainen, M., Jalava, P., Makkonen, U., Teinilä, K., Saarnio, K., Hillamo, R., Hirvonen, M.R. and Jokiniemi, J. 2011. Physicochemical characterization of fine particles from small-scale wood combustion. Atmospheric Environment. 45(40), pp.7635–7643.

Lanz, V.A., Hueglin, C., Buchmann, B., Hill, M., Locher, R., Staehelin, J., Reimann, S. and Science, C. 2008. Receptor modelling of C 2 – C 7 hydrocarbon sources at an urban background site in Zurich , Switzerland : changes between 1993 – 1994 and 2005 – 2006. Atmospheric Chemistry and Physics. 8, pp.2313–2332.

Li, M., Wang, X., Lu, C., Li, R., Zhang, J., Dong, S., Yang, L., Xue, L., Chen, J. and Wang, W. 2020. Nitrated phenols and the phenolic precursors in the atmosphere in urban Jinan, China. Science of the Total Environment. 714, p.136760.

Liu, C., Chung, C.E., Zhang, F. and Yin, Y. 2016. The colours of biomass burning aerosols in the atmosphere. Scientific Reports. 6(1), pp.1–9.

Liu, C., Chung, E.C., Yin, Y. and Schnaiter, M. 2018. The absorption Ångström exponent of black carbon: from numerical aspects. Atmospheric Chemistry and Physics. 18(9), pp.6259–6273.

Lu, H., Zhu, L. and Zhu, N. 2009. Polycyclic aromatic hydrocarbon emission from straw burning and the influence of combustion parameters. Atmospheric Environment. 43(4), pp.978–983.

Magnone, E., Park, S. and Park, J.H. 2016. Effects of Moisture Contents in the Common Oak on Carbonaceous Aerosols Generated from Combustion Processes in an Indoor Wood Stove Effects of Moisture Contents in the Common Oak on in an Indoor Wood Stove. Combustion Science and Technology. 188(6), pp.982–996.

Mante, O.D., Butcher, T.A., Wei, G., Trojanowski, R. and Sanchez, V. 2015. Evaluation of biomass-derived distillate fuel as renewable heating oil. Energy and Fuels. 29(10), pp.6536–6543.

Mason, P.E., Darvell, L.I., Jones, J.M. and Williams, A. 2016. Observations on the release of gas-phase potassium during the combustion of single particles of biomass. Fuel. 182, pp.110–117.

Maxwell, D., Gudka, B.A., Jones, J.M. and Williams, A. 2020. Emissions from the combustion of torrefied and raw biomass fuels in a domestic heating stove. Fuel Processing Technology. 199.

Mcdonald, J.D., Zielinska, B., Fujita, E.M., Sagebiel, J.C., Chow, J.C. and Watson, J.G. 2000. Fine particle and gaseous emission rates from residential wood combustion. Environmental Science and Technology. 34(11), pp.2080–2091.

McDonald, R. 2009. Evaluation of gas, oil and wood pellet fuelled residential heating system emissions characteristics.

Min, S., Ryong, H., Joo, Y., Yeun, S. and Hyuck, K. 2011. Mutation Research / Genetic Toxicology and Environmental Mutagenesis Organic extracts of urban air pollution particulate matter ($PM_{2.5}$) -induced genotoxicity and oxidative stress in human lung bronchial epithelial cells. Mutation Research - Genetic Toxicology and Environmental Mutagenesis. 723(2), pp.142–151.

Mitchell, E.J.S., Lea-Langton, A.R., Jones, J.M., Williams, A., Layden, P. and Johnson, R. 2016a. The impact of fuel properties on the emissions from the combustion of biomass and other solid fuels in a fixed bed domestic stove. Fuel Processing Technology. 142, pp.115–123.

Mitchell, E.J.S., Ting, Y., Allan, J., Spracklen, D. V, Mcfiggans, G., Coe, H., Routledge, M.N., Williams, A., Jones, J.M., Ting, Y., Allan, J. and Spracklen, D. V 2019. Pollutant Emissions from Improved Cookstoves of the Type Used in Sub-Saharan Africa Pollutant Emissions from Improved Cookstoves of the Type Used in Sub-Saharan Africa. Combustion Science and Technology., pp.1–21.

Mohr, C., Lopez-Hilfiker, F.D., Zotter, P., Prévoît, A.S.H., Xu, L., Ng, N.L., Herndon, S.C., Williams, L.R., Franklin, J.P., Zahniser, M.S., Worsnop, D.R., Knighton, W.B., Aiken, A.C., Gorkowski, K.J., Dubey, M.K., Allan, J.D. and Thornton, J.A. 2013. Contribution of nitrated phenols to wood burning brown carbon light absorption in Detling, United Kingdom during winter time. Environmental Science and Technology. 47(12), pp.6316–6324.

Morville, S., Scheyer, A., Mirabel, P. and Millet, M. 2006. Spatial and geographical variations of urban, suburban and rural atmospheric concentrations of phenols and nitrophenols. Environmental Science and Pollution Research. 13(2), pp.83–89.

Nishad, P.M. 2013. Various colour spaces and colour space conversion. Journal of Global Research in Computer Science. 4(1), pp.44–48.

Nowakowski, D.J. and Jones, J.M. 2008. Uncatalysed and potassium-catalysed pyrolysis of the cell-wall constituents of biomass and their model compounds. Journal of Analytical and Applied Pyrolysis. 83(1), pp.12–25.

Nowakowski, D.J., Jones, J.M., Brydson, R.M.D. and Ross, A.B. 2007. Potassium catalysis in the pyrolysis behaviour of short rotation willow coppice. Fuel. 86(15), pp.2389–2402.

Obaidullah, M., Bram, S., Verma, K. and De Ruyck, D. 2012. A review on particle emissions from small scale biomass combustion. International Journal of Renewable Energy Research. 2(1).

Obernberger, I., Brunner, T. and Bärnthaler, G. 2006. Chemical properties of solid biofuels-significance and impact. Biomass and Bioenergy. 30(11), pp.973–982.

Obernberger, I., Brunner, T. and Joller, M. 2001. Characterisation and formation of aerosols and fly-ashes from fixed-bed biomass combustion. Aerosols in Biomass Combustion., pp.67–74.

Olsson, J.G., Pettersson, J.B.C. and Hald, P. 1997. Alkali Metal Emission during Pyrolysis of Biomass.

Orasche, J., Schnelle-Kreis, J., Schön, C., Hartmann, H., Ruppert, H., Arteaga-Salas, J.M. and Zimmermann, R. 2013. Comparison of emissions from wood combustion. Part 2: Impact of combustion conditions on emission factors and characteristics of particle-bound organic species and polycyclic aromatic hydrocarbon (PAH)-related toxicological potential. Energy and Fuels. 27(3), pp.1482–1491.

Oros, D.R. and Simoneit, B.R.T. 2001. Identification and emission factors of molecular tracers in organic aerosols from biomass burning Part 1. Temperate climate conifers. Applied Geochemistry. 16(13), pp.1513–1544.

Ozgen, S., Caserini, S., Galante, S., Giugliano, M., Angelino, E., Marongiu, A., Hugony, F., Migliavacca, G. and Morreale, C. 2014. Emission factors from small scale appliances burning wood and pellets. Atmospheric Environment. 94, pp.144–153.

Pandey, K. and Sahu, L.K. 2014. Emissions of volatile organic compounds from biomass burning sources and their ozone formation potential over India. Current Science. 106(9), pp.1270–1279.

Pervez, S., Verma, M., Tiwari, S., Chakrabarty, R.K., Watson, J.G., Chow, J.C., Panicker, A.S., Deb, M.K., Siddiqui, M.N. and Pervez, Y.F. 2019. Household solid fuel burning emission characterization and activity levels in India. Science of the Total Environment. 654, pp.493–504.

Pettersson, E., Boman, C., Westerholm, R., Bostrom, D. and Nordin, A. 2011. Stove Performance and Emission Characteristics in Residential Wood Log and Pellet Combustion, Part 2: Wood Stove. Energy Fuels. 25, pp.315–323.

Phillips, D., Mitchell, E.J.S., Lea-Langton, A.R., Parmar, K.R., Jones, J.M. and Williams, A. 2016. The use of conservation biomass feedstocks as potential

bioenergy resources in the United Kingdom. Bioresource Technology. 212, pp.271–279.

Price-Allison, A., Lea-Langton, A.R., Mitchell, Edward J. S. Gudka, B., Jones, J.M., Mason, P.E. and Williams, A. 2019. Emissions Performance of High Moisture Wood Fuels Burned in a Residential Stove. Fuel. 239, pp.1038–1045.

Purvis, C.R. and McCrillis, R.C. 2000. Fine Particulate Matter (PM) and Organic Speciation of Fireplace Emissions. Environmental Science and Technology. 34, pp.1653–1658.

Raitila, J., Heiskanen, V.P., Routa, J., Kolström, M. and Sikanen, L. 2015. Comparison of Moisture Prediction Models for Stacked Fuelwood. Bioenergy Research. 8(4), pp.1896–1905.

Rau, J.A. 1989. Composition and size distribution of residential wood smoke particles. Aerosol Science and Technology. 10(1), pp.181–192.

Reid, J.S., Koppmann, R., Eck, T.F. and Eleuterio, D.P. 2005. A review of biomass burning emissions part II: intensive physical properties of biomass burning particles. Atmos. Chem. Phys. 5, pp.799–825.

Rogge, W.F., Hildemann, L.M., Mazurek, M.A. and Cass, G.R. 1998. Sources of Fine Organic Aerosol. 9. Pine, Oak , and Synthetic Log Combustion in Residential Fireplaces. Environmental Science and Technology. 32(1), pp.13–22.

Russell, P.B., Bergstrom, R.W., Shinozuka, Y., Clarke, A.D., DeCarlo, P.F., Jimenez, J.L., Livingston, J.M., Redemann, J., Dubovik, O. and Strawa, A. 2010. Absorption Angstrom Exponent in AERONET and related data as an indicator of aerosol composition. Atmospheric Chemistry and Physics. 10(3), pp.1155–1169.

Sadezky, A., Mucjenhuber, H., Grothe, H., Niessner, R. and Poschl, U. 2005. Raman microspectroscopy of soot and related carbonaceous materials: Spectral analysis and structural information. Carbon. 43, pp.1731–1742.

Schmidl, C., Marr, I.L., Caseiro, A., Kotianova, P., Berner, A., Bauer, H., Kasper-giebl, A. and Puxbaum, H. 2008. Chemical characterisation of fine particle emissions from wood stove combustion of common woods growing in mid-European Alpine regions. Atmospheric Environment. 42(1), pp.126–141.

Seong, H.J. and Boehman, A.L. 2013. Evaluation of Raman Parameters Using Visible Raman Microscopy for Soot Oxidative Reactivity. Energy and Fuels. 27, pp.1613–1624.

Shen, G., Tao, S., Wei, S., Zhang, Y., Wang, R., Wang, B., Li, W., Shen, H., Huang, Y., Chen, Y., Chen, H., Yang, Y., Wang, W., Wang, X., Liu, W. and Simonich, S.L.M. 2012. Emissions of Parent, Nitro, and Oxygenated Polycyclic Aromatic Hydrocarbons from Residential Wood Combustion in Rural China. Environmental Science and Technology. 46, pp.8123–8130.

Shen, G., Wei, S., Wei, W., Zhang, Y., Min, Y., Wang, B., Wang, R., Li, W., Shen, H., Huang, Y., Yang, Y., Wang, W., Wang, X., Wang, X. and Tao, S. 2012. Emission factors, size distributions, and emission inventories of carbonaceous particulate matter from residential wood combustion in rural China. Environmental Science and Technology2. 46(7), pp.4207–4214.

Shen, G., Xue, M., Wei, S., Chen, Y., Zhao, Q., Li, B., Wu, H. and Tao, S. 2013. Influence of fuel moisture, charge size, feeding rate and air ventilation conditions on the emissions of PM, OC, EC, parent PAHs, and their derivatives from residential wood combustion. Journal of Environmental Sciences (China). 25(9), pp.1808–1816.

Simoneit, B.R.T. 2002. Biomass burning - A review of organic tracers for smoke from incomplete combustion.

Sippula, O. 2010. Fine particle formation and emissions in biomass combustion.

Sippula, O., Hokkinen, J., Puustinen, H., Yli-Pirilä, P. and Jokiniemi, J. 2009. Comparison of particle emissions from small heavy fuel oil and wood-fired boilers. Atmospheric Environment. 43(32), pp.4855–4864.

Tihay-Felicelli, V., Santoni, P.A., Gerandi, G. and Barboni, T. 2017. Smoke emissions due to burning of green waste in the Mediterranean area: Influence of fuel moisture content and fuel mass. Atmospheric Environment. 159, pp.92–106.

Tissari, J., Lyyränen, J., Hytönen, K., Sippula, O., Tapper, U., Frey, A., Saarnio, K., Pennanen, A.S., Hillamo, R., Salonen, R.O., Hirvonen, M.R. and Jokiniemi, J. 2008. Fine particle and gaseous emissions from normal and smouldering wood combustion in a conventional masonry heater. Atmospheric Environment. 42(34), pp.7862–7873.

Tuinstra, F. and Koenig, J.L. 1970. Raman Spectrum of Graphite. Journal of Chemical Physics. 53(3), pp.1126–1130.

Vakkilainen, E.K. 2017. Steam Generation from Biomass. Oxford: Butterworth-Heinemann.

Wagner, F., Wagner, F., Amann, M., Bertok, I., Cofala, J. and Heyes, C. 2010. Baseline emission projections and further cost-effective reductions of air pollution impacts in Europe – a 2010 perspective NEC Scenario Analysis Report Nr. 7 Baseline Emission Projections and Further Cost-effective Reductions of Air Pollution Impacts in. Laxenburg: International Institute for Applied Systems Analysis.

Wiinikka, H. and Gebart, R. 2004. Critical parameters for particle emissions in small-scale fixed-bed combustion of wood pellets. Energy and Fuels. 18(4), pp.897–907.

Wilton, E. and Bluett, J. 2012. Factors influencing particulate emissions from NEW compliant woodburners in Nelson, Rotorua and Taumarunui 2007.

Wöhler, M., Andersen, J.S., Becker, G., Persson, H., Reichert, G., Schön, C., Schmidl, C., Jaeger, D. and Pelz, S.K. 2016. Investigation of real-life operation of biomass room heating appliances - Results of a European survey. Applied Energy. 169, pp.240–249.

Yokelson, R.J., Griffith, D.W.T. and Ward, D.E. 1996. Open-path Fourier transform infrared studies of large-scale laboratory biomass fires. Journal of Geophysical Research: Atmospheres. 101(D15), pp.67–80.

Yuntenwi, E.A.T. and Ertel, J. 2008. Laboratory study of the effects of moisture content on heat transfer and combustion efficiency of three biomass cook stoves. Energy for Sustainable Development. 12(2), pp.66–77.

Zhao, W., Li, Z., Zhao, G., Zhang, F. and Zhu, Q. 2008. Effect of air preheating and fuel moisture on combustion characteristics of corn straw in a fixed bed. Energy Conversion and Management. 49(12), pp.3560–3565.

Chapter 7
The Effect of Cold-Start Operation on Combustion Conditions and Pollutant Formation

7.1 Introduction

Combustion testing of residential room-heating appliances utilising solid fuels, mineral fuels and fuelwood, is often undertaken in accordance with BS EN 13240:2001 + A2: 2004. The testing of domestic heating appliances to the standard method requires the stove device to be heated to a nominal operating condition prior to the start of the testing sequence. As such, an ignition load is applied to the device followed by a pre-test batch of test-fuel material which is combusted under different cold-start conditions. The pre-test batch, or batches (when required), are applied to ensure nominal combustion conditions and the formation of a suitable hot-firebed for subsequent test-batch ignition. Similar pre-test procedures are applied when testing domestic heating appliances using bituminous coal fuels (BS PD 6434:1969), solid fuel in space heating appliances (AS/NZS 4012:1999; CSA B415.1-10:2010; NS 3058:1994), residential cooker appliances (EN 12815:2001 + A1:2004), insert appliances for an open fireplace (EN 13229:2001 + A2:2004) and larger boiler systems (<500 kW) burning fossil fuels or biogenic material (BS EN 303-5:2012). As such, stove testing practices are generally applied in order to ensure repeatability of performance and repeatability of emission results under well-defined, or idealised, combustion conditions. Subsequently, the results generated by means of standardised testing practices generally present combustion values that are not representative or real-world domestic application (Houck et al., 2008; Reichert and Schmidl, 2018). Increased smoke formation is often observed during cold-start operation in response to lower combustion temperatures (Fachinger et al., 2017). The effect of high smoke formation, generally observed during start-up and cold-start operation, is therefore negated from the experimental procedure and quantified emission factor results (Houck et al., 2008). Furthermore, the development of emission inventories applying results from only warm-start stove operation may contribute in an underestimation of true domestic combustion emissions. For example, a poorly operated heating appliance utilised for aesthetics or short-term heating may only apply a cold-start batch and a single warm-start batch. The resulting emission profile would suggest that the majority of emissions from the combustion reaction originated from the ignition and cold-start period. The daily period of stove operation is known to vary across the UK with London and the North West presenting 1 h and 24 h of use per week respectively (BEIS, 2016). If stove appliances are only used periodically or for a reduced duration, the effect of

the cold-start would be significant in terms of total emissions produced. Emission inventories may therefore underestimate the true pollutant formation when testing under pre-heated conditions only. Several testing methods have been developed which attempt to provide information on combustion efficiency and emission monitoring under real-world operating conditions. For example, the beReal testing procedure, designed to test residential combustion appliances under real-world operating conditions, utilises a series of different operating conditions within a testing series including ignition and pre-heating conditions (Reichert et al., 2013). The majority of combustion testing presented within the literature maintains an ignition and pre-test phase which is generally disregarded from the experimental conclusions with only warm-start data quantified for application in emission inventories (Mitchell et al., 2016). The following work aims to assess the effect of cold-start operating conditions on stove performance and pollutant emission formation, the effect of cold-start data on emission factor repeatability and conclusions, and the effect of ignition materials on combustion characteristics.

7.2 Literature Review

Combustion testing in accordance with BS EN 13240:2001 + A2: 2004 is undertaken while the heating appliance is operating under nominal conditions with ignition and cold-start operation generally neglected from the testing procedure. Cold-start operation involves the ignition, start-up and combustion of a single or series of fuel batches while warm-start operation is the process of applying additional fuel to the appliance following the formation of a hot grate. When testing to a standard operating procedure the cold-start process is applied for the purpose of developing a hot grate only meaning that start-up performance and emissions are discounted from the experimental results (Houck et al., 2008). Previous research has identified increased combustion emissions during cold-start operation (Fachinger et al., 2017; Gonçalves et al., 2011; Houck et al., 2008; Hueglin et al., 1997; Nussbaumer et al., 2008; Ozgen et al., 2013; Tissari et al., 2008) with such processes often occurring in response to reduced combustion temperatures (Fachinger et al., 2017; Tissari et al., 2008). The majority of combustion testing within the literature is undertaken under warm-start operation only meaning that cold-start values are generally not incorporated within contemporary emission inventories (McCrillis et al., 1992). The testing of appliances under such conditions results in as much as 33% of the total emissions being disregarded when cold-start data is negated (Tiegs, 1995).

Particulate emission formation is commonly observed under poor combustion conditions when the operating temperature is low. Cool temperatures under cold-

start operation therefore result in an increase in PM_t formation prior to the onset of nominal combustion conditions. Previously, Shelton & Gay (1986) identified an increase in PM_t emissions during cold-start operation by a factor of five when compared to stove operation under nominal operation. Nussbaumer et al. (2008) also identifies as much as 50% of the total PM_t emission formation occurring during the initial 20 min of stove operation equating to just 7% of the total burning cycle. In addition, Ozgen et al. (2013) characterises as much as 46% of the total PM_t formation occurring during the primary ignition phase. Similar work undertaken by Fachinger et al. (2017) shows this effect during the combustion of a variety of softwood and hardwood fuels under cold-start and warm-start operation. PM_t emission is shown to be 15.7 mg/MJ and 4.3 mg/MJ during the cold-start and warm-start operation of beech fuelwood combustion. Similarly, during the combustion of ash and spruce the PM_t emission is shown to be 17.7 mg/MJ and 12.3 mg/MJ under cold-start operation and 3.7 mg/MJ and 7.7 mg/MJ under warm-start operation respectively. Such processes are observed in closed-stove, open-fireplace and cookstove appliances where inhibited combustion conditions during cold-start operation result in higher PM_t emissions (Gonçalves et al., 2011; Maddalena et al., 2012). These emissions are generally neglected from standard operating procedures and emission indexes given the complexity of operating stove appliances during start-up (Shelton & Gay, 1986) and the inherent variability in cold-start operation which can result in a significant error of quantified emission factor results (McCrillis et al., 1992).

The number of cold-start batches applied is often climate dependant; in cooler locations where fuelwood is burned as a primary method of heating the number of cold-starts is likely to be minimal. In locations where wood burning is not the primary method of heating the number of cold-starts is likely to be higher meaning the method of determining emissions is not representative of real-world use (Houck et al., 2008; Gabriel Reichert & Schmidl, 2018; Shelton & Gay, 1986). **Figure 7.1** presents findings of a 2016 BEIS study investigating the average number of hours which different combustion appliances are operated per week (BEIS, 2016). Results identify the majority of appliances currently used within the UK are open fireplace and closed stove systems located within urban locations. In addition, a significant fraction of all appliances are used less than 12 hours per week. As such, it is likely that urban combustion appliances are only used for a limited number of hours per combustion event. A similar pattern of stove used has been identified in the USA where an average operation period of 5.8 h (HPBA, 2004) and 4.8 h (BPBA, 2006) is presented (Houck et al., 2008). This suggests that, particularly in urban locations, the use of stove appliances is likely to present a significant number of cold-start phases (Houck et al., 2008). Therefore, both commercial and academic emission

inventories devised in accordance with BS EN 13240:2001 + A2: 2004 may underestimate the effect of domestic combustion appliances in response to the effect of a high frequency of cold-start operation.
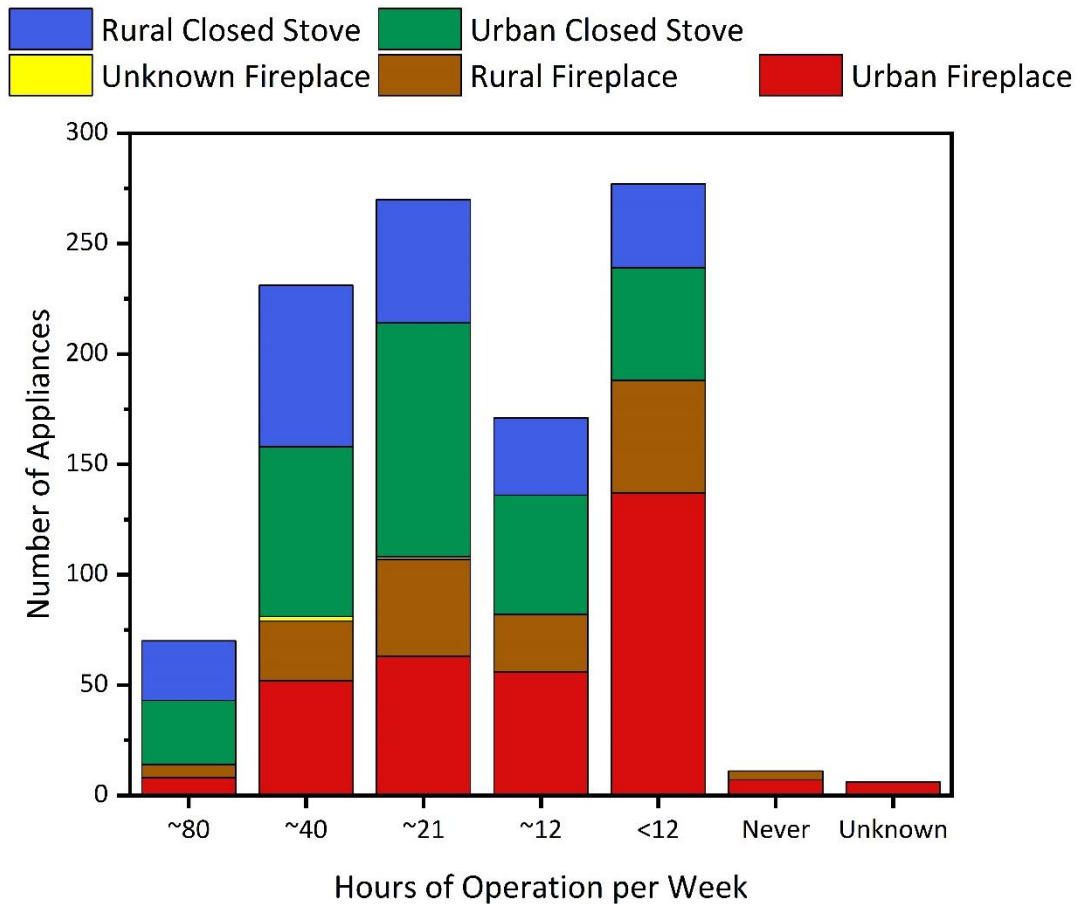
Figure 7.1 Variation in the hourly stove use within the UK during winter months. The figure presents variation in terms of duration (hours) for both closed-stove appliances and insert open-fireplace installations (BEIS, 2016).

7.3 Materials and Methods

A HETAS approved Waterford Stanley Oisin multi-fuel heating stove was used during combustion testing as previously identified (Maxwell et al., 2020; Mitchell et al., 2016; Phillips et al., 2016; Price-Allison et al., 2018). Information relating to equipment and operating procedures is presented in **Chapter 3** Combustion testing was undertaken using two methods. In the first, combustion testing was undertaken in a method similar to that presented in BS EN 13240 for the purpose of evaluating the effect of cold-start and warm-start operation on emissions. In the second, a series of kindling piles where combusted from room temperature with the aid of different firelighter materials so as to evaluate the effect of ignition materials on

emissions and start-up performance. Fuel characterisation for fuelwood and kindling is presented in **Table 7.1**. Zip[TM] firelighter and If You Care[TM] firelighter is manufactured in accordance with BS 7952-2001 and BS 1860-3 where the aromatic content (<25% m/m), sulphur content (<0.2% m/m) and smoke point (>20mm) is controlled.

Table 7.1 Proximate and ultimate analysis of test fuel, kindling and firelighter materials

Fuel Type	Beech Fuelwood (Price-Allison et al., 2021)	Pine Kindling [Homefire] (Phyllis2, 2021)
Volatile Matter (% db)	75.8±0.4	81.83
Ash	10.5±0.6	1.03
Fixed Carbon	13.7±0.4	17.14
Bulk MC (% ar)	12.92±1.32	16.48±1.36
C (% db)	46.1±0.6	50.87
H	5.7±0.1	6.27
N	0.4±0.01	0.18
S	0.00*	0.04
O	37.3±0.9	41.58

* values recorded below the detection limit

7.3.1 Cold-Start (CS) and Warm-Start (WS) Combustion Testing Method

Combustion testing was undertaken using kiln-dried hardwood beech (Fagus sylvatica L.) logs sourced from a local supplier [Ashtrees Ltd, Leeds, West Yorkshire]. The moisture content of the fuelwood was determined in accordance with BS EN 1813-1 and was found to be 12.92±1.32. All bark was removed from the fuel prior to analysis and combustion testing. Each experimental batch maintained a bulk mass between 1.18 kg and 1.35 kg on an as fired basis (μ = 1.26±0.1 kg). Combustion testing was undertaken in accordance with BS EN 13240 with gaseous and particulate sampling undertaken as identified in **Chapter 3**.

Stove operation incorporated a single cold-start batch followed by a series of warm-start batches under nominal combustion conditions. A cold-start batch was constructed on the grate in a manner which ensured repeatability in start-up conditions. A pre-weighed sample of kerosene-based firelighter material [ZipTM, High Performance] maintaining a mass of 50.01±0.08 g was placed on the centre of the grate. Subsequently, a pre-weighed batch of softwood kindling maintaining a

mass of 102.41±1 g was arranged around the firelighter so as to ensure maximum exposure. Two logs where placed above the kindling pack based upon a bottom-up ignition approach (Nussbaumer et al., 2008). The duration of cold-start operation was identified on a mass basis. Subsequent warm-start batches where applied onto the hot-grate without de-ashing allowing for ease of ignition.

7.3.2 Firelighter Combustion Testing Method

Combustion testing was undertaken using techniques previously identified (**Chapter 3**). A test pile batch was constructed on a cold-grate in a manner which ensured repeatability in start-up conditions. A pre-weighed sample of firelighter was placed on the centre of the grate and a pile of softwood kindling was constructed above. Ignition was undertaken following a bottom-up method as described in Maxwell et al. (2020). If You Care[TM] firelighter testing incorporated a mass of 53.7±2.2 g of the ignition aid and 302.1±2.9 g of pine kindling. Zip[TM] testing incorporated a mass of 50.1±0.5 g of the ignition aid and 302.4±2.5 g of pine kindling. The combustion duration was determined on a visual basis with the end of combustion testing identified at 5 min following the end of the flaming phase. A total of three tests were undertaken for each of the firelighter materials with each test beginning at room temperature or cold-start conditions. The primary supplement associated with If You Care[TM] firelighter material is vegetable oil maintaining an estimated HHV of 40.5 MJ/kg while Zip[TM] firelighter material includes kerosene as a supplement maintaining an estimated HHV of 46.2 MJ/kg (Demirbaş, 2003; TheEngineeringToolbox.com, 2003). Furthermore, the chemical structure of vegetable oil and kerosene is known to differ. Vegetable oil generally comprises triglycerides which include a molecule of glycerol and three molecules of fatty acids in the form of a carboxyl group (Blin et al., 2013). Alternatively, kerosene is a petroleum-based substance comprising a complex mixture of hydrocarbons in the form of 10-16 carbon atoms per molecule with additional inclusions of benzene, hexane and naphthalene (Gad & Pham, 2014; Lam et al., 2012). Cetane number (CN) is often applied as a measure of ease of ignition and material flammability (Sidibé et al., 2010). The CN of vegetable oil is dependent upon the parent feedstock and is generally found within the range of 29 and 45. Alternatively, diesel and other petroleum-based substances maintain a higher CN value often greater than 50 (Blin et al., 2013; Sidibé et al., 2010). Previous work has identified higher emissions and improved performance during the combustion of kerosene-based fuels in contrast to vegetable oil-based derivatives (Dinesha et al., 2019) however there has been limited evaluation of the effect of such substances as combustion aids within a residential heating appliance.

7.4 Results and Discussion

7.4.1 Burning Rate and Combustion Temperature

The rate of fuel conversion and temperature may be applied as a method of determining combustion conditions within the stove appliance. Higher combustion temperatures generally correspond with an increase in the fuel conversion rate while lower combustion temperatures may correspond with a reduction in the burning rate and detrimental combustion conditions (Alves et al., 2011; Fachinger et al., 2017). Further information of the determination of combustion temperature and burning rate is shown in **Chapter 3**. The rate of fuel conversion is shown to vary throughout the combustion experiment. Similar findings have been presented within the literature where the rate is dependent upon the phase of the combustion reaction (Mitchell et al., 2016; Fachinger et al., 2017; Maxwell et al., 2020). Additionally, the burning rate has been shown to vary depending upon fuel type and appliance (Mcdonald et al., 2000). A lower burning rate is generally presented during the combustion of fuelwood under cold-start conditions. Under cold-start conditions a maximum burning rate of 3.9 kg/hour was observed following ignition and generally represented the combustion of firelighter material and kindling as well as processes of water loss from the fuel particle during the pre-ignition or drying phase. Under warm-start conditions a maximum burning rate of 5.1 kg/hour was observed during the peak flaming phase and succeeding a 6 min drying period following reloading. The average conversion rate is presented as 1.29±0.31 g/kg$_{fuel}$ and 1.87±0.40 g/kg$_{fuel}$ for cold-start and warm-start operation respectively. In addition, a difference in the burning rate is presented during different phase of combustion (start-up, flaming and smouldering combustion) for both cold-start and warm-start batches. Cold-start operation results in an initial peak in the conversion rate followed by a prolonged period of reduced mass loss. Warm-start operation generally presents a significant burning rate peak following the addition of fuel to the combustion appliance. The rapid loss of mass is likely in response to fuel particle moisture loss and initial devolatalisation during heating (Price-Allison et al., 2018). Under cold-start conditions the peak conversion rate occurred between 3 min and 9 min following ignition. Under warm-start conditions the peak conversion rate occurred between 2 min and 9 min following reloading. As such, the period of peak-burning rate under cold-start conditions is likely controlled by the rate-limiting drying phase (Price-Allison et al., 2018). Alternatively, the period of peak-burning rate under warm-start conditions us likely controlled by the rate of volatile loss and onset of peak-flaming combustion (Mitchell et al., 2016). This process is likely dependent upon the initial temperature of the grate during reloading. A similar

pattern is presented in Maxwell et al. (2020) whereby a peak in the burning rate is presented following the addition of new fuel to the combustion reaction.

Temperature within the combustion zone is known to vary throughout the reaction and is controlled by a number of factors previously discussed. Given the difficulty in measuring the temperature within a small domestic heating appliance, primarily in response to the dynamic variability of the combustion reaction, flue gas temperature has been applied as a representative proxy of conditions within the firebox as identified within the literature (Lamberg et al., 2011; Fachinger et al., 2017; Price-Allison et al., 2018; Maxwell et al., 2020). **Figure 7.2** presents the variation in combustion temperature during cold-start and warm-start batch testing. Results indicate a process of rapid heating during ignition followed by a plateau in the combustion temperature throughout the flaming phase. A subsequent reduction in the temperature is observed throughout the smouldering phase in response to a slowed combustion reaction. A similar trend is observed during both cold-start and warm-start operation. The average combustion temperature measured across a complete batch cycle is shown to vary between different stove operating conditions. Intuitively, the cold-start batch presents a lower combustion temperature than that of the warm-start burning cycles. The average temperature is shown to be 250±39 ºC and 363±48 ºC under cold-start and warm-start conditions respectively. Similarly, the maximum attained temperature was higher during warm-start operation. The maximum temperature was observed within the range of 273 ºC and 342 ºC under cold-start conditions and between 379 ºC and 580 ºC under warm-start conditions. A large error in the average combustion temperature, 250±39 ºC, is presented under cold-start conditions indicating the effect of poor ignition on both the temperature and heating rate. In addition, under warm-start operation the average and maximum temperature is shown to increase with each batch of fuel applied to the stove. A similar process is identified during the combustion of fuelwood and fuel briquettes in response to the increased energy throughput during prolonged stove operation (**Chapter 8**).
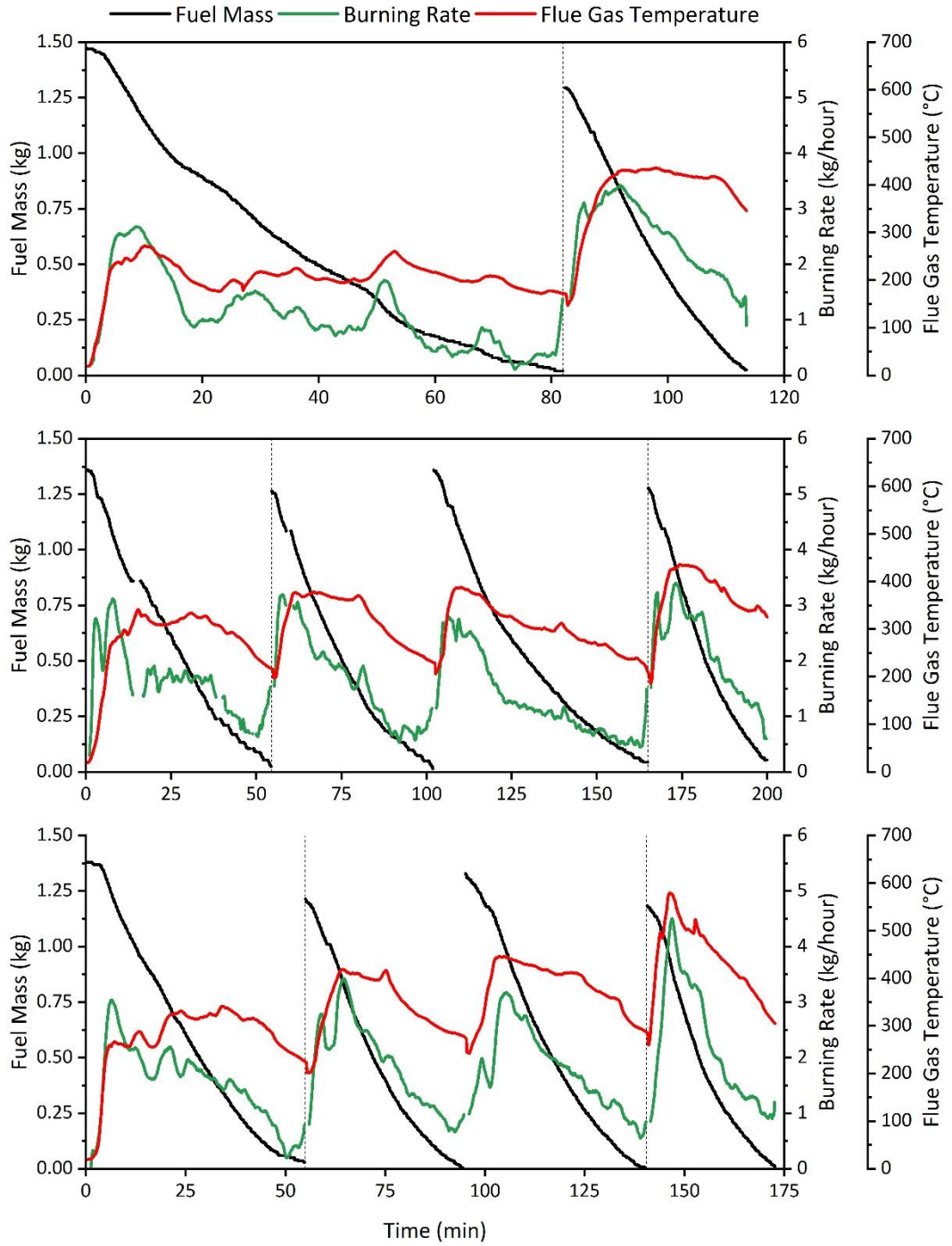
Figure 7.2 Variation in mass loss (kg), fuel burning rate (kg/hour) and combustion temperature (^{o}C). Temperature is represented by the flue gas temperature (^{o}C). Fuel mass and burning rate is presented in kg/hour on an as-fired basis.

Fuelwood conversion rate is shown to be dependent upon the combustion temperature while the temperature differs depending upon stove operational conditions. As such, cold-start operation, synonymous with reduced operating temperatures, results in a reduced burning rate. Analysis of the Pearson Correlation Coefficient (r) between combustion temperature and fuel conversion rate shows a positive and statistically significant correlation (r is 0.91) whereby an increase in temperature leads to an increase in the rate of conversion. A similar correlation is also presented between flame temperature and burning rate (r is 0.92). **Figure 7.3** presents the relationship between temperature and burning rate during cold-start and warm-start operating conditions. Cold-start operation is generally associated with a reduced combustion temperature resulting in a lower burning rate. Warm-start operation is generally associated with an increased combustion temperature resulting in a high burning rate. A review of the convex-hull definition suggests a shift in an up (↑) and right (→) direction following the addition of subsequent warm-start test batches. As such, the temperature and burning rate generally increase with each batch of fuel applied to the stove. Cold-start operation is also shown to be the most variable presenting a convex-hull regional area of 929 in contrast to smaller areas of 777, 441 and 627 for WS1, WS2 and WS3 respectively. Such processes are likely in response to the inherent variability in fuel particle ignition, heat distribution across the fuel pack and low temperatures during the early stages of combustion.
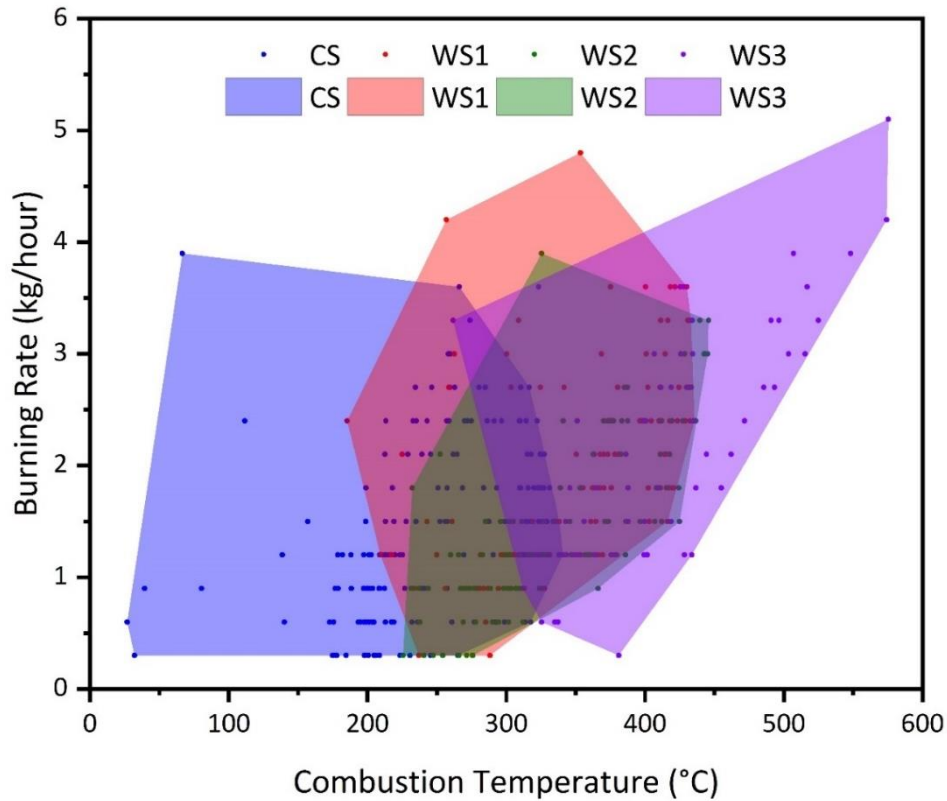
Figure 7.3 The effect of combustion temperature (ºC) on fuel conversion rate (kg/hour) during cold-start and warm-start stove operation. Each test batch is represented within a series where CS is cold-start, WS1 is warm-start batch 1, WS2 is warm-start batch 2 and WS3 is warm-start batch 3. The shaded area is a convex-hull and represents the total region where data is present for CS, WS1, WS2 and WS3. Burning rate values present the average rate sampled on a min/min basis.

Operating conditions are shown to vary significantly during the operation of the stove appliance under cold-start and warm-start conditions. Combustion temperature (flue gas and flame temperature) is presented as a rate limiting factor effecting the burning rate, average O_2 availability within the combustion zone and batch duration (min). A prolonged heating duration is required when warming domestic heating appliances due to the structural and material properties of the device. The estimated energy requirement for heating the stove (q) from 20ºC to 100ºC is 2723.2 kJ assuming an appliance mass of 74 kg and a predominantly cast-iron composition. The energy requirement is calculated (**Equation 7.1**) as a function of the specific heat of cast iron (C_p) which is estimated to be 0.46 kJ/kgC, the mass of the appliance (m) in kg and the heating range (d_t) in degrees Celsius (ºC) (TheEngineeringToolbox.com, 2003).

$$(7.1) \quad q = C_p \times m \times d_t$$

Table 7.2 presents a summary of the average combustion conditions presented during each of the cold-start and warm-start testing series on a complete batch-basis. As previously suggested, there is a strong positive correlation between combustion temperature and the rate of fuel conversion. Cold-start testing, under low heating conditions, presents a prolonged combustion and burn-out duration (63.83±15.73 min) where warm-start operation, associated with a higher burning rate, presents a reduced duration (42.10±11.13 min). A strong negative correlation is associated with combustion temperature and batch duration where r is -0.923 and –0.938 for flue gas and flame temperature respectively. In addition, the O_2 concentration is shown to vary between cold-start and warm-start conditions and is closely correlated with burning rate (*r* is -0.979) and temperature (*r* is -0.863). Similar processes are observed by Ozgen et al. (2013) whereby varying O_2 availability under cold-start (16.6%) and warm-start (13.4%) operation occurs in response to high combustion temperatures in the latter likely resulting in a higher rate of fuel conversion. As such, cold-start operation is generally associated with a lower combustion temperature in response to the method of ignition (Nussbaumer et al., 2008), user behaviour (Fachinger et al., 2017), energy loss during the drying period (Shen et al., 2012; Price-Allison et al., 2018), difficulty in ignition in response to specific fuel properties, the cooling effect of water vapour within the combustion zone and the thermal mass of the appliance (Tryner et al., 2014). Such processes lead to a reduction in the burning rate effecting both the O_2 availability and the duration of the combustion reaction. Such processes are generally negated following the application of additional test batches.

Table 7.2 Variation in average combustion conditions during cold-start and warm-stove operation

Test Phase	Burning Rate (kg/hour)	Ave. Flue Gas Temp. (°C)	Ave. Flame Temp. (°C)	Ave. O_2 Conc. (vol-%)	Combustion Period (min)
CS	1.29±0.31	250±39	360±62	16.48±0.03	63.83±15.73
WS-1	1.94±0.43	349±33	505±134	14.94±2.11	39.67±8.01
WS-2	1.50±0.35	340±56	483±127	16.35±1.62	54.25±12.37
WS-3	2.15±0.06	409±51	587±67	14.00±0.51	33.58±2.00
WS-Ave.	1.87 ± 0.40	363 ± 48	522 ± 107	15.05±1.70	42.10±11.13

7.4.2 Variation in Emission Concentrations During Stove Operation Under Cold-Start and Warm-Start Conditions

Gaseous emissions monitoring was undertaken during the combustion of each batch of fuel and during each phase of combustion. **Figure 7.4**, **7.5** and **7.6** present the emissions measurements for organic and inorganic gaseous species in mg/Nm^3. It should be noted that pollutants identified as benzene (C_6H_6) and Formaldehyde (CH_2O) are likely to include a series of other trace species. The nature and pattern of the emission profiles were found to generally correspond with similar measurements presented in earlier works (Esbjörn Pettersson et al., 2011; Mitchell et al., 2016; Maxwell et al., 2020). There is a 120 sec data-gap in the emission profile at the point of manual reloading. The measurements in this period are invalidated by the effect of air inundation within the firebox while the stove door is opened.

Nitrogen oxide (NOx) measurements were made throughout the complete combustion cycle thereby incorporating aspects of ignition, flaming combustion and smouldering. NOx generally consists of Nitric oxide (NO) and Nitrogen dioxide (NO_2). NO is identified as the major fraction incorporating between 90% and 95% of the total NOx composition (Koppejan and van Loo, 2008; Khan et al., 2009; Mladenović et al., 2016). As such, NO and NOx may be applied interchangeably during the combustion of biomass (Amand and Leckner, 1991). The emission formation is shown to vary depending upon the phase of combustion with the flaming phase generally presenting a higher concentration (mg/m^3). NOx formation in small domestic heating appliances generally occurs in response to the thermal decomposition of nitrogen-containing compounds within the fuel particle during devolatalisation. Given the relatively low combustion temperatures (<1400ºC) observed within the testing series (**Table 7.2**) the formation of NO is likely in response to the release of nitrogen via the fuel NOx mechanism only (Glarborg et al., 2003; Koppejan and van Loo, 2008; Bugge et al., 2015). It is also likely that a small fraction of the total NOx may be derived via the prompt NOx route however it is thought to be a minor contribution (Johnsson, 1994). During biomass heating the nitrogenic compounds are released in the form of NH_3 and HCN with the former being decomposed to NH_2 and NH radicals which are subsequently oxidised to form NO. In addition, NH_2 and NH may react with radicals of NO and OH allowing for the formation of N_2 (Johnsson, 1994; Werther et al., 2000). HCN is also oxidised to form NCO which reacts with NO in the gas phase resulting in the formation of N_2O (Miller and Bowman, 1989; Werther et al., 2000).The average NO concentration (mg/m^3) observed during cold-start operation was 59.3±19.8 mg/m^3 while the average concentration observed during warm-start operation was 67.5±16.1 mg/m^3.

The average emission concentration does not vary significantly under different temperature conditions during cold-start and warm-start operation or between each of the individual warm-start batches suggests Fuel NOx as a primary formation route. The rate of NOx formation also appears to correlate with the combustion temperature and, as a result, the burning rate, suggesting a higher concentration during periods of increase fuel conversion. Following the ignition of a fuel batch the NO concentration increases to a peak followed by a period of steady decline. Such processes occur in response to the devolatalisation and consumption of nitrogenic compounds within the fuel volatile fraction during the flaming phase. Following the loss of the fuel volatile fraction the rate of NO formation slows. Nitrogen compounds remaining in the char may be combusted during the smouldering phase (Khan et al., 2009) however the total formation is relatively low. Char bound nitrogen is likely burned towards the end of the combustion reaction leading to the formation of NO, N_2O and N_2 (Klein and Rotzoll, 1994; Werther et al., 2000).

As with the formation of NOx, Sulphur oxide (SOx) species formation is directly linked to the inherent sulphur content of the fuel material. As such, SOx concentration levels are dependent upon the inherent sulphur content of the fuel material. SOx generally consists of sulphur dioxide (SO_2) and sulphur trioxide (SO_3). SO_2 is identified as the primary constituent incorporating more than 95% of the total SOx emission. SO_3 is found in lower concentrations (<5%) and is associated with lower temperature combustion (Koppejan and van Loo, 2008). Following devolatalisation, sulphur reacts with O_2 leading to the formation of a variety of SOx species. The subsequent SOx pollutant is based upon the O_2 availability within the combustion zone. Where the oxygen availability is high the sulphur will react to form SO, SO_2 and SO_3. Where the oxygen availability is low the sulphur will react to form H_2S, S_2 and SH (FLUENT, 2009). The average SO_2 concentration (mg/m^3) observed during cold-start operation was 52.0 ± 2.9 mg/m^3 while the average concentration observed during warm-start operation was 52.8 ± 5.7 mg/m^3. The limited variation in emission concentration suggests the oxidation of fuel bound sulphur as the primary route of formation. Like NO, the rate of SO_2 formation appears to be affected by the burning rate and combustion temperature whereby periods of higher burning intensity result in an increase in emissions. As such, the ignition and flaming combustion phases generally produce a higher concentration of SOx due to the increased rate of fuel sulphur loss. The SO_2 formation during the smouldering phase is generally lower in response to the limited fuel sulphur availability within the char phase.

Variation in the concentration of VOC pollutants was observed throughout the combustion cycle and between differing stove operational conditions. Carboxylic

acid group pollutants are formed during the breakdown of each of the primary constituents of biomass with high concentrations produced during the deacetylation of hemicellulosic material due to the abundance of O-acetyl group compounds attached to the xylem-chain structure (Shen et al., 2010; Shen et al., 2015; Lu et al., 2019). Acetic acid ($C_2H_4O_2$) is identified as the most common carboxylic product derived from the pyrolysis of biomass (Lu et al., 2019). The formation of $C_2H_4O_2$ may occur through the dissociation of O-acetyl side chains during pyrolysis or via the breakdown of uronic acid group compounds depending upon combustion temperature and retention time (Wang et al., 2015). The formation of $C_2H_4O_2$ is dependent upon pyrolysis temperature but generally occurs within the range of 192-429 ºC (Shen et al., 2015). The average $C_2H_4O_2$ concentration observed during cold-start operation was 125.8±116.0 mg/m^3 while the average concentration observed during warm-start operation was 25.8±20.1 mg/m^3. The formation of $C_2H_4O_2$ is shown to be higher during cold-start operation where the concentration is reduced in response to an increase in the combustion temperature and during the smouldering phase. Emission concentrations are shown to be significantly lower during the combustion of fuelwood under warm-start conditions. An initial spike in $C_2H_4O_2$ formation occurs following reloading likely in response to the effect of moisture within the fuel particle resulting in a delay in ignition. Following the onset of the flaming phase the emission concentration is negligible suggesting $C_2H_4O_2$ is consumed under the hotter combustion conditions.

Aldehyde formation occurs in response to the breakdown of cellulose and hemicellulose during the combustion reaction (Kopczyński et al., 2015). During biomass combustion more than 50% of the total aldehyde emittance is Formaldehyde (CH_2O) and Acetaldehyde (CH_3CHO) where an increase in concentration occurs during low temperature combustion conditions (Koppmann et al., 2005). The average CH_2O concentration observed during cold-start operation was 71.0±35.3 mg/m^3 while the average concentration observed during warm-start operation was 30.1±17.0 mg/m^3. The formation of CH_2O appears to follow a similar trend to that of other oxygenated hydrocarbons ($C_2H_4O_2$) whereby concentrations are high during cold-start operation and low during warm-start operation. In addition, an initial peak in CH_2O formation generally occurs following reloading with a subsequent reduction during the high temperature flaming combustion phase. A such, the emittance of oxygenated hydrocarbon species appears to correspond with a decrease in the combustion temperature (Koppmann et al., 2005). Aldehyde monitoring is often undertaken given the detrimental effects of high concentration exposure on human health. In addition, CH_2O may react with HCl within the atmosphere leading to the formation of bis(chloromethyl) ether ($(CH_2Cl)_2O$), a compound maintaining carcinogenic properties (Llpari et al., 1984).
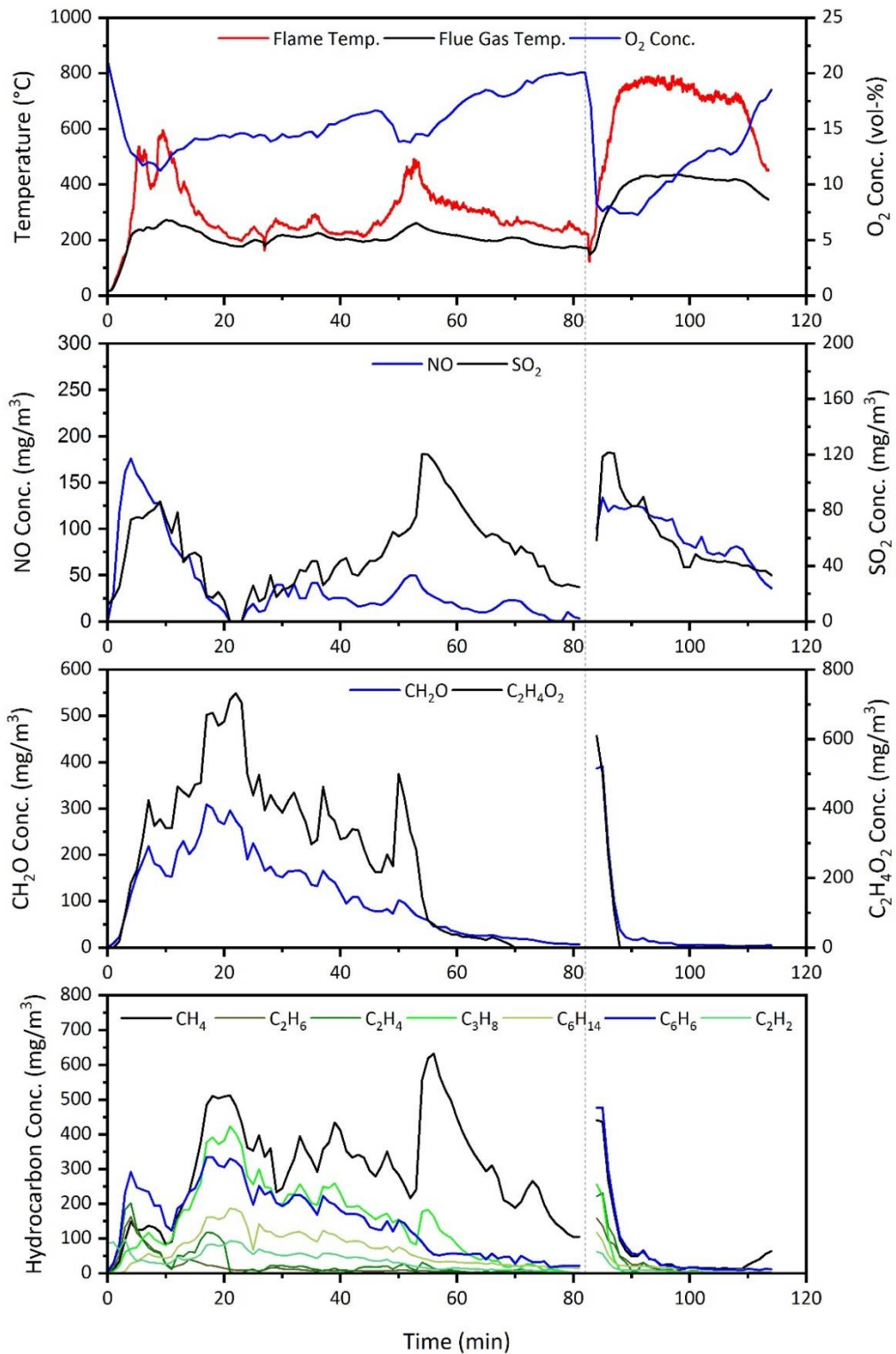
Figure 7.4 Temperature (^{o}C) and pollutant emission concentrations (mg/m^3) during the combustion of kiln-dried beech fuelwood (testing series one). Emission concentrations are presented at 0°C and 101.325 kPa. The cold-start batch was ignited via the application of 101.8 g kiln-dried pine kindling and 50.1 g kerosene-based firelighter material. Vertical dashed lines indicate periods of fuel reloading.

Figure 7.5 Temperature ($^{\circ}$C) and pollutant emission concentrations (mg/m^3) during the combustion of kiln-dried beech fuelwood (testing series two). Emission concentrations are presented at 0°C and 101.325 kPa. The cold-start batch was ignited via the application of 103.6 g kiln-dried pine kindling and 49.9 g kerosene-based firelighter material. Vertical dashed lines indicate periods of fuel reloading.
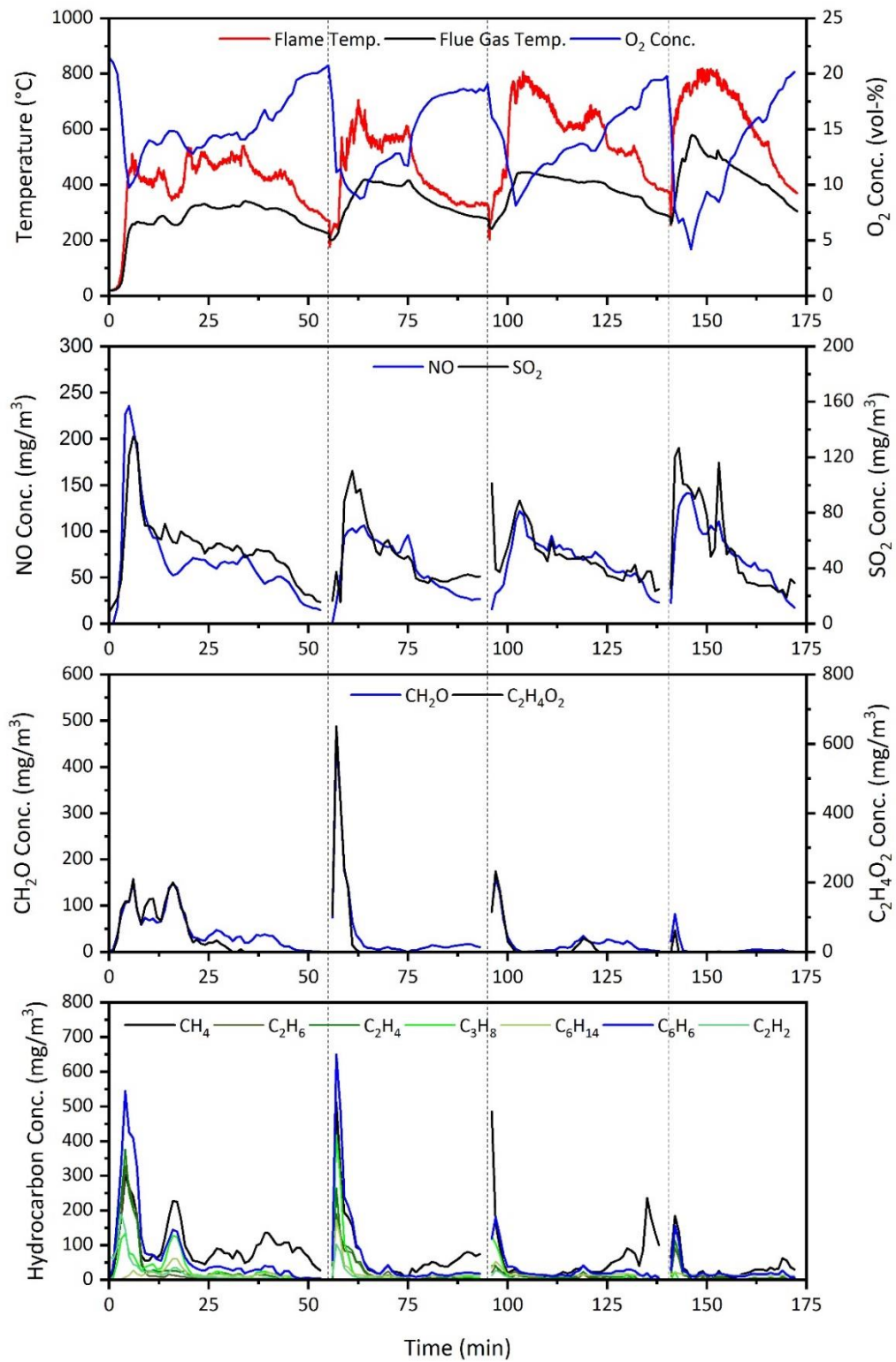
Figure 7.6 Temperature (^{o}C) and pollutant emission concentrations (mg/m^3) during the combustion of kiln-dried beech fuelwood (testing series three). Emission concentrations are presented at 0°C and 101.325 kPa. The cold-start batch was ignited via the application of 101.8 g kiln-dried pine kindling and 50.1 g kerosene-based firelighter material. Vertical dashed lines indicate periods of fuel reloading.

Hydrocarbon emission monitoring was undertaken during the combustion of each batch of fuel and during each phase of particle combustion. The concentration of hydrocarbon species is shown to vary throughout the combustion cycle and under different operating conditions. **Figure 7.4, 7.5** and **7.6** present the emissions measurements for Methane (CH_4), Ethane (C_2H_6), Ethylene (C_2H_4), Propane (C_3H_8), Hexane (C_6H_{14}), Benzene (C_6H_6) and Acetylene (C_2H_2) pollutants in mg/Nm^3. CH_4 and other hydrocarbon species are generally regarded as an intermediate between fuel carbon and CO_2 as well as fuel hydrogen and H_2O assuming complete combustion (Koppejan and van Loo, 2008). The formation of CH_4 and other hydrocarbon products occur in response to reduced combustion temperatures, a reduced residence time and inhibited O_2 availability within the combustion zone (Koppejan and van Loo, 2008). CH_4 and C_6H_6 were found to be the most prevalent hydrocarbon species presenting a concentration of 166±113 mg/m^3 and 104±38 mg/m^3 during cold-start operation and 75±35 mg/m^3 and 47±18 mg/m^3 under warm-start operation. Similar findings have been presented within the literature whereby CH_4 and other low molecular weight compounds presents the higher emission concentration (E Pettersson et al., 2011). Under warm-start conditions the hydrocarbon species presenting a higher molecular weight where generally found in lower concentrations likely in response to the thermal cracking of larger compounds under higher combustion temperatures. Alternatively, under cold-start conditions and in response to lower combustion temperatures, C_2-C_3 chain hydrocarbon species where recorded in the lowest concentration. The emission concentration of all hydrocarbon species is shown to spike during ignition followed by a period of decline during the onset of flaming combustion. In addition, an increase in the emission concentration is also observed at the end of the batch during the smouldering phase in response to a reduction in temperature and during the pyrolysis or remaining fuel particle fragments on the grate.

Figure 7.7 presents the variation in total hydrocarbon emissions under cold-start operation and during each of the subsequent warm-start batches. The total hydrocarbon concentration is calculated as the sum of each monitored pollutant species in mg/Nm^3 (CH_4, C_2H_6, C_2H_4, C_3H_8, C_6H_{14}, C_6H_6 and C_2H_2). The range is presented as the difference in emission concentration observed under each experiment at a specific time (min) during the combustion reaction. The average concentration is the numerical average emission concentration calculated from each of the three combustion experiments. Cold-start operation presents the highest hydrocarbon emission with an average concentration of 510 mg/m^3. The average concentration is shown to decrease with each batch of fuel applied to the stove suggesting the effect of an increase in the combustion temperature on emission formation. Similarly, **Figure 7.4**, **7.5** and **7.6** present variation in individual

concentration subject to temperature and depending upon the phase of combustion. The average concentration for WS-1, WS-2 and WS-3 was 249 mg/m^3, 217 mg/m^3 and 112 mg/m^3 respectively. The average emission concentration observed during warm-start operation was 205 mg/m^3. The formation of total hydrocarbon pollutants generally follows the same trend under both cold-start and warm-start operation. The concentration is shown to peak during ignition followed by a period of decline during flaming combustion where the temperature is highest. A second peak is observed during the smouldering phase in response to the late devolatalisation of remaining fuel under cooler combustion conditions. The peak in concentration during ignition and smouldering combustion is shown to decrease with each batch of fuel applied to the stove suggesting the effect of the stove operating duration on temperature and combustion conditions.
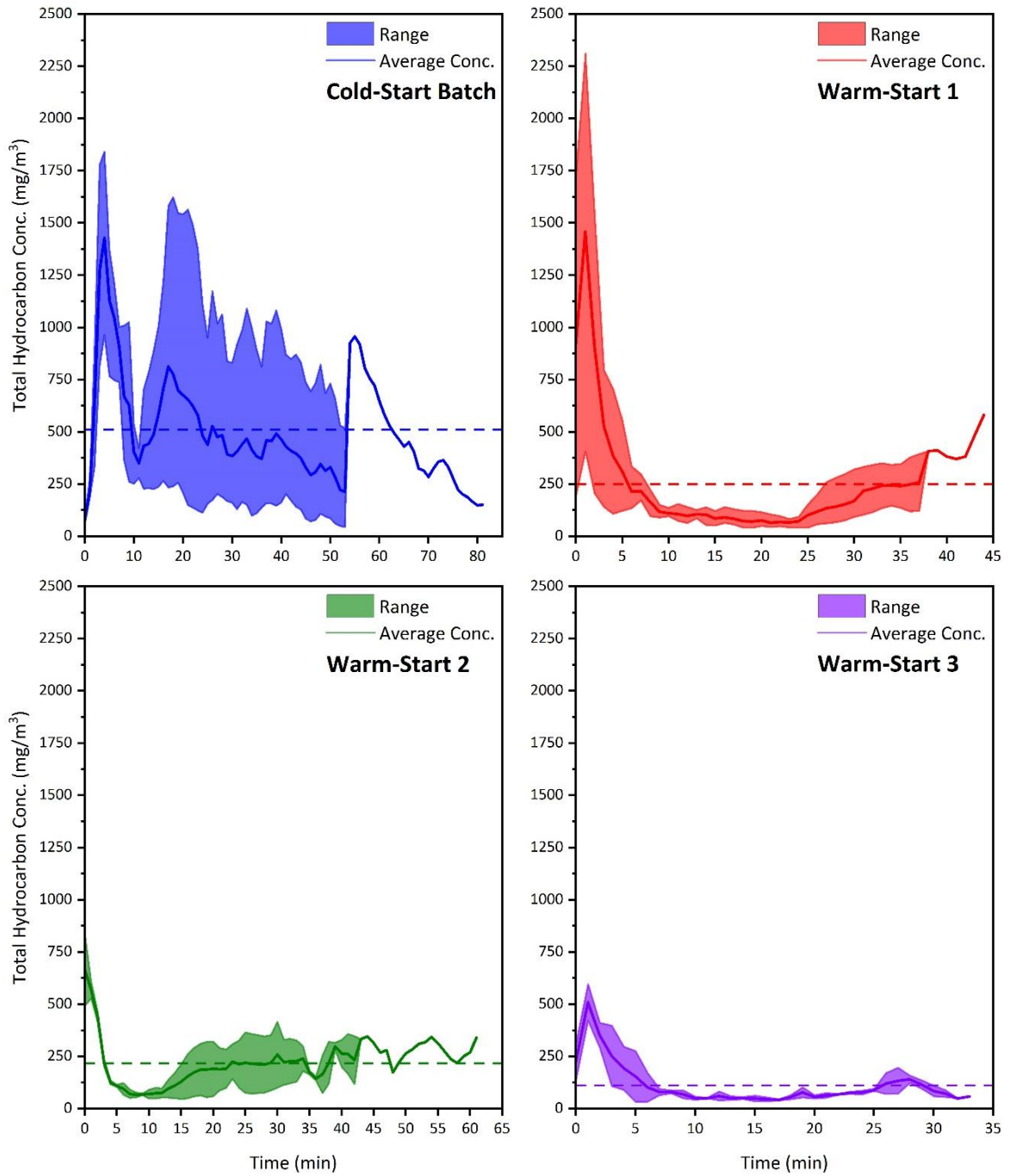
Figure 7.7 Variation in Total Hydrocarbon emission concentration (mg/m^3) during cold-start and warm-start stove operation. Emission concentrations are presented at 0°C and 101.325 kPa. Total Hydrocarbon concentration is presented as the sum of hydrocarbon species CH_4, C_2H_6, C_2H_4, C_3H_8, C_6H_{14}, C_6H_6 and C_2H_2. - - - presents the average emission concentration in mg/m^3 for all testing series.

7.4.3 Variation in Combustion Efficiency under Cold-Start and Warm-Start Conditions

The Modified Combustion Efficiency (MCE) may be calculated as an indication of the fuel carbon fraction converted into CO_2 during a combustion reaction (Fachinger et al., 2017). **Figure 7.8** presents the variation in MCE and CO under cold-start and warm-start operation. The average MCE is shown to vary between methods of operation and phase of combustion. Cold-start operation presents an average MCE of 0.90±0.06 while warm-start operation presents and average MCE of 0.95±0.01. The range of MCE values for cold-start operation is between 0.83 and 0.94 while the range of average MCE values for warm-start operation is between 0.93 and 0.97. The MCE is shown to be significantly more variable under cold-start conditions in response to difficulty in ignition.

The average CO concentration was shown to be similar during stove operation under cold-start and warm-start conditions. The average emission concentration was shown to be 3250±256 mg/m³ and 3294±290 mg/m³ for cold-start and warm-start operation respectively. Under both conditions the pattern of CO formation appears to follow a similar trend whereby the emission concentration reaches a peak during the ignition of the cold-start batch or the addition of new fuelwood to the grate. The presence of the initial peak suggests incomplete combustion of volatile material under cold-start or reduced operating temperatures. CO is known to peak following fuel reloading in response to rapid devolatalisation of the fuel particles during heating in absence of a flame. High CO formation is therefor likely to occur in response to limited mixing of combustion products with O_2, rapid devolatalisation of fuel particles and low combustion temperatures (Vicente et al., 2015). Following the ignition of the fuel particles, and the onset of flaming combustion conditions, the CO concentration is shown to decline and often plateau. The reduced CO concentration occurs in response to an increase in the combustion temperature results in the complete burnout of volatile compounds and the oxidation of CO to CO_2 (Mitchell et al., 2016). The concentration is also shown to increase towards the end of the combustion cycle signifying the onset of fuel smouldering and char combustion at lower temperatures (Mitchell et al., 2016). The effect of poor ignition of fuel particles on CO formation is presented in **Figure 7.4**: Series 1 whereby the average emission concentration was 3545 mg/m³ under cold-start conditions. Poor ignition contributes in a reduction in the firebox temperature subsequently inhibiting the oxidation of volatile compounds within the combustion zone. Cold-start operation appears to provide a greater variability in emission results with average concentrations appearing to be dependent upon the ignition process.

Both CO concentration and the efficiency of the combustion reaction appear to be affected by the temperature conditions. Pearson's correlation analysis indicates a coefficient of 0.779 for flue gas temperature and MCE. Similarly, a correlation coefficient of 0.771 is indicated for burning rate and MCE. These correlations of temperature with fuel conversion rate and MCE are shown to be statistically significant to a level of $P = <0.01$. Cold-start combustion is generally associated with lower temperatures resulting in a higher CO fraction and reduced combustion efficiency. Alternatively, warm-start combustion is generally associated with higher temperatures resulting in a lower CO fraction and increased combustion efficiency. In addition, the variation in temperature observed throughout the course of a single test-batch, irrespective of cold-start or warm-start conditions, is shown to effect both CO formation and the MCE value. Similar findings have been reported within the literature whereby cold-start operation generally presents reduced combustion temperatures leading to high CO concentrations and reduced combustion efficiency. Tissari et al. (2008) identifies relatively low combustion temperatures during cold-start operation followed by a subsequent increase in temperature with each additional batch of fuelwood applied to the appliance. Resultant changes in the combustion conditions correspond with an increase in CO formation by a factor of 3.5 (Tissari et al., 2008). Ozgen et al. (2013) presents further variability in CO formation under cold-start (63 g/kg$_{fuel}$) and warm-start (42 g/kg$_{fuel}$) operation. In addition, CO formation has been shown to be significantly higher during all phases of combustion; the formation was shown to be higher by a factor of 1.6 during the ignition, 1.3 during flaming and 1.6 during smouldering (Ozgen et al., 2013). Similarly, Vicente et al.) 2015) presents higher CO during periods of low temperature conditions indicative of both ignition and char burnout phases. The char burnout phase generally occurs at the end of the combustion reaction at temperatures $<500 \,^{\circ}C$. Such processes have been shown to correspond with a reduction in the combustion efficiency and a shift in the flame colour from yellow, during flaming combustion, to a light blue (Calvo et al., 2014). As such, the CO formation and MCE is affected by both the phases of combustion (Tissari et al., 2008; Calvo et al., 2014; Mitchell et al., 2016) and the combustion temperature (Tarelho et al., 2005; Calvo et al., 2014) with both processes varying under cold-start and warm-start operation.
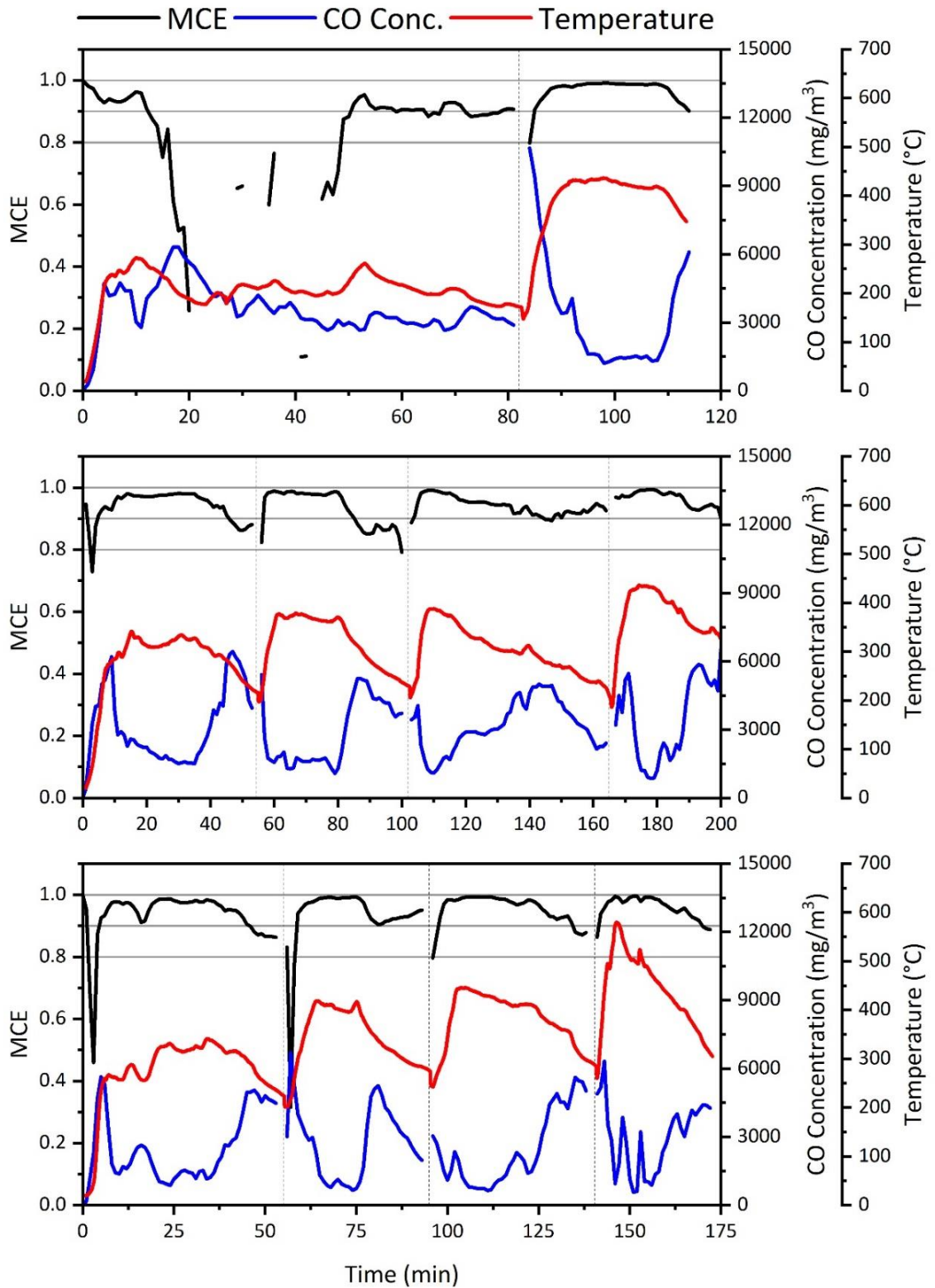
Figure 7.8 Variation in MCE, CO concentration and temperature during cold-start and warm-start stove operation. Emission concentrations are presented at 0ºC and 101.325 kPa. - - - presents the batch reloading point (min).

7.4.4 Variation in Gaseous Emissions under Cold-Start and Warm-Start Conditions

Gaseous emission factors (g/kg$_{fuel}$) were calculated for each of the pollutant species measured on a complete batch basis thereby including aspects of ignition, flaming combustion and smouldering. **Table 7.3** presents the numerical average emission factor values calculated for the two/three test batches where the stated error is the standard deviation of the sample. The average warm-start emission factor values represent the average emission for all of the warm-start experiments (WS-1, WS-2 and WS-3).

High emission factor values are generally presented under cold-start operation while the subsequent emission formation is shown to be relatively low following the development of warm-start conditions. The average CO emission factor is 76.91±23.35 g/kg$_{fuel}$ under cold-start operation and 54.11±10.28 g/kg$_{fuel}$ under warm-start operation. Such processes are likely in response to low temperatures during ignition and throughout the cold-start combustion reaction contributing in the onset of a smouldering-like combustion reaction. The reduced CO formation during warm-start operation suggests an improved efficiency in the combustion reaction where CO is oxidised during the formation of CO_2. CH_4 and C_6H_6 are shown to be the most prevalent hydrocarbon species under both stove operating conditions. The average CH_4 and C_6H_6 emission factor values are shown to reduce significantly following the onset of stable combustion conditions under a higher temperature. The average CH_4 emission factor is shown to be 4.24±3.86 g/kg$_{fuel}$ under cold-start operation and 1.41±0.91 g/kg$_{fuel}$ under warm-start operation. The average C_6H_6 emission factor is shown to be 2.54±1.57 g/kg$_{fuel}$ under cold-start operation and 0.83±0.37 g/kg$_{fuel}$ under warm-start operation. A similar trend is presented for other hydrocarbon species, CH_2O and Acetic acid. NOx and SO_2 emission factor values appear relatively unaffected by the cold-start and warm-start conditioning. A slightly higher emission is presented under cold-start conditions however this is likely in response to a higher mass of fuel within the appliance during ignition considering the presence of firelighter and kindling materials.

The variability in emission factor values is shown to be more significant during cold-start operation while values are often more similar when the stove is heated. A large standard deviation (σ) is observed during the combustion of fuelwood during cold-start conditions in response to issues affecting the ignition of the test fuel. This error is derived from a poor ignition event observed during the testing of CS-1. Poor ignition, likely in response to fuel placement, the exposure of fuel particles to the heated grate and fuel moisture content, resulted in slow ignition. This results in a lower burning rate, inhibited combustion temperatures and the onset of a

smouldering combustion reaction. As such, CS-1 suggests increased CO formation, in contract to warm-start operation, by a factor of 2.5. CS-2 and CS-3 present more successful ignition reactions resulting in improved combustion conditions. The cold-start emission values for these series were only higher by a factor of 1.1 and 1.7 when compared with respective warm-start operation.

Table 7.3 Emission Factor values for Cold-Start and Warm-Start stove operation. WS-Average is the average Warm-Start emission factor values for WS-1, WS-2 and WS-3. THC is the total emission of hydrocarbon species (CH_4, C_2H_6, C_2H_4, C_3H_8, C_6H_{14}, C_6H_6 and C_2H_2). Emission factor values are presented in g/kg_{fuel}.

Pollutant Species	CS (g/kg_{fuel})	WS-1 (g/kg_{fuel})	WS-2 (g/kg_{fuel})	WS-3 (g/kg_{fuel})	WS-Ave. (g/kg_{fuel})
CO	76.91±23.35	50.65±7.56	64.83±13.92	48.60±0.19	54.11±10.28
SO_2	1.18±0.22	0.79±0.03	1.03±0.30	0.79±0.06	0.86±0.17
NOx	1.36±0.21	1.05±0.13	1.16±0.0	1.10±0.04	1.10±0.09
CH_4	4.24±3.86	1.50±0.47	2.12±1.44	0.57±0.19	1.41±0.91
C_2H_6	1.88±2.14	0.52±0.14	0.44±0.39	0.01±0.0	0.35±0.29
C_2H_4	0.85±0.10	0.40±0.10	0.28±0.14	0.17±0.04	0.30±0.14
C_3H_8	0.89±0.98	0.39±0.08	0.44±0.23	0.21±0.03	0.35±0.15
C_6H_{14}	0.74±0.35	0.16±0.0	0.12±0.07	0.03±0.0	0.11±0.07
C_2H_2	0.59±0.04	0.31±0.12	0.17±0.03	0.20±0.09	0.24±0.11
C_6H_6	2.54±1.57	1.08±0.09	0.86±0.49	0.42±0.15	0.83±0.37
THC	11.72±8.84	4.36±0.39	4.44±2.80	1.61±0.51	3.60±1.80
CH_2O	1.78±1.31	0.81±0.14	0.63±0.36	0.12±0.06	0.56±0.35
$C_2H_4O_2$	3.35±3.72	0.88±0.14	0.41±0.12	0.03±0.01	0.50±0.40

A high degree of variability may also be observed during warm-start operation. Both cold-start and warm-start emissions are affected by the temperature of the combustion reaction. As such, high emissions may be observed under warm-start operation if there is a reduction in the combustion temperature. Such processes may result in emissions being as high, or higher, during warm-start operation to that observed when the stove is cold. WS-2 presents a high standard deviation (σ) for gaseous pollutant species in response to higher emission values observed during warm-start combustion testing. **Figure 7.9** presents the effect of a reduction in temperature on emission formation under warm-start operation observed during Series Two. The average combustion temperature observed during cold-start operation was 273.1ºC while the average temperature observed during WS-2 was

300.3ºC. This value is lower than that observed during other warm-start batches within the series (WS-1 was 318.9ºC; WS-3 was 372.8ºC. As such the emission factor values are shown to increase by a factor of 1.16 for CO and 1.52 for CH_4 during WS-2 when compared with cold-start operation. This effect is masked by the addition of further batches when quantifying average emission factor values but remains prevalent when assessing the error. Though such values may appear as anomalous results it is important that they are considered, as with cold-start emissions, in the quantification of emission factor values given that they demonstrate the dynamic nature of the combustion reaction within small residential heating appliances.
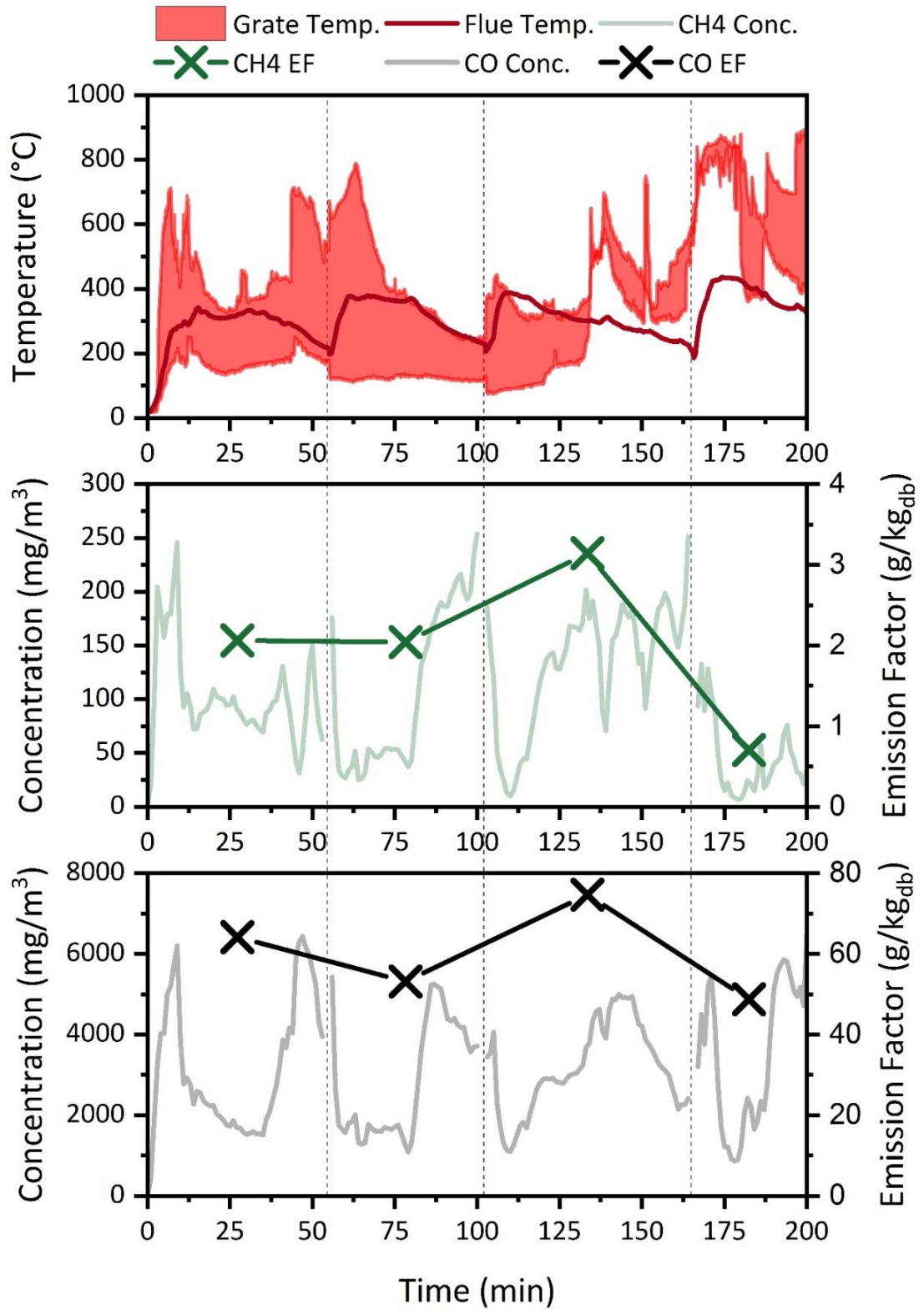
Figure 7.9 The effect of combustion temperature on concentration and emission factor of CO and CH$_4$. Data is derived from Series 2. - - - presents the batch reloading point (min). ■ presents the observed range in grate temperature (^{o}C) dependent upon location on the grate.

A scaling factor is calculated to numerically quantify the variation in average emission factor values between test batch types. The factor is calculated as a ratio of the emission factor from cold-start operation and warm-start operation ($EF_{CS}:EF_{WS}$). Factors are calculated for average emission factor values whereby WS-1ave is the average scaling factor observed during the combustion of WS-1 batches in Series One, Series Two and Serie Three. Scaling factor values for each of the monitored gaseous emission species is presented in **Table 7.4**. Average emission factor values are shown to be higher during the operation of the stove under cold-start conditions and lower when an increase in the combustion temperature is observed. CO presents a high emission during cold-start operation with an average emission factor of 76.91±23.35 g/kg$_{fuel}$. CO formation is shown to reduce during the operation of the stove appliance under warm-start conditions. The average emission factor was found to be 50.65±7.56 g/kg$_{fuel}$, 64.83±13.92 g/kg$_{fuel}$ and 48.60±0.19 g/kg$_{fuel}$ for WS-1ave, WS-2ave and WS-3ave respectively. A correlation may be observed between the combustion temperature and CO emission factor value. The average combustion temperature was low during cold-start operation with an average value of 250±39 ºC. The addition of subsequent fuel led to an increase in combustion temperatures with average conditions found to be 349±33 ºC, 340±56 ºC and 409±51 ºC for WS-1ave, WS-2ave and WS-3ave respectively. As such, the emission of CO is shown to be higher by a factor of 1.42 between cold-start and average warm-start test batches. Similarly, the formation of CH_4 was found to be 4.24±3.86 g/kg$_{fuel}$ during cold-start operation while an emission factor of 1.50±0.47 g/kg$_{fuel}$, 2.12±1.44 g/kg$_{fuel}$ and 0.57±0.19 g/kg$_{fuel}$ was calculated for the combustion of fuelwood during WS-1ave, WS-2ave and WS-3ave batches respectively. As such, the average CH_4 emission is shown to increase by a factor of 3.01 during the operation of the stove under cold-start conditions. This trend is observed across each of the observed hydrocarbon species while the THC formation is shown to increase by a factor of 3.26 during cold-start operation. Aldehyde formation is also shown to reduce during the onset of high temperature combustion. CH_2O presents a high emission during cold-start operation with an average emission factor of 1.78±1.31 g/kg$_{fuel}$. CH_2O formation is shown to reduce during the operation of the stove appliance under warm-start conditions. The average emission factor was found to be 0.81±0.14 g/kg$_{fuel}$, 0.63±0.36 g/kg$_{fuel}$ and 0.12±0.06 g/kg$_{fuel}$ for WS-1ave, WS-2ave and WS-3ave respectively. Subsequently, the average CH_2O emission is shown to increase by a factor of 2.20, 2.83 and 14.83 for WS-1ave, WS-2ave and WS-3ave respectively. The most significant difference is observed during WS-3ave when the maximum combustion temperature is observed suggesting a more complete burnout of gaseous pollutants. A similar trend is observed for the formation of $C_2H_4O_2$ whereby

increased combustion temperatures observed during warm-start operation correspond with a reduction in emissions. The emission of $C_2H_4O_2$ was shown to be 3.35 ± 3.72 g/kg$_{fuel}$ during cold-start operation with warm-start conditions resulting in the formation of 0.88 ± 0.14 g/kg$_{fuel}$, 0.88 ± 0.14 g/kg$_{fuel}$ and 0.03 ± 0.01 g/kg$_{fuel}$ for WS-1_{ave}, WS-2_{ave} and WS-3_{ave} respectively. The average emission during warm-start operation was found to be 0.50 ± 0.40 g/kg$_{fuel}$ therefore suggesting an increase by a factor of 6.70 during cold-start operation. Some variation is observed in SO_2 and NOx emissions during cold-start and warm-start operation. The emission of these species is shown to increase by a factor of 1.37 and 1.24 during cold-start operation of SO_2 and NOx respectively. In response to the generally linear relationship between the elemental sulphur and nitrogen composition and the SO_2 and NOx emittance it stands to reason that the variance should be small (Glarborg et al., 2003; Koppejan and van Loo, 2008; Sommersacher et al., 2012). The minor variation observed between the methods of operation is likely in response to the presence of firelighter and kindling material within the firebox during the initial start-up. Furthermore, in response to reduced combustion temperatures and an increased residence time due to a slowed flue gas velocity, the O_2 availability within the combustion zone is shown to be higher during cold-start operation (**Table 7.2**). As such, an increase in SO_2 and NOx formation may occur in response to excess air conditions within the combustion zone resulting in an increased O_2 availability (Glarborg et al., 2003; ANSYS FLUENT, 2009).

Table 7.4 Emission factor scaling values for Cold-Start and Warm-Start stove operation. WS-Average is the average Warm-Start emission factor values for WS-1, WS-2 and WS-3 observed during Series One, Series Two and Series Three. Scaling factor values are calculated as the ratio of Cold-Start and Warm-Start emission factor values.

Pollutant Species	WS-1 Ave. (EF_{CS}/EF_{WS-1})	WS-1 Ave. (EF_{CS}/EF_{WS-2})	WS-1 Ave. (EF_{CS}/EF_{WS-3})	WS-1 Ave. ($EF_{CS}/EF_{WS-Ave.}$)
CO	1.52	1.19	1.58	1.42
SO_2	1.49	1.15	1.49	1.37
NOx	1.30	1.17	1.24	1.24
CH_4	2.83	2.00	7.44	3.01
C_2H_6	3.62	4.27	188.00	5.37
C_2H_4	2.13	3.04	5.00	2.83
C_3H_8	2.28	2.02	4.24	2.54
C_6H_{14}	4.63	6.17	24.67	6.73
C_2H_2	1.90	3.47	2.95	2.46
C_6H_6	2.35	2.95	6.05	3.06
THC	2.69	2.64	7.28	3.26
CH_2O	2.20	2.83	14.83	3.18
$C_2H_4O_2$	3.81	8.17	111.67	6.70

Gaseous emissions are shown to be higher during cold-start operation and lower during warm-start operation. A similar process is presented within the literature whereby a reduction in the combustion temperature under cold-start operation corresponds with an increase in gaseous emission formation. Ozgen et al. (2013) identifies an increase in CO and organic gaseous carbon (OGC) species under cold-start conditions by a factor of 1.5 and 3.2 respectively with higher emissions also presented across all phases of combustion. For example, during the combustion of beech fuelwood within a closed-fireplace appliance, the emission of OGC is reported to be 8.8×10^3 mg/kg, 3.1×10^3 mg/kg and 4.7×10^3 mg/kg during ignition, flaming combustion and smouldering under warm-start operation. The equivalent emission under cold-start operation was shown to be 1.9×10^4 mg/kg, 7.2×10^3 mg/kg and 2.7×10^4 mg/kg. Such processes occur in response to inhibited combustion temperature whereby an average flue gas temperature of 211 ºC was reported under cold-start operation and 279 ºC under warm-start operation. **Figure 7.10** presents similar findings whereby an increase in the combustion temperature, generally observed under warm-start operation, results in a reduction in gaseous emission formation. The figure presents the gaseous emission formation observed during cold-start and warm-start combustion for beech fuelwood logs and biomass

briquettes (**Chapter 8**). The method of ignition differs between combustion experiments where BB (●) represents biomass briquettes ignited using Zip^{TM} Firelighter only, BL+BB (■) represents beech logs ignited using a mixture of Zip^{TM} Firelighters and biomass briquettes, and BL+K (▲) represents beech logs ignited using a mixture of Zip^{TM} Firelighter and pinewood kindling. A negative correlation is presented between combustion temperature and pollutant species CO, CH_4, C_6H_6 and CH_2O where an R^2 value of 0.52, 0.67, 0.70 and 0.69 is reported respectively. Similar to the findings presented in Ozgen et al. (2013), an increase in the combustion temperature during warm-start operation corresponds with a reduction in gaseous pollutant emissions. In all cases pollutant emissions where highest during cold-start operation. CO formation during BB combustion testing was shown to increase by a factor of 1.43-2.00 during cold-start operation. Similarly, BL+BB and BL+K present an increase by a factor of 1.52-1.55 and 1.09-2.46 respectively. CH_4 is shown to increase by a factor of 3.51-3.78, 2.96-3.97 and 1.05-7.66 for BB, BL+BB and BL+K under cold-start operation respectively. C_6H_6 is shown to increase by a factor of 4.45-5.66, 3.30-4.48 and 1.92-3.85 for BB, BL+BB and BL+K under cold-start operation respectively. CH_2O is shown to increase by a factor of 8.32-12.01, 3.03-5.32 and 1.70-4.37 for BB, BL+BB and BL+K under cold-start operation respectively.

Analysis of the Pearson's Correlation Coefficient (*r*) between combustion temperature and pollutant species formation shows a negative and statistically significant correlation whereby an increase in temperature leads to a reduction in emissions. Pearson's correlation analysis indicates a coefficient of -0.675, -0.844, -0.819 and -0.817 for CO, CH_4, C_6H_6 and CH_2O respectively. The correlation of gaseous pollutant species formation and combustion temperature is shown to be statistically significant to a level of P = <0.01.
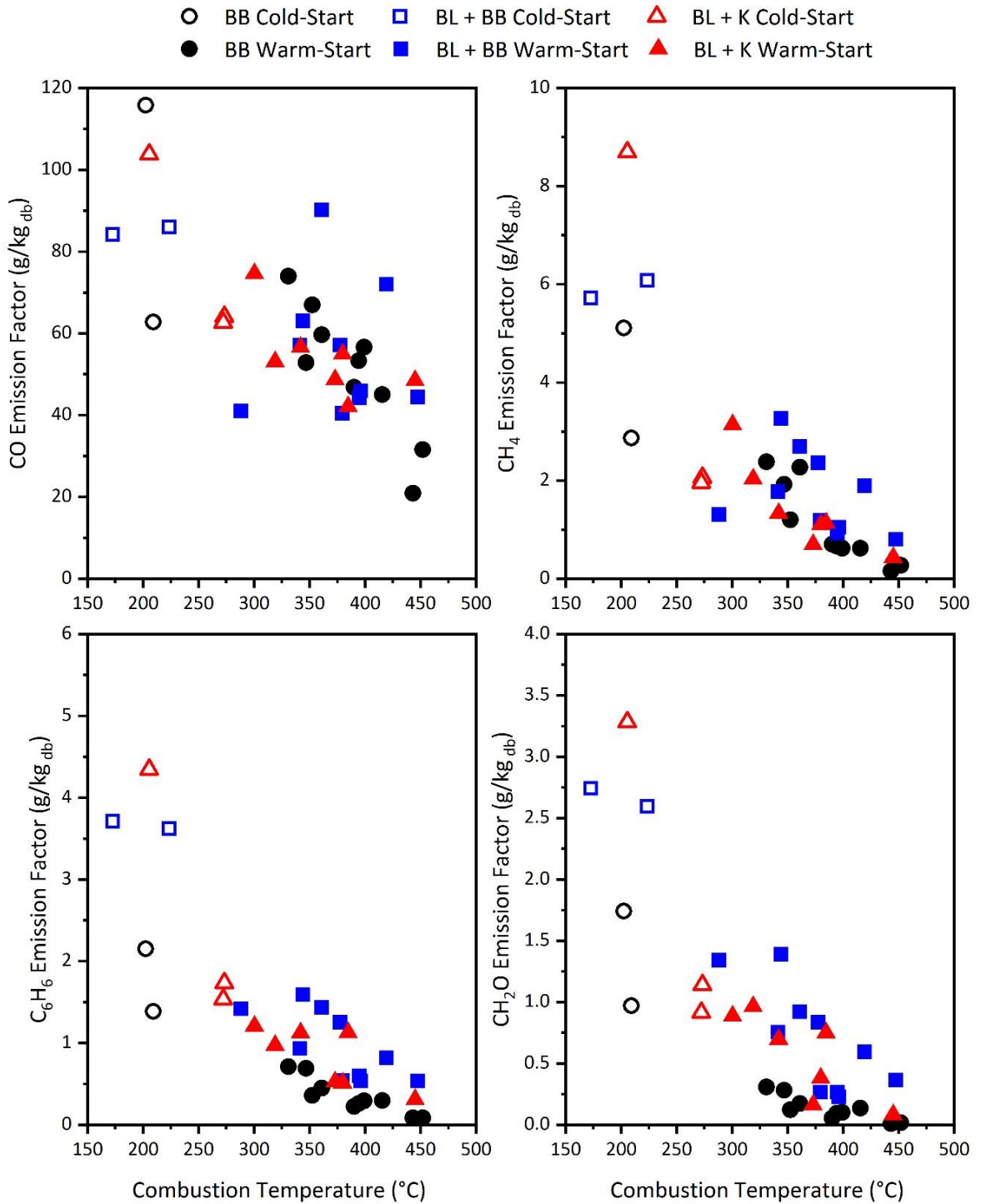
Figure 7.10 Variation in emission factor values (g/kg_fuel) and combustion temperature (°C) during cold-start and warm-start stove operation. Temperature is represented by the flue gas temperature (°C). BB is biomass briquettes, BL is beech logs and K is kindling.

7.4.5 Variation in Particulate Emissions under Cold-Start and Warm-Start Conditions

Total particulate emission (PM_t) sampling was undertaken via impaction with size separation as per the specific gravity of aerosol constituents. In accordance with BS EN 13240, the current legislative limits of PM_t emissions within smoke control areas is 5.5 g/kg$_{fuel}$. PM_t emission limits are proposed to be 55% lower than current standards following the implementation of Ecodesign 2022. Under the new legislation PM_t emission limits are limited to 2.4 g/kg$_{fuel}$. Soot emission factors were found to vary during stove operation under cold-start and warm-start conditions with the former being higher by a factor of 2.1 Emission factors for each of the test batches are presented in **Table 7.5**. The emission of PM_t is shown to be within the range of 2.63 g/kg$_{fuel}$ and 9.99 g/kg$_{fuel}$ during cold-start operation and between 1.83 g/kg$_{fuel}$ and 3.20 g/kg$_{fuel}$ during warm-start operation. The highest PM_t formation (9.99 g/kg$_{fuel}$) is observed during cold-start operation where the lowest combustion temperature is observed (205 ºC). The average emission factors are shown to be 5.2±4.1 g/kg$_{fuel}$ and 2.5±0.5 g/kg$_{fuel}$ for cold-start and warm-start operation respectively. PM_t under cold-start operation presents the greatest error with a standard deviation of 4.1 g/kg$_{fuel}$ in contrast to the lower deviation of 0.5 g/kg$_{fuel}$ observed during warm-start conditions. PM_t formation is shown to reduce with each batch of fuel applied during warm-start operation. The average formation during WS-1 is 2.5±0.5 g/kg$_{fuel}$ and the average formation during WS-2 operation is 2.2±0.4 g/kg$_{fuel}$. WS-3 operation indicates an increase in PM_t formation (2.83±0.5 g/kg$_{fuel}$) likely in response to the presence of non-combusted particles remaining upon the grate from previous batches. In addition, an increase in the combustion temperature during the final batch of operation may result in an increase in velocity thereby reducing retention time within the combustion zone and promoting incomplete combustion.

Similar findings are presented within the literature where cold-start operation generally observes increased particulate loading under lower combustion temperatures (Nussbaumer et al., 2008; Gonçalves et al., 2011). Nussbaumer et al. (2008) identifies higher PM loading during cold-start operation with a subsequent reduction during the development of nominal warm-start operation. $PM_{2.5}$ emission have been reported within the range of 5.62 g/kg$_{fuel}$ and 25.8 g/kg$_{fuel}$ during cold-start operation and between 1.66 g/kg$_{fuel}$ and 16.0 g/kg$_{fuel}$ during warm-start operation for woodstove appliances (Gonçalves et al., 2011). Similarly, $PM_{2.5}$ emission has been reported within the range of 8.11 g/kg$_{fuel}$ and 29.0 g/kg$_{fuel}$ during cold-start operation and between 0.84 g/kg$_{fuel}$ and 21.7 g/kg$_{fuel}$ during warm-start operation for fireplace appliances (Gonçalves et al., 2011). Hueglin et al. (1997)

similarly identified a higher particle number during the initial start-up phase of combustion testing with a reduction in the PM count by a factor of 5.6 and 2.9 during the subsequent flaming and smouldering phases. Furthermore, Fachinger et al. (2017) presents emission factor values of 1.22 g/kg_{fuel} under cold-start operation and 0.55 g/kg_{fuel} under warm-start operation providing a scaling factor of 2.2. $PM_{2.5}$ formation is also likely higher throughout all phases of combustion when comparing cold-start and warm-start operation. Fachinger et al. (2017) presents $PM_{2.5}$ emission factor values of 0.75 g/kg_{fuel} and 0.05 g/kg_{fuel} under the flaming and smouldering phases of cold start operation in contrast to values of 0.37 g/kg_{fuel} and 0.02 g/kg_{fuel} observed under warm-start conditions. Similar processes have also been identified during the combustion of coal (Maddalena et al., 2012) and the operation of cookstove appliances (Maddalena et al., 2012) however results have not been shown to be statistically significant when testing the latter in response to the small thermal mass of the appliances (Chen et al., 2016; Shen et al., 2017).

Table 7.5 PM_t emission factor values (g/kg_{fuel}), mass of soot collection (mg), emission concentration (mg/m^3) and particle size distribution (%). Emission concentrations are presented at $0^\circ C$ and 101.325 kPa.

Series	Test Batch	Emission factor (g/kg_{fuel})	Mass (mg)	$PM_{10}>$ (%)	$PM_{2.5}$-PM_{10} (%)	PM_1-$PM_{2.5}$ (%)	$<PM_1$ (%)	Temp. (°C)
1	CS	9.99	14.72	0.54	0.68	4.76	94.02	205
	WS-1	2.73	4.52	0.88	1.77	4.20	93.14	385
2	CS	3.04	4.64	0.65	1.08	7.33	90.95	273
	WS-1	1.83	2.79	0.72	1.08	5.38	92.83	319
	WS-2	1.88	3.07	0.33	1.30	6.19	92.18	300
	WS-3	2.46	3.96	0.25	2.02	5.81	91.92	373
3	CS	2.63	4.34	0.46	3.23	8.06	88.25	272
	WS-1	2.81	3.99	1.25	0.50	5.51	92.73	342
	WS-2	2.45	4.02	0.75	1.24	6.72	91.29	380
	WS-3	3.20	4.73	-	2.33	6.55	91.12	445

Figure 7.11 presents the effects of combustion temperature on PM_t (this work) and PM_{10} (Fachinger et al., 2017). A linear fit may be applied to both datasets whereby an increase in the combustion temperature generally corresponds with a reduction in PM_t and PM_{10} formation. In addition, cold-start operation, synonymous with low combustion temperatures, present higher particulate formation when compared with that observed during onset of warm-start conditions. In this work the average PM_t

under cold-start operation was 5.2±4.1 g/kg$_{fuel}$ when fuel particles are combusted at an average temperature of 250±39 ºC. Alternatively, the average PM$_t$ under warm-start operation was 2.5±0.5 g/kg$_{fuel}$ when fuel particles are combusted at an average temperature of 363±48 ºC. Similarly, Fachinger et al. (2017) presents an average PM$_{10}$ formation of 21.03±11.32 mg/MJ and an average combustion temperature of 130±32 ºC under cold-start operation with an average PM$_{10}$ formation of 7.73±6.09 mg/MJ and an average combustion temperature of 224±29 ºC under warm-start conditions. This work presents an R^2 value of 0.40 and a Pearson Correlation Coefficient (*r*) value of -0.63 when evaluating the relationship between combustion temperature and PM$_t$ formation. Similarly, Fachinger et al. (2017) presents an R^2 value of 0.47 and a *r* value of -0.69. Limited variation is presented in the particle size distribution for soot samples collected during cold-start and warm-start operation.

PM$_t$ formation occurs in response to the incomplete combustion of volatile hydrocarbon compounds during the pyrolysis reaction. During devolatalisation hydrocarbon species are liberated within the combustion zone under heating. Such processes occur in response to low temperatures within the combustion zone. Hydrocarbon fragments undergo a complex reaction of cracking and accumulation resulting in the formation of aromatic rings in the form of PAH (Obaidullah et al., 2018). The growth of PAH rings in response to low combustion temperature, and other factors, results in the formation of soot particles. Soot formation therefore occurs when combustion temperatures are low thereby inhibiting the complete oxidation of particles (Vicente et al., 2015). As such, the ignition phase can be responsible for up to 46% of the total nanoparticle formation of a test-batch (Ozgen et al., 2013). The composition of PM$_t$ generated under low temperature and high temperature combustion is also shown to vary with the former presenting a higher organic carbon (OC) content and the later presenting a higher elemental carbon (EC) content (Bond et al., 2004; Gonçalves et al., 2011; Mitchell et al., 2016; Obaidullah et al., 2018). In addition, the variation in temperature dependent PM$_t$ composition is shown to effect cytotoxicity thereby relating to human health (Bølling et al., 2012). Prakash and Murray (1972) present limited variation in PM$_t$ formation between 454 ºC and 537 ºC with a noticeable reduction during high temperature combustion when the reaction temperature exceeded 593 ºC. Vicente et al. (2015) also suggests significantly higher PM$_t$ emissions can occur during low temperature combustion particularly during cold-start operation. The level of PM$_t$ formation during cold-start operation is shown to vary depending upon fuelwood moisture content, particle size and material density (Koppmann et al., 2005; Vicente et al., 2015). Alternatively, PM$_t$ has been shown to increase at high combustion temperatures (Venkataraman et al., 2004) likely in response to limitations in stove

design resulting in a limited O_2 availability and retention time under a higher burning rate.
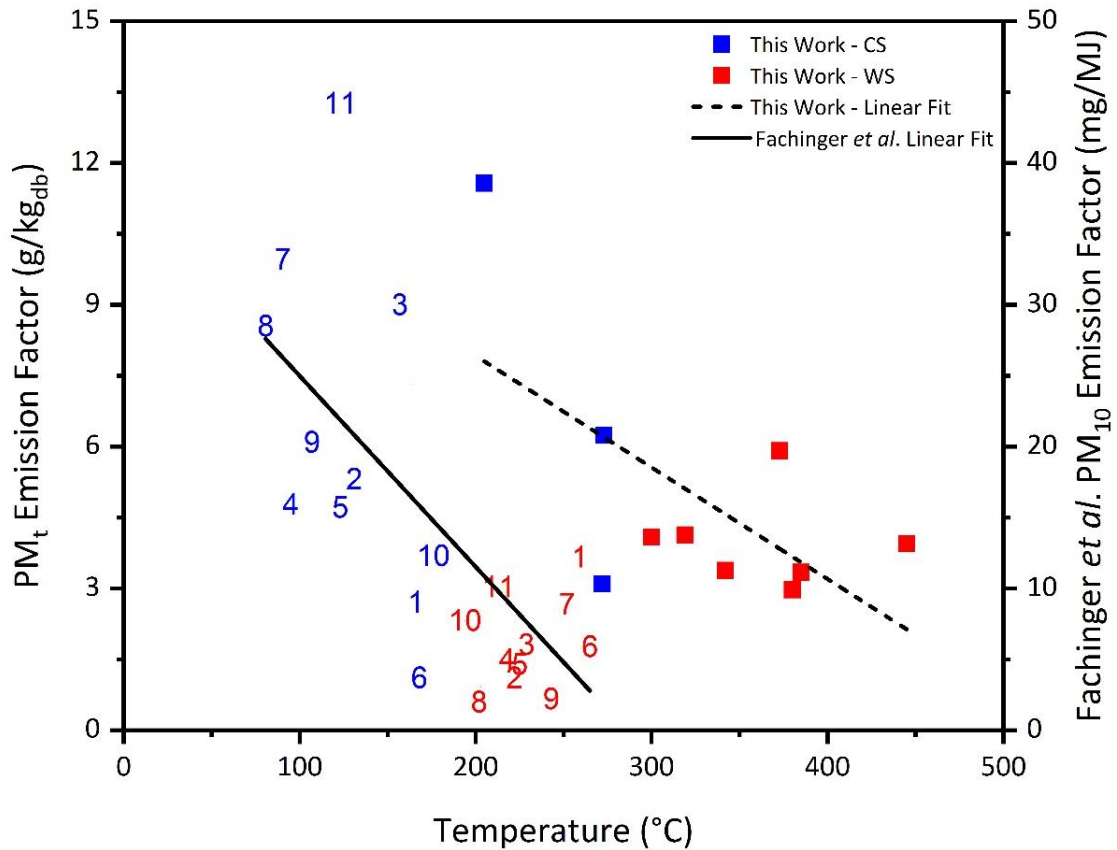
Figure 7.11 The effect of combustion temperature on particle formation. Temperature is presented as the average flue gas temperature (^{0}C). PM_t emission factors for this study are presented in g/kg$_{fuel}$. PM_{10} from (Fachinger et al., 2017) is presented in mg/MJ. From Fachinger et al. the fuelwood is presented as; Apple (1), Ash (2), Bangkirai (3), Birch (4), Beech (5), Cherry (6), Hickory (7), Oak (8), Plum (9), Spruce (10) and Spruce and Fir mixture (11). Blue and Red numeration identifies cold-start and warm-start operation respectively. The fuelwood is combusted in a contemporary high efficiency log burning appliance.

7.4.6 Effect of Cold-Start Inclusion on Results Repeatability and Emission Limit Criteria

As previously suggested, the testing of domestic heating appliances under standardised method conditions requires the stove device to be heated to a nominal operating condition prior to the start of the testing sequence. The onset of warm-start operation requires stove conditioning through the application of a cold-start batch(s). This results in official test types generally presenting combustion values that are not representative of real-world domestic application (Houck et al., 2008;

Reichert and Schmidl, 2018) given that increased smoke formation is generally observed during cold-start operation in response to lower combustion temperatures (Fachinger et al., 2017). In addition, cold-start data is often negated from emission factor indexes given the high degree of variability associated with stove operation at lower temperatures. The inclusion of cold-start data can therefore result in poor repeatability and a high degree of error (Fachinger et al., 2017). Given the high degree of inherent variability generally associated with biomass combustion the inclusion of cold-start data is known to cause problems when drawing statistically significant conclusions (McCrillis et al., 1992).

Figure 7.12 presents the variation in the emission factor sample population including only warm-start (WS) data and when the cold-start (CS) data is included. The associated error is calculated as ±1 standard deviation (σ) of the numerical mean ($\bar{x}$). Population variance is measured as the predicted value of the squared deviation from the numerical mean (σ^2). The analysis of WS data only is representative of methods followed in accordance with BS EN 13240:2001 + A2: 2004 while inventory data including both CS and WS data is more likely to representative real-world operating practices. The following findings have been identified for PM_t, CO, CH_4 and THC pollutant species.

i. Average PM_t emission observed during warm-start operation only was found to be 2.5±0.5 g/kg_{fuel}. The inclusion of the cold-start emission values results in a higher PM_t emission factor value of 3.3±2.4 g/kg_{fuel}. As such, the average PM_t emission factor value is shown to increase by 27.6% following the inclusion of cold-start emission data. PM_t emission factor values derived from warm-start operation only are reported within the range of 1.8 g/kg_{fuel} and 2.73 g/kg_{fuel}. The inclusion of cold-start emission factor values within the inventory results in a wider distribution of values within the range of 1.83 g/kg_{fuel} and 9.99 g/kg_{fuel}. The distribution of the PM_t within the inventory containing only warm-start data small ($\sigma = 0.5$ g/kg_{fuel}) in contrast to inventory data including both cold-start and warm-start data ($\sigma = 2.4$ g/kg_{fuel}). Similarly, the population variance is found to be small ($\sigma^2 = 0.24$ g/kg_{fuel}^2) when only warm-start data is included within the inventory and larger ($\sigma^2 = 5.72$ g/kg_{fuel}^2) when both cold-start and warm-start data are considered.

ii. Average CO emission observed during warm-start operation only was found to be 54.11±10.28 g/kg_{fuel}. The inclusion of the cold-start emission values within the emission inventory results in a higher CO emission factor value of 60.95±17.69 g/kg_{fuel}. As such, the average CO emission factor value is shown to increase by 12.6% following the inclusion of

cold-start emission data. CO emission factor values derived from warm-start operation only are reported within the range of 42.15 g/kg_{fuel} and 74.67 g/kg_{fuel}. The inclusion of cold-start emission factor values within the inventory results in a wider distribution of values within the range of 42.15 g/kg_{fuel} and 103.85 g/kg_{fuel}. The distribution of the CO within the inventory containing only warm-start data small (σ = 10.28 g/kg_{fuel}) in contrast to inventory data including both cold-start and warm-start data (σ = 17.69 g/kg_{fuel}). Similarly, the population variance is found to be small (σ^2 = 90.65 g/kg_{fuel}^2) when only warm-start data is included within the inventory and larger (σ^2 = 281.53 g/kg_{fuel}^2) when both cold-start and warm-start data are considered.

iii.   Average CH_4 emission observed during warm-start operation only was found to be 1.41±0.91 g/kg_{fuel}. The inclusion of the cold-start emission values within the emission inventory results in a higher CH_4 emission factor value of 2.26±2.39 g/kg_{fuel}. As such, the average CH_4 emission factor value is shown to increase by 60.3% following the inclusion of cold-start emission data. CH_4 emission factor values derived from warm-start operation only are reported within the range of 0.44 g/kg_{fuel} and 3.14 g/kg_{fuel}. The inclusion of cold-start emission factor values within the inventory results in a wider distribution of values within the range of 0.44 g/kg_{fuel} and 8.70 g/kg_{fuel}. The distribution of the CH_4 within the inventory containing only warm-start data small (σ = 0.91 g/kg_{fuel}) in contrast to inventory data including both cold-start and warm-start data (σ = 2.39 g/kg_{fuel}). Similarly, the population variance is found to be small (σ^2 = 0.72 g/kg_{fuel}^2) when only warm-start data is included within the inventory and larger (σ^2 = 5.16 g/kg_{fuel}^2) when both cold-start and warm-start data are considered.

iv.   Average THC emission observed during warm-start operation only was found to be 3.60±1.80 g/kg_{fuel}. The inclusion of the cold-start emission values within the emission inventory results in a higher THC emission factor value of 6.03±5.91 g/kg_{fuel}. As such, the average THC emission factor value is shown to increase by 67.5% following the inclusion of cold-start emission data. THC emission factor values derived from warm-start operation only are reported within the range of 1.25 g/kg_{fuel} and 6.42 g/kg_{fuel}. The inclusion of cold-start emission factor values within the inventory results in a wider distribution of values within the range of 1.25 g/kg_{fuel} and 21.92 g/kg_{fuel}. The distribution of the THC within the inventory containing only warm-start data small (σ = 1.80 g/kg_{fuel}) in contrast to inventory data including both cold-start and warm-start data

(σ = 5.91 g/kg$_{fuel}$). Similarly, the population variance is found to be small (σ^2 = 2.79 g/kg$_{fuel}^2$) when only warm-start data is included within the inventory and larger (σ^2 = 31.44 g/kg$_{fuel}^2$) when both cold-start and warm-start data are considered.
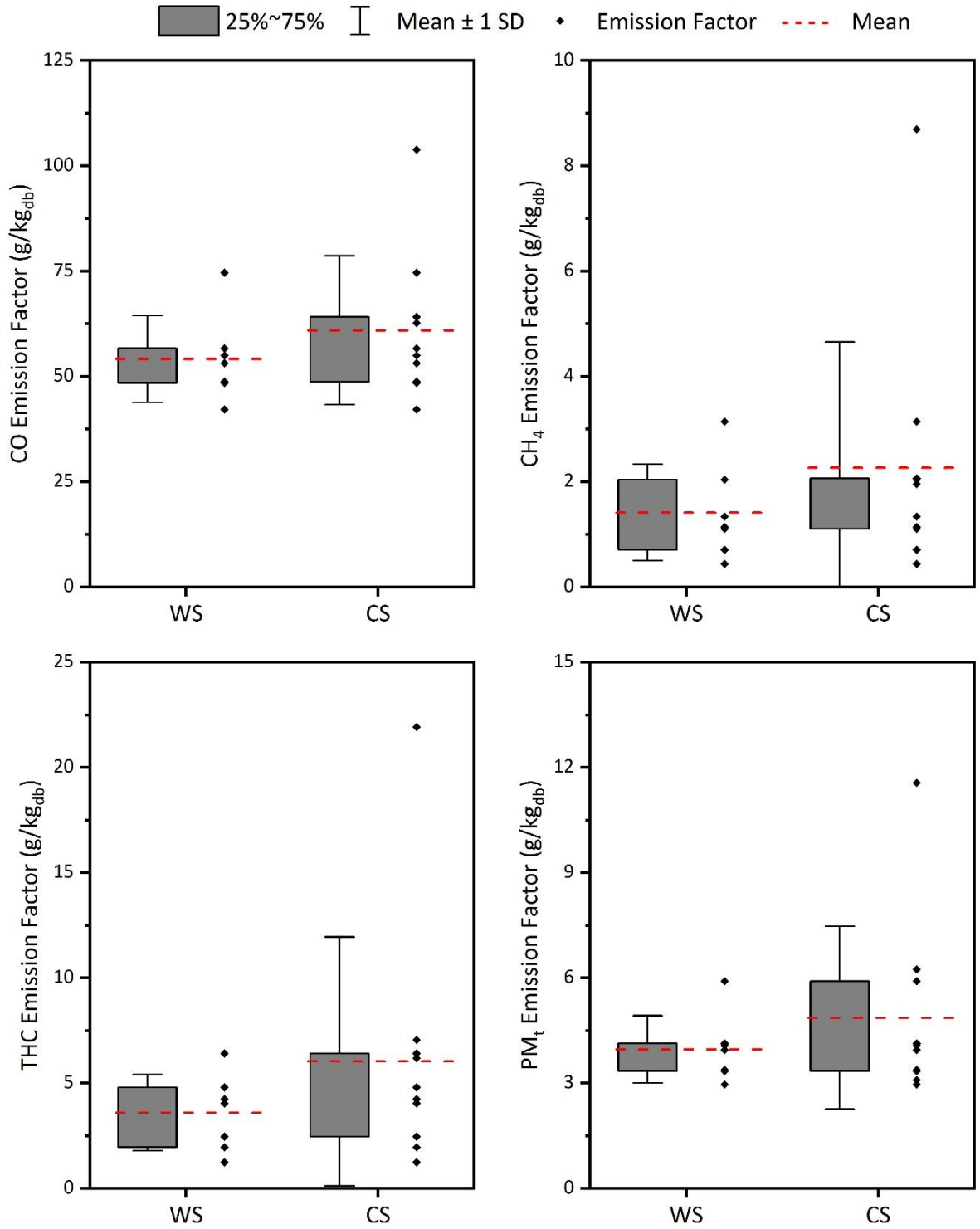
Figure 7.12 Effect of cold-start data inclusion on the distribution of emission factor values and the quantified error. Error is presented as ±1 standard deviation of the numerical mean.

A non-parametric Mann-Whitney U test is applied as a method of quantifying the significance of variation between both inventories at a statistical level. The Mann-Whitney U statistic indicates that the inventory including only warm-start data and inventory including both cold-start and warm-start data are not statistically different ($\rho = 0.05>$). PM_t, CO, CH_4 and THC present a ρ value of 0.669, 0.417, 0.475 and 0.364 respectively. Such findings are likely in response to relatively low emission factor value observed during cold-start operation in Series One and Series Two with high emission factor values identified in the warm-start operation of Series Two. As such, the inherent variability in biomass combustion makes the statistical assessment of variance difficult (McCrillis et al., 1992).

7.4.7 Effect of Cold-Start Emission Data on Ecodesign Limits

Combustion emission limits have been identified in new Ecodesign 2022 for PM_t, CO, organic gaseous carbon (OGC), which is identified as THC in this work, and NOx. An emission limit of 2.4-5.0 g/kg_{fuel} is established for PM_t. A large range in PM_t emission limits is presented in response to the different methods of PM sampling under standardised conditions. Emission limits are set at 996 g/GJ, 80 g/GJ and 113 g/GJ for CO, THC and NOx (Mitchell, Phillips, et al., 2019). These values have been converted from g/GJ too g/kg_{fuel} using a HHV value of 18.46 MJ/kg for beech logs as identified in (Phyllis2, 2020). Pollutant emission formation is known to be higher during the operation of stove appliances under cold-start conditions (Fachinger et al., 2017). Combustion testing under standard operational practices negate the presence of cold-start emissions with only nominal operating conditions contributing into the formation of emission factor values (Houck et al., 2008). **Table 7.6** presents the emission limits as identified under Ecodesign 2022 standards, the average emission factor value derived from warm-start operation only and the average emission factor value derived from both cold-start and warm-start operation.

Average PM_t emission during both warm-start testing (2.48±0.5 g/kg_{fuel}) and combustion testing that included both cold-start and warm-start operation (3.30±2.4 g/kg_{fuel}) is shown to exceed the limit outlined in Ecodesign regulation (2.4 g/kg_{fuel}). Previous testing has identified PM_t emission values which exceed the limit recommendations using the same stove appliance meaning that formation is likely in response to stove design, fuel properties and user behaviour (Maxwell et al., 2020). Similarly, NOx is identified below the emission threshold and shown to be similar during cold-start and warm-start operation likely in response to the mechanism of formation previously discussed. Biomass combustion has been shown to generally produce NOx at levels below that of the Ecodesign threshold

(Bäfver et al., 2011; Du et al., 2017) with examples of exceedances generally associated with the combustion of higher fuel-nitrogen materials (Mitchell et al., 2016). As such, NOx formation is more associated with the fuel properties than the stove design or operating practices. CO is shown to be higher for the emission inventory including both cold-start and warm-start results. This is likely in response to the increase in smouldering combustion observed under lower combustion temperatures during cold-start operation (Vicente et al., 2015). Both inventories are shown to exceed the emission limits identified under Ecodesign 2022 legislation. Similarly, THC is shown to be higher during cold-start operation in response to lower combustion temperatures resulting in the incomplete combustion of pyrolysis derived hydrocarbon species (Tissari et al., 2008; Vicente et al., 2015). Average THC emission factor values derived from warm-start only as well as values derived from both cold-start and warm-start operation are shown to exceed the Ecodesign 2022 limits.

Table 7.6 Comparison of emission factor values (g/kg$_{fuel}$) selected from warm-start only data and a complete inventory including both cold-start and warm-start data. Data is also compared against emission limits stipulated in Ecodesign 2022 (Mitchell, Phillips, et al., 2019).

Pollutant Species	Ecodesign 2022 Limit (g/kg$_{fuel}$)	WS (g/kg$_{fuel}$)	CS + WS (g/kg$_{fuel}$)
PM$_t$	2.4	2.48	3.30
CO	18.4	54.1	61.0
OGC (THC)	1.48	3.6	6.0
NOx (NO + 10%)	2.5	1.1	1.2

Average emission factor values in contemporary indexes are expected to reduce in response to an improvement in combustion appliance design following the implementation of Ecodesign 2022 (Savolahti et al., 2019). Such processes would increase the relative number of low emission appliances currently in use within the UK resulting in air quality benefits (Mitchell, Phillips, et al., 2019). The stove appliance used within this study in a Waterford Stanley Oisin multifuel stove maintaining a heat output of 5.7 kW and an efficiency of 79%. The appliance is HETAS approved however it is not a DEFRA approved appliance and is not except from use in smoke control areas under the Clean Air Act. The appliance maintains a cast-iron structure incorporating a high thermal mass and a single primary air supply. Ecodesign appliances are likely to include secondary and tertiary are supplies designed to ensure more complete burnout of combustion products

thereby resulting in a higher efficiency. The principal design of the Oisin appliance, specifically the limited air supply, results in limitations in air and fuel mixing resulting in the incomplete combustion (Sun et al., 2018). Exceedances in both CO and OGC is likely in response to such processes. Previous work has identified the effect of improved air supply and the application of two-stage combustion appliances on increased efficiency and reduced emissions (MacCarty et al., 2010; Nussbaumer et al., 2008; Sun et al., 2018).

7.4.8 Emission Formation Using Different Firelighter Materials

Emissions generated during the ignition phase and cold-start operation are shown to be a primary source of total gaseous and particulate pollutants (Fachinger et al., 2017; Nussbaumer et al., 2008; Ozgen et al., 2013). Previous works have also explored the effect of different methods of start-up on pollutant formation and stove performance (Nussbaumer et al., 2008; G. Reichert et al., 2017; Vicente et al., 2015). A variety of start-up aids are commonly used during the ignition of kindling piles within a stove. A variety of firelighter materials are currently available and vary in physiochemical composition. Combustion analysis was undertaken to assess the effect of ignition aid design and composition during the kindling phase of stove operation. ZipTM [High Performance] is an example of a HETAS approved petroleum-based firelighter material primarily incorporating kerosene as an ignition aid. This type of ignition material is commonly used during the ignition, kindling and cold-start operation during stove testing (Maxwell et al., 2020; Mitchell, Ting, et al., 2019; Price-Allison et al., 2018; Ting et al., 2018). If You CareTM is an example of a natural ignition aid material consisting of FCS approved and responsibly forested wood with natural vegetable oil. The firelighter is USDA approved as a natural and biobased material.

7.4.8.1 Effect of Firelighter Composition on Emissions and Start-up Performance

Variation in combustion conditions is shown to be limited between natural (If You Care[TM]) and kerosene (ZIP[TM]) firelighter materials. The average burning rate observed during the combustion reaction was 1.03±0.06 kg/hour for If You Care[TM] and 0.91±0.04 kg/hour for Zip[TM]. In addition, If You Care[TM] and Zip[TM] present an average conversion rate within the range of 0.96-1.08 kg/hour and 0.88-0.95 kg/hour respectively. Similarity in the burning rate is present in response to limited variation in combustion temperature between the fuel materials. The average flue gas and flame temperature during the combustion of natural firelighter material with kindling was 206±8 ºC and 257±17 ºC respectively. Average combustion

temperatures were found to be similar during the combustion of kerosene firelighter material with kindling in both the flue gas (187±7 ºC) and the flame (226±26 ºC).

Figure 7.13 presents variation in gaseous pollutant concentration during the combustion reaction. In response to similarities in the burning rate and combustion temperature the emission concentration trends (mg/m^3), and emission factor values (g/kg$_{fuel}$) are shown to be similar. Trends in CO, organic compounds and hydrocarbon species are shown to correspond with change in the combustion temperature across the duration of the reaction. For example, CO is shown to increase with a reduction in temperature with a maximum observed at lower temperatures during char burnout. The average CO formation is shown to be higher during natural firelighter combustion with an emission factor of 64.03±0.89 g/kg$_{fuel}$. CO formation during kerosene combustion is generally lower with an average value of 58.69±6.00 g/kg$_{fuel}$ however individual batches are found within the range presented during natural firelighter testing. Organic (CH$_2$O) and hydrocarbon (CH$_4$) concentration trends are shown to increase during the pyrolysis phase during the devolatalisation of the kindling particles. In both cases the concentration is shown to reach a maximum during the onset of the smouldering phase followed by a decline in formation during burnout. There is not significant difference presented during the start-up phase signifying similarities in emission between both firelighter materials. In addition, average emission factor values are shown to be similar for both fuels. If You Care^{TM} firelighter material presents emission factor values within the range of 0.69-1.06 g/kg$_{fuel}$ and 0.96-1.72 g/kg$_{fuel}$ for CH$_2$O and CH$_4$ respectively. Similarly, Zip^{TM} firelighter material presents emission factor values within the range of 0.87-1.12 g/kg$_{fuel}$ and 1.05-1.56 g/kg$_{fuel}$ for CH$_2$O and CH$_4$ respectively.
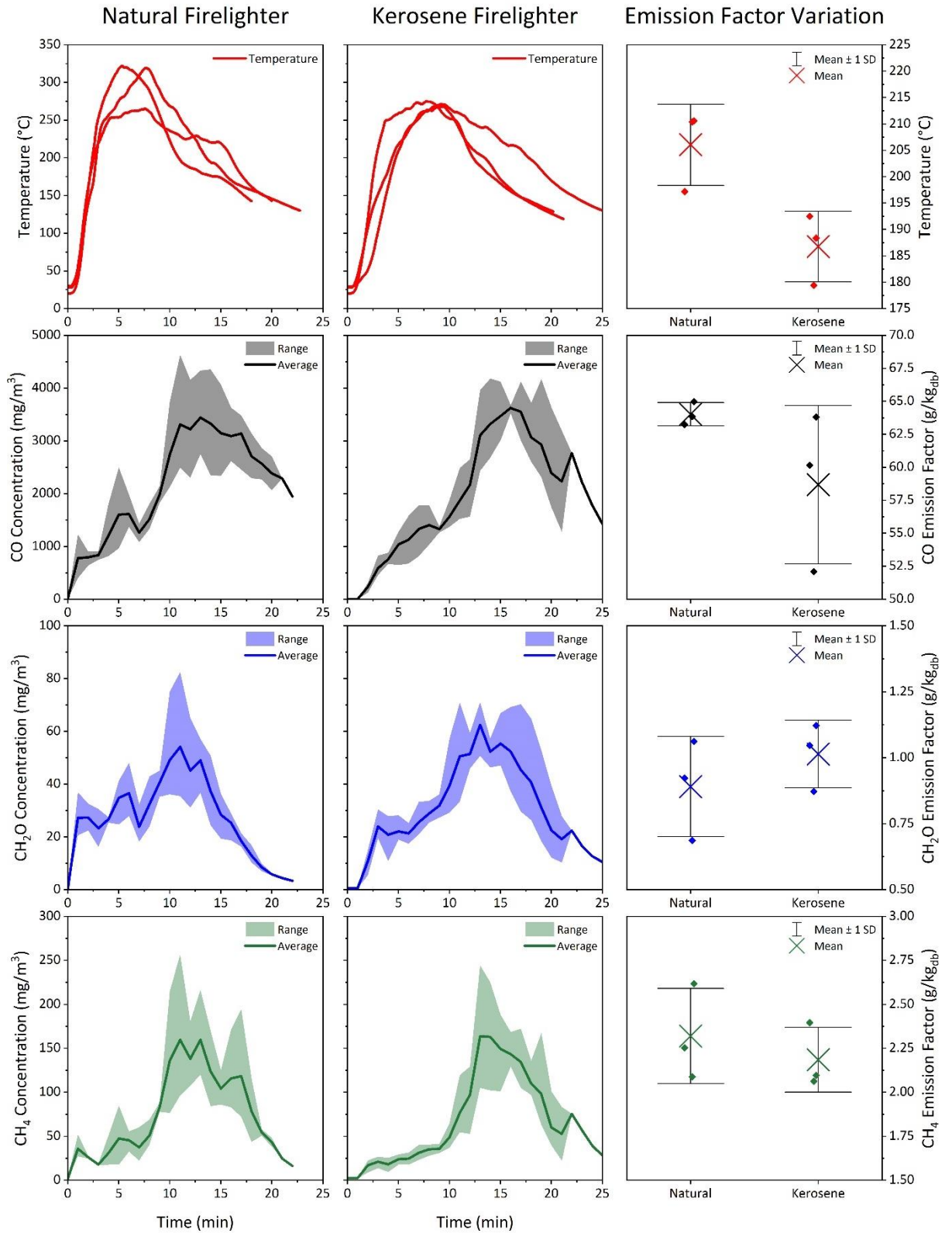
Figure 7.13 Variation in gaseous pollutant concentration (mg/m^3) and emission factor (g/kg$_{fuel}$) between natural firelighter and kerosene firelighter materials. ♦ represent emission factor values for each test undertaken.

7.4.8.2 Statistical Variation in Emission Formation from Different Firelighter Materials

Table 7.7 presents variation in average combustion conditions (burning rate, flue gas temperature and flame temperature), gaseous pollutant emissions and PM_t for kindling ignited via natural and kerosene-based firelighter materials. A scaling factor is applied to identify similarities in the average condition or emission factor value. Scaling values within the range of 0.9 and 1.1 are identified a minor and are likely in response to the inherent variability of biomass combustion in small domestic appliances. The scaling value is calculated as a ratio of natural firelighter/kerosene firelighter values. The average PM_t is shown to be similar for both methods of ignition. PM_t is identified within the range of 3.55-7.97 g/kg_{fuel} and 4.54-5.69 g/kg_{fuel} for kindling batches ignited via natural and kerosene-based firelighters respectively. Emission factor values observed at the top of the range during natural firelighter combustion are not in response to loss of temperature or increase in burning rate and is likely the result of natural variance in fuel pile combustion. Emission factor values for CH_4, C_2H_6, C_2H_4, C_3H_8, C_2H_2 and C_6H_6 are shown to be similar. In addition, THC is found to be similar during both combustion reactions. THC is identified within the range of 4.97-7.88 g/kg_{fuel} and 5.96-7.67 g/kg_{fuel} for kindling batches ignited via natural and kerosene-based firelighters respectively. $C_2H_4O_2$ presents a high scaling value however emissions factor values are identified at trace levels only for both fuels.

C_6H_{14} is shown to be significantly higher during the combustion of kindling ignited via kerosene-based material. This is likely in response to the presence of complex hydrocarbon inclusions within the kerosene matrix with naphthalene, benzene and n-hexane formations often associated (Lam et al., 2012). NOx formation is shown to vary between test fuels with emission factor values presented within the range of 1.79-2.10 g/kg_{fuel} and 0.56-0.66 g/kg_{fuel} for natural and kerosene firelighter materials respectively. Combustion temperature is shown to be similar and relatively low for both fuel types indicating the fuel NOx mechanism as the primary route of NOx formation (Bugge et al., 2014; Glarborg et al., 2003; Koppejan & Loo, 2008).

Table 7.7 Variation in combustion conditions and emissions during the combustion of natural firelighter and kerosene firelighter materials within kindling.

Fuel	Natural Firelighter (If You Care™)	Kerosene Firelighter (ZIP™)	Scaling factor (Natural/Kerosene)
Burning Rate (kg/hour)	1.03±0.06	0.91±0.04	1.1
Flue Temperature (°C)	206±8	187±7	1.1
Flame Temperature (°C)	257±17	226±26	1.1
MCE	0.94±00	0.94±0.01	1.0
CO (g/kg$_{fuel}$)	64.03±0.89	58.69±6	1.1
SO_2	1.14±0.05	1.19±0.02	0.96
NOx	0.62±0.05	1.98±0.17	0.31
CH_4	2.32±0.27	2.19±0.18	1.06
C_2H_6	0.69±0.24	0.77±0.03	0.90
C_2H_4	0.66±0.16	0.63±0.07	1.00
C_3H_8	0.35±0.13	0.35±0.10	1.00
C_6H_{14}	0.47±0.12	1.14±0.20	0.41
C_2H_2	0.47±0.22	0.39±0.10	1.21
C_6H_6	1.28±0.39	1.36±0.28	0.94
THC	6.23±1.54	6.82±0.96	0.91
CH_2O	0.89±0.19	1.01±0.13	0.88
$C_2H_4O_2$	0.07±0.09	0.05±0.03	1.40
PM_t	5.17±2.44	5.23±0.61	1.00

Combustion conditions are shown to be similar following the use of natural and kerosene-based firelighter materials during ignition. In response to similarities in the combustion conditions the emission of smoke and specific gaseous pollutant species is also shown to be similar. The following conclusions may therefore be presented in response to the described similarities with regards to combustion performance and emission formation.

i.   The use of natural firelighter material comprising biogenic substances and vegetable oil as an ignition aid presents combustion conditions similar to that of kerosene-based firelighter materials. The ignition of a kindling pile is shown to be indifferent during the application of both combustion materials. As such, the selection of firelighter materials is not of significant importance during the ignition and a cold-start batch. This presents significance for both residential stove use and commercial testing application where the use of different firelighter materials does not vary the performance of the combustion appliance.

ii. The start-up process is shown to be similar for both natural and kerosene-based firelighter materials. The capacity for igniting the kindling pile is also shown to be similar. Given the differences in structural and chemical composition of vegetable oil and kerosene it is likely that variation in emission formation is likely. Where differences in emission is expected the similarities in pollutant formation may be in response to a masking effect associated with the combustion of the kindling pile. As such, the emissions generated during the combustion of the firelighter materials are relatively small to that observed during the simultaneous combustion of the kindling. If so, the use of different firelighter materials for reducing emissions is again nullified given that the majority of emissions observed during start-up originate from the combustion of biomass on the grate.

iii. The use of different firelighter materials is shown to present only a minor effect on the total start-up emission with the majority of pollutant formation occurring in response to kindling combustion. Therefore, the use of different ignition aids does not affect the performance of the appliance or inhibit the formation of pollutant species.

iv. Other processes associated with the start-up operation present a much more significant impact on the cold-start performance of the appliance. Factors such as fuelwood moisture content (Price-Allison et al., 2018), fuel placement and orientation of ignition (Vicente et al., 2015), fuel properties (Mitchell et al., 2016) and user behaviour (Fachinger et al., 2017) are much more likely to affect the performance of the appliance than the type of ignition material.

7.5 Conclusions

A study was undertaken to investigate the effect of cold-start operation on gaseous and particulate pollutant formation from a small fixed-bed residential heating stove. A series of combustion experiments where undertaken using a method based upon BS EN 13240. Combustion testing was principally undertaken to assess the variance between cold-start and warm-start operation on emissions. In addition, a second study assessed the effect of different firelighter materials on emissions during start-up. Fuels used within this study include softwood kindling and beech fuelwood logs maintaining a moisture content of 12.92±1.32%. Firelighter materials included within this study include Zip^{TM} High Performance as an example of a kerosene-based ignition aid and If You Care^{TM} as an example of a biogenic-based ignition aid. Gaseous emissions where monitored throughout the combustion cycle

via an online FTIR analyser. Size-separated soot particles where collected within a dilution tunnel using a gravimetric impaction device. The following conclusions have been made.

i. The burning rate and combustion temperature where shown to differ throughout the combustion reaction. The burning rate observed under cold-start conditions was significantly lower than that observed when a nominal combustion condition was reached. The average conversion rate is presented as 1.29±0.31 kg/hour and 1.87±0.40 kg/hour for cold-start and warm-start operation respectively. Similarly, the combustion temperature observed under cold-start conditions was lower than that observed under warm-start operation. The average temperature is shown to be 250±39 °C and 363±48 °C under cold-start and warm-start conditions respectively. The rate of fuel conversion is shown to be affected by the combustion temperature whereby an increase in the temperature results in an increase in the burning rate. Low combustion temperatures under cold-start conditions result in a lower burning rate. High combustion temperatures under warm-start operation result in a higher burning rate. The temperature and burning rate are also shown to increase with each batch of fuelwood applied to the stove appliance under warm-start operation.

ii. Cold-start operation presents a relatively low average MCE (0.90±0.06) and a high CO average emission factor (76.91±23.35 g/kg_{fuel}). Warm-start operation presents a higher average MCE (0.95±0.01) and a lower CO average emission factor (54.11±10.28 g/kg_{fuel}). This is in response to the low combustion temperatures observed under cold-start operation resulting in smouldering combustion. Under warm-start operation the CO is likely oxidised under higher combustion temperatures leading to the formation of CO_2 and a lower MCE. Both MCE and CO formation is shown to be statistically correlated with combustion temperature.

iii. NOx and SOx emission are shown to vary throughout the combustion cycle under both cold-start and warm-start operation likely in response to the devolatalisation of the fuel nitrogen content. Both NOx and SOx emission factor values presented on a complete batch-basis are relatively unaffected by cold-start and warm-start operation with small variance likely in response to the combustion of firelighter material and kindling during initial start-up.

iv. Formaldehyde (CH_2O) and Acetic acid emission ($C_2H_4O_2$) is shown to vary dependent upon mode of operation. The average emission factor of CH_2O was 1.78±1.31 g/kg_{fuel} under cold-start operation and 0.56±0.35

g/kg$_{fuel}$ under warm-start operation. Similarly, the average emission factor of $C_2H_4O_2$ was 3.35±3.72 under cold-start operation and 0.50±0.40 under warm-start operation. Cold-start operation resulted in an increase in the formation of CH_2O and $C_2H_4O_2$ by a factor of 3.2 and 6.7 respectively. In both cases, an increase in the combustion temperature observed under warm-start operation results in a reduction in emission.

v.   Hydrocarbon species formation is shown to vary under cold-start and warm-start conditions. Methane (CH_4) and Benzene (C_6H_6) are found to be the most prevalent hydrocarbon species under both conditions. The average emission factor of CH_4 was 4.24±3.86 g/kg$_{fuel}$ under cold-start conditions and 1.41±0.91 g/kg$_{fuel}$ under warm-start conditions. Similarly, the average emission factor of C_6H_6 was 2.54±1.57 g/kg$_{fuel}$ under cold-start conditions and 0.83±0.37 g/kg$_{fuel}$ under warm-start conditions. Cold-start operation resulted in an increase in the formation of CH_2O and $C_2H_4O_2$ by a factor of 3.0 and 3.0 respectively. Total hydrocarbon (THC) formation was found to vary throughout the combustion cycle during both cold-start and warm-start conditions. Generally, formation was shown to peak following initial reloading in response to the pyrolysis of fuelwood particle under flameless conditions prior to ignition and during periods where the combustion temperature was low. The average emission of THC was found to be 11.72±8.84 g/kg$_{fuel}$ and 3.60±1.80 g/kg$_{fuel}$ under cold-start and warm-start conditions respectively. As such, cold-start operation resulted in an increase in the formation of THC by a factor of 3.3. Hydrocarbon formation is also shown to be controlled by the combustion temperature. Low temperatures observed during cold-start operation result in a high emission factor value while higher temperatures observed during warm-start operation result in a lower emission factor value.

vi.   Total particulate emission (PM_t) was shown to vary during cold-start and warm-start operation. The emission of PM_t is shown to be within the range of 3.04 g/kg$_{fuel}$ and 9.99 g/kg$_{fuel}$ during cold-start operation and between 1.83 g/kg$_{fuel}$ and 3.20 g/kg$_{fuel}$ during warm-start operation. The average PM_t emission under cold-start operation was 5.2±4.1 g/kg$_{fuel}$ when fuel particles are combusted at an average temperature of 250±39 ºC. Alternatively, the average PM_t emission under warm-start operation was 2.48±0.5 g/kg$_{fuel}$ when fuel particles are combusted at an average temperature of 363±48 ºC. The emission of PM_t appears to be controlled by the combustion temperature. Relatively low combustion temperatures

observed under cold-start operation results in high PM_t formation. Following the addition of subsequent test batches under warm-start conditions the formation of PM_t is generally shown to reduce.

vii. High emission factor values are also observed under warm-start conditions in response to inhibited combustion processes. The average combustion temperature observed during the cold-start phase of Series Two was 273.1^{o}C while the average temperature observed during WS-2 of the series was 300.3^{o}C. This value is lower than that observed during other warm-start batches within the series where the average combustion temperature during WS-1 and WS-3 was 318.9^{o}C and 372.8^{o}C respectively. Such processes occur in response to the dynamic nature of biomass combustion in small residential heating appliances contributing in a high degree of error. Lower temperatures observed under WS-2 resulted in higher gaseous emissions than what was observed under cold-start operation. Though anomalous results such as this may occur under nominal operating conditions it is likely that this process is commonly associated with warm-start operation and the application of combustion analysis in triplicate effectively masks such results. Notwithstanding, such processes should be considered when attributing emission factor values for new stove appliances and fuels.

viii. When testing stove appliances in accordance with BS EN 13240:2001 or other standardised conditions the cold-start results are often negated. Under such conditions the cold-start operational phase is designed to ensure nominal stove conditioning only with the results not contributing to emission inventory datasets. Such processes are often undertaken in order to attain repeatable results and reduce the high degree of variability in stove performance and emission formation generally observed under cold-start operation. Domestic stove use must include cold-start operation and may contribute a significant fraction of the total emissions produced meaning that such results should be considered in order to reproduce applicable values. Emission factor values where shown to be higher during cold-start operation in response to the lower efficiency and combustion temperature. Two inventories are therefore developed. In the first, only emission factor values generated under warm-start operation and in the second, emission factor values generated under both cold-start and warm-start operation. The inclusion of cold-start results leads to the formation of higher average emission factor values within the inventory including total stove use:

- Average PM_t emission observed during warm-start operation only was found to be 2.48±0.5 g/kg$_{fuel}$. The inclusion of the cold-start emission values results in a higher PM_t emission factor value of 3.30±2.4 g/kg$_{fuel}$. As such, the average PM_t emission factor value is shown to increase by 28.4% following the inclusion of cold-start emission data.

- Average CO emission observed during warm-start operation only was found to be 54.11±10.28 g/kg$_{fuel}$. The inclusion of the cold-start emission values within the emission inventory results in a higher CO emission factor value of 60.95±17.69 g/kg$_{fuel}$. As such, the average CO emission factor value is shown to increase by 12.6% following the inclusion of cold-start emission data.

- Average CH_4 emission observed during warm-start operation only was found to be 1.41±0.91 g/kg$_{fuel}$. The inclusion of the cold-start emission values within the emission inventory results in a higher CH_4 emission factor value of 2.26±2.39 g/kg$_{fuel}$. As such, the average CH_4 emission factor value is shown to increase by 60.3% following the inclusion of cold-start emission data.

- Average THC emission observed during warm-start operation only was found to be 3.60±1.80 g/kg$_{fuel}$. The inclusion of the cold-start emission values within the emission inventory results in a higher THC emission factor value of 6.03±5.91 g/kg$_{fuel}$. As such, the average THC emission factor value is shown to increase by 67.5% following the inclusion of cold-start emission data.

ix. The variability in emission factor values was shown to be lower in the inventory including only warm-start operation in response to the nominal stove conditioning and limited variation in performance. Alternatively, following the addition of cold-start results the error is shown to increase as the repeatability is greatly affected. A non-parametric Mann-Whitney U test is applied as a method of quantifying the significance of variation between both inventories at a statistical level. The Mann-Whitney U statistic indicates that the inventory including only warm-start data and inventory including both cold-start and warm-start data are not statistically different ($\rho = 0.05>$).

x. NOx emission limits were found to be below the emission limits presented under Ecodesign 2022 legislation for residential combustion appliances. Emission of PM_t, THC and CO were shown to be above the limits however this was found to be true for both inventories containing only warm-start data and both cold-start and warm-start data. Such

processes are likely in response to the limitation in the stove design. The stove appliance used within this study in a Waterford Stanley Oisin multifuel stove maintaining a heat output of 5.7 kW and an efficiency of 79%. The appliance is HETAS approved however it is not a DEFRA approved appliance and is not except from use in smoke control areas under the Clean Air Act. The appliance maintains a cast-iron structure incorporating a high thermal mass and a single primary air supply. Ecodesign appliances are likely to include secondary and tertiary are supplies designed to ensure more complete burnout of combustion products thereby resulting in a higher efficiency.

xi. Combustion testing was undertaken to assess the effect of firelighter material on emission and performance during initial start-up. As previously discussed, the variance in performance and emission was shown to be limited during the combustion of kerosene-based and biogenic-based firelighter materials. This suggests that the type of ignition aid applied does not affect the cold-start results.

xii. Cold-start operation is shown to affect both combustion efficiency and pollutant formation. Such processes are observed but not presented during the testing of combustion appliances in accordance with BS EN 13240:2001 or other standardised conditions. Given that cold-start operation is prevalent in almost all cases of residential combustion practices the formation of inventories containing only warm-start data may correspond with an underestimation of the true scale of emissions from domestic sources. The inclusion of cold-start data results in a higher degree of variation within the inventory resulting in a higher degree of error however such processes are also synonymous with domestic application. It therefore stands to reason that modification to combustion testing practices are required which should allow the analysis of start-up and cold-start operation. This would allow for the formation of inventories and certified emission values for stove appliances to be more representative of what is observed under real-world application.

7.6 References

Akagi, S.K., Yokelson, R.J., Wiedinmyer, C., Alvarado, M.J., Reid, J.S., Karl, T., Crounse, J.D. and Wennberg, P.O. 2011. Emission factors for open and domestic biomass burning for use in atmospheric models. Atmospheric Chemistry and Physics. 11(9), pp.4039–4072.

Alves, C., Gonçalves, C., Fernandes, A.P., Tarelho, L. and Pio, C. 2011. Fireplace and woodstove fine particle emissions from combustion of western Mediterranean wood types. Atmospheric Research. 101(3), pp.692–700.

Amand, L.E. and Leckner, B. 1991. Influence of Fuel on the Emission of Nitrogen Oxides (NO and N_2O) From an 8-MW Fluidized Bed Boiler. Combustion and Flame. 84, pp.181–196.

ANSYS FLUENT 2009. SOx Formation. ANSYS FLUENT 12.0 Theory Guide. [Online], 13.2.1. [Accessed 27 May 2020]. Available from: https://www.afs.enea.it/project/neptunius/docs/fluent/html/th/node220.htm.

BEIS 2016. Summary results of the domestic wood use survey [Online]. Available from: www.gov.uk/government/statistics/digest-of-united-kingdom-energy-statistics-dukes-2014-printed-version.

Bølling, A.K., Totlandsdal, A.I., Sallsten, G., Braun, A., Westerholm, R., Bergvall, C., Boman, J., Dahlman, H.J., Sehlstedt, M., Cassee, F., Sandstrom, T., Schwarze, P.E. and Herseth, J.I. 2012. Wood smoke particles from different combustion phases induce similar pro-inflammatory effects in a co-culture of monocyte and pneumocyte cell lines. Particle and Fibre Toxicology. 9(1), p.45.

Bond, T.C., Streets, D.G., Yarber, K.F., Nelson, S.M., Woo, J.H. and Klimont, Z. 2004. A technology-based global inventory of black and organic carbon emissions from combustion. Journal of Geophysical Research: Atmospheres. 109(14), pp.1–43.

Bugge, M., Skreiberg, Ø., Haugen, N.E.L., Carlsson, P. and Seljeskog, M. 2015. Predicting NOx Emissions from Wood Stoves using Detailed Chemistry and Computational Fluid Dynamics In: Energy Procedia. Elsevier Ltd, pp.1740–1740.

Calvo, A.I., Tarelho, L.A.C., Alves, C.A., Duarte, M. and Nunes, T. 2014. Characterization of operating conditions of two residential wood combustion appliances. Fuel Processing Technology. 126, pp.222–232.

Chen, Y., Shen, G., Su, S., Du, W., Huangfu, Y., Liu, G., Wang, X., Xing, B., Smith, K.R. and Tao, S. 2016. Efficiencies and pollutant emissions from forced-draft biomass-pellet semi-gasifier stoves: Comparison of International and Chinese water boiling test protocols. Energy for Sustainable Development. 32, pp.22–30.

Fachinger, F., Drewnick, F., Gieré, R. and Borrmann, S. 2017. How the user can influence particulate emissions from residential wood and pellet stoves: Emission

factors for different fuels and burning conditions. Atmospheric Environment. 158, pp.216–226.

FLUENT 2009. ANSYS FLUENT 12.0 Theory Guide - 13.2.1 Overview. 13.2 SOx Formation. [Online]. [Accessed 26 April 2020]. Available from: https://www.afs.enea.it/project/neptunius/docs/fluent/html/th/node220.htm.

Glarborg, P., Jensen, A.D. and Johnsson, J.E. 2003. Fuel nitrogen conversion in solid fuel fired systems. Progress in Energy and Combustion Science. 29(2), pp.89–113.

Gonçalves, C., Alves, C., Fernandes, A.P., Monteiro, C., Tarelho, L., Evtyugina, M. and Pio, C. 2011. Organic compounds in $PM_{2.5}$ emitted from fireplace and woodstove combustion of typical Portuguese wood species. Atmospheric Environment. 45(27), pp.4533–4545.

Houck, J.E., Pitzman, L.Y. and Tiegs, P. 2008. Emission Factors for New Certified Residential Wood Heaters In: Proceedings of the 17th International Emission Inventory Conference, Inventory Evaluation-Portal to Improved Air Quality.

Hueglin, C., Gaegauf, C., Künzel, S. and Burtscher, H. 1997. Characterization of wood combustion particles: Morphology, mobility, and photoelectric activity. Environmental Science and Technology. 31(12), pp.3439–3447.

Johnsson, J.E. 1994. Influence of Fuel on the Emission of Nitrogen Oxides (NO and N_2O) From an 8-MW Fluidized Bed Boiler. Fuel. 73(9), pp.1398–1415.

Khan, A.A., de Jong, W., Jansens, P.J. and Spliethoff, H. 2009. Biomass combustion in fluidized bed boilers: Potential problems and remedies. Fuel Processing Technology. 90(1), pp.21–50.

Klein, M.R. and Rotzoll, G. 1994. N_2O und NO bildung beim kohle und kokskornabbrand in laborwirbelschichten. VGB Kraftwerkstechnik. 74(12), pp.1072–1080.

Kopczyński, M., Plis, A. and Zuwała, J. 2015. Thermogravimetric and kinetic analysis of raw and torrefied biomass combustion. Chemical and Process Engineering - Inzynieria Chemiczna i Procesowa. 36(2), pp.209–223.

Koppejan, J. and van Loo, S. 2008. The Handbook of Biomass Combustion and Co-firing. London: Routledge.

Koppmann, R., von Czapiewski, K. and Reid, J.S. 2005. A review of biomass burning emissions, part I A review of biomass burning emissions, part I: gaseous emissions of carbon monoxide, methane, volatile organic compounds, and nitrogen containing compounds. Atmos. Chem. Phys. Discuss. 5, pp.10455–10516.

Lamberg, H., Nuutinen, K., Tissari, J., Ruusunen, J., Yli-Pirilä, P., Sippula, O., Tapanainen, M., Jalava, P., Makkonen, U., Teinilä, K., Saarnio, K., Hillamo, R., Hirvonen, M.R. and Jokiniemi, J. 2011. Physicochemical characterization of fine

particles from small-scale wood combustion. Atmospheric Environment. 45(40), pp.7635–7643.

Llpari, F., Dasch, J.M. and Scruggs, W.F. 1984. Aldehyde Emissions from Wood-Burning Fireplaces. Environmental Science and Technology. 18(5), pp.326–330.

Lu, Q., Wu, Y. ting, Hu, B., Liu, J., Liu, D. jia, Dong, C. qing and Yang, Y. ping 2019. Insight into the mechanism of secondary reactions in cellulose pyrolysis: interactions between levoglucosan and acetic acid. Cellulose. 26(15), pp.8279–8290.

Maddalena, R., Lunden, M., Wilson, D., Ceballos, C., Kirchstetter, T., Slack, J. and Dale, L. 2012. Quantifying stove emissions related to different use patterns for the Silver-Mini (small Turkish) space heating stove. Berkeley.

Maxwell, D., Gudka, B.A., Jones, J.M. and Williams, A. 2020. Emissions from the combustion of torrefied and raw biomass fuels in a domestic heating stove. Fuel Processing Technology. 199.

McCrillis, R.C., Watts, R.R. and Warren, S.H. 1992. Effects of operating variables on PAH emissions and mutagenicity of emissions from woodstoves. Journal of the Air and Waste Management Association. 42(5), pp.691–694.

Mcdonald, J.D., Zielinska, B., Fujita, E.M., Sagebiel, J.C., Chow, J.C. and Watson, J.G. 2000. Fine particle and gaseous emission rates from residential wood combustion. Environmental Science and Technology. 34(11), pp.2080–2091.

Miller, J.A. and Bowman, C.T. 1989. Influence of Fuel on the Emission of Nitrogen Oxides (NO and N_2O) From an 8-MW Fluidized Bed Boiler. Prog. Energy Combust. Sci. 15, pp.287–338.

Mitchell, E.J.S., Coulson, G., Butt, E.W., Forster, P.M., Jones, J.M. and Williams, A. 2017. Heating with Biomass in the United Kingdom: Lessons from New Zealand. Atmospheric Environment. 152, pp.431–454.

Mitchell, E.J.S., Lea-Langton, A.R., Jones, J.M., Williams, A., Layden, P. and Johnson, R. 2016. The impact of fuel properties on the emissions from the combustion of biomass and other solid fuels in a fixed bed domestic stove. Fuel Processing Technology. 142, pp.115–123.

Mladenović, M.R., Dakić, D. v., Nemoda, S., Paprika, M.J., Komatina, M.S., Repić, B.S. and Erić, A.M. 2016. The combustion of biomass - The impact of its types and combustion technologies on the emission of nitrogen oxide. Hemijska Industrija. 70(3), pp.287–298.

Nussbaumer, T., Doberer, A., Klippel, N., Bühler, R. and Vock, W. 2008. Influence of ignition and operation type on particle emissions from residential wood combustion In: 16th European Biomass Conference and Exhibition.

Obaidullah, M., Bram, S. and Ruyck, J. de 2018. An Overview of PM Formation Mechanisms from Residential Biomass Combustion and Instruments Using in PM

Measurements. International Journal of Energy and Environment. 12(May), pp.41–50.

Ozgen, S., Cernuschi, S. and Giugliano, M. 2013. Experimental evaluation of particle number emissions from wood combustion in a closed fireplace. Biomass and Bioenergy. 50(0), pp.65–74.

Pettersson, Esbjörn, Boman, C., Westerholm, R., Boström, D. and Nordin, A. 2011. Stove performance and emission characteristics in residential wood log and pellet combustion, part 2: Wood stove. Energy and Fuels. 25(1), pp.315–323.

Pettersson, E, Boman, C., Westerholm, R., Bostrom, D. and Nordin, A. 2011. Stove Performance and Emission Characteristics in Residential Wood Log and Pellet Combustion, Part 2: Wood Stove. Energy Fuels. 25, pp.315–323.

Prakash, C.B. and Murray, F.E. 1972. Combustion Science And Technology Studies on Air Emissions from the Combustion of Wood-Waste Studies on Air Emissions from the Combustion of Wood-Waste. Combustion Science and Technology. 6, pp.81–88.

Price-Allison, A., Mason, P.E., Jones, J.M., Barimah, E.K., Jose, G., Brown A.E. and Williams, A. 2021. The impact of fuelwood moisture content on the emission of gaseous and particulate pollutants from a wood stove. Combustion Science and Technology.

Price-Allison, A., Lea-Langton, A.R., Mitchell, Edward J. S.Gudka, B., Jones, J.M., Mason, P.E. and Williams, A. 2018. Emissions Performance of High Moisture Wood Fuels Burned in a Residential Stove.

Phyllis2. ECN Phyllis classification (wood, pine, #128). [Accessed 5 August 2021]. Available from: https://phyllis.nl/browse/standard/ecn-phyllis#pine.

Reichert, G. and Schmidl, C. 2018. Advanced Test Methods for Firewood Stoves Report on consequences of real-life operation on stove performance.

Reichert, G., Sturmlechner, R., Stressler, H., Schwabl, M., Schmidl, C., Oehler, H., Mack, R. and Hartmann, H. 2013. Definition of Suitable Measurement Methods and Advanced Type Testing Procedure for Real Life Conditions [Online]. Available from: www.bioenergy2020.eu.

Reid, J.S., Koppmann, R., Eck, T.F. and Eleuterio, D.P. 2005. A review of biomass burning emissions part II: intensive physical properties of biomass burning particles. Atmos. Chem. Phys. 5, pp.799–825.

Shen, D.K., Gu, S. and Bridgwater, A. v. 2010. Study on the pyrolytic behaviour of xylan-based hemicellulose using TG-FTIR and Py-GC-FTIR. Journal of Analytical and Applied Pyrolysis. 87(2), pp.199–206.

Shen, D., Zhang, L., Xue, J., Guan, S., Liu, Q. and Xiao, R. 2015. Thermal degradation of xylan-based hemicellulose under oxidative atmosphere. Carbohydrate Polymers. 127, pp.363–371.

Shen, G., Gaddam, C.K., Ebersviller, S.M., vander Wal, R.L., Williams, C., Faircloth, J.W., Jetter, J.J. and Hays, M.D. 2017. A laboratory comparison of emission factors, number size distributions, and morphology of ultrafine particles from eleven different household cookstove-fuel systems. Environmental Science and Technology. 51(11), pp.6522–6532.

Shen, G., Tao, S., Wei, S., Zhang, Y., Wang, R., Wang, B., Li, W., Shen, H., Huang, Y., Chen, Y., Chen, H., Yang, Y., Wang, W., Wang, X., Liu, W. and Simonich, S.L.M. 2012. Emissions of parent, nitro, and oxygenated polycyclic aromatic hydrocarbons from residential wood combustion in rural China. Environmental Science and Technology. 46(15), pp.8123–8130.

Sommersacher, P., Brunner, T. and Obernberger, I. 2012. Fuel indexes: A novel method for the evaluation of relevant combustion properties of new biomass fuels In: Energy and Fuels. American Chemical Society, pp.380–390.

Tarelho, L.A.C., Matos, M.A.A. and Pereira, F.J.M.A. 2005. Axial and radial CO concentration profiles in an atmospheric bubbling FB combustor. Fuel. 84(9), pp.1128–1135.

TheEngineeringToolbox.com 2003. Specific Heat of some Metals. [Accessed 23 April 2020]. Available from: https://www.engineeringtoolbox.com/specific-heat-metals-d_152.html.

Tissari, J., Lyyränen, J., Hytönen, K., Sippula, O., Tapper, U., Frey, A., Saarnio, K., Pennanen, A.S., Hillamo, R., Salonen, R.O., Hirvonen, M.R. and Jokiniemi, J. 2008. Fine particle and gaseous emissions from normal and smouldering wood combustion in a conventional masonry heater. Atmospheric Environment. 42(34), pp.7862–7873.

Tryner, J., Willson, B.D. and Marchese, A.J. 2014. The effects of fuel type and stove design on emissions and efficiency of natural-draft semi-gasifier biomass cookstoves. Energy for Sustainable Development. 23(1), pp.99–109.

Venkataraman, C., Joshi, P., Sethi, V., Kohli, S. and Ravi, M.R. 2004. Aerosol and Carbon Monoxide Emissions from Low-Temperature Combustion in A Sawdust Packed-Bed Stove. Aerosol Science and Technology. 38(1), pp.50–61.

Vicente, E.D., Duarte, M.A., Calvo, A.I., Nunes, T.F., Tarelho, L. and Alves, C.A. 2015. Emission of carbon monoxide, total hydrocarbons and particulate matter during wood combustion in a stove operating under distinct conditions. Fuel Processing Technology. 131, pp.182–192.

Wang, S., Ru, B., Lin, H. and Sun, W. 2015. Pyrolysis behaviours of four O-acetyl-preserved hemicelluloses isolated from hardwoods and softwoods. Fuel. 150, pp.243–251.

Werther, J., Saenger, M., Hartge, E.-U., Ogada, T. and Siagi, Z. 2000. Influence of Fuel on the Emission of Nitrogen Oxides (NO and N_2O) From an 8-MW Fluidized Bed Boiler. Progress in Energy and Combustion Science. 26, pp.1–27.

Yokelson, R.J., Griffith, D.W.T. and Ward, D.E. 1996. Open-path Fourier transform infrared studies of large-scale laboratory biomass fires. Journal of Geophysical Research: Atmospheres. 101(D15), pp.67–80.

Chapter 8
Impact of Replicate Number on Repeatability of Results and the Minimisation of Error when Calculating Emission Factors from a Domestic Stove

8.1 Introduction

The operational performance and pollutant emissions from domestic heating appliances is known to be highly variable. The testing of such devices is commonly associated with a high degree of discrepancy when evaluating emission data leading to poor repeatability and reproducibility (Trojanowski et al., 2018). Consequently, poor repeatability in combustion data results in a large range of emission factor values observed within emission inventories. Biomass combustion is a complex process involving interactions between heat and mass transfer as well as chemical reactions and fluid flow (Jenkins et al., 1998). A number of variables may affect the combustion process which are somewhat external to the fundamental reaction. The inherent fuel properties, including moisture content, chemical composition and material features including size or shape (Mcdonald et al., 2000; Simoneit, 2002; Mando, 2013; Jones et al., 2014; Mitchell et al., 2016; Trojanowski et al., 2018; Price-Allison et al., 2019; Trubetskaya et al., 2021) may result in poor conditions within a stove device leading to incomplete combustion (Koppejan and Loo, 2008). In addition, variables relating to the operator (Trojanowski et al., 2018) and factors relating to the stove device, including primary air availability (Fachinger et al., 2017), can result in further variability between both individual batches and tests. As such, relatively minor alterations between different combustion reactions can result in notable variability in observed emissions and the performance of the stove. These combined variables, and the inherent complexity of the combustion reaction, result in difficulty when attempting to produce repeatable results (Haslett et al., 2018). In response to the complexity of stove operation there persists a high likelihood of changeable results. Such processes, result in the considerable range in emissions data presented within inventories. An assessment of the quality of emission inventories may therefore be required (Klauser et al., 2020).

The most common method of evaluating stove or fuel performance is through the calculation of emission factors. These factors are a numerical estimate of the mass of a specific emission likely to arise following a combustion event. Such factors are often presented in mass of emission per mass of fuel consumed (g/kg_{fuel}), per energy of fuel (g/MJ), or across a temporal period (kg/day). A number of methods for deriving emission factors across a combustion period are presented within the

literature (Ballard-Tremeer and Jawurek, 1996; Zhang et al., 2000; Shen et al., 2010; Fachinger et al., 2017; Price-Allison et al., 2019); each is associated with inherent difficulties and limitations inhibiting universal application of a standardised method (GACC, 2014). Though emission factors may be calculated for specific periods within an individual combustion event (Mitchell et al., 2016), the majority of factors are calculated from an average emission concentration taken from the complete combustion cycle of a batch of fuel. This method presents a value more applicable for real-world stove operation, but it may result in reduced, or masked, emission events. For example, higher emission events during flaming combustion may be masked by notable reductions in emissions during the smouldering phase (Koppejan and Loo, 2008; Ozgen et al., 2014; Haslett et al., 2018). It is therefore important that stove testing understands the effect of stove operational practices, methodology limitations and the complexity of the combustion reaction upon the changeable nature of emission results. Poor reproducibility therefore affects results confidence and the ability to draw significant conclusions with regards to combustion performance and emissions. Undertaking additional batch testing could allow for improved confidence in derived emission results and minimise the inherent variability relating to operational practices, methodology limitations and the complexity of the combustion reaction.

Though the number of replicates tested presents a significant control on result confidence, there is discrepancy within the literature as to the number applied, which may range between one and seven, with the majority of investigations applying around three batches per fuel or per stove (Kinsey et al., 2009; Vu et al., 2012; Cerqueira et al., 2013; Ozgen et al., 2013; Calvo et al., 2014; Phillips et al., 2016; Seljeskog et al., 2017). Previous work by Schmidl et al. (2011) identified the need for additional batch tests when firing a manually-fed stove device compared with automated systems. Furthermore, a somewhat restrictive approach is presented within BS EN 13240:2001 which specifies that only two batches of logs or solid fuel are required during the testing of stoves during continuous operation (BSi, 2001). Notwithstanding, it is mathematically correct to calculate statistical conclusions from a sample population of three or more values however smaller populations can result in false-positives, decreased predictability and low accuracy when statistically evaluating a hypothesis (Hernandez et al., 2006; Wang et al., 2014). It is believed by some researchers that the very nature of combustion testing means that simply increasing the sample size (increasing the number of tests) will not lead to a reduction in variation between emission factor values and, as a result, error. Alternatively, given the capacity for error and poor repeatability of emission results, it stands to reason that more replicates are necessary. This idea has been previously explored when addressing repeatability issues in cookstove devices

(Wang et al., 2014) and pellet-stove space heating appliances (Trojanowski et al., 2018). However little work has been done in the quantification of error in domestic heating stoves. Given the disparity in testing approaches and the limited reproducibility of emission results future legislation and the regulation of testing procedures must account for a complete range of potential emission outcomes where a defined emission factor is unachievable (Coulson et al., 2015).

As discussed above, the homogeneity of fuels maintains significant impact on variability in emissions. Fuelwood is described as highly inhomogeneous materials, while briquetted and coal-based materials are of a more uniform composition and dimension (Tabarés et al., 2006). It therefore stands to reason that a more homogeneous fuel such as a biomass-based briquette or coal should produce more repeatable emission results, assuming consistent operational practices, and therefore require fewer repeated tests than other heterogeneous fuels. This hypothesis is explored in this Chapter.

8.2 Literature Review

The U.S. EPA (2016) have recently discussed the need for an operating protocol which can deliver precise and repeatable results so as to improve data confidence (U.S. EPA, 2016). A number of standardised testing procedures have been developed for stove testing and emission monitoring in Europe: NS 3058/NS 3059, Din-Plus and BS PD 6434 for Norway, Austria-Germany and the UK respectively and EN 13240 applied as a European standard. The Norwegian standard method (NS 3059) requires combustion testing for a cycle of four runs, while the Austrian-German (Din-plus) and European methods (EN 13240) employ a series of two-test-batches-per-experiment following an initial ignition batch. In contrast, the UK standard for solid fuel burning in domestic appliances (BS PD 6434) recommends that five repeat tests are undertaken per experiment (BSi, 2009; Mitchell et al., 2017). The number of repeats undertaken in published work is highly variable ranging between one and seven tests (Nakamura et al., 1981; Kinsey et al., 2009; Vu et al., 2012; Cerqueira et al., 2013; Ozgen et al., 2013; Calvo et al., 2014; Phillips et al., 2016). Nevertheless, poor repeatability and high degrees of error remain persistent problems within the literature. In addition, there is limited definition of the stove operation period in both UK and European testing standards. Though field-based emissions monitoring provides real-word emissions information, limitations in reproducibility mean that laboratory stove-testing under standardised laboratory conditions will remain the preferred method (Chen et al., 2012).

The fundamental cause of incomplete combustion is outlined in Smith (1987) and may be affected by the stove operator. The principal factors affecting combustion

include: the ratio of well-mixed air and mass of fuel within the combustion chamber, the temperature of the fuel and gas, and the residence time of products within the combustion zone. The impact of operator influence on stove performance is widely reported within the literature with standardised operating and test procedures designed to minimise its effect Such controls relate to processes regarding the fuel, methods of stove ignition, the regularity of use, the overall intensity of use and the operation of air supply or control (Wöhler et al., 2016). Operator error is shown to be lower when testing automated systems as identified by Fachinger et al. (2017) where only a 5% variability in emission factors were operator-derived.

Operators can choose the properties of the fuel applied within a heating stove device which is shown to affect performance (Wöhler et al., 2016). Previous work undertaken by Fachinger et al. (2017) reported the capacity for minimising emissions through the selection of appropriate fuels and burning patterns. . The selection of fuelwood species can result in varied thermal performance and emissions. Evtyugina et al (2014) identified variable levels of trace gas emissions following the combustion of European beech, Pyrenean oak and black poplar within a domestic heating stove with a difference in emissions also often presented between hardwood and softwood species (Mcdonald et al., 2000). Similarly, Mitchell et al (2016) identified differences in particulate emissions and burning rates between a series of biomass and coal based solid fuels combusted within the same heating stove under similar operating conditions (Mitchell et al., 2016). A number of factors affect the combustion performance of such fuels, with fuelwood combustion noted as being the most complex. The inherent moisture content of a fuel can inhibit initial combustion by increasing the drying period before ignition, which results in intermittent and incomplete combustion (Koppejan and Loo, 2008; Price-Allison et al., 2019). Moisture is also noted to reduce the thermal performance of a heating stove device in response to this additional energy loss during early phases (Mando, 2013). An investigation of the effect of fuelwood moisture content is presented in **Chapter 5** and **Chapter 6**.

The method of fuel loading and fuel-bed structure may affect the performance of a combustion appliance while variation in such practices can result in lower reproducibility (Trubetskaya et al., 2021). The number, size and mass of fuel particles is also shown to affect performance and emissions (Wöhler et al., 2016). The mass of fuel applied is generally subject to the HHV and moisture content as outlined in BS EN 13240. Overloading and underloading of a grate influences combustion conditions. Previous work by Fachinger et al. (2017) reported higher PM_1 emissions when burning fuel on an overloaded grate. Though combustion temperatures could be higher, leading to improved combustion conditions, the

limited oxygen-to-fuel- ratio and residence time of derived products may inhibit complete combustion. This leads to an increase in gaseous and particulate emissions where primary air supply is not sufficient. Such processes can lead to increased emissions for a longer period of time throughout the combustion reaction (Tissari et al., 2009). The size of fuel particles is also a factor, with the combustion of smaller logs often resulting in higher emissions when compared with larger logs of an equal total mass . This may be the result of rapid combustion of smaller particles (due to the larger surface area) resulting in faster gasification of volatile material. Where the air supply is constant, the rapid devolatilisation of smaller logs can result in incomplete combustion, while higher particulate emissions occurs in response to higher temperatures within the combustion zone (Tissari et al., 2009). Alternatively, Dasch (1982) identified higher emissions during the combustion of larger logs in response to limited oxygen availability and reduced combustion temperatures (Dasch, 1982).

The stove operator can also influence stove performance through the structural placement of the fuel, the point at which the stove is reloaded, and the control of primary air flow through the stove damper (Wöhler et al., 2016). The physical arrangement of fuel particles and firelighter materials prior to ignition can affect the formation of a hot-bed and, as a result, contribute in variation in combustion conditions between testing series (Trubetskaya et al., 2021). Excess air within the combustion chamber often results in enhanced flaming combustion. However, in response of a reduced residence time, emission factors may be higher as reported in Fachinger et al. (2017). Standard operating procedures during stove testing and emission monitoring attempt to mitigate variance in operator practices between both individual experiments and between testing facilities.

Heterogeneity of both individual particles and batches of a fuel may be an additional source of error during heating stove testing. Biomass derived fuels are heterogeneous - incorporating a mixture of cellulose, hemicellulose, lignin, bark and extractive compounds - which can vary between species and fuel particle samples of the same tree or source (Goldstein, 1991; Perré and Turner, 2002). Other aspects of the fuel material such as moisture content can vary depending upon the initial location of the fuel within the tree structure (Espenas, 1951). The heterogeneous nature of fuelwood logs in particular has resulted in may accredited testing facilities using standardised fuel materials selective sampling to remove barked and knotted logs. In addition, every endeavour is made to ensure the material under test is similar to that which is commercially available and conforms to those types recommended by the stove manufacturer (Stewart, 2017). Briquetted and pelletized fuels may be developed from a range of lignocellulosic biomass.

Unlike fuelwood logs, these processed materials are more homogeneous, with reduced variation between samples (Tabarés et al., 2006). It therefore stands to reason that the combustion of a more homogenous fuel should result in more reproducible combustion conditions thereby improving repeatability of derived emissions data.

The combustion of biomass in small residential heating appliances is complex often resulting in the development of unforeseeable and unavoidable events which induce poor repeatability and offset fuel sampling and stove operating practices designed to maintain consistency (Haslett et al., 2018). These events may include the collapse of a fuel stack prior to adequate heating meaning that a proportion of the fuel particles remain unexposed to the combustion reaction for a prolonged period. Such events can have a significant impact upon the combustion of a fuel batch and subsequent emission formation. Ignition, burning rate and devolatilisation of fuel may vary depending upon access to the heated grate often meaning that fuel types comprising smaller particles, such as pelletised and briquetted biomass , burn more evenly than logs because of the uniformity in thermal exposure (Stewart, 2017). Though the majority of fuel within a firebox is expected to burn, non-uniform thermal exposure may result in delayed or inhibited combustion of fuel; a process which will almost certainly lead to varied emission patterns under batch testing. Unforeseeable events within a combustion process are often minor and difficult to quantify but provide for notable differences in emissions profiles. A simple shift in the fuel pack or the falling of a log from a stack of particles can result in an emission spike as particulate matter is liberated from the bed. Alternatively, it could inhibit the rate of fuel consumption if the material is isolated from the heated grate. Though increased control of stove testing has been attempted in the literature (Fachinger et al., 2017), the unpredictable nature of combustion means that some variability is both expected and unavoidable.

As discussed earlier, repeated batch testing is a potential method of reducing error when measuring emissions from residential heating appliances (Scott, 2005; Wilton, 2012; Wilton and Bluett, 2012; Wang et al., 2014; Stewart, 2017). The success of using arithmetic averaging of emission results, and subsequent communication of stove performance values, is limited by the number of replicates applied within a test study. Though debate is presented within the literature on the number of repeated tests that should be applied, few dedicated studies have been undertaken which attempt to quantify the degree of confidence associated with standardised testing procedures (Wang et al., 2014).

Wang et al. (2014) investigated the effect of repeated testing on the statistical significance (standard deviation (σ), standard error (SE), cumulative distribution

function (CDF), and result confidence) of emission results from two cookstove devices. Stove operation practices and device performance were standardised as much as possible. Results are summarised in **Figure 8.1** where a specific number of replicates is identified so as to achieve a confidence of 0.01, 0.05 and 0.1 or 90%, 95% and 99% confidence respectively. An increase in the confidence is presented with an increase in the number of repeated tests undertaken. Applying this to stove testing, it is clear that increased batch testing would reduce uncertainty and mitigate misleading results. The application of additional testing will not reduce the standard deviation of values, principally because of the inherent variance of results, but will reduce the standard error (Wang et al., 2014). Though numerically valid, the application of three test batches may not be sufficient to representatively measure a true stove performance. Alternative international standard testing procedures (AS/NZS 4012/3) outline the need for as many as nine replicates so as to achieve more certainty of results, while a reduction in this value may infer error due to poor reproducibility (Scott, 2005).

A collation and review of real-world woodstove emission factors taken from a series of testing exercises is developed by Coulson et al. (2015). The study identifies variability in emission factor values generated during individual batch testing and between testing regimes. From a total of 390 in-situ combustion experiments the range of emission factors identified during a single experiment was sometimes found to be similar to the range of values from all experiments. A log-normal distribution was shown for each of the stove datasets each presenting a geometric mean of 4.9±3.8 g/kg$_{fuel}$ (all stoves), 3.9±3.8 g/kg$_{fuel}$ (NES compliant stoves) and 9.8±2.4 g/kg$_{fuel}$ (pre-1994 stoves). The study concluded that an increase in the total number of tests applied within an investigation fails to reduce the variability in emission factor results. As such, a coefficient of variance of around 1.0 is consistently observed for both larger and smaller population sizes. No relationship therefore observed between the variation in emission factor values and the size of the population meaning that an increase in the number of tests did not reduce observed variation (Coulson et al., 2015). The paper focuses on real-world and in-situ testing within urban locations in New Zealand and does not implement standardised testing under laboratory conditions. As such, further testing into the effect of reproducibility under laboratory conditions is therefore required so as to assess the impact of repetitive testing upon the statistical significance of results.
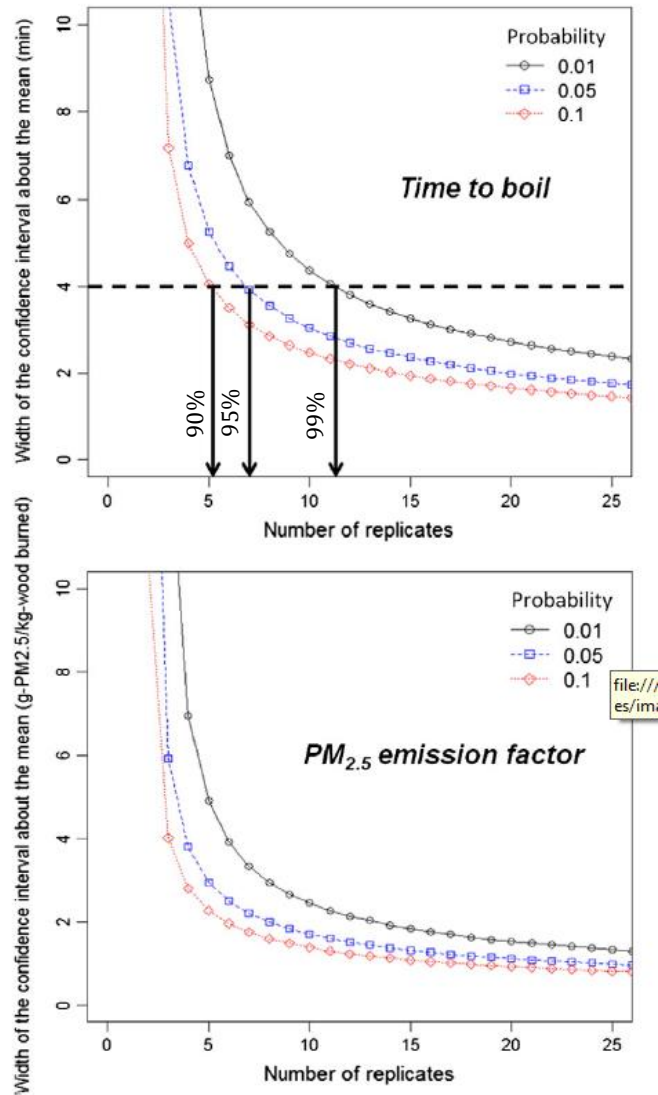
Figure 8.1 The effect of additional replicant testing on the confidence interval at 90%, 95% and 99% confidence while testing small cookstove devices. Taken from Wang et al. (2014).

Fachinger et al. (2017) investigated variability and uncertainty when calculating emission factors during fuelwood combustion in a 6 kW wood burning stove. The investigation analysed the impact of (*i*) experimental uncertainty, or uncertainty derived by minor differences in stove operation between experimental batches, (*ii*) day-to-day variability, or the difference in emission results across each experimental procedure, (*iii*) fuel variability in response to change of fuel supplier. **Figure 8.2** displays the magnitude of uncertainty for each of the three factors for each investigated pollutant. Experimental results showed a lower degree of uncertainty for pollutants which maintain a higher concentration. As such, pollutants with a lower concentration present a higher degree of uncertainty. Variability derived from the stove operator is believed to account for the majority of uncertainty

during the experimental work and is suggested to account for up to 30% of change in final emission factor values (Fachinger et al., 2017).

An evaluation of previously published emission values from accredited laboratories is presented by Curkeet and Ferguson (2010) where general repeatability was shown to be very poor: an average emission factor of 3.1 g/h corresponded with a standard deviation of ±5.4 g/h and a range of ±5.4 g/h (Curkeet and Ferguson, 2010; Trojanowski et al., 2018). Poor repeatability therefore inhibits confidence in results making it difficult to draw conclusions which are statistically significant.
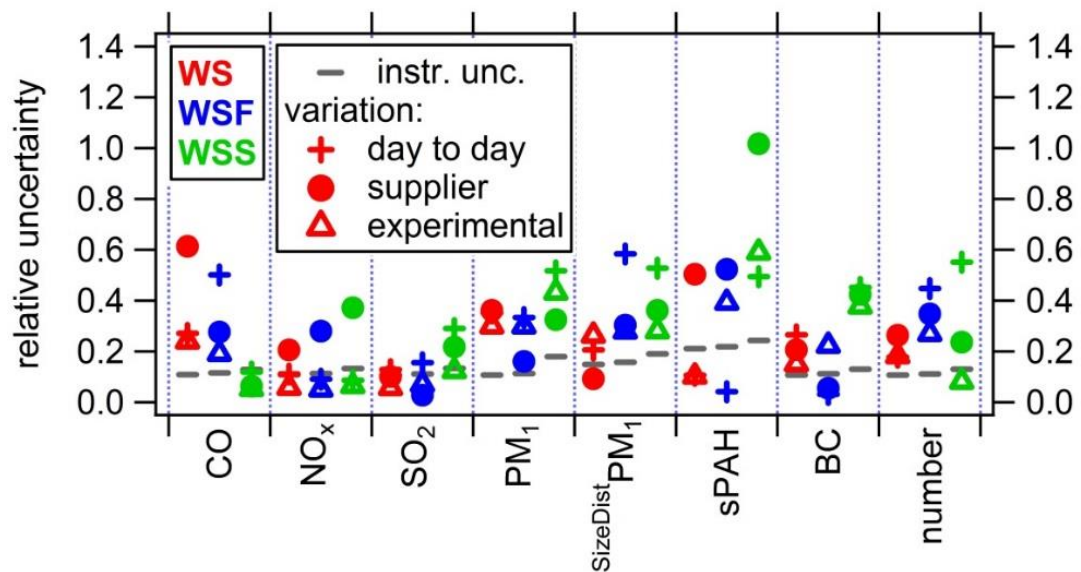
Figure 8.2 Sources of uncertainty associated with the combustion of Beech logs under ideal combustion conditions in a 6 kW wood burning stove. Uncertainty is provided for each of the three combustion phases investigated in the study were WS is warm start, WSF is flaming combustion phase and WSS is smouldering combustion phase. Taken from Fachinger et al. (2017, Supplimentry Information).

Previous work has identified the need for additional replicate testing when calculating emission factors. Given the potential impact of replicate number upon results confidence it stands to reason that further testing is required. Additional research should therefore be twofold and include; (*i*) the impact of batch repetition on confidence in emission factors and (*ii*) the impact of fuel heterogeneity on the requirement of replicant testing.

8.3 Materials and Methods

8.3.1 Test Fuel Information

Three typical fuels were studied as identified in **Table 8.1**. The fuels are commonly available within the UK market and include; (*i*) kiln-dried beech (hardwood), prepared in accordance with Ready to Burn certification, was studied to test the impact of fuel heterogeneity on emission repeatability. These fuelwood logs where kiln dried for a period of 24 hours at 50°C before being stored under a high tunnel to reduce the moisture content to between 15-20%. After receipt, the logs were kept in a covered outdoor store before being transferred to the indoor testing facility. All bark on the fuelwood logs was removed so as to mitigate potential sources of contamination and increased emissions from secondary sources: the processing of the fuelwood logs in this way increased the uniformity of the testing material (Obernberger et al., 2006; Phillips et al., 2016). In addition, all logs were cut to the dimensions presented in **Table 8.2**. [ii] Torrefied olive stone briquettes [Arigna], previously characterised by Trubetskaya et al. (2019), and (*iii*) HETAS approved biomass briquettes [Hotmax], incorporating pine sawdust residue, were applied as examples of more homogenous fuel materials. Both biomass and torrefied briquettes were stored in plastic bags before being air dried for a period of 24 hours prior to combustion testing. Each of the test fuels are presented in **Figure 8.3**.

Table 8.1 Details of the fuels used in this study

Fuel	Fuel Type	Physical Properties	Number of Replicates
Beech Logs (Ashtrees Ltd)	Fuelwood	Kiln-dried fuelwood Fuelwood dried at 50°C for 24 hours Stored in High Tunnel prior to collection Stored in outdoor shelter prior to testing All bark removed and fuel dimensioned HETAS and Ready to Burn approved	10
Biomass Briquettes (Hotmax)	Biomass Briquette	Pine sawdust residue briquette without binder Stored in plastic bags prior to testing HETAS and Ready to Burn approved	10
Grovoids (Arigna Fuels)	Torrefied Briquettes	Washed olive pit (Olea europaea) derived feedstock torrefied at 280°C> and briquetted Stored in plastic bags prior to testing	9

Figure 8.3 (a) debarked kiln-dried beech fuelwood logs, (b) torrefied olive briquettes [Arigna] and (c) biomass briquettes [Hotmax].

Table 8.2 Fuel characterisation and analysis

Fuel Type	Fuelwood	Biomass Briquettes	Torrefied Briquettes
VM (% db)	75.8	76.0	43.5
Ash	10.5	4.9	16.8
FC	13.7	19.1	39.8
Bulk MC (% ar)	17.45	5.48	13.8
C (% daf)	51.5	52.3	67.0
H	6.7	6.4	6.1
N	0.4	0.5	1.1
S	0.0	0.0	0.0
O	41.4	40.7	25.8
HHV (MJ/kg db)	17.8	19.8	21.2
LHV	13.21	17.35	17.05

*db – dry basis, daf – dry ash free

8.3.2 Multi-Fuel Stove Operation

Combustion testing was undertaken on a HETAS approved Waterford Stanley Oisin multi-fuel heating stove. Full details of the combustion testing facility, procedure and instrumentation is presented in **Chapter 3**.

Each batch of fuel was selected so as to improve homogeneity, where possible; as such material that differed in terms of size and mass was disregarded. The mass of each applied fuelwood batch (B_{fl}) was determined following BS EN 13240 as identified in **Chapter 3**, and as listed in **Table 8.3**:

i. The mass of each fuelwood (F) batch was in the range of 1.373 kg ±10%. In addition, a single test batch, at a reduced mass of 1.037 kg, was studied to examine the effect of underloading at high stove temperatures.

ii. Previous testing of the biomass briquettes (B) [Hotmax] briquetted fuel revealed reduced O_2 concentrations within the flue gas in response to high combustion temperatures resulting in a high burning rate. A reduced fuel load of 1 kg ±10% was subsequently applied during testing.

iii. Torrefied olive briquettes (T) [Arigna] were tested in batches of 1.5 kg ±10% as per the manufacturer recommendation.

Stove testing was performed following a method similar to BS EN 13240 for a heating stove burning under nominal intermittent conditions, as follows:

1. A pre-test batch of fuel was placed across the bottom grate in a manner designed to ensure reproducibility of ignition. The fuel batch was ignited using a mixture of 40 g ±10% of firelighters (Zip, Original) and 40 g ±10% kindling [Hotmax Briquettes] with the placement designed to ensure repeatable start-up conditions. The pre-test batch was identified as complete when the mass of fuel and ash remaining in the stove reached a specified mass (~50g).

2. A series of five subsequent test batches were applied to investigate the repeatability of results under hot start conditions. A reload point was determined for each of the warm-start batches based upon the mass of unburned fuel and ash residue remaining within the stove. The reload points for each batch where maintained across testing series. The operation of the stove and placement of the fuel was designed to ensure repeatability of results and uniform combustion of the fuel pack. The dimensions and masses used in each test are given in **Table 8.3**, together with burning time of each reload batch.

3. Each of the fuels were investigated across two combustion series on two separate days. Each series included a single cold-start batch followed by up to five warm-start reload batches in each day.

Table 8.3 Fuel characterisation and analysis

Fuel (Batch No.)	No. of Particles	Ave. Length, Width (cm)	*Total Mass (Ave. Fuel Particle Mass) (g)	Batch Time (min)
B (1.1)	4	5.8, 7.5	978 (245)	34.3
B (1.2)	4	5.5, 7.5	928 (232)	35.28
B (1.3)	4	5.8, 7.5	999 (250)	34.3
B (1.4)	4	5.8, 7.5	1056 (264)	33.31
B (1.5)	4	6.0, 7.5	1044 (261)	28.42
B (2.1)	4	5.8, 7.5	1072 (268)	35
B (2.2)	4	5.9, 7.5	1092 (273)	39
B (2.3)	4	5.4, 7.5	1022 (255.58)	35
B (2.4)	4	5.4, 7.5	1049 (262.41)	30
B (2.5)	4	5.5, 7.5	1031 (257.98)	31
T (1.1)	27	-	1521.6	54
T (1.2)	27	-	1538.0	50
T (1.3)	27	-	1472.5	53
T (1.4)	29	-	1516.5	66
T (1.5)	30	-	1570.2	78.28
T (2.1)	30	-	1456.75	54
T (2.2)	31	-	1501.23	56
T (2.3)	31	-	1495.59	64
T (2.4)	33	-	1363.18	78
F (1.1)	2	24, 9	1419.77 (709.89)	40
F (1.2)	2	23.75, 9.25	1456.01 (728.01)	43
F (1.3)	2	23.75, 9	1312.86 (656.43)	32.5
F (1.4)	2	23.25, 9.5	1268.85 (634.43)	30.5
F (1.5)	2	23.75, 10	1439.90 (719.95)	34.5
F (2.1)	2	24.25, 8.25	1343.26 (671.63)	38
F (2.2)	2	23.5, 8.25	1403.75 (701.88)	35
F (2.3)	2	23.75, 9	1311.06 (665.53)	33.5
F (2.4)	2	24.25, 8	1412.58 (706.29)	44.5
F (2.5)	2	24, 6.25	1037.04 (518.52)	25.75

*mass presented on an as-fired (af) basis

8.3.3 Statistical Analysis

Results of two testing series incorporating a pre-test batch followed by four/five warm-start test batches were considered in the quantification of stove start-up conditions and emission factor results. Given the likely variation in stove conditions

influencing the combustion process, as a function of both time and mass of fuel applied, the batch results were applied within the sample population in the order in which they were recorded. The effect of emission factor population sample size was evaluated following a method outlined in Wang et al. (2014). The standard deviation about an arithmetic mean ($\bar{x}$), as identified in **Equation 8.1**, is applied as an indication of the spread of measured results and, as a result, the likely variability within the population (Berthouex and Brown, 2002; Altman and Bland, 2005). Unlike standard error around a mean, the standard deviation will not necessarily reduce given a larger sample size and is instead dependent upon the recorded emission factor values (Wang et al., 2014). As such, the standard deviation is a measure of the scatter of observed sample values about an observed mean while the standard error is a measure of precision when estimating a true mean value from the deviation of observed data points (Berthouex and Brown, 2002).

$$(8.1) \quad \sigma = \sqrt{\frac{1}{n-1}\sum(x_i - \bar{x})^2}$$

σ is the standard deviation

n is the inventory sample size

$\bar{x}$ is the mean of observations within the inventory

x_i inventory value

Confidence intervals are applied as a method of quantifying a likely interval within which the true mean of a population may be located. The interval about the arithmetic average is described as $\bar{x} \pm E$ where E is the centred half-length value; as such, the full confidence interval may be calculated as 2E. The upper-bound and lower-bound intervals, about the arithmetic mean, may be calculated as $\bar{x} + E$ and $\bar{x} - E$ respectively. For large sample sizes, generally larger than 30, a z-statistic is applied as a method of calculating E. An appropriate estimation for the z-statistic values may be applied dependent upon the accuracy of the interval. Given the relatively small sample size in this study, a more appropriate t-statistic is applied which can be simply calculated in excel using the =TINV function, a calculation of the inverse of the two-tailed Student's T Distribution. Generally, the value of the dimensionless t-statistic decreases with an increase in the sample size as shown in **Table 8.4**.

Table 8.4 Examples of t-statistic variation depending upon sample size (*n*) and confidence level (*CL*)

Sample Size	t-statistic		
	CI=90%	CI=95%	CI=99%
3	2.920	4.303	9.925
4	2.353	3.182	5.841
5	2.132	2.776	4.604
10	1.833	2.262	3.250
15	1.761	2.145	2.977
20	1.729	2.093	2.861
25	1.711	2.064	2.797
50	1.677	2.010	2.680
100	1.660	1.984	2.626

The full-interval (2E) may be calculated using **Equation 8.2** where tα/2 is the t-statistic, σ is the standard deviation and n is the sample size. Values were calculated for three common confidence intervals where 1–α is 0.99, 1–α is 0.95 and 1–α is 0.90 (Berthouex and Brown, 2002; Wang et al., 2014).

$$(\mathbf{8.2}) \quad 2E = 2\frac{t\frac{\alpha}{2} \cdot \sigma}{\sqrt{n}}$$

A correlation is a measure of the statistical linier dependence between variable x and variable y. Typically, convergence must be measured across the same scale however due to the different variables investigated as part of this study a scaleless convergence, or correlation coefficient, is required. **Equation 8.3** identifies the method of calculating the Pearson's correlation coefficient (*r*) where positive or negative correlation is measured between -1 and +1 where a value of zero indicates complete independence of both variables. A probability normal-theory value (*P*) of 0.05 and 0.01, corresponding with a 95% and 99% confidence interval, is applied to assess the statistical significance of correlation results (Berthouex and Brown, 2002). Pearson's correlation analysis is a parametric statistical test meaning that data must be normally distributed. Given that data may not normally distributed in all cases, a bootstrapping method is applied to confirm the statistical significance of results for a bias corrected 95% confidence interval. Bootstrapping applies a method of repeated sampling of the data variables; up to 1,000 samples are selected under the current experimental procedure, using random sampling conditions (Wang et al., 2014).

$$(\mathbf{8.3}) \quad \sigma = \sqrt{\frac{1}{n-1}\sum(x_i - \bar{x})^2}$$

xi   each value of the x-variable within the inventory

x̄   is the mean of observations of the x-variable within the inventory

yi   each value of the y-variable within the inventory

ȳ   is the mean of observations of the y-variable within the inventory

8.4 Experimental Results

8.4.1 Variation in Combustion Conditions

Combustion experiments for each of the fuels were undertaken across two testing series. Each of these series incorporated an ignition phase, or cold start batch and these results are presented but not analysed in this chapter. The subsequent series of warm-start batches were used to derive emission factor values and were included within the statistical analysis. Control measures were applied to ensure reproducibility of the combustion reaction and inhibit the establishment of operator influence. Variability in emissions and combustion characteristics is therefore a function of prolonged operation of the stove, the thermal mass of the firebox relative to the mass of fuel consumed, and inherent burning variability. Each of these processes is defined in response to the period of stove use with prolonged combustion testing resulting in notably different conditions to those observed under standard testing conditions.

Previous research has identified a relationship between combustion zone temperature and pollutant emission formation (Smith, 1987; Fachinger et al., 2017) with flue gas temperature ($Flue_t$) providing a representative indication of heating conditions within the firebox (Alves et al., 2011). The combustion of biomass briquettes provided the highest temperatures while torrefied briquettes and fuelwood were similar. Average combustion temperatures were 388±40°C, 373±40°C and 374±44°C for biomass briquettes, torrefied briquettes and fuelwood respectively. Variability in combustion temperature between warm-start test batches is shown in **Table 8.4**. $Flue_t$ is in agreement with the range previously identified within the literature (Ozgen et al., 2014; Fachinger et al., 2017). A general increase in temperature is observed with each subsequent warm-start batch of fuelwood and biomass briquettes applied to the stove. Minor reduction in $Flue_t$ are observed and attributed to individual combustion events where fuel particles are displaced from the hot-grate thereby inhibiting flaming combustion. This process was particularly prevalent when testing fuelwood where the fuel pack is composed of a small

number of large fuel particles. The increased temperatures observed during later batches are likely in response to the total throughput of material into the combustion chamber. As such, the combustion temperatures are likely affected not only by the current fuel load but also by the combustion conditions observed during previous batches. A general decrease in temperature is observed with each subsequent warm-start batch of torrefied briquettes applied to the stove. The reduced temperatures are likely in response to a prolonged ignition time following fuel reloading. The delayed ignition was a result of fuel moisture content, ash formation on the grate and inhibited O_2 availability during heavy smouldering of the previous test batch. Flue gas velocity ($Flue_v$) is changeable and dependent upon the combustion temperature with higher velocities generally corresponding with a higher total fuel throughput. Increased flue gas velocity may result in a reduction in the residence time of combustion products within the flaming phase subsequently impacting pollutant formation.

Table 8.4 Average flue gas temperature (°C) observed during batch phase testing

Batch No.	B S1	B S2	T S1	T S2	F S1	FS2
1	330.9	346.7	376.9	379.9	288.0	341.1
2	352.4	390.0	442.7	381.7	343.9	379.5
3	360.9	394.1	418.7	354.5	377.4	395.8
4	399.1	415.5	365.5	303.6	447.3	360.9
5	451.9	443.2	340.1	-	419.0	394.5

The rate of fuel conversion was found to be similar to those observed during previous testing (Mitchell et al., 2016). Some variation in the burning rate of torrefied briquettes is observed which is likely due to the higher moisture content. **Figure 8.3** presents a trend between the fuel conversion rate and the average temperature observed across a complete batch cycle where higher combustion temperatures correspond within an increase in the burning rate as identified in Fachinger et al. (2017). An increase in the temperature occurred with each batch of fuel applied to the stove leading to a corresponding increase in the burning rate for fuelwood and biomass briquette fuels. A reduction in the conversion rate of the torrefied briquette material is likely a result of reduced temperatures in the combustion chamber. Burning rates (kg/hour) were found to be 1.71±0.2, 1.44±0.2 and 2.09±0.6 for biomass briquettes, torrefied briquettes and fuelwood logs respectively. A reduction in $Flue_t$ is often observed and attributed to individual combustion events. Such events are considered random and unavoidable and include the shifting of fuel particles from the hot-grate during the combustion

reaction thereby inhibiting energy availability subsequently leading to reduced stove temperatures and slowed fuel conversion rates.

Average O_2 concentrations are similar for biomass briquettes and fuelwood and are shown to be within the range of 12.04-15.69 vol-%. A reduction in oxygen availability is observed as a function of stove operating time with lower concentrations observed during high temperature combustion where the fuel conversion rate is also highest. O_2 concentrations are significantly higher during torrefied briquette combustion and are within the range of 15.72-17.82 vol-%. In response to the slowed burning rate the O_2 availability is shown to increase as a function of stove operating period with higher O_2 concentrations observed when combustion temperature and burning rate are reduced.
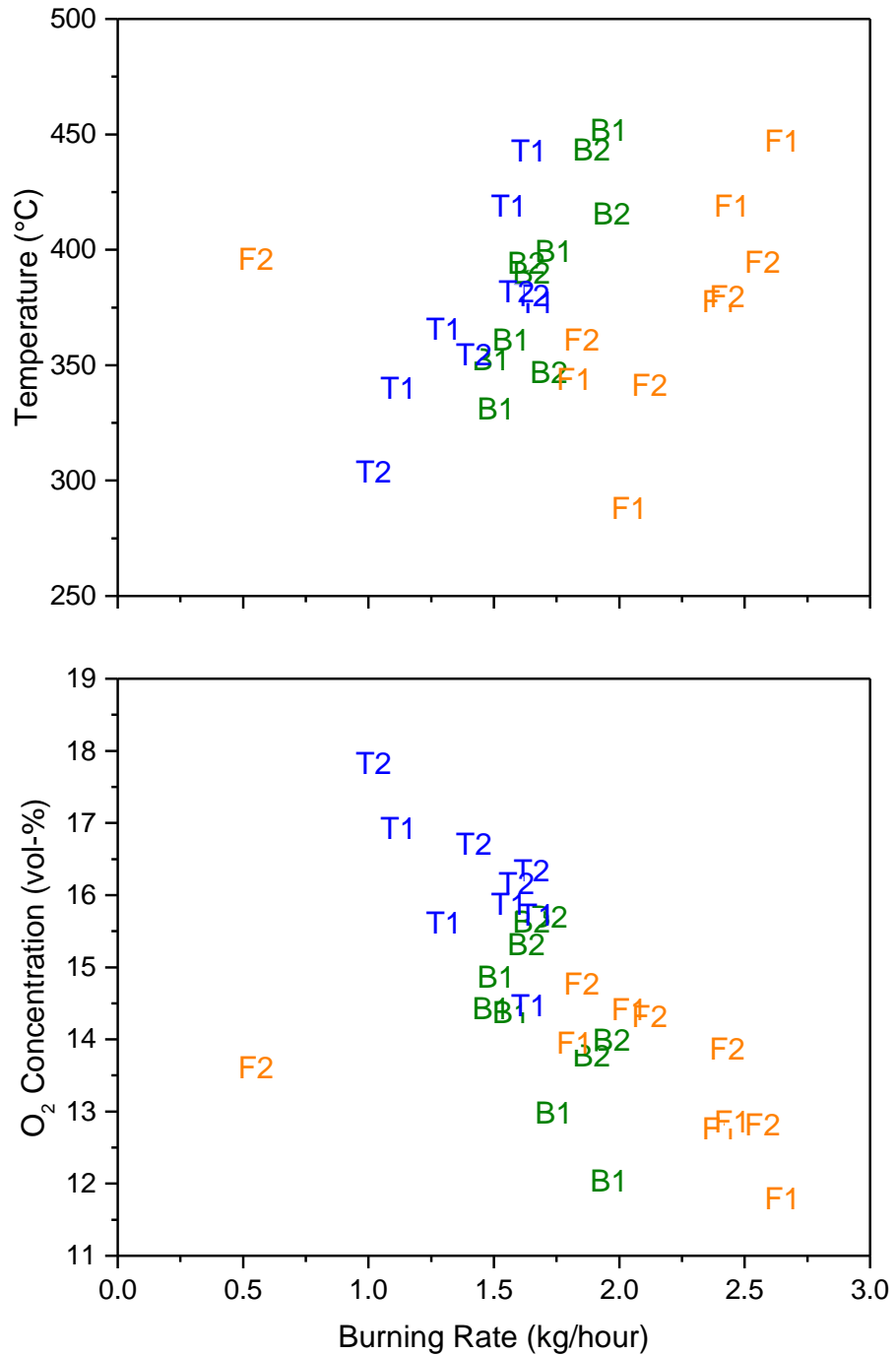
Figure 8.3 Variation in fuel burning rate (kg/hour) on an as fired basis as a function of flue gas temperature (°C) and O_2 availability (vol-%). Burning rate, flue gas temperature and O_2 concentrations are calculated as an average across the complete batch cycle. B is biomass briquettes, T is torrefied briquettes and F is fuelwood logs where 1 and 2 refer to the testing series number.

8.4.2 Summary of gaseous emission results

Emission Factor values are calculated using different constants in this Chapter. To convert these values into the same condition that is presented in the rest of the

thesis a correction factor of 0.88 may be applied. Emission factor results for this chapter have been updated within **Chapter 9** for direct comparison with other results.

Continuous gaseous emission monitoring was undertaken throughout the combustion experiments with emission factor values calculated across a complete batch cycle . Emission factor results were within the range found in the literature (Purvis and McCrillis, 2000; Hedberg et al., 2002; Bafver et al., 2011; Pettersson et al., 2011; Ozgen et al., 2014; Fachinger et al., 2017). **Table 8.5** outlines the emission factor values derived from individual warm-start batches and the average emission results calculated for each of the fuel materials.

Table 8.5 Average gaseous emission factors calculated from the complete combustion cycle. Emission factor values presented in g/kg_{fuel} unless otherwise stated.

Fuel	CO	CH_4	CH_2OCH_2O	C_6H_6	SO_2	NOx	NH_3 (mg/g)	MCE
B	50.8±15.8	1.1±0.8	0.1±0.1	0.3±0.2	0.9±0.1	1.5±0.2	85.8±39.3	0.96
T	163.6±29.0	1.8±1.0	0.6±0.2	1.7±1.0	1.4±0.3	1.9±0.3	415.9±71.8	0.84
F	55.6±16.0	1.7±0.8	0.7±0.4	1.0±0.4	0.6±0.2	1.0±0.2	144.2±30.7	0.94

8.4.2 Summary of particulate emission results

Particulate collection was undertaken under dilution by impaction as shown in **Chapter 3**. High PM loading generally occurs during ignition and flaming phases with significantly lower concentrations generally observed during smouldering combustion (Mitchell et al., 2016). As such, the calculation of PM_t across a complete batch cycle may mask very high PM loading during early phases of combustion if the smouldering phase is extended (Calvo et al., 2015; Mitchell, 2017).

In response to the method of particulate matter sampling [PM_{10} Impactor, Dekati] the emission inventory sample size remains small for PM_t emission factors ($n = <5$). As such, the PM_t values are not included in the statistical analysis. **Table 8.6** summaries the PM_t emission factor values and particulate size distribution for each of the test fuels under warm-start operation.

Table 8.6 Average particle size distribution of PM material under diluted conditions as a percentage (%) of PM_t.

Particle Size Fraction (µm)	B	T	F
n	5	5	6
PM_t (g/kg$_{fuel}$)	2.4±0.7	0.7±0.2	1.2±0.5
Range (g/kg$_{fuel}$)	1.5-3.1	0.6-1.1	0.6-2.0
PM_{10} >	0.7±0.4	2.6±3.0	0.7±0.6
$PM_{2.5}$ - PM_{10}	2.7±1.6	0.9±0.9	1.2±1.0
PM_1 - $PM_{2.5}$	4.6±1.2	4.6±6.7	2.5±1.6
<PM_1	92.1±2.4	91.9±5.5	95.5±2.8

8.4.3 Effect of stove operational period on emission formation

Pollution emission concentrations are shown to reduce during repeated batch testing. Higher emission factors are generally presented during pre-test, cold-start, batch combustion however these values are likely skewed by instrument error and contamination during the combustion of kerosene ignition material. Emission concentrations and corresponding emission factors are presented in **Figure 8.4-8.6**. The repeated tests of biomass briquettes indicate a reduction in pollutant formation as a function of total fuel throughput. Higher emission factor values are observed during batches 1, 2 and 3 with lower values observed during the combustion of batches 4 and 5. The improvement in emissions is likely the result of increased temperatures within the combustion zone following a prolonged heating period and combustion of a larger fuel mass. Flue gas and grate temperatures were in the range of 330-394 °C and 450-555 °C for batches 1-3 with 399-451 °C and 483-617 °C for batches 4-5. O_2 concentration trends are also noted to vary with increased temperatures. This is likely in response to more energetic combustion under hotter stove conditions leading to a higher O_2 demand during the thermal conversion reaction. The MCE trend is similar between batches with higher values (0.90-1.00) and lower values (0.80-0.90) corresponding to flaming and smouldering combustion phases respectively (Akagi et al., 2011). However, MCE values during latter test batches are notably higher suggesting higher CO_2 concentrations and lower CO concentrations. CO formation is generally a function of combustion phase and temperature and is an intermediate species of CO_2 formed during the oxidation of hydrocarbon fuels (Sartor et al., 2014; Olave et al., 2017). The reduction in CO emission factors during these batches also suggests more significant flaming combustion compared to smouldering phases. It is therefore likely that the

temperature within the combustion zone had a significant effect on pollutant emission concentrations.

CH_4 emission arising from the combustion of biomass briquettes and fuelwood reduced following the addition of subsequent test batches. The average emission of CH_4 derived from the initial three batches of biomass briquettes was 1.53±0.77 g/kg$_{fuel}$. Subsequently, the average emission was reduced to 0.42±0.24 g/kg$_{fuel}$ during the combustion of batches 4 and 5. A similar trend is observed during the combustion of fuelwood whereby a higher emissions (1.83±0.85 g/kg$_{fuel}$) are observed during the initial three batches followed by lower emissions (1.58±0.89 g/kg$_{fuel}$) during batches 4 and 5. The reduction in CH_4 is less significant during the combustion of fuelwood in response to fuelwood particles becoming displaced from the hot-grate leading to an increase in smouldering and lower combustion temperatures. Similar trends were found for benzene species and formaldehyde. The higher combustion temperatures observed in this work, resulting in lower emission concentrations, would not generally be observed when following standard testing practices – i.e. applying three batches of fuel. NOx and SO_2 emissions appear unaffected by increased combustion temperatures suggesting the majority of the pollutant formation is dependent on fuel nitrogen and sulphur contents.

The combustion of torrefied briquettes appears to show an alternative trend with increased emissions presented with an increase in total fuel throughout as shown in **Figure 8.5a,b**. CH_4 emission was 1.3±0.4 g/kg$_{fuel}$ following the combustion of a single test batch, and 3.0±0.6 g/kg$_{fuel}$ recorded during test batches 4 and 5. A similar pattern is identified for alkane species, benzene and formaldehyde. Increased emission concentrations correspond with reduced combustion temperatures. A possible cause of reduced temperatures within the combustion zone relate to the prolonged ignition period following reloading and high moisture content. In addition, the onset of heavy smouldering and continued devolatilisation of hydrocarbon products inhibited ignition. In some cases, this initial ignition period was as much as 150 seconds thereby causing the peaks presented in **Figure 8.5a**.

Figure 8.4-8.6 present gaseous emission profiles for each of the combustion experiments including both cold-start and warm-start operation. Emission profiles are shown for series 1 (S1) and series 2 (S2) for each of the fuels. Gas emission concentrations are presented in mg/m^3 on a dry basis at STP. Pollutant emission factor values are presented in g/kg$_{fuel}$. O_2 concentrations are presented in vol-%$_{db}$.
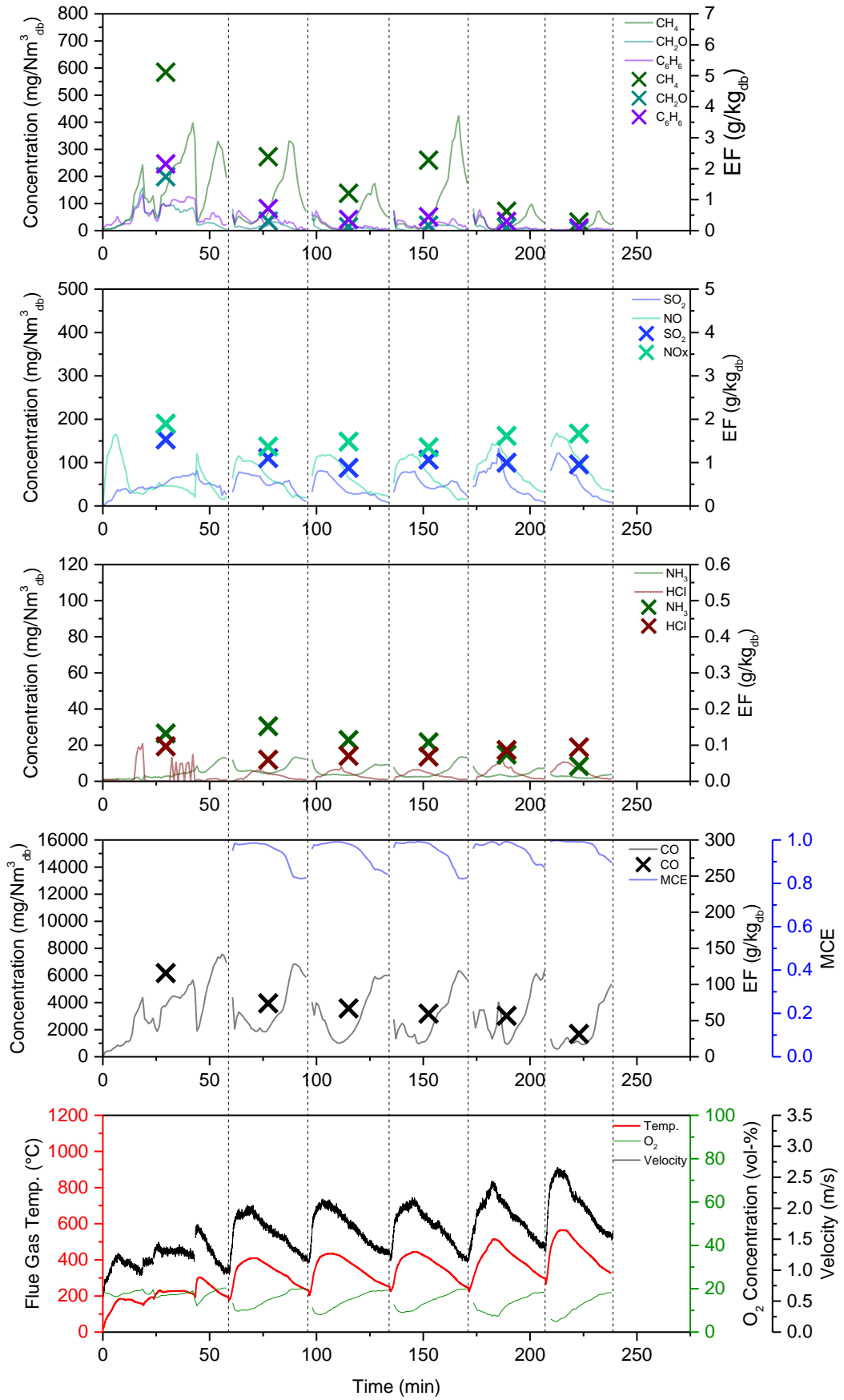
Figure 8.4a Biomass briquette S1: Gaseous pollutant emission profile
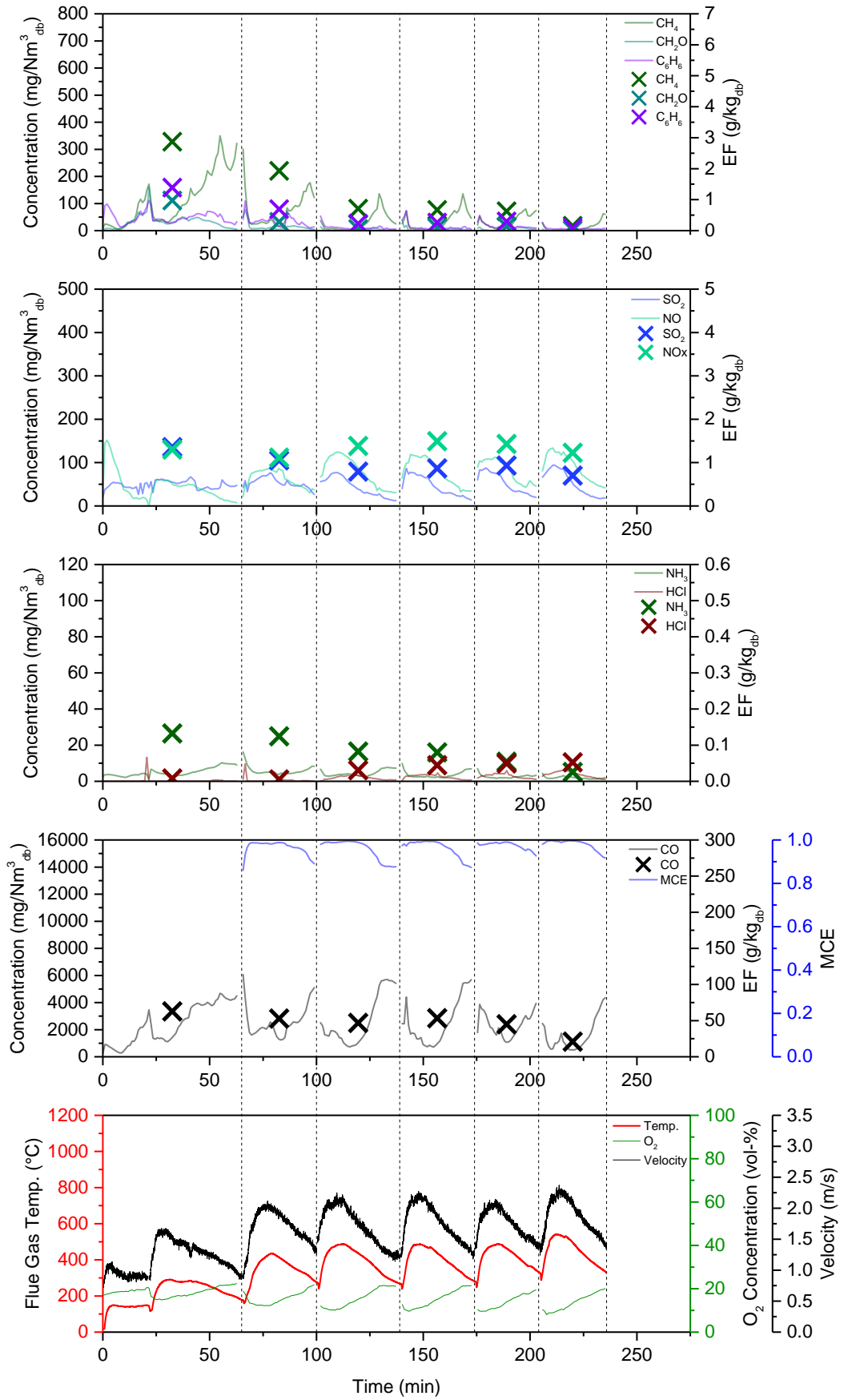
Figure 8.4b Biomass briquette S2: Gaseous pollutant emission profile
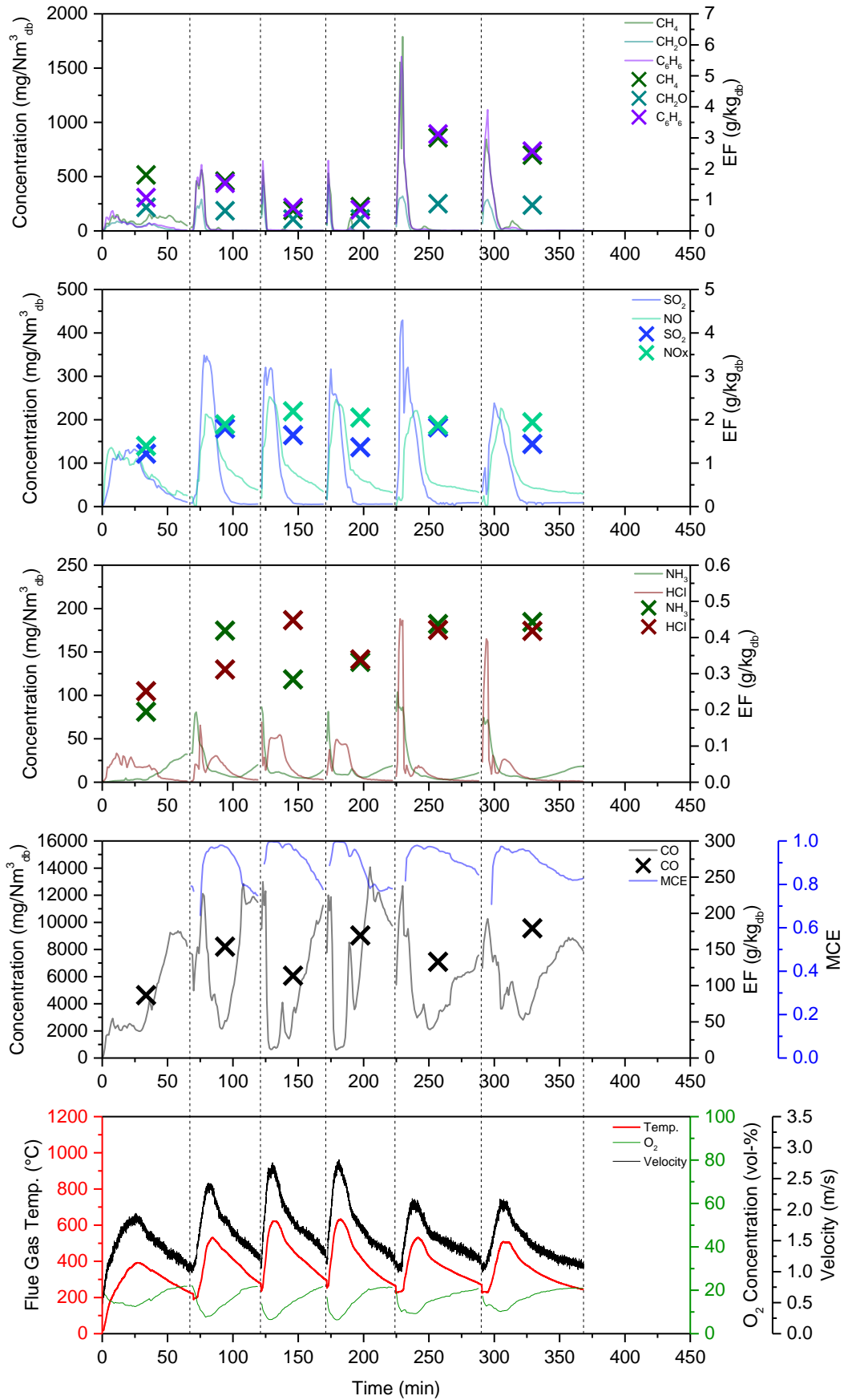
Figure 8.5a Torrefied briquette S1: Gaseous pollutant emission profile
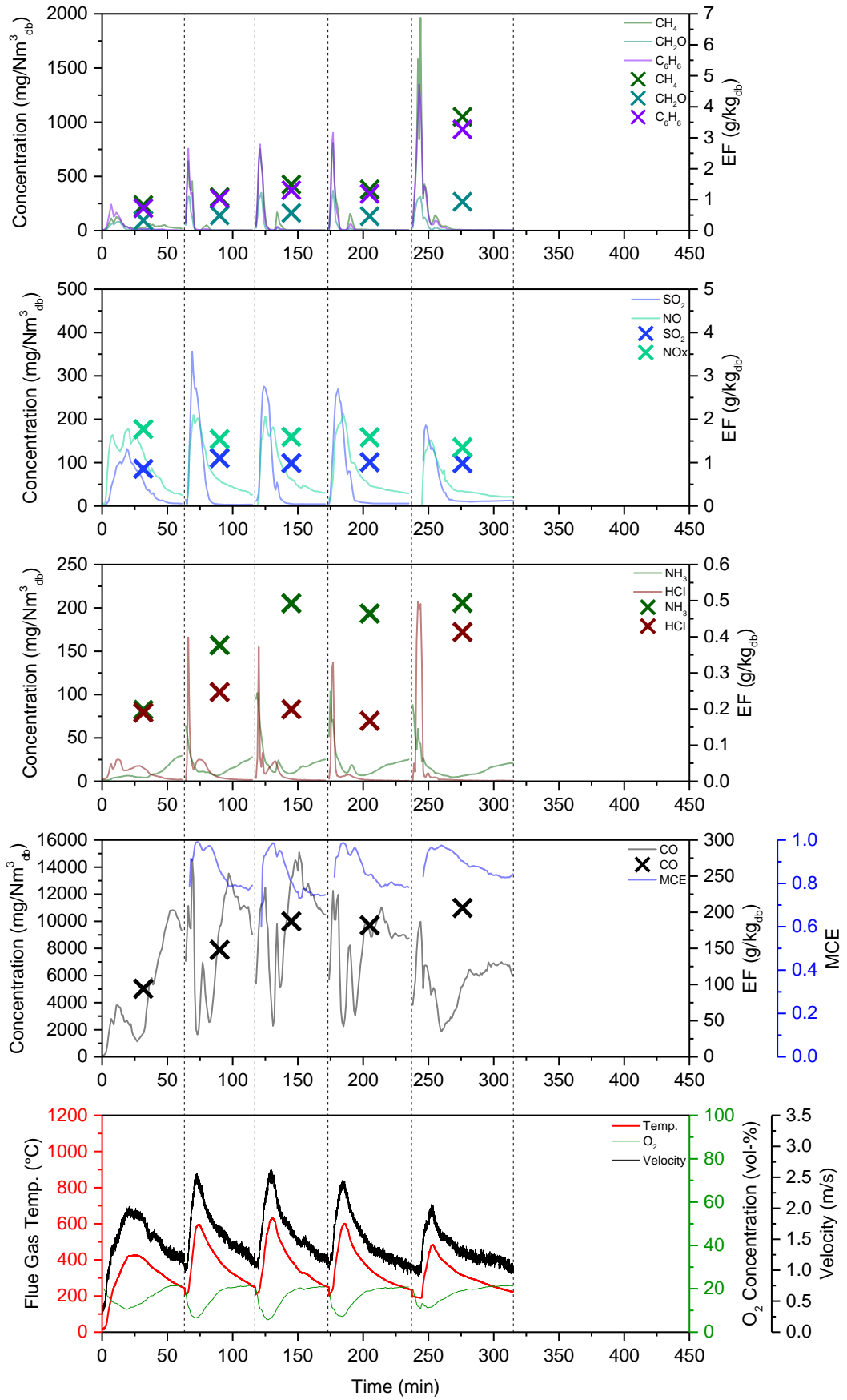
Figure 8.5b Torrefied briquette S2: Gaseous pollutant emission profile
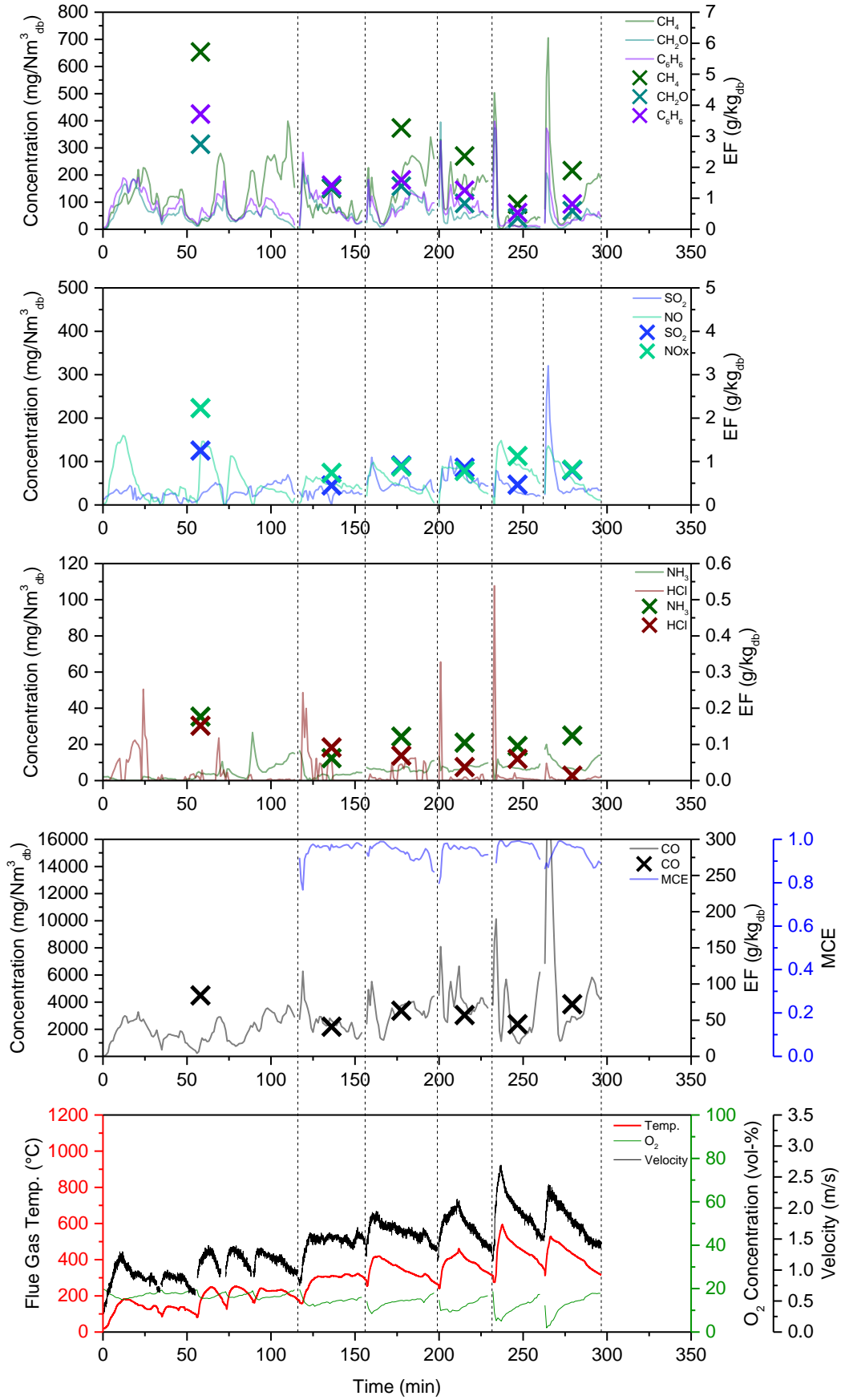
Figure 8.6a Fuelwood S1: Gaseous pollutant emission profile
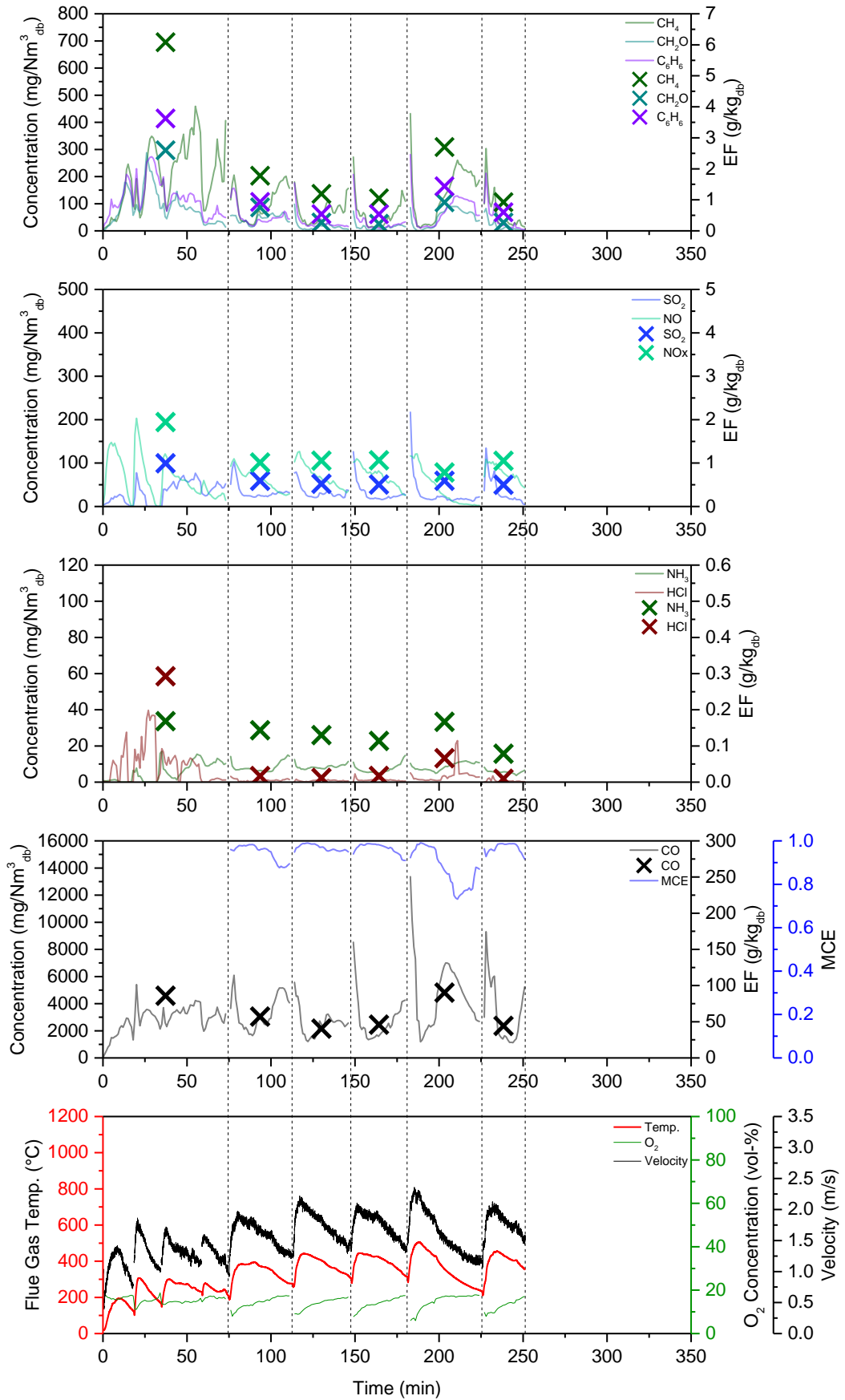
Figure 8.6b Fuelwood S2: Gaseous pollutant emission profile

8.4.4 Influence of Combustion Events upon Repeatability

Variance in pollutant concentrations are presented between test batches with significant differences in the burning processes for torrefied and raw biomass fuel materials. **Figure 8.7a** shows trends in concentrations during different combustion cycles. As mentioned previously, the combustion of torrefied briquettes resulted in high emission peaks following fuel reloading and higher concentrations generally presented during prolonged stove use. Such peaks arise from residual fuel material remaining on the grate during reloading. During this process remaining flames are extinguished when new fuel is added resulting in continued devolatilisation on the heated grate for a prolonged period without the presence of a flame. Thus, prolonged ignition, reduced temperatures, high bottom ash accumulation and inhibited O_2 availability all contribute to the significant smoking of the extinguished batch.

There were also instances of significantly higher emission concentrations during the combustion of fuelwood logs (**Figure 8.7b**). A general increase in the average combustion temperature is observed with each batch of fuel combusted within a testing series. Increased temperatures generally correspond with improved combustion conditions are lower concentrations of pollutants. However, an increase in emission is shown during a latter batch within the testing series in response to a reduction in temperature. The peak observed during the combustion of batch four was a result of a log falling from the heated grate onto a cooler section of the stove thereby increasing smoke and reducing combustion temperatures. As a result, higher emission factors are displayed during a period when optimum combustion conditions are expected. The impact of such processes can affect the standard deviation of emission factors about the mean value. This is an inherent consideration of biomass combustion whereby fuel properties and unplanned operation processes have an influence on stove performance and burn conditions.
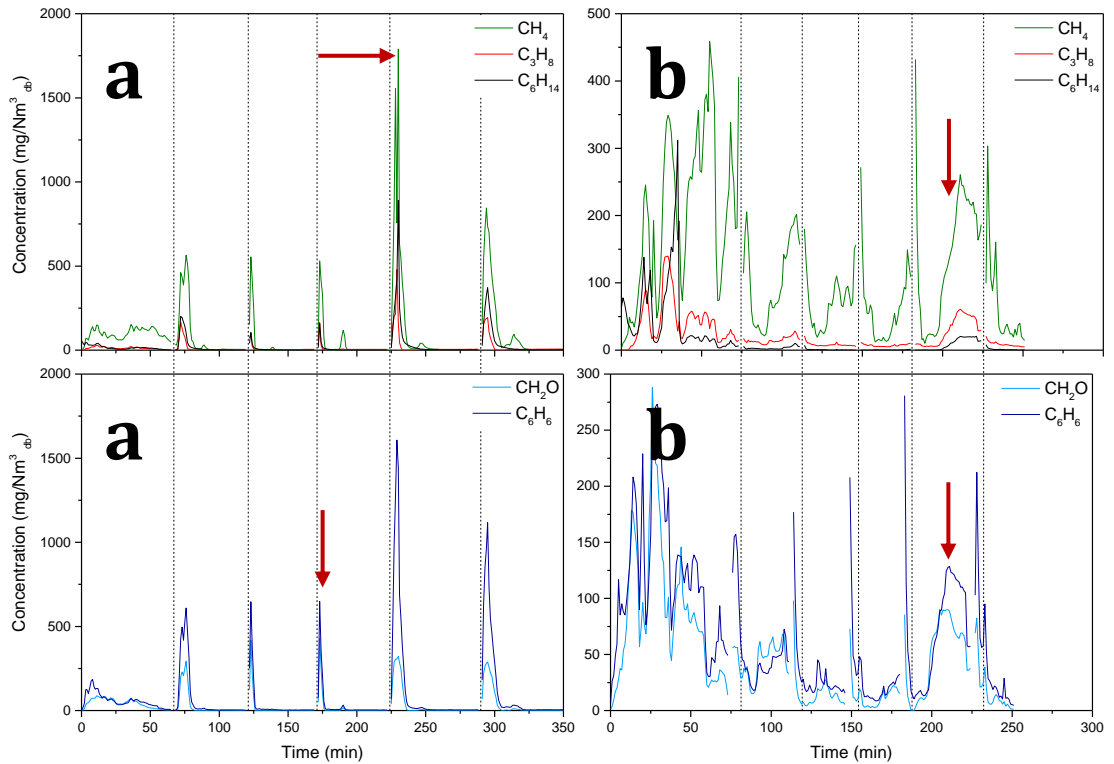
Figure 8.7 Variation in pollutant concentration during repeated combustion events for (a) torrefied briquette and (b) fuelwood test runs. → identifies periods where combustion events provide a significant control on emission factor quantification while --- indicates the point of fuel reloading.

The combustion of solid fuel within a domestic stove is a complex process incorporating several dynamic variables. **Table 8.7-8.9** provide a correlation matrix for each of the test fuels which examines statistically significant relationships between each of the combustion variables. The correlation coefficient is calculated from the method outlined in **Equation 8.3** where r is an indication of the linearity of the correlation measured between -1 and +1. The significance of the correlation is estimated from P and bootstrapping analysis as identified in Wang et al., (2014). The matrix is a cross comparison of each of the combustion variables against all other combustion parameters. Cells marked in dark green identify correlations that are significant to a P=0.01 (99%) confidence interval. Cells marked in a light green identify correlations that are significant to a P=0.05 (95%) confidence interval. Cells which are blank suggest a limited relationship which is not statistically significant.

Repeated combustion testing results in an increase in the flue gas temperature in response to a higher total fuel throughput. A significant correlation between flue gas temperature and O_2 concentration is reported for each of the test fuels. A negative relationship is presented whereby an increase in the recorded flue gas temperature results in a decrease in the O_2 concentration. A strong correlation is observed for

torrefied briquettes and fuelwood where the correlation was found to be significant at P=0.01 confidence. The negative correlation was shown to be significant at a P=0.05 confidence interval for biomass briquette combustion. A similar trend is observed between O_2 and fuel conversion rate where an increase in conversion corresponds with a reduction in O_2. However, the Pearson's correlation coefficients of -0.579, -0.716 and -0.436 for biomass briquettes, torrefied briquettes and fuelwood respectively indicate that this relationship is not statistically significant.

A significant positive correlation is also presented between temperature and flue gas velocity whereby increased temperatures generally correspond with an increase in rate, particularly for biomass briquette and torrefied briquette fuels where r is equal to +0.852 and +0.807 respectively. A weaker correlation is presented between these variables during fuelwood combustion which is likely due to significant variation in conversion rates as identified in **Figure 8.7**.

Flue gas temperature is an important indicator during the formation of gaseous emissions where an increase in temperature generally corresponds with a reduction in pollutant formation. For example, the correlation between combustion temperatures, HN_3, CH_4 and CO is shown to be statistically significant during biomass briquette combustion. In addition, variation in the recorded average batch temperature is shown to correlate with reductions in CH_4, CH_2O and C_6H_6 emissions during torrefied briquette combustion . This indicates that improved conditions within the combustion chamber results in more complete burnout of combustion products.

Given the complexity of fuelwood combustion, the flue gas temperature appears to maintain a limited control on certain pollutant formation indicating that alternative factors are controlling combustion conditions and emissions. Generally, a limited correlation between temperature, NOx and SO_2 is presented further indicating that these pollutants are derived from fuel nitrogen and sulphur only and not through alternative thermal mechanisms. Only a weak correlation between O_2 and pollutants is present for each of the fuels indicating that the significance of O_2 availability was not sufficient to effect combustion conditions. Correlations between each of the pollutants formed during the combustion experiments is likely due to the change in combustion conditions only and is not indicative of an interaction between different pollutants.

The statistical correlation for each of the examined combustion variables is shown in **Table 8.7** for biomass briquettes, **Table 8.8** for torrefied briquettes and **Table 8.9** for fuelwood. Statistical significance is presented as Pearson's Correlation Coefficient for combustion parameters and emission results. r is the coefficient with values measured in terms of strength of correlation between -1 and +1. P is the

probability value (or P-value) applied as a measure of statistical significance. If the P-value is <0.05 the null hypothesis may be rejected (assuming that the null hypothesis states that there is no correlation between two variables). Upper and Lower relate to the upper and lower Bootstrapping for a 95% confidence interval and are applied as a secondary measure of statistical significance.

Table 8.7 Biomass briquettes, correlation matrix for combustion variables.

		Burning Rate	O₂	Flue Temp.	Flue Velocity	CO	CH₄	CH₂O	C₆H₆	SO₂	NOx	NH₃
Burning Rate	r		-.579	.852**	.755*	-.833**	-.676*	-.491	-.578	-.281	.166	-.846**
	P		.080	.002	.012	.003	.032	.150	.080	.432	.647	.002
	Lower		-.813	.358	.493	-.953	-.867	-.903	-.911	-.867	-.639	-.935
	Upper		-.185	.992	.950	-.657	-.440	.279	-.060	.519	.733	-.735
O₂	r	-.579		-.661*	-.825**	.417	.477	.521	.547	-.075	-.674*	.595
	P	.080		.037	.003	.230	.164	.122	.102	.837	.033	.070
	Lower	-.813		-.888	-.927	-.347	-.111	-.007	.041	-.541	-.914	-.003
	Upper	-.185		-.203	-.525	.785	.861	.868	.897	.469	-.056	.917
Flue Temp.	r	.852**	-.661*		.875**	-.896**	-.886**	-.845**	-.905**	-.543	.414	-.979**
	P	.002	.037		.001	.000	.001	.002	.000	.105	.234	.000
	Lower	.358	-.888		.708	-.984	-.955	-.990	-.979	-.931	-.429	-.992
	Upper	.992	-.203		.974	-.647	-.810	-.185	-.750	.277	.886	-.976
Flue Velocity	r	.755*	-.825**	.875**		-.747*	-.722*	-.735*	-.743*	-.209	.568	-.806**
	P	.012	.003	.001		.013	.018	.015	.014	.562	.087	.005
	Lower	.493	-.927	.708		-.957	-.881	-.934	-.905	-.929	-.502	-.952
	Upper	.950	-.525	.974		-.399	-.608	-.308	-.554	.587	.958	-.689
CO	r	-.833**	.417	-.896**	-.747*		.749*	.711*	.765**	.617	-.008	.889**
	P	.003	.230	.000	.013		.013	.021	.010	.057	.983	.001
	Lower	-.953	-.347	-.984	-.957		.375	.249	-.002	.016	-.723	.684
	Upper	-.657	.785	-.647	-.399		.941	.919	.974	.888	.712	.975
CH₄	r	-.676*	.477	-.886**	-.722*	.749*		.908**	.879**	.741*	-.477	.916**
	P	.032	.164	.001	.018	.013		.000	.001	.014	.164	.000
	Lower	-.867	-.111	-.955	-.881	.375		.782	.720	.414	-.853	.804
	Upper	-.440	.861	-.810	-.608	.941		.975	.989	.949	.139	.980
CH₂O	r	-.491	.521	-.845**	-.735*	.711*	.908**		.965**	.722*	-.548	.852**
	P	.150	.122	.002	.015	.021	.000		.000	.018	.101	.002
	Lower	-.903	-.007	-.990	-.934	.249	.782		.872	.370	-.971	.564
	Upper	.279	.868	-.185	-.308	.919	.975		.993	.955	.371	.963
C₆H₆	r	-.578	.547	-.905**	-.743*	.765**	.879**	.965**		.673*	-.499	.909**
	P	.080	.102	.000	.014	.010	.001	.000		.033	.142	.000
	Lower	-.911	.041	-.979	-.905	-.002	.720	.872		.295	-.939	.747
	Upper	-.060	.897	-.750	-.554	.974	.989	.993		.930	.579	.977
SO₂	r	-.281	-.075	-.543	-.209	.617	.741*	.722*	.673*		.050	.622
	P	.432	.837	.105	.562	.057	.014	.018	.033		.891	.055
	Lower	-.867	-.541	-.931	-.929	.016	.414	.370	.295		-.623	.168
	Upper	.519	.469	.277	.587	.888	.949	.955	.930		.850	.880
NOx	r	.166	-.674*	.414	.568	-.008	-.477	-.548	-.499	.050		-.357
	P	.647	.033	.234	.087	.983	.164	.101	.142	.891		.311
	Lower	-.639	-.914	-.429	-.502	-.723	-.853	-.971	-.939	-.623		-.848
	Upper	.733	-.056	.886	.958	.712	.139	.371	.579	.850		.352
NH₃	r	-.846**	.595	-.979**	-.806**	.889**	.916**	.852**	.909**	.622	-.357	
	P	.002	.070	.000	.005	.001	.000	.002	.000	.055	.311	
	Lower	-.935	-.003	-.992	-.952	.684	.804	.564	.747	.168	-.848	
	Upper	-.735	.917	-.976	-.689	.975	.980	.963	.977	.880	.352	

Correlation is significant at the 95% level (2-tailed)   *

Correlation is significant at the 99% level (2-tailed)   **

Table 8.8 Torrefied briquettes, correlation matrix for combustion variables.

		Burning Rate	O_2	Flue Temp.	Flue Velocity	CO	CH_4	CH_2O	C_6H_6	SO_2	NOx	NH_3
Burning Rate	r		-.716*	.807**	.867**	-.534	-.867**	-.803**	-.856**	.180	.338	-.545
	P		.030	.009	.002	.139	.002	.009	.003	.643	.374	.129
	Lower		-.947	.303	.522	-.844	-.957	-.952	-.963	-.593	-.506	-.841
	Upper		.027	.966	.977	-.021	-.620	-.375	-.639	.758	.836	-.210
O_2	r	-.716*		-.902**	-.870**	.883**	.624	.546	.534	-.658	-.779*	.737*
	P	.030		.001	.002	.002	.072	.128	.138	.054	.013	.023
	Lower	-.947		-.983	-.981	.311	-.380	-.469	-.405	-.817	-.964	-.016
	Upper	.027		-.646	-.589	.991	.936	.914	.922	-.492	-.346	.980
Flue Temp.	r	.807**	-.902**		.975**	-.707*	-.844**	-.802**	-.791*	.379	.726*	-.848**
	P	.009	.001		.000	.033	.004	.009	.011	.314	.027	.004
	Lower	.303	-.983		.870	-.935	-.975	-.977	-.972	-.353	-.328	-.974
	Upper	.966	-.646		.999	-.206	-.547	-.392	-.442	.949	.967	-.621
Flue Velocity	r	.867**	-.870**	.975**		-.658	-.852**	-.792*	-.813**	.398	.696*	-.823**
	P	.002	.002	.000		.054	.004	.011	.008	.289	.037	.006
	Lower	.522	-.981	.870		-.915	-.981	-.978	-.968	-.338	-.259	-.976
	Upper	.977	-.589	.999		-.158	-.550	-.307	-.497	.933	.969	-.603
CO	r	-.534	.883**	-.707*	-.658		.418	.334	.302	-.722*	-.674*	.729*
	P	.139	.002	.033	.054		.263	.379	.429	.028	.046	.026
	Lower	-.844	.311	-.935	-.915		-.625	-.612	-.659	-.908	-.924	.049
	Upper	-.021	.991	-.206	-.158		.919	.885	.901	-.438	-.117	.987
CH_4	r	-.867**	.624	-.844**	-.852**	.418		.970**	.986**	-.015	-.449	.684*
	P	.002	.072	.004	.004	.263		.000	.000	.970	.225	.042
	Lower	-.957	-.380	-.975	-.981	-.625		.866	.	-.608	-.878	-.286
	Upper	-.620	.936	-.547	-.550	.919		.998	.	.647	.468	.988
CH_2O	r	-.803**	.546	-.802**	-.792*	.334	.970**		.983**	.124	-.340	.661
	P	.009	.128	.009	.011	.379	.000		.000	.751	.371	.052
	Lower	-.952	-.469	-.977	-.978	-.612	.866		.903	-.516	-.826	-.048
	Upper	-.375	.914	-.392	-.307	.885	.998		.999	.690	.457	.968
C_6H_6	r	-.856**	.534	-.791*	-.813**	.302	.986**	.983**		.109	-.334	.622
	P	.003	.138	.011	.008	.429	.000	.000		.780	.380	.074
	Lower	-.963	-.405	-.972	-.968	-.659	.	.903		-.531	-.834	-.214
	Upper	-.639	.922	-.442	-.497	.901	.	.999		.678	.431	.969
SO_2	r	.180	-.658	.379	.398	-.722*	-.015	.124	.109		.771*	-.430
	P	.643	.054	.314	.289	.028	.970	.751	.780		.015	.249
	Lower	-.593	-.817	-.353	-.338	-.908	-.608	-.516	-.531		-.366	-.799
	Upper	.758	-.492	.949	.933	-.438	.647	.690	.678		.989	-.056
NOx	r	.338	-.779*	.726*	.696*	-.674*	-.449	-.340	-.334	.771*		-.748*
	P	.374	.013	.027	.037	.046	.225	.371	.380	.015		.020
	Lower	-.506	-.964	-.328	-.259	-.924	-.878	-.826	-.834	-.366		-.923
	Upper	.836	-.346	.967	.969	-.117	.468	.457	.431	.989		-.351
NH_3	r	-.545	.737*	-.848**	-.823**	.729*	.684*	.661	.622	-.430	-.748*	
	P	.129	.023	.004	.006	.026	.042	.052	.074	.249	.020	
	Lower	-.841	-.016	-.974	-.976	.049	-.286	-.048	-.214	-.799	-.923	
	Upper	-.210	.980	-.621	-.603	.987	.988	.968	.969	-.056	-.351	

Correlation is significant at the 95% level (2-tailed)   *

Correlation is significant at the 99% level (2-tailed)   **

Table 8.9 Fuelwood, correlation matrix for combustion variables.

		Burning Rate	O_2	Flue Temp.	Flue Velocity	CO	CH_4	CH_2O	C_6H_6	SO_2	NOx	NH_3
Burning Rate	r		-.436	.207	.270	-.058	-.089	-.034	-.074	.070	-.034	-.154
	P		.208	.566	.450	.873	.806	.926	.839	.847	.927	.671
	Lower		-.910	-.566	-.497	-.775	-.897	-.918	-.951	-.712	-.804	-.699
	Upper		-.233	.977	.990	.355	.381	.465	.431	.526	.941	.131
O_2	r	-.436		-.810**	-.846**	.325	.413	.514	.542	-.057	-.402	.402
	P	.208		.004	.002	.359	.236	.129	.106	.875	.249	.250
	Lower	-.910		-.923	-.942	-.482	-.282	-.343	-.549	-.730	-.843	-.459
	Upper	-.233		-.638	-.678	.770	.805	.878	.926	.482	.383	.950
Flue Temp.	r	.207	-.810**		.976**	-.013	-.352	-.757*	-.700*	-.010	.545	.111
	P	.566	.004		.000	.972	.318	.011	.024	.979	.103	.759
	Lower	-.566	-.923		.881	-.657	-.813	-.900	-.849	-.692	-.104	-.690
	Upper	.977	-.638		.997	.538	.180	-.480	-.506	.620	.878	.668
Flue Velocity	r	.270	-.846**	.976**		-.187	-.436	-.777**	-.750*	-.082	.656*	.015
	P	.450	.002	.000		.606	.208	.008	.013	.822	.039	.967
	Lower	-.497	-.942	.881		-.766	-.848	-.901	-.858	-.675	.123	-.763
	Upper	.990	-.678	.997		.374	.023	-.644	-.654	.555	.916	.625
CO	r	-.058	.325	-.013	-.187		.745*	.351	.523	.502	-.545	.722*
	P	.873	.359	.972	.606		.013	.320	.121	.139	.103	.018
	Lower	-.775	-.482	-.657	-.766		.461	-.278	-.124	-.011	-.953	.073
	Upper	.355	.770	.538	.374		.980	.959	.958	.981	-.046	.967
CH_4	r	-.089	.413	-.352	-.436	.745*		.714*	.827**	.813**	-.622	.494
	P	.806	.236	.318	.208	.013		.020	.003	.004	.055	.146
	Lower	-.897	-.282	-.813	-.848	.461		.237	.456	.499	-.935	-.059
	Upper	.381	.805	.180	.023	.980		.983	.992	.965	-.302	.913
CH_2O	r	-.034	.514	-.757*	-.777**	.351	.714*		.954**	.450	-.759*	-.039
	P	.926	.129	.011	.008	.320	.020		.000	.192	.011	.914
	Lower	-.918	-.343	-.900	-.901	-.278	.237		.886	-.241	-.943	-.738
	Upper	.465	.878	-.480	-.644	.959	.983		.995	.916	-.503	.808
C_6H_6	r	-.074	.542	-.700*	-.750*	.523	.827**	.954**		.518	-.817**	.112
	P	.839	.106	.024	.013	.121	.003	.000		.125	.004	.758
	Lower	-.951	-.549	-.849	-.858	-.124	.456	.886		-.062	-.977	-.681
	Upper	.431	.926	-.506	-.654	.958	.992	.995		.930	-.597	.850
SO_2	r	.070	-.057	-.010	-.082	.502	.813**	.450	.518		-.470	.235
	P	.847	.875	.979	.822	.139	.004	.192	.125		.171	.513
	Lower	-.712	-.730	-.692	-.675	-.011	.499	-.241	-.062		-.953	-.456
	Upper	.526	.482	.620	.555	.981	.965	.916	.930		.076	.917
NOx	r	-.034	-.402	.545	.656*	-.545	-.622	-.759*	-.817**	-.470		-.003
	P	.927	.249	.103	.039	.103	.055	.011	.004	.171		.994
	Lower	-.804	-.843	-.104	.123	-.953	-.935	-.943	-.977	-.953		-.665
	Upper	.941	.383	.878	.916	-.046	-.302	-.503	-.597	.076		.590
NH_3	r	-.154	.402	.111	.015	.722*	.494	-.039	.112	.235	-.003	
	P	.671	.250	.759	.967	.018	.146	.914	.758	.513	.994	
	Lower	-.699	-.459	-.690	-.763	.073	-.059	-.738	-.681	-.456	-.665	
	Upper	.131	.950	.668	.625	.967	.913	.808	.850	.917	.590	

Correlation is significant at the 95% level (2-tailed)　*

Correlation is significant at the 99% level (2-tailed)　**

8.4.5 Impact of Repeatability upon Results Confidence

Statistical variance in the emission of gaseous species is shown in **Figure 8.8-8.15** for each of the three test fuel materials. The confidence interval plot is formulated as a function of the standard deviation for the sampled population. Unlike standard error, the standard deviation will often not reduce with an increase in population size and is instead dependent upon the emission factor values within the sample (Wang et al., 2014).

The quantified emission of each pollutant species is generally shown to reduce with an increase in combustion temperature and this in turn is dependent upon total fuel mass throughput. Flue gas temperature increases with an increase in the mass throughput of fuelwood and biomass briquettes. As previously discussed, some oscillation is temperature is identified during the combustion of torrefied briquettes. Box plot series diagrams describe the effect of repeated batch testing on the distribution of emission factor results within an inventory sample.

Width of confidence interval about the mean (*CI*) plots are applied as a measure of identifying the ideal number of batches required to determine the most accurate estimation of pollutant emission factor. Confidence curves representing confidence level (*CL*)=90% (*P*=0.1), *CL*=95% (*P*=0.05) and *CL*=99% (*P*=0.01) are applied for each of the pollutant species. As previously discussed, such curves are dependent upon sample values and the deviation of selected populations about the emission factor mean. The width of the confidence interval (*CI*) is affected by both the *CL* parameter and the sampling error. The sampling error is affected by both the sample size (*n*) and the variation in sample values. In response, the width of the *CI* generally (*i*) decreases with an increase in *n*, (*ii*) decreases when the sample standard deviation is reduced and (*iii*) increases with an increase in the *CL* (Giannoulis, 2019). A CL of 95% is generally applied during statistical evaluation and will be used as a method of comparison in this work (du Prel et al., 2009).

8.4.5.1 Biomass Briquettes

Results show a smaller width of the confidence interval with an increase in the CL. The *CI* is generally shown to reduce with an increase in the number of repeated test batches; this is evident at all CL parameters. The CI following three repeated batches is 53.4 g/kg$_{fuel}$, 3.0 g/kg$_{fuel}$, 1.0 g/kg$_{fuel}$, 0.6 g/kg$_{fuel}$, 0.1 g/kg$_{fuel}$, 1.0 g/kg$_{fuel}$, 0.5 g/kg$_{fuel}$ and 0.2 g/kg$_{fuel}$ for CO, CH_4, NOx, SO_2, NH_3, C_6H_6, CH_2O and HCl respectively where CI=95%. The minimum CI for CH_4 (CI=1.18 g/kg$_{fuel}$), CH_2O (CI=0.15 g/kg$_{fuel}$) and HCl (CI=0.04 g/kg$_{fuel}$) was observed following 10 repeat batches. The minimum CI for C_6H_6 was observed following 2 repeat batches in

response to the small standard deviation in emission factor values (σ=0.015 g/kg$_{fuel}$). The minimum *CI* values for other gaseous species where 16.4 g/kg$_{fuel}$ for CO following 8 repeats, 0.16 g/kg$_{fuel}$ for SO_2 following 9 repeats and 0.05 g/kg$_{fuel}$ for NH_3 following 7 repeats. An increase in the CI of CO was observed during TB9-10 and thereby affecting the CI values of the remaining series. This occurs in response to reduced emission factor values during high temperature combustion. The average temperature observed between TB1-8 was 373±30°C with a corresponding average emission of 57±10 g/kg$_{fuel}$. The combustion temperature continued to increase during latter repeats. The average temperature observed during TB9-10 was 448±6°C with a corresponding average emission of 26±8 g/kg$_{fuel}$. The increased temperature results in improved combustion conditions thereby inhibiting CO formation; low emission values are thereby presented during the latter repeats as shown in **Figure 8.8a** which correspond with an increase in the stand deviation. A similar process is displayed for SO_2 and NH_3. The increase in CI is therefore attributed to improved combustion conditions during prolonged stove operation. A minimum uncertainty of ±0.265 g/kg$_{fuel}$ is presented after only two test batches when quantifying C_6H_6 emission during biomass briquette combustion. The result is in response to the initial two test batches producing very similar emission factor results thereby inferring a very small standard deviation. A subsequent increase in the uncertainty is presented in **Figure 8.13a** following the addition of further test batches. As such, the standard deviation may increase significantly with a notably changed combustion conditions in response to prolonged stove operation or unpredictable combustion events.

8.4.5.2 Torrefied Briquettes

Similar to the results previously discussed, a lower CI is displayed with an increase in the CL; additionally, the CI is generally shown to reduce with an increase in the number of repeated tests undertaken. The CI following three repeated batches is 107.6 g/kg$_{fuel}$, 2.3 g/kg$_{fuel}$, 1.7 g/kg$_{fuel}$, 1.8 g/kg$_{fuel}$, 0.3 g/kg$_{fuel}$, 2.0 g/kg$_{fuel}$, 0.7 g/kg$_{fuel}$ and 0.5 g/kg$_{fuel}$ for CO, CH_4, NOx, SO_2, NH_3, C_6H_6, CH_2O and HCl respectively where CI=95%. The minimum confidence interval is generally found to occur within the largest sample size. The minimum CI for CO (CI=44.6 g/kg$_{fuel}$), NOx (CI=0.45 g/kg$_{fuel}$), SO_2 (CI=0.53), NH_3 (CI=0.11) and HCl (CI=0.16 g/kg$_{fuel}$) was observed following 9 repeat batches. The minimum CI for CH_4 and was observed following 6 repeat batches while the minimum CI for C_6H_6 was observed following 7 batches. The increase in the width of the CI for these organic species occurs in response to an increase in the standard deviation caused by significantly higher emission factor values during the TB7-9. In contrast to more efficiently burning biomass briquettes,

the increase in CI is attributed to inhibited combustion conditions during prolonged stove operation.

8.4.5.3 Fuelwood

The CI following three repeated batches is 56.6 g/kg$_{fuel}$, 5.1 g/kg$_{fuel}$, 0.7 g/kg$_{fuel}$, 1.2 g/kg$_{fuel}$, 0.2 g/kg$_{fuel}$, 1.7 g/kg$_{fuel}$, 1.8 g/kg$_{fuel}$ and 0.2 g/kg$_{fuel}$ for CO, CH$_4$, NOx, SO$_2$, NH$_3$, C$_6$H$_6$, CH$_2$O and HCl respectively where CI=95%. The minimum confidence interval is generally found to occur within the largest sample size. The minimum CI for CH$_4$ (CI=1.18 g/kg$_{fuel}$), NOx (CI=0.22 g/kg$_{fuel}$), SO$_2$ (CI=0.24 g/kg$_{fuel}$), NH$_3$ (CI=0.04 g/kg$_{fuel}$), C$_6$H$_6$ (CI=0.61 g/kg$_{fuel}$), CH$_2$O (CI=0.62 g/kg$_{fuel}$) and HCl (CI=0.04 g/kg$_{fuel}$) was observed following 10 repeat batches. The minimum CI for CO was observed following 7 repeat batches due to the presence of higher emissions during TB8 . The presence of this outlying emission factor values increases the standard deviation of the larger inventory thereby increasing the CI.
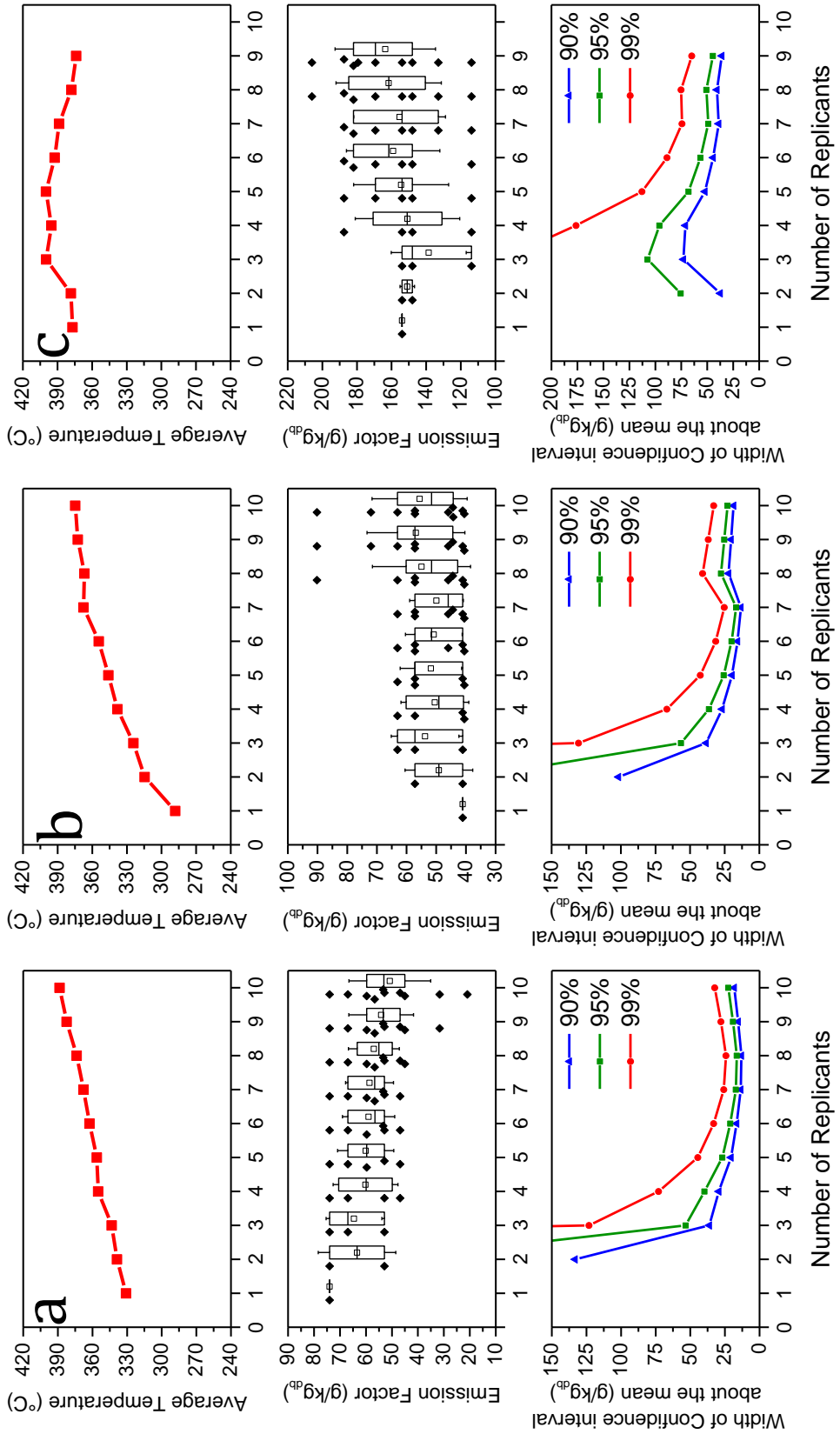
Figure 8.8 Variation in CO emission (g/kg$_{fuel}$) dependent upon number of test repeats (*n*) and combustion temperature (°C). Whisker intervals present values one standard deviation from the numerical mean. (a) Biomass briquettes, (b) Fuelwood and (c) Torrefied briquettes.
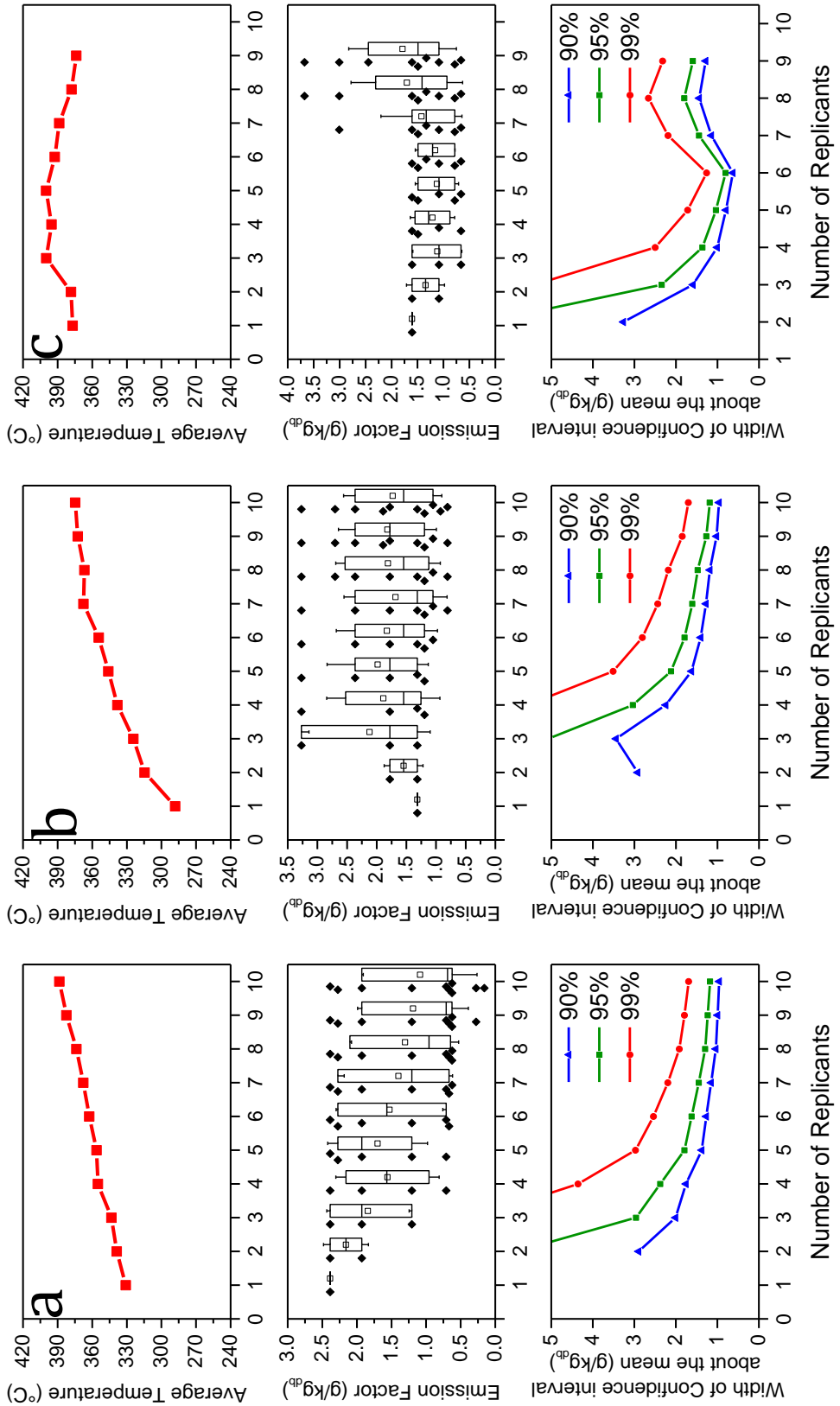
Figure 8.9 Variation in CH₄ emission (g/kg_fuel) dependent upon number of test repeats (*n*) and combustion temperature (°C). Whisker intervals present values one standard deviation from the numerical mean. (a) Biomass briquettes, (b) Fuelwood and (c) Torrefied briquettes.
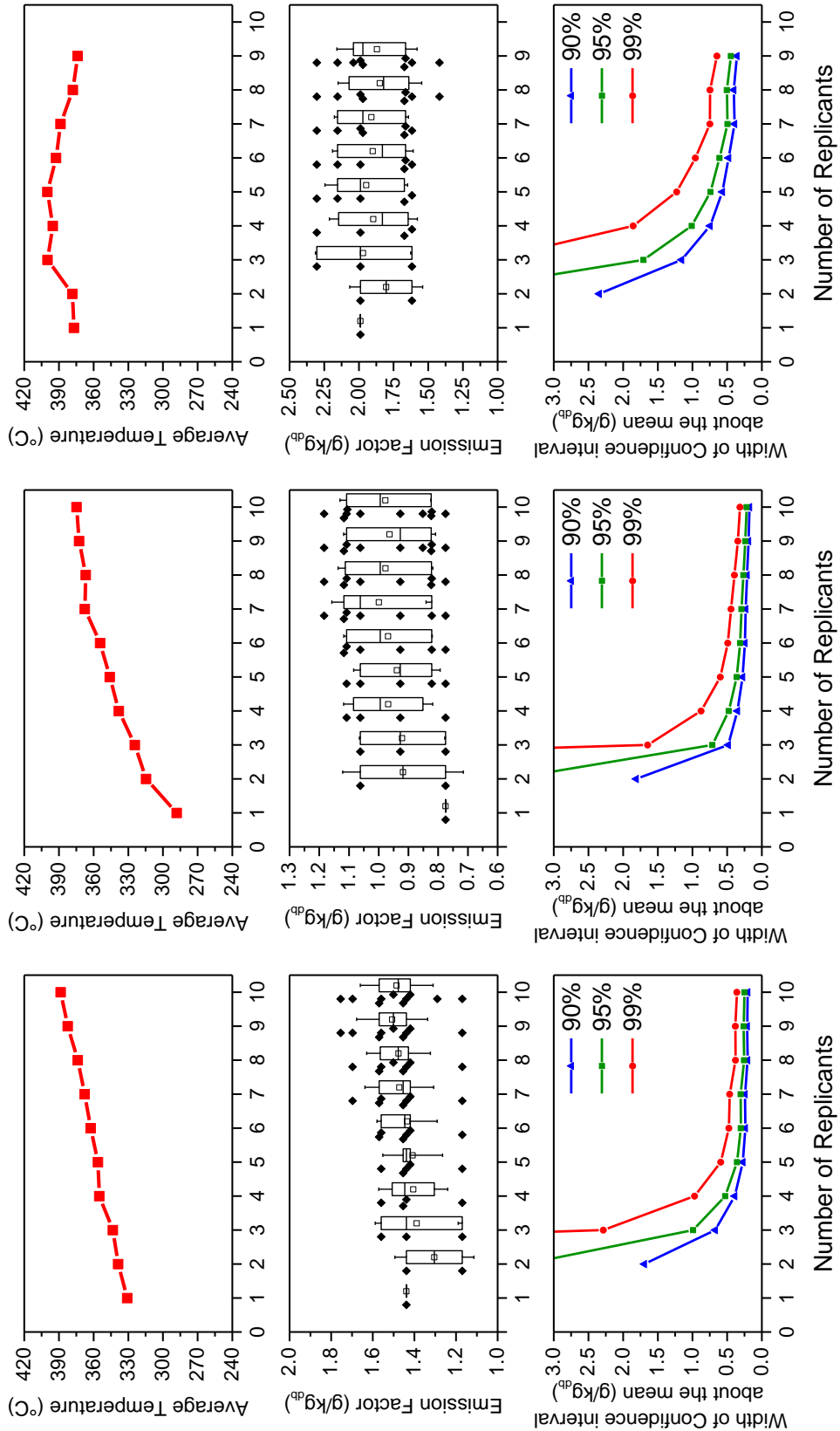
Figure 8.10 Variation in NOx emission (g/kg_fuel) dependent upon number of test repeats (*n*) and combustion temperature (°C). Whisker intervals present values one standard deviation from the numerical mean. (a) Biomass briquettes, (b) Fuelwood and (c) Torrefied briquettes.
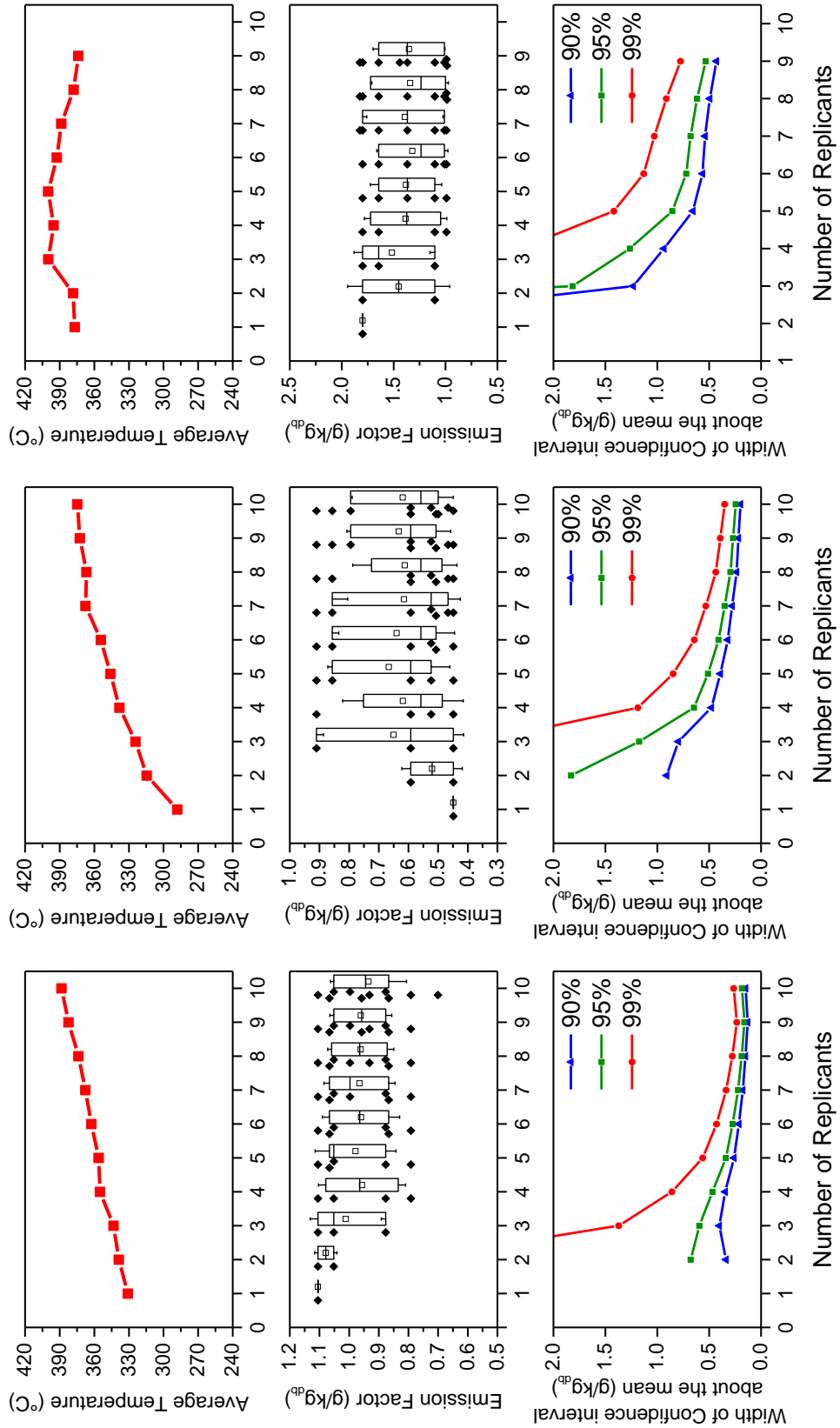
Figure 8.11 Variation in SO₂ emission (g/kg$_{fuel}$) dependent upon number of test repeats (*n*) and combustion temperature (°C). Whisker intervals present values one standard deviation from the numerical mean. (a) Biomass briquettes, (b) Fuelwood and (c) Torrefied briquettes.
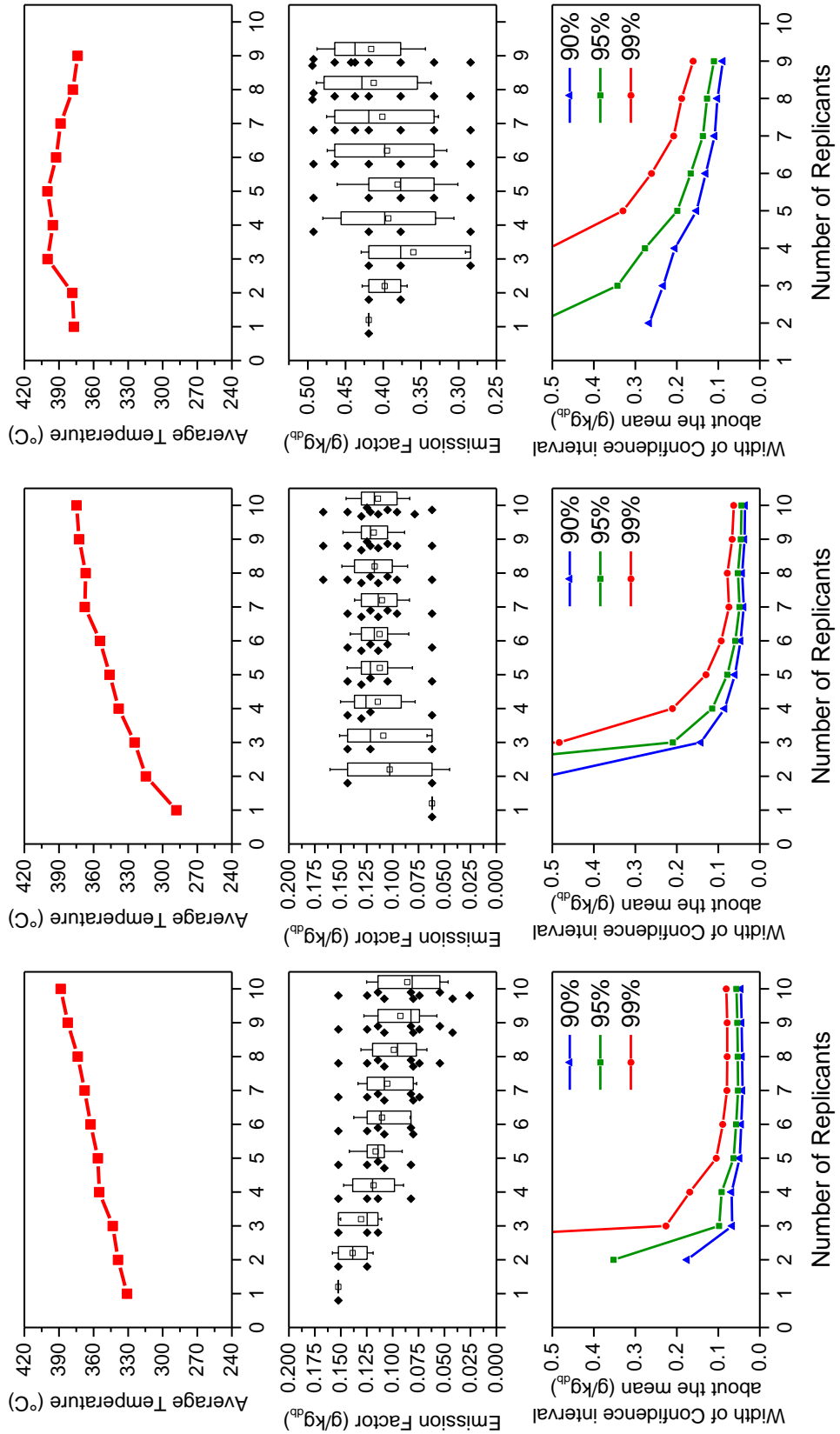
Figure 8.12 Variation in NH₃ emission (g/kg_fuel) dependent upon number of test repeats (*n*) and combustion temperature (°C). Whisker intervals present values one standard deviation from the numerical mean. (a) Biomass briquettes, (b) Fuelwood and (c) Torrefied briquettes.
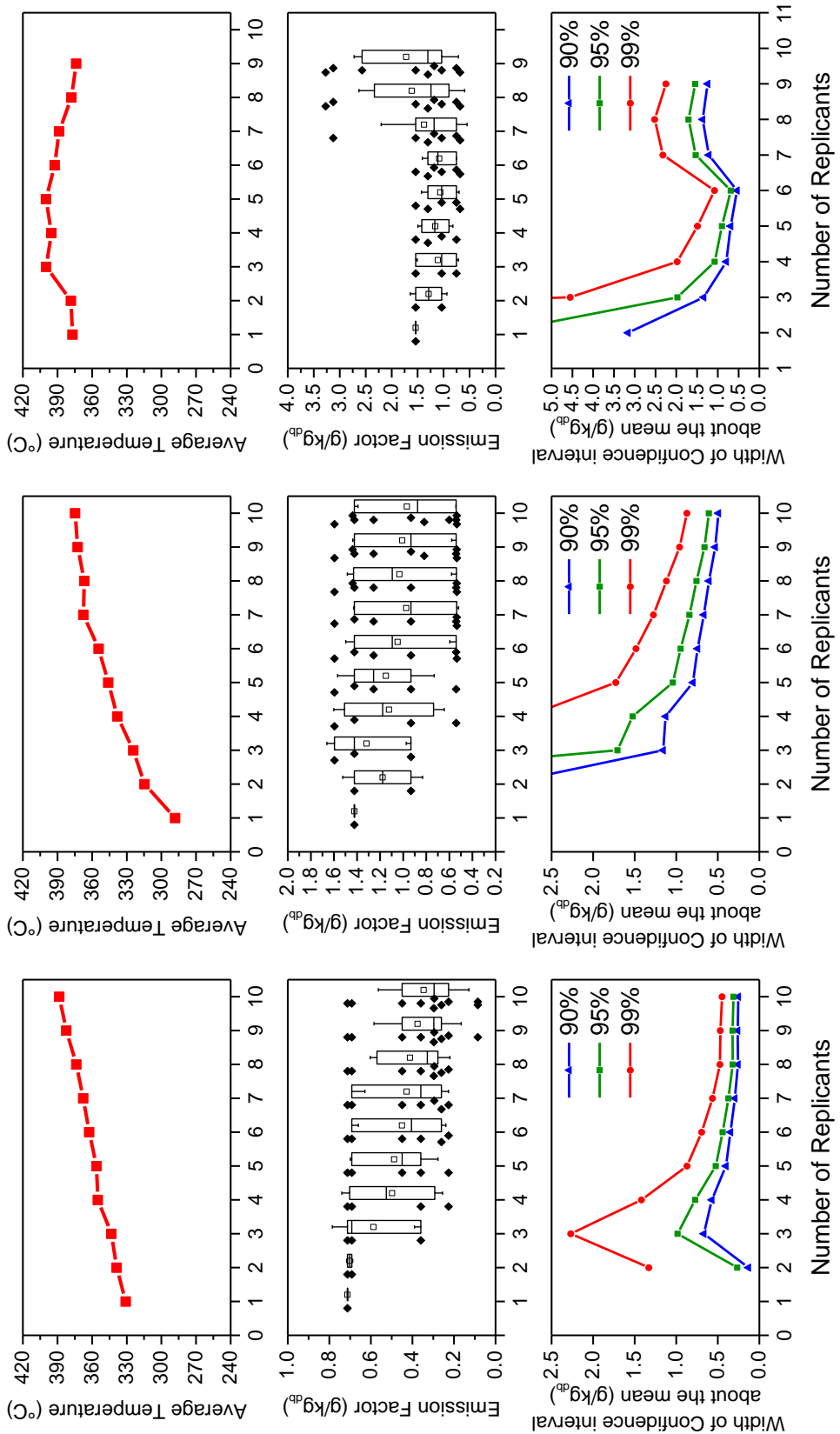
Figure 8.13 Variation in C_6H_6 emission (g/kg$_{fuel}$) dependent upon number of test repeats (*n*) and combustion temperature (°C). Whisker intervals present values one standard deviation from the numerical mean. (a) Biomass briquettes, (b) Fuelwood and (c) Torrefied briquettes.
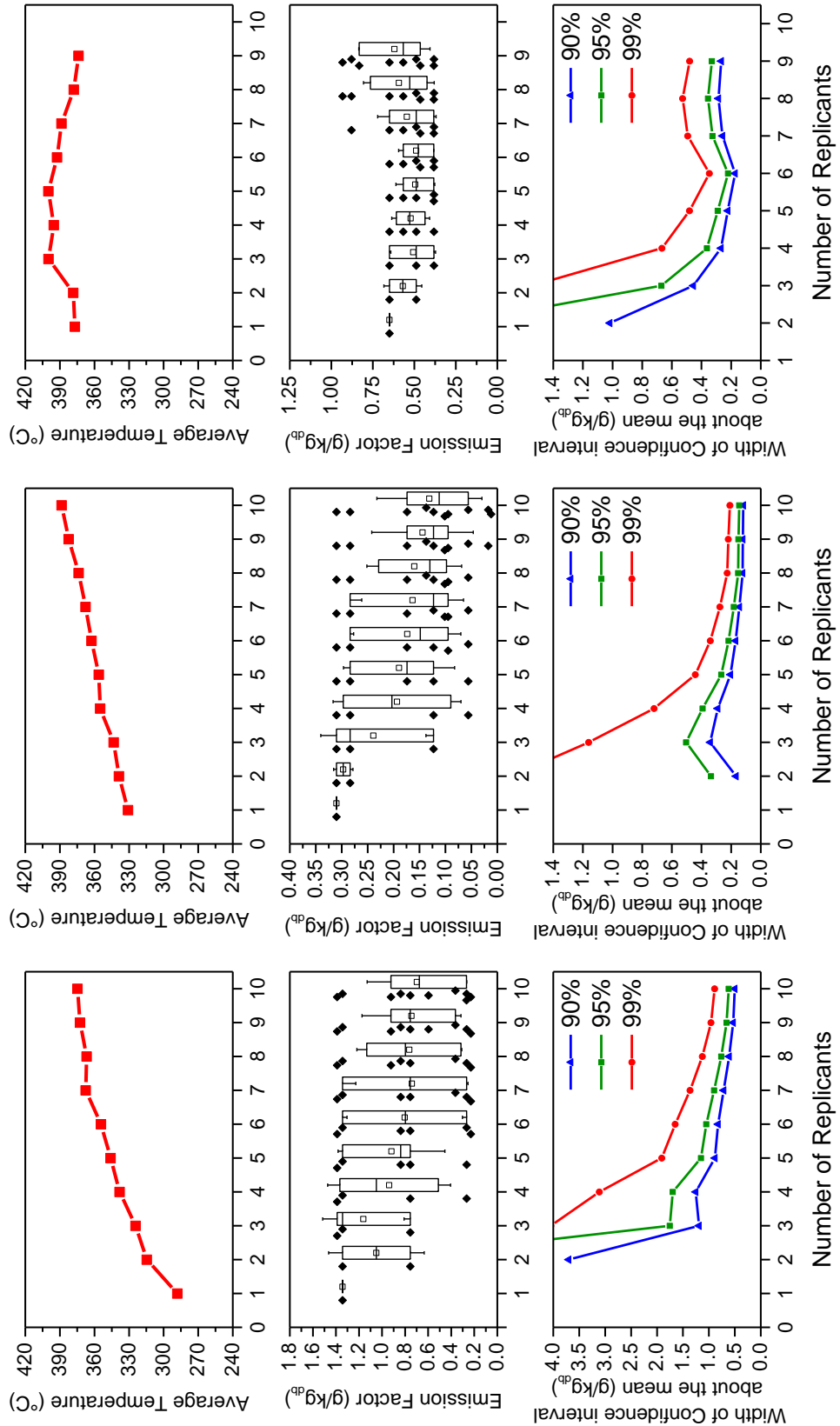
Figure 8.14 Variation in CH$_2$O emission (g/kg$_{fuel}$) dependent upon number of test repeats (*n*) and combustion temperature (°C). Whisker intervals present values one standard deviation from the numerical mean. (a) Biomass briquettes, (b) Fuelwood and (c) Torrefied briquettes.
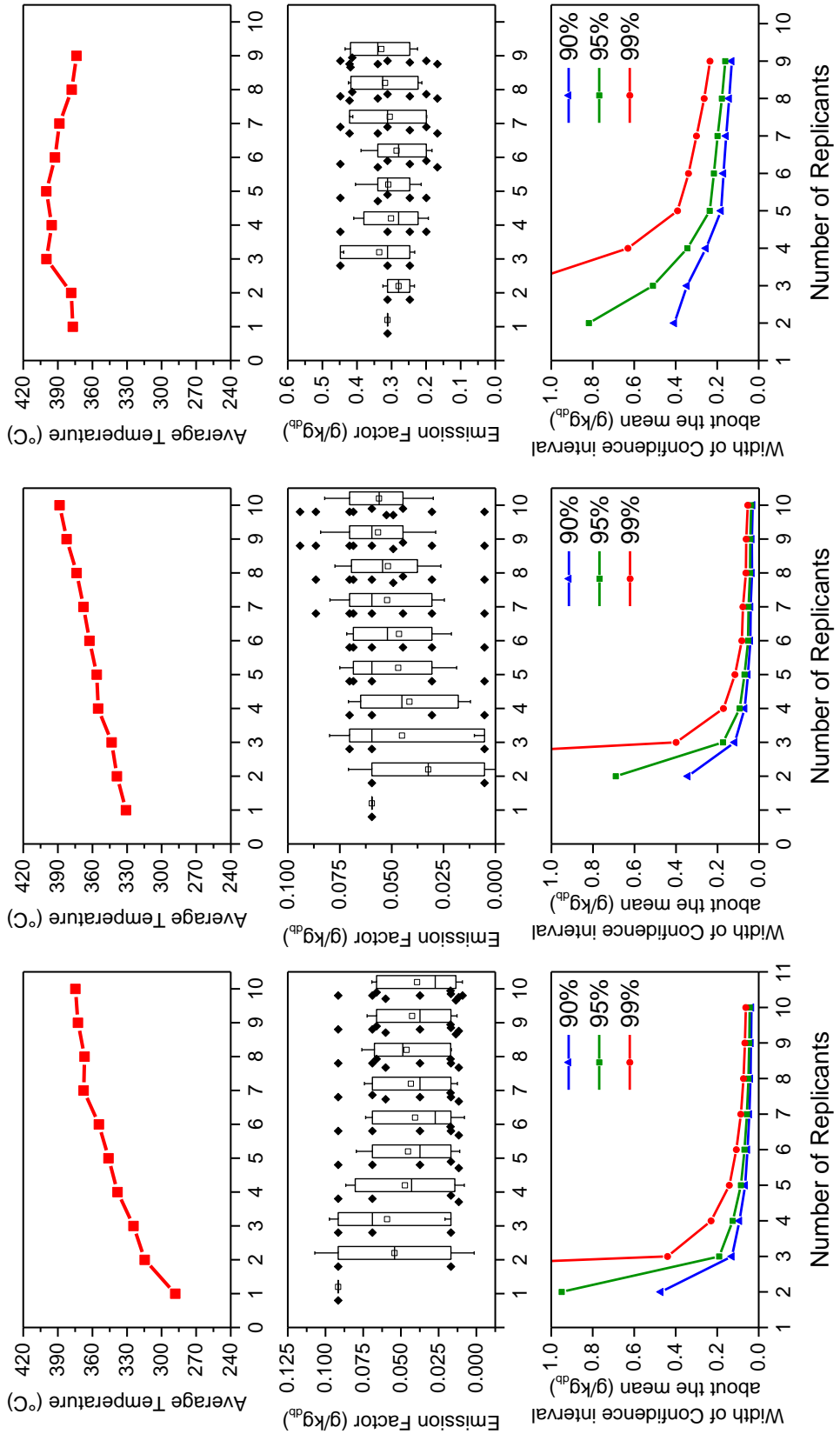
Figure 8.15 Variation in HCl emission (g/kg_fuel) dependent upon number of test repeats (*n*) and combustion temperature (°C). Whisker intervals present values one standard deviation from the numerical mean. (a) Biomass briquettes, (b) Fuelwood and (c) Torrefied briquettes.

8.5 Discussion

8.5.1 Variance in Combustion Conditions

The combustion of biomass in small domestic appliances is a complex process which may be influenced by number of variables some of which may be directly attributed to the user. Notwithstanding, undertaking combustion experiments under standardised conditions attempts to impose uniformity and generate repeatable results. Experimental accuracy and precision refers to the closeness of measured values to a true and representative value as well as the repeatability of such results (Trojanowski et al., 2018). Increasing the number of tests undertaken may therefore be applied as a method of improving the validity of emission inventories.

In this work, combustion conditions have been shown to change significantly between testing batches. Temperatures within the firebox where noted to be significantly higher during prolonged stove testing in contrast with temperatures observed following standard testing practices, and were found to be within the range outlined in previous work (Ozgen et al., 2014; Fachinger et al., 2017). The recorded combustion temperature was found to be similar between fuelwood and biomass briquettes (**Figure 8.16**). The combustion of torrefied briquettes leads to high temperatures which are comparable to that of the other fuels however the temperature was found to decrease during prolonged stove use. In addition, the temperature profiles are significantly different between the torrefied and biomass fuels. Biomass materials appear to combust at high flaming temperatures and moderate smouldering temperatures, while torrefied fuels provide for hotter initial temperatures followed by a prolonged period of cooler smouldering combustion. This profile is presented in **Figure 8.16** where the process is likely related to the high volatile content of biomass fuels in contrast to torrefied materials as identified in **Table 8.2** and presented within the literature (Maxwell et al., 2020). The higher maximum combustion temperatures observed for briquetted fuels is likely related to the large surface of the constituent particles, and friability of the material structure. Flue gas temperatures, applied as a proxy for combustion temperature, measured in this work are higher than those presented in the literature likely because of the prolonged heating time and higher total fuel throughput. Ozgen et al. (2013), Fachinger et al. (2017) and Maxwell et al. (2020) present average flue gas temperatures in the range of 182-360°C from a three-test batch cycle for torrefied, briquetted and fuelwood materials. Significantly lower temperatures are presented for materials similar to those used in this study following a single batch of fuel in the same combustion device (Mitchell et al., 2016). Previous work has also noted increased temperatures during the combustion larger batches of fuel, however little

work has been undertaken on the cumulative heating effect of multiple batches on emissions and, in the case of this study, repeatability of results.

Burning rates (kg/hour) were shown to vary between fuels and as a function of the combustion temperature. Fuelwood logs burned at a rate similar to those outlined during previous work (Mitchell et al., 2016) while torrefied briquettes burned at a slower rate than during previous testing (Maxwell et al., 2020). Though O_2 availability is most commonly identified as a rate-limiting factor affecting fuel conversion there is also a relationship between combustion zone temperature and burning rate where the primary air supply is sufficient (Koppejan and Loo, 2008). Figure 8.16-8.18 identifies the time series profiles of burning rate, combustion temperature and O_2 availability. Burning rate generally follows combustion temperature which is shown to increase as a function of the period of stove use for biomass briquette and fuelwood. In contrast, burning rates were shown to reduce during prolonged stove operation when torrefied briquettes were applied. Previous work by Calvo et al. (2015) outlined the relationship between combustion temperature and the rate of fuel conversion and also noted the influence of these processes on the formation of pollutant emissions. Generally stated, an increase in the combustion temperature causes, and is caused by, an increase in the fuel conversion rate. Given appropriate O_2 availability, such processes result in improved conditions and so decrease pollutant emission.

Fuel moisture content is often identified as a control on burning rate during the combustion of biomass (Price-Allison et al., 2019). Biomass briquettes, presenting a lower MC% (5.45±0.1) generally burn at a similar temperature with similar O_2 availability when compared with fuelwood maintaining a higher MC% (17.45±1.43). The high O_2 availability during biomass briquette combustion may be in response to stove underloading. Fachinger et al. (2017) highlights the potential detrimental consequences of fuel loading on stove performance and emission formation during the flaming phase of combustion. An increase in the air-to-fuel ratio within the combustion zone, likely observed during biomass briquette combustion, may lead to reduced temperatures and improved oxygen availability. An increase in the load capacity during biomass briquette combustion may have resulted in higher combustion temperatures resulting in the rapid conversion of fuel thereby inhibiting O_2 availability. The impact of this is often an increase emission formation. Variation in burning rate between individual batches is presented in **Figure 8.18**. In cases where very dry fuel is combusted, or stoves are overloaded the increased burning rate and temperature may inhibit O_2 availability and product retention time within the combustion zone resulting in higher pollutant formation (Nussbaumer et al., 2008; Pettersson et al., 2011; Shen et al., 2013; Ozgen et al., 2014; Fachinger et al.,

2017). Higher burning rates are generally not observed when testing to a standard procedure when the total fuel throughput is limited to just three test batches.
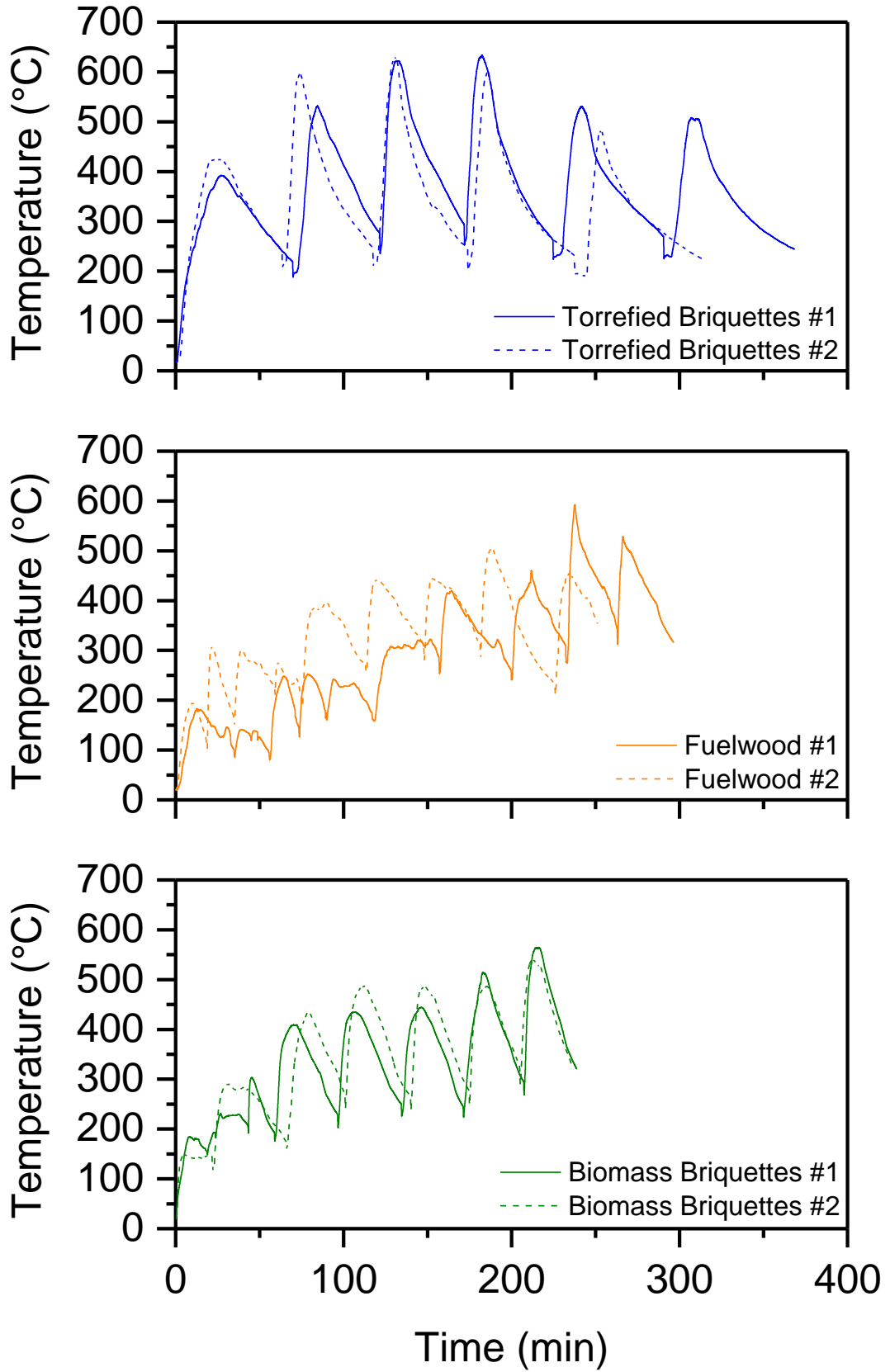
Figure 8.16 Variation in flue gas temperature (°C) as a function of time.
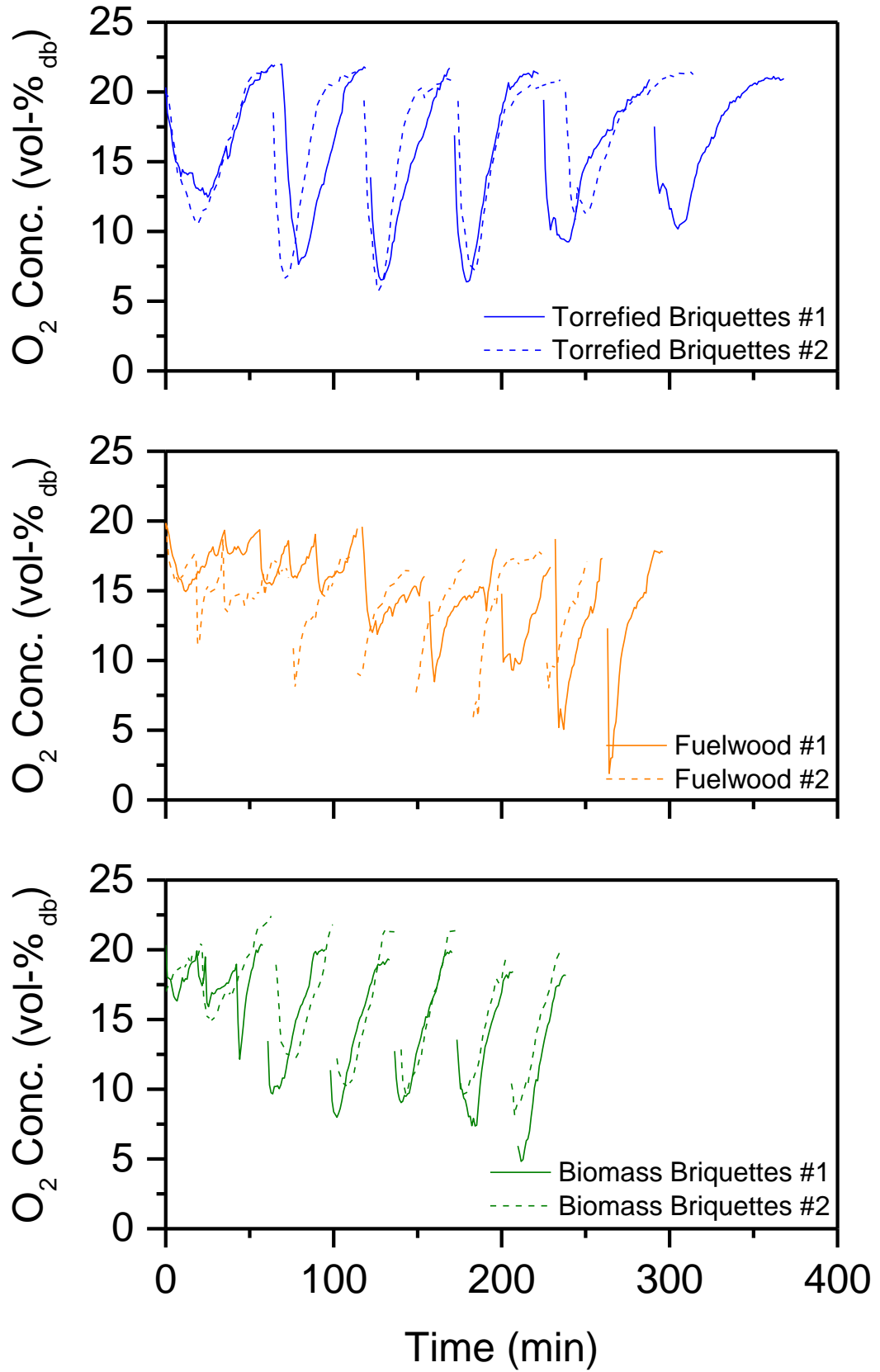
Figure 8.17 Variation in O₂ concentration (vol-%) as a function of time.
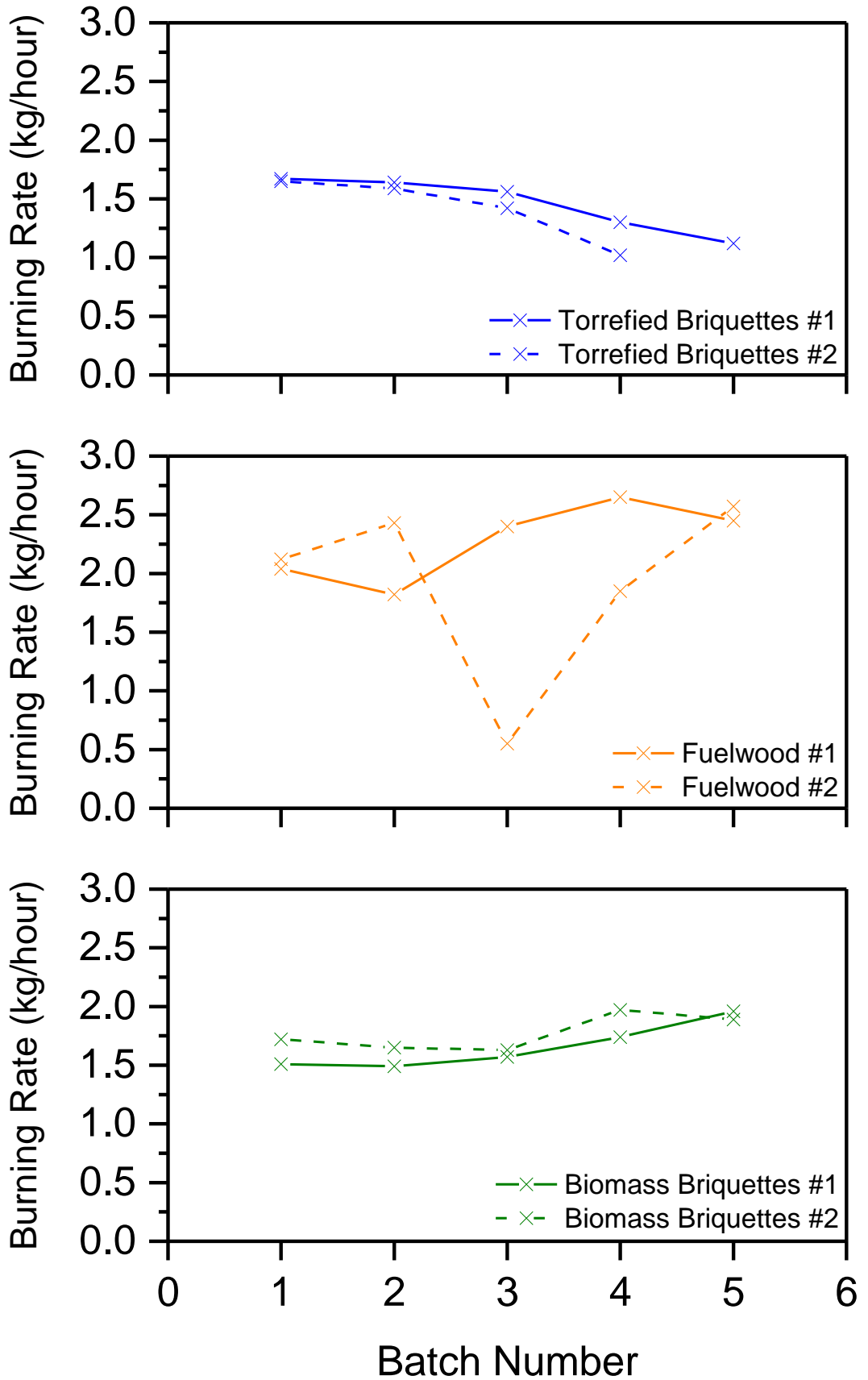
Figure 8.18 Variation in the average fuel burning rate (kg/hour) as a function of time.

The influence of fuel conversion rate, stove temperature and O_2 availability on pollutant emission formation has been widely discussed within the literature (Nussbaumer et al., 2008; Pettersson et al., 2011; Ozgen et al., 2014; Fachinger et al., 2017; Olave et al., 2017). Specifically, Olave et al. (2017) identifies the relationship between increased combustion temperatures and reduced pollutant formation. Changes in such conditions affect the fundamental processes influencing the extent to which combustion products are completely consumed in the oxidation reaction as outlined in Smith (1987). CO fluctuation between batches is in response to variation in conditions within the combustion zone. CO formation during the combustion of biomass briquettes and fuelwood is generally shown to decline with an increase in fuel throughput due to an increase in the combustion temperature. Parallels between CO formation, combustion temperature and MCE suggest that a greater fraction of the fuel carbon is converted as CO_2 when combustion temperatures are increased. The presence of such conditions shows a prolonged period of flaming combustion for higher fuel throughputs. It is likely that reduced CO emissions would not be observed during standard testing practices before an optimum stove temperature is reached. CO formation was generally higher during torrefied briquette combustion. Given the lower volatile content associated with torrefied materials (Ibrahim et al., 2013), the material burns more similar to coal, allowing for a short flaming phase and a prolonged smouldering phase. Notwithstanding, the combustion of torrefied fuel and resulting CO formation is still influenced by combustion conditions and temperature. Similarly, variability in alkane, benzene and aldehyde species between test batches is due to changes in combustion conditions over the testing period, which promotes their oxidation to form CO_2 and H_2O.

NOx and SO_2 formation was related to the fuel nitrogen and sulphur content. Given the relatively low average combustion temperatures (Mitchell et al., 2016), fuel-NOx is identified as the dominant source. Only limited fluctuation in emission levels between test batches is identified suggesting that the NOx and SO_2 formation pathway is unaffected by changes in combustion conditions brought about by an increase in stove operation time. In addition, combustion temperatures are not suitably high for the formation of significant quantities of thermal NOx (Koppejan and Loo, 2008) as identified in **Table 8.10**. Skreiberg et al. (1997) and Houshfar et al. (2011) show that excess air and increased O_2 availability can increase NO and NOx formation. In the current work, though O_2 availability is known to fluctuate within the stove during testing, there is very little variance in NOx. This process is described in **Figure 8.19** showing the fluctuation in O_2 and temperature as well as the rate of NO and SO_2 formation. Correlation results do indicate a positive effect of increased O_2 availability on NOx formation in biomass briquette and torrefied fuel

combustion, however not in fuelwood logs. Given that all combustion variables differ significantly between batches and increased NOx is also identified during later batches where combustion temperatures are highest it is likely that for the current conditions, variance in NOx and SOx emission factors remain unaffected by temperature, O_2 availability and burning rate fluctuation. An example of the non-dependency relationship between temperature, NOx and SO_2 is presented in **Table 8.10**. Torrefied briquette fuel has the highest N-content, and lower values are found in the biomass fuels, with similar findings commonly presented in the literature (Sommersacher et al., 2012). Corresponding NOx emission factors are presented whereby those for torrefied fuel are the highest, followed by fuelwood and biomass briquette fuel.

Table 8.10 Temperature, NOx and SO_2 results observed during each test during biomass briquette combustion.

Batch No.	Ave. Flue Gas Temp. (°C)	NOx (g/kg$_{fuel}$)	SO_2 (g/kg$_{fuel}$)
1	330.9	1.4	1.1
2	346.7	1.17	1.05
3	352.4	1.6	0.9
4	390.0	1.45	0.79
5	360.9	1.4	1.1
6	394.1	1.57	0.87
7	399.1	1.7	1.0
8	415.5	1.50	0.93
9	451.9	1.8	1.0
10	443.2	1.29	0.70

Here, NO and SO_2, are measured as an approximation of NOx and SOx, and these are higher during the flaming phase of combustion compared to significantly lower levels during the smouldering phase (char combustion). Mitchell et al. (2016) identifies similar findings whereby flaming phase NOx was between 46-56% higher than smouldering phase NOx during the combustion of fuelwood. Analysis of average combustion conditions and subsequent pollutant emission factors revealed a limited relationship whereby in most cases correlations between temperature, NOx and SO_2 are not significant. Similarities in the variation in temperature trends and pollutant formation are observed however the fluctuation in emissions is likely only in response to the rate of fuel conversion, a factor which is both controlled and controlled by the temperature.
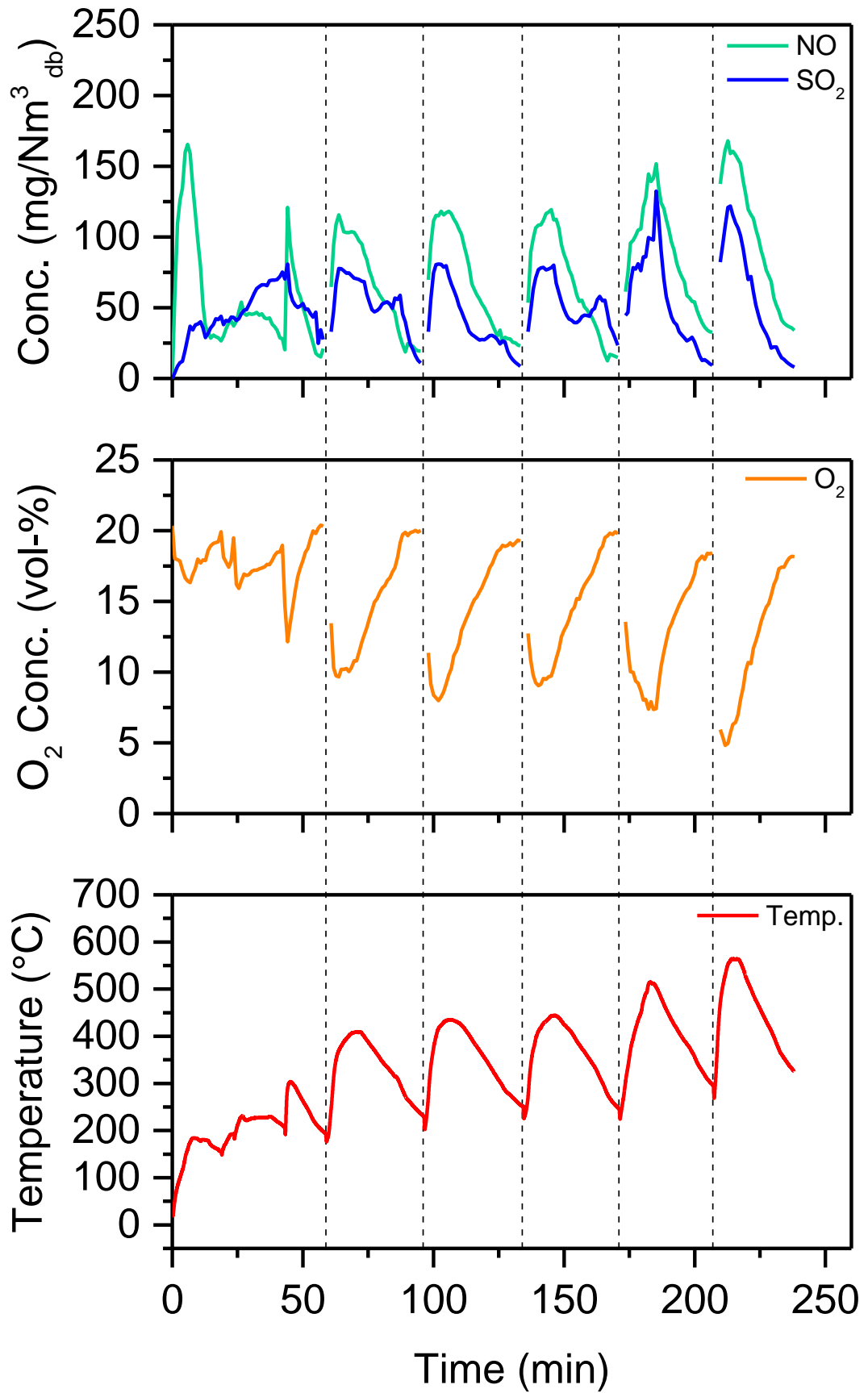
Figure 8.19 Variation in NO, SO₂ and O₂ concentration and temperature during the combustion of biomass briquettes.

Hydrocarbon and VOC emissions are shown to reduce with an increase in combustion temperature. As such, higher concentrations are present during the initial phases of combustion and when the stove is in the process of heating up. Given appropriate combustion conditions, CH_4 and other non-methane volatile organic compounds (NMVOC) species behave as an intermediate between fuel carbon and fuel hydrogen and, during complete combustion, CO_2 and H_2O (Koppejan and Loo, 2008). The combustion temperature is a rate limiting factor in the reaction rates of hydrocarbon species and, as a result, in the total emission. Other combustion parameters, including residence time within the combustion zone, also affect hydrocarbon emissions; where adequate O_2 is available, the temperature is identified as the rate limiting control (Koppejan and Loo, 2008). Olsson et al. (2003) studied CH_4 emission between different combustion devices with higher concentrations generally associated with lower combustion temperatures. Similarly, Evtyugina et al. (2014) identifies significant differences in VOC formation during the combustion of three fuelwood species producing a range of combustion temperatures. The combustion of oak fuelwood produced a low temperature of 307°C and the highest emission, poplar combustion produced a moderate temperature of 371°C and moderate emission formation and beech produced a high temperature of 441°C and the lowest emission.

High VOC emission concentrations (**Figure 8.20**) were observed following the addition of subsequent test material onto a bed of char. During the initial stages, the new batch of fuel is undergoing low temperature endothermic pyrolysis which results in the formation of high emission concentrations, since temperatures are below the temperature threshold required for ignition and more efficient combustion (Evtyugina et al., 2014). This was also seen by Ozgen and Caserini (2018) and high emissions during reloading were explained by lower combustion temperatures and high excess air. These observations were present throughout the testing series illustrating the potential impact of fuel properties, for example fuel moisture content, on temperature and emissions. **Figure 8.20a,b** provides a summary of the effect of combustion temperature on pollutant emissions . The reduction in emissions during prolonged testing is in response to improved combustion conditions predominantly controlled by an increase in combustion temperature.
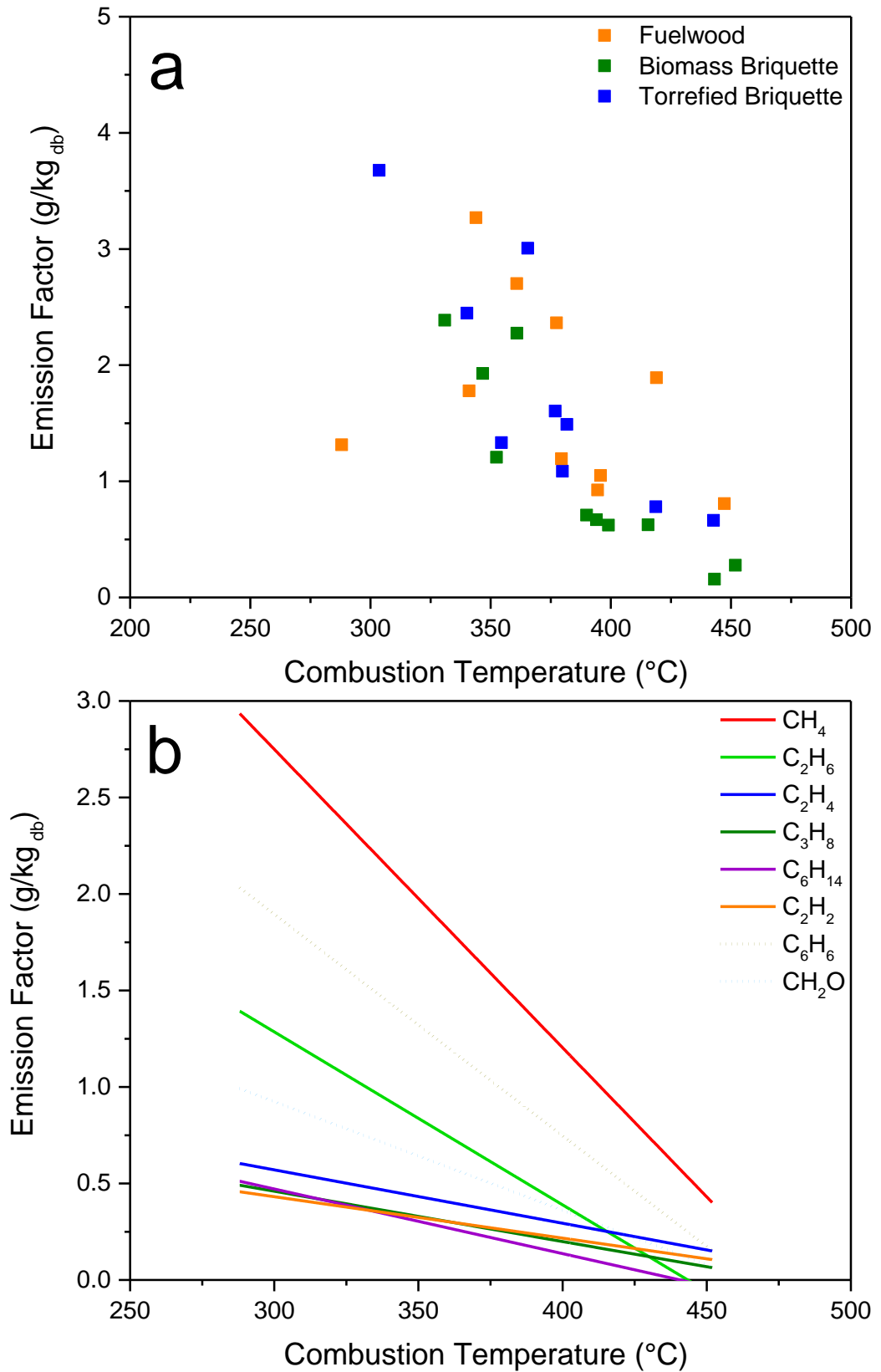
Figure 8.20 The effect of combustion temperature (°C) on emissions from VOC and hydrocarbon species. The effect of temperature on CH_4 emissions (a) is presented for each of the test fuels which the linearity of decay (b) incorporates all fuels.

8.5.2 Effect of number of repeats upon results confidence

Figure 8.21 displays the variation in the width of the confidence interval where P=0.05 between different fuel types. Similarly, the CI for individual fuel types is presented in **Figure 8.8-8.15**. As previously discussed, the CI is affected by the number of repeats undertaken with both improved and inhibited combustion conditions affecting the result confidence. Significant improvement in the combustion conditions during prolonged stove use can lead to lower emission formation the level of which is below that observed during previous batches; this leads to an increase in σ thereby affecting the CI. Inversely, significant inhibition in the combustion conditions can lead to higher emission formation the level of which is above that observed during previous batches; this leads to an increase in σ thereby affecting the CI.
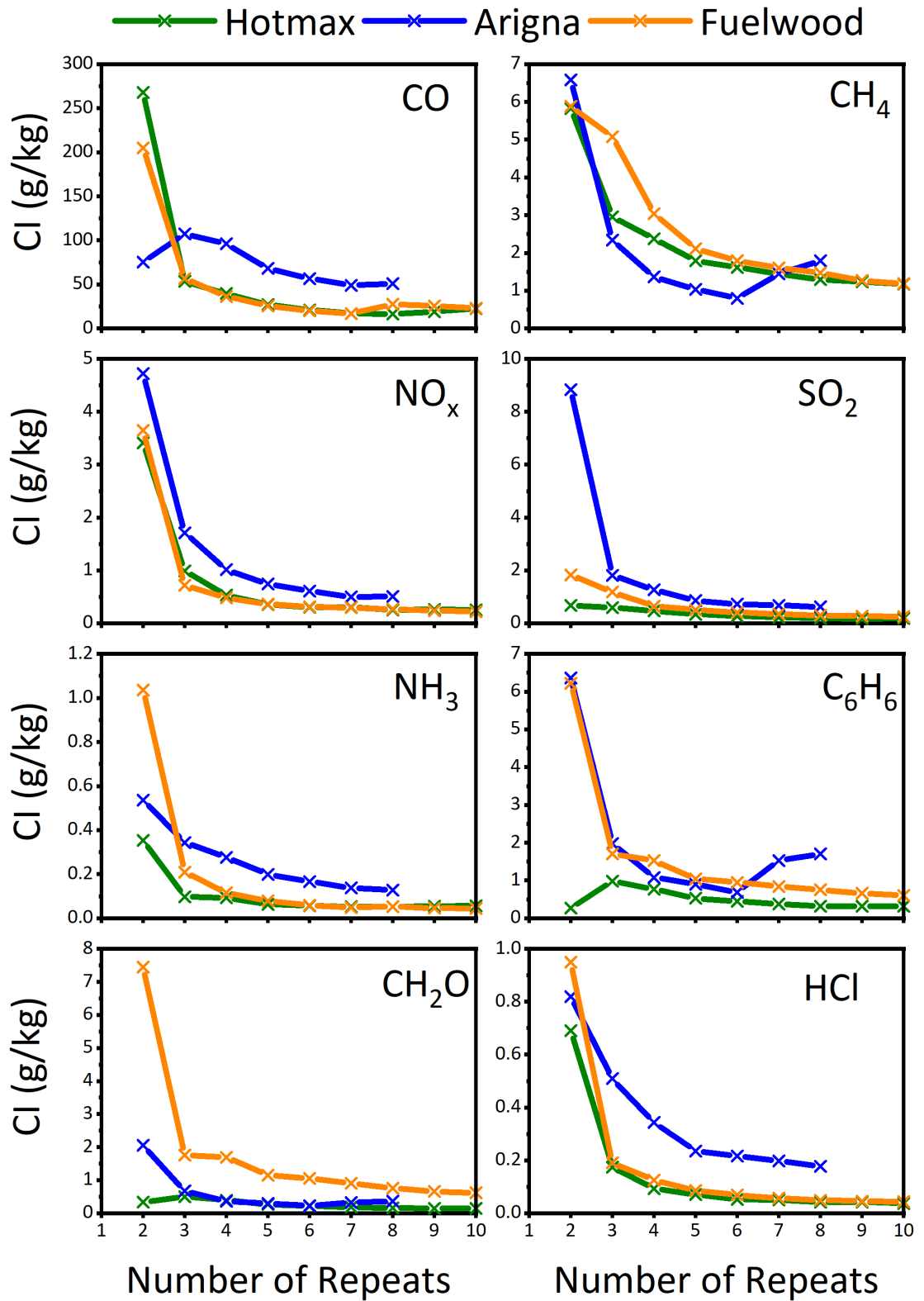
Figure 8.21 Variation in the width of the confidence interval about the mean (*CI*) where *P*=0.05 (*CL*=95%)

8.5.2.1 Impact of inventory sample size upon repeatability

The CI is shown to reduce with an increase in the number of test batches. Generally, the most significant reduction in the CI is presented following the introduction of a third test-batch while subsequent test-batches provide a less significant reduction in the CI. This trend is generally observed for each of the fuels and for each pollutant species. The CI is affected by the size of the sample inventory and the CL (Giannoulis, 2019). It is assumed that the larger the size of the sample inventory the greater the statistical precision and the narrower the CI; the inverse is therefore presented for inventories maintaining a smaller sample size (Gupta, 2015). Inventory values for biomass briquettes (**Chapter 8.4.5.1**) and fuelwood (**Chapter 8.4.5.3**) appears to follow the trend outlined within the literature whereby an increase in n results in a reduction in CI (Gupta, 2015; Matsuyama, 2018; Giannoulis, 2019). The trend in CI relative to n is more variable with regards to the torrefied briquette fuel as shown in **Chapter 8.4.5.2**. An increase in the CI is presented following the addition of TB7 and TB8. This process is particularly prevalent for hydrocarbon and formaldehyde species. In this case, the CI is inversely proportional to the standard deviation of inventory values about the mean. The formation of outlier emission results during prolonged stove operation, including values both significantly higher and lower than the mean value, result in an increase in the standard deviation thereby reducing the precision of statistical estimations. Less significant increases in the CI are also found during prolonged stove testing of biomass briquettes and fuelwood.

8.5.2.2 Impact of fuel type upon repeatability

Biomass briquettes were tested as an example of a highly homogeneous fuel material while fuelwood was tested due to variability in particle size and mass. Torrefied fuel briquettes were composed of small cobbles which where variable in size and composition (Trubetskaya et al., 2019). The torrefied fuel created a uniform bed which was simple to replicate because of the small size of the cobble particles. As such, it was assumed that the combustion reaction would be similar between test-batches. The initial hypothesis was that the changeable structure of the fuelwood would lead to significant differences in the emissions during the combustion reaction while the biomass briquettes would lead to more repeatable results. Given the homogeneity of briquetted materials and heterogeneity of fuelwood logs it postulated that combustion emissions would be more variable in logs than in briquetted fuels. The numerical range of emission factor results are presented in **Table 8.11** for each of the three fuel materials.

Table 8.11 Numerical range (g/kg$_{fuel}$) of emission factor results for each fuel.

Fuel	CO	CH$_4$	CH$_2$O	C$_6$H$_6$	SO$_2$	NOx	NH$_3$ (mg/g)	PM$_t$
Biomass Briquettes	53.07	2.23	0.30	0.63	0.40	0.58	0.13	1.59
Torrefied Briquettes	92.19	3.01	0.55	2.59	0.84	0.88	0.21	0.57
Fuelwood Logs	49.71	2.46	1.16	1.06	0.46	0.41	0.10	1.41

The combustion of biomass briquette and fuelwood materials resulted in the formation of a lower quantity of CO when compared with torrefed fuel. Mitchell et al. (2016) identified a uniform rate of thermal conversion and emission formation during the combustion of torrefied fuels when compared to a raw biomass material. The process of torrefaction results in the decomposition of highly reactive components, within a biomass material (Prins et al., 2006), resulting in a loss of volatile matter and an increase in the fraction of fixed carbon as shown in **Table 8.2**. Both Mitchell et al. (2016) and Maxwell et al. (2020) observed a reduction in CO emissions during the combustion of torrefied materials. In contrast, in the current work, higher CO emissions were observed across a wider numerical range together with a reduced flaming phase and a prolonged smouldering phase (a consequence of the lower volatile matter). The high moisture content of the torrefied fuel studied here is a contributing factor in this, resulting in poor ignition and lower combustion temperatures. A similar finding is shown for other gaseous pollutants whereby difficult ignition and extended smouldering phases results in higher pollutant formation and a greater range in emission factor results.

The biomass briquettes present the most consistent characteristics, in terms of size and mass, however a large range in results is still observed. It is thought that this is because of the incremental increase in the combustion temperature which results in improved combustion conditions. Fuelwood logs are the most inconsistent in terms of shape and mass and these also show a large range of emission factor values. **Figure 8.22** shows the distribution of emission factor values and standard error for each of the fuel materials. Though initially hypothesised that fuel type will present a significant control on combustion repeatability, the inherent combustion process appears to maintain the greatest impact. Generally, homogenous fuels appear to burn more consistently however changes in the stove conditions during an experiment result in greater discrepancy and, as a result, a reduction on repeatability. Generally, the combustion of biomass briquettes leads to the

formation of reduced emissions in contract to fuelwood and torrefied briquettes. In addition, the observed range in emission factor values is generally lower in response to the homogeneity of the material resulting in uniformity of the combustion reaction between batches. Though torrefied briquettes are also an example of a homogeneous fuel the impact of a higher moisture content may have inhibited combustion conditions and uniformity of the combustion reaction between batches. Mitchell (2017) provides a summary of the range and variation in emission factor values reported within the literature. Though some correlation of stove conditions and pollutant formation is reported there. The current work highlights the importance of stove processes, specifically combustion temperature, on emission factor values.
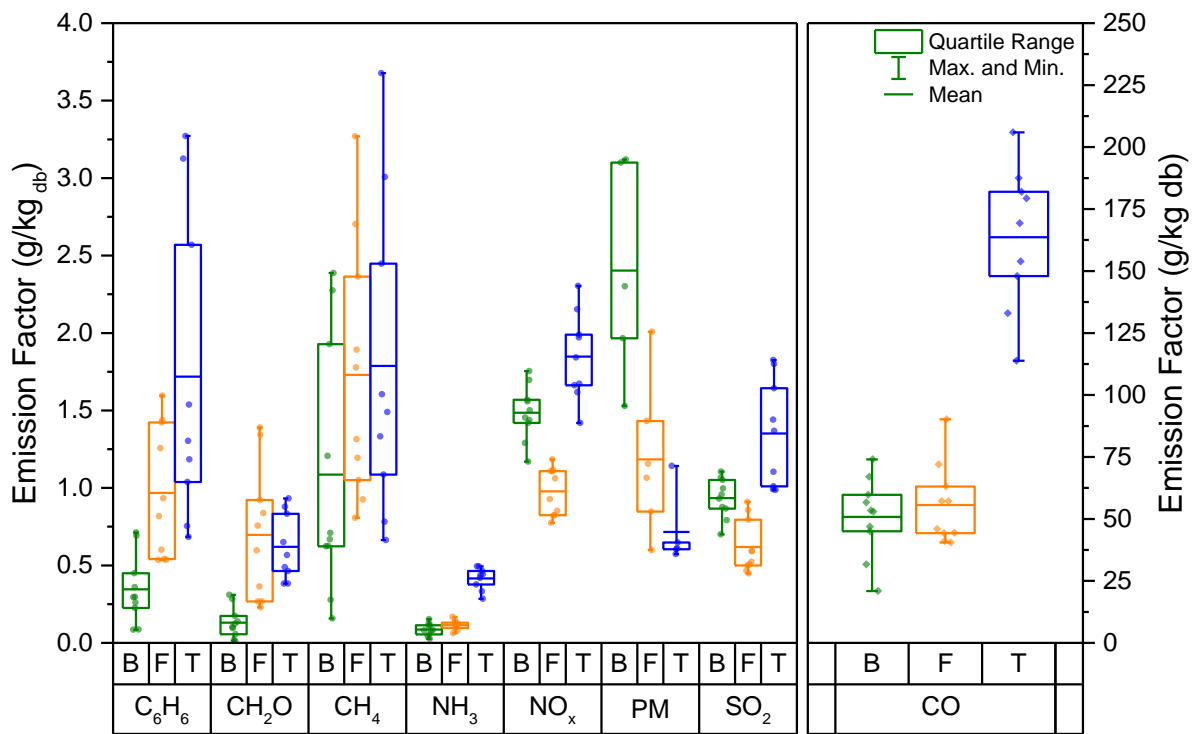
Figure 8.22 Variation in emission factor (g/kg_fuel) results for PM and gaseous species. The upper and lower whisker bound present the maximum and minimum recorded emission factor while the box identifies the standard error. • presents individual recorded emission factor results. B is biomass briquettes, F is Fuelwood and T is Torrefied briquettes.

8.5.2.3 Impact of burn quality upon repeatability

An increase in the CI occurs in response to an increase in the standard deviation of the sample population. An increase in the standard deviation occurs when there is a statistically significant increase or decrease in the emission factor within the sample. As such, a combustion reaction which is significantly improved or inhibited

during prolonged testing can lead to the formation of outliers within the emission factor series thereby affecting the CI. Both improved and degraded combustion conditions can have this affect. The development of variable quality of combustion conditions during a prolonged combustion reaction can have a statistically significant impact on the formation of outlier results and, as a result, the CI. **Figure 8.20** outlines the importance of combustion temperature on emission formation while **Figure 8.19** displays the effect of prolonged stove operation on combustion temperature. Prolonged combustion testing of fuelwood and biomass briquettes, described in **Figure 8.16**, corresponds with a gradual increase in the combustion temperature leading to a reduction in emission formation with an increase in fuel throughput. As a result, prolonged stove testing can result in an increase in the CI however the effect is not pronounced. Alternatively, a reduction in the combustion temperature is observed with an increase in the throughput of torrefied briquettes due to the higher moisture content. Detrimental combustion conditions displayed during prolonged testing result in emission formation significantly different from the statistical average. In response, the standard deviation of values about the statistical average result in a broadening of the CI; this leads to a reduction in precision.

The complexity of biomass combustion inhibits repeatability in small-scale combustion experiments. Consequently, there is in significant range of emission factor values presented within the literature (Mitchell, 2017). Previous work has outlined the need for large sample sizes when attributing emission factor values as a method of reducing error (Pettersson et al., 2011; Wang et al., 2014; Stewart, 2017). Alternatively, the inherent variability of biomass combustion may mean that increasing the number of costly and time-consuming tests will not improve confidence in emission factor results (Coulson et al., 2015). As previously discussed, a series of 9-10 combustion experiments were undertaken for each of the three test fuels with resulting emission factors displayed in **Figure 8-15**. The pollutant emission is influenced by temperature, burning rate and O_2 availability, and combustion conditions vary as a function of operating period and fuel mass throughput. Biomass briquette and fuelwood combustion appears to produce generally consistent results whereby pollutant formation is reduced with an increase in stove operating period. Even so, results which vary significantly from the mean value may occur with an increase in the number of batches which can be attributed to either improved or inhibited combustion conditions. Difficulty in torrefied briquette ignition contributed to significantly higher emissions during prolonged batch testing indicating that the number of batches applied within an individual test should be specific to the type of fuel combusted.

The variance in torrefied briquette emissions during prolonged combustion creates outlier results thereby skewing the standard deviation of the population around the mean. This happens both when the stove is cool and producing very high emissions, and when the stove is hot and producing very low emissions. Though standard error is likely to reduce with an increase in the sample size, the standard deviation is unaffected and varies in response to the fluctuation in individual emission factor values (Wang et al., 2014). As such, an increase in the width of confidence may occur with an increase in the number of tests undertaken in response to significantly different combustion conditions. Though variation is observed during prolonged heating, the confidence is significantly improved when compared to the standard three batch testing results commonly applied with the literature.

Estimating emission factor confidence by the application of replicant testing is shown to be a complex process with accuracy centred primarily on combustion temperature. An increase in the combustion temperature is generally observed during prolonged stove operation thereby creating favourable combustion conditions and minimising emissions. Alternatively, independent combustion events may affect the combustion process at any point during the experimental procedure resulting in variance in the derived emission factor results. It therefore stands to reason that similarly undertaking three test batches is not enough for accurate emission factor estimation given the prolonged heating requirements of small-scale combustion devices. However, attributing a specific number is impossible given the inherent dynamicity of the combustion reaction. Results from this work appear to suggest that an increase in the number of batches leads to an increase in results confidence, however that confidence is dependent upon both changes in stove conditions and independent combustion events. As such, combustion experiments should be undertaken until (a) average combustion temperatures (recorded on a batch basis) are maintained at a constant rate and (b) enough test batches are completed for the complete series to be considered statistically significant. In the case of small-scale domestic combustion, the number of completed batches should only incorporate values which are consistent amongst other batch testing results where anomalous events are disregarded from the series.

8.6 Conclusion

operational performance and pollutant emissions from domestic heating appliances is known to be highly variable. The testing of such devices is commonly associated with a high degree of discrepancy when evaluating emission data leading to poor repeatability and low results confidence. The following chapter assesses the

variability in emissions and stove performance when a repetitive testing approach is applied. A review of variation in emission factors is presented for three different materials common to the UK fuels market. A total of two testing series were undertaken for each of the fuels with a series incorporating a pre-test batch followed by four-five subsequent test batches. Results suggest notable variation in the combustion conditions during an experiment with combustion temperature identified as a significant control. An increase in temperature was observed with an increase in the total throughput of fuel through the stove device. It was found that higher temperatures generally corresponded with a reduction in pollutant emissions. Several unforeseeable combustion events were observed during the testing series leading to outlier results. An increase in the number of repeats undertaken leads to an increase in results confidence however results can become unclear during prolonged stove testing in response to changing stove conditions and the presence of outlier results. Results of the investigation suggest that undertaking three test batches, a method most commonly applied with the literature, may lead to an over-estimate in emission factor values given the effect of prolonged heating requirements in small-scale devices. Increasing the number of replicants is therefore advisable however results should be presented in conjunction with corresponding stove conditions. The following conclusions are outlined as:

i. Combustion conditions are shown to change significantly between batches during prolonged stove testing. Such changes mean that the testing parameters are not consistent between fuel batches. Stove testing is shown to be complex and unpredictable with unpredictable events potentially skewing results, thereby limiting confidence. Combustion temperature is shown to be a controlling factor in pollutant formation with higher combustion temperatures observed during an increase in the throughput of fuel material.

ii. NOx and SOx emissions are governed by the $Fuel_N$ and $Fuel_S$ respectively.

iii. Emission factors are fundamentally controlled by the combustion temperature and independent, or uncontrollable, events.

iv. The torrefied briquette fuel studied here was not typical since it had high moisture content which meant combustion conditions were poor and emissions consequently higher than expected. For the other two fuels studied, the wood briquettes gave the most consistent combustion repeatability (in terms of emission factors of pollutants), and the fuelwood logs the worst. So, it does appear that fuel type impacts on emission factors, not least since it is intimately linked to the consistency of combustion conditions, including temperatures.

v.   Regarding repeatability, increased stove temperatures, likely caused by long term stove operation, presents a detrimental effect. Prolonged combustion activity results in conditions that differ significantly from those observed during the application of earlier test batches. It is therefore likely that the testing of stove emission performance with three or less test batches may not be sufficiency to ensure optimal temperature. As such, the derived emission factor values may over-estimate likely pollutant emissions when compared with stove devices operated over a prolonged period of time. Similarly, only burning a small number of batches, a process commonly applied in the UK, may result in higher emissions due to lower combustion temperatures meaning that accredited emission factor values could be considered an under-estimate.

vi.   An increase in the number of test-batches generally results in a reduction in the width of the confidence interval thereby increasing the statistical precision of the emission result. However, changes in the condition of the combustion zone during prolonged testing can positively or negatively affect the emission formation. This can lead to highly changeable emissions which can affect the CI thereby negating the effect of repetitive batch testing. Therefore, it is the quality of the combustion reaction (per batch) which has a greater effect on repeatability than the type of fuel combusted.

vii.   Stove testing procedures should consider the impact of applied fuel mass, on both an individual batch and a batch-by-batch basis, on the impact upon combustion temperatures and formation of derived pollutant products. The recommended solution would thereby be that stove users should continue to implement the pre-test-batch followed by x3 test-batch standard procedure however a greater number of tests should be undertaken. This would negative the effect of prolonged stove testing on the combustion zone. However, this method would only be representative of controlled operating conditions and not be representative of stove performance in cool countries where a device may run for a prolonged period.

8.6 References

Akagi, S.K., Yokelson, R.J., Wiedinmyer, C., Alvarado, M.J., Reid, J.S., Karl, T., Crounse, J.D. and Wennberg, P.O. 2011. Emission factors for open and domestic biomass burning for use in atmospheric models. Atmospheric Chemistry and Physics. 11(9), pp.4039–4072.

Altman, D.G. and Bland, J.M. 2005. Standard deviations and standard errors. British Medical Journal. 331, p.2005.

Alves, C., Gonçalves, C., Fernandes, A.P., Tarelho, L. and Pio, C. 2011. Fireplace and woodstove fine particle emissions from combustion of western Mediterranean wood types. Atmospheric Research. 101(3), pp.692–700.

Bafver, L., Leckner, B., Tullin, C. and Berntsen, M. 2011. Particle emissions from pellets stoves and modern and old-type wood stoves. Biomass and Bioenergy. 35(8), pp.3648–3655.

Ballard-Tremeer, G. and Jawurek, H.H. 1996. Comparison of five rural, wood-burning cooking devices: Efficiencies and emissions. Biomass and Bioenergy. 11(5), pp.419–430.

Berthouex, P.M. and Brown, L.C. 2002. Statistics for Environmental Engineers Second Edi. Lewis Publishers.

BSi 2001. BS EN 13240:2001+A2:2004 - Roomheaters Fired by Solid Fuel - Requirements and Test Methods.

BSi 2009. DD CEN/TS-15883:2009 - Residential Solid Fuel Burning Appliances - Emission Test Methods.

Calvo, A.I., Martins, V., Nunes, T., Duarte, M., Hillamo, R., Teinilä, K., Pont, V., Castro, A., Fraile, R., Tarelho, L. and Alves, C. 2015. Residential wood combustion in two domestic devices: Relationship of different parameters throughout the combustion cycle. Atmospheric Environment. 116, pp.72–82.

Calvo, A.I., Tarelho, L.A.C., Alves, C.A., Duarte, M. and Nunes, T. 2014. Characterization of operating conditions of two residential wood combustion appliances. Fuel Processing Technology. 126, pp.222–232.

Cerqueira, M., Gomes, L., Tarelho, L. and Pio, C. 2013. Formaldehyde and acetaldehyde emissions from residential wood combustion in Portugal. Atmospheric Environment. 72, pp.171–176.

Chen, Y., Roden, C.A. and Bond, T.C. 2012. Characterizing biofuel combustion with Patterns of Real-Time Emission Data (PaRTED). Environmental Science and Technology. 46(11), pp.6110–6117.

Coulson, G., Bian, R. and Somervell, E. 2015. An investigation of the variability of particulate emissions from woodstoves in New Zealand. Aerosol and Air Quality Research. 15(6), pp.2346–2356.

Curkeet, R. and Ferguson, R. 2010. EPA Wood Heater Test Method Variability Study - Analysis of Uncertainty, Repeatability and Reproducibility based on the EPA Accredited Laboratory Proficiency Test Database [Online]. Available from: http://www.familiesforcleanair.org/wp-content/uploads/2015/02/Wood-Heater-Emission-Test-Method-Variability-Paper-06.Oct_.10-2.pdf.

Dasch, J.M. 1982. Particulate and Gaseous Emissions from Wood-Burning Fireplaces. Environmental Science and Technology. 16(10), pp.639–645.

EPA, U.S. 2016. Process for Developing Improved Cordwood Test Methods for Wood Heaters [Online]. Available from: https://www.epa.gov/sites/production/files/2016-03/documents/discussion_paper_-_process_for_dev_imp_cwtm_030916.pdf.

Espenas L. D. (United States Department of Agriculture Forest Service) 1951. Some Wood-Moisture Relations. Wisconsin.

Evtyugina, M., Alves, C., Calvo, A., Nunes, T., Tarelho, L., Duarte, M., Prozil, S.O., Evtuguin, D. V. and Pio, C. 2014. VOC emissions from residential combustion of Southern and mid-European woods. Atmospheric Environment. 83, pp.90–98.

Fachinger, F., Drewnick, F., Giere, R. and Borrmann, S. 2017. How the user can influence particulate emissions from residential wood and pellet stoves: Emission factors for different fuels and burning conditions. Atmospheric Environment. 158, pp.216–226.

GACC 2014. The Water Boiling Test (Version 4.2.3): Cookstove Emissions and Efficiency in a Controlled Laboratory Setting [Online]. Available from: https://cleancookstoves.org/binary-data/DOCUMENT/file/000/000/399-1.pdf.

Giannoulis, C. 2019. How to interpret the width of a confidence interval. The Analysis Factor. [Online]. Available from: https://www.theanalysisfactor.com/interpret-width-of-confidence-interval/.

Goldstein, I.S. 1991. Overview of the Chemical Composition of Wood In: M. Lewin and I. S. Goldstein, eds. Wood Structure and Composition. New York: Marcel Dekker, Inc, pp.1–7.

Gupta, A. 2015. Interpreting research findings with confidence interval. Journal of Orthodontics. 1(1), p.8.

Haslett, S.L., Thomas, J.C., Morgan, W.T., Hadden, R., Liu, D., Allan, J.D., Williams, P.I., Keita, S., Liousse, C. and Coe, H. 2018. Highly controlled, reproducible measurements of aerosol emissions from combustion of a common African biofuel source. Atmospheric Chemistry and Physics. 18(1), pp.385–403.

Hedberg, E., Kristensson, A., Ohlsson, M., Johansson, C., Johansson, A., Swietlicki, E., Vesely, V., Wideqvist, U. and Westerholm, R. 2002. Chemical and physical characterization of emissions from birch wood combustion in a wood stove.

Hernandez, P.A., Graham, C.H., Master, L.L. and Albert, D.L. 2006. The effect of sample size and species characteristics on performance of different species distribution modelling methods. Ecography. 29(5), pp.773–785.

Houshfar, E., Skreiberg, Ø., Løv, T. and Sørum, L. 2011. Effect of Excess Air Ratio and Temperature on NOx Emission from Grate Combustion of Biomass in the Staged Air Combustion Scenario. Energy and Fuels. 25, pp.4643–4654.

Ibrahim, R.H.H., Darvell, L.I., Jones, J.M. and Williams, A. 2013. Physicochemical characterisation of torrefied biomass. Journal of Analytical and Applied Pyrolysis. 103, pp.21–30.

Jenkins, B.M., Baxter, L.L., Miles, T.R. and Miles, T.R. 1998. Combustion properties of biomass. Fuel Processing Technology. 54(1–3), pp.17–46.

Jones, J.M., Lea-Langton, A.R., Ma, L., Pourkashanian, M. and Williams, A. 2014. Pollutants Generated by the Combustion of Solid Biomass Fuels. London: Springer.

Kinsey, J.S., Kariher, P.H. and Dong, Y. 2009. Evaluation of methods for the physical characterization of the fine particle emissions from two residential wood combustion appliances. Atmospheric Environment. 43(32), pp.4959–4967.

Klauser, F., Carlon, E., Kistler, M., Schmidl, C., Schwabl, M., Sturmlechner, R., Haslinger, W. and Kasper-giebl, A. 2020. Emission characterization of modern wood stoves under real-life oriented operating conditions. Atmospheric Environment. 192, pp.257–266.

Koppejan, J. and Loo, S. van 2008. The Handbook of Biomass Combustion and Co-firing. London: Routledge.

Mando, M. 2013. Biomass Combustion and Co-Firing In: L. Rosendahl, ed. Biomass Combustion Science, Technology and Engineering. Oxford: Woodhead Publishing.

Matsuyama, T. 2018. An application of bootstrap method for analysis of particle size distribution. Advanced Powder Technology. 29(6), pp.1404–1408.

Maxwell, D., Gudka, B.A., Jones, J.M. and Williams, A. 2020. Emissions from the combustion of torrefied and raw biomass fuels in a domestic heating stove. Fuel Processing Technology. 199.

Mcdonald, J.D., Zielinska, B., Fujita, E.M., Sagebiel, J.C., Chow, J.C. and Watson, J.G. 2000. Fine particle and gaseous emission rates from residential wood combustion. Environmental Science and Technology. 34(11), pp.2080–2091.

Mitchell, E. 2017. Emissions from Residential Solid Fuel Combustion and Implications for Air Quality and Climate Change. University of Leeds.

Mitchell, E.J.S., Coulson, G., Butt, E.W., Forster, P.M., Jones, J.M. and Williams, A. 2017. Heating with Biomass in the United Kingdom: Lessons from New Zealand. Atmospheric Environment. 152, pp.431–454.

Mitchell, E.J.S., Lea-Langton, A.R., Jones, J.M., Williams, A., Layden, P. and Johnson, R. 2016. The impact of fuel properties on the emissions from the combustion of biomass and other solid fuels in a fixed bed domestic stove. Fuel Processing Technology. 142, pp.115–123.

Nakamura, K., Hatakeyama, T. and Hatakeyama, H. 1981. Studies on heat capacity of cellulose and lignin by differential scanning calorimetry. Polymer. 51(9), pp.607–613.

Nussbaumer, T., Doberer, A., Klippel, N., Bühler, R. and Vock, W. 2008. Influence of ignition and operation type on particle emissions from residential wood combustion In: 16th European Biomass Conference and Exhibition.

Obernberger, I., Brunner, T. and Bärnthaler, G. 2006. Chemical properties of solid biofuels-significance and impact. Biomass and Bioenergy. 30(11), pp.973–982.

Olave, R.J., Forbes, E.G.A., Johnston, C.R. and Relf, J. 2017. Particulate and gaseous emissions from different wood fuels during combustion in a small-scale biomass heating system. Atmospheric Environment. 157, pp.49–58.

Olsson, M., Kjallstrand, J. and Petersson, G. 2003. Specific chimney emissions and biofuel characteristics of softwood pellets for residential heating in Sweden. Biomass and Bioenergy. 24, pp.51–57.

Ozgen, S. and Caserini, S. 2018. Methane emissions from small residential wood combustion appliances : Experimental emission factors and warming potential. Atmospheric Environment. 189(June), pp.164–173.

Ozgen, S., Caserini, S., Galante, S., Giugliano, M., Angelino, E., Marongiu, A., Hugony, F., Migliavacca, G. and Morreale, C. 2014. Emission factors from small scale appliances burning wood and pellets. Atmospheric Environment. 94, pp.144–153.

Ozgen, S., Cernuschi, S. and Giugliano, M. 2013. Experimental evaluation of particle number emissions from wood combustion in a closed fireplace. Biomass and Bioenergy. 50(0), pp.65–74.

Perré, P. and Turner, I.W. 2002. A heterogeneous wood drying computational model that accounts for material property variation across growth rings. Chemical Engineering Journal. 86(1–2), pp.117–131.

Pettersson, E., Boman, C., Westerholm, R., Bostrom, D. and Nordin, A. 2011. Stove Performance and Emission Characteristics in Residential Wood Log and Pellet Combustion, Part 2: Wood Stove. Energy Fuels. 25, pp.315–323.

Phillips, D., Mitchell, E.J.S., Lea-Langton, A.R., Parmar, K.R., Jones, J.M. and Williams, A. 2016. The use of conservation biomass feedstocks as potential bioenergy resources in the United Kingdom. Bioresource Technology. 212, pp.271–279.

du Prel, J.B., Hommel, G., Rohrig, B. and Blettner, M. 2009. Confidence interval or p-value?: Part 4 of a series on evaluation of scientific publications. Dtsch Arztebl. 106(19), pp.335–339.

Price-Allison, A., Lea-Langton, A.R., Mitchell, Edward J. S.Gudka, B., Jones, J.M., Mason, P.E. and Williams, A. 2019. Emissions Performance of High Moisture Wood Fuels Burned in a Residential Stove. Fuel. 239, pp.1038–1045.

Prins, M.J., Ptasinski, K.J. and Janssen, F.J.J.G. 2006. Torrefaction of wood Part 2 . Analysis of products. Journal of Analytical and Applied Pyrolysis. 77, pp.35–40.

Purvis, C.R. and McCrillis, R.C. 2000. Fine Particulate Matter (PM) and Organic Speciation of Fireplace Emissions. Environmental Science and Technology. 34, pp.1653–1658.

Sartor, K., Restivo, Y., Ngendakumana, P. and Dewallef, P. 2014. ScienceDirect Prediction of SOx and NOx emissions from a medium size biomass boiler. Biomass and Bioenergy. 65, pp.91–100.

Schmidl, C., Luisser, M., Padouvas, E., Lasselsberger, L., Rzaca, M., Ramirez-Santa Cruz, C., Handler, M., Peng, G., Bauer, H. and Puxbaum, H. 2011. Particulate and gaseous emissions from manually and automatically fired small scale combustion systems. Atmospheric Environment. 45(39), pp.7443–7454.

Scott, A. 2005. Real-life emissions from residential wood burning appliances in New Zealand [Online]. Available from: http://www.crc.govt.nz/publications/Reports/air-report-emissions-residential-wood-burning-appliances-nz-000805.pdf.

Seljeskog, M., Sevault, A., Østnor, A. and Skreiberg, Ø. 2017. Variables Affecting Emission Measurements from Domestic Wood Combustion. Energy Procedia. 105(1876), pp.596–603.

Shen, G., Xue, M., Wei, S., Chen, Y., Zhao, Q., Li, B., Wu, H. and Tao, S. 2013. Influence of fuel moisture, charge size, feeding rate and air ventilation conditions on the emissions of PM, OC, EC, parent PAHs, and their derivatives from residential wood combustion. Journal of Environmental Sciences (China). 25(9), pp.1808–1816.

Shen, G., Yang, Y., Wang, W., Tao, S., Zhu, C., Min, Y., Xue, M., Ding, J., Wang, B., Wang, R., Shen, H., Li, W., Wang, X. and Russell, A.G. 2010. Emission factors of particulate matter and elemental carbon for crop residues and coals burned in typical household stoves in China. Environmental Science and Technology. 44(18), pp.7157–7162.

Simoneit, B.R.T. 2002. Biomass burning - A review of organic tracers for smoke from incomplete combustion.

Skreiberg, Ø., Hustad, J. and Karlsvik, E. 1997. Empirical NOx-Modelling and Experimental Results from Wood Stove Combustion In: Developments in Thermochemical Biomass Conversion. Dordrecht: Springer, pp.1462–1476.

Smith, K.R. 1987. Biofuels, Air Pollution and Health. New York: Plenum Press.

Sommersacher, P., Brunner, T. and Obernberger, I. 2012. Fuel indexes: A novel method for the evaluation of relevant combustion properties of new biomass fuels In: Energy and Fuels. American Chemical Society, pp.380–390.

Stewart, R. 2017. Assessment of particulate emissions from wood log and wood pellet heating appliances [Online]. Harwell. Available from: https://uk-air.defra.gov.uk/assets/documents/reports/cat07/1801291425_170201_Defra_NAEI _appliance_testing_summary_Issue1_Final_copy.pdf.

Tabarés, J.L., Granada, E., Moran, J., Porteiro, J., Murillo, S. and López González, L.M. 2006. Combustion behaviour of Spanish lignocellulosic briquettes. Energy Sources, Part A: Recovery, Utilization and Environmental Effects. 28(6), pp.501–515.

Tissari, J., Hytönen, K., Sippula, O. and Jokiniemi, J. 2009. The effects of operating conditions on emissions from masonry heaters and sauna stoves. Biomass and Bioenergy. 33(3), pp.513–520.

Trojanowski, R., Butcher, T., Wei, G. and Celebi, Y. 2018. Repeatability in Particulate and Gaseous Emissions from Pellet Stoves for Space Heating. Energy and Fuels. 32(3), pp.3543–3550.

Trubetskaya, A., Leahy, J.J., Yazhenskikh, E., Müller, M., Layden, P., Johnson, R., Ståhl, K. and Monaghan, R.F.D. 2019. Characterization of woodstove briquettes from torrefied biomass and coal. Energy. 171, pp.853–865.

Trubetskaya, A., Lin, C., Ovadnevaite, J., Ceburnis, D., O'Dowd, C., Leahy, J.J., Monaghan, R.F.D., Johnson, R., Layden, P. and Smith, W. 2021. Study of Emissions from Domestic Solid-Fuel Stove Combustion in Ireland. Energy and Fuels. 35, p.4978.

Vu, B., Alves, C.A., Gonçalves, C., Pio, C., Gonçalves, F. and Pereira, R. 2012. Mutagenicity assessment of aerosols in emissions from wood combustion in Portugal. Environmental Pollution. 166, pp.172–181.

Wang, Yungang, Sohn, M.D., Wang, Yilun, Lask, K.M., Kirchstetter, T.W. and Gadgil, A.J. 2014. How many replicate tests are needed to test cookstove performance and emissions? - Three is not always adequate. Energy for Sustainable Development. 20(1), pp.21–29.

Wilton, E. 2012. Review - particulate emissions from wood burners in New Zealand [Online]. Available from: https://www.niwa.co.nz/sites/niwa.co.nz/files/WoodburnerReportFinal.pdf.

Wilton, E. and Bluett, J. 2012. Wood Burner Testing Christchurch 2009 : Diurnal variation in emissions , wood use , indoor temperature and factors influencing start-up Prepared for Ministry of Science and Innovation [Online]. Available from:

https://www.niwa.co.nz/sites/niwa.co.nz/files/2 - AKL 2012-020 Woodburner testing Chch 2009.pdf.

Wöhler, M., Andersen, J.S., Becker, G., Persson, H., Reichert, G., Schön, C., Schmidl, C., Jaeger, D. and Pelz, S.K. 2016. Investigation of real life operation of biomass room heating appliances - Results of a European survey. Applied Energy. 169, pp.240–249.

Zhang, J., Smith, K.R., Ma, Y., Ye, S., Jiang, F., Qi, W., Liu, P., Khalil, M.A.K., Rasmussen, R.A. and Thorneloe, S.A. 2000. Greenhouse gases and other airborne pollutants from household stoves in China: A database for emission factors. Atmospheric Environment. 34(26), pp.4537–4549.

Chapter 9
Concluding Remarks and Future Work

9.1 Conclusions

9.1.1 Measurement of Moisture in Fuelwood

Fuelwood MC is determined via an oven-drying approach outlined in BS EN ISO 18134-2 and using a digital moisture probe. MC is highly variable within logs with values noted to change across the dimensions of a single log. Discrepancy in particle MC using a probe may occur depending on particle size, location of sampling point and placement within a storage pile. It is difficult to accurately determine the moisture content of fuelwood for the purpose of combustion testing. The destructive nature of accurate MC% determination by proximate analysis means that the particles sampled for analysis are not the same as the fuelwood logs applied during combustion experiments. Therefore, there is a high likelihood that the MC value will not be representative of the fired fuelwood. This is a significant limitation in the application of oven-drying of fuels to be characterised for the purpose of combustion testing given the substantial effect of moisture upon the combustion reaction. As such, the use of moisture probe devices should be considered for all proximate and fired fuelwood particles to assess approximate homogeneity of moisture content.

9.1.2 Impact of Moisture on Combustion Conditions

Combustion conditions were found to be directly affected by the fuelwood MC. Evidence of this affect is presented in **Chapter 5**-**Chapter 8**. Generally, an increase in fuelwood MC resulted in a reduction in combustion temperature and a slowed burning rate. In addition, MCE was shown to be lower when MC was increased while O_2 was shown to be higher. Combustion temperature is controlled by fuel MC and is outlined as the most significant factor affecting pollutant emission formation in this study.

9.1.3 Impact of Moisture on Gaseous Emissions

Ecodesign Directive (2009/125/EC) sets limits for particulate and gaseous emissions from domestic biomass combustion appliances . The current limits outlined in EU 2015/1185 and under the directive are 2.4 g/kg$_{fuel}$ for PM emissions (may be 5 g/kg$_{fuel}$ depending upon sampling method), 996 g/GJ (~18.4 g/kg$_{fuel}$) for

CO, 80 g/GJ (~1.48 g/kg$_{fuel}$) for total hydrocarbons and 113 g/GJ (~2.09 g/kg$_{fuel}$) for NOx.

A summary of the primary findings relating to the effect of MC on gaseous emissions is presented below. All data refers to the combustion of fuelwood when the stove is operating under nominal conditions. It should be noted that the appliance used in this study is of an older design which predates the current Ecodesign legislation. As such, the stove is generally not expected to meet the emission requirements under EU emission directives.

Emission factors are presented in g/kg$_{fuel}$ dry at STP. A correction factor of 0.88 is applied for results collected in **Chapter 8** for direct comparison with other data.

9.1.3.1 CO

Carbon monoxide emissions were found within the range identified within the literature. The emission of CO is generally associated with poor combustion quality and smouldering-type reactions (Mitchell et al., 2016). CO is an intermediate species in the formation of CO_2 were the rate of conversion is dependent upon temperature (Koppejan and van Loo, 2008). As discussed, the combustion of wet fuelwood results in a lower combustion temperature and slowed burning rate. In response, the emission of CO increases with an increase in MC, as identified in **Figure 9.1**.The average CO emission identified for fuelwood in this study was 73.6±29.4 g/kg$_{fuel}$ with values found within the range of 35.7-133.8 g/kg$_{fuel}$. The combustion of dry fuelwood with an MC of <20% emitted an average of 59.0±22.4 g/kg$_{fuel}$ while the combustion of wet fuelwood with an MC of >20% emitted an average of 105.6±12.3 g/kg$_{fuel}$. As a result, increasing the MC to a content more than 20% resulted in an increase of CO emission by a factor of 1.76. Similar findings have been outlined within the literature. Shelton and Gay (1986) found an increase in CO emission from 304.3±48.9 g/kg$_{fuel}$ to 567.0±64.6 g/kg$_{fuel}$ when the MC was increased from 21% to 41% equating to an increase by a factor of 1.86. Additionally, Purvis et al. (2000) shown in an increase in emission by a factor of 1.58 when the MC is increased beyond 20%. CO emission for both wet and dry fuelwood were more than the limitations outlined in Ecodesign 2015/1185.

9.1.3.2 CH$_4$ and NMVOC

Few studies have specifically evaluated CH$_4$ emissions from residential combustion appliances (Ozgen and Caserini, 2018) with research often including only cookstove devices (Zhang et al., 2000; S.C. Bhattacharya et al., 2002). In the current work it was found that extent of CH$_4$ and NMVOC emission from a

residential heating appliance was significantly dependent upon the fuel MC value. Fuelwood combustion resulted in a CH_4 emission within the range of 0.29-11.32 g/kg_{fuel} with an average emission of 2.48±2.28 g/kg_{fuel} during fuelwood combustion in the test appliance. The emission of NMVOC was found within the range of 0.47-14.31 g/kg_{fuel} with an average emission of 3.41±3.32 g/kg_{fuel}. The combustion of wet fuelwood with a MC of >20% resulted in CH_4 and NMVOC emissions that were 115% and 116% higher than that observed during the combustion of dry fuelwood (<20% moisture). The CH_4 and NMVOC emissions from dry fuelwood combustion were 1.32±0.75 g/kg_{fuel} and 1.84±1.03 g/kg_{fuel} while the same emissions were 5.01±2.48 g/kg_{fuel} and 6.84±4.02 g/kg_{fuel} from wet fuelwood. **Figure 9.1** presents these findings as well as similar values identified within the literature. Similar findings are presented in Mitchell et al. (2019) who identified an increase in CH_4 formation by a factor of 2.8-7.6 when the MC was increased from 5.1% to 27.9%. CH_4 was found to be the most common VOC, accounting for 79±37% of the total emission. CH_4 is commonly identified as the most common VOC during biomass combustion (Tissari et al., 2019). These findings are of specific importance as atmospheric CH_4 emission may account for as much as 30% of global warming since the pre-industrial period (UNEP, 2022). The average organic gaseous compound (OGC) emission (CH_4 + NMVOC) was 11.85 g/kg_{fuel} and 3.15 g/kg_{fuel} for wet and dry fuelwood respectively. OGC emission for both wet and dry fuelwood were more than the limitations outlined in Ecodesign 2015/1185.

9.1.3.3 CH_2O

High concentrations of formaldehyde are often identified during the combustion of fuelwood. CH_2O is presented as the most common aldehyde species with concentrations between 2-3 times higher than that of acetaldehyde (Cerqueira et al., 2013). An assessment of aldehyde formation from residential combustion is required given the toxic or carcinogenic nature with likely adverse effects on human health (Pilidis et al., 2009). Additionally, aldehyde emissions may affect tropospheric chemistry as a precursor to ozone and peroxiacynitrate formation (Carlier et al., 1986). Relatively few studies have investigated the emission of CH_2O from fuelwood combustion (Cerqueira et al., 2013) and there are limited reviews on the relative effect of moisture content. In this present study, CH_2O emissions were recorded within the range of 0.08-4.31 g/kg_{fuel} with an average emission of 0.96±0.97 g/kg_{fuel} for fuelwood. The extent of emissions is shown to be dependent upon fuel MC as identified in **Figure 9.1**.The combustion of dry fuelwood (<20% MC) corresponded with a lower emission of 0.48±0.35 g/kg_{fuel} while wet fuelwood (>20% MC) produced a higher average emission of 2.00±1.09 g/kg_{fuel}. These values

are within the range presented in the literature as shown in **Figure 9.1**. A similar trend is observed in Liparl et al. (1984) and Mcdonald et al. (2000) where the combustion of higher MC fuelwood resulted in higher CH_2O emissions.

9.1.3.4 NOx and SO$_2$

The emission of NOx is shown to be unaffected by the fuelwood MC value, as shown in **Figure 9.1**. The statistical significance of the correlation is very weak presenting an R^2 value of <0.01. Similarly, SO_2 formation appears unaffected by change in the fuelwood MC content. The average emission of NOx and SO_2 was found to be 1.05±0.24 g/kg$_{fuel}$ and 0.64±0.24 g/kg$_{fuel}$. NOx emission is shown to be unaffected by MC where dry and wet fuelwood emission factors are 1.02±0.18 g/kg$_{fuel}$ and 1.11±0.33 g/kg$_{fuel}$ respectively; this accounts for an 8% difference in NOx emission formation. A minor increase in SO_2 emission is observed were dry and wet emission factors are 0.60±0.24 g/kg$_{fuel}$ and 0.72±0.24 g/kg$_{fuel}$; this accounts for an 18% difference in SO_2 formation. A review of the statistical distribution (σ) of SO_2 emission factor results indicates limited effect of MC on pollutant formation. Given the low combustion temperatures observed during the test reactions it is likely that the extent of NOx and SO_2 formation are solely related to the fuel nitrogen and sulfur concentrations. NOx emission for both wet and dry fuelwood were less than the limitations outlined in Ecodesign 2015/1185.
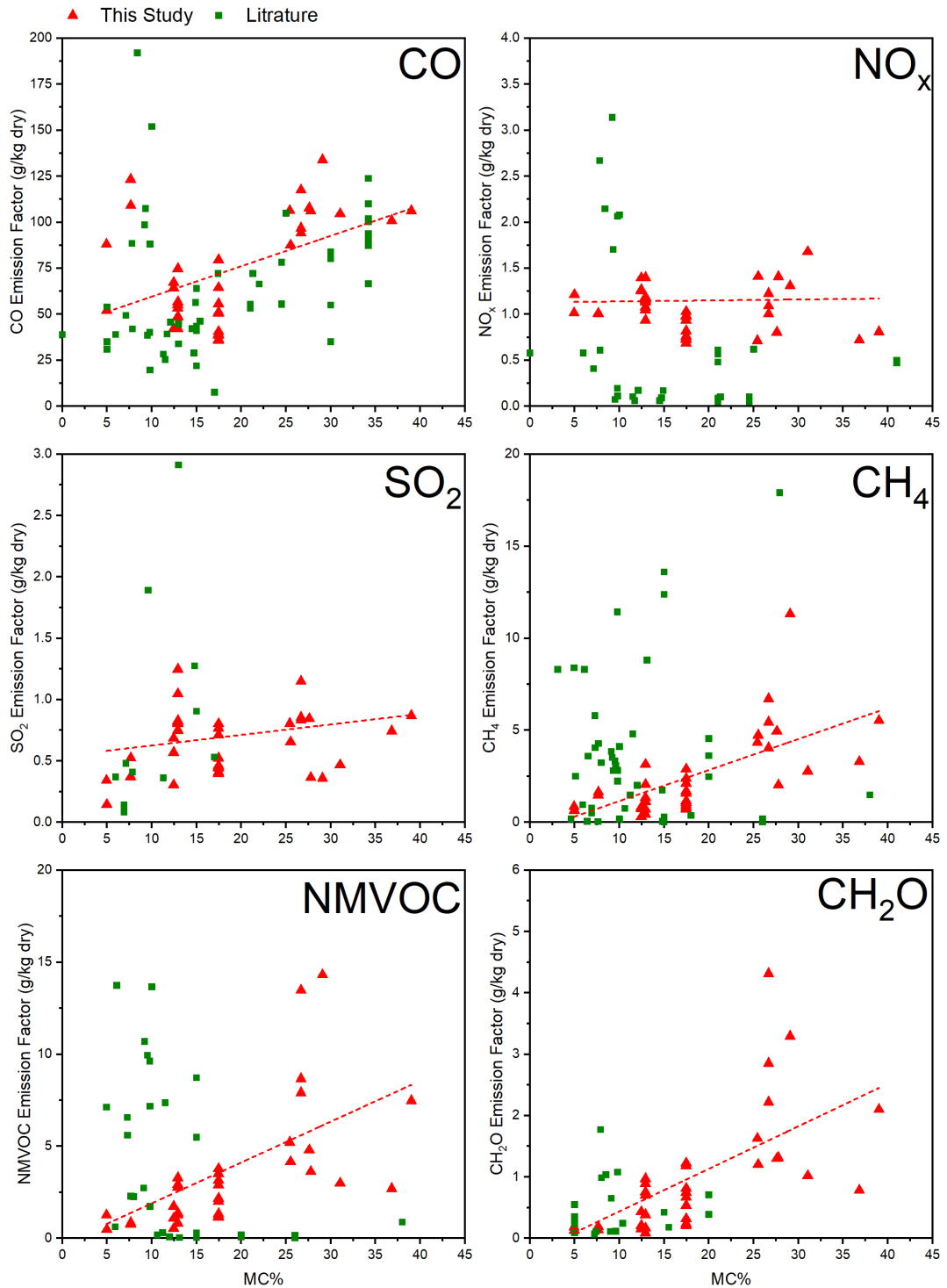
Figure 9.1 Summary of the effect of MC on gaseous emissions. Additional values from the literature are representative of fuelwood and woodchip combustion in various combustion appliances (Liparl et al., 1984; Shelton and Gay, 1986; Zhang et al., 2000; Mcdonald et al., 2000; S. Bhattacharya et al., 2002; Hedberg et al., 2002; Johansson et al., 2004; Koyuncu and Pinar, 2007; Wang et al., 2009; Orasche et al., 2012; Cerqueira et al., 2013; Hayashi et al., 2014; Duarte et al., 2014; Ozgen et al., 2014; Reda et al., 2015; Mitchell et al., 2016; Cereceda-balic et al., 2017; Ozgen and Caserini, 2018; Mitchell et al., 2019; Guerrero et al., 2019; Maxwell et al., 2020; Martens et al., 2021)

9.1.4 Impact of Moisture on PM Emissions

Note : PM values in the Conclusions Chapter have been corrected slightly from those identified in previous chapters. Values in this Chapter are presented in STP. A correction of 0.84 is applied to convert the values in the previous chapters to the current condition.

The effect of fuelwood moisture content on PM emissions is reviewed in **Chapter 5** and **Chapter 6**. Additionally, fuelwood maintaining differing MC values were tested in **Chapter 7** and **Chapter 8**. The average PM emission factor for all fuelwood combusted under warm-start conditions was 3.88 ± 3.86 g/kg$_{fuel}$ with a range of 14.43 g/kg$_{fuel}$. Burning kiln dried fuelwood (<20% MC) resulted in the lowest emission of 2.03 ± 1.06 g/kg$_{fuel}$. Subsequently, fuelwood characterised as seasoned (Rolls, 2013) with an MC of 20-30% presented an emission factor of 7.56 ± 5.19 g/kg$_{fuel}$. Finally, high moisture fuelwood which was had undergone inadequate seasoning or was freshly cut with an MC of >30% presented an emission of 6.37 ± 4.87 g/kg$_{fuel}$. These results agree with findings presented within the literature as shown in **Figure 9.2**.

Previous work undertaken by Wilton and Bluett (2012) reported a possible increase in PM emission during the combustion of either very dry or wet fuelwood with low emissions identified during fuelwood within a MC of 20-30%. Similar findings have been reported by Huangfu et al. (2014), L'Orange et al. (2012) and Tissari et al. (2019) where PM emission was reduced with an increase in MC (**Figure 2.8**). The reason for such processes is due to the control that MC maintains across the combustion reaction. Water in the fuelwood slows the reaction and the burning rate preventing the onset of an O_2 deficiency (Rogge et al., 1998) and increasing the residence time of liberated volatiles within the combustion zone (Yuntenwi and Ertel, 2008). The results of this study, as presented in **Figure 9.2**, do not identify a significant increase in PM formation during the combustion of dry fuelwood although the polynomial fit does suggest a possible increase in intensity of particulate generation when wetter materials are combusted. As a result, the findings of this work are more similar that Guofeng Shen et al. (2013) and Butcher and Sorenson (1979) where low MC fuelwood produces low emissions and high MC fuelwood produces high emissions.
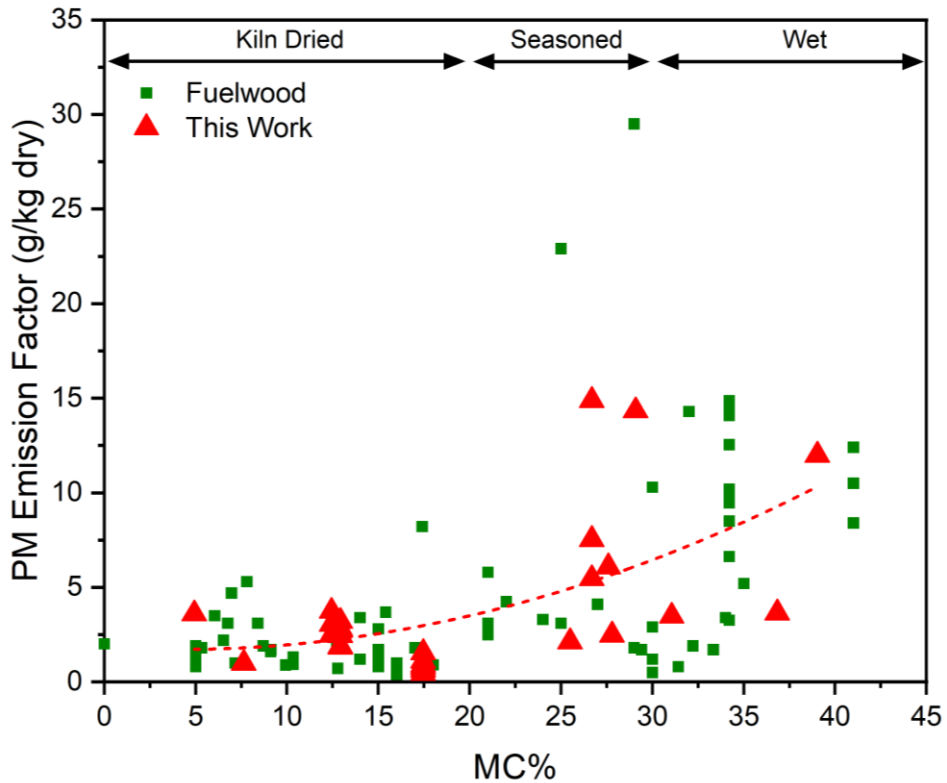
Figure 9.2 Summary of the effect of MC on PM emissions. Additional values from the literature are representative of fuelwood and woodchip combustion in various combustion appliances including cookstoves and residential heating appliances. The parametric fitting function is for results from This Work only (Shelton and Gay, 1986; Purvis et al., 2000; Yuntenwi and Ertel, 2008; Emily Wilton and Bluett, 2012; Shen et al., 2012; Guofeng Shen et al., 2013; Mitchell et al., 2016; Magnone, S.K. Park, et al., 2016; Guerrero et al., 2019).

Recent recognition of the impact of high MC fuel combustion on PM emissions has resulted in the 2019 Clean Air Strategy recommending that only materials <20% moisture should be supplied to the domestic market. Subsequently, the Ready to Burn certification scheme encourages control of high MC fuel for residential consumption. **Figure 9.3** presents the distribution of PM emission factors reported in this study. The results have been categorised into two groups in accordance with the DEFRA and Ready to Burn moisture limit guidelines (20%). Results from this thesis support this 20% guideline limit where fuel containing <20% MC produce lower PM emissions (2.03±1.06 g/kg$_{fuel}$) than fuelwood containing a MC in excess of 20% (7.20±4.85 g/kg$_{fuel}$). Additionally, the combustion of high MC fuelwood produces a larger variance in emissions due to the complexity and inconsistency of combustion conditions when water content is increased. PM emission for dry fuelwood (<20% MC) was less than the limitations outlined in Ecodesign 2015/1185. Burning fuelwood with a MC of >20% led to PM emission in excess of this limit.
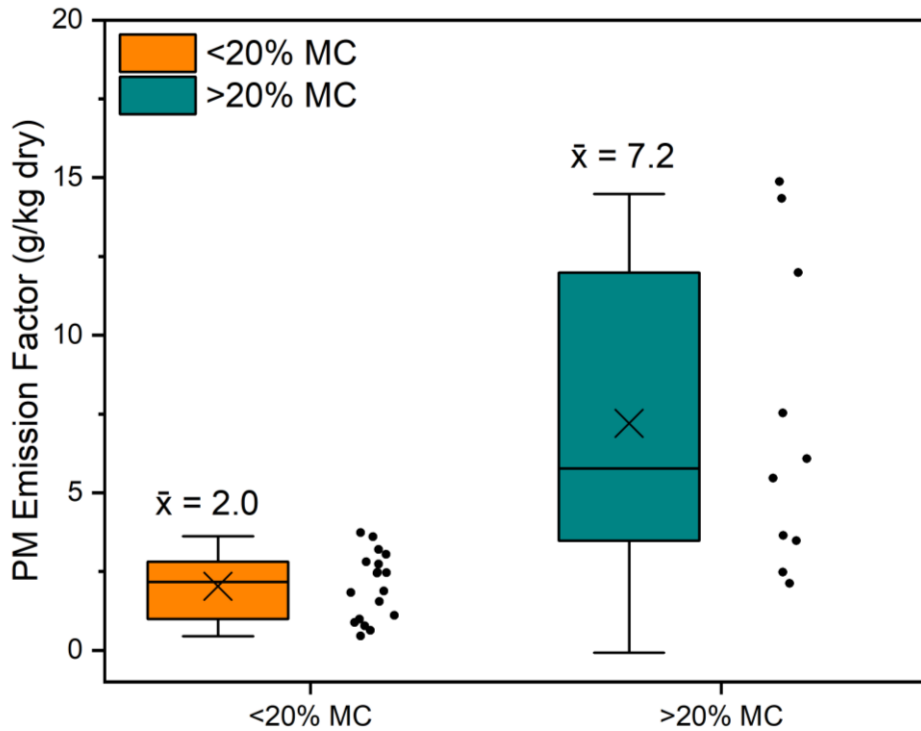
Figure 9.3 Summary of the distribution of PM emission factors for fuelwood combusted with a MC below the approved DEFRA limit (<20% MC) and above the DEFRA limit (>20% MC). Whisker bars represent values which are within 1.5 standard deviations of the mean.

9.1.4.1 Impact of Moisture on EC and OC Fractionation

Chapter 5 and **Chapter 6** show the effect of fuelwood moisture content on the formation of EC and OC fractions during combustion. The EC and OC fractions are analysed as a carbon ratio (TC) for comparison with previous work. The fraction of EC was observed within the range of 2.5% and 92.9% of the total carbon while OC was measured between 7.1% and 97.5%. The EC/TC ratio was found to be heavily dependent upon the fuelwood moisture content with the combustion of wet material resulting in a higher OC fraction.

Fuelwood maintaining an MC of <25% promoted the formation of soot with a smaller OC fraction thereby providing a higher EC/TC of 0.66±0.26 and a range of 0.28-0.93. Alternatively, soot generated from fuelwood with a MC value more than 25% provided a lower EC/TC of 0.18±0.09 and a range of 0.02-0.27. Soot generated during dry fuelwood combustion is most similar to that of diesel combustion (Gillies and Gertler, 2000) while wet fuelwood produced soot maintaining an EC/TC fraction more similar to open burning reactions (Santiago-De La Rosa et al., 2018). The EC/TC ratio values are in good agreement with other results presented within the literature (Mitchell et al., 2016). **Figure 9.4** describes

the effect of MC on EC/TC fractionation as found within the literature combined with findings identified in **Chapter 5** and **Chapter 6**. This trend is in agreement with other findings within the literature whereby high MC fuel results in the formation of a high OC fraction (G. Shen et al., 2013; Magnone, S. Park, et al., 2016).

The fractionation of carbon in soot is dependent upon the temperature of the combustion reaction. High temperature combustion results in a higher EC fraction while high OC formation is observed under cooler reactions (Bølling et al., 2009). This affect was presented during the combustion of fuelwood maintaining differing MC values. The combustion of dry fuelwood corresponds with low OC formation leading to higher EC/TC results. Alternatively, the combustion of wet fuelwood corresponds with high OC formation leading to lower EC/TC results.
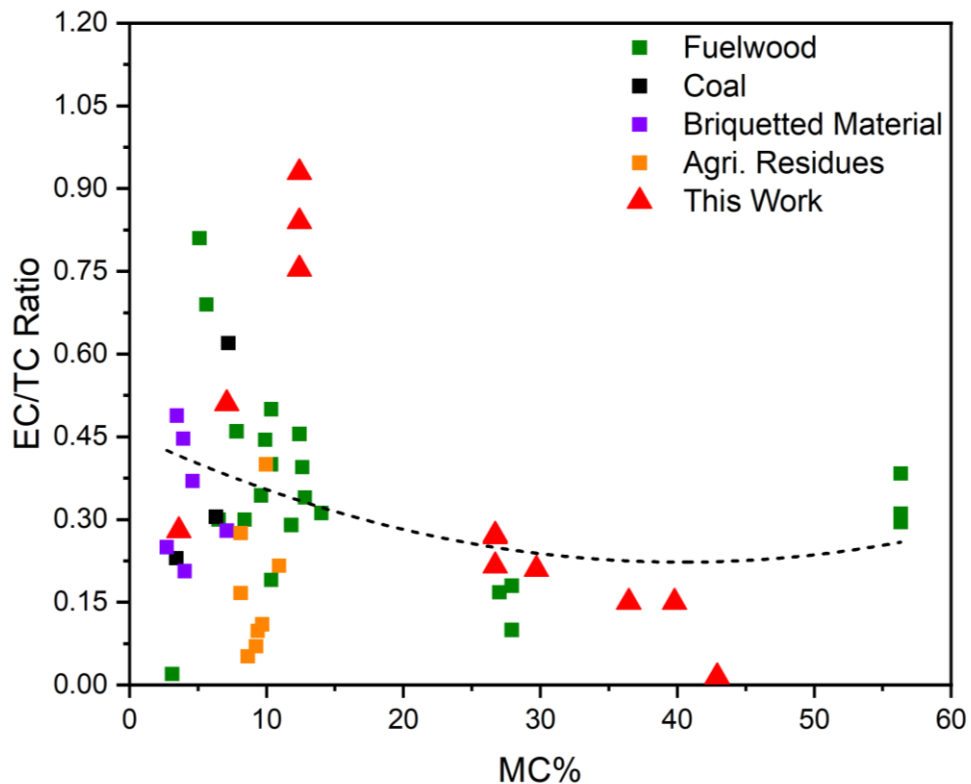
Figure 9.4 Summary of the effect of MC on EC/TC. Addition values provided from literature sources for fuelwood and other materials combusted in stove, cookstove and controlled burner devices (G. Shen et al., 2013; Vicente et al., 2015; Mitchell et al., 2016; Magnone, S.K. Park, et al., 2016; Atiku et al., 2016; Nystrom et al., 2017; Santiago-De La Rosa et al., 2018; Mitchell et al., 2019; Czaplicka et al., 2019)

A possible source of uncertainty in these results relates to the likely effect of different measurement techniques (Bølling et al., 2009). The methods applied in this study are TGA (**Chapter 6**) and optical absorbance (**Chapter 5**) as defined by

Birch and Cary (1996). A number of other techniques are currently available for EC and OC determination including the IMPROVE ECOC method or total optical reflectance (TOR) approach (Chow et al., 2001) and the NIOSH ECOC method (NIOSH, 1996) with primary differences relating to peak temperature and O_2-free heating stages (Schauer, 2003). As a result, it remains difficult to quantify EC/TC correlations within emission inventories due to the differing practices of analysis.

9.1.4.2 Impact of Moisture on PM Size Distribution

PM sample material was principally extracted from a Dilution Tunnel using a Dekati PM_{10} Impactor. The impaction device allowed for the sampling of particulate emission by size fractionation (<PM_1, PM_1-$PM_{2.5}$, $PM_{2.5}$-PM_{10} and >PM_{10}). The PM size fraction distribution was relatively consistent between fuels suggesting that MC maintains a limited impact upon particle size, although there is some evidence for larger particle formation during low moisture fuel combustion in **Chapter 6**.

Ultrafine particles (<1µm) are found to be most common with <PM_1 maintaining 93.1±3.5% of the total PM emittance across all fuel types. When burning kiln dried fuelwood (<20% moisture), the <PM_1 contribution was 93.4±2.2%. Similarly, the average <PM_1 emittance of seasoned fuelwood (20-30% moisture) and wet fuelwood (>30% moisture) was 96.9±1.9% and 96.8±2.7%, respectively. These values are in good agreement with other findings (Johansson et al., 2004; Tissari et al., 2008; Maxwell et al., 2020) where the <1µm size fraction was dominant.

Recent studies have evaluated the effect of soot particles with a nominal diameter of <2.5µm on human health (Heßelbach et al., 2017). Particles of this diameter are small and capable of bypassing the mucociliary defence system resulting in subsequent deposition in the peripheral airways (Heßelbach et al., 2017; Montgomary et al., 2020). Results from this thesis indicate that between 90.4% and 100% of PM emission generated through domestic combustion is of a size fraction (<2µm) determined to be harmful.

9.1.4.3 Impact of Moisture on PM Morphology Characteristics

Optical analysis of PM emissions generated during the combustion of low MC and high MC fuelwood revealed notable differences in material structure and composition. The results of this investigation are presented in **Chapter 5** and **Chapter 6**. SEM analysis of soot samples generated during the combustion of wet fuelwood revealed a significant amorphous tar-like structure forming strands and globules in line with the high OC fraction. Alternatively, soot generated during the combustion of dry fuelwood was comprised of long chains of spherical particulate

matter maintaining a diameter of approximately 50 nm characteristic of the EC fraction.

The colour of soot has been noted in several papers (Rau, 1989; Mitchell et al., 2016; Jones et al., 2018) and is shown to be dependent upon combustion conditions. Wet fuelwood burns at lower temperatures a larger OC fraction is accumulated on sampling filter papers. High OC incorporation often leads to soot samples presenting a dark brown colouration. Alternatively, the low OC fractions observed during dry fuelwood combustion mean that soot material presents a black colouration. An assessment of colour was also undertaken throughout different stages of combustion with results differing depending upon MC. Dry fuelwood combustion generally results in formation of darker and higher density samples whereby the colour is dark brown or black. The combustion of high moisture fuelwood or fuels under cold-start conditions results in the formation of soot samples presenting lower density and light brown or tan colouration. The shift in colouration of soot from black to brown is proportional to the combustion temperature and subsequent accumulation of amorphous tar on the filter paper. These findings have a significant influence on the Absorption Ångström Exponent (AAE) which is an optical indicator affecting absorption in the visible and near-infrared spectral region.

Raman analysis was undertaken to evaluate the effect of MC on the physiochemical structure of soot. The first order Raman spectra of soot generated during the combustion of high and low moisture fuelwood consisted of the same two overlapping peaks located at approximately $1350 cm^{-1}$ and $1585 cm^{-1}$. These peaks are commonly attributed with soot structures and are referred to as the D-peak ($1350 cm^{-1}$) characterised as disordered carbon and the G-peak ($1585 cm^{-1}$) characterised as graphitic carbon (Dippel et al., 1999; Sadezky et al., 2005; Ess et al., 2016). Differences in the intensity of both the GD-peak and G-peak are noted depending on MC. Notably, the average I_D/I_G ratio of soot generated from high MC fuelwood combustion was 0.90 ± 0.05 while a lower value of 0.69 ± 0.03 was presented for soot generated during the combustion of wet fuelwood. An increase in the D-band observed during wet fuelwood combustion is associated with amorphous carbon formations while a heightened G-band during the combustion of dry fuelwood is synonymous with ideal graphitic lattice-type structures.

9.1.5 Stove Operating and Testing Practices

Stove testing and accreditation is required prior to market availability within the UK. A number of standardised testing methods are available offering different conditions and requirements with BS EN 13240 most commonly applied in the UK.

9.1.5.1 Cold Start Operation

Combustion testing in accordance with BS EN 13240 requires only that a stove is operating under nominal conditions prior to emissions and efficiency analysis. This is identified as a limitation as cold-start conditions are negated from the testing procedure. Furthermore, the derived emission factors are commonly used in emission inventories which are subsequently applied in climate models. Previous work has highlighted high emissions during cold-start or ignition procedures (Shelton and Gay, 1986; Nussbaumer et al., 2008; Ozgen et al., 2013; Fachinger et al., 2017) with such phases accounting for as much as 33% of the total emission (Tiegs, 1995). The extent of cold-start operation is likely to vary depending upon region. A significant proportion of stove use in the UK is recreational with evidence suggesting that operational duration of ≤12 h per week (BEIS, 2016a). This indicates that a notable fraction of stove use is associated with cold-start operation only. This is likely more relevant in urban locations where residential combustion is not a primary heating practice.

An investigation into the effect of cold-start operation is presented in **Chapter 7**. Testing was undertaken to provide evidence on the differences in combustion conditions and pollutant formation under cold-start and warm-start operation. Additionally, the use of differing ignition aids on the start-up reaction was examined. Cold-start operation resulted in a lower flue gas combustion temperatures (205 ±39°C) when compared to warm-start operation (363±48°C). Similarly, the burning rate was affected by the stove condition with rates measured at 1.29±0.31 g/kg$_{fuel}$ and 1.87±0.4 g/kg$_{fuel}$ for cold-start and warm-start operation respectively. Low combustion temperature commonly results in inhibited combustion conditions (Venkataraman et al., 2004). The effect of the reduced combustion temperatures was an increase in gaseous emissions by a factor of 3.3 and an increase in PM emissions by a factor of 2.1. The correlation between combustion temperature and pollutant formation is shown in **Figure 7.11**. Incremental increases in combustion temperature are observed with each batch of fuelwood applied to the stove. However, in response to the dynamic nature of the biomass combustion in small closed-fronted heating appliances, reductions in efficiency and temperature can occur after the stove has been in operation for a prolonged period of time. This can mean that warm-start operation produces higher emissions than cold-start operation however this is generally deemed anomalous with such values generally often being masked within the averaged results by during repetitive testing approaches.

This study is important given the current practices associated with stove and heating appliance testing under standardised conditions. Table 9.1 shows the

influence of the addition of cold-start (CS) data within an emission inventory and how this relates to emission limitations as presented in Ecodesign 2015/1185. CO, THC and PM concentrations are all in exceedance of the values outlined in the legislation however the test appliance is a Waterford Stanley Oisin SF NB stove designed in 2012 prior to the establishment of the revised (reduced) emission limits. NOx remains below the emission limit and is unaffected by the phase of operation. The inclusion of cold-start data within an emission inventory increases the average emission by a factor of 0.4-2.9 depending upon species. From this several conclusions can be made. Firstly, given the likelihood of cold-start operation maintaining a significant proportion of total stove use within the UK, CS values should be incorporated for relevance to real-world conditions. Additionally, the inclusion of CS data within an inventory significantly increases the projected emission associated with a specific device or fuel. This is of importance given the intended use of inventories for modelling atmospheric and climatic change. Cold-start operation is neglected in the majority of testing methods including BS EN 13240. Given the complexity of the combustion reaction and significant effect of cold-start inclusion within inventories it is recommended that future standards should include all emission data including start-up conditioning. Similar approaches have been implemented within BS ISO 19867-1:2008 for cookstove testing and the BeReal testing procedure (BeReal, 2013).

Table 9.1 Comparison of emission limits and result inventory values dependent upon cold start inclusion.

Emission	Ecodesign 2015/1185 Limit	WS* Emission (g/kg_{fuel})	CS* and WS* Emission $(g/kg_{fuel}$	Factor **
CO	18.4	54.1	61.0	2.9
THC	1.48	3.6	6.0	2.4
NOx	2.5	1.1	1.2	0.4
PM	2.4	2.5	3.3	1.0

* Average emission factor for warm-start (WS) operation only and for both warm-start and cold-start (CS) data in included.

** The factor represents the ratio increase when both CS and WS data is considered within an emission inventory.

9.1.5.2 Repeatability and Operational Duration

Biomass combustion is a complex process (Jenkins et al., 1996). Combustion testing in small heating appliances is commonly acknowledged to produce notable variability in results and poor reproducibility (Trojanowski et al., 2018). As

discussed, stove testing is generally undertaken in accordance with a standardised operating method. The number of repeated tests identified in standardised methods and within the literature is noted to vary. Furthermore, the duration of stove testing remains generally unknown and is often variables across European countries. Recent surveys have suggested that stove operational duration within the UK is likely short with only 29% of stove consumers utilising their appliance for 40 hours or more (BEIS, 2016b). This emphasises the importance of cold-start conditions within emission inventories however in colder European nations the operational duration is likely much longer (Wöhler et al., 2016).

Chapter 8 reviews the effect of operational duration and the processes which affect reproducibility in terms of stove performance. The outcomes of the research identify three processes. Firstly, the effect of inventory sample size on results confidence. Secondly, the impact of fuel type on repeatability. Finally, the impact of operational duration on combustion conditions.

A confidence interval (CI) is formulated to identify the impact of sample size (n) on results confidence. It is assumed that the larger the size of the sample inventory (i.e. the number of fuel reloads in the test) the greater the statistical precision and the narrower the CI; the inverse is therefore presented for inventories maintaining a smaller sample size (Gupta, 2015). Inventory values for biomass briquettes (**Chapter 8.4.5.1**) and fuelwood (**Chapter 8.4.5.3**) appears to follow the trend outlined within the literature whereby an increase in n results in a reduction in CI (Gupta, 2015; Matsuyama, 2018; Giannoulis, 2019). The trend in CI relative to n is more variable with regards to the torrefied briquette fuel as shown in **Chapter 8.4.5.2**. An increase in the number of test-batches generally results in a reduction in the width of the confidence interval thereby increasing the statistical precision of the emission result. However, changes in the condition of the combustion zone during prolonged testing can positively or negatively affect the emission level. For some fuels this can lead to highly changeable emissions which can affect the CI thereby negating the effect of repetitive batch testing. Therefore, it is the quality of the combustion reaction (per batch) which has a greater effect on repeatability than the type of fuel combusted. Wood briquettes were found to provide the most consistent results due to the regularity of their physical structure and combustion performance. Fuelwood, identified as the most heterogeneous material, provided the poorest repeatability. Increased temperatures during long-term stove operation often contribute in a reduction in repeatability as the improved efficiency is distinctively different from what is observed during previous batches.

Combustion conditions are generally shown to improve with each batch of fuel applied to the stove in response to an increase in the combustion temperature.

Maximum temperatures are generally observed after prolonged stove operation beyond the common testing duration of many standard test procedures. The higher temperatures generally correspond with lower emissions. Prolonged testing scenarios should therefore be considered given the longevity of daily stove operation in many European countries. It therefore stands to reason that the accredited emission values for an appliance may be an over-estimation given that ideal temperatures are not always attained relative to real-world operating conditions.

Stove testing procedures should consider the impact of applied fuel mass, on both an individual batch and a batch-by-batch basis, on the combustion temperatures and formation of derived pollutant products. The recommended solution would thereby be that stove users should continue to implement the pre-test-batch followed by 3 test-batch standard procedure however a greater number of tests should be undertaken. This would overcome the effect of prolonged stove testing on the combustion zone. However, this method would only be representative of controlled operating conditions and not be representative of stove performance in cool countries where a device may run for a prolonged period.

9.2 Future Work

9.2.1 Correlation between Soot Colouration and Composition

It was observed that soot samples collected on filter papers present different colouration depending upon composition, notably the EC and OC fractionation. EC and OC are important variables in the determination of AAE which have a notable influence in climatological simulations (Bond et al., 2002; Bond and Bergstrom, 2006). Previous research has illustrated the differences in soot colouration (Rau, 1989; Mitchell et al., 2016; Jones et al., 2018; Price-Allison et al., 2021). An example of the difference in colour is shown in **Figure 9.5**. Simple methods of measuring emission concentration via photometric determination are applied in other industries including DIN 51402-1 and ASTM D 2156-94 methods for measuring soot emission from oil burning systems. This approach has been successfully applied in emission concentration research related to biofuel blend resources (Estevez et al., 2019), emission testing for waste incinerator research (Kardono, 2016) and cookstove combustion testing (Singh and Poudel, 2013). Currently the method has only been applied for estimating concentration based upon sample darkness and density using the Bacharach Smoke Scale. Future work may apply this sampling method as a way of high-frequency collecting soot from a flue. The colouration of the soot is likely to vary depending upon the phase of

combustion (Jones et al., 2018) and the fuel MC (Price-Allison et al., 2021). A review of the colouration of soot via low-cost techniques, including RGB surveys, could be combined with EC/OC analysis to generate a new scale. The proposed EC/OC scale would give an indication of amorphous and graphitic carbon contents which are synonymous with black carbon and brown carbon fractions. These qualitative values could feed into climatological simulation research. This method would be of use in cookstove testing research currently being undertaken in developing countries where traditional methods of EC/OC determination are unavailable. The idea for this work was from useful discussion concerning soot measurement with Mr. Glynn Hughes [Hughes Design Ltd].

Figure 9.5 Likely variability in the colouration of soot collected during the combustion of biomass. Differences in colouration are subject to combustion conditions including temperature and burning rate.

9.2.1 The Impact of Soot Inhalation on Human Health

Air quality in urban locations has declined in recent years with biomass combustion identified as a probable source of increased PM concentrations (Fuller et al., 2013; Fuller et al., 2014). Degradation of indoor and outdoor air quality from biomass and solid fuel combustion is known to affect human health with approximately 3.8 million premature deaths identified globally as a result of noncommunicable diseases including ischaemic heath disease, chronic obstructive pulmonary disease, pneumonia and lung cancer (WHO, 2021). It is estimated that up to 40,000 premature deaths are attributed to biomass smoke in Europe annually (Tomlin, 2021). The impact of deteriorating air quality is of significant importance in developing nations with more than 2.6 billion people reliant upon biomass and solid fuel combustion for cooking (Leary et al., 2021). Several studies have evaluated the

effect of PM$_{2.5}$ inhalation on human health (Matzenbacher et al., 2017; Uski et al., 2018; Mitchell et al., 2019). Comet assay is commonly applied as a method of determining cellular DNA damage via electrophoresis. The method provides a quantitative indication of the effect of toxic compounds on eukaryotic cells and the extent of the DNA damage. This thesis has shown that moisture content in fuelwood affects the OC and EC fractions in emitted particulate. Components in the OC fractions could be active in inducing cellular damage. Given the likely high quantities of wet fuelwood currently consumed within the UK (BEIS, 2016a) and the contemporary decline in urban air quality (Fuller et al., 2014), it is proposed that further work is required to assess the effect of high moisture fuelwood combustion on human health.

9.2.2 Methods of Clean Residential Combustion

The results of this thesis have revealed that contemporary combustion appliances are inefficient and have a high pollutant output. Nevertheless, the use of such devices remains a common practice in Northern Europe and the UK. As a result, change in the design of combustion systems or fuels may be required to abate the production of emissions and curve the detrimental impact on air quality. Future work may include an investigation into the effect of electrostatic precipitators (ESP) on woodstove flue systems for the direct collection of PM emittance (Bologa et al., 2009). Similarly, the use of O$_2$ monitoring with automated primary-airflow correction may be investigated for gauging ideal combustion conditions (feeding rates, burning rate and air supply) for reducing emissions (Valente et al., 2020). Finally, the use of alternative fuels may be applied as a replacement for high polluting materials. Fuels including pre-treated torrefied biomass (Maxwell et al., 2020; Trubetskaya et al., 2021) and briquettes derived from sustainably sourced waste or residues (Morales-Maximo et al., 2022) may be investigated as a low-emission alternative to fuelwood and coal.

9.1 References

Atiku, F.A., Mitchell, E.J.S., Lea-Langton, A.R., Jones, J.M., Williams, A. and Bartle, K.D. 2016. The Impact of Fuel Properties on the Composition of Soot Produced by the Combustion of Residential Solid Fuels in a Domestic Stove. Fuel Processing Technology. 151, pp.117–125.

BEIS 2016a. Special feature - Domestic wood use survey [Online]. [Accessed 18 May 2020]. Available from: www.gov.uk/government/statistics/digest-of-united-kingdom-energy-statistics-dukes-2014-printed-version.

BEIS 2016b. Summary results of the domestic wood use survey [Online]. Available from: www.gov.uk/government/statistics/digest-of-united-kingdom-energy-statistics-dukes-2014-printed-version.

BeReal 2013. beReal - Advanced testing methods for better real life performance of biomass heating appliances. Available from: http://www.bereal-project.eu/.

Bhattacharya, S.C., Albina, D.O. and Myint Khaing, A. 2002. Effects of selected parameters on performance and emission of biomass-fired cookstoves.

Bhattacharya, S.C., Albina, D.O. and Salam, P.A. 2002. Emission factors of wood and charcoal-fired cookstoves. Biomass and Bioenergy. 23, pp.453–469.

Birch, M.E. and Cary, R.A. 1996. Elemental carbon-based method for monitoring occupational exposures to particulate diesel exhaust. Aerosol Science and Technology. 25, pp.221-241.

Bologa, A., Paur, H.R., Seifert, H. and Woletz, K. 2009. Particle collection by an electrostatic precipitator from the exhaust gas of a wood combustion stove In: Proceedings of the European Combustion Meeting.

Bølling, A.K., Pagels, J., Yttri, K.E., Barregard, L., Sallsten, G., Schwarze, P.E. and Boman, C. 2009. Health effects of residential wood smoke particles: the importance of combustion conditions and physicochemical particle properties. Particle and Fibre Toxicology. 6(1), pp.1–20.

Bond, T.C. and Bergstrom, R.W. 2006. Aerosol Science and Technology Light Absorption by Carbonaceous Particles: An Investigative Review Light Absorption by Carbonaceous Particles: An Investigative Review. Aerosol Science and Technology. 40(1), pp.27–67.

Bond, T.C., Covert, D.S., Kramlich, J.C., Larson, T.V. and Charlson, R.J. 2002. Primary particle emissions from residential coal burning: Optical properties and size distributions. Journal of Geophysical Research: Atmospheres. 107(D21).

Butcher, S.S. and Sorenson, E.M. 1979. A Study of Wood Stove Particulate Emissions. Journal of the Air Pollution Control Association. 29(7), pp.724–728.

Carlier, P., Hannachi, H. and Mouvier, G. 1986. The chemistry of carbonyl compounds in the atmosphere - A review. Atmospheric Environment. 20(11), pp.2079–2099.

Cereceda-balic, F., Toledo, M., Vidal, V., Guerrero, F., Diaz-robles, L.A., Petit-breuilh, X. and Lapuerta, M. 2017. Science of the Total Environment distributions from the combustion of wood species using a new controlled combustion chamber 3CE. Science of the Total Environment. 584–585, pp.901–910.

Cerqueira, M., Gomes, L., Tarelho, L. and Pio, C. 2013. Formaldehyde and acetaldehyde emissions from residential wood combustion in Portugal. Atmospheric Environment. 72, pp.171–176.

Chow, J.C., Watson, J.G., Crow, D., Lowenthal, D.H. and Merrifield, T. 2001. Comparison of IMPROVE and NIOSH carbon measurments. Aerosol Science and Technology. 34(1), pp.23–34.

Czaplicka, M., Cieslik, E., Komosinski, B. and Rachwal, T. 2019. Emission factors for biofuels and coal combustion in a domestic boiler of 18 kW. Atmosphere. 10(12), p.771.

Dippel, B., Jander, H. and Heintzenberg, J. 1999. NIR FT Raman spectroscopic study of Ñame soot. phys. 1, pp.4707–4712.

Duarte, M., Vicente, E., Calvo, A., Nunes, T., Tarelho, L. and Alves, C. 2014. Gaseous and particulate emissions from the combustion of wood in a Portuguese stove In: SPEIC14 - Towards Sustainable Combustion.

Ess, M.N., Ferry, D., Kireeva, E.D., Niessner, R., Ouf, F. and Ivleva, N.P. 2016. In situ Raman microspectroscopic analysis of soot samples with different organic carbon content : Structural changes during heating. Carbon. 105, pp.572–585.

Estevez, R., Aguado-Deblas, L., Posadillo, A., Hurtado, B., Bautista, F.M., Hidalgo, J.M., Luna, C., Calero, J., Romero, A. and Luna, D. 2019. Performance and emission quality assessment in a diesel engine of straight castor and sunflower vegetable oils, in diesel/gasoline/oil triple blends. Energies. 12(2181).

Fachinger, F., Drewnick, F., Gieré, R. and Borrmann, S. 2017. How the user can influence particulate emissions from residential wood and pellet stoves: Emission factors for different fuels and burning conditions. Atmospheric Environment. 158, pp.216–226.

Fuller, G.W., Sciare, J., Lutz, M., Moukhtar, S. and Wagener, S. 2013. New Directions: Time to tackle urban wood burning? Atmospheric Environment. 68, pp.295–296.

Fuller, G.W., Tremper, A.H., Baker, T.D., Espen, K. and Butter, D. 2014. Contribution of wood burning to PM 10 in London. Atmospheric Environment. 87, pp.87–94.

Giannoulis, C. 2019. How to interpret the width of a confidence interval. The Analysis Factor. [Online]. Available from: https://www.theanalysisfactor.com/interpret-width-of-confidence-interval/.

Gillies, J.A. and Gertler, A.W. 2000. Comparison and evaluation of chemically speciated mobile source $PM_{2.5}$ particulate matter profiles. Journal of the Air & Waste Management Association. 50, pp.1459–1480.

Guerrero, F., Yanez, K., Vidal, V. and Cereceda-Balic, F. 2019. Effects of wood moisture on emission factors for $PM_{2.5}$, particle numbers and particulate-phase PAHs from Eucalyptus globulus combustion using a controlled combustion chamber for emissions. Science of the Total Environment. 648, pp.737–744.

Gupta, A. 2015. Interpreting research findings with confidence interval. Journal of Orthodontics. 1(1), p.8.

Hayashi, K., Ono, K., Kajiura, M., Sudo, S., Yonemura, S., Fushimi, A., Saitoh, K., Fujitani, Y. and Tanabe, K. 2014. Trace gas and particle emissions from open burning of three cereal crop residues: Increase in residue moistness enhances emissions of carbon monoxide, methane, and particulate organic carbon. Atmospheric Environment. 95, pp.36–44.

Hedberg, E., Kristensson, A., Ohlsson, M., Johansson, C., Johansson, A., Swietlicki, E., Vesely, V., Wideqvist, U. and Westerholm, R. 2002. Chemical and physical characterization of emissions from birch wood combustion in a wood stove.

Heßelbach, K., Kim, G.-J., Flemming, S., Haupl, T., Bonin, M., Dornhof, R., Gunther, S., Merfort, I. and Humar, M. 2017. Disease relevant modifications of the methylome and transcriptome by particulate matter ($PM_{2.5}$) from biomass combustion. Epigenetics. 12(9), pp.779–792.

Huangfu, Y., Li, H., Chen, X., Xue, C., Chen, C. and Liu, G. 2014. Effects of moisture content in fuel on thermal performance and emission of biomass semi-gasified cookstove. Energy for Sustainable Development. 21, pp.60–65.

Jenkins, B.M., Baxter, L.L., Miles, T.R. and Miles Jr, T.R. 1996. Combustion properties of biomass In: Proceedings of Biomass Usage for Utility and Industrial PPower.

Johansson, L.S., Leckner, B., Gustavsson, L., Cooper, D., Tullin, C. and Potter, A. 2004. Emission characteristics of modern and old-type residential boilers fired with wood logs and wood pellets. Atmospheric Environment. 38, pp.4183–4195.

Jones, J., Mitchell, E., Williams, A., Jose, G., Hondow, N., Lea-langton, A., Jones, J., Mitchell, E., Williams, A., Jose, G., Hondow, N. and Combustion-generated, A.L.E. 2018. Examination of Combustion-Generated Smoke Particles from Biomass at Source : Relation to Atmospheric Light Absorption Examination of Combustion-Generated Smoke Particles from Biomass at Source : Relation to Atmospheric Light Absorption. Combustion Science and Technology. 00(00), pp.1–14.

Kardono, K. 2016. Environmental performance test of hazardous waste incinerator in Indonesia. KMUTNB International Journal of Science and Technology. 9(2), pp.79–90.

Koppejan, J. and van Loo, S. 2008. The Handbook of Biomass Combustion and Co-firing. London: Routledge.

Koyuncu, T. and Pinar, Y. 2007. The emissions from a space-heating biomass stove. Biomass and Bioenergy. 31(1), pp.73–79.

L'Orange, C., DeFoort, M. and Willson, B. 2012. Influence of testing parameters on biomass stove performance and development of an improved testing protocol. Energy for Sustainable Development. 16(1), pp.3–12.

Leary, J., Leach, M., Batchelor, S., Scott, N. and Brown, E. 2021. Battery-supported eCooking: A transformative opportunity for 2.6 billion people who still cook with biomass. Energy policy. 159(112619).

Liparl, F., Dasch, J.M. and Scruggs, W.F. 1984. Aldehyde emissions from wood-burning fireplaces. Environmental Science and Technology1. 18(5), pp.326–330.

Magnone, E., Park, S.K. and Park, J.H. 2016. Effects of Moisture Contents in the Common Oak on Carbonaceous Aerosols Generated from Combustion Processes in an Indoor Wood Stove. Combustion Science and Technology. 188(6), pp.982–996.

Martens, P., Czech, H., Tissari, J., Ihalainen, M., Suhonen, H., Sklorz, M., Jokiniemi, J., Sippula, O. and Zimmermann, R. 2021. Emissions of gaseous and volatile organic compounds from residential heating: A comparison of brown coal briquettes and logwood combustion. Energy and Fuels. 35(17), pp.14010–14022.

Matsuyama, T. 2018. An application of bootstrap method for analysis of particle size distribution. Advanced Powder Technology. 29(6), pp.1404–1408.

Matzenbacher, C.A., Garcia, A.L.H., dos Santos, M.S., Nicolau, C.C., Premoli, S., Correa, D.S., de Souza, C.T., Niekraszewicz, L., Dias, J.F., Delgado, T.V., Kalkreuth, W., Grivicich, I. and da Silva, J. 2017. DNA damage induced by coal dust, fly and bottom ash from coal combustion evaluated using the micronucleus test and comet assay in vitro. Journal of Hazardous Materials. 324(Part B), pp.781–788.

Maxwell, D., Gudka, B.A., Jones, J.M. and Williams, A. 2020. Emissions from the combustion of torrefied and raw biomass fuels in a domestic heating stove. Fuel Processing Technology. 199.

Mcdonald, J.D., Zielinska, B., Fujita, E.M., Sagebiel, J.C., Chow, J.C. and Watson, J.G. 2000. Fine particle and gaseous emission rates from residential wood combustion. Environmental Science and Technology. 34(11), pp.2080–2091.

Mitchell, E.J.S., Lea-Langton, A.R., Jones, J.M., Williams, A., Layden, P. and Johnson, R. 2016a. The impact of fuel properties on the emissions from the

combustion of biomass and other solid fuels in a fixed bed domestic stove. Fuel Processing Technology. 142, pp.115–123.

Mitchell, E.J.S., Lea-Langton, A.R., Jones, J.M., Williams, A., Layden, P. and Johnson, R. 2016b. The impact of fuel properties on the emissions from the combustion of biomass and other solid fuels in a fixed bed domestic stove. Fuel Processing Technology. 142, pp.115–123.

Mitchell, E.J.S., Ting, Y., Allan, J., Spracklen, D. V, Mcfiggans, G., Coe, H., Routledge, M.N., Williams, A., Jones, J.M., Ting, Y., Allan, J. and Spracklen, D. V 2019. Pollutant Emissions from Improved Cookstoves of the Type Used in Sub-Saharan Africa Pollutant Emissions from Improved Cookstoves of the Type Used in Sub-Saharan Africa. Combustion Science and Technology., pp.1–21.

Montgomary, M.T., Sajuthi, S.P., Cho, S.H., Everman, J.L., Rios, C.L., Goldfarbmuren, K.C., Jackson, N.D., Saef, B., Cromie, M., Eng, C., Medina, V., Elhawary, J.R., Oh, S.S., Rodriguez-Santana, J., Valadar, E.K., Burchard, E.G. and Seibold, M.A. 2020. Genome-wide analysis reveals mucociliary remodelling of the nasal airway epithelium induced by urban $PM_{2.5}$. American Journal of Cell and Molecular Biology. 63(2), pp.172–184.

Morales-Maximo, M., Tutiaga-Quinones, J.G., Masera, O. and Ruiz-Garcia, V.M. 2022. Briquettes from Pinus spp. Residues: Energy saving and emissions mitigation in the rural sector. Energies. 15(9), p.3419.

NIOSH 1996. Elemental carbon (diesel particulate): Method 5040. Cincinatti.

Nussbaumer, T., Doberer, A., Klippel, N., Bühler, R. and Vock, W. 2008. Influence of ignition and operation type on particle emissions from residential wood combustion In: 16th European Biomass Conference and Exhibition.

Nystrom, R., Lindgren, R., Avagyan, R., Westerholm, R., Lundstedt, S. and Boman, C. 2017. Influence of wood species and burning conditions on particle emission characteristics in a residential wood stove. Energy and Fuels. 31(5), pp.5514–5524.

Orasche, J., Seidel, T., Hartmann, H., Schnelle-Kreis, J., Chow, J.C. and Ruppert, H. 2012. Comparison of emissions from wood combustion. Part 1: Emission factors and characteristics from different small-scale residential heating appliances considering particulate matter and polycyclic aromatic hydrocarbon (PAH)-related toxicological potential o. Energy Fuels. 26, pp.6695–6704.

Ozgen, S. and Caserini, S. 2018. Methane emissions from small residential wood combustion appliances : Experimental emission factors and warming potential. Atmospheric Environment. 189(June), pp.164–173.

Ozgen, S., Caserini, S., Galante, S., Giugliano, M., Angelino, E., Marongiu, A., Hugony, F., Migliavacca, G. and Morreale, C. 2014. Emission factors from small scale appliances burning wood and pellets. Atmospheric Environment. 94, pp.144–153.

Ozgen, S., Cernuschi, S. and Giugliano, M. 2013. Experimental evaluation of particle number emissions from wood combustion in a closed fireplace. Biomass and Bioenergy. 50(0), pp.65–74.

Pilidis, G., Karakitsios, S.P., Kassomenos, P.A., Kazos, E.. and Stalikas, C.D. 2009. Measurments of benzene and formaldehyde in a medium sized urban environment. Indoor/outdooe health risk implications on special population groups. Environmental Monitoring and Assessment. 150, pp.285–294.

Price-Allison, A., Mason, P.E., Jones, J.M., Barimah, E.K., Jose, G., Brown, A.E., Ross, A.B. and Williams, A. 2021. The Impact of Fuelwood Moisture Content on the Emission of Gaseous and Particulate Pollutants from a Wood Stove. Combustion Science and Technology.

Purvis, C.R., Mccrillis, R.C. and Kariher, P.H. 2000. Fine particulate matter (PM) and organic speciation of fireplace emissions. Environmental Science and Technology. 34(9), pp.1653–1658.

Singh, R.M. and Poudel, M.S. 2013. Briquette fuel - An option for management of Mikania micrantha. Nepal Journal of Science and Technology. 14(1), pp.109–114.

Rau, J.A. 1989. Composition and size distribution of residential wood smoke particles. Aerosol Science and Technology. 10(1), pp.181–192.

Reda, A.A., Czech, H., Schnelle-Kreis, J., Sippula, O., Orasche, J., Weggler, B., Abbaszade, G., Arteaga-Salas, J.M., Kortelainen, M., Tissari, J., Jokiniemi, J., Streibel, T. and Zimmermann, R. 2015. Analysis of gas-phase carbonyl compounds in emissions from modern wood combustion appliances: Influence of wood type and combustion appliances. Energy and Fuels. 29(6), pp.3897–3907.

Rogge, W.F., Hildemann, L.M., Mazurek, M.A. and Cass, G.R. 1998. Sources of Fine Organic Aerosol . 9 . Pine , Oak , and Synthetic Log Combustion in Residential Fireplaces. Environmental Science and Technology. 32(1), pp.13–22.

Rolls, W. 2013. The Log Book. East Meon: Permanent Publications.

Sadezky, A., Mucjenhuber, H., Grothe, H., Niessner, R. and Poschl, U. 2005. Raman microspectroscopy of soot and related carbonaceous materials: Spectral analysis and structural information. Carbon. 43, pp.1731–1742.

Santiago-De La Rosa, N., González-Cardoso, G., Figueroa-Lara De Jesús, J., Gutiérrez-Arzaluz, M., Octaviano-Villasana, C., Ramírez-Hernández, I.R. and Mugica-Álvarez, V. 2018. Emission factors of atmospheric and climatic pollutants from crop residues burning. Journal of the Air & Waste Management Association. 68(8), pp.849–865.

Schauer, J.J. 2003. Evaluation of elemental carbon as a marker for diesel particulate matter. Journal of Exposure Science and Environmental Epidemiology. 13, pp.443–453.

Shelton, J.W. and Gay, L.W. 1986. Evaluation of low-emission wood stoves [Online]. Sacramento, California. [Accessed 12 June 2020]. Available from: https://ww2.arb.ca.gov/sites/default/files/classic//research/apr/past/a3-122-32_exsum.pdf.

Shen, G., Tao, S., Chen, Y., Zhang, Y., Wei, S., Xue, M., Wang, B., Wang, R., Lv, Y., Shen, H., Huang, Y. and Chen, H. 2013. Emission characteristics for polycyclic aromatic hydrocarbons from solid fuels burned in domestic stoves in rural China. Environmental Science and Technology. 47(24), pp.14485–14494.

Shen, G., Wei, S., Wei, W., Zhang, Y., Min, Y., Wang, B., Wang, R., Li, W., Shen, H., Huang, Y., Yang, Y., Wang, W., Wang, Xilong, Wang, Xuejun and Tao, S. 2012. Emission factors, size distributions, and emission inventories of carbonaceous particulate matter from residential wood combustion in rural China. Environmental Science and Technology. 46(7), pp.4207–4214.

Shen, Guofeng, Xue, M., Wei, S., Chen, Y., Zhao, Q., Li, B., Wu, H. and Tao, S. 2013. Influence of fuel moisture, charge size, feeding rate and air ventilation conditions on the emissions of PM, OC, EC, parent PAHs, and their derivatives from residential wood combustion. Journal of Environmental Sciences (China). 25(9), pp.1808–1816.

Tiegs, P.E. 1995. Design and Operating Factors Which Affect Emissions from Residential Wood-Fired Heaters: Review and Update.

Tissari, J., Lyyränen, J., Hytönen, K., Sippula, O., Tapper, U., Frey, A., Saarnio, K., Pennanen, A.S., Hillamo, R., Salonen, R.O., Hirvonen, M.R. and Jokiniemi, J. 2008. Fine particle and gaseous emissions from normal and smouldering wood combustion in a conventional masonry heater. Atmospheric Environment. 42(34), pp.7862–7873.

Tissari, J., Väätäinen, S., Leskinen, J., Savolahti, M., Lamberg, H., Kortelainen, M., Karvosenoja, N. and Sippula, O. 2019. Fine particle emissions from sauna stoves: effects of combustion appliances and fuel, and implications for the Finnish Emission Inventory. Atmosphere. 10(12), p.775.

Tomlin, A.S. 2021. Air quality and climate impacts of biomass use as an energy source: A review. Energy and Fuels. 35(18), pp.14213–14240.

Trojanowski, R., Butcher, T., Wei, G. and Celebi, Y. 2018. Repeatability in Particulate and Gaseous Emissions from Pellet Stoves for Space Heating. Energy and Fuels. 32(3), pp.3543–3550.

Trubetskaya, A., Lin, C., Ovadnevaite, J., Ceburnis, D., O'Dowd, C., Leahy, J.J., Monaghan, R.F.D., Johnson, R., Layden, P. and Smith, W. 2021. Study of Emissions from Domestic Solid-Fuel Stove Combustion in Ireland. Energy and Fuels. 35, p.4978.

UNEP 2022. Methane emissions are driving climate change. Here's how to reduce them. [Accessed 2 May 2022]. Available from: https://www.unep.org/news-and-stories/story/methane-emissions-are-driving-climate-change-heres-how-reduce-them#:~:text=Methane is also a powerful, keeping began in the 1980s.

Uski, O., Rankin, G., Lindgren, R., Lopez, N., Blomberg, A.C., Muala, A., Bosson Damewood, J.A. and Sandstrom, T. 2018. In vitro toxicity of particulate matter derived from biomass cook stoves used in developing countries In: A70 Environmental Stressors, Gases, and Host Responses. American Thoratic Society, pp.A2281–A2281.

Valente, L., Tarelho, L.A.C. and Costa, V.A.F. 2020. Emissions mitigation by control of biomass feeding in an industrial biomass boiler. Energy Reports. 6(1), pp.483–489.

Venkataraman, C., Joshi, P., Sethi, V., Kohli, S. and Ravi, M.R. 2004. Aerosol and Carbon Monoxide Emissions from Low-Temperature Combustion in A Sawdust Packed-Bed Stove. Aerosol Science and Technology. 38(1), pp.50–61.

Vicente, E.D., Duarte, M.A., Calvo, A.L., Nunes, T.F., Tarelho, L.A.C., Custodio, D., Colombi, C., Gianelle, V., Sanchez de la Campa, A. and Alves, C.A. 2015. Influence of operating conditions on chemical composition of particulate matter emissions from residential combustion. Atmospheric Research. 166(1), pp.92–100.

Wang, S., Wei, W., Du, L., Li, G. and Hao, J. 2009. Characteristics of gaseous pollutants from biofuel-stoves in rural China. Atmospheric Environment. 43(27), pp.4148–4154.

WHO 2021. Household air pollution and health. Available from: https://www.who.int/news-room/fact-sheets/detail/household-air-pollution-and-health.

Wilton, E. and Bluett, J. 2012. Factors influencing particulate emissions from NEW compliant woodburners in Nelson, Rotorua and Taumarunui 2007.

Wilton, Emily and Bluett, J. 2012. Wood Burner Testing Christchurch 2009 : Diurnal variation in emissions , wood use , indoor temperature and factors influencing start-up Prepared for Ministry of Science and Innovation [Online]. Available from: https://www.niwa.co.nz/sites/niwa.co.nz/files/2 - AKL 2012-020 Woodburner testing Chch 2009.pdf.

Wöhler, M., Andersen, J.S., Becker, G., Persson, H., Reichert, G., Schön, C., Schmidl, C., Jaeger, D. and Pelz, S.K. 2016. Investigation of real life operation of biomass room heating appliances - Results of a European survey. Applied Energy. 169, pp.240–249.

Yuntenwi, E.A.T. and Ertel, J. 2008. Laboratory study of the effects of moisture content on heat transfer and combustion efficiency of three biomass cook stoves. Energy for Sustainable Development. 12(2), pp.66–77.

Zhang, J., Smith, K.R., Ma, Y., Ye, S. and Jiang, F. 2000. Greenhouse gases and other airbourne pollutants from household stoves in China: A database for emission factors. Atmospheric Environment. 34(26), pp.4537–4549.